# ON THE MECHANICAL BEHAVIOUR OF HUMAN TOOTH STRUCTURES:

## An Application of The Finite Element Method of Stress Analysis.

Thesis presented in Two Volumes

for the Degree of Doctor of Philosophy

by

K.W.J. Wright, B. Tech.

VOLUME ONE

DEPARTMENT OF MECHANICAL ENGINEERING

BRUNEL UNIVERSITY

MARCH 1975

## ABSTRACT

The Finite Element Method of stress analysis is employed in axisymmetric, two and three-dimensional forms, to investigate the mechanical behaviour of dental structures under simulated oral loading conditions. Stress distributions which are examined, include those occuring in the crowns of normal teeth due to masticatory loading and in restored teeth as a consequence of the restoration's setting and thermal expansions. The force distributions occuring on roots of individual teeth and on teeth used as abutments for various bridge constructions are also investigated for both axial and non-axial loading and various alveolar bone support conditions. The instantaneous centres of rotation of teeth when subjected to orthodontic loading are also determined.

The Finite Element Method is employed to examine various published hypotheses which attempt to correlate the mechanical behaviour of bone structures with that tissue's biological response characteristics. The cases examined include the remodelling of the alveolar process subsequent to orthodontic treatment and the remodelling or so-called straightening of the malaligned long bone.

Utilising published experimental data, the Finite Element Method is also employed in a reverse mode to enable some hitherto unknown mechanical properties of the periodontal membrane and cortical bone tissues to be determined. Indeed, due to the flexibility of the method, it was possible to

represent these tissues as orthotropic materials.

The work is presented in two volumes. While the first volume contains all the results of the analyses, the second contains an outline of the relevant finite element theory. Nevertheless, where the theory has been extended, in particular in the area of non-isotropic material analysis, it is developed in greater depth. The second volume also contains both a thorough description and a listing of all the computer programs developed.

# PREFACE

Biomedical Engineering describes the activity of those who employ engineering principles and techniques to solve problems in, or associated with, medicine and biology. As the name suggests, Biomedical Engineering is necessarily multi-disciplinary and requires co-operation and understanding between the clinician and the engineer. This thesis describes mechanical engineering stress analyses of some typical although idealised dental structures. The aim is to improve the understanding of how the dental tissues react to various forms of mechanical loading. This was done by utilising the Finite Element Method which is a far more accurate method of analysis than those which have been used hitherto in this field.

The work is presented in two parts. The first part, Volume One, contains all the details and results of the dental structural analyses, whereas the second part, Volume Two, contains all the analytical theory and a detailed exposition of the computer programs. This layout was chosen purposely so that the clinician or biological research worker interested in only the results and conclusions of the analyses, would not be confronted with unnecessary mathematics and programming detail. Similarly, the reader who is interested in only the analytical aspects of the work can refer to Volume Two which is almost completely free of

clinical involvement. In addition, the discussion on the computer programs developed (which are general programs and can be employed to solve a wide variety of stress analysis problems), is extensive so that a prospective user should be able to successfully employ and develop them further with the minimum of difficulty. Of course, this approach has necessitated a certain amount of repetition which has consequently increased the bulk of the thesis.

The work reported herein was commenced in 1969, before the S.I. system of units had been formally adopted. Consequently, because the work was developed using the Imperial system of units, all the results obtained are presented in this system.

## ACKNOWLEDGEMENTS

I wish to thank Professor G. Jackson of Brunel University and Professor H.M. Pickard of The Royal Dental Hospital, London, for instigating the research programme and for their support and encouragement. Grateful thanks are also due to Professor Pickard for making the facilities of The Royal Dental Hospital available to me and for assisting with the MEDLARS search.

I would like to express my sincerest thanks to Mr. A.L. Yettram, for all his guidance, help and enthusiasm.

I am also indebted to a number of people who have willingly given both time and thoughtful discussion during the course of the research. In particular, the members of staff of The Royal Dental Hospital, especially Professor H.M. Pickard, Professor W.J.B. Houston and Dr. N.E. Waters.

I am especially grateful to Dr. C.E. Renson of The Dental School of The London Hospital Medical College and Dr. A.G. Cartwright of Surrey University who allowed me access to their data before they had published their results.

I wish also to thank Jennifer Wood, Margaret Trew and Margaret Sumner for their help with the typing and reproduction of the thesis.

Finally, my acknowledgements would not be complete without me expressing warmest thanks to my wife Barbara, for her patience and continuous support and encouragement.

# LIST OF SYMBOLS

The following list defines the principal symbols used in this thesis. Other symbols are defined in context. Rectangular and square matrices are indicated by square brackets [ ], and column vectors by braces { }.

| | |
|---|---|
| X,Y,Z: | Right-hand Cartesian coordinate axis |
| $\bar{X},\bar{Y},\bar{Z}$: | systems. |
| X!Y!Z! | |
| $E_z$ | Young's Modulus of elasticity in Z coordinate direction. |
| $\mu_{zx}$ | Poisson's ratio. Ratio of strain (passive) induced in X direction and the stress induced strain (active) in the Z direction. |
| $G_{xy}$ | Modulus of rigidity in the XY plane. |
| $\sigma_{xx}$ | Normal stress component in X coordinate direction. |
| $\varepsilon_{yy}$ | Normal strain component in Y coordinate direction. |
| $\tau_{xy}$ | Shear stress component in the XY plane. |
| $\gamma_{yz}$ | Shear strain component in the YZ plane. |
| u,v,w | Nodal displacement components in the directions of the corresponding Cartesian coordinate directions. |
| $\alpha_n$ | Generalized coordinate. |
| $\{f\}$ | Column vector of displacement components. |
| [A] | Matrix of element nodal point coordinates. |
| $\{q\}$ | Column vector of element nodal point displacements. |
| $N_n$ | Interpolation function. |
| $\delta,\eta,\xi$ | Local element coordinate directions. |

| | |
|---|---|
| $\{F\}$ | Column vector of element nodal point forces which are equivalent statically to the boundary stresses and internal distributed loading acting on the element. |
| $[k]$ | Element stiffness matrix. |
| $\{F_d\}$ | Column vector of element nodal point forces required to balance any internal distributed loading acting on the element. |
| $\{F_t\}$ | Column vector of element nodal point forces required to balance any initial internal strains in the element. |
| $[B]$ | Matrix relating element nodal point displacements and the internal element strains. |
| $[D]$ | Material elasticity matrix. |
| $\{R\}$ | Column vector of structural nodal point forces. |
| $[K]$ | Structural stiffness matrix. |
| $\{d\}$ | Column vector of structural nodal point displacements. |
| $[MBK]$ | Modified arrangement of the structural stiffness matrix. |
| $[J]$ | Jacobian transformation matrix. |

# CONTENTS

VOLUME 1

# CHAPTER ONE

## INTRODUCTION TO VOLUME ONE

### WHY DENTAL STRUCTURAL STRESS ANALYSIS?

# 1. INTRODUCTION TO VOLUME ONE.

## WHY DENTAL STRUCTURAL STRESS ANALYSIS?

A great deal of today's dental practice and procedure is based upon empirical laws and 'rule of thumb' criteria which have evolved over the years as a result of clinical experience. Although this 'common sense' approach has produced the high standard of dental practice and technique which we, as patients, have grown to accept and expect, an increasing number of dental research workers and clinicians are beginning to question some of these long standing ideas and are seeking to place their profession on a more scientific basis.

Many different methods have been employed to investigate the development, growth, function and pathogenesis of the dental tissues. Similarly, diverse approaches have been used to study the effects of dental treatment. Although clinical study and observation are still extensively used, more and more emphasis is being placed upon techniques in which the specimens, environment and conditions can be more carefully selected and controlled.

It is not a new idea that the study of dental practice and procedures using engineering analysis techniques could improve the understanding and consequently the development and design of dental restorations. Although some of the earlier work in this field dates back to the beginning of this century, it has been primarily during the past two decades that the relevance and importance of the engineering type of approach has become more commonly recognised. A survey of the literature on past

engineering type analyses of dental struc tures will not be given here as this will appear in the relevant sections of later chapters. However, it should be emphasized that the engineering type of approach does not eliminate the need for clinical experiment and observation but should rather be used to complement them.

The purpose of any scientific investigation is to achieve some eventual goal. Sometimes the reason may be to acquire and to build up the store of basic scientific knowledge, or to simply unravel a hitherto unsolved mystery. Alternatively, the purpose may be to gain an understanding of certain phenomena, thereby enabling man to construct new apparatus or machines; hopefully, to enhance his well-being or environment.

The reasons for attempting dental structural stress analyses can be chosen to fall into all of the categories outlined above. Firstly, dental stress analysis could provide basic information on how the dental tissues react to mechanical stimuli, such as for example the forces of normal mastication. Also by studying the stress, strain and deformation behaviour of the tooth supporting structures, a better understanding of the mechanism or mechanisms governing alveolar bone remodelling could possibly be attained. Similarly, a better structural understanding of the behaviour of a restoration or prosthesis should also indicate ways for its further development and hence to the possible improvement into either its function or design.

From the above it is apparent that the study of the mechanical behaviour of dental structures could have wide and far reaching implications clinically. Indeed, bearing

in mind the fact that everyone at some stage in their lives experiences dental problems of one sort or another, the successful application of engineering techniques of structural analysis could also have important and considerable economic consequences.

# CHAPTER TWO

## THE GENERAL ANATOMY AND HISTOLOGY

## OF THE DENTAL TISSUES

# 2 THE GENERAL ANATOMY AND HISTOLOGY OF THE DENTAL TISSUES

## 2.1 INTRODUCTION

The mouth or oral cavity, is the gateway to the alimentary canal and through it must pass all the food which we require for our nutrition and well-being. The basic function of the dental structures and tissues is to form the masticatory apparatus, a machine by which all the solid food that enters the mouth is chopped, ground and mixed with saliva in preparation for swallowing. Another very important function of the dental structures is the significant contribution they make to speech production. As well as these purely physical roles, the aesthetic appeal of a pleasant and natural dentition has important psychological consequences.

In this chapter the general anatomy and histology of the face and dental tissues pertaining to the dental structural analysis are briefly described.

## 2.2 THE FACIAL SKELETON

The bony framework of the mouth is composed largely of the two maxillae which are immovably attached to the calvaria, and the horseshoe shaped mandible which articulates about the temporomandibular joint, FIG. 2.1. It is by the movement of the mandible in relation to the fixed maxillae through the action of the muscles of mastication, (and by the tongue and cheeks), that chewing and speech activities are achieved.

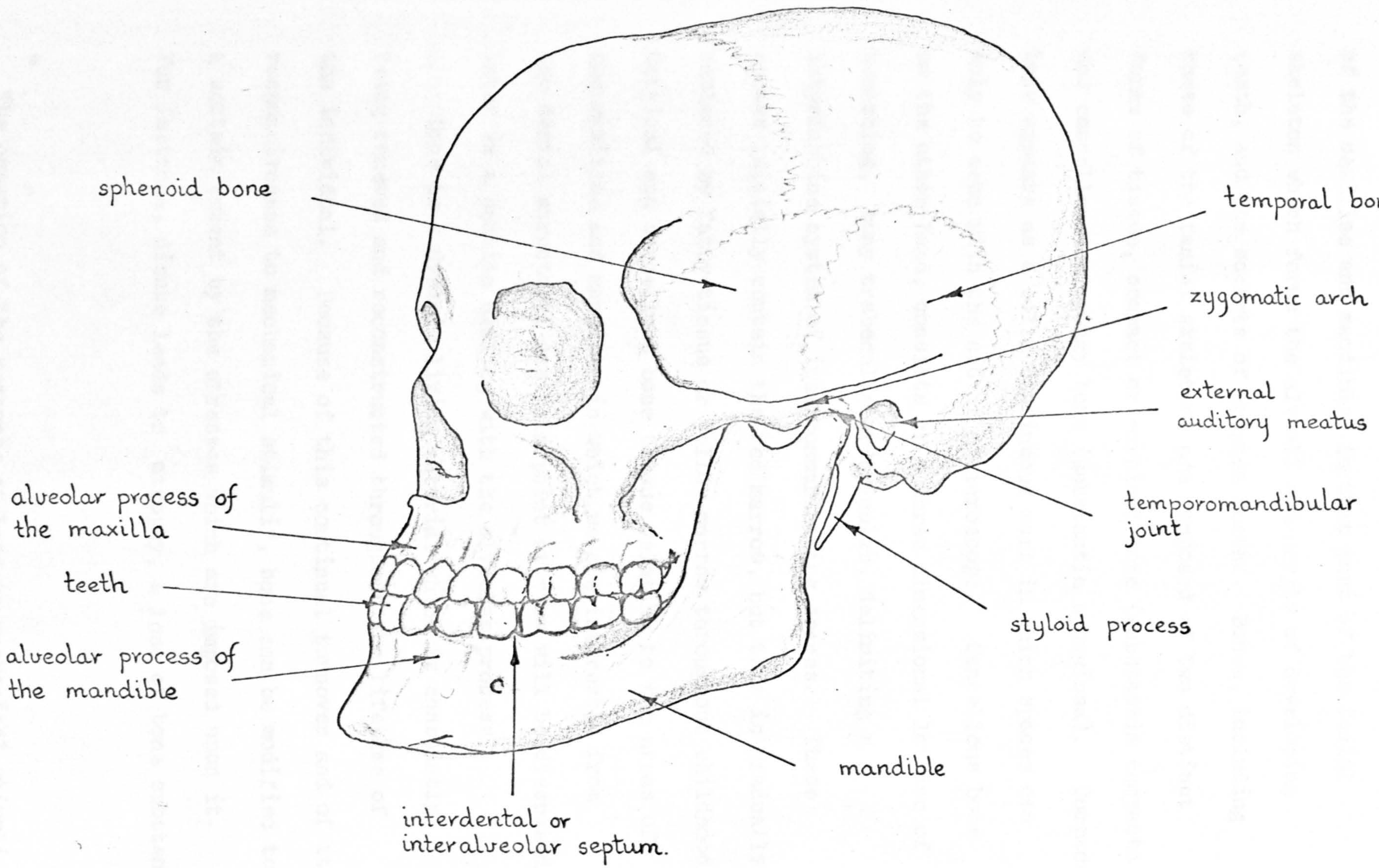


FIG. 2.1 The bony framework of the mouth

Alveolar bone, which comprises the alveolar processes of the maxillae and mandible, is that part of the facial skeleton which forms the alveoli and crypts of developing teeth, and the sockets of erupted teeth. Bones, including those of the facial skeleton, are composed of two distinct forms of tissue, compact or cortical bone (substantia compacta) and cancellous or spongy bone (substantia spongiosa). Compact bone appears as a solid continuous mass in which spaces can only be seen with the aid of a microscope. Cancellous bone on the other hand, consists of a three dimensional lattice of branching, bony trabeculae or spicules, delimiting a labyrinthine system of intercommunicating spaces. These spaces initially contain the red marrow, but this is gradually replaced by fatty-tissue or yellow marrow throughout childhood. Cortical and cancellous bone tissue relating to the areas of the maxillae and mandible in which we are interested from the dental structural analysis point of view will be discussed later in a section dealing with the alveolar process.

Bone is a dynamic living material which is constantly being renewed and reconstructed throughout the lifetime of the individual. Because of this continual turnover and of its responsiveness to mechanical stimuli*, bone can be modified to a certain extent by the stresses which are imposed upon it. For instance, disuse leads to atrophy, a loss of bone substance

* The question of the response of bone to mechanical stimuli is the centre of a great deal of controversy. It is one of the areas which has been investigated in this project and is covered in a later chapter.

whereas an increase in use or function is accompanied by hypertrophy, an increase in bone mass.

## 2.3 THE TEETH

### 2.3.1 Dentitions and Normal Tooth Relationships

Man, like most mammals, has two natural sets of teeth during his lifetime. The first set is called the primary, milk or deciduous teeth of childhood and number twenty teeth in all, whereas the second set, called the permanent teeth, totals thirty two. Both sets of teeth are divided equally between the upper (maxilla), and lower (mandibular), arches. In each arch the teeth are arranged symmetrically on either side of the median or sagittal plane with the teeth on one side being the mirror image of those on the other side, FIG. 2.2. Although the microscopic structure of both sets of teeth is basically similar, the permanent dentition reaches a higher state of development and the teeth are slightly larger than their deciduous counterparts.

The deciduous teeth in each side of each jaw starting from the sagittal plane and progressing laterally and posteriorly, are called respectively: central (medial) incisor, lateral incisor, canine (cuspid), first molar and finally the second molar. The permanent teeth starting at the sagittal plane and progressing as before are called: central incisor, lateral incisor, canine, first premolar (bicuspid), second premolar

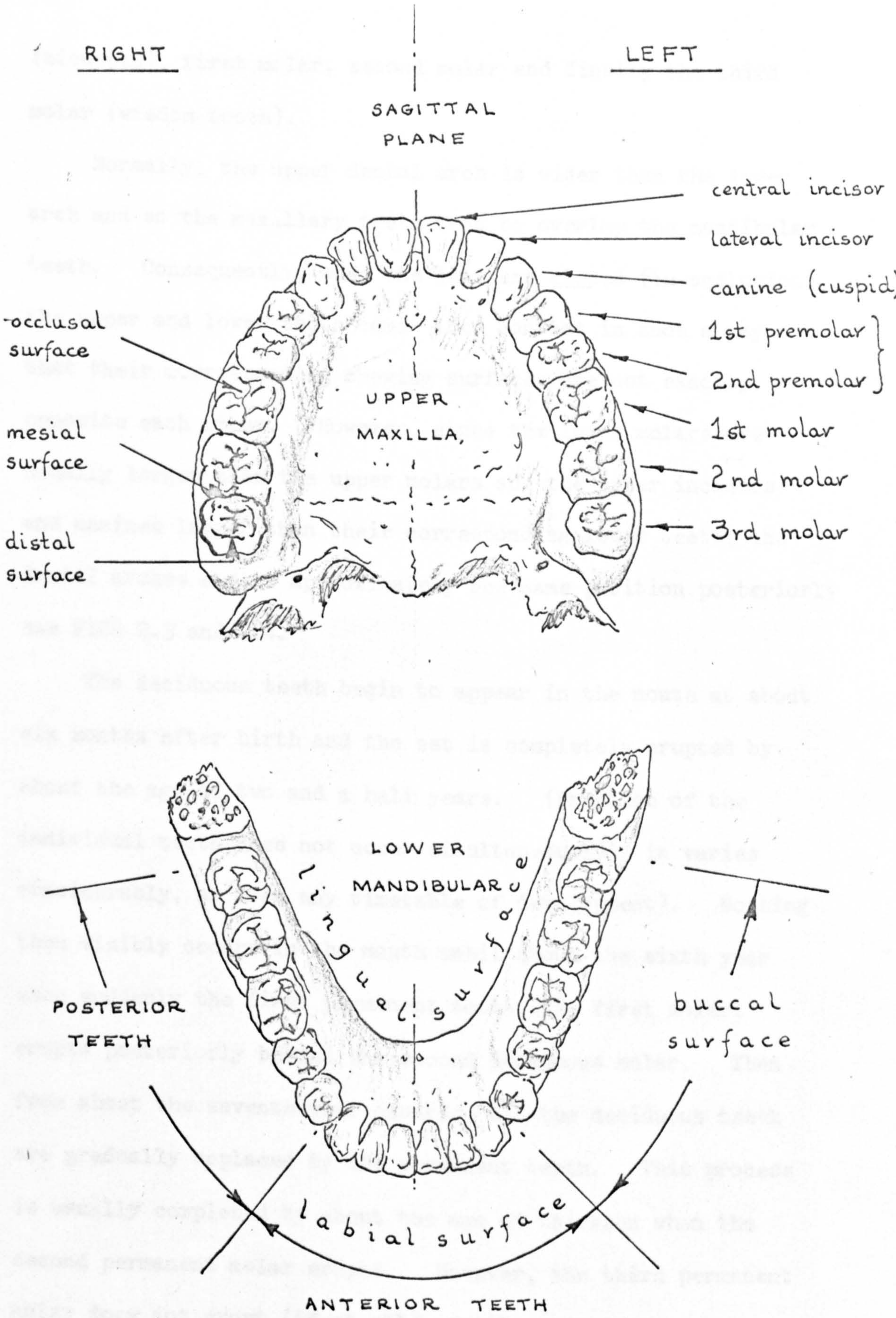


FIG. 2.2 The permanent dentition.

(bicuspid), first molar, second molar and finally the third molar (wisdom tooth).

Normally, the upper dental arch is wider than the lower arch and so the maxillary teeth tend to overlap the mandibular teeth. Consequently, when the jaws are closed (in occlusion), the upper and lower teeth come into contact in such a way that their corresponding chewing surfaces are not exactly opposite each other. However, since the lower molars are usually larger than the upper molars and the upper incisors and canines larger than their corresponding lower teeth, the dental arches end at approximately the same position posteriorly see FIGS 2.3 and 2.4.

The deciduous teeth begin to appear in the mouth at about six months after birth and the set is completely erupted by about the age of two and a half years. (Eruption of the individual teeth does not occur simultaneously; it varies considerably, as does any timetable of development). Nothing then visibly occurs in the mouth until about the sixth year when suddenly the first permanent tooth, the first molar, erupts posteriorly behind the second deciduous molar. Then from about the seventh year onwards, all the deciduous teeth are gradually replaced by the permanent teeth. This process is usually completed by about the age of thirteen when the second permanent molar erupts. However, the third permanent molar does not erupt (if at all), until several years later.

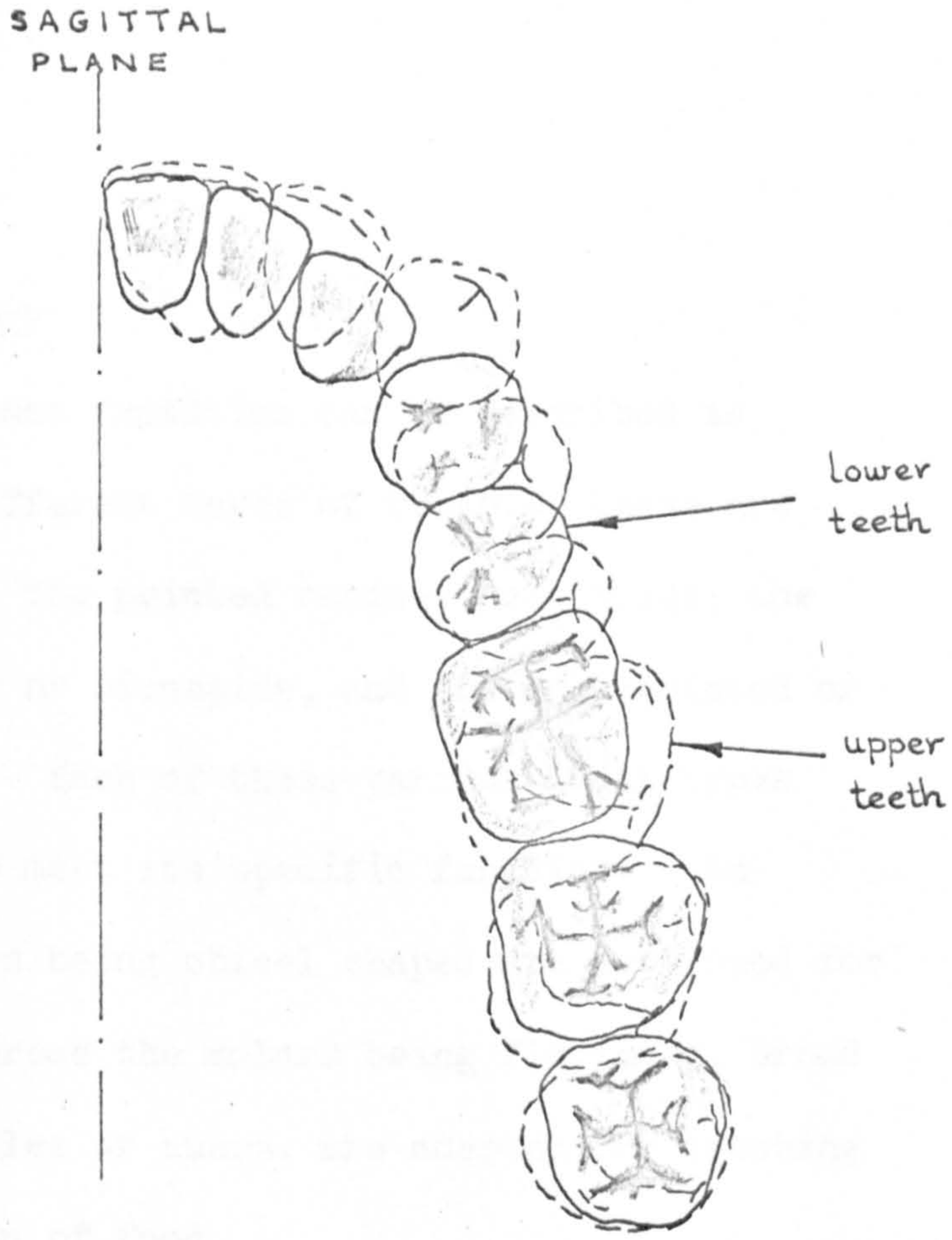


FIG. 2.3 Ideal occlusion of the permanent dentition.

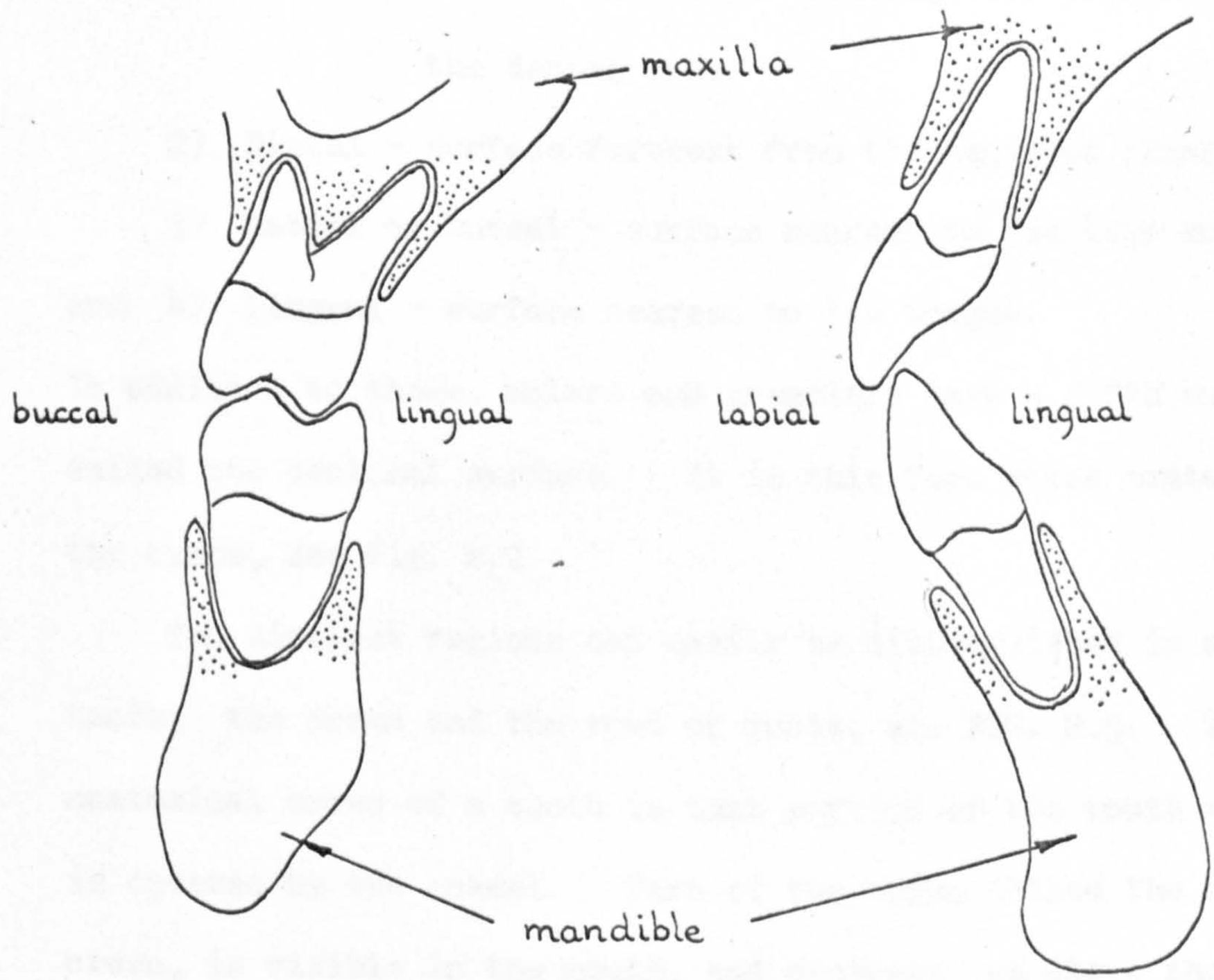


FIG. 2.4 Diagramatic illustration of the occlusal relationship through the molar and incisal regions respectively.

### 2.3.2 Tooth Morphology

The permanent human dentition can be described as consisting of four different types of teeth. These are the cutting incisors, the pointed canines or cuspids, the two-pointed premolars or bicuspids, and the many-pointed or multi-cuspid molars. Each of these various tooth types is adapted in form to meet its specific function. As examples, the incisors being chisel shaped are developed for biting or cutting whereas the molars being flattened, broad and containing tubercles or cusps, are adapted for crushing and for the dimunition of food.

Each tooth has four external surfaces; these have been designated as follows:

1) Mesial - nearest surface to the sagittal plane of the dental arch.

2) Distal - surface furthest from the sagittal plane.

3) Labial or buccal - surface nearest to the lips or cheeks.

and 4) Lingual - surface nearest to the tongue.

In addition to these, molars and premolars have a fifth surface called the occlusal surface. It is this face which contains the cusps, see Fig. 2.2

Two distinct regions can easily be distinguished in any tooth; the crown and the root or roots, see FIG. 2.5. The anatomical crown of a tooth is that portion of the tooth which is covered by the enamel. Part of the crown called the clinical crown, is visible in the mouth, and projects up above the gum (gingiva). Tooth roots are not normally visible in

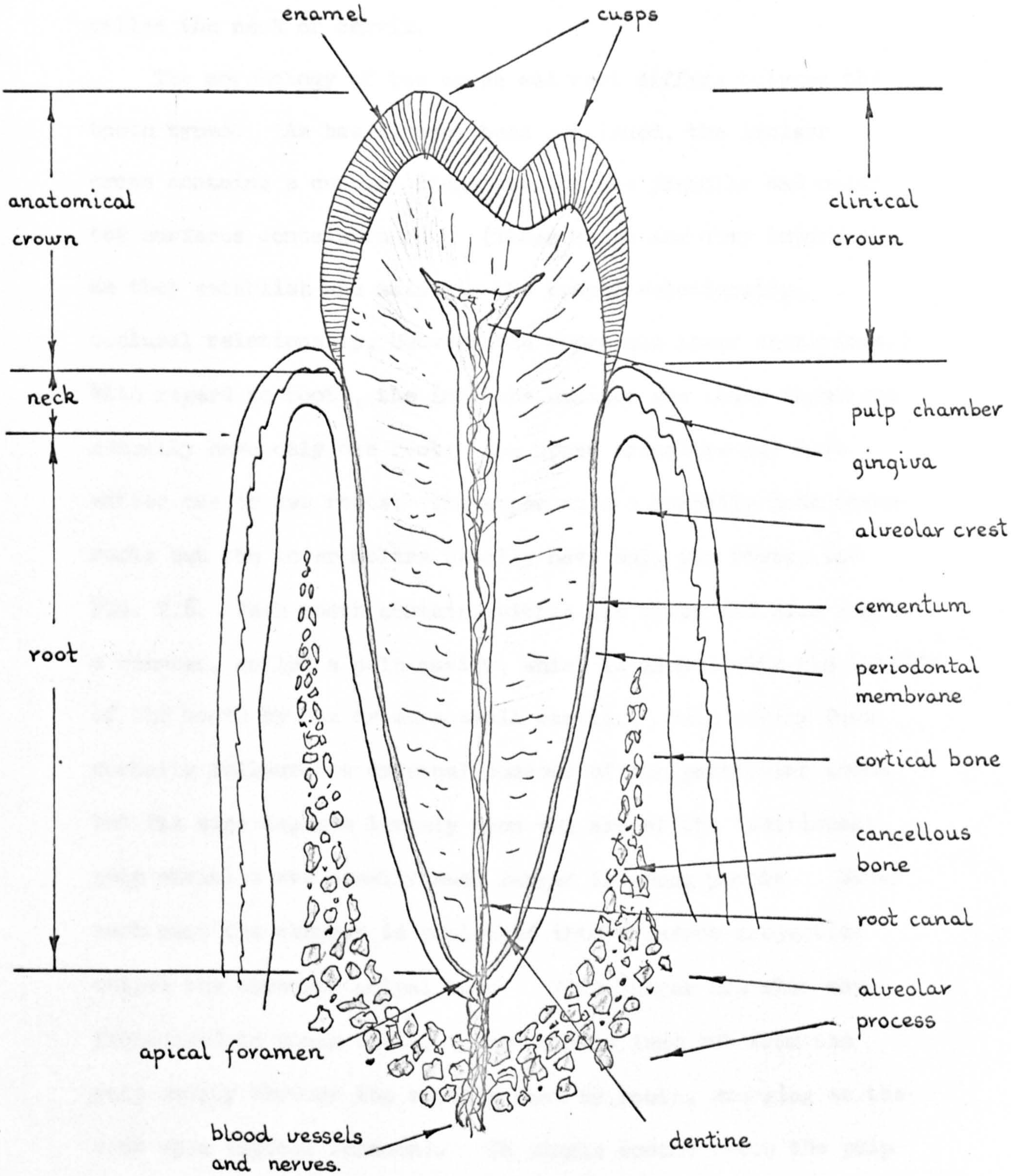


FIG. 2.5 Bucco-lingual cross-section of a mandibular premolar showing general tooth morphology and the dental tissues.

the mouth as they are that portion of the tooth which is embedded in the alveolar bone. The short intermediate portion of the tooth connecting the crown and root areas is called the neck or cervix.

The morphology of the crown and root differs between the tooth types. As has already been mentioned, the incisor crown contains a cutting ridge whereas the premolar and molar top surfaces contain cusps. (These cusps are very important as they establish and maintain the proper relationship, occlusal relationship, between the upper and lower dentitions.) With regard to roots, the incisors, canines and lower premolars normally have only one root; the upper premolars may have either one or two roots; the upper molars normally have three roots but the lower molars usually have only two roots, see FIG. 2.6. Each tooth contains within its crown and neck region a chamber, called a pulp cavity, which is linked with the outside of the tooth by one or more small canals. Pulp cavity form normally follows the external contour of the particular tooth but its size depends largely upon the age of the individual; pulp cavities are usually much larger in young people. Under each cusp the chamber is prolonged into a narrow projection called the cornu or pulpal horn. These horns are also more pronounced in young teeth. Root canals lead out from the pulp cavity through the tooth's root or roots, emerging at the root apex (apical foramen). In single rooted teeth the pulp cavity usually merges imperceptably into the root canal, which

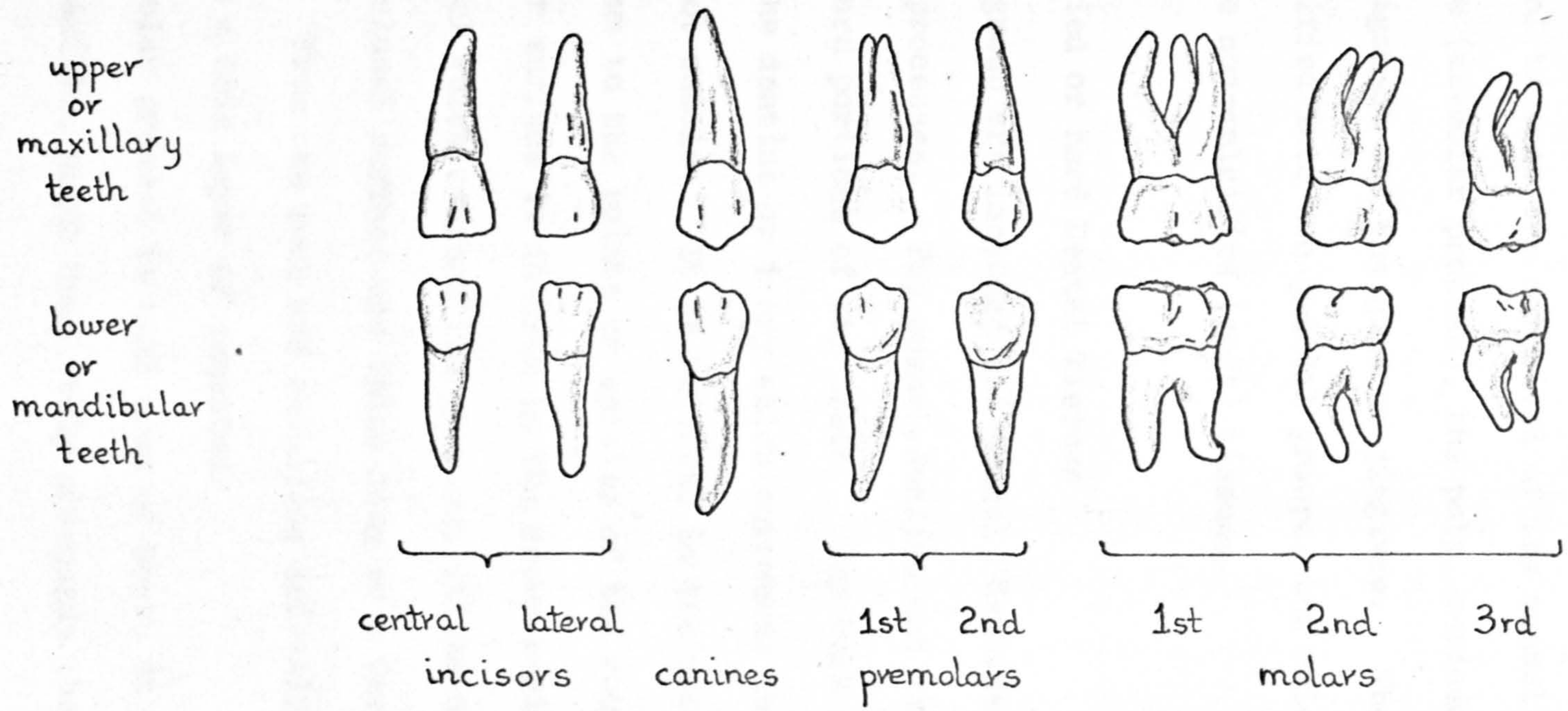


FIG. 2.6 The left upper and lower permanent teeth viewed from the labiobuccal aspect.

tapers gradually to its small opening at the apical foramen. However, in molar and in some premolar teeth the large pulp chamber is readily distinguishable from the fine narrow root canals.

## 2.4 THE DENTAL TISSUES

The dental tissues are comprised of the enamel, dentine, cementum, bone (alveolar process), the pulp, periodontal membrane or ligament and the gums or gingivae. These are usually classified into two general groups, the calcified (hard) and the non-calcified (soft) tissues.

### 2.4.1 Calcified or Hard Dental Tissues

In this group are included the enamel, dentine, cementum and alveolar processes. The enamel, dentine and cementum make up the hard portions of the teeth. The bulk of any tooth consists of the dentine or ivory which surrounds the pulp cavity and root canals. It is thickest in the crown region and tapers down to the points or apicies of the roots. The dentine's outer surface is covered in the crown region by a layer of enamel which reaches its greatest thickness on the incisal or occlusal surface and thins down to a feather edge at the neck. From the neck and extending apically, the dentine is covered by a thin layer of cementum.

The alveolar process is that area of bone, in either the mandible or maxilla, which completely surrounds the tooth roots

and extends up in the normal healthy condition at the alveolar crests to within two or three millimetres of the cemento-enamel junction.

### 2.4.1.1 Enamel

Enamel is the hardest and the most densely calcified tissue in the body. It consists almost entirely of calcium salts in the form of large apatite crystals. Consequently, it is very resistant to wear and is therefore suitably positioned on the anatomical crowns of the teeth, the surfaces subjected to severe abrasion. Its thickness varies with position on the crown being thickest, up to 2.5 mm, on the occlusal and cutting surfaces. Unlike dentine,cementum and bone, enamel is not formed or remodelled throughout life; having attained its normal thickness it is cut off from any cellular elements and no more is produced. Hence unlike the other three calcified tissues it has no power to react to injury by means of the cellular tissues related to it. Although enamel does not change physiologically once formed, changes can take place on a chemical level.

Structurally,enamel is comprised of thin globulated rods or prisms held together by a small amount of interstitial cementing substance. Each prism runs uninterruptedly through the whole thickness of the enamel layer, standing approximately upright on the dentine surface and finishing almost perpendicular to the tooth surface. However, the prisms are not straight, they are particularly gnarled and twisted in the cusp and

occlusal areas, see FIG 2.7 Enamel prisms are about 5 microns in diameter but due to the increase in area at the enamel surface over that at the dentine-enamel interface, the size of the prisms varies throughout the enamel thickness. Because the interstitial cementing substance is much weaker than the prism material, prisms separate easily along the cleavage planes. This is why enamel offers little resistance to shear stress, particularly when it is unsupported by sound dentine.

All restorations involve the removal of some enamel and in certain cases, e.g. for a jacket crown, all the enamel is removed.

### 2.4.1.2 Dentine

Primary dentine forms the bulk and consequently gives the basic shape to each tooth. Although slightly harder than cementum and bone, it is not as brittle as enamel and possesses a high degree of elasticity. Dentine is a very sensitive tissue; consequently, it is not normally exposed in the mouth being covered on the crown with enamel and on the root area with cementum. As with bone and cementum, dentine formation can continue throughout life. However, because this formation is restricted to the pulpal surface, dentine is unable to replace lost substance.

Dentine is composed of cells (odontoblasts), and a calcified intercellular ground substance. The ground substance is only intercellular in the sense that it surrounds the protoplasmic

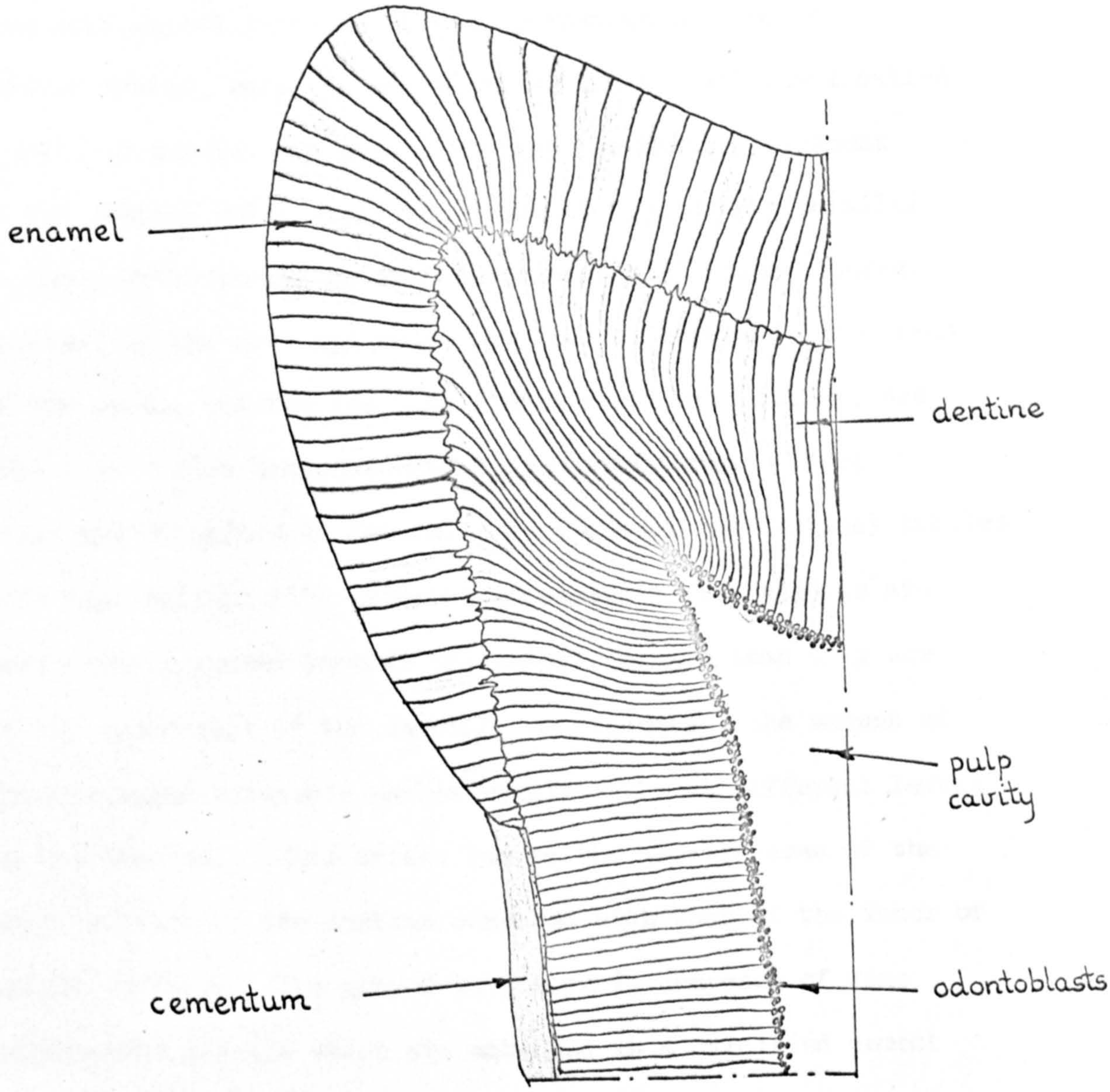


FIG. 2.7 Diagrammatic illustration of the tissues of the teeth.

processes of the odontoblasts. The odontoblasts are arranged to form a layer of cells on the pulpal surface of the dentine. Each odontoblast possesses a thin protoplasmic process (Tomes' fibre), which is contained within a small canal called a dentinal tubule, and passes through the entire thickness of the dentine wall. All the dentinal tubules run parallel to one another and in general describe an 'S' shaped course. However, in the root and under the incisal edge and cusp areas of the crown, the tubules take a much straighter course, see FIG. 2.7. Fine branches extend from each Tomes' fibre; these are contained in lateral extensions of the dentinal tubules with many uniting with adjacent processes. The tubules are more closely packed towards the pulpal surface than they are in the outer part of the dentine, consequently, the amount of intercellular substance varies considerably at different levels in the dentine. This arises due to the greater area of the outer surface of the dentine compared with that of the inner or pulpal surface. The ground substance is composed of fine collagenous fibrils which are embedded in a calcified cement substance. The fibrils are bound together to form dense bundles of fibres and are arranged in a lattice-like fashion around and between the dentinal tubules.

Even though the dentine is very sensitive to mechanical, thermal and chemical irritation, the innervation of the dentine is not completely understood. Although some nerve fibres from the dental pulp have been observed to penetrate into the dentinal tubules, it is generally believed that the Tomes' fibres

transmit the sensory stimulation to the dental pulp. Once stimulated further dentine (secondary dentine), is produced on the pulpal surface. Consequently, by old age secondary dentine may be so extensive as to fill the pulp cavity completely.

### 2.4.1.3 The Cement or Cementum

The cement or cementum is a very thin layer of tissue which normally covers the whole tooth root, extending from the cement-enamel junction down to the apical foramina. It has two main functions. Firstly, it protects the dentine; this is a very important feature as in later life the gingiva generally recedes and therefore this very sensitive tissue would be otherwise left exposed. Secondly, it retains the tooth in its socket by attaching to the root surfaces the periodontal membrane fibres which span across from the alveolar bone.

Cementum is very similar to bone tissue both chemically and histologically, and it is not greatly different in its physiological behaviour. Although it is much less readily resorbed than bone, cementum is highly responsive to mechanical stimuli and to changes in conditions in its environment. Because it obtains its nourishment from the periodontal membrane, it readily undergoes necrosis when the membrane is damaged and subsequent resorption by the surrounding connective tissues. On the other hand, cementum can be deposited at any time, consequently, it can attach new periodontal fibres to the tooth root or can make up at the root apex for lost tooth substance, e.g. for enamel lost due to wear (attrition).

Cementum consists of an organic matrix and an inorganic element. The organic matrix comprises of collagenous fibrils embedded in a ground substance. Calcium salts, which constitute the inorganic element, are in the form of apatite molecules which are deposited in the ground substance between and around the collagenous fibrils of the matrix.

There are two forms of cementum. The type depends upon the absence or presence of cells (cementocytes), and is known as either the acellular (primary), or cellular (secondary) cementum respectively. The first cement layed down is the acellular variety. This forms as a thin homogenous layer over the entire root surface. The secondary cementum is generally found in the apical region where the cementum assumes a thickness several times greater than it does at the neck of the tooth. However, one of the characteristics of the tissue is that its total thickness varies due to the variation in thickness of each layer, and not by a difference in the number of layers. The cementocyte cells are contained in spaces or lucanae, similar to the osteocytes in bone tissue. Processes from the cementocytes spread out from the lucanae through canaluculi towards the periodontal membrane. These processes anastomose with those of neighbouring cells.

Since the formation of cementum continues throughout life, the attach ment of the periodontal membrane fibres (Sharpey's fibres) can be altered or shifted in response to changes in the functional stresses. This ability for reattachment is of prime

importance in orthodontic practice. However, if the functional forces or irritants are beyond the compensatory powers of the cementum, resorption and the subsequent loosening of the teeth results.

2.4.1.4 Bone and the Alveolar Process

Bone in common with other connective tissues consists of cells, fibres and a ground substance. However, unlike the others its extracellular components are calcified.

Four basic constituents are employed in the construction of bone. The first constituent provides a network of collagenous fibres; the individual fibres themselves are made up of a large number of finer fibrils. This fibre network is embedded in the second constituent, namely, a ground substance which chemically consists of a protein-carbohydrate complex. The third component, which together with the previous two comprises the extracellular substance of bone, is the crystaline bone mineral. It is this component, a complex chemical made primarily from calcium and phosphate, which imparts to bone its hardness and rigidity. Bone mineral is deposited in the form of slender needles throughout the collagen network of the organic matrix. Cells called osteocytes form the fourth and final constituent of bone. It is these cells which are the living part of the bone tissue. Although three different kinds of cells have been identified in bone, (osteocytes, osteoblasts and osteoclasts), there is strong evidence to suggest that a transformation takes place from

one cell type to another. It is therefore reasonable to regard them as being the different functional state of the same cell type. Osteocytes are bone-inhabiting cells with each cell occupying its own cavity or lucana. Radiating from the lucanae in all directions are fine branching tubular passages called canaliculi. Canaliculi from one lucana anastomose with those from neighbouring lucanae, hence these cavities are connected by a continuous network of minute canals.

The proportions and histological arrangement of the bone constituents are combined in man to produce two types of bone tissue, namely, woven or coarse-fibre and lamellar or fine-fibre bone respectively. Both woven and lamellar bone may enclose only a few small vascular channels, giving rise to cortical bone, or they may contain numerous large vascular spaces forming cancellous bone, FIG 2.8.

Bones are composed of an outer skin or layer of cortical bone and an internal network of trabeculae forming areas of cancellous tissue. External bone surfaces are invested with a layer of highly specialised connective tissue called the periosteum. Internal surfaces however, are covered with a more delicate tissue layer called the endosteum. Both the periosteum and the endosteum possess osteogenic properties, that is to say, they have the ability to lay down new bone tissue.

Woven bone is basically a provisional material which is usually replaced by the more permanent type of lamellar tissue. Structurally woven bone consists of large irregular sac-like

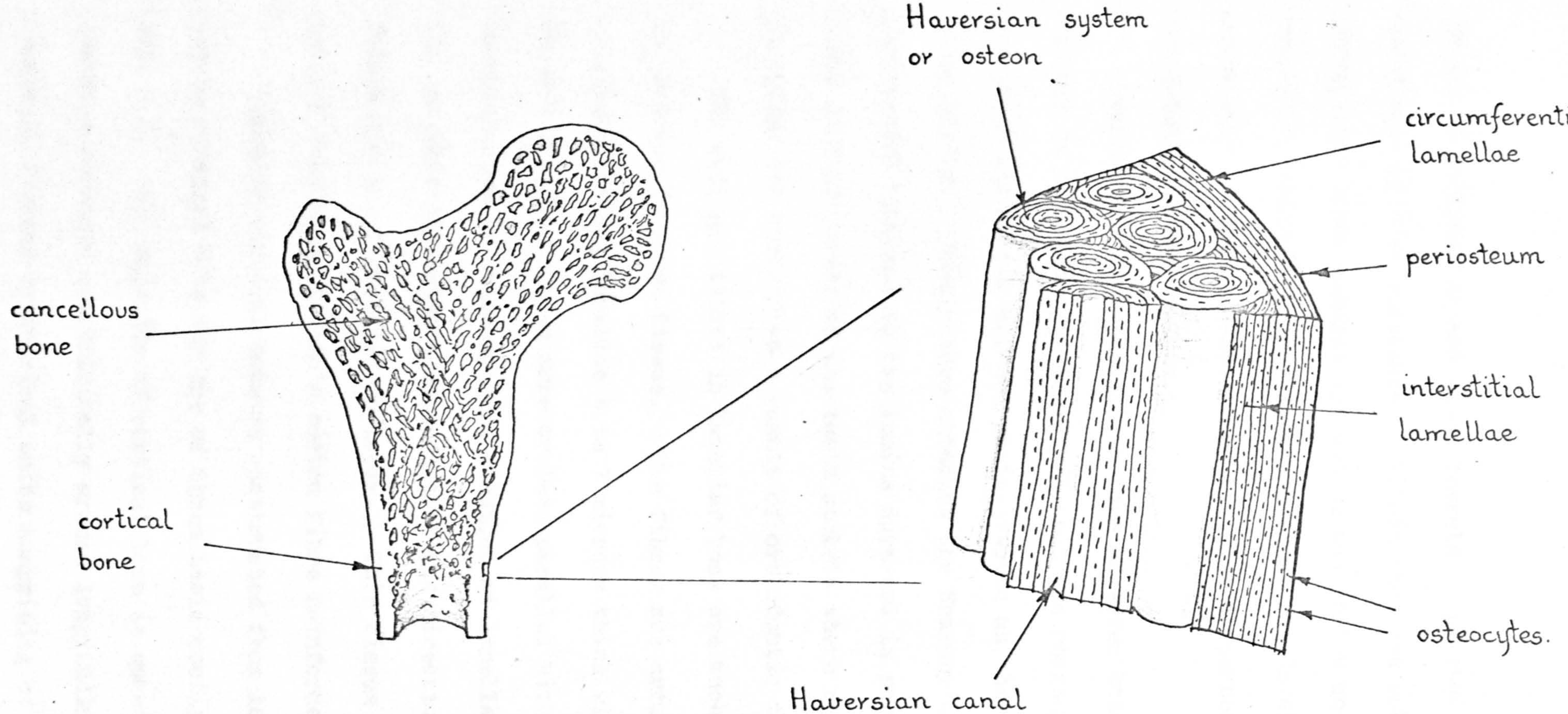


FIG. 2.8 Diagrammatic illustration of cancellous and cortical bone.

spaces containing fat and blood vessels, separated by walls and plates of bone substance. Within the bone substance the collagenous fibre bundles are coarse and follow no orderly pattern. Generally, they interweave and run in all spatial directions. The osteocytes are likewise dispersed randomly throughout the bone matrix.

Bundle bone is a particular form of woven bone. Although similar in structure it differs in that the coarse collagen fibres of its matrix are not so interwoven as they are in the woven tissue. Bundle bone attaches the Sharpey's fibres of the periodontal membrane to the lamina dura and is particularly found in those areas of the tooth sockets where recent bone formation has occured as a result of orthodontic tooth movement.

The collagen fibres in lamellar bone are much finer than those found in woven tissue. The fibres are arranged in layers or sheets forming lamellae 4 to 7 microns thick with the fibres in each lamella running more or less parallel with one another. Lamellar bone is built up from a number of lamellae. However, the lamellae are orientated such that the direction of the collagen fibres changes from layer to layer. This tissue is therefore natures forerunner to man's carbon fibre reinforced plastic.

Lamellar cortical bone is constructed from lamellae which can be arranged into any one of three basic configurations, FIG. 2.8. The majority of cortical bone is constructed from lamellae arranged concentrically around longitudinal vascular channels, forming cylindrical units comprising of between 4 and 20 lamellae. This type of structure is called a Haversian system or osteon. The central channel is on average

about 50 microns in diameter and is known as the Haversian canal. The second type of arrangement is found to lie between the complete Haversian systems. It consists of lamellae arranged into irregularly shaped units called interstitial systems or lamellae. It has been postulated that the interstitial lamellae are the remnants of complete osteones which have undergone the natural process of bone turnover. The demarcation lines between the osteones and the interstitial systems are known as cementing lines. The third type of lamellar bone arrangement is found on bone surfaces beneath the periosteum and endosteum membranes. It consists of several continuous lamellae which extend uninterruptedly around the periphery of the external and internal surfaces. This is consequently known as circumferential lamellar bone.

The Haversian canals, which contain blood vessels, are connected to one another and with the external and internal bone surfaces by transverse passages called Volkmann's canals. These canals which are not surrounded by lamellae, allow blood vessels from the periosteum and endosteum to communicate with those of the Haversian systems.

Lamellar cancellous bone is composed of trabeculae which consist of one or more lamellae surrounding the recticular, a vascular tissue of medullary substance. The trabeculae which are covered by endosteum, undergo continual reconstruction with lamellae being removed or added depending upon the decrease or increase of the imposed functional stresses.

The alveolar process is that part of the bone tissue which is immediately adjacent to the roots of the teeth. No distinct boundary exists between the alveolar processes and the rest of the so-called basal bone which makes up the maxilla and the mandible. Both blend together naturally forming one continuous structure.

The function of the alveolar process is to give support to the teeth and to react the transmitted forces of mastication. Consequently, the structure is in harmony with the functional forces that are imposed upon it. Naturally, the bone size and arrangement varies between individuals but the general or normal structural configuration is as illustrated in FIG 2.9.

The alveolar process is composed mainly of lamellar type bone. Both the maxilla and the mandible possess an outer layer or shell of stiff cortical bone. This is usually much thicker in the mandible than it is in the maxilla. At the alveolar crests the surface cortical alveolar bone is continuous with the thinner layer of cortical bone lining the tooth sockets. This bone is called the lamina dura and it is held by some authorities as being the alveolar process proper. It is in the lamina dura that the Sharpey's fibres of the periodontal membrane are embedded, providing the teeth with their attachment and support.

Although the deeper regions of the surface alveolar cortical bone and of the lamina dura consist of Haversian systems, the layers below the periosteum and adjacent to the periodontal membrane are made up of surface lamellae. Where the Sharpey's

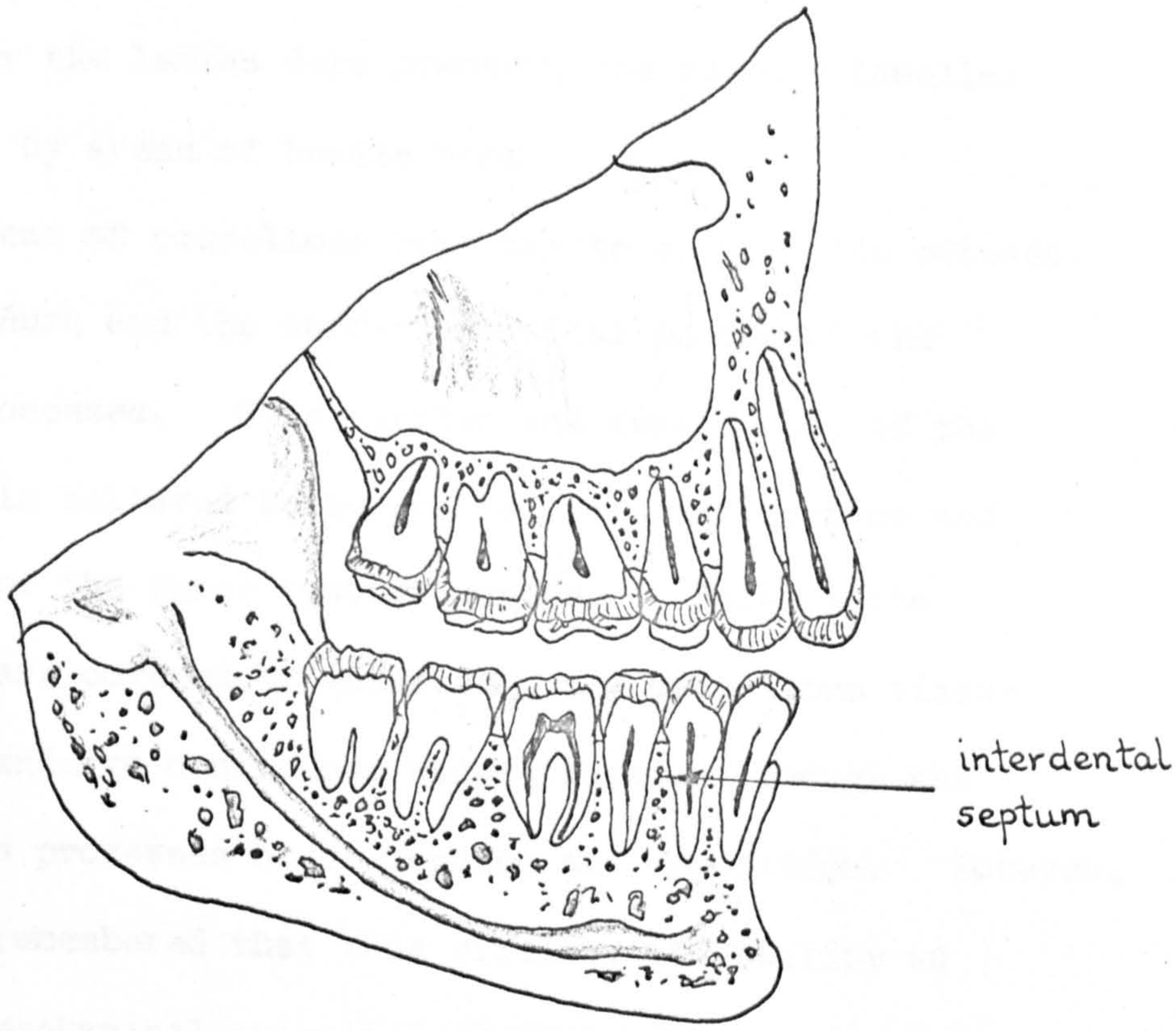


Sagittal section through the maxilla and the mandible.

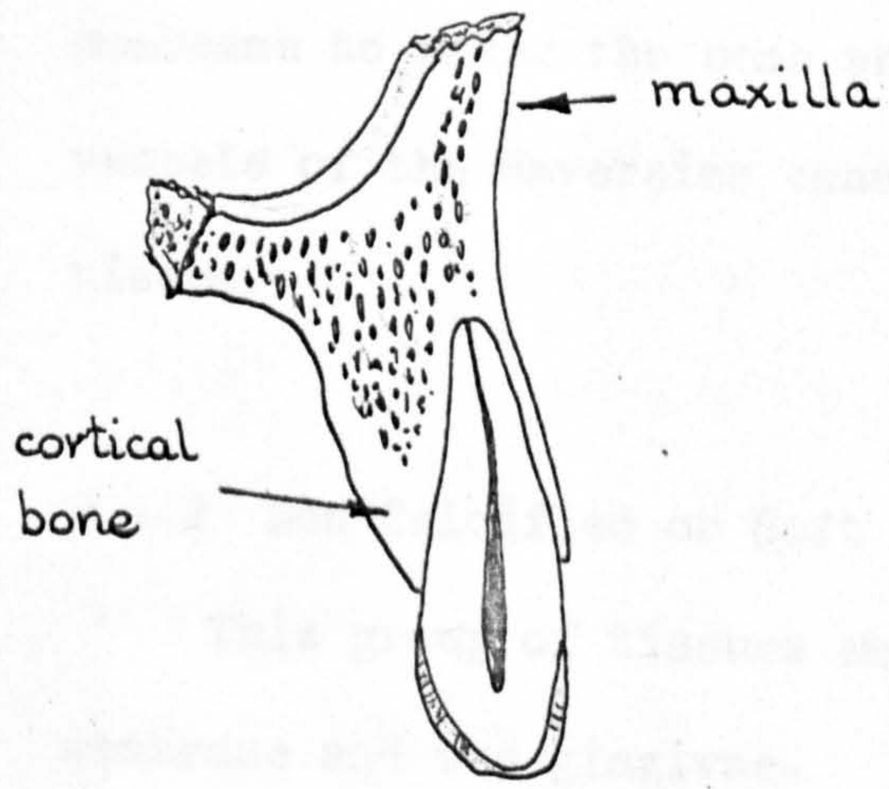


Labiolingual section through upper canine.

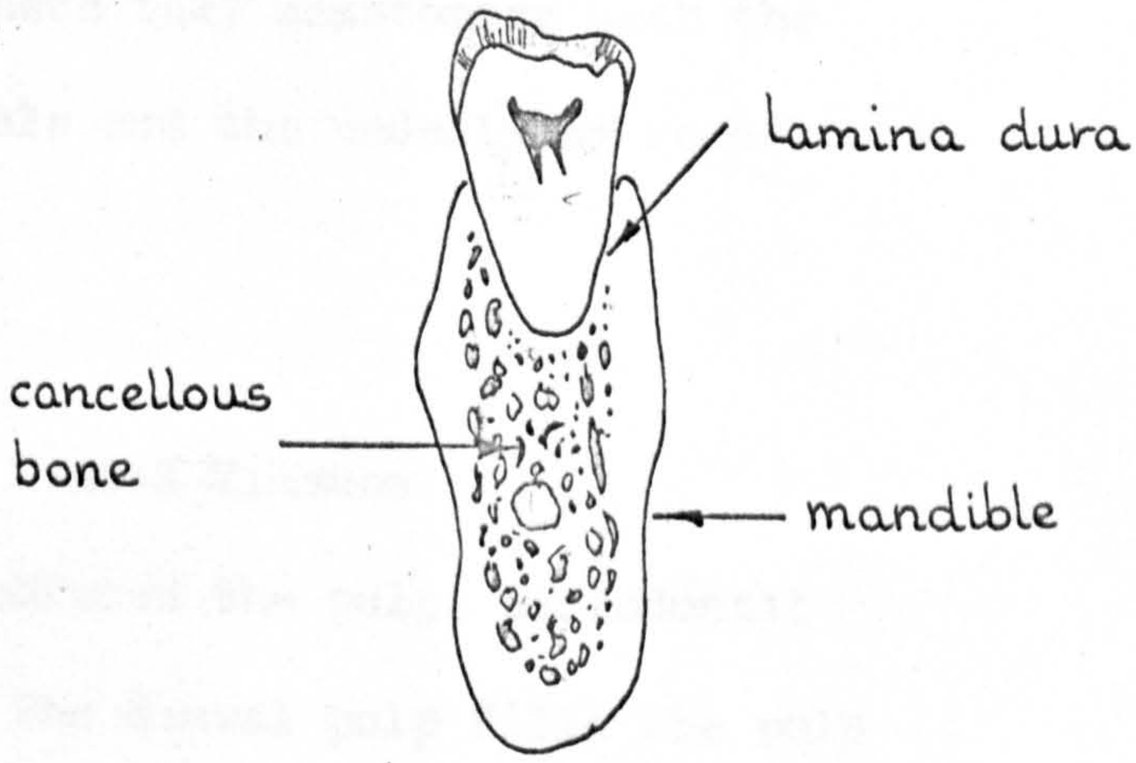


Buccolingual section through lower first molar.

FIG. 2.9 Typical structural arrangement of the alveolar processes.

fibres enter the lamina dura however, the surface lamellae are covered by areas of bundle bone.

The areas of cancellous bone can be seen to lie between the lamina dura and the surface cortical plates of the alveolar processes. Size, number and development of the trabeculae is believed to be related to the direction and magnitudes of the force systems imposed. Because the trabeculae are covered by endosteum, the cancellous tissue is able to undergo continuous reconstruction through the simultaneous processes of resorption and apposition. However, it must be remembered that this vitality and ability to respond to mechanical stimuli decreases with age.

Both the periosteal surface of the alveolar process and the periodontal membrane surface of the lamina dura are perforated by numerous Volkmann's canals. These canals allow blood vessels and nerves from the periosteum and periodontal membrane to enter the bone where they anastomose with the vessels of the Haversian canals and the underlying cancellous tissue.

### 2.4.2 Non-Calcified or Soft Dental Tissues

This group of tissues embraces the pulp, periodontal membrane and the gingivae. The dental pulp fills the pulp cavity and root canals and many of its small arteries and vessels enter via the tooth's apical foramina. The periodontal membrane, a thin layer of fibrous tissue, connects the cementum

covered root surfaces to the supporting alveolar bone processes. The gingiva, which is a part of the oral mucous membrane, surrounds and is normally attached to the enamel of each tooth. However, with increasing age the gingiva generally recedes so that in old people it is usually attached to the cementum.

### 2.4.2.1 The Dental Pulp

The dental pulp occupies the pulp cavity, a chamber enclosed by dentine and located centrally within the body of each tooth. Dental pulp is composed of cells and an intercellular substance. The cells of the pulp include odontoblasts, fibroblasts and certain defence type cells whereas the intercellular substance consists of fibres and a ground substance of gelatinous consistency. In addition it includes blood vessels, nerves and lymphatics which enter the pulp cavity via the apical foramina and root canals.

The pulp is derived from the dental papilla, of which it is the part remaining after the formation of the dentine. Because of this developmental connection the pulp is involved with the response of the dentine to stimuli. The pulp is a very sensitive tissue and reacts to mechanical, thermal and chemical irritation. If the stimulation is moderate it reacts by laying down secondary dentine and if severe it responds like all other connective tissues by undergoing inflammatory changes.

As well as being involved with the deposition of secondary dentine as a form of defensive action, the pulp has also nutritive and sensory functions. These functions are supported by the blood vessels and nerves combined within it. However, the only form of sensation displayed by the pulp in response to any stimulation is that of pain.

### 2.4.2.2 The Periodontal Membrane

The periodontal membrane attaches the roots of the teeth to the alveolar bone forming the tooth sockets and thereby transmits all the forces applied to the teeth to the supporting bone structure. The thickness of the periodontal membrane is dependent on the functional stresses which are imposed upon it. In a normal functioning tooth it is about 0.20 to 0.30 mm. The thickness however, is not uniform over the whole tooth root, being slightly thicker in the neck and apical regions it gives rise to a characteristic hour-glass shape. In non-functioning teeth the membrane undergoes atrophy and can become as a result, half its normal thickness.

Although the periodontal membrane serves as the periosteum to the lamina dura, it differs from the usual periosteum by the absence of any elastic fibres. The membrane consists of bundles of thick collagenous non-elastic fibres, cells, blood vessels, lymphatics and nerves.

The most important constituent of the periodontal membrane is the bundles of fibres, known as the principal fibres, which pass from the cementum of the tooth root out into the adjacent

tissues. These principal fibres are divided into groups according to the direction in which they run and to their specific function. The orientation of the fibre bundles varies at different levels in the alveolus. The bundles have been classified as either apical, oblique, horizontal or cervical, transceptal, crest and gingival fibres respectively, FIG 2.10. In the relaxed or non-functioning state, the fibre bundles have a slightly wavy course. Consequently, they permit a very small tooth movement upon the application of a small applied force. This 'give' in the membrane acts like a shock absorber and tends to smooth out any shock or suddenly applied loading.

The great majority of the principal periodontal fibres form the group known as the oblique fibres, which run obliquely inward and downward from the lamina dura to the tooth cementum. These fibres suspend the tooth in its socket.and by their arrangement transform axial tooth loads into tensile surface stresses on the socket wall.

The periodontal fibres in the apical region of the membrane, called the apical fibres, forms a cushion of fairly loose tissue with the fibre bundles mainly radiating out from the root apex.

In the region of the neck of the tooth the fibre bundles follow a more or less horizontal course. These horizontal or cervical fibres form an almost continuous ligament between the root and the rim of the alveolar bone at the mouth of the socket. The more superficial fibres of this group on the mesial and distal surfaces, pass over the interdental septum and connect with the

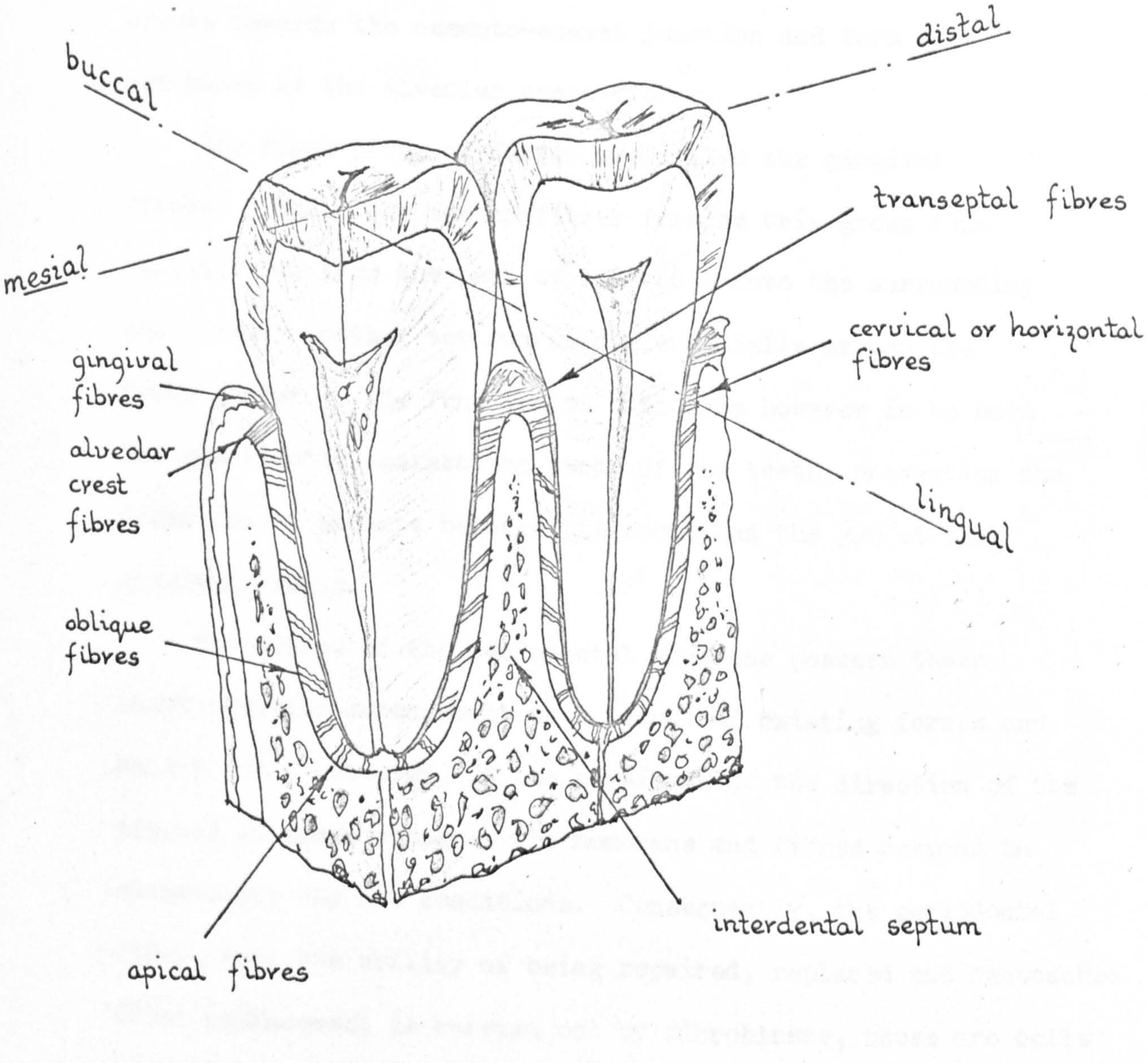


FIG. 2.10 Diagrammatic illustration showing the arrangement of the principal periodontal membrane fibres.

necks of the adjacent teeth. These transceptal fibres are continuous with the periosteum of the bony septum and tie together the individual teeth in the arch into one functional unit. However, on the lingual and labial or buccal surfaces, the superficial fibres run obliquely upwards from the alveolar crests towards the cemento-enamel junction and form what are known as the alveolar crest fibres.

The final group of fibres are called the gingival fibres. While one set of fibres forming this group runs radially out from the neck of the tooth into the surrounding gum tissue, another set runs circumferentially around the tooth socket. The function of both sets however is to hold the gum tightly against the necks of the teeth, preventing the formation of pockets between the tooth and the gum at the gingival margin.

The fibres of the periodontal membrane possess their characteristic arrangement as a result of existing forces and conditions. However, if the magnitude or the direction of the imposed stresses changes, the membrane and fibres respond to accommodate the new conditions. Consequently, the periodontal fibres have the ability of being repaired, replaced and reattached. Fibre replacement is carried out by fibroblasts, these are cells which lie on and around the collagenous bundles. Attachment of these fibres is achieved by the deposition of new bone to the walls of the socket and by the deposition of cementum to the root surface. These functions are controlled by the osteoblast

and the cementoblast cells respectively. If horizontal or lateral forces exceeding the physiological limits compress and crush the soft periodontal tissues between the tooth root and the alveolar bone, nature will again repair and reattach new tissues to regain normal function. However, if these abnormal forces are excessive or recurrent, necrosis of the soft tissues and bone resorption will occur.

### 2.4.2.3 The Gingiva or Gum

The oral mucous membrane is primarily a soft tissue that lines the surfaces of the oral cavity. Like the skin, it is composed of a surface epithelium and a deeper connective tissue layer. Although it has the same basic structure throughout, it exists in different forms in different parts of the mouth. In the gum and hard palate areas it is described as a masticatory or cornified mucosa, whereas over the cheeks, lips, soft palate and the floor of the mouth it forms a much simpler lining mucosa.

The gingiva or gum is that part of the oral mucous membrane which is related to the teeth and the alveolar bone. It is firmly connected with the periosteum at the alveolar crests and is also attached, via the epithelial attachment to the enamel on the crowns of the teeth. However, in later years the gum recedes and the connection with the teeth moves apically, forming an attachment to the cementum covered root surfaces.

The function of the oral mucous membrane is both to cover the underlying tissues and also to help to protect the teeth from infection. The teeth are particularly vulnerable in the neck region where the junction of the gingivae and the teeth forms a peripheral pocket called the gingival crevice or sulcus.

# CHAPTER THREE

# THE PHYSICAL PROPERTIES OF THE DENTAL TISSUES AND SOME RESTORATIVE MATERIALS

# 3 THE PHYSICAL PROPERTIES OF THE DENTAL TISSUES AND SOME RESTORATIVE MATERIALS

## 3.1 INTRODUCTION

A physical property of a material or tissue can be defined as being some measurable quantity of its physical condition, which relates its state, change of state or function, with respect to a certain aspect of its environment. Usually, physical properties are classified into smaller subgroups. Mechanical properties for instance, are physical properties which relate to the behaviour of the material when it is subjected to mechanical stresses or loads. In order to carry out static stress analysis of dental structures, it is necessary to have a knowledge of some of the physical properties, (in particular the mechanical properties), of the materials involved. This applies not only to the restorative materials but also to the dental tissues as well.

While several books and many articles in the dental journals have been written on the physical properties of the restorative materials, comparatively little work has been published on the physical properties of the biological materials. This at first glance may seem very strange. Unless the properties of the dental tissues are known, upon what criteria can a restorative material, (whose function afterall is to replace and imitate lost or diseased tissue), be selected? Although there are many other significant factors to consider,

mechanical compatibility is just as important as is biological compatibility. For example,if the mechanical properties of a restorative material are significantly different from those of the natural tissue which it is replacing, the response of the restored structure to the same mechanical stimuli will likewise be significantly different from that of the original structure. This effect will be clearly demonstrated in a later chapter.

One of the main reasons why there is a lack of tissue property data available can be attributed to the difficulty of the measurement task involved. While the problem of obtaining a supply of normal sound human tissue can be overcome by using a 'similar' animal substitute, most of the property measuring equipment available has been designed to be used with fairly large, inanimate, dry and standard shaped laboratory type specimens. Consequently, the initial difficulty to arise when attempting to measure some particular tissue property is the need to construct a suitable testing apparatus. Even if all the difficulties are surmounted and measurements are obtained, one is still faced with the question of how applicable the data is to the function of the tissue in the natural <u>in-vivo</u> environment. Other reasons for the paucity of tissue data perhaps could be that its significance has not yet been fully realised and that techniques of analysis available have not required or necessitated their determination.

Because of gaps in the knowledge with regard to certain tissue data, the technique of analysis employed in this project has been used as a research tool to obtain analytically some overall tissue properties. This has been achieved by modelling clinical experiments and then matching the analytical and the clinical results.

The object of this chapter is to review the literature for the physical properties of each of the dental tissues and materials which are involved in the dental structures to be analysed. Because the restorative materials are in general well documented, the properties required for this project have been extracted from the authoritative work of Skinner and Phillips (1)*. The review is followed by a short discussion on the data which has been presented and property values are proposed which will be used in the subsequent stress analyses. However, before investigating the tissue and material properties, some terms relating to general material behaviour are defined. This will be helpful as some of these terms are often used too loosely, ambiguously or incorrectly. This section is succeeded by a short account of some of the factors which have an influence on the experimental data presented.

* Selected reference number.

## 3.2 SOME GENERAL DEFINITIONS OF TERMS WHICH RELATE TO MATERIAL PHYSICAL BEHAVIOUR

Certain terms have been ascribed to particular features of material behaviour which are observable in experimental tests on most common everyday engineering materials, e.g. steel, concrete and timber. These terms are equally applicable in describing the behaviour of living tissues even though cells and fluid form a significant part of their construction.

### 3.2.1 Force

All materials and structures deform or deflect under load; nothing is completely rigid. Just as a building or a bridge deforms under loading so the teeth and the jaws deflect under the forces of mastication. The magnitude of the deflection depends upon the magnitude of the applied forces, the mechanical properties of the structural materials and the design of the structure. It is through the process of deformation; moving the atoms or molecules either further apart or closer together, that materials are able to generate the internal forces required to balance and oppose the externally applied loads.

### 3.2.2 Stress

Stress, or mechanical stress (to distinguish it from emotional or psychological stress), is a measure of the intensity of the internal reacting forces which materials develop in order to resist the action of the externally applied loads or forces. It can be one of two types, namely tangential

or normal, and is expressed in units of force per unit area, e.g. pounds per square inch.

Normal stress can be either tensile or compressive in nature and is the intensity of force which acts perpendicularly to a surface. Shear stress on the other hand, is produced by forces which act parallel to the surface causing a slipping type action and is therefore neither tensile nor compressive in character.

In looking at the stresses acting at a particular point in a loaded structure, a three-dimensional or triaxial state of stress generally exists. To define this state explicitly three normal stresses acting orthogonally to one another and three corresponding shear stresses are required. Because stress is a second order tensor quantity, the stresses acting at a point can be transformed and planes found where the stress components reduce to a situation consisting purely of normal stresses. Planes on which these occur are called principal planes and the corresponding stresses principal stresses. Some structures however, possess a far more simplified stress system with stress components acting only in two dimensions or biaxially, or even more simply in one dimension or uniaxially, FIG. 3.1

### 3.2.3 Strain

As has already been stated, materials and structures deflect and deform under the action of applied forces. It is through the action of deformation that the structure or material is able to generate the internal resisting stresses required to support

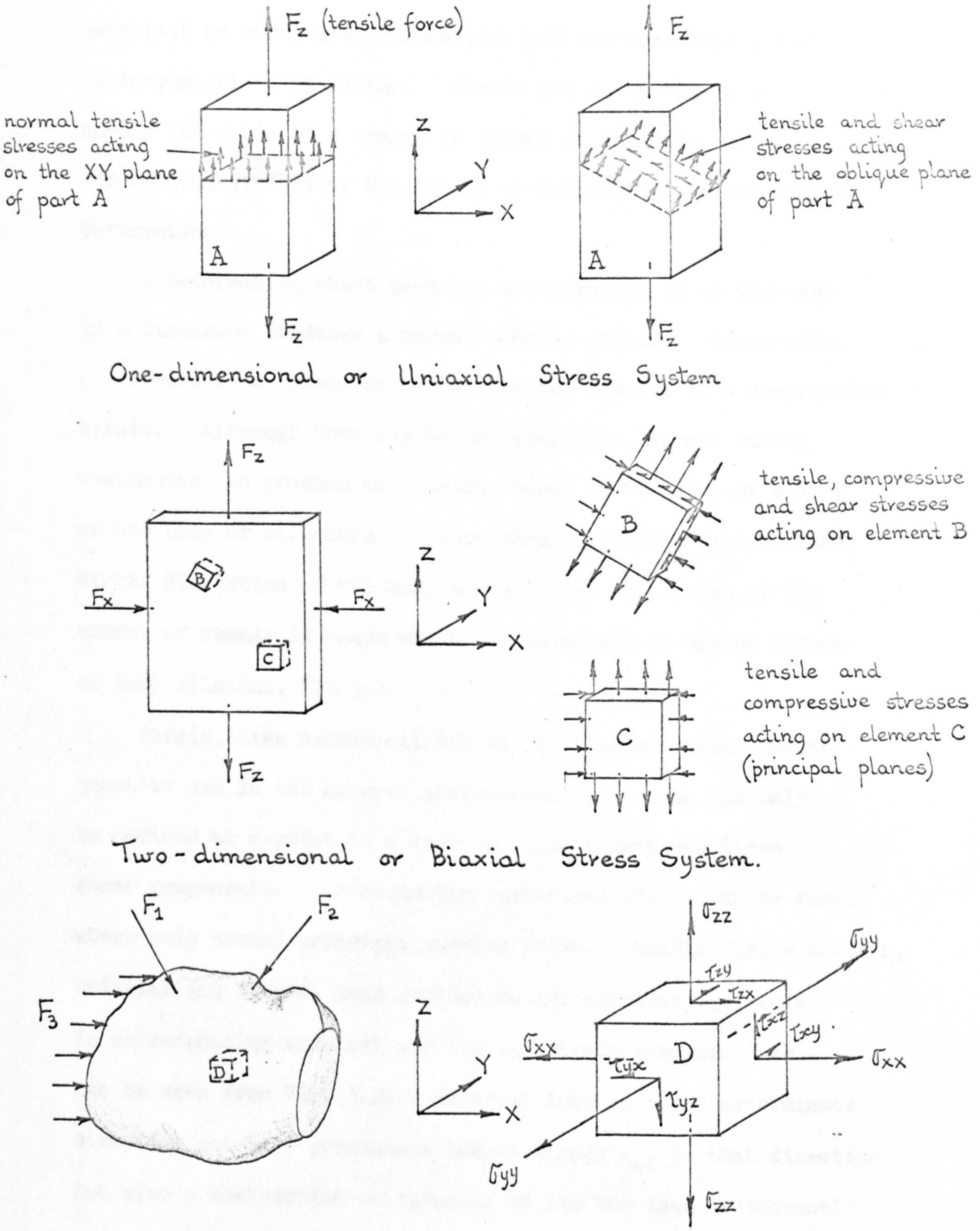


One-dimensional or Uniaxial Stress System




Two-dimensional or Biaxial Stress System.




Three-dimensional or Triaxial Stress System.

FIG. 3.1 Illustration of uniaxial, biaxial and triaxial stress systems.

these imposed loads. Mechanical strain is a measure of the materials or structures deformation and can be either normal or tangential in character. Strain has no units, it is merely the ratio of a change in length or dimension after deformation divided by the length or original dimension before deformation*.

A deformation which produces an extension or an increase in a dimension produces a normal tensile strain. Conversely, a decrease in a dimension or contraction results in a compressive strain. Although they may be imperceptible, normal strain components can produce an overall change in the size or volume of the body or structure. Shear strain however, is a measure of the distortion of the body and gives an indication of the amount of change in shape which has occurred, it has no effect on body dilation, FIG 3.2.

Strain, like mechanical stress, is a second order tensor quantity and in the general three-dimensional case can only be defined at a point in a body by three normal and three shear components. Consequently, principal planes can be found where only normal principal strains exist. Unlike stress however, uniaxial and biaxial load systems do not necessarily result in corresponding uniaxial and biaxial strain systems. As can be seen from FIG. 3.2, a uniaxial load in the $\hat{z}$ co-ordinate direction not only produces a normal strain $\varepsilon_{z\hat{z}}$ in that direction but also a contraction or thinning of the bar (and consequently compressive strains), in both the X and Y co-ordinate directions as well.

* Strictly speaking strain has units of inches per inch or mm/mm.

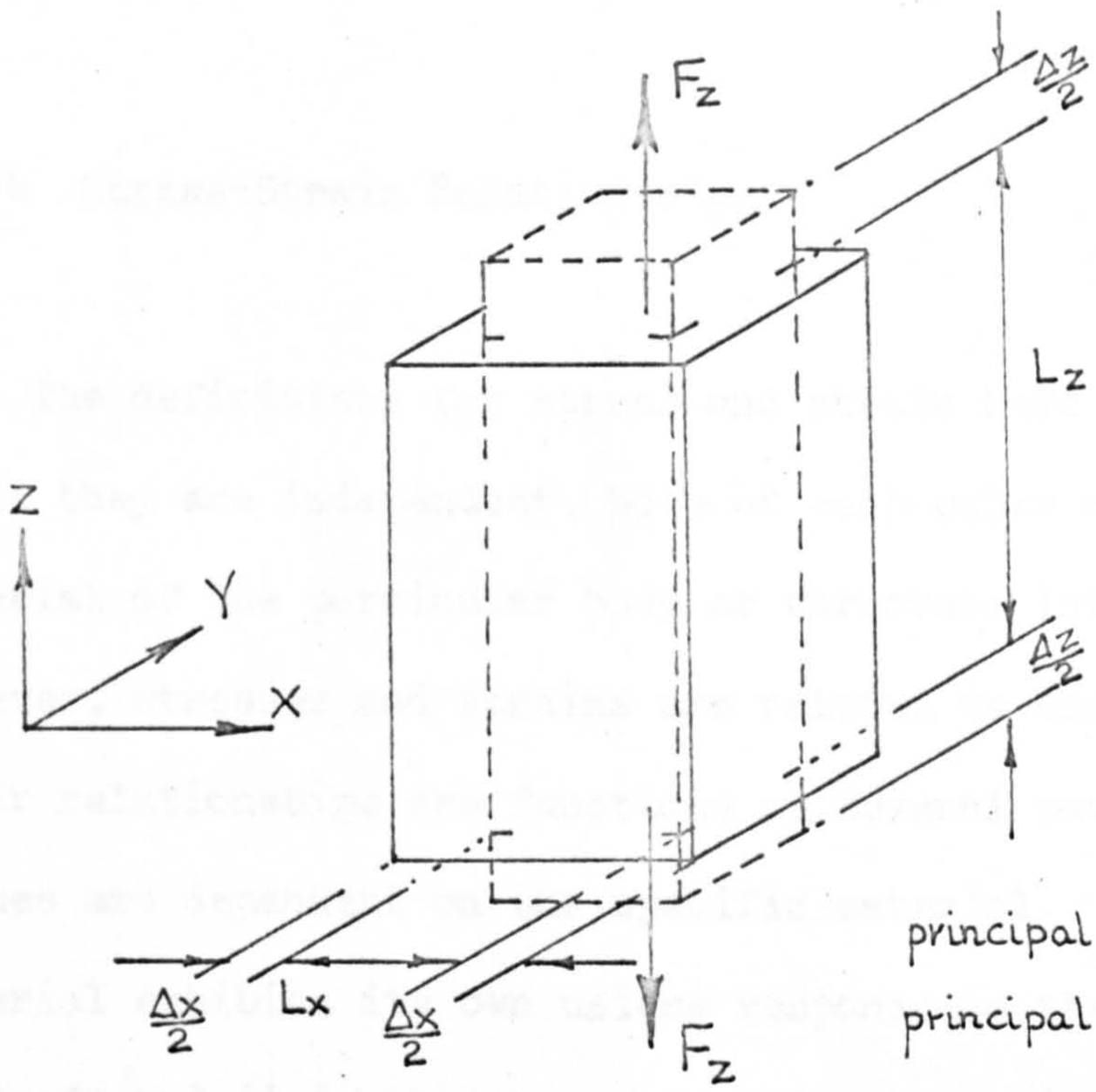


principal normal strain $\epsilon_{zz} = \frac{\Delta z}{L_z}$

principal normal strain $\epsilon_{xx} = -\frac{\Delta x}{L_x}$

Normal Strain

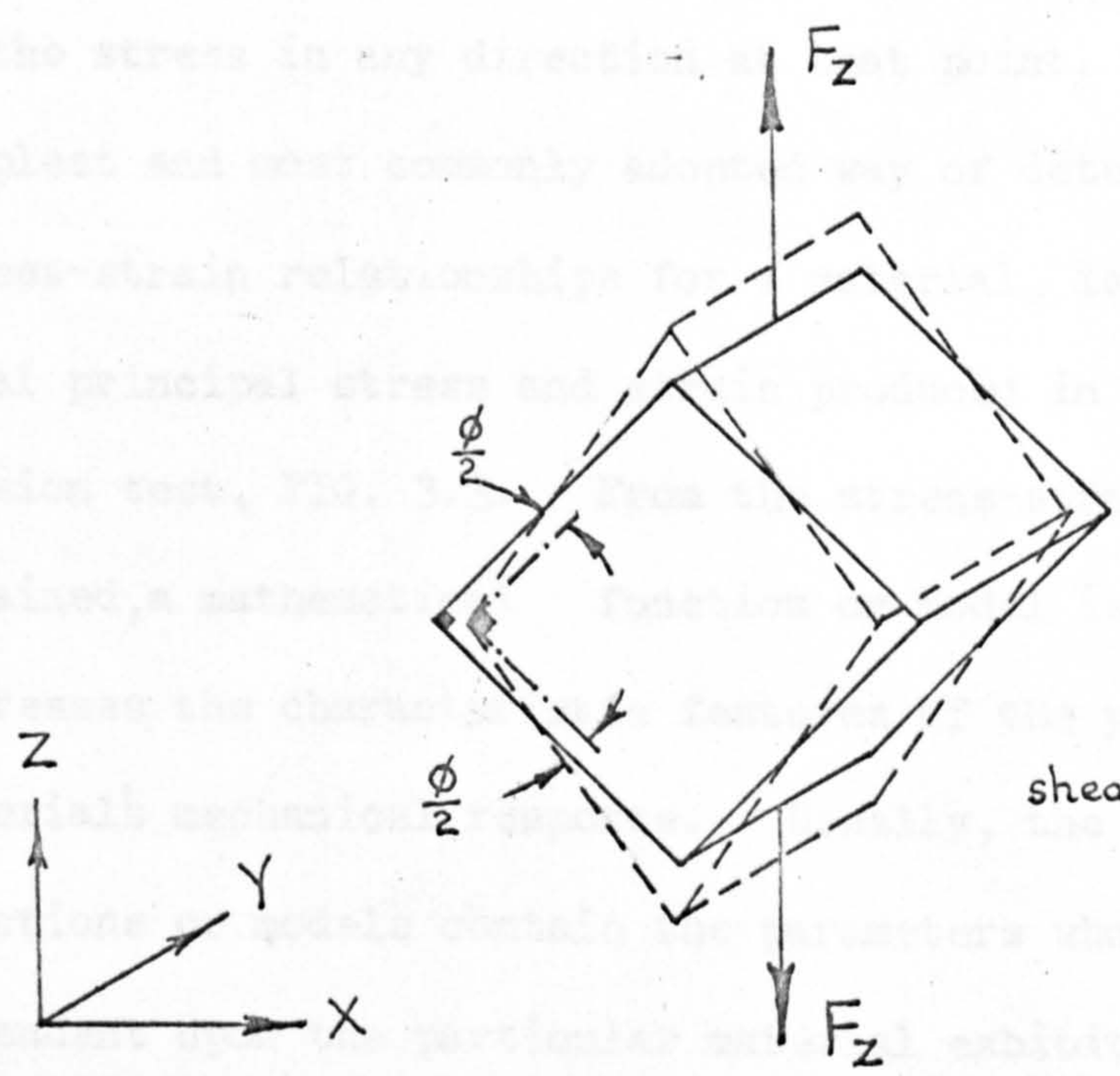


shear strain $\gamma_{xz} = \phi$

Shear Strain

FIG. 3.2 Diagrammatic illustration of normal and shear strain components.

### 3.2.4 Stress-Strain Relationships

The definitions for stress and strain have been given as if they are independent, both of each other and of the material of the particular body or structure involved. However, stresses and strains are related to each other and their relationships are functions of several parameters whose values are dependent on the specific material. Every material exhibits its own unique response to the application of loads and it is this response which mechanically distinguishes one material from another.

All strains at a point in a loaded body may be influenced by the stress in any direction at that point. However, the simplest and most commonly adopted way of determining the stress-strain relationships for a material, is to relate the axial principal stress and strain produced in a uniaxial tension test, FIG. 3.3. From the stress-strain diagram obtained, a mathematical function or model is derived which expresses the characteristic features of the particular materials mechanical response. Usually, the mathematical functions or models contain the parameters whose values are dependent upon the particular material exhibiting the response. The expression determined, which relates the stress to the strain for all possible types of loading, is called the constitutive equation or relationship for the material.

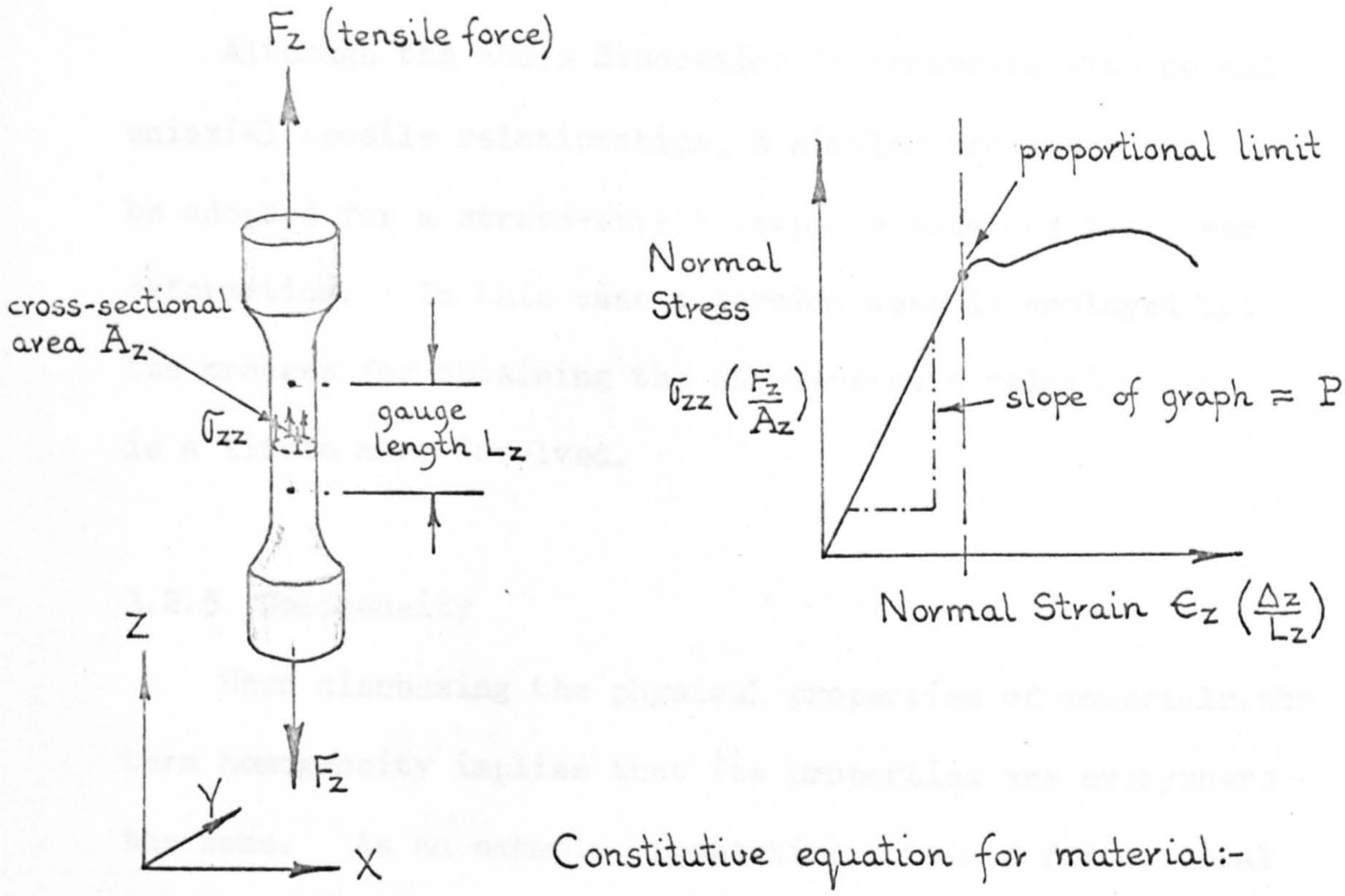


Constitutive equation for material:-

$$\sigma_{zz} = P\epsilon_{zz}$$

FIG. 3.3 Determination of the stress-strain relationship of a material from a uniaxial tensile test.

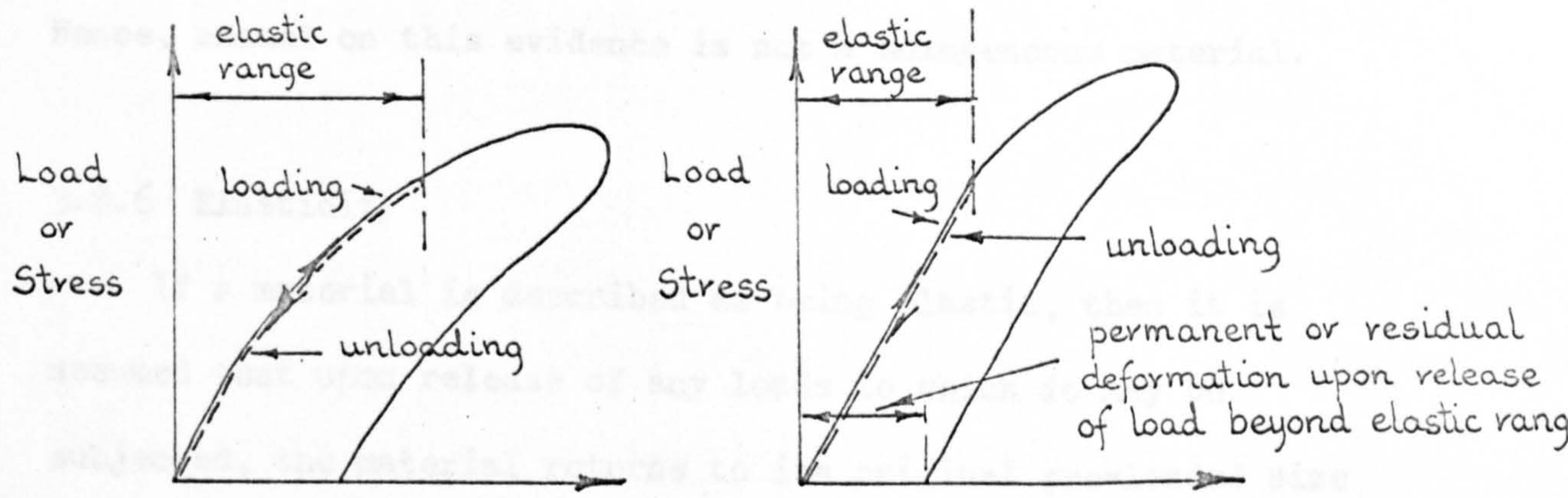


N.B. Loading and unloading curves should be coincident in elastic range.

FIG. 3.4 Non-linear and linear forms of elasticity.

Although the above discussion is concerned with normal uniaxial tensile relationships, a similar procedure can be adopted for a stress-strain response obtained for shear deformation. In this case a torsion test is employed but the process for obtaining the stress-strain relationship is a little more involved.

### 3.2.5 Homogeneity

When discussing the physical properties of materials, the term homogeneity implies that its properties are everywhere the same. As an example, properties obtained for cortical bone have been obtained from experiments using specimens taken from femora; in this work these properties have also been assumed to apply to the cortical bone of the alveolar processes. Again, certain properties for human enamel have been found to vary over different areas of the same crown. Hence, enamel on this evidence is not a homogeneous material.

### 3.2.6 Elasticity

If a material is described as being elastic, then it is assumed that upon release of any loads to which it may be subjected, the material returns to its original pre-loaded size and shape. Common engineering materials have what is termed an elastic range. The elastic range defines a limit of stress beyond which the material will fail to regain its original form and will have undergone permanent deformation.

Many materials exhibit a particular form of elastic action known as linear elasticity. In this case, the material deforms in direct proportion to the magnitude of the applied load. Such a material is said to possess a linear stress-strain relationship and is a manifestation of the familiar Hooke's Law, FIG 3.4

### 3.2.7 Young's Modulus or Modulus of Elasticity

From the stress-strain diagram for the uniaxial tension test in FIG. 3.3, it can be seen that the material is linearly elastic for the first part of the graph. Consequently, the constitutive stress-strain relationship for this region is

$$\sigma_{zz} = P\ \epsilon_{zz}$$

where $\sigma_{zz}$ and $\epsilon_{zz}$ represent the normal stress and strain components in the Z co-ordinate direction. The constant P is the slope of the linear portion of the graph and has the units of force per unit area (the same units as stress). P, a constant of proportionality, is called the Young's modulus or modulus of elasticity and is often denoted by the symbol E. Strictly speaking E should have a subscript and be written Ez to show that the value refers to the material in the Z co-ordinate direction. If instead of a tensile test the specimen were subjected to a compressive force, a similar stress-strain relationship would be obtained. However, in this case, the slope of the initial linear portion of the curve, although still denoted by Ez, would be the compressive modulus of elasticity of the material. For many engineering materials such as steel,

the modulus of elasticity in compression is the same as it is in tension.

Young's modulus is a measure of the stiffness or flexibility of the material. Taking as an example the two tensile uniaxial stress-strain curves shown in FIG. 3.5a it can be seen that material B requires twice the normal stress of material A in order to produce the same deformation. Hence, material B is twice as stiff as material A and consequently has a modulus of elasticity such that

$$Ez\ (B) = 2Ez(A)$$

Some materials possess either a very small or no distinguishable linear elastic region, FIG. 3.5b. Consequently, properties referred to as the tangent and secant moduli are sometimes used in the constitutive equations in these non-linear regions. The tangent modulus is the slope of the stress-strain curve at any point beyond the proportional limit. The secant modulus however, is the ratio of the total stress and the corresponding total strain at any point beyond the linear elastic range.

### 3.2.8 Shear Modulus or Modulus of Rigidity

As was mentioned in section 3.2.4, a stress-strain curve can be obtained for a material subjected to shear loading. For this case a torsion test on a specimen of uniform circular cross-section, is employed and a graph of torque (equivalent to force), versus specimen rotation (deflection) is obtained. From the linear elastic region

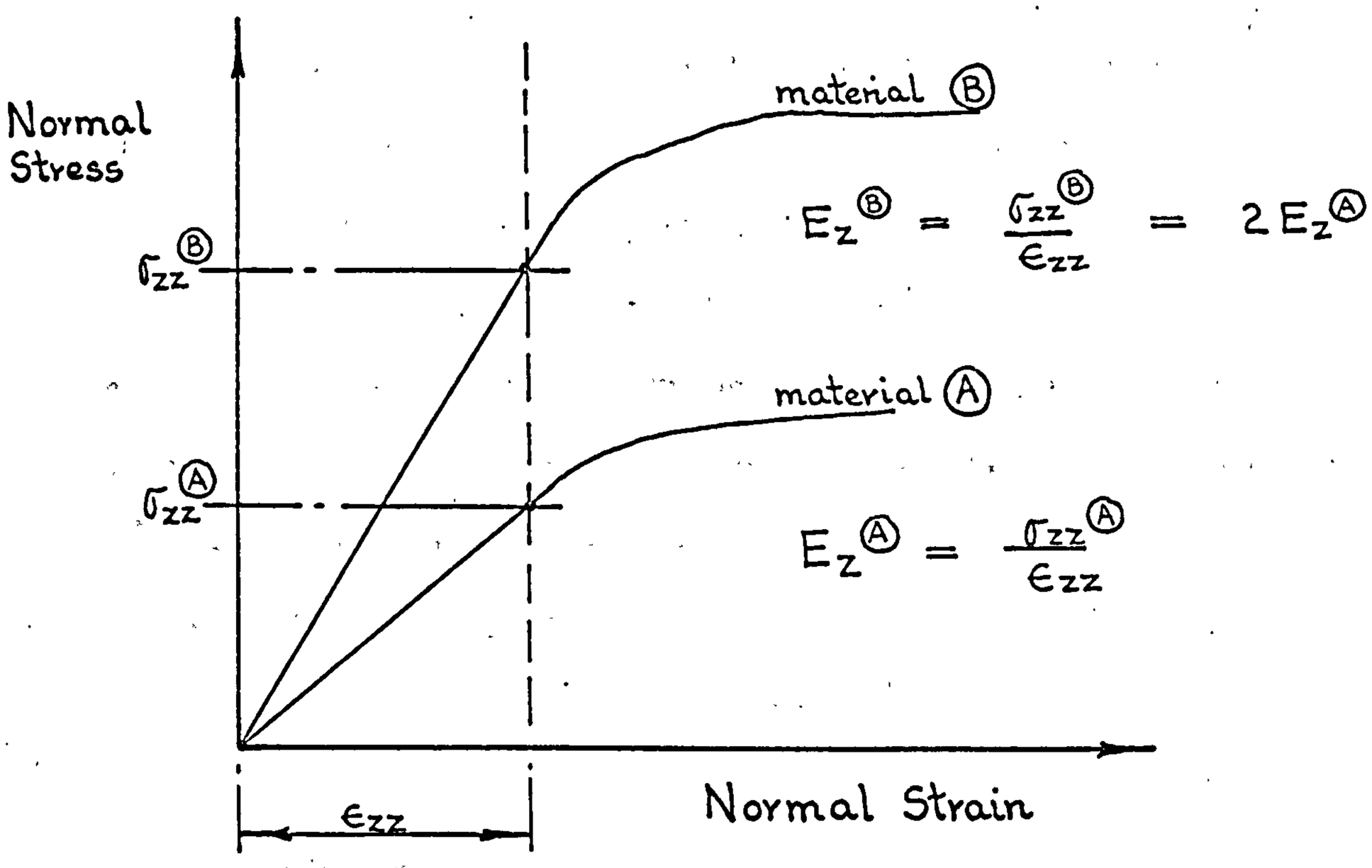


a) Determination of the Young's modulus of elasticity

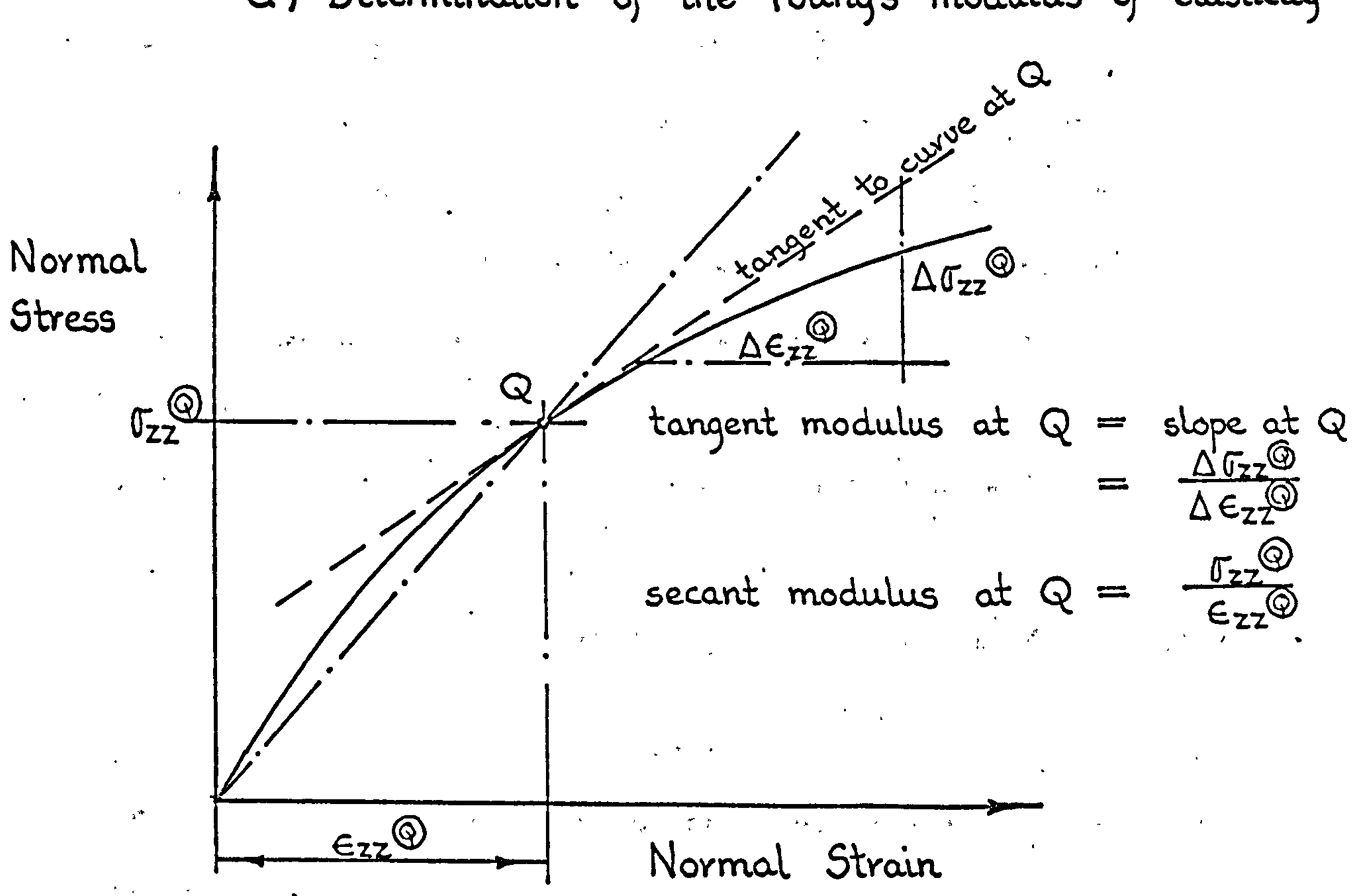


b) Determination of the tangent and secant moduli

FIG. 3.5 Determination of the Young's modulus of elasticity for linear elastic materials and the tangent and secant moduli for non-linear elastic materials.

of this curve the ratio of the shear stress and the shear strain is determined. This ratio, often denoted by the symbol G is called the shear modulus or the modulus of rigidity of the material. Again,like the modulus of elasticity, G should be subscripted and written as say $G_{xy}$. Here the subscripts indicate that the shear modulus is a measure of the shearing stiffness of the material in the XY plane. The shear modulus Gxy relates the shear stress $\tau_{xy}$ and the shear strain $\gamma_{xy}$, in the XY plane, by the constitutive relationship

$$\tau_{xy} = G_{xy} \cdot \gamma_{xy}$$

### 3.2.9 Bulk Modulus

Another elastic constant which is sometimes useful for comparing different materials is the bulk modulus. The bulk modulus is defined as being the average of the three normal stresses at a point divided by the cubical dilation. The cubical dilation is the change in volume per original unit volume. Hence,if an element of the material originally has sides of length dx, dy and dz, and deforms into an element with sides $dx(1 + \varepsilon_{xx})$, $dy(1 + \varepsilon_{yy})$, and $dz(1 + \varepsilon_{zz})$ the dilation becomes

$$\text{Dilation} = \frac{(1 + \varepsilon_{xx})(1 + \varepsilon_{yy})(1 + \varepsilon_{zz})dxdydz - dxdydz}{dx\ dy\ dz}$$

$$= \varepsilon_{xx} + \varepsilon_{yy} + \varepsilon_{zz}$$

if products of strain are considered negligible compared with the strains themselves.

Thus, by definition the bulk modulus $K_b$ becomes

$$K_b = \frac{\frac{\sigma xx + \sigma yy + \sigma zz}{3}}{\varepsilon xx + \varepsilon yy + \varepsilon zz}$$

### 3.2.10 Poisson's Ratio

When discussing mechanical strains it was shown how a uniaxially applied force to a bar in the Z co-ordinate direction not only produced a normal strain $\varepsilon_{zz}$ in that direction, but also normal strains in the X and Y co-ordinate directions as well. It can be shown experimentally that the normal passive induced strain occurring in the X direction is directly proportional to the active stress produced strain $\varepsilon_{zz}$ in the Z direction for stresses below the proportional limit.

Hence, $\varepsilon_{xx}$ (passive) $\alpha$ $\varepsilon_{zz}$ (active)

or $\varepsilon_{xx}$ (passive) = $\varepsilon_{zz}$ (active) x constant

The constant in the above equation is called the Poisson's ratio and is often denoted by $\mu$. Like the moduli of elasticity and rigidity, Poisson's ratio should be subscripted. For the above case

$$\text{Poisson's ratio} = \frac{\varepsilon_{xx\ (passive)}}{\varepsilon_{zz\ (active)}} = \mu_{zx}$$

where $\mu_{zx}$ refers to the ratio of the passive resulting strain in the X direction and the active stress induced strain occurring in the Z direction. Similarly, the ratio of the induced passive strain in the Y co-ordinate direction due to the active stress induced strain in the Z direction can be expressed as

$$\mu_{zy} = \frac{\varepsilon_{yy\ (passive)}}{\varepsilon_{zz\ (active)}}$$

It must be remembered that all Poisson's ratios are associated with a sign depending upon whether the strains induced are extensions, assumed positive, or contractions assumed negative. Generally,materials when stretched or extended in one Cartesian co-ordinate direction, shrink or contract in the other two.directions. This implies, using the above equation, that $\mu$ is negative and also that the material tends to reduce in volume under load. However, convention has it that Poisson's ratios are usually ascribed positive values. Consequently, equations in which this parameter occurs are automatically written to take account of the minus sign. This point has to be very carefully watched when dealing with biological materials as the actual or real sign of the Poisson's ratio is very often uncertain.

### 3.2.11 Isotropy and Anisotropy

A material is said to be isotropic if its physical properties are not dependent upon the direction in the material along which they are measured. For example, if a material is isotropic with respect to its tensile Young's modulus, then no matter in what direction the specimen is taken from the material for the tensile test, the same value of the modulus of elasticity will be obtained. Consequently, a homogeneous, linear elastic, isotropic material has only two completely independent elastic constants or properties. Thus from the four properties previously discussed, namely, Young's modulus, shear modulus, bulk modulus and Poisson's ratio, only two are

independent of one another.

An anistropic material however, is a material in which the physical properties are different in different directions. In the general case of anisotropy the material possesses no kind of elastic symmetry whatsoever and it has twenty one independent elastic constants. Fortunately, materials when considered on a macroscopic scale, exhibit some elastic symmetry and so the number of independent constants is greatly reduced.

One very special class of anisotropic materials is that which possesses . . axes of elastic symmetry which are orthogonal to one another, FIG. 3.6. This type of material, which has in the general three-dimension case nine independent elastic constants, is consequently known as an orthotropic material. Cortical bone and certain kinds of timber are typical examples of materials that are approximately orthotropic.

### 3.2.12 Thermal Expansion

When the temperature of a material is either raised or lowered, a change usually occurs in the material's dimensions. With many materials, and particularly with metals, the changes in dimensions have been found experimentally to be directly proportional to the original dimensions of the body and also to the relative temperature changes which the material has experienced. Hence, the change in dimension of a material in say the $x$ co-ordinate direction can be expressed as:

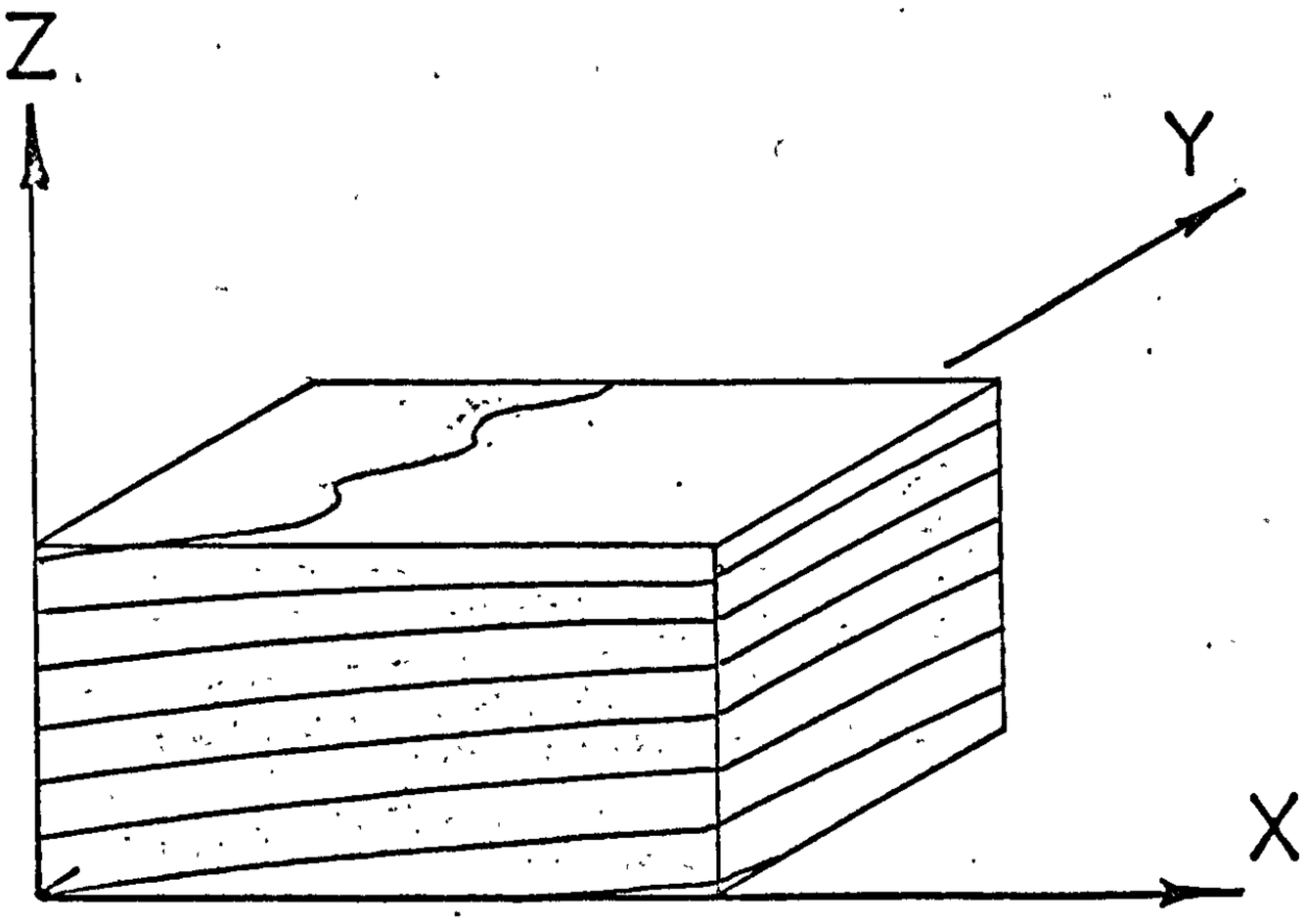


a) Element of timber.

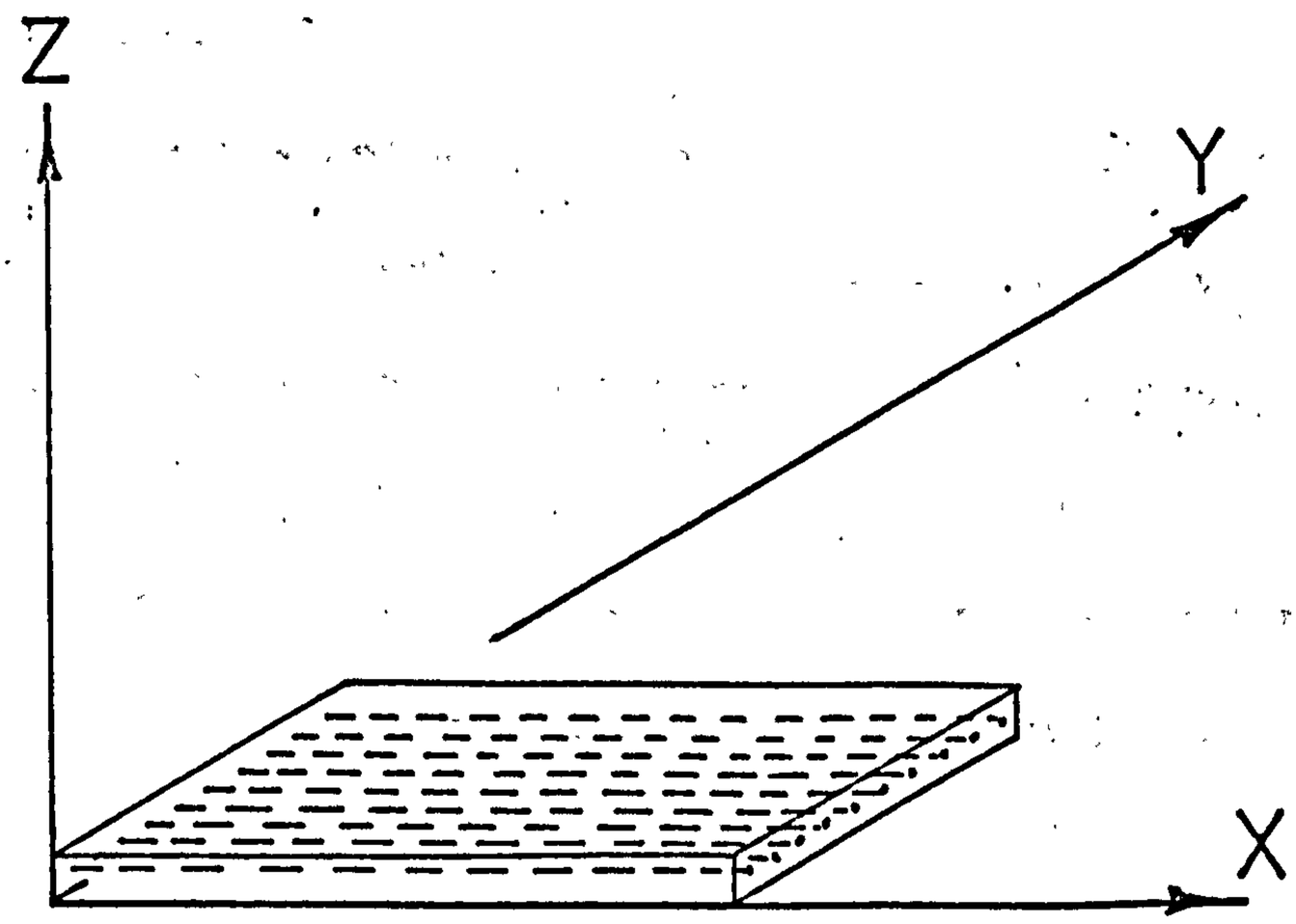


b) Carbon-fibre reinforced plastic.
(The fibres are all parallel to one another.)

FIG. 3.6 Illustrating grained type orthotropic materials which possess axes of elastic symmetry which are orthogonal to one another.

change in Z dimension $\alpha$ original Z dimension x temperature change

or $\delta Z = Z$ x temperature change x constant

The constant in the above equation is known as the coefficient of linear thermal expansion for the material in the Z co-ordinate direction. The actual value of the constant depends upon the temperature range being considered. It has the units of length per degree of temperature change per unit of length. Although the coefficient of thermal expansion is dependent upon material direction, for most metals this property is isotropic.

The coefficient of linear thermal expansion is generally a much higher value for metals than it is for non-metals. For example, the constant is two to three times larger for amalgam than it is for tooth substance over the same oral temperature range.

Although the coefficient of linear thermal expansion is the property most easily determined experimentally, the volumetric expansion of a material is also important. However, for most practical purposes the coefficient of volumetric thermal expansion may be considered to be approximately three times the value for linear thermal expansion over the same temperature range.

### 3.2.13 Thermal Conductivity

The thermal conductivity of a material is a measure of its ability to transfer heat by the mode of conduction. Metals are generally very much better thermal conductors than are plastics and other non-metals. Enamel and dentine are relatively poor conductors and could therefore be classified as being thermal insulators. Hence, bearing in mind that the dental pulp is very sensitive to thermal stimulation, it is apparant that the insertion of a large metal restoration into a tooth could have deleterious biological consequences. Also, the high thermal expansion of most restorative materials coupled with their ability to readily transfer heat, could similarly lead to serious structural failures.

### 3.2.14 Piezoelectricity

The application of mechanical stress produces in certain dielectrics an electrical polarisation (an electric dipole moment), proportional to the applied stress. If the dielectric is isolated, polarisation manifests itself as a voltage across the material. However, if the material is on short circuit,a flow of charge occurs during the loading phase. This phenomenon is called the direct piezoelectric effect. On the other hand,if a voltage is applied to the same material (in a particular direction), a corresponding mechanical strain or distortion cccurs.

Consequently, this is known as the converse piezoelectric effect.

It has been proposed that bone and other biological tissues are piezoelectric materials. It has also been suggested that this property provides one of the regulating or controlling mechanisms in tissue repair and replacement.

### 3.2.15 Viscoelasticity

In the sections dealing with elastic action and the determination of the elastic constants, namely the Young's modulus, the shear modulus, the bulk modulus and the Poisson's ratios, no mention was made in the discussions of the effect of time on the materials behaviour. In fact, by its omission it was automatically assumed that the stress-strain relationship was unaffected by the time scale of the experiment, or in other words, by the rate at which the stress or strain was applied. Perfect elasticity implies that the stress-strain relationship is independent of time and the elastic constants independent of the rate of deformation.

While these elastic assumptions are generally applicable to the majority of materials when they are subjected to fairly small strains for reasonably short periods of time at normal ambient or room temperatures, they are not usually valid for plastics and for soft materials. Consequently, other models have been developed in order to describe these particular materials behaviour.

A particular class of material; and biological tissues may well fall into that class, are time dependent. That is to say the material response is not only dependent upon the load magnitude, but also upon the load history. For instance, if a constant tensile load was applied to such a material in a uniaxial test, then the corresponding tensile strain would be found to increase with time. This is the same as saying that the material creeps with time. Similarly, if the same material were to be extended and held clamped in this elongated state, the tensile stress generated in the specimen would reduce or relax with time. This type of behaviour, where the material tends to flow, is more characteristic of a highly viscous liquid than it is of an elastic solid. Consequently, materials exhibiting this type of stress-strain-time behaviour are classified as being viscoelastic. The two typical linear viscoelastic material response characteristics described above, are illustrated in greater detail in FIG. 3.7.

## 3.3 SOME FACTORS WHICH INFLUENCE THE DETERMINATION OF THE PHYSICAL PROPERTIES OF THE DENTAL TISSUES

It would be preferable if all the tissue property data required in the analyses could be determined from in-vivo measurements. Unfortunately however, this is not possible at the moment and so in-vitro measurements on small test samples are employed*. It is therefore necessary to be aware of the factors which may affect the small tissue samples

* Modern ultrasonic techniques of measurement are currently under development and so it may be possible, when these methods are perfected, to determine the tissue properties in-vivo.

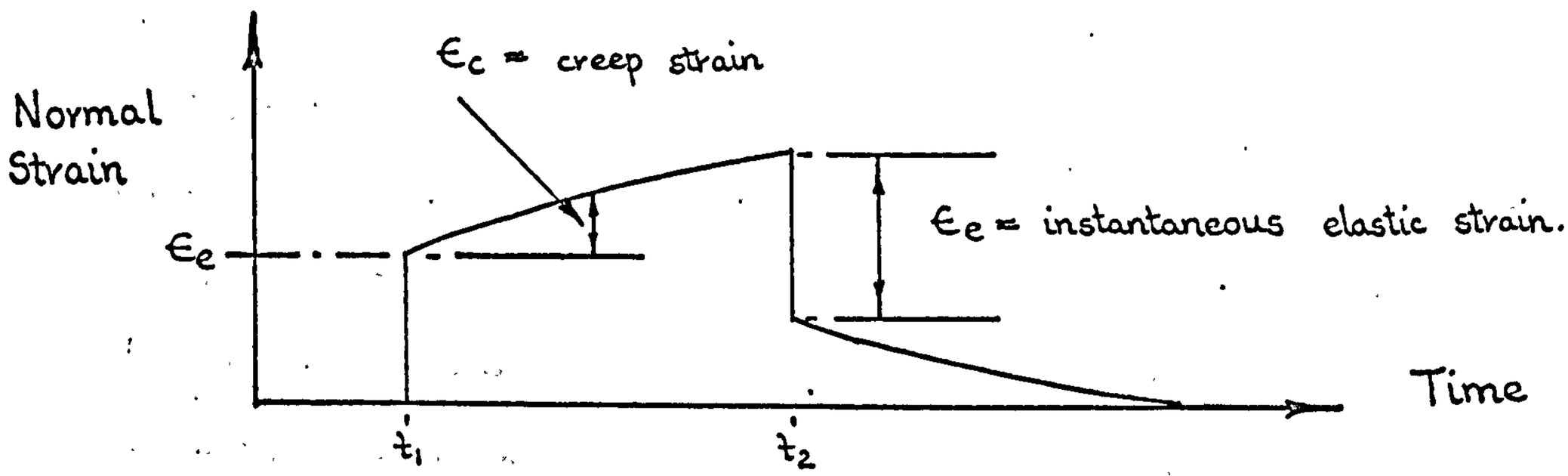


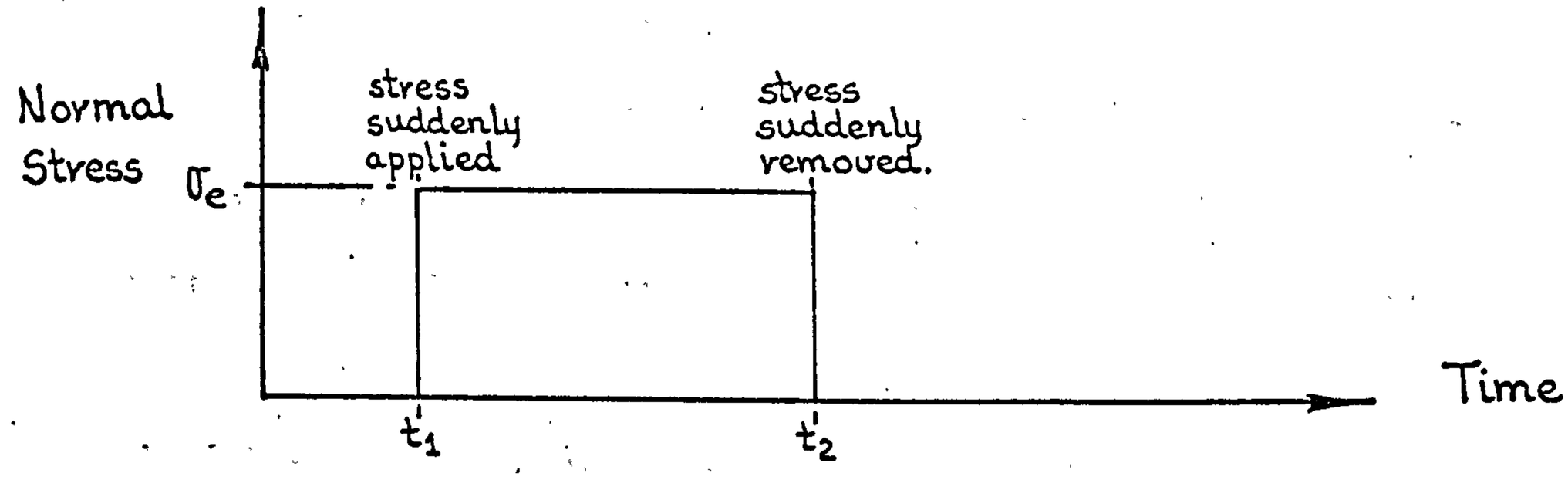


Normal strain response to normal stress step input.

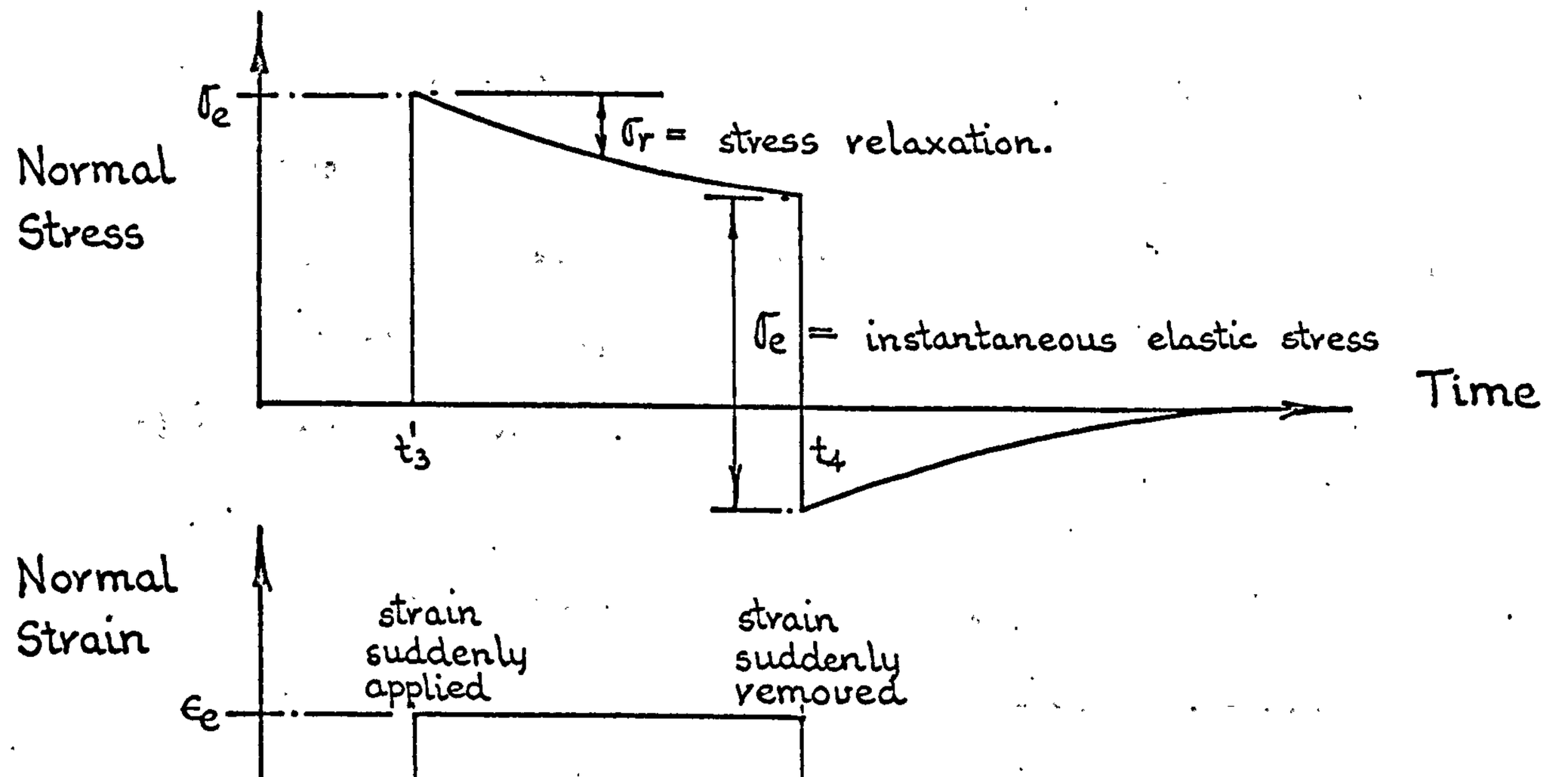


Normal stress response to normal strain step input.

FIG. 3.7 Linear viscoelastic material response characteristics for simple uniaxial test specimen.

(and consequently the physical properties which are obtained from them), once they are removed from their natural living environment. While some of the more obvious factors which may influence the in-vitro measurements have been investigated, others exist which have not been fully examined. Tissues afterall are living materials; they have their own blood supply and unlike common materials are partly composed of cells and intercellular fluids. Although Swanson and Freeman (2) concluded from their work on whole femora that bone was not hydraulically strengthened, it is not reasonable to assume that this doctrine applies to other tissues or to small test samples. The periodontal membrane is a particularly relevant example*; it has a copious blood supply and contains many cells and vessels. Moreover, in its natural environment it is somewhat enclosed, having the stiff alveolar socket wall on one side and the equally stiff tooth root on the other. Consequently, it is extremely doubtful if any simple experiment on this tissue in-vitro would produce meaningful data with regard to its function and behaviour under stress in-vivo.

### 3.3.1 Variations between Specimen Species

Because of the obvious difficulty of obtaining sound human specimen material, many authors have investigated the properties of animal tissue. Although this is admirable material for developing the experimental apparatus and technique, it is dangerous to assume that the tissues are both

* WILLS, D.J., PICTON, D.C.A. and DAVIES W.I.R. indicated at a meeting of the I.A.D.R. (British Div.) held at King's College, London in 1972, that the properties of the periodontium in monkeys were affected by alterations in blood supply.

histologically and mechanically the same for all species. A good example of the differences which can exist was clearly shown by McLeish and Habboobi (3). These authors demonstrated that the Young's modulus for cortical bone in the ox is approximately twice the value of the human tissue taken from the equivalent anatomical position.

### 3.3.2 Specimen Condition

The condition of the specimen being tested has a direct bearing on the property values obtained from in-vitro measurements. It is very important that the tissue is not dehydrated. Numerous authors have demonstrated how the stiffness of bone, dentine and enamel, increases significantly with increased dehydration, Evans and Lebow (4), and Tyldesley (5). Another equally important aspect to consider is whether the material is of pathological or of normal origin. Stanford et al (6), concluded that the modulus of elasticity was much lower for carious enamel than it was for sound tissue.

### 3.3.3 Type and Mode of Test

The method of structural stress analysis employed in this investigation assumes that the tissue property data are obtained under static or near-static loading conditions. The significance of the rate of loading on the mechanical properties of tissues has been clearly demonstrated by McElhaney et al (7), who found that the E value for cortical

bone increased considerably with the rate of loading. It is therefore essential that the mode of test employed is compatible with the static analyses.

A further point which has to be borne in mind is whether the tissues exhibit the same mechanical response in tension as they do in compression as this is conventionally assumed to be the case in most methods of stress analysis. Consequently, it is important to investigate the properties of the tissues under both types of loading conditions if it is required to take into account any significant differences.

## 3.4 LITERATURE SURVEY OF THE PHYSICAL PROPERTIES OF THE DENTAL TISSUES

The literature survey was conducted to obtain both qualitative and quantitative data on the dental tissues and materials required in the subsequent stress analyses. The gingiva and dental pulp however, were not included in the survey. Being soft tissues and because of their anatomical positions, they play no significant role mechanically in the structures considered in this investigation. Consequently, they have been ignored.

In examining the data presented in the literature, due attention has been paid to the influencing factors which were discussed in the previous section. As a consequence of this,many data have been discarded because information concerning the actual tests, type and condition of the specimen material was not clearly documented.

### 3.4.1 The Enamel

Because the amount of enamel available on the normal human tooth is small, it is very difficult to obtain samples of this tissue which are physically large enough to test. Consequently, very little work has been done on enamel to determine its mechanical properties. Of the properties which are required in the stress analyses, only the modulus of elasticity has really been seriously measured.

Stanford et al in 1958 (6) determined the Young's modulus of enamel in compression from circular cross-section human specimens obtained from freshly extracted teeth. Between their preparation and actual testing, the specimens were stored in distilled water. The authors observed that the E values determined varied considerably, and depended upon the location on the crown where the specimens were obtained. Cusp enamel was found to be much stiffer than side and occlusal surface material. They concluded that the high stiffness of the cusp enamel could be attributed to the gnarled and twisted configuration of the enamel rods.in these areas. The low value for occlusal enamel was suggested as being due to decalcification. This seems very reasonable because the occlusal surfaces are particularly vulnerable to the onset of caries.

In 1959 Tyldesley (5), published his work and reaffirmed the extreme difficulties of obtaining suitable enamel material. He resorted to using compound dentine and enamel specimens which were ground down from the labial surfaces

of the upper incisors. The author reports to have kept his specimens 'wet', right from extraction through to machining and testing. The specimens which were in the form of rectangular bars, were loaded by a four point bending apparatus. Hence, the enamel was subjected to both compression and tension. From the load versus beam deflection readings, and using the Young's modulus for dentine, Tyldesley calculated the E value for enamel by employing simple compound bar theory. His value of $19 \times 10^6$ p.s.i. is very high in comparison with Stanford's result. In fact, it seems from his paper that he made an error in his calculation, for he assumed that the stress in the compound bar would be the same in both the enamel and the dentine. Although the specimen data and recorded results are not too clearly presented, by interpreting the data and re-working the calculation, a value for E of $7.2 \times 10^6$ p.s.i. can be obtained.

Stanford et al in 1960 (8), modified and slightly improved their procedure of 1958, and obtained more compression values for the Young's modulus of enamel. As before, they found that crown position was important; properties were dependent upon specimen location. The specimens taken from the side of the tooth also showed that the modulus values determined were dependent upon the prism or tubule orientation. The average E obtained with the prisms parallel to the specimen's axis was $4.7 \times 10^6$ p.s.i. while that for specimens with the prisms perpendicular to the axis was found to be only $1.4 \times 10^6$ p.s.i.

In some cases, the authors found that the E value for enamel, obtained from a similar tooth position and having the same prism direction, was much higher for teeth originating from an area where fluoride was endemic.

Craig et al in 1961 (9), published their work on the compressive modulus of human enamel. Using freshly extracted human molars they produced circular shaped prism test specimens whose longitudinal axes were approximately parallel to the direction of the enamel rods. The specimens which were prepared under a continuous stream of water, were stored in water up to the time of testing. The tests were conducted using a discontinuous loading rate, the strain being measured after each load increment. This procedure, the authors claimed, was possible because no flow in the enamel was observed to occur. The average value of E obtained from twelve cusp samples, having a length to diameter ratio greater than two, was $12.2 \times 10^6$ p.s.i. However, the average value for seventeen side enamel specimens having a length to diameter ratio greater than 1.4, was slightly lower at $11.3 \times 10^6$ p.s.i.

From compression tests on whole teeth, Haines 1968 (10), reports on two values he obtained for the effective Poisson's ratio of human enamel. However, his paper gives no clear explanation of how these values were determined. He states that enamel has two distinct loading phases. For low loads or the first loading phase, the Poisson's ratio is for most practical purposes zero whereas for the second phase

| Author and Reference | Type of Test | Property | Remarks and Observations |
|---|---|---|---|
| Stanford et.al 1958 (6) | Compression (no strain-rate given) | $E = 8{\cdot}2 \times 10^6$ p.s.i | Cusp material - no prism direction |
| | | $E = 6{\cdot}0 \times 10^6$ p.s.i | Side material - no prism direction |
| | | $E = 1{\cdot}8 \times 10^6$ p.s.i. | Occlusal surface material |
| Tyldesley 1959 (5) | 4 point bending on composite specimen | $E = 19 \times 10^6$ p.s.i | Error in Tyldesley's calculation |
| | | $E = 7{\cdot}2 \times 10^6$ p.s.i | Value calculated from given data. |
| Stanford et.al. 1960 (8) | Compression (no strain-rate given) | $E = 4{\cdot}7 \times 10^6$ p.s.i | Side material - Prisms parallel to specimen axis |
| | | $E = 1{\cdot}4 \times 10^6$ p.s.i | Side material - Prisms perpendicular to specimen axis. Stanford et. al. conclude that enamel is anisotropic. |
| Craig et. al. 1961 (9) | Compression (intermittent loding) | $E = 12{\cdot}2 \times 10^6$ p.s.i | Cusp material - Prisms parallel to specimen axis. Specimen Length/Diameter > 2 |
| | | $E = 11{\cdot}3 \times 10^6$ p.s.i. | Side material - Prisms parallel to specimen axis. Specimen Length/Diameter > 1·4 |
| Haines 1968 (10) | Compression (on whole teeth) | $\mu = 0$ | For 'low' loads. |
| | | $\mu \simeq 0{\cdot}3$ | For 'high' loads. |
| Lees and Rollins. 1972 (11) | Ultrasonic Method (on bovine whole teeth) | $\mu \simeq 0{\cdot}28$ | $\mu$ refers to no specific prism orientation. Lees and Rollins conclude that enamel is anisotropic. |

TABLE 3.1 Published mechanical properties of enamel.

or higher loads he reports the value to be approximately 0.3.

Although Lees and Rollins in 1972 (11), investigated the properties of the hard dental tissues of intact bovine incisors, it is relevant to point out that their findings strongly suggest enamel to be a highly anistropic material. Even though the specimen condition is not stated in their paper, the teeth examined were embedded in an acrylic plastic prior to testing. Hence, it must be assumed that some dehydration must have occured. However, from their experiments the authors estimated the Poisson's ratio for bovine enamel to be in the region of 0.28.

### 3.4.2 The Dentine

Of all the dental tissues, the dentine is the one which has been most extensively investigated. This can be attributed to the relative abundance of the tissue in the teeth thereby enabling a more reasonable sized specimen to be obtained.

Peyton et al 1952 (12), investigated the value of E for dentine using cylindrical compression specimens obtained from human molars. The material was taken from freshly extracted teeth and was kept moist throughout preparation. Prior to testing the specimens were stored in water. From ten separate tests the average value of E was $1.67 \times 10^6$ p.s.i. Although the authors concluded that the variables such as tubule direction, loading rate and specimen length to diameter ratio affected the results, no single variable was isolated in the tests in order to determine its singular effect.

In 1958, Craig and Peyton (13) reported on an improved and slightly modified series of experiments using the same technique as described above. This time the effects of specimen length to diameter ratio, tubule orientation and rate of tissue loading were investigated. Although they did not state the specimen condition as being either wet or dry, their E value ranged from 1.84 x $10^6$ p.s.i. to 2.41 x $10^6$ p.s.i., a value slightly higher than that obtained from their previous study. They also concluded that tubule orientation and length to diameter ratios above 1:1, had no influence upon the modulus value. In further experiments where small dentine specimens were loaded very rapidly with large loads (in excess of 100 lbf) for long periods of time (greater than 20 minutes), a considerable amount of creep occurred. (In fact,their specimen response curves are identical to the characteristic linear viscoelastic material response curves discussed and illustrated in section 3.2.15). Craig and Peyton described this creep strain as being retarded elastic deformation.

Stanford et al in their 1958 paper (6), obtained the compressive Young's modulus of dentine for human wet cylindrical specimens. Their average value over several tests was 2.2 x $10^6$ p.s.i. The authors did not record the tubule orientation in the tissue specimens. However, in their later paper in 1960 (8), with their improved and modified technique, cognizance was taken of this and other influencing factors. From these studies they concluded that neither tooth type whether vital or pulpless, or tubule direction, affected the stiffness of the dentine. However, slightly smaller values of E were obtained for

root dentine than were obtained for coronal material. The values determined fell within the overall range.of $1.0 \times 10^6$ p.s.i. to $2.4 \times 10^6$ p.s.i.

Tyldesley in 1959 (5), was able to obtain specimen bars of sufficient size in dentine for his four point bending experiments. The average value of E determined was $1.79 \times 10^6$ p.s.i. Although Tyldesley was unable to investigate accurately the effect of tubule orientation, (his relatively large specimens contained tubules running in most directions), he did examine other important factors. He concluded that age, sex and tooth type had little effect on the value of E. A similar modulus value was obtained for sound dentine originating from otherwise carious teeth. Tyldesley is one of the few authors who investigated the effect of moisture content on the dentine properties. He found that dehydration measurably affected the results of his experiments. Consequently, he conducted his tests within five to ten minutes of the specimens being removed from their water storage bath.

In 1968 Haines (10) from his compression tests on whole teeth, obtained for dentine a Young's modulus of $1.6 \times 10^6$ p.s.i. and a Poisson's ratio of 0.014. However, like his work on enamel, very little explanation was given as to how these properties were determined or of the condition of the tissue when the measurements were taken.

Probably the most thorough and systematic study of the mechanical properties of human dentine was the work of Renson in 1970 (14). He measured both the Young's and the shear moduli. For the Young's modulus measurements he employed both compression and tension tests while for the rigidity modulus he used a simple torsion experiment. The average values determined for E were $1.74 \times 10^6$ p.s.i. in tension and $1.86 \times 10^6$ p.s.i. in compression. His average value for the shear modulus was $1.16 \times 10^6$ p.s.i. Renson concluded from his work that age, sex, tooth type and specimen location does not significantly affect the mechanical properties. He also concluded that dentine can be regarded as an isotropic material. Consequently, he calculated the Poisson's ratio for the tissue using the relationship which links it with E and G* From his table of results he calculates $\mu$ to be almost zero thereby agreeing with the result of Haines (10). However, there seems to be some error in his calculations at this point because using the values tabulated and the equation relating E, G and $\mu$ one obtains:-

$$G = \frac{E}{2(1 + \mu)}$$ (applicable for isotropic homogeneous materials only)

and $$\mu = \frac{E}{2G} - 1$$

$$= \frac{1.74 \times 10^6}{2 \times 1.16 \times 10^6} - 1$$

$$= 0.75 - 1$$

$$\therefore \mu = -0.25$$

* The subscripts for the elastic constants have been omitted as the dentine is assumed to be an isotropic material.

| Author and Reference | Type of Test | Property | Remarks and Observations |
|---|---|---|---|
| Peyton et. al. 1952(12) | Compression (no strain-rate given) | $E = 1{\cdot}67 \times 10^6$ p.s.i. | Average obtained from 10 tests. Authors concluded that E was affected by tubule orientation. |
| Craig and Peyton. 1958(13) | Compression (low strain-rate) | $E = 1{\cdot}84 \rightarrow 2{\cdot}41 \times 10^6$ p.s.i | Tubule orientation not significant. |
| | Compression (high strain-rate) | | High loads applied for times greater than 20 minutes produced VISCOELASTIC response. |
| Stanford et.al. 1958 (6) | Compression. | $E = 2{\cdot}2 \times 10^6$ p.s.i. | Tubule orientation not known. Average value obtained from many tests. |
| 1960 (8) | Compression | $E = 1{\cdot}0 \rightarrow 2{\cdot}4 \times 10^6$ p.s.i. | Tubule orientation not significant. |
| Tyldesley 1959(5). | 4 point bending test | $E = 1{\cdot}79 \times 10^6$ p.s.i. | Dehydration increases E value obtained for specimen. Random tubule distribution. |
| Haines 1968(10) | Compression | $E = 1{\cdot}6 \times 10^6$ p.s.i<br>$\mu = 0{\cdot}014$ | Whole tooth specimens. Specimen condition not given. |
| Renson 1970(14) | Tension | $E = 1{\cdot}74 \times 10^6$ p.s.i. | Concluded dentine is an isotropic material. Properties are the same in parts of tooth. |
| | Compression | $E = 1{\cdot}86 \times 10^6$ p.s.i. | |
| | Torsion | $G = 1{\cdot}16 \times 10^6$ p.s.i. | |
| | | $\mu \simeq 0$ | Calculated by Renson from E and G. However, error in calculations. |
| | | $\mu \simeq -0{\cdot}25$ | Correct calculation using $G = \frac{E}{2(1+\mu)}$ |

TABLE 3.2 Published mechanical properties of dentine.

a value which is distinctly different from zero*. However, as Renson himself states in his thesis, this is a very unsatisfactory way of obtaining $\mu$ because a very small experimental error in the measured values of E and G (say 3%), leads to a very large error in the calculated value for $\mu$ (approximately 25%).

### 3.4.3 The Cementum

No references can be found which deal with the mechanical properties of the cementum required in the stress analyses. The reason for this can probably be attributed to the fact that the tissue only appears in the form of a thin surface layer. Consequently, it is not available in a sufficient quantity to enable a normal experimental specimen to be obtained. Even the results of hardness measurements (determined using indentation techniques) are open to question, as this method is critically dependent upon the specimen thickness.

### 3.4.4 The Periodontal Membrane

A number of authors have investigated the rotation of the teeth within their sockets and the resulting stress distributions in the periodontal membrane. However, only one reference has been traced where actual experimental physical data of the periodontal membrane tissue have been measured. This single work dates back to 1935 when Dyment and Synge (15), measured the tensile

* Bearing in mind the sign convention for $\mu$ this result implies that in a tension test, the specimen of dentine would expand in the transverse direction.

| Author and Reference | Type of Test | Property | Remarks and Observations |
|---|---|---|---|
| Dyment and Synge. 1935(15) | Tension | E = 210·0 p.s.i. | Average value obtained from 4 wet strips of calf and lamb membrane material. Linear load versus extension curve obtained. However, creep occurred when load maintained for several minutes. |
| | | $\mu = 0.5$ | Membrane assumed to be incompressible. |
| | | G = 70·0 p.s.i. | Value calculated from $G = \frac{E}{2(1+\mu)}$ using E and $\mu$. Membrane assumed isotropic. |

TABLE 3.3 Published mechanical properties of periodontal membrane.

Young's modulus of four wet strips of membrane which had been taken from freshly killed calves and lambs. The authors assumed that the membrane was incompressible (implying that $\mu = 0.5$), homogeneous and isotropic. Hence, using the relationship

$$G = \frac{E}{2(1+\mu)}$$

they were able to calculate the shear modulus. Average values obtained from their experiments were E = 210 p.s.i. and G = 70 p.s.i. respectively. However, as Dyment and Synge point out, due to the obvious limitations of their tests, these values must be regarded as circumspect. Although a linear load versus extension response was obtained for all specimens, when the load was maintained for several minutes the tissue was observed to flow. This flow was also manifest when the samples were unloaded by the residual extensions which remained.

It must also be remembered that these experiments were conducted on specimens which were free, whereas, in the natural environment, the periodontal membrane is enclosed between the alveolar bone on one side and the tooth root on the other. The normal situation would therefore appear superficially to be less conducive to flow.

### 3.4.5 Bone

More mechanical properties and data have been published for bone in the last two decades than have probably been published for all the other tissues together. While numerous authors have conducted studies on cortical bone, few references have been

found where the mechanical properties of the cancellous tissue have been investigated. Because of the relatively large mass of bone which is available in the long bones,most workers have concentrated their efforts on tissue from this source and in particular on material obtained from the shaft of the femur. However, with the ever increasing concern, particularly in the United States of America, over head injuries resulting from automotive accidents, more and more attention is being paid to the study of the cranial tissue. (McElhaney (16) and Wood (17)).

### 3.4.5.1 Cortical Bone

Because the literature concerned with the mechanical properties of cortical bone is legion ,only a few pertinent references relevant to the present work will be discussed. For a more detailed and historical account of the quantification of the physical properties of cortical bone ,the reader is recommended the general review articles of Kraus (18), Welch (19) and Swanson (20). Sedlin's work (21), on the overall structural behaviour of bone is also worthy of detailed study.

Evans and Lebow in 1951 (4), conducted tensile tests on femoral cadaveric material. The specimens were cut such that their axes were parallel with the long axis of the femur and approximately parallel also with the fibre or osteon orientation. The authors tested samples taken from the four quadrants of each of the right and left hand bones and from the proximal, middle

and distal thirds. Where possible,adjacent specimens were treated in either one of two ways. While one was maintained in the wet condition prior to testing by storing the specimen in water, the other was oven dried. The results of Evans and Lebow show that the average value of the Young's modulus for the wet specimens is about 17% lower than it is for the corresponding dry tissue. Their average normal wet E value was approximately $2 \times 10^6$ p.s.i. The authors could find very little regional differences in the E values from the same bone and concluded also that increasing patient age had very little, if any, modifying effect.

In 1952 Dempster and Liddicoat (22), proposed cortical bone to be a non-isotropic material. Although they used macerated museum material in their tests,they re-wetted some samples by soaking them overnight in water. The authors conducted both tensile and compressive tests on longitudinal or parallel-grain orientated specimens and found that the modulus for compression was on average slightly higher than that obtained in tension. The average E values recorded for the re-wetted tissue were $2.06 \times 10^6$ p.s.i. in compression and $1.73 \times 10^6$ p.s.i. in tension. Dempster and Liddicoat agreed with Evans and Lebow's findings in that dry specimens gave higher modulus values than did the wet material.

For their second series of experiments, to compare the elastic modulus for different grain orientations, the authors had to rely solely on compression tests on small cube shaped specimens. This was because of the limited thickness of the

femoral cortex in the radial direction. From their results Dempster and Liddicoat concluded that for wet cortical tissue the elastic modulus was the same in directions radial and tangential to the bone grain. Its numerical value was approximately half that of the E value recorded for the longitudinal grain direction. Although the authors believed that the actual numerical results of these three orthogonal E values were modified by end effects, (caused by the small specimen length to cross-section ratio), they proposed that the respective ratios were valid as the end effects were the same for all three tests. Thus,

$$E_{\text{(longitudinal to bone grain)}} = 2 \times E_{\text{(tangential to bone grain)}} = 2 \times E_{\text{(radial to bone grain)}}$$

Bonfield and Li determined some mechanical properties for cortical tissue obtained from bovine femora and tibia. All specimens were kept refrigerated in between preparation and testing. In their first paper in 1966 (23), the authors conducted tensile tests on specimens whose axes coincided with that of the axis of the long bone. Thus, assuming that the grain orientation was parallel to the long bone axis, the average Young's modulus value of $3.8 \times 10^6$ p.s.i., obtained at a strain rate of 0.00033 per second, shows that the bovine bone, with all other conditions being equal, is approximately twice as stiff as its human counterpart. In their later paper in 1967 (24), the same authors employed a torsion test procedure to filament type specimens. Because of the small size of the specimens involved, Bonfield and Li were able to conduct tests both with

and against the bone grain. Hence, by measuring the torque applied and the resulting specimen rotation, they calculated, using simple torsion theory, the tissue's shear moduli. The average values they obtained were:-

G (parallel grain specimens) = $0.85 \times 10^6$ p.s.i.

G (transverse grain specimens) = $1.9 \times 10^6$ p.s.i.

However, because the simple torsion theory adopted is based upon the assumption that the structure of the material is symmetrical with the specimen axis about which the torque is applied, the value of G determined for the transverse grain orientated case is not strictly the transverse shear modulus. Obviously, from FIG. 3.8 it can be seen that the grain direction differs from the top or bottom of the specimen to that of its sides. However, Bonfield and Li's data and results will be used in chapter 6 to determine theoretically, using the finite element method, the transverse shear modulus of the bovine tissue.

Wood in 1971 (17), determined the Young's modulus for human compact cranial bone in tension. He investigated the properties of the outer and inner cortical tables in directions tangential to the skull surface for different strain rates. Although he found, like other authors, that E was dependent upon the strain rate, he could find no significant differences due to the orientation of the specimens. Wood's average E value for both the inner and outer layers was $1.7 \times 10^6$ p.s.i. at

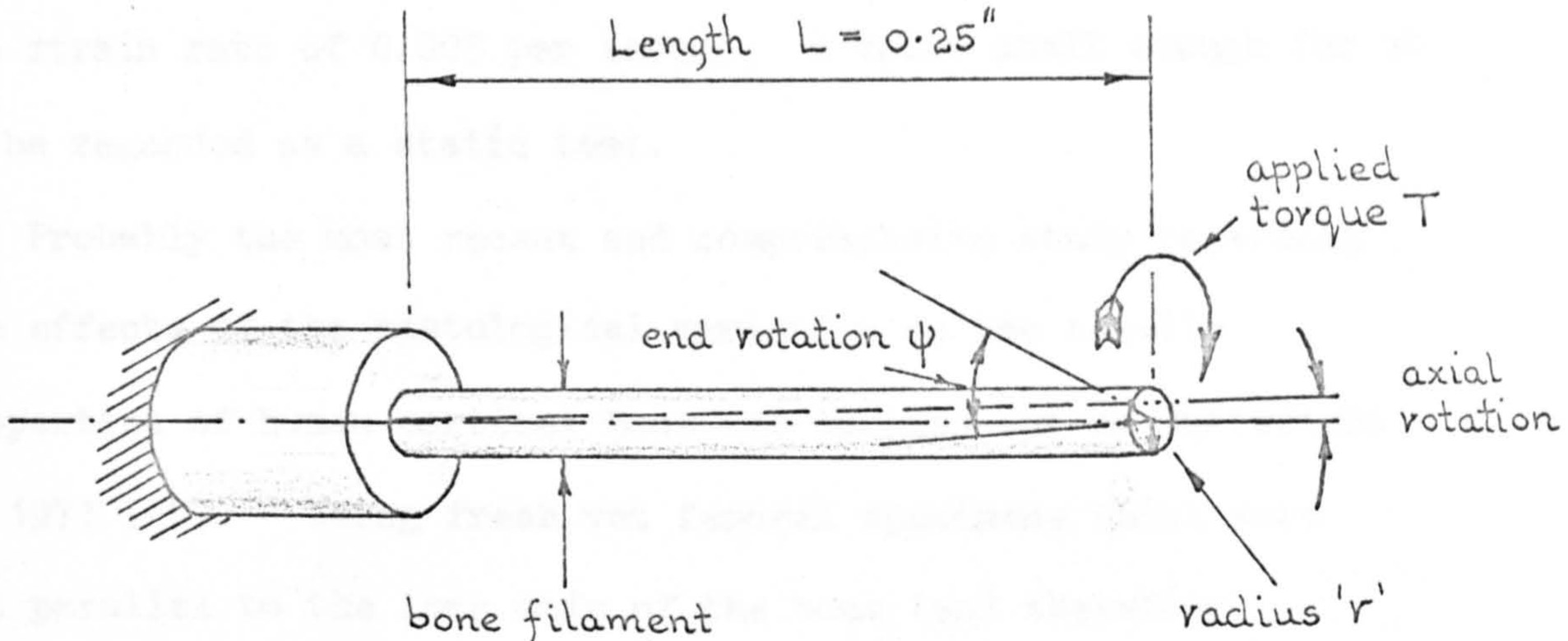


Governing Equation $\frac{T}{J} = \frac{G\Psi}{L} = \frac{q}{r}$

where G = shear modulus of elasticity

J = polar moment of area $\left(\frac{\pi d^4}{64}\right)$

q shear stress at radius r

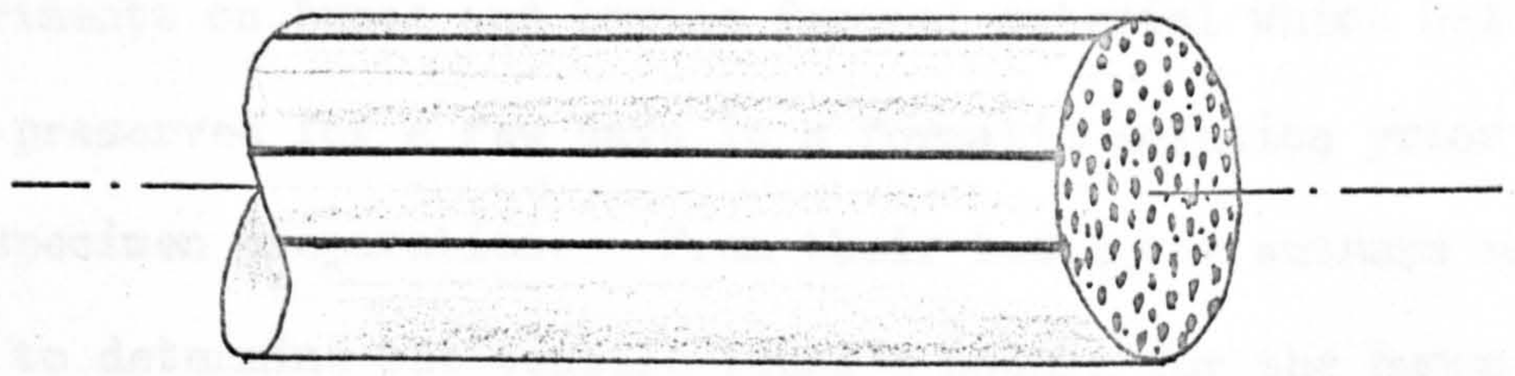

Bone grain parallel to specimen axis

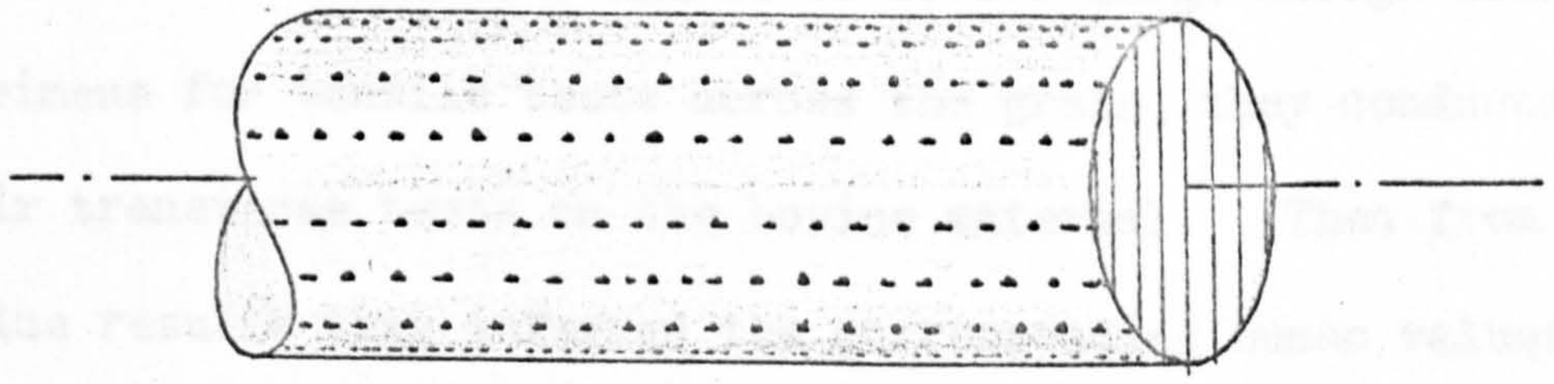

Bone grain transverse to specimen axis.

FIG. 3.8 Experimental method and details used by Bonfield and Li (24).

the strain rate of 0.005 per second; a value small enough for it to be regarded as a static test.

Probably the most recent and comprehensive study regarding the effects of the histological variation on the tensile properties of human cortical bone was carried out by Cartwright in 1971 (25). Using fresh wet femoral specimens which were cut parallel to the long axis of the bone (and therefore approximately parallel to the bone grain), Cartwright determined the Young's modulus at a strain rate of 0.0001 per minute. This rate is again well within that approximating to a static test. His average value however, of $1.17 \times 10^6$ p.s.i., is considerably lower than other published results for the tensile modulus.

McLeish and Habboobi in 1971 (3), carried out some tensile experiments on human and bovine femoral material which had been preserved for a few days in a formalin solution prior to the specimen preparation. From their tests,the authors were able to determine the tensile Young's moduli for the human tissue both with and across the grain, and also the two Poisson's ratios associated with these two directions, see FIG. 3.9. Because the authors were unable to obtain large enough human specimens for tensile tests across the grain, they conducted their transverse tests on the bovine material. Then from these bovine results they inferred the corresponding human values by assuming that the ratios of the moduli and the Poisson's ratios were the same for both species. All their tests were carried out at a crosshead velocity of 0.02 inches per second.

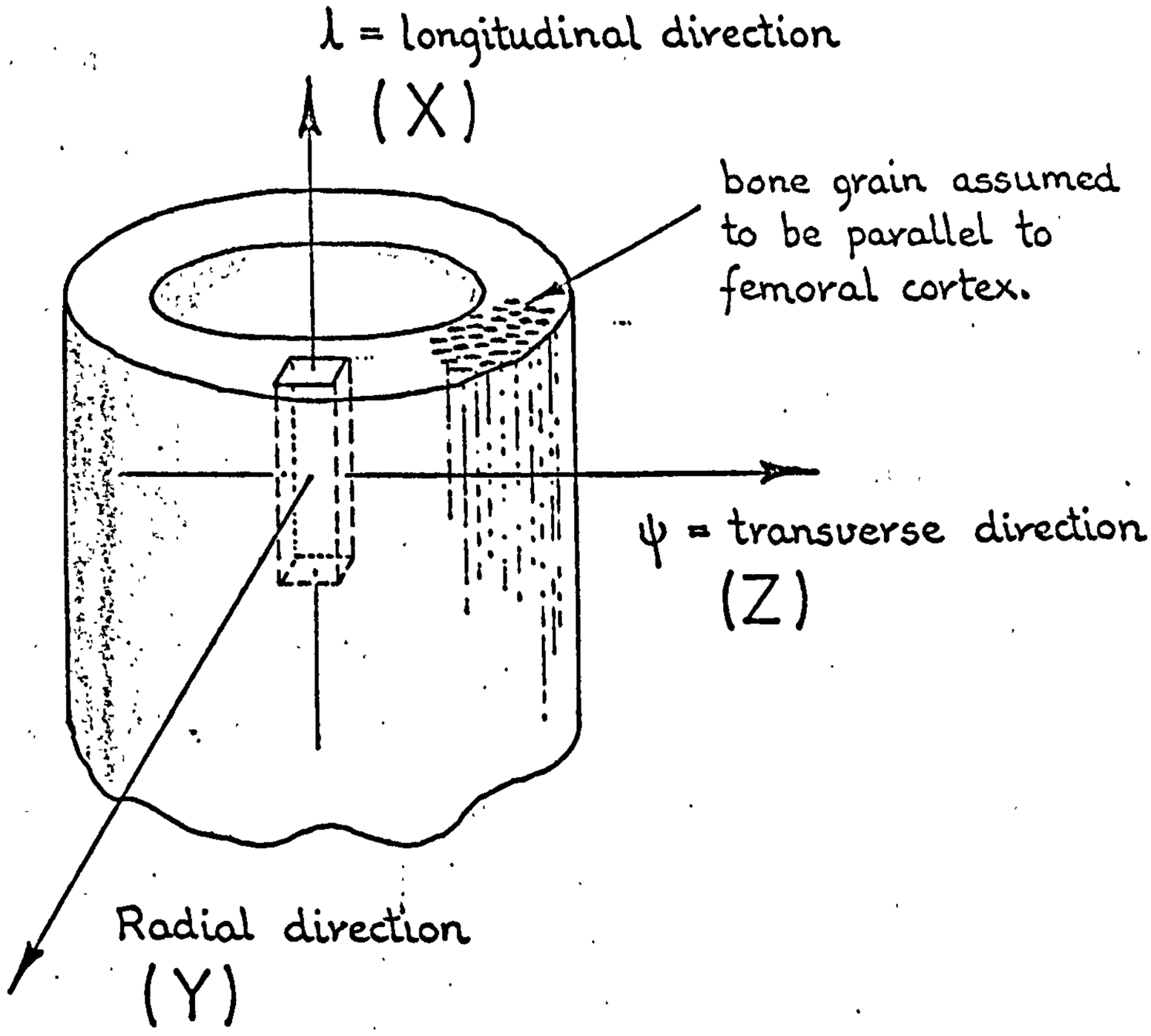


$E_\lambda$ = Young's modulus in the longitudinal direction.

$E_\psi$ = Young's modulus in the transverse direction.

$\mu_\lambda$ = Poisson's ratio – ratio of tangential to longitudinal strains for loading in the longitudinal direction.

i.e. $$\mu_\lambda = \frac{\epsilon_\psi \text{ (passive)}}{\epsilon_\lambda \text{ (active)}}$$

Thus $$\epsilon_\psi \text{(passive)} = \mu_\lambda \epsilon_\lambda \text{(active)}$$
$$= \mu_\lambda \frac{\sigma_\lambda}{E_\lambda}$$

N.B. $\mu_\lambda \equiv \mu_{xy} \equiv \mu_{xz}$ for authors notation.

$\mu_\psi$ = Poisson's ratio – ratio of longitudinal to tangential strains for loading in the tangential direction.

N.B. $\mu_\psi \equiv \mu_{zx} \equiv \mu_{yx}$ for authors notation.

FIG. 3.9 Illustrating the notation employed by McLeish and Habboobi (3).

Average results for human bone, which were obtained by direct measurement were :-

$$E_1 = 2.22 \times 10^6 \text{ p.s.i.}$$

and $$\mu_1 = 0.29$$

The average values obtained directly for the bovine tissue were:-

$$E_1 = 4.05 \times 10^6 \text{ p.s.i.}$$

$$E_\phi = 2.09 \times 10^6 \text{ p.s.i.}$$

$$\mu_1 = 0.25$$

and $$\mu\phi = 0.18$$

Hence,by assuming that

$$\left.\frac{E_1}{E\phi}\right|_{\text{bovine}} \equiv \left.\frac{E_1}{E\phi}\right|_{\text{human}}$$

McLeish and Habboobi calculated the value of $E\phi$ for human bone. This simple sum yields the result of:-

$$E\,\phi = 1.11 \times 10^6 \text{ p.s.i.}$$

Similarly, if

$$\left.\frac{\mu 1}{\mu\phi}\right|_{\text{bovine}} \equiv \left.\frac{\mu 1}{\mu\phi}\right|_{\text{human}}$$

then a value of $\mu\phi$ for the human tissue of 0.21 can be determined.

### 3.4.5.2 Cancellous Bone

As previously mentioned, published work on the physical properties of cancellous bone is very sparse. In fact,only two references have been obtained which deal with this tissue.

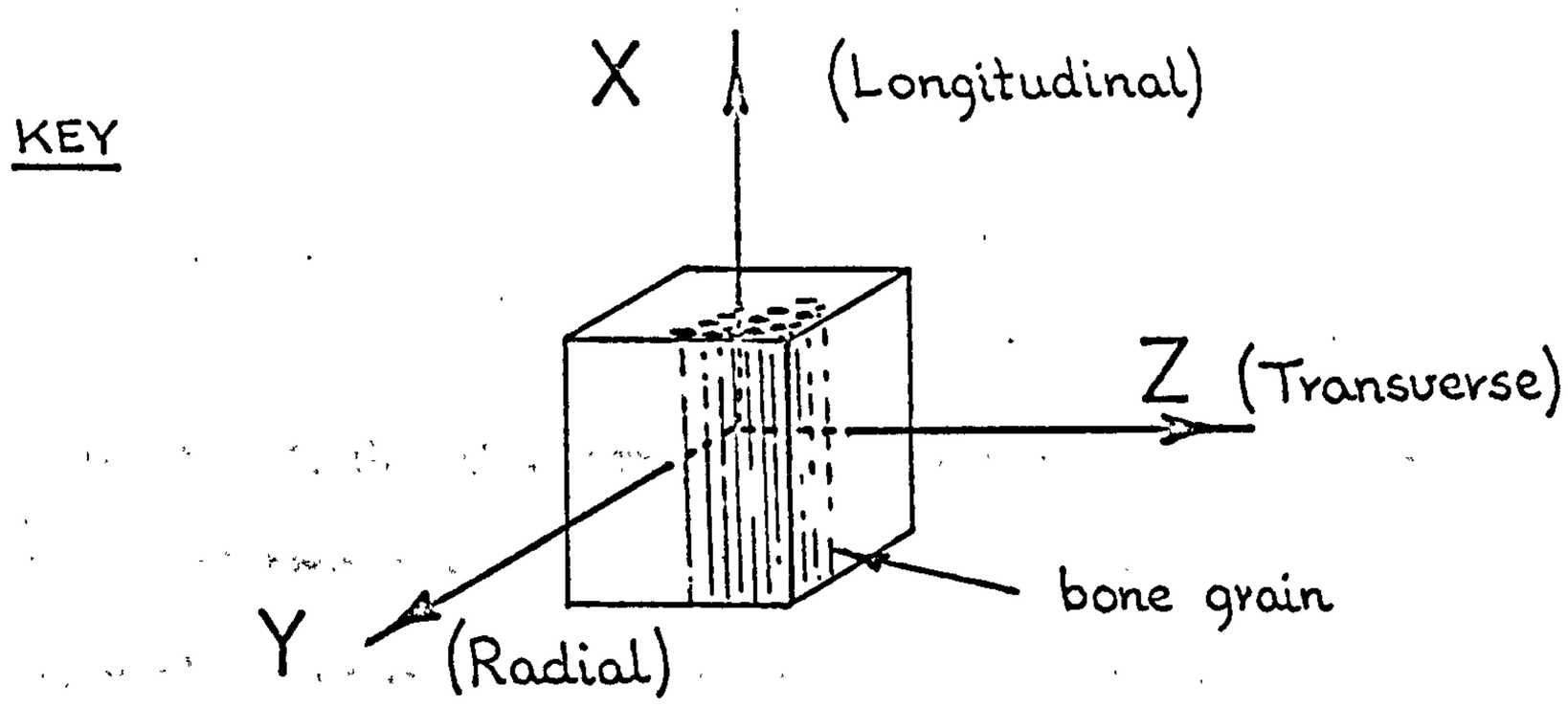


| Author and Reference | Type of Test | Property | Remarks and Observations |
|---|---|---|---|
| Evans and Lebow. 1951 (4). | Tension | $E_x = 2{\cdot}0 \times 10^6$ p.s.i | Re-wetted cadaveric femoral material. Ex for oven-dried tissue 17% greater than for the wet tissue. |
| Dempster and Liddicoat 1952 (22) | Compression | $E_x = 2{\cdot}06 \times 10^6$ p.s.i | Re-wetted macerated museum material. Authors concluded cortical bone to be anisotropic |
| | Tension | $E_x = 1{\cdot}73 \times 10^6$ p.s.i | |
| | Compression | $E_y = E_z$<br>$E_x = 2E_y$ | Bone in 'wet' condition. |
| Bonfield and Li 1966 (23) 1967 (24) | Tension | $E_x = 3{\cdot}8 \times 10^6$ p.s.i | Bovine tissue |
| | Torsion (see FIG. 3.8) | $G = 0{\cdot}85 \times 10^6$ p.s.i | Bone grain parallel with axis of torsion specimen. |
| | | $G = 1{\cdot}9 \times 10^6$ p.s.i | Bone grain transverse with axis of torsion specimen. |
| Wood 1971 (17) | Tension. (strain-rate 0·005 per sec.) | $E = 1{\cdot}7 \times 10^6$ p.s.i | Human compact cranial bone. E dependent upon strain-rate. No grain orientation given |
| Cartwright 1971 (25) | Tension (strain-rate 0·001 per min.) | $E_x = 1{\cdot}17 \times 10^6$ p.s.i. | Fresh wet human femoral tissue. |
| McLeish and Habboobi. 1971 (3) | Tension (cross-head velocity 0·02 ins/sec) | $E_x = 2{\cdot}22 \times 10^6$ p.s.i | Human femoral material stored prior to testing in formalin solution. |
| | | $\mu_{xz} = 0{\cdot}29$<br>$(\mu_{xz} = \mu_{xy})$* | |
| | | $E_x = 4{\cdot}05 \times 10^6$ p.s.i. | Bovine tissue.<br>*N.B. $\mu_{xz} = \mu_{xy}$ and $\mu_{zx} = \mu_{yx}$ for material isotropic in ZY plane. |
| | | $E_z = 2{\cdot}09 \times 10^6$ p.s.i. | |
| | | $\mu_{xz} = 0{\cdot}25$ * | |
| | | $\mu_{zx} = 0{\cdot}18$ * | |

TABLE 3.4 Published mechanical properties of cortical bone.

Although the trabeculae comprising the cancellous tissue are constructed from the same material as the cortical bone, because the trabeculae form a network type structure, the macroscopic mechanical properties of the spongy bone are vastly different from the macroscopic properties of the compact tissue. Obviously, the properties are dependent upon the size, number and configuration of the trabeculae making up the cancellous bone. Consequently, as the trabeculae are believed to be influenced by the force system imposed on the tissue, the properties will vary not only from bone to bone but also from point to point within the same bone. However, as the following results will show, the stiffness of the cancellous bone is generally an order of magnitude below that of the cortical tissue.

Yokoo in 1952 (26), measured the compressive modulus of elasticity of wet human cancellous bone taken from the lumbar vertebrae. He found that the modulus depended upon the age of the person, the value being much higher for the younger individual. The author recorded an average value for E of 12800 p.s.i. for the 40 to 49 year age group.

McElhaney et al in 1970 (16), in their paper dealing with the mechanical properties of the cranial tissues, measured the compressive modulus of a complete section or plug of the parietal bone. The plug consisted of a sandwich formed by the outer and inner cortical tables and the core of spongy bone filling (diploe), see FIG 3.10. Although the specimens consisted of both cortical and cancellous tissue, because the former is an order of magnitude stiffer than the latter, the modulus obtained

| Author and Reference | Type of Test | Property | Remarks and Observations |
|---|---|---|---|
| Yokoo 1952 (26). | Compression | E = 12 800 p.s.i. | Specimens taken from lumbar vertebrae of 40 - 49 year old people. 'Wet' material. |
| McElhaney et. al. 1970 (16) | Compression (cross-head velocity 0·01 ins/min) | E = 0·57 → 3·99 $\times 10^5$ p.s.i. | 'Wet' plug of cranial tissue consisting of outer and inner layers of cortical tissue and a core of spongy bone See FIG. 3.10. |

TABLE 3.5 Published mechanical properties of cancellous bone.

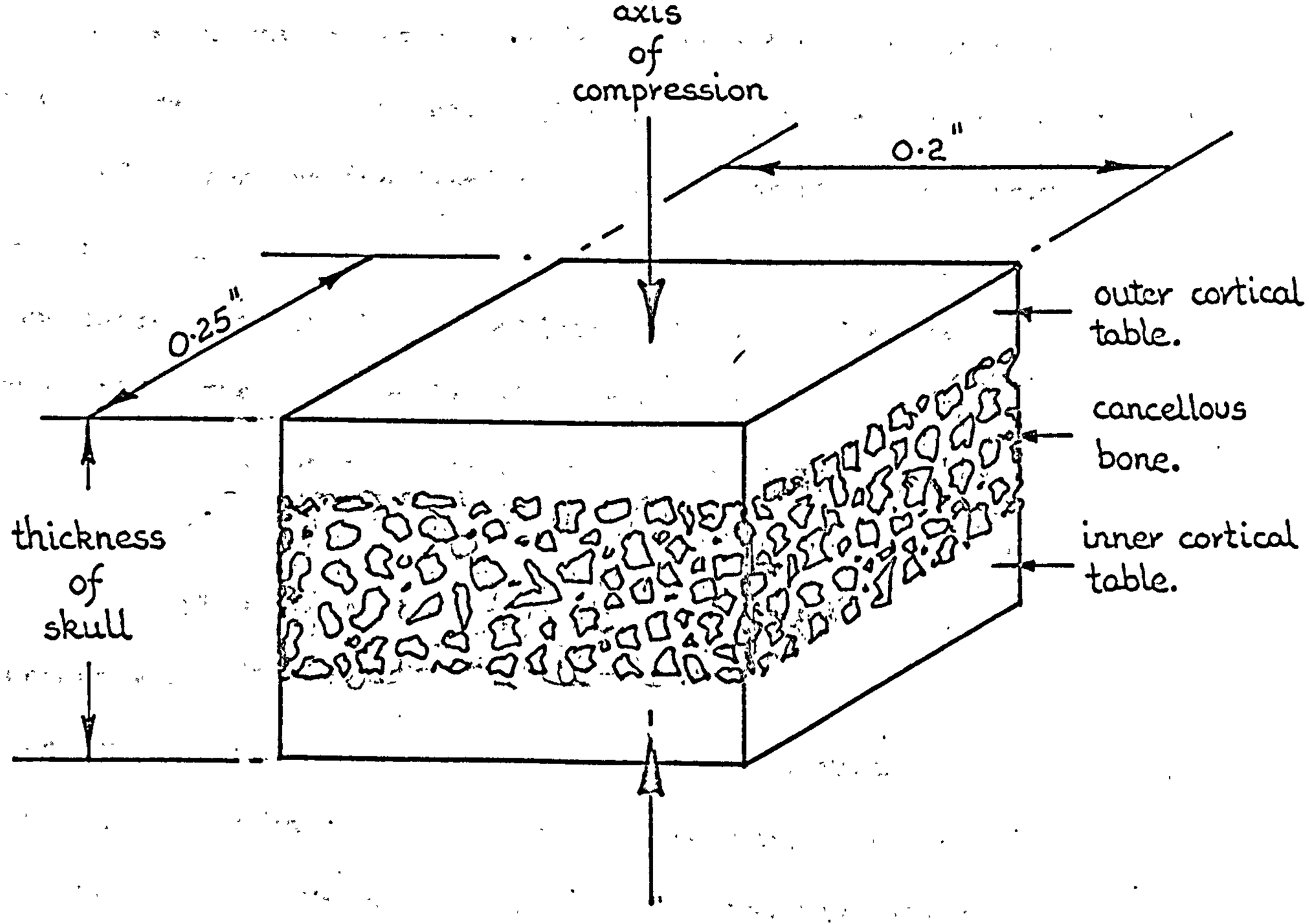


FIG 3.10 Cranial specimens used by McElhaney (16) to determine the compressive Young's modulus of cancellous bone.

from the compressive test would be primarily that of the spongy bone. The authors kept their specimen material in a moist condition throughout preparation, and applied the load at a constant velocity of 0.01 inches per minute. Again, these authors found that the modulus depended upon the arrangement and configuration of the trabeculae in the diploe. Consequently, their E values varied considerably from specimen to specimen but fell within the general range of $0.57 \times 10^5$ to $3.99 \times 10^5$ p.s.i.

### 3.4.6 The Physical Properties of the Dental Materials Required in the Structural Analyses

The dental materials are generally considered to comprise those materials which are employed in the mechanical procedures included in restorative dentistry, such as prosthetics, crown and bridge and operative dentistry. Because of the obvious importance of materials in dentistry, the science of dental materials forms an essential element of the training programme of all dental schools. Consequently, this has stimulated research and so the behaviour and the physical properties of the common dental materials have been widely investigated and documented. (In fact, standards and specifications have been formulated by which the value of any particular dental material can be gauged). Therefore, the properties required in this project have been taken directly from the work of Skinner and Phillips (1).

| Material | Type of Test | Property | Remarks and Observations |
|---|---|---|---|
| Amalgam | Compression | $E = 2{\cdot}0 \times 10^{6}$ p.s.i. | Properties dependent upon composition, preparation and operative technique. Isotropic. |
| | | $\alpha = 25{\cdot}0 \times 10^{-6}/°C$ (coefficient of linear thermal expansion) | For normal oral temperature range. |
| Zinc Phosphate Cement. | Compression | $E = 1{\cdot}3 \times 10^{6}$ p.s.i | Isotropic |
| Dental Gold | Compression | $E = 11{\cdot}3 \times 10^{6}$ p.s.i | Isotropic |

TABLE 3.6 Published physical properties of some dental materials.
Skinner and Phillips (1)

## 3.5 DISCUSSION AND DATA ANALYSIS

From an analysis of the tissue and material data presented, average or general overall physical properties are proposed which will be used in the subsequent structural analyses.

### 3.5.1 Enamel

It can be concluded from the data presented in Table 3.1 and from the histology of the enamel that it is approximately an orthotropic material. It is much stiffer in the direction parallel to the prisms than it is against them. The ratio of the stiffness is indicated by Stanford *et al* (8) to be about 3:1. However, there is a considerable scatter in the results given for the Young's modulus values obtained in the direction of the prisms which cannot easily be explained. It therefore seems reasonable to select an average value from those tabulated. Consequently, an E of $10.2 \times 10^6$ p.s.i. (which makes enamel exactly six times stiffer than the dentine), seems a very reasonable value to assume. However, it is apparent from the table that enamel does not appear to be a homogeneous material, being more flexible on the crown sides than it is in the cusp areas. It may therefore be more reasonable to take a lower E value of $6.8 \times 10^6$ p.s.i. (a value four times stiffer than dentine), for analyses where the stress distribution in the enamel is not critical.

### 3.5.2. Dentine

The data presented for the dentine in Table 3.2, shows a remarkable degree of consistency. Most authors agree that the tissue is isotropic and that it possesses a linear elastic response over the normally expected load range. As Renson (14) showed the mechanical response to be similar in both tension and compression, an average value for the Young's modulus of $1.7 \times 10^6$ p.s.i. can be assumed. However, if Renson's value for the shear modulus is employed it results in a negative value being obtained for the Poisson's ratio. This result implies that when a tensile specimen of dentine is stretched, it does not contract in the transverse direction but instead expands. Although this is possible physically, it is none-the-less somewhat unusual. If the Poisson's ratio of 0.3 is used (a value common for many materials), it would suggest an error of approximately 50% in Renson's G (or E) value. However, due to the bulk of evidence supporting the value for the Young's modulus, it seems reasonable to accept the E and to examine the effects of the variation of $\mu$ and G. (In fact, in 2-D finite element analyses, the value of Poisson's ratio does not significantly affect the resulting stress distribution patterns.)

### 3.5.3 Cementum

Because of the cementum's minimal existence on the tooth roots and of the lack of properties available, it seems logical to amalgamate this tissue with the dentine. Consideration of the physical likeness of the two tissues suggests that the effect of this simplification should not be too severe.

### 3.5.4 Periodontal Membrane

The mechanical properties presented for the periodontal membrane in Table 3.3 were obtained from experiments so far removed from the natural human environment that no serious analysis can be based upon them. The only significant contribution of the data is that it gives an idea of the expected overall magnitude of the stiffness of the membrane tissue. It is apparent that it is very flexible and could possibly exhibit a considerable flow characteristic. Considering the membrane's fibrous structure it is highly probable that the tissue is also non-isotropic. However, this and other effects relating to the properties of the periodontal membrane will be the subject of an analytical study in Chapter 6.

### 3.5.5 Cortical Bone

Consideration of table 3.4 and the histology of cortical bone clearly suggests that this tissue is approximately an orthotropic material. The major stiffness axis being parallel to the osteon or bone 'grain' direction. However, in the other two orthogonal directions the stiffness appears to be the same. This implies that cortical bone is isotropic in the plane perpendicular to the bone grain. The stiffness in this plane has been found to be approximately half of the stiffness of the bone in the grain direction. Therefore assuming the cortical bone of the alveolar process to be similar to that of the femoral and cranial bones, then the values of the Young's moduli can be taken as:-

E (in direction of bone grain) = $2.0 \times 10^6$ p.s.i.

E (in transverse and radial directions orthogonal to bone grain) = $1.0 \times 10^6$ p.s.i.

Assuming that the stiffness of bovine material is exactly twice that of the human tissue, then using Bonfield and Li's (24) data for the shear modulus for bovine bone, a value of $G = 0.4275 \times 10^6$ p.s.i. for human bone in the longitudinal-transverse (or radial) plane can be determined. The values for the shear moduli in the other two planes cannot be used directly. However, these will be evaluated in Chapter 6. The corresponding Poisson's ratio values given by McLeish and Habboobi (3) similarly cannot be used as given because, as will be shown in Chapter 6, they violate the Maxwell-Betti reciprocal relationships.

### 3.5.6 Cancellous Bone

As the number, size and arrangement of the trabeculae comprising the cancellous bone depends upon the stress environment, no specific or general mechanical properties can be ascribed to this tissue. The data given in Table 3.5 illustrates the wide variations in the macroscopic samples of the tissue examined. However, it is evident, (or at least from the two cases given), that the stiffness of the tissue is generally of an order of magnitude lower than that for cortical bone. Therefore, structurally it should be less significant. Consequently, it seems appropriate to allot a stiffness value of $E = 2 \times 10^5$ p.s.i. and to assume that the tissue behaves isotropically. Hence,

by assuming a value for the Poisson's ratio (say $\mu = 0.3$),

G can be calculated using the formula:

$$G = \frac{E}{2(1+\mu)}$$

### 3.5.7 Dental Materials

The only mechanical property given for the dental materials required for the stress analyses are the compressive Young's moduli. However, it is reasonable to assume that these are basically isotropic materials and that their Poisson's ratios are approximately the same as for the common metals, i.e. $\mu = 0.3$. Thus employing the formula

$$G = \frac{E}{2(1+\mu)}$$

the shear modulus of each of the dental materials can be determined.

| Tissue/ Material. | Characteristic Behaviour | Isotropic or Anisotropic | Property | Remarks |
|---|---|---|---|---|
| Enamel | Linear Elastic | Assume Orthotropic | $E = 10{\cdot}2 \times 10^6$ p.s.i | In direction of enamel prisms. |
| | | | $E = 3{\cdot}4 \times 10^6$ p.s.i | Perpendicular to direction of enamel prisms |
| | | Isotropic | $E = 6{\cdot}8 \times 10^6$ p.s.i | Simple material model used for economic reasons in analyses where enamel behaviour is not critical. |
| Dentine | Linear Elastic | Isotropic | $E = 1{\cdot}7 \times 10^6$ p.s.i | |
| | | | $\mu = -0{\cdot}25 \rightarrow 0{\cdot}3$ | $\mu$ determined using E and G |
| | | | $G = 1{\cdot}16 \rightarrow 0{\cdot}654 \times 10^6$ p.s.i | |
| Periodontal Membrane | ? | ? | $E = 210{\cdot}0$ p.s.i.<br>$\mu = 0{\cdot}5$<br>$G = 70{\cdot}0$ p.s.i. | Values obtained assuming membrane to be isotropic and incompressible. Investigate mechanical properties in Chapter Six. |
| Cortical Bone | Linear Elastic | Orthotropic | $E = 2{\cdot}0 \times 10^6$ p.s.i | In direction of bone grain |
| | | | $E = 1{\cdot}0 \times 10^6$ p.s.i | Perpendicular to direction of bone grain |
| | | | $G = 0{\cdot}4275 \times 10^6$ p.s.i | In planes parallel to bone grain direction, see Table 3.4 and Fig 3.8 Investigate mechanical properties in Chapter Six. |
| Cancellous Bone | Linear Elastic | Assume Isotropic (considered macroscopically) | $E \simeq 2{\cdot}0 \times 10^5$ p.s.i | E dependent upon trabecula size shape and configuration. Generally very much less stiff than cortical tissue when considered macroscopically. |
| Amalgam | Linear Elastic | Isotropic | $E = 2{\cdot}0 \times 10^6$ p.s.i<br>$\mu = 0{\cdot}3$<br>$G = 0{\cdot}77 \times 10^6$ p.s.i | Value assumed for $\mu$ and G determined using $G = \frac{E}{2(1+\mu)}$<br>$(\alpha = 25 \times 10^{-6}/°C)$ |
| Zinc Phosphate Cement | Linear Elastic | Isotropic | $E = 1{\cdot}3 \times 10^6$ p.s.i.<br>$\mu = 0{\cdot}3$<br>$G = 0{\cdot}5 \times 10^6$ p.s.i | Value assumed for $\mu$ and G determined using $G = \frac{E}{2(1+\mu)}$ |
| Dental Gold | Linear Elastic | Isotropic | $E = 11{\cdot}3 \times 10^6$ p.s.i<br>$\mu = 0{\cdot}3$<br>$G = 4{\cdot}34 \times 10^6$ p.s.i | Value assumed for $\mu$ and G determined using $G = \frac{E}{2(1+\mu)}$ |

TABLE 3.7 Some tissue and material mechanical properties used in the structural analyses.

# CHAPTER FOUR

# MASTICATORY AND ABNORMAL LOADING OF DENTAL STRUCTURES

# 4. MASTICATORY AND ABNORMAL LOADING OF DENTAL STRUCTURES

## 4.1 INTRODUCTION

The chief physical role of dental structures is to apply forces or loads to the food which enters the oral cavity. The human occlusion is characterised by the omnivorous type of mastication which combines both the shearing and milling actions of the teeth. While the shearing action is achieved by the relative movement of the cusps and marginal ridges, the milling of the food is accomplished by the cusps as they approach their positions in their respective fossae.

The forces required to bring about the communition of food are generated by the masticatory muscles and are transmitted through the dental structures of the jaws to the food. Therefore, every time the jaws close and the teeth make contact with either food or each other, the dental structures are deformed. Consequently, as pointed out in the previous chapter, stresses are induced in the tissues and restorative materials. Since nature responds to function or loading (within physiological limits), by increased circulation and tissue vitality, mechanical stress is a prerequisite for dental health. However, the introduction of restorative materials and prostheses in place of the natural dental structures can produce abnormal loading conditions on the remaining tissues which can subsequently lead to their necrosis and destruction.

In this chapter, the type and forms of loading to which the dental structures are generally subjected, are discussed. These range from the normal masticatory loads or forces imposed on the natural structures and tissues, to the abnormal loads due to restorative procedures and the introduction of restorative materials and prostheses.

## 4.2 NORMAL MASTICATORY FORCES

It is pertinent at this juncture to distinguish between static and dynamic forces. Static loads or forces are forces which are applied under conditions of static equilibrium. In other words, the whole structure is at rest and the stresses and strains are constant. Although during the application of a load to a material or structure the force varies from zero up to its final magnitude, if the force is applied sufficiently slowly it is possible that the deformation (and induced stresses), will not exceed the values obtained when the full force is achieved and the state of static equilibrium attained. Dynamic loads on the other hand are loads which generally vary with time. Consequently, the kinetic energy associated with the impacting bodies is either transferred and/or converted and stress waves or transients are set up. Crudely speaking, a dynamic or impact load would induce higher instantaneous stresses in the structure than would a static load of the same magnitude.

Although masticatory forces are mostly dynamic in character, the work reported in this thesis relating to this type of loading, considers them to be static or quasi-static in nature. However, this seemingly unnatural approach can be justified because the work is primarily concerned with general patterns and trends in the stress and deformation behaviour of the dental structures and not with absolute numerical values.

The teeth are the immediate agents through which the work of mastication is achieved. The reaction of the teeth to the forces of mastication is determined both by the magnitude of the forces exerted and by the nature of the surfaces in contact. For example, if the incisal surfaces were flat and were at right angles to both the long axes of the teeth and the direction of the forces applied, then the tooth reactions would also be in the direction of their long axes. However, the opposing surfaces of the teeth are curved convexly and their long axes are not parallel to one another. Consequently, during mastication both axial and lateral force components are imposed, FIG 4.1. Friction between tooth and tooth or between tooth and food will also affect the inclination of the reactionary forces. However, the significance of friction is unknown as it is difficult to determine the lubricating properties of the saliva and the food.

Although the maximum total force that can be generated by the normal musclature has been estimated to be in the region of three hundred pounds, the range of static loads obtainable on any one tooth under conscious muscular effort

has been reported to lie between twenty and two hundred pounds. Table 4.1 gives some typical values which have been averaged from various literature sources. The wide variations which exist in the published results can be attributed not only to the differences in the structure and function of the individuals examined but also to the different measurement techniques employed. While some instruments measured the axial components of the whole tooth loads, others recorded the whole tooth loads in the direction normal to the occlusal plane. However, during the mastication of the normal diet the maximum amplitude of the bite forces on any one tooth has been found to rarely exceed twenty five pounds and generally falls within the range of one and ten pounds, Howell & Brudevold (27) and Yurkstas & Curby (28). The results of these workers were obtained from transducers which were incorporated in either artificial or restored natural teeth. Consequently, the values recorded are approximately the whole tooth masticatory axial forces.

## 4.3 ABNORMAL MASTICATORY FORCES

The normal dental structures maintain their state of health and equilibrium only so long as they remain in a condition of dynamic balance. The presence of all of the natural teeth, or their properly constructed substitutes with their occlusal surfaces correctly interrelated, is one of the prime factors which helps to maintain this balance. Consequently, as soon as the condition of balance is broken or disturbed, the function and health of the dental structures are impaired. One of the major causes of structural imbalance is the introduction

| MALE | | | | | | | | | | | | | | | |
|---|---|---|---|---|---|---|---|---|---|---|---|---|---|---|---|
| 8 | 7 | 6 | 5 | 4 | 3 | 2 | 1 | 1 | 2 | 3 | 4 | 5 | 6 | 7 | 8 |
| MAXILLARY | | | | | | | | | | | | | | | |
| 38 | 107 | 114 | 71 | 66 | 51 | 37 | 40 | 39 | 33 | 51 | 66 | 74 | 108 | 114 | 59 |
| MANDIBULAR | | | | | | | | | | | | | | | |
| 112 | 76 | 83 | 61 | 71 | 56 | 48 | — | 40 | 52 | 59 | 72 | 63 | 67 | 71 | 64 |

| FEMALE | | | | | | | | | | | | | | | |
|---|---|---|---|---|---|---|---|---|---|---|---|---|---|---|---|
| 8 | 7 | 6 | 5 | 4 | 3 | 2 | 1 | 1 | 2 | 3 | 4 | 5 | 6 | 7 | 8 |
| MAXILLARY | | | | | | | | | | | | | | | |
| — | 80 | 90 | 54 | 60 | 88 | 37 | 40 | 37 | 28 | 50 | 45 | 53 | 58 | 63 | 55 |
| MANDIBULAR | | | | | | | | | | | | | | | |
| 51 | 54 | 59 | 51 | 53 | 26 | 34 | 30 | 38 | 85 | 32 | 52 | 54 | 53 | 53 | 44 |

TABLE 4.1 Maximum bite forces in pounds on individual teeth. The values given above are the averages obtained from several data sources.

into the oral cavity of restorations and prostheses. If not properly designed and constructed,these can create abnormal loading conditions on the dental structures simply from the normal function of mastication. Hence, adverse stresses are thereby imposed on the supporting tissues which can result in their breakdown and eventual destruction.

### 4.3.1 Differences in the Mechanical Properties of the Restorative and Natural Materials

As mentioned in an earlier chapter, differences between the mechanical properties of the restorative materials and those of the natural or biological materials which they are replacing, can greatly affect <u>per se</u> the stress distributions occurring in the surrounding dental tissues. These abnormal stress distributions can subsequently lead to tissue irritation and necrosis. A particular example of this condition is discussed in sub-section 4.3.5

### 4.3.2 Occlusal Surface Restorative Design

The design and construction of the occlusal surface of a restoration will obviously affect the tooth's reaction to normal masticatory function. While the restoration height, for example a high or low spot, will result in an occlusal imbalance, the inclination of the cusp or contact surfaces will affect the magnitude of the lateral force component. Normally, the lateral or transverse force components on the

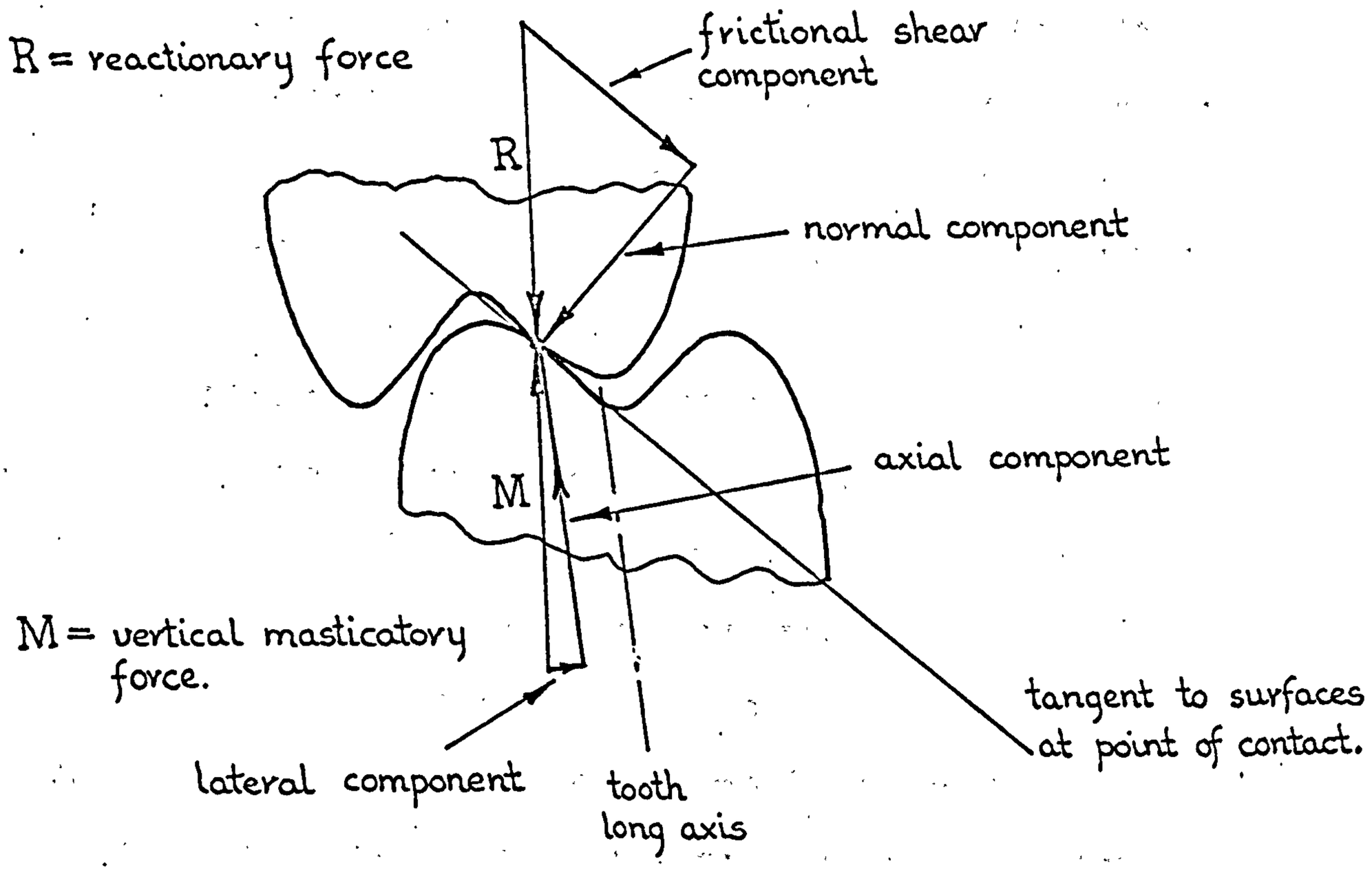


FIG. 4.1 Resolution of tooth-to-tooth contact reactionary forces.

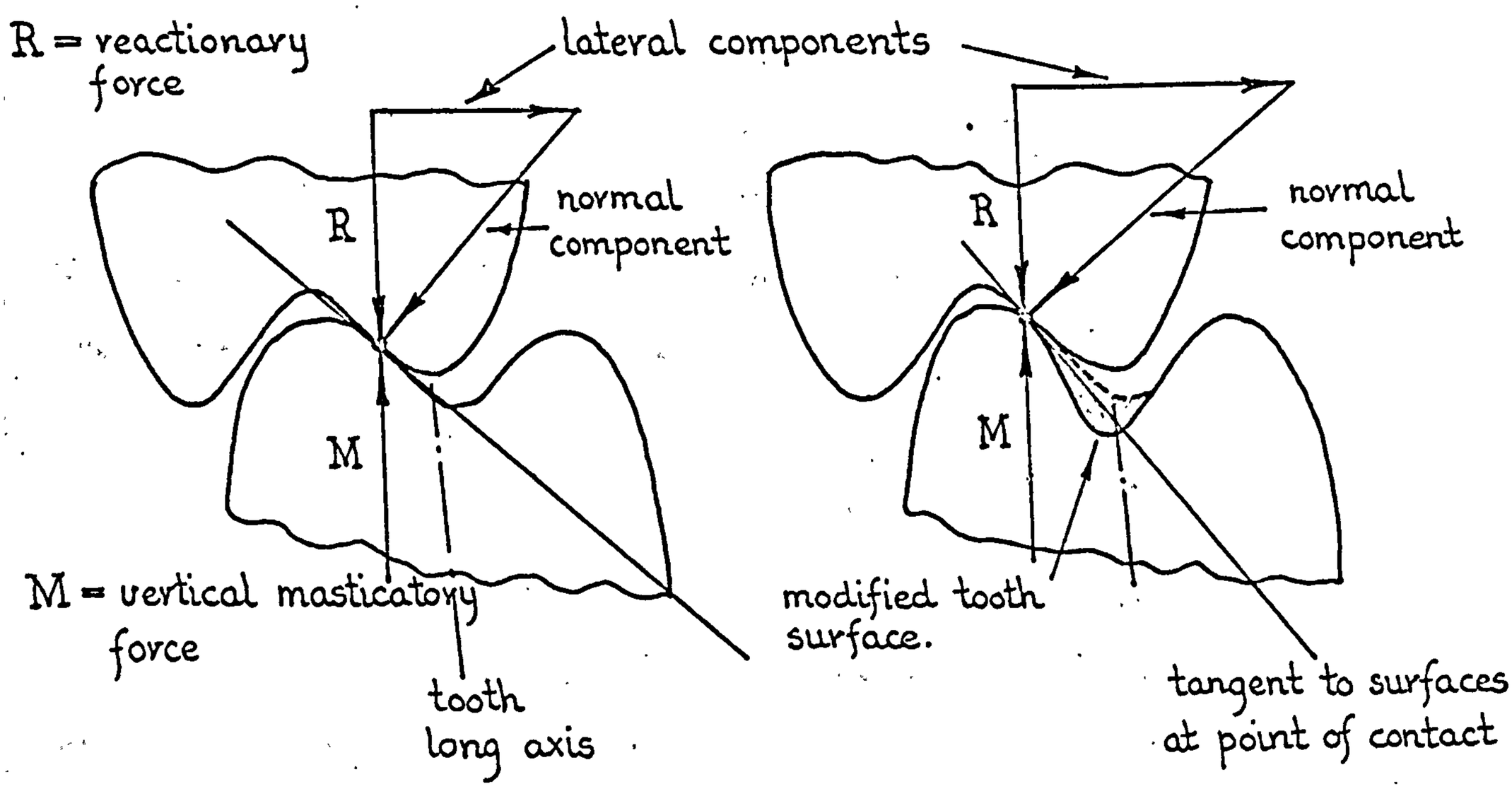


a) Original contact surfaces. b) Modified contact surfaces.

FIG. 4.2 Illustrating the increase in the lateral force component as a result of modifying the slope of the contact surfaces.

posterior teeth are relatively small in comparison with the axial components, see FIG 4.1. Consequently, if a restoration is constructed such that the cusp inclination is increased, then in general the lateral force component will be similarly increased. FIG 4.2 shows a simplified case where the effect of friction between the tooth surfaces has been ignored. Here the lateral force component has been increased by the change in the inclination of the contact surfaces. In this case, the increased lateral force component produces an increased tipping or turning moment on the tooth which in turn creates corresponding areas of increased tensile and compressive stresses in the periodontal membrane. If these stresses are increased above certain biological limits* the tooth will subsequently move and the result will be a modified occlusion.

To reduce the magnitude of the lateral force components generated, the practice of cusp reduction is often employed. This procedure, which tends to flatten the cusps, reduces the slope of the contact surfaces.

### 4.3.3 Bridge Abutments

Teeth used to form bridge abutments or to receive precision attachments are probably susceptible to the severest forms of abnormal loading. As shown diagrammatically in the bridge illustrated in FIG 4.3, the abutment teeth are subjected

* Although this phrase is often quoted in the dental literature, no quantitative data has been ascribed to this so-called limit. In fact, the causation of tooth movement is still fairly vague.

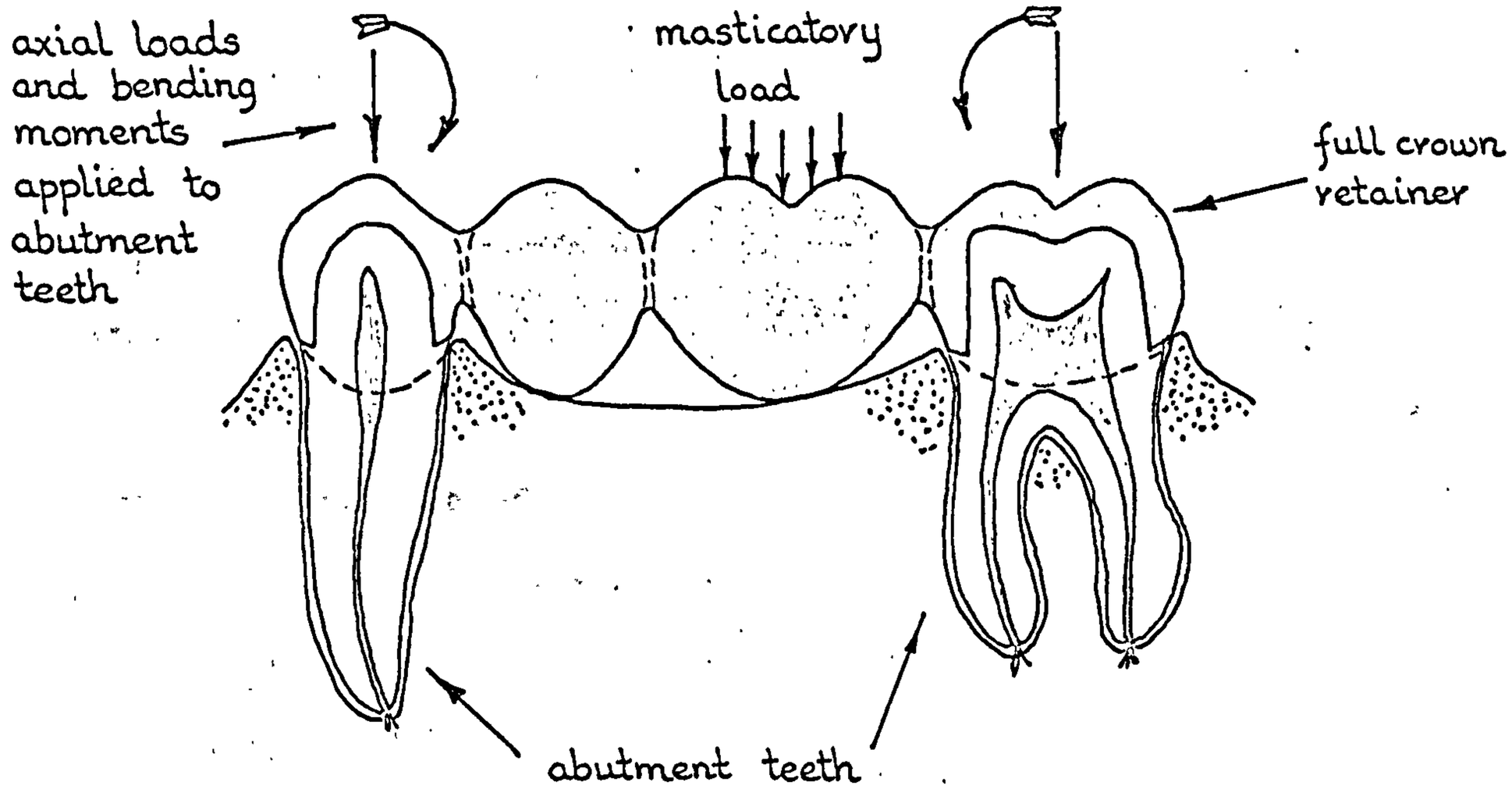


FIG. 4.3 Diagrammatic illustration showing how the abutment teeth of a bridge can be subjected to axial loads and abnormal bending moments.

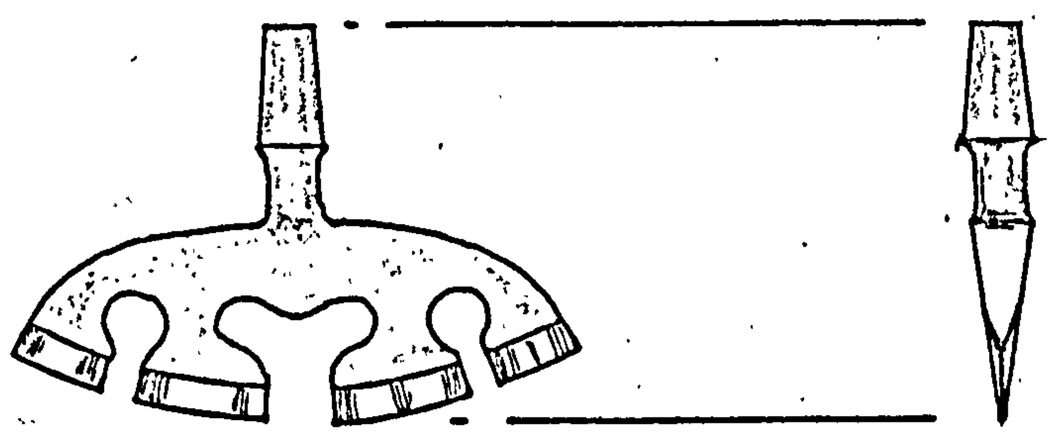

FIG. 4.4 Typical blade type endosseous implant.

to both axial loads and abnormal bending moments. This combination of loading not only leads to stress concentrations occurring at the interface of the natural and restorative materials, but also around the tooth roots in the supporting alveolar bone. Consequently, teeth used to form such abutments have to be very carefully selected with regard to the condition and quality of their supporting tissues, and the type and form of bridge retainer employed appropriately matched and designed.

### 4.3.4 Endosseous Implants

Recently, a number of different types of metal implants have been introduced which are either driven or screwed directly into the bone of the maxillar or mandible. The artificial tooth crown or bridge prosthesis is then attached to this metal substructure, see FIG 4.4. Because of the relative stiffnesses of the metal and bone and the almost impossible task of making the combination a perfect fit, the transfer of the masticatory forces to the supporting tissue inevitably occurs at a number of small select areas. Consequently, these points are subjected to very high stresses.

The problem of uneven stress transfer between materials of different moduli was manifested in the total hip prosthesis implant. However, in this case the situation was improved by inserting a flexible buffer or filler material between the metal stem of the implant and the femoral cortex, Charnley 1965 (29).

### 4.3.5 Partial and Complete Dentures

Dentures often apply unexpected and abnormal loads to their supporting oral tissues. Sometimes, the alveolar ridges possess high spots which lead both to denture instability and to stress concentrations occurring in the mucosa and underlying bone. The patient experiences rocking of the denture about these pivotal points and also suffers extreme soreness and irritation. A simple remedy for this condition is to insert a soft lining material between the denture base and the oral tissue. This has a cushioning effect and distributes the masticatory forces more evenly over the denture supporting structures.

## 4.4 ABNORMAL NON-MASTICATORY FORCES

So far, the discussion has concentrated on the normal and abnormal forces and loads which are imposed on the dental structures and tissues as a consequence of the natural process of mastication. The following sections however, examine some of the abnormal forces and stresses which are applied to the tissues whether as a form or as a result of dental rehabilitation and treatment.

### 4.4.1 Orthodontic Treatment

Malocclusion is defined as the deviation from the normal, the relation of the teeth in the same arch to each other and to those in the opposing arch. Orthodontics is that branch of dental science which is concerned with the correction of the malocclusion of the teeth.

The tissues supporting the teeth react to changes in the forces and the stresses which are imposed upon them. Consequently, orthodontic treatment consists of applying controlled and precise force systems to these tissues so as to invoke a response such that the teeth will move to a more normal orientation and position. Orthodontic appliances can provide force systems which will produce either tooth body movements or tooth rotation or tipping movements. Tipping movements of the teeth are associated with the rotation of the teeth about their long axes and occur about a centre of rotation which is generally located towards the root apex, FIG. 4.5A. Body tooth movement however, involves movement of the whole tooth in some particular direction. There are four different varieties of body tooth movement namely, horizontal, depression, elevation and rotation around the tooth long axis, see FIG 4.5.

The force systems employed for tooth movements are applied either continuously or intermittently. Although the magnitude of the force depends largely on the tooth type, it is usually in the order of a few grammes. This allows the tissues time to respond favourably and minimises the risk of the teeth becoming excessively loose or painful. Methods of transmitting the orthodontic forces include the use of fine springs which may be attached to a plate, activator or archwire. Brackets and staples attached to metal bands may also be employed. These are generally fitted onto anchor teeth and sometimes to the teeth being moved, see FIG 4.6. In the case

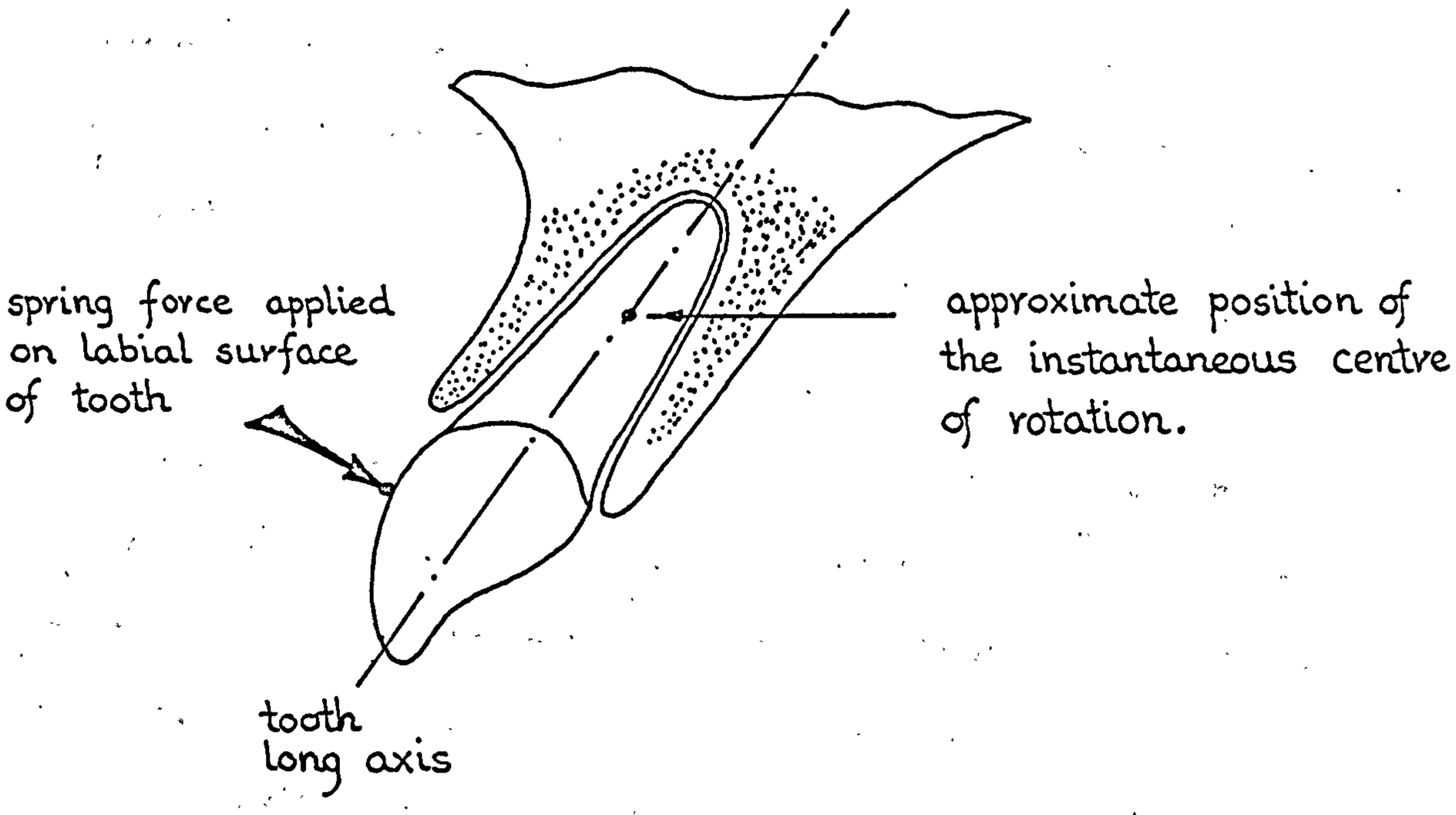


a) Tipping tooth movement.

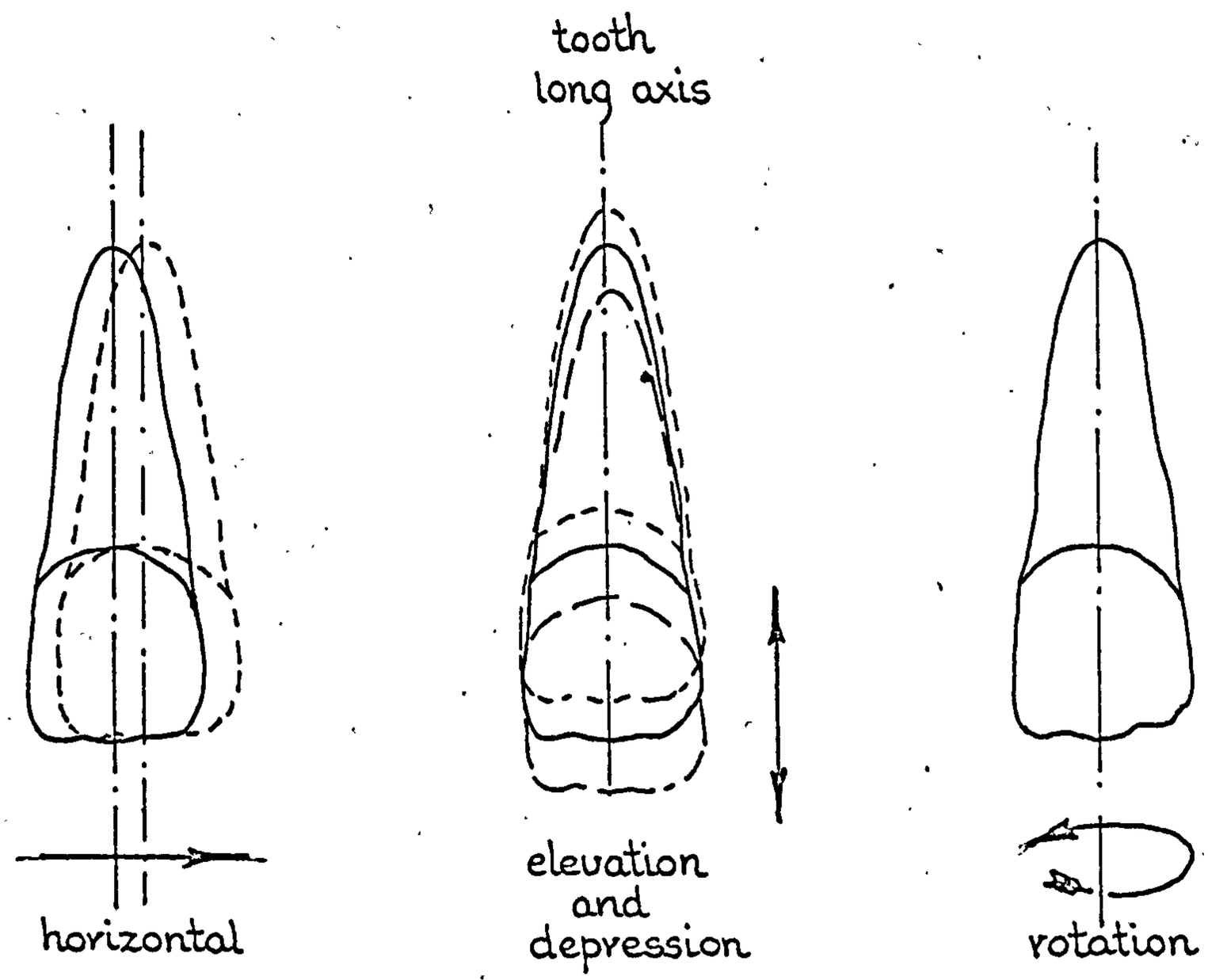


b) Body tooth movements.

FIG. 4.5 Diagrammatic representation of orthodontic tipping and body tooth movements.

illustrated, a main archwire is utilized which is formed into a shape to suit the particular malocclusion. These latter forms of appliances can produce both tipping and bodily tooth movements.

4.4.2 Filling Setting Expansion

In general,most filling materials rely on a mechanical fit between the margins of the restoration and the tooth tissues to provide an adequate seal against the ingression of the oral fluids. Therefore, it is desirable that the restorative material expands slightly during the setting process,thereby ensuring a more intimate contact between the restoration and the enamel and dentine of the tooth. Hence,as the tooth tissues are somewhat elastic, they will also expand due to the expansion of the restoration. Thus, a situation is created where the tooth tissues are being stressed by the expansion of the filling material, and the restoration stressed by the tooth tissues as they tend to resist the expansion.

Although the amount of setting expansion is affected by the composition and ratio of the constituents, method and degree of mixing and the manipulative technique employed, general standardised limits have been laid down for many of the restorative materials. For instance, the standard specification for amalgam allows for an expansion of between 0 to 20 microns per centimetre to occur during the first 24 hour period after condensation.

LABIAL

LINGUAL

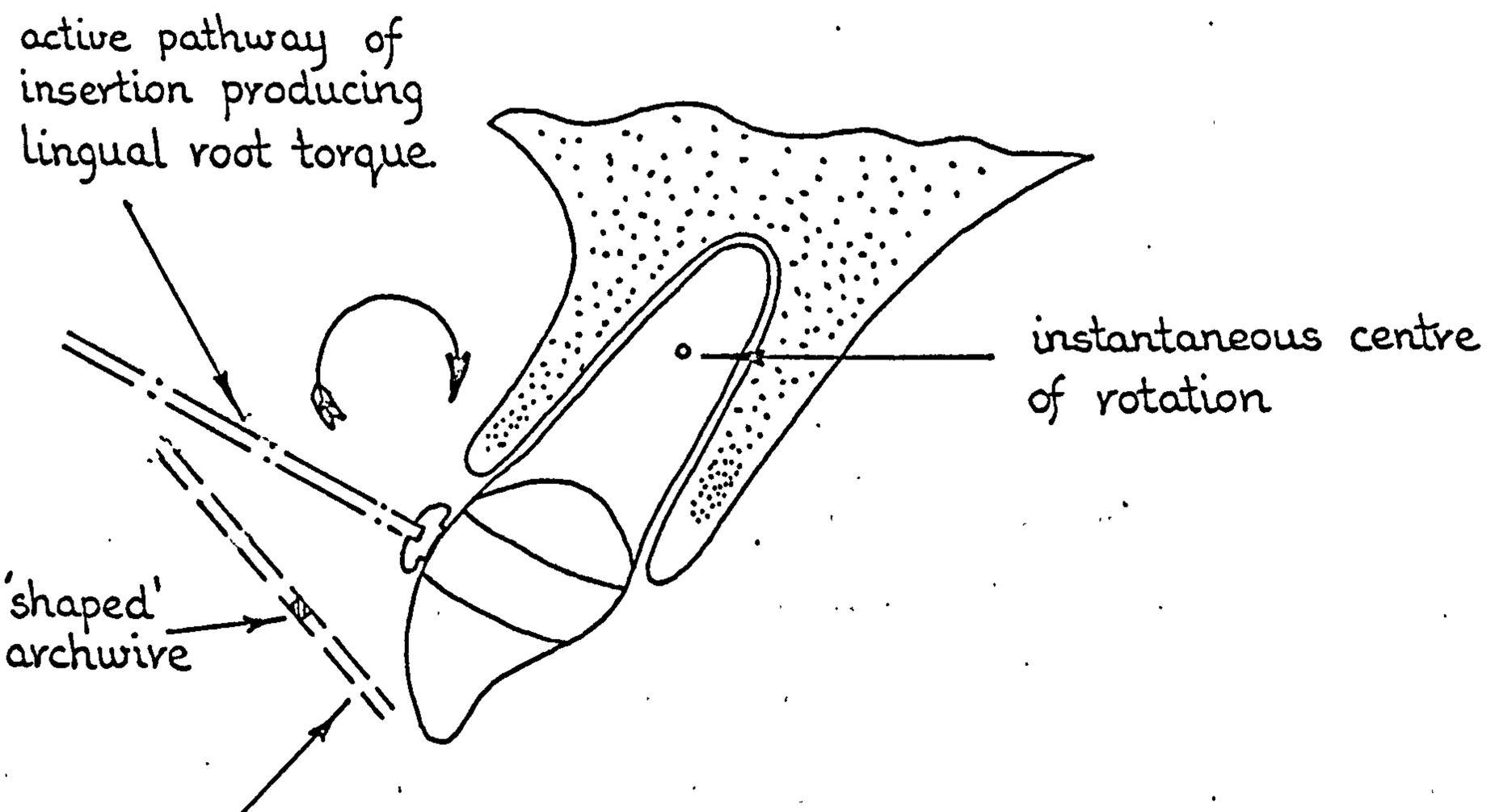


FIG. 4.6 Body movement of a tooth can be obtained by applying a force at the instantaneous centre of rotation. However, the centre of rotation is inaccessible. Therefore, a torque is applied to a bracket attached to the tooth's crown in order to produce a resultant which passes through the instantaneous centre of rotation.

### 4.4.3. Differential Thermal Expansion

Differences in the thermal expansion of the restorative materials and the tooth tissues result in the generation of internal stress systems when the composite structure is subjected to temperature variations. Because the metal filling materials possess a higher coefficient of thermal expansion than do the tooth enamel and dentine, they tend to expand more on heating. Hence, stress systems are created in the combined structure which are similar to those caused by the filling material setting expansion discussed in the previous section.

The actual magnitude and pattern of the stresses generated in the structure depend upon the differences in the coefficients of thermal expansion, the relative changes in the temperature distribution and the thermal conductivities of the materials and tissues involved. Although the oral temperatures are generally of a transient or dynamic nature, the overall temperature range of the modern diet may exceed $60^{o}C$, Pickard 1970 (30).

# CHAPTER FIVE

# METHODS FOR THE ANALYSIS OF DENTAL STRUCTURES

# 5. METHODS FOR THE ANALYSIS OF DENTAL STRUCTURES

## 5.1 INTRODUCTION

The objective of many clinicians and research workers has been to study natural dental structures, modified structures due to the introduction of restorations and prostheses, and the reaction of the tissues to various treatment procedures, employing diverse non-clinical engineering type techniques of analysis. Indeed, during the past few years it has been common place for physicists, engineers, material scientists and mathematicians to assist the teams of clinical workers researching into dental problems. Consequently, because of this multi-disciplined attack, the analysis of dental structures has experienced many changes and different approaches. This can be readily seen from the published literature of the past decade. Methods and techniques of analysis employed range from simple mathematical or analytical models, physical two and three-dimensional model simulations through to pseudo-model representations involving photoelastic materials. All of these approaches have been used with varying degrees of success to study both qualitatively and quantitatively different forms of dental behaviour. The interested reader is recommended to look at the excellent standard texts of Gabel and Tylman & Tylman (titles appear under the heading of general references), where all of these methods are discussed and are employed to illustrate different aspects of dental structural design.

The object of this chapter is to review some of the techniques and methods of analysis which have been presented in the dental literature, to introduce the method of analysis to be used in the current investigation and to discuss some of their relative advantages and disadvantages.

The Finite Element Method has not been used previously for dental structural analysis. However, it is non-the-less a very powerful technique and enables prcblems to be investigated which have hitherto been thought intractable.

## 5.2 MATHEMATICAL OR ANALYTICAL MODELS OF ANALYSIS

Mathematical or analytical models generally represent exact and precise descriptions of ideal or theoretical material or structural behaviour and are usually expressed in terms of equations. These equations can be in either differential, partial differential or algebraic form and contain parameters, or functions of parameters, which are either known or unknown. (See for example sections 3.2.4 and 3.2.7 where a mathematical model is employed to explain linear elastic material behaviour.) In general,the number of equations derived is made equal to the number of unknown quantities. Consequently, a solution of the entire set of equations renders the values of all of the unknown parameters.

In constructing mathematical models, it is usual for certain simplifying assumptions to be made in order that the resulting equations derived can in fact be solved. Hence, mathematical models are no better than the assumptions on which

they are based. Therefore, it is essential that calculations resulting from the use of such models should be checked and verified wherever possible with physical or clinical experiment and observation.

Probably the first mathematical model ever derived for analysing the centre of rotation, displacement and pressure distributions of a tooth supported in the periodontal membrane and bone structure, can be attributed to the eminent mathematician Synge (31) in 1933. Synge's model consisted of a rigid tooth and bone structure separated by a thin elastic, homogeneous, isotropic and incompressible membrane. The model, as conceived by Synge, proposed that the periodontal membrane under no load was under a state of atmospheric hydrostatic pressure. Under load, some zones in the membrane would increase in pressure while others would fall below that of the atmosphere. Synge derived equations for the distribution of pressure in the periodontal membrane as a function of load and root surface location.

Synge set up and solved the equilibrium equations for two simple test cases. The first model assumed the structure to be two-dimensional and having a uniform thickness of 0.24 inches. The root part of the model was in the form of a wedge, see FIG. 5.1a. For this model the centre of rotation of the tooth was calculated to be approximately half way between the root apex and the cervix when the tooth was subjected to a transverse load applied at the incisal edge. Synge's second model considered the tooth root to be axisymmetric and in the form of a cone.

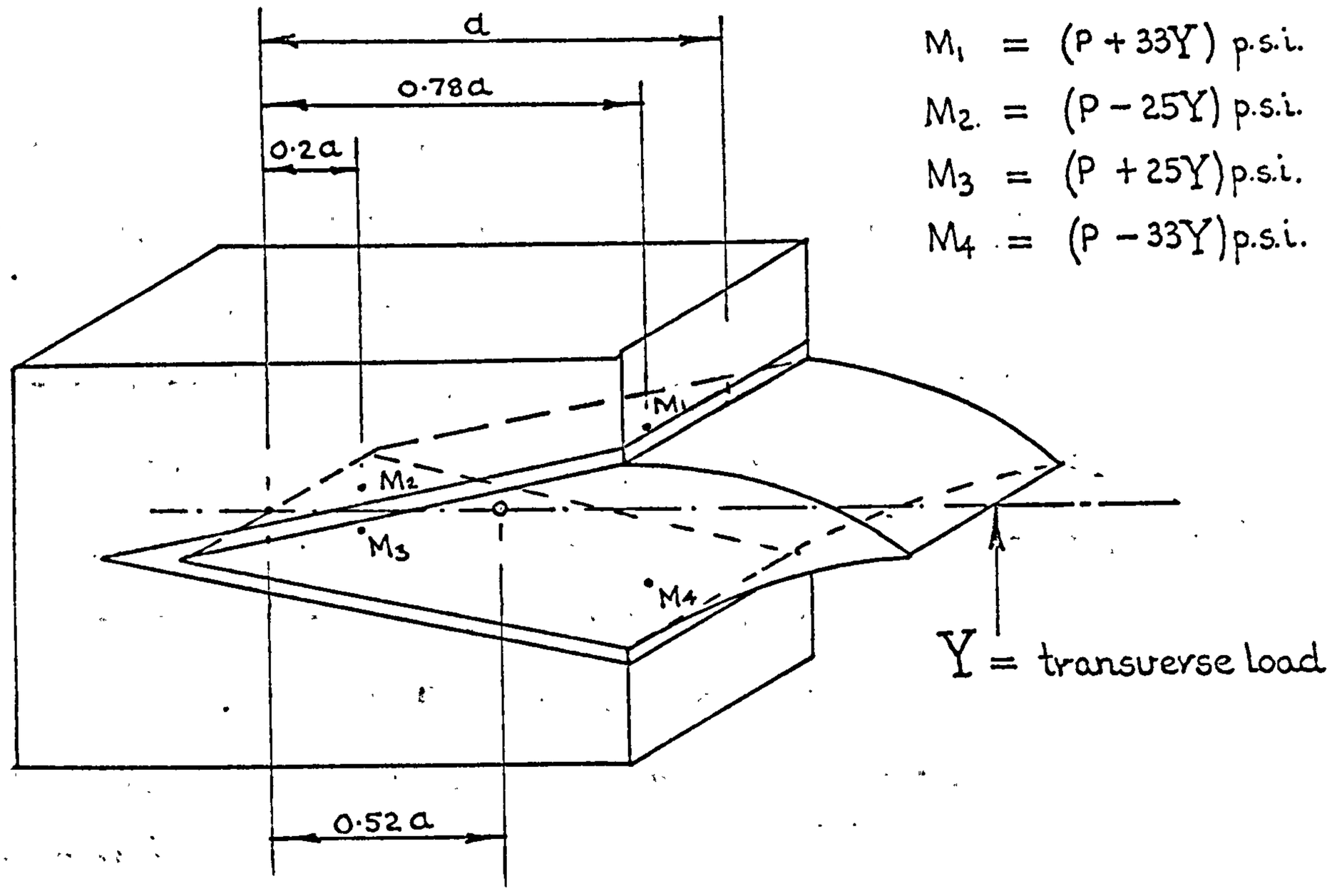


$M_1 = (P + 33Y)$ p.s.i.
$M_2 = (P - 25Y)$ p.s.i.
$M_3 = (P + 25Y)$ p.s.i.
$M_4 = (P - 33Y)$ p.s.i.

a) 2-D wedge model.

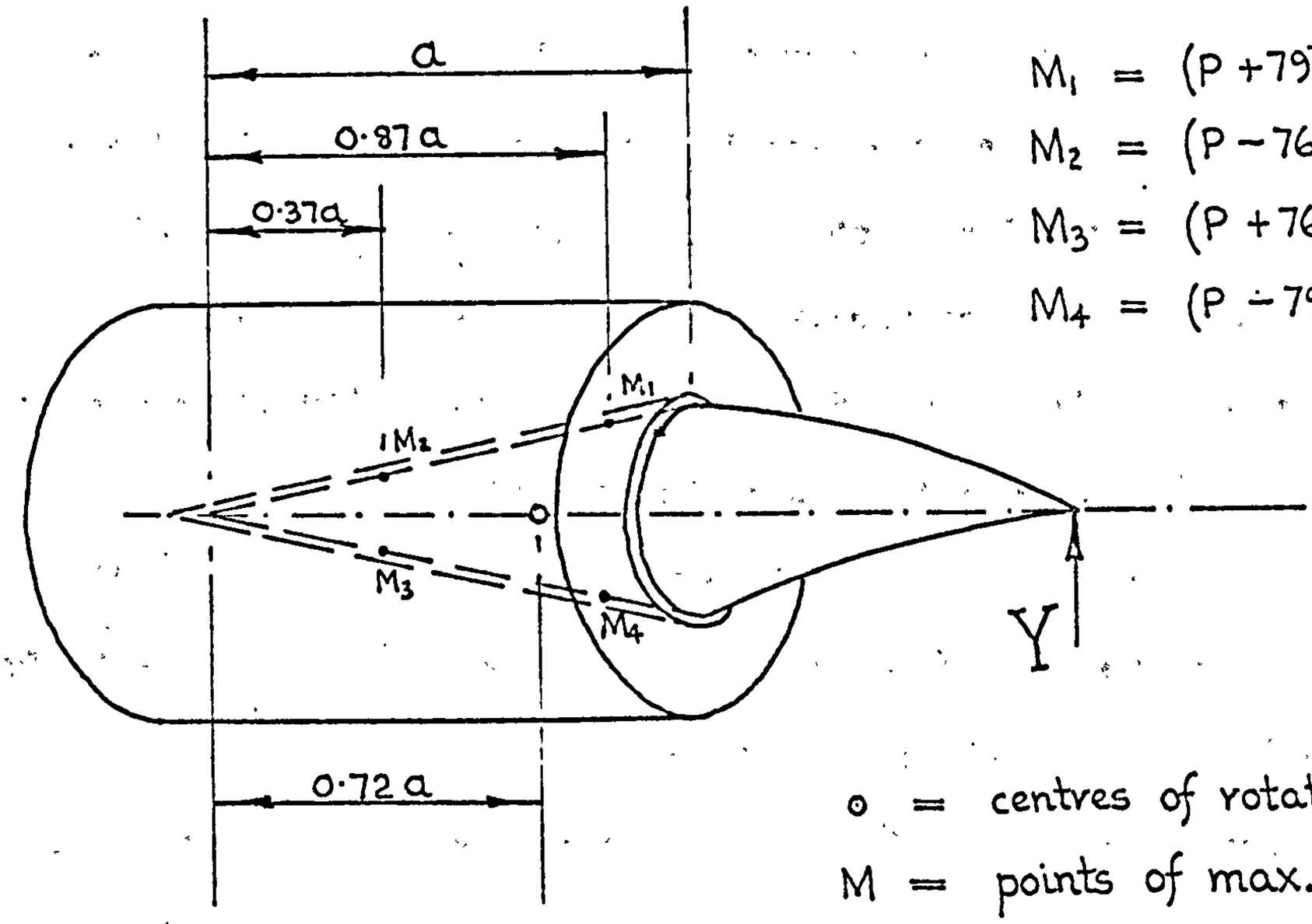


$M_1 = (P + 79Y)$ p.s.i.
$M_2 = (P - 76Y)$ p.s.i.
$M_3 = (P + 76Y)$ p.s.i.
$M_4 = (P - 79Y)$ p.s.i.

o = centres of rotation.
M = points of max. pressure.
P = atmospheric pressure.

b) Axisymmetric or cone model.

FIG. 5.1 The results of Synge (31). Obtained by assuming the periodontal membrane to be a linear elastic, homogeneous, isotropic and incompressible material.

In this case, the centre of rotation was found to occur coronally, at a position approximately three quarters of the distance between the root apex and the cervix, FIG 5.1b. Assuming a rigidity modulus value of rubber (G = 230 p.s.i.), Synge calculated the transverse deflection of the tooth's incisal edge to be $8.9 \times 10^{-6}$ inches (approx. 0.22 microns), for a transverse load of 0.19 pounds. A corollary of this theory is that the tooth's transverse displacement is directly proportional to the periodontal membrane thickness raised to the third power.

In 1939 Hay (32), modified Synge's theory to cater for the compressibility of the periodontal membrane. He proposed that because the membrane consisted mainly of water, the small compressibility of the fluid must be taken into account. Hay calculated the stress patterns, displacements and the centres of rotation for a conical rooted tooth under six different loading conditions. He assumed the membrane to be of uniform thickness of 0.0098 inches and employed the shear modulus value (G = 70 p.s.i.) given by Dyment and Synge in their paper in 1935 (15). For a transverse load of 0.0626 pounds (1 oz.) applied at the incisal edge, Hay calculated the corresponding transverse deflection to be $1.25 \times 10^{-5}$ inches (approx. 0.3 microns). Thus, this result gives a slightly larger deflection than Synge's but for approximately only one third of the applied load. However, Hay concluded that his results were not very sensitive to changes in the compressibility of the membrane but were directly proportional to the shear modulus. Hence, the

significant difference in the flexibilities indicated by these two author's results can be attributed to the difference in the values employed for the shear moduli. The centre of rotation calculated by Hay agreed closely with Synge's result and occurred coronally at approximately two thirds of the distance between the root apex and the cervix.

Further work on determining the stresses in the periodontal membrane has been recently published by Haack et al (33), who took for their model a paraboloid of revolution. Like Synge and Hay, the authors assumed the membrane to be of a uniform thickness, homogeneous, linear elastic and isotropic material. However, they did consider different compressibilities and varied Poisson's ratio from 0.0 in steps of 0.15 up to 0.45. Haack et al derived the Navier or equilibrium equations for their model and employed the boundary conditions:-

1) the outer bone surface was fixed and was completely rigid

and 2) that the tooth was completely rigid but moveable.

They solved the resulting equations using finite difference techniques for four different loading conditions. These were:-

1) Unit axial torque

2) Unit lateral force applied at the root's centre of resistance (assumed to be coronally 0.6 of the distance between apex and cervix)

3) Unit axial pull

and 4) Unit lateral couple.

The authors found that in general, the stresses in the membrane increased for increasing values of Poisson's ratio, (i.e. as the membrane approached incompressibility) and were higher at the tooth surface than at the bone surface. From their lateral torque (transverse load) calculations, the centre of rotation was also found to vary with Poisson's ratio, being respectively 0.53 for $\mu = 0$ and 0.56 for $\mu = 0.45$. (The 0.53 and 0.56 signify the proportion of the apex to cervix dimension measured coronally from the root apex to the centre of rotation.)

In 1956 Gabel (34), mathematically looked at the support mechanism of the teeth. He proposed a compromise between the two distinct schools of thought which proclaim that the periodontal membrane provides either a fibre support system or a compressible or incompressible membrane support system. Gabel suggested that probably both types of tooth support existed simultaneously. From his calculations, the author deduced that if the waviness of the periodontal fibres accounted for more than 4% of their overall straightened length then they would remain unstressed during a tooth intrusion of 0.025 mm. Thus, he concluded that the fibre support theory was not credible and that compression of the parenchyma of the membrane must therefore give some support. Gabel also calculated that the displaceable blood in the periodontal membrane was approximately equal to the change in the socket volume which occurred during the tooth intrusion. However, he claimed that the fibres were there for a purpose and proposed that the pressure created in the membrane could possible produce a tangential displacement of the tissue against the fibre network. This tissue displacement

forced the fibres to assume the shape of carteneries thereby inducing tensile stresses in them.

Ledley in 1968 (35), put forward a mathematical analysis and computational method using engineering theories, whereby, the force distribution on the tissues supporting complete dentures during normal masticatory function could be determined. However, Ledley's method required the mechanical properties of the mucosa to be determined experimentally but he gave no indication as to how this was to be achieved.

The kernel of Ledley's approach lay in the analytical determination of the relative displacements of discrete points on the denture at the end of a particular activity. The displacements were calculated by subtracting from the Cartesian co-ordinates of the discrete points on the denture after it had received a rigid body movement, the original co-ordinates of the same points before displacement. The original co-ordinates of the surface of the denture base were obtained by first embedding the base in an acrylic resin, slicing it into sections through the desired points and then measuring the X,Y, and Z co-ordinates from some selected origin. Thus assuming a state of static equilibrium to exist and knowing the pressure-displacement relationship of the supporting tissue, the normal reactive tissue force for each differential area of the denture base can be determined. The theory assumes however, that all points on the denture base compress the tissue, (a condition that not always necessarily occurs in practice), and also that the shear force reactionary components are negligible.

Using the same ideas and principles presented in the paper just discussed, Ledley and Huang in 1968 (36) and in 1969 (37), carried out some numerical analyses on the displacement of teeth subjected to various loading conditions. Again, a linear stress-strain relationship for the periodontal membrane was employed but the surface of the root was approximated by a series of facets which were constructed so as to lie parallel with one of the three planes of the Cartesian co-ordinate system. The most important point that the authors made however, was that a general tooth displacement does not necessarily possess a unique centre of rotation. In fact, in moving from its initial to final position, the movement could be achieved in an infinite number of different ways. (The idea of a centre of rotation is merely a mathematical concept which produces a single point about which the tooth 'could' be rotated in order to achieve the required overall displacement.)

Tsao in 1970 (38), employed a mathematical approach to determine the size and geometry of the occlusal rests for removable partial denture designs. Using simple beam theory, the maximum masticatory bite forces and the mechanical properties of the dentine and restorative materials involved, the author calculated the diameter and depth of head required for a spherical type attachment.

Burstone in 1962 (39), derived a formula for determining the position of the centre of rotation of two-dimensional parabolic shaped single rooted teeth, see FIG 5.2. In his derivation, the author assumed the tooth to be in a state of

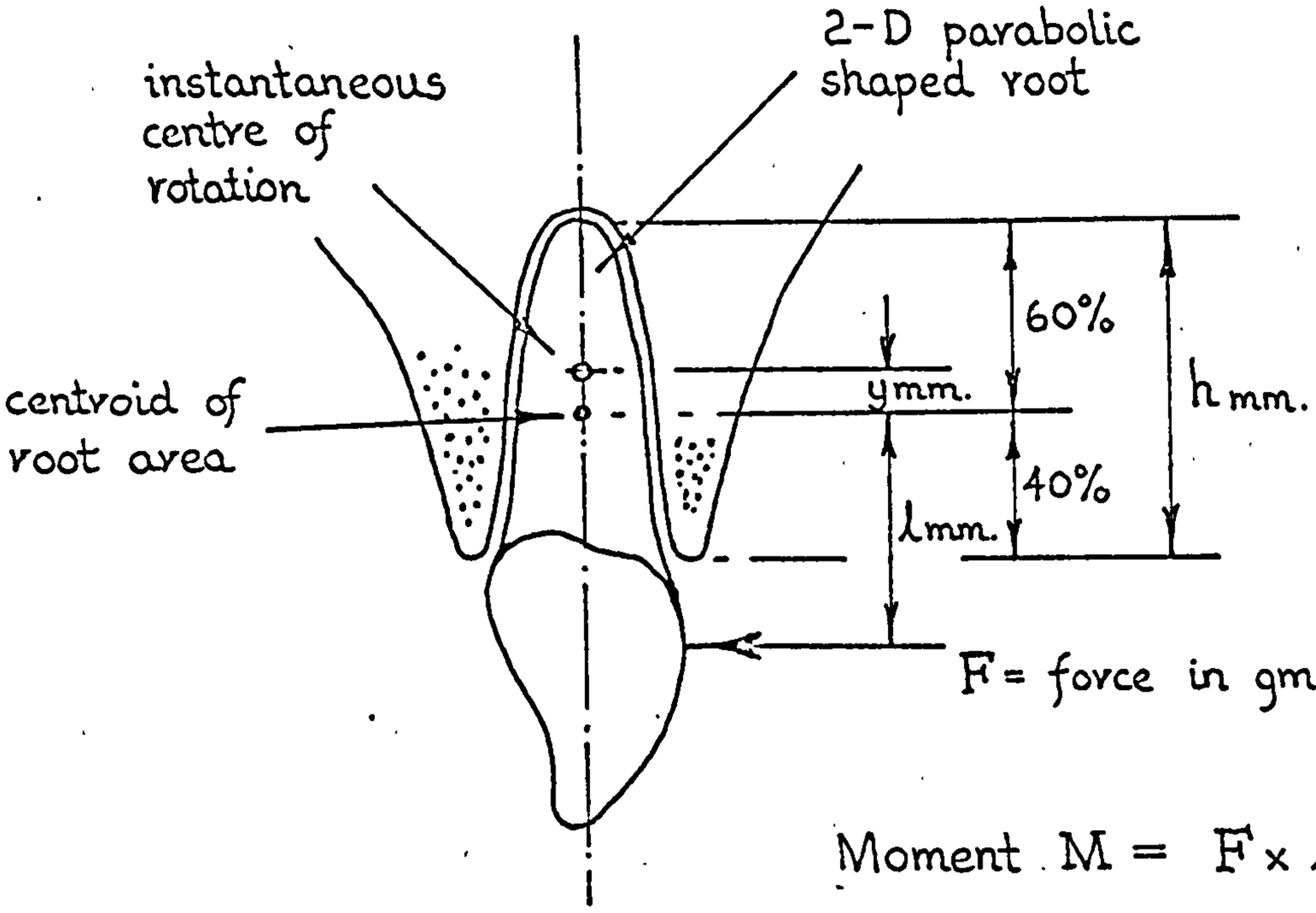


FIG. 5.2 Illustrating Burstone's formula for determining the instantaneous centre of rotation of a 2-D single rooted parabolic shaped tooth.

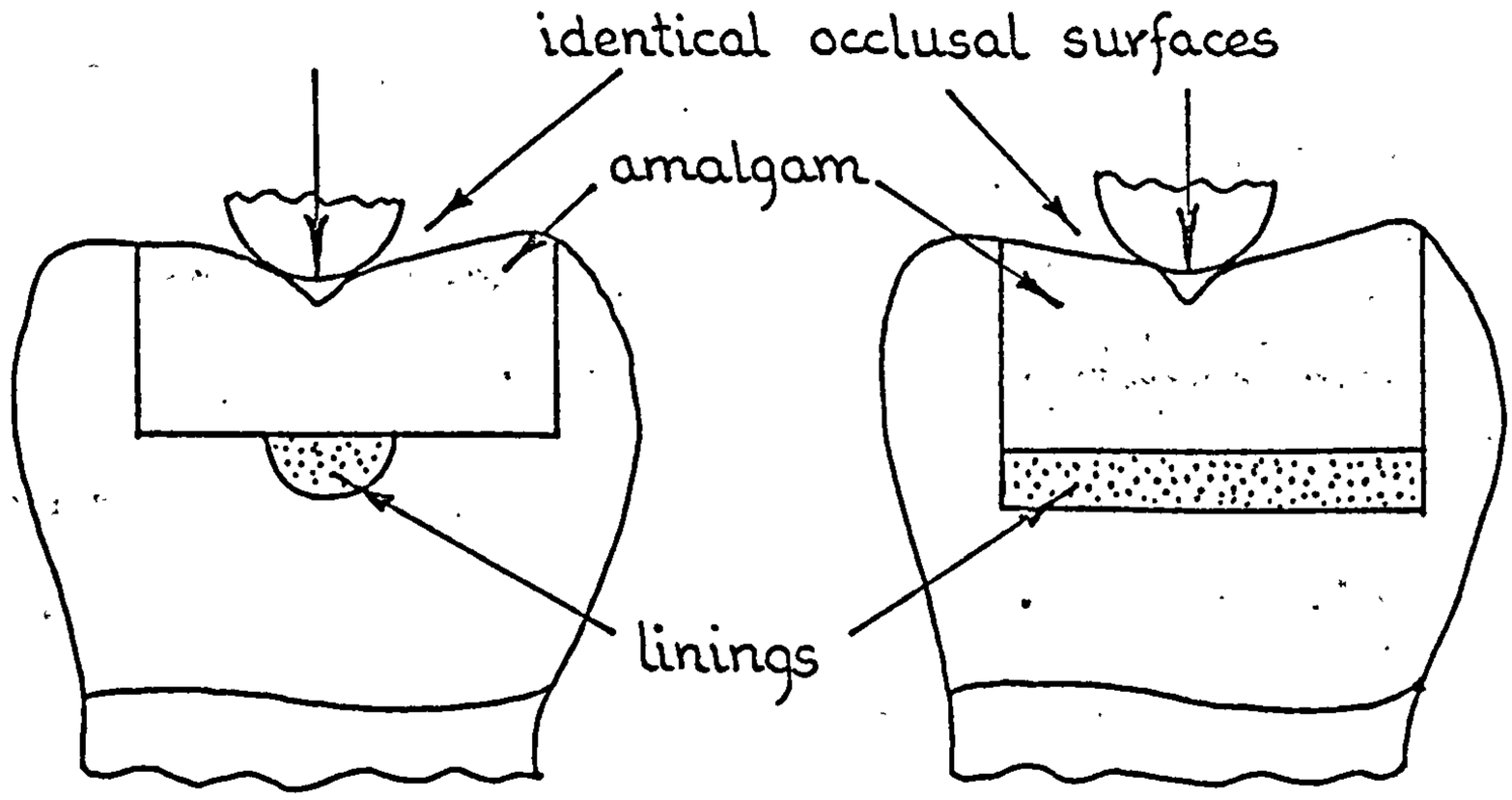


FIG. 5.3 Model cavity preparations. Hoppenstand and McConnell (41).

static equilibrium and the stress distribution along the root surface to be uniform. He also assumed the periodontal membrane to possess a linear stress-strain relationship. In 1969 Christiansen and Burstone (40) compared the analytical results obtained using this formula with some results determined experimentally with a considerable degree of success.

## 5.3 MODEL SIMULATIONS

The use of physical models to simulate the dental structures has been employed by numerous investigators in order to study dental structural behaviour. While this approach gives a visible appreciation of the overall structural model response, as with the analytical models previously discussed, the results obtained are no better than the models themselves. In other words, unless the model materials and components are truly representative of those which they are attempting to simulate, their behaviour need not be anything like that which would occur with real structures.

Hoppenstand and McConnell in 1960 (41), used a model simulation technique to study the mechanical failure of class I type amalgam restorations with two different cement bases. Using plastic tooth models two forms of cavities were cut, one being a shallow cavity and the other a deep one, FIG 5.3. As several teeth were prepared of each cavity form, a jig was employed to ensure uniformity of design. The shallow cavities were prepared with a hemispherical excavation cut in the centre of the pulpal floor to receive the lining base material. For the deeper cavities however, the underbase lining material was

deposited in the form of a continuous layer over the entire cavity floor. The lining materials used in the tests were zinc oxide/eugenol and zinc phosphate cement. Control teeth of both cavity forms were employed in which all of the cavity was filled with amalgam. The occlusal surfaces of all of the restored teeth were manufactured using a steel die. All teeth were subsequently loaded to destruction via a 1/8 inch diameter steel ball positioned on the occlusal surface.

The authors concluded from their tests that very little difference in tooth breaking strength occurred with either of the lining materials for the shallow cavities. However, for the deeper cavities the zinc oxide/eugenol restoration was found to be much weaker than the corresponding zinc phosphate restoration. Even so, the zinc phosphate restoration was still weaker than the equivalent control restoration which only contained amalgam.

In 1961 Mahler et al (42), used a similar technique to the previous authors to investigate design aspects of amalgam class II restorations. Mahler et al employed models composed of amalgam restorations condensed in prepared cavities in natural teeth, amalgam restorations condensed in identical cavities in the same teeth reproduced in technic metal and plaster restorations cast in prepared cavities in densite model teeth, eight times full size. Twenty of each of the three model types were constructed having four different forms of restoration design. All teeth were statically loaded axially until fracture occurred.

From their results,the authors concluded that the models consisting of amalgam and technic metal showed a greater variability in the breaking loads than did the amalgam-natural tooth combination. They attributed this to greater adhesion between the restoration and the metal tooth than between the amalgam and the natural tooth structure. Thus, it is evident that in using models of this kind,the introduction of extraneous influences can greatly affect the simulated structural behaviour.

Haack and Weinstein in 1963 (43), published their work which employed a two-dimensional sagittal slice model of a central maxillary incisor composed of a timber tooth and alveolar bone support separated by a thin elastic foam sponge periodontal membrane FIG 5.4. Hence, by applying different force systems to the crown of the tooth analogue, the authors were able to demonstrate visually the areas of compression and tension in the 'periodontal membrane' and the approximate centres of 'tooth' rotation. Although, as Haack and Weinstein pointed out, the model has obvious limitations, the use of such analogues for pedagogic purposes, (providing of course they are truly representative of the clinical situation), can be equivalent to many hours of verbal explanation.

In 1964 Dempster and Duddles (44), used a similar approach to Haack and Weinstein to investigate tooth statics. Dempster and Duddles employed two-dimensional chipboard models of a mandibular molar tooth and socket but unlike the previous authors did not include a 'periodontal membrane' material. Instead,

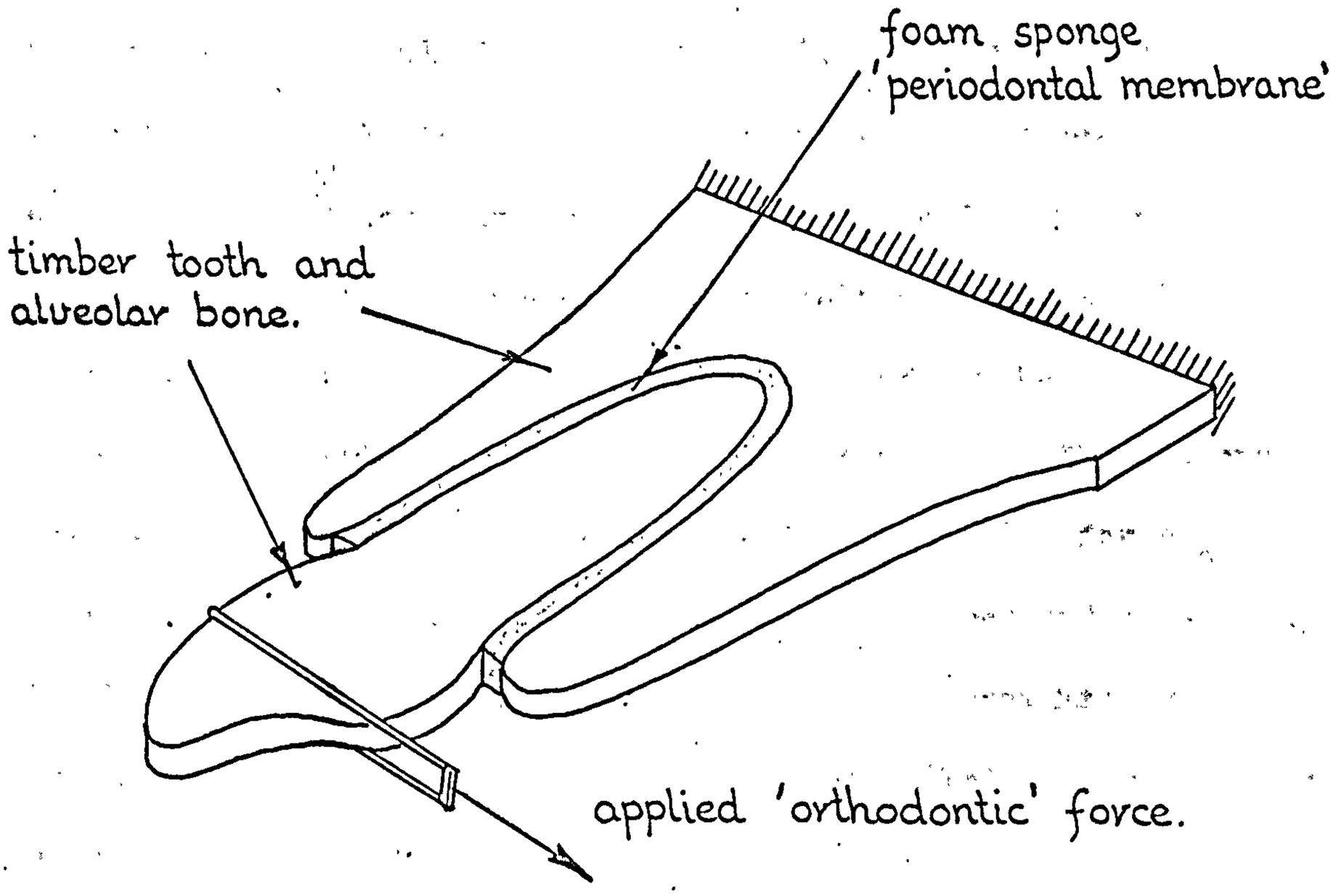


FIG. 5.4 Two-dimensional timber and foam sponge analogue. Haack and Weinstein (43).

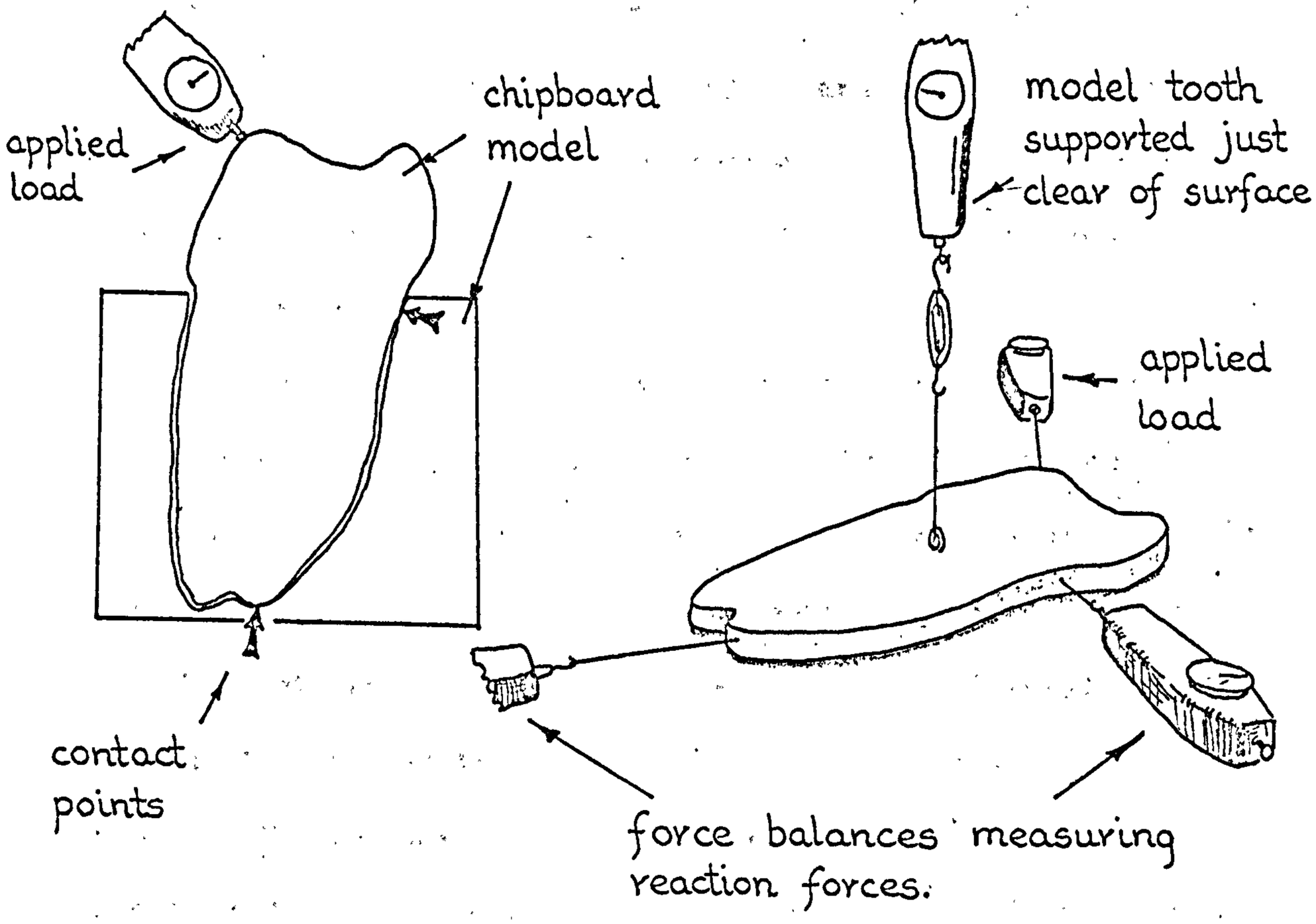


FIG. 5.5 Two-dimensional chipboard model of mandibular molar without 'periodontal membrane'. Dempster and Duddles (44).

they coated with chalk the 'socket wall', (which was machined accurately to scale to fit the tooth profile). Hence, on applying coronal force systems the 'tooth' moved or rocked in the 'socket' making contact with it only at a number of discrete points. These points of course, were marked on the 'tooth root' by the chalk from the 'socket wall'. The authors then separated their model analogue and by attaching force balances to the contact points, in a direction perpendicular to the 'roct' surface, were able to recreate approximately the static equilibrium conditions which prevailed in the complete model, FIG 5.5.

The biggest disadvantage with this ingenious approach lies in the fact that having no 'membrane' all the reactive forces are considered to flow out through the 'tooth' at points. Consequently, the 'alveolar side walls' are unable to react any intrusive components of the load systems and therefore these loads would simply flow straight down the 'tooth' and out at the 'root apices'.

Henderson et al in 1970 (45), reported on two types of models they had developed in order to study the behaviour of teeth used to form adbutments for fixed partial dentures. Their first model, FIG 5.6, consisted of 'teeth', which were represented by lengths of studding, which were embedded in a 'periodontal membrane' of rubber-based impression material in a timber block. The 'abutment teeth' were connected as required for the experiments by means of a rigid bar or 'bridge' which was secured to either three, two or to just one of the 'teeth'

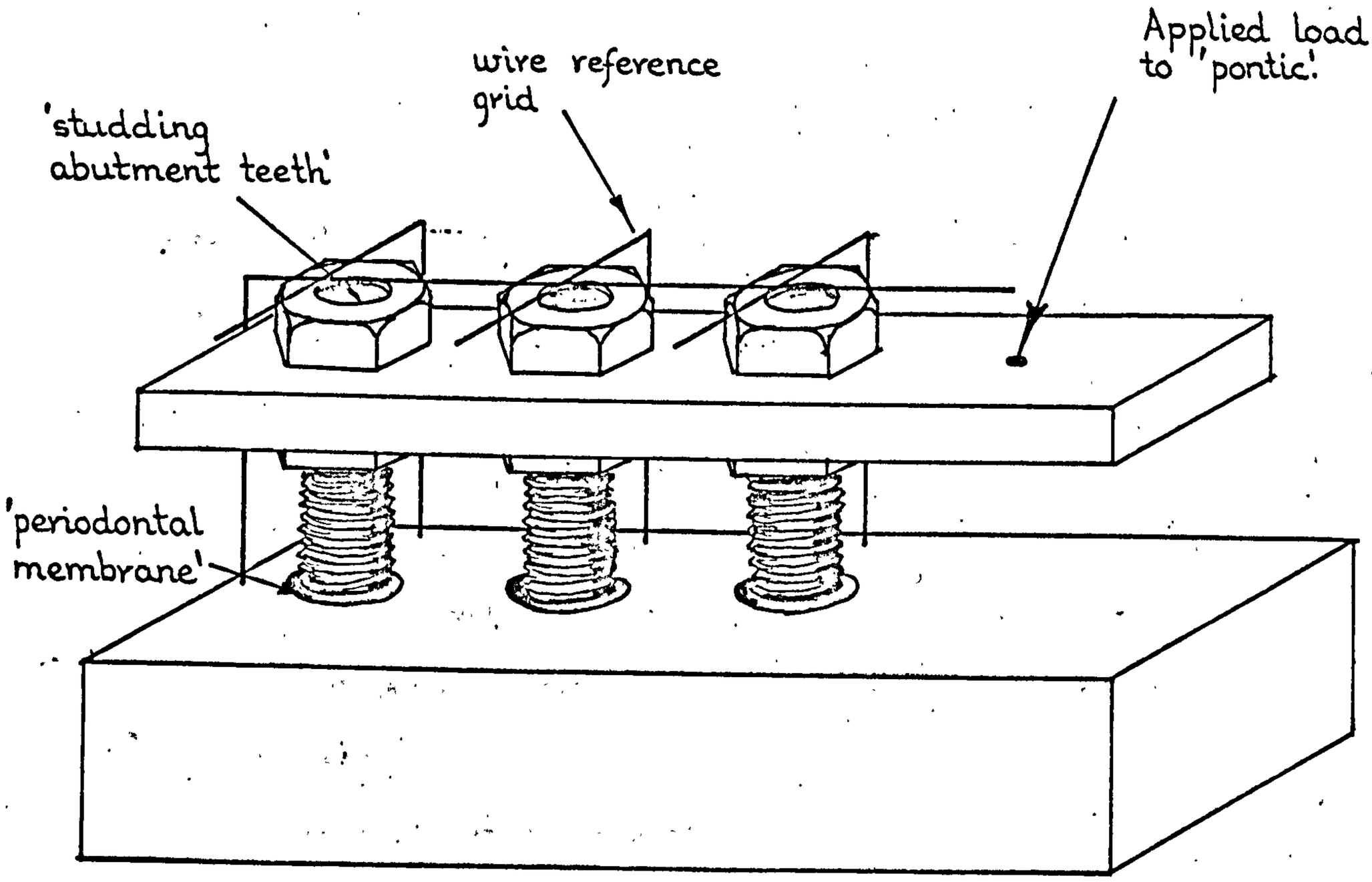


FIG. 5.6 'Nuts and bolts' type model of cantilever bridge. Henderson (45).

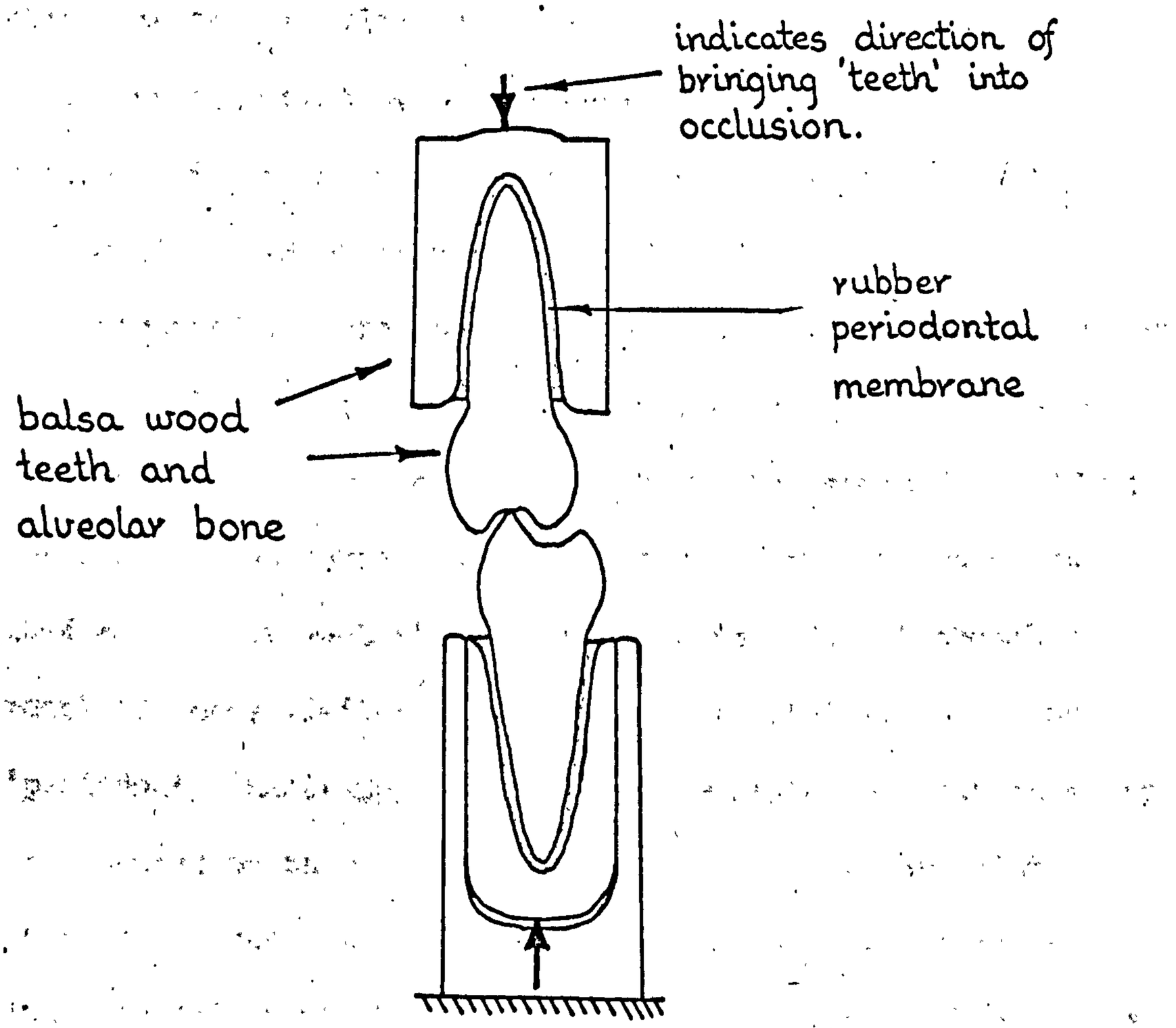


FIG. 5.7 Balsa wood and rubber slice model of posterior teeth in centric closure. Dickson (46).

respectively, via nuts screwed onto the appropriate studs. A wire reference grid spanned the entire model and by simultaneously taking 'occlusal' and 'lateral' photographs of the loaded set-up, the structural displacement pattern was obtained. Thus, the authors were able to study the movement of the whole 'prosthesis' for various loadings applied to the 'first molar pontic' when different numbers of abutment teeth were employed.

In the same paper the authors report on a more refined technique where ivorine teeth, surrounded by a rubber-base 'periodontal membrane', were supported in an acrylic denture base. The teeth, the canine, first and second premolars which had been previously prepared to receive three-quarter gold crowns, were then loaded separately both axially and obliquely in order to determine their corresponding load versus displacement characteristics. The same teeth were then combined to form abutments for a cantilever bridge carrying a first molar pontic. Hence, when the pontic was loaded and the resulting deflections of the abutments recorded, by using the calibration curves for each tooth, the proportion of the load accrued by each abutment was determined. Although the model has many limitations, e.g. type and thickness of the 'periodontal membrane', the authors demcnstrated that this type of restoration should be used with only limited optimism. This is because the abutment teeth are subjected to severe loads caused by the bending moments or leverage action of the cantilever type prosthesis.

In 1972 Dickson (46), published his work in which he used models to study the tipping of the posterior teeth in centric closure. Dickson's models were two-dimensional buccolingual slice sections of posterior teeth constructed from balsa wood and rubber. The balsa wood formed the 'tooth' and 'alveolar bone' and the elastic rubber the 'periodontal membrane,' FIG 5.7. From his experiments and subsequent analyses, the author demonstrated the tipping or rotation of the teeth and the trends of the forces involved in centric occlusion.

## 5.4 EXPERIMENTAL STRESS ANALYSIS

While the model simulations previously discussed were primarily concerned with overall external structural behaviour, the study of the internal structural or tissue reactions, i.e. the internal stresses, has been attempted using other various experimental methods. Indeed, it is probably in this area that the bulk of the work concerned with the mechanical analysis of the dental structures has been carried out. Experimental methods of stress analysis employed include photoelastic model and layer analysis, brittle lacquer coatings and electrical resistance strain gauge techniques.

The photoelastic model technique requires a replica scale model of the actual structure to be analysed, to be constructed in a photoelastic material. Photoelastic materials, when loaded, polarise impinging light rays into components (which are subsequently transmitted through the material), in the directions of the principal stresses. Furthermore, the light

waves are transmitted with different velocities, consequently they emerge with one ray possibly being retarded with respect to another. This retardation, which is directly proportional to the difference between the principal stresses at each point in the material and to the thickness of the slice, (when considering two-dimensional models), can be observed when the model is viewed in a polariscope. The retardation throughout the photoelastic model is manifest as an interference pattern. From the 'fringe' pattern in the model structure, the corresponding stress system can be determined.

While two-dimensional photoelastic models can be loaded and observed directly in the polariscope, for three-dimensional models, a 'frozen' stress technique is usually adopted. In this case, the three-dimensional scale model is slowly heated up to the particular materials critical temperature, whereupon, it becomes 'rubbery'. If the model is then loaded and slowly cooled down to ambient temperature, the interference or stress patterns caused by the loading are 'frozen' into the model. Thus the model can then be sliced and viewed as were the two-dimensional models in the polariscope.

The photoelastic layer technique consists of attaching a layer of the photoelastic material to the surface of the actual structure under investigation. When the structure is subsequently loaded, the interference pattern in the layer is observed directly. This is achieved by passing the light beam through the layer and reflecting it back from the surface of the structure. The reflected light obviously then passes

yet again through the layer before reaching the polariscope.

The brittle lacquer coating technique is similar in principle to that of the photoelastic layer method. Again, a surface coating is applied to the unloaded actual structure. However, with this technique, when the structure is subsequently loaded after the layer has dried, the brittle coating cracks at right angles to the directions of the principal surface strains. Hence, knowing the strain sensitivity of the lacquer material, the strain in the structure at the time and point at which the cracks appeared can be determined.

While both the layer techniques discussed can only investigate surface effects, they have the added advantage of being able to analyse the actual structure under consideration. However, this advantage cannot easily be utilized for in-vivo dental analysis. Consequently, simulated models of the dental structures must first be constructed in order to employ either of these techniques.

Resistance strain gauges are electrical transducers which change their electrical resistance when a change occurs in their physical dimensions. Hence, if these devices are attached to structures prior to their being loaded, a measure of the surface deformation under the imposed loading can be obtained. Unfortunately, like the layer techniques, these are not very convenient for in-vivo dental work.

The comments relating to the validity of the mathematical and model simulation results discussed earlier are equally applicable to these experimental methods. For unless the

experimental models are accurate simulations of the real life structures they represent,then completely misleading results can ensue. This is clearly demonstrated in a subsequent section in this chapter where a simple two-dimensional analysis, used to introduce the Finite Element Method, shows how the incorrectly matched photoelastic model materials, representing a compound dental structure, drastically affect the overall model's behaviour.

For further background information pertaining to the experimental methods of stress analysis outlined in this section, the interested reader is referred to the standard texts of Holister (47) and Frocht (48).

Mahler and Peyton in 1955 (49), pointed out the need to determine the optimum design or structural configuration for dental restorations. Analysis, they concluded, instead of empirical rules and criteria, was the only means of achieving this goal. The authors proclaimed that because of the irregular shapes of dental restorations, "experimental methods of stress analysis is indicated since mathematical theories can only be applied to certain regular shapes". Hence,they proposed the method of photoelasticity.

The authors employed the two-dimensional technique to buccolingual sections of a molar model subjected to an occlusal load. Mahler and Peyton clearly showed the differences in the internal reactions of normal models, models 'filled' with a class I type amalgam restoration, and models 'restored with a gold inlay preparation'. However, they did not take into

account in their models, the difference between the enamel and dentine mechanical properties in the real structure, but instead, constructed their models from just one photoelastic material. Consequently, as will be shown later, the stress patterns obtained from their analyses are not truly representative of the actual real life situation.

In his paper in 1958 Mahler (50), employed almost an identical approach to that described above to investigate various aspects of the design of proximo-occusal restorations in mandibular first molars. Mahler again used Catalin 61-893 for his photoelastic model but this time used it in conjunction with dental stone as a supporting material. As before, no distinction was made in the models to simulate the enamel/dentine tooth structure combination. It is also extremely doubtful whether the dental stone provides the same support to the restoration as would the dentine in the actual tooth. Hence, it is unlikely that the stress distributions Mahler obtained from his experiments are pertinent to actual proximo-occlusal restorations in normal molars.

In a long series of articles during the past six years, Craig's team of researchers at the University of Michigan, have reported on various studies using two-dimensional photoelastic techniques which were concerned with different aspects of restoration design. The first two articles in the series Craig et al (51, 52), investigated the stress distributions occurring in inlays and crowns for different loading conditions. Their models consisted of a photoelastic restoration supported on an aluminium base. The aluminium base represented the area

of the dentine and this was luted to the 'restoration' by means of improved stone. Thus, the authors made no attempt to match the modulus ratios of their model materials with those of. the dental tissues which they were representing. As will be shown later in this chapter, failure to do this can seriously affect the resulting stress analyses.

In the next five parts of the series, El-Ebrashi *et al* (53, 54, 55, 56, 57), endeavoured to match the ratios of the moduli of their photoelastic materials with those of the tooth structure. However, they can be criticized through the fact that they used an average modulus of elasticity for tooth structure of $8.5 \times 10^6$ p.s.i. instead of the modulus for dentine of only $1.7 \times 10^6$ p.s.i., (see chapter three). This of course, makes a considerable difference to the ratio of the moduli of gold/tooth structure as opposed to that of gold/ dentine. Also, the models reported in this series of papers, did not simulate either the 'enamel-dentine' tooth structural combination or the pulp chambers. All of these factors seriously affect the models' structural behaviour and consequently the photoelastic analyses. This has been clearly demonstrated recently in an article by Tanner (58).

In the most recent article in the series Nally *et al* 1971 (59), investigated restorations in which porcelain was bonded to gold crowns. The authors employed three different photoelastic materials in an attempt to match the dentine/ gold/procelain stiffness combination. To do this, one of the materials was modified but it was found subsequently to creep under load. Another serious drawback experienced

was that the material used to lute the 'crown' to the 'tooth' substructure seriously affected the resulting stress patterns. In fact,it was found to act as a buffer or stress distributer.

Lehman in 1966 (60), used the three-dimensional frozen stress technique of photoelastic analysis to investigate the contact stresses occurring at the contact areas of both adjacent teeth and at points of contact between teeth and metal orthodontic clasps. Although Lehman did not include in his models the pulp chamber, he did try to take into account the enamel/dentine combination of the dental tissues by using silicone rubber to form the softer or less-stiff dentine core. From the stress patterns frozen into his slices, the author concluded that the much stiffer 'enamel' crown bore the main burden of the contact forces applied to the teeth. He also proposed that as the areas of high stress concentration are coincident with the areas associated with carious lesions, they could be instrumental in the onset of dental caries.

In 1968 Johnson et al (61), used the three-dimensional photoelastic frozen stress technique in order to study five different designs of class I cavities in models of the mandibular first molar. The models, which were six times full size, were cast in an aluminium mould and were produced with both normal shaped and crudely shaped rectangular type pulp chambers. The cavities were prepared in the models with the aid of a template but were left 'unfilled'. Loading of the test specimens was carried out realistically using another

model simulating the opposing maxillary teeth. Obviously, load was only applied to the simulated tooth structure and not to the 'restorations'. Although the authors clearly show in their results the benefits to be gained by rounding the internal line angles, their conclusions must be open to question as their models did not represent the actual enamel/dentine/filling combination of the normal dental situation.

Lehman also in 1968 (62), employed the frozen stress method to investigate the stresses which occur in the alveolar bone due to occlusal loading of the teeth. However, the author's models did not simulate either the periodontal membrane or the areas of cancellous tissue in the maxillar and mandibular processes. Assuming contact to take place between the 'tooth' and 'socket wall', Lehman applied the theory relating to the stresses induced by two stiff cylinders in contact, in order to estimate the stresses in the 'alveolar wall'. Although he concluded that the alveolar bone was "well able to cope with all the normal masticatory efforts and even maximum exertions", the serious limitations of the author's models certainly leave open to question the applicability of his results to the natural functioning dental structures.

In 1971 Farah and Craig (63), employed the reflective photoelastic technique to look at the surface strains in a fixed partial denture under load. The prosthesis, a four unit bridge having two central pontics, was supported by first bicuspid and second mandibular molar abutments, FIG. 5.8. By using this method, an actual or typical bridge was employed;

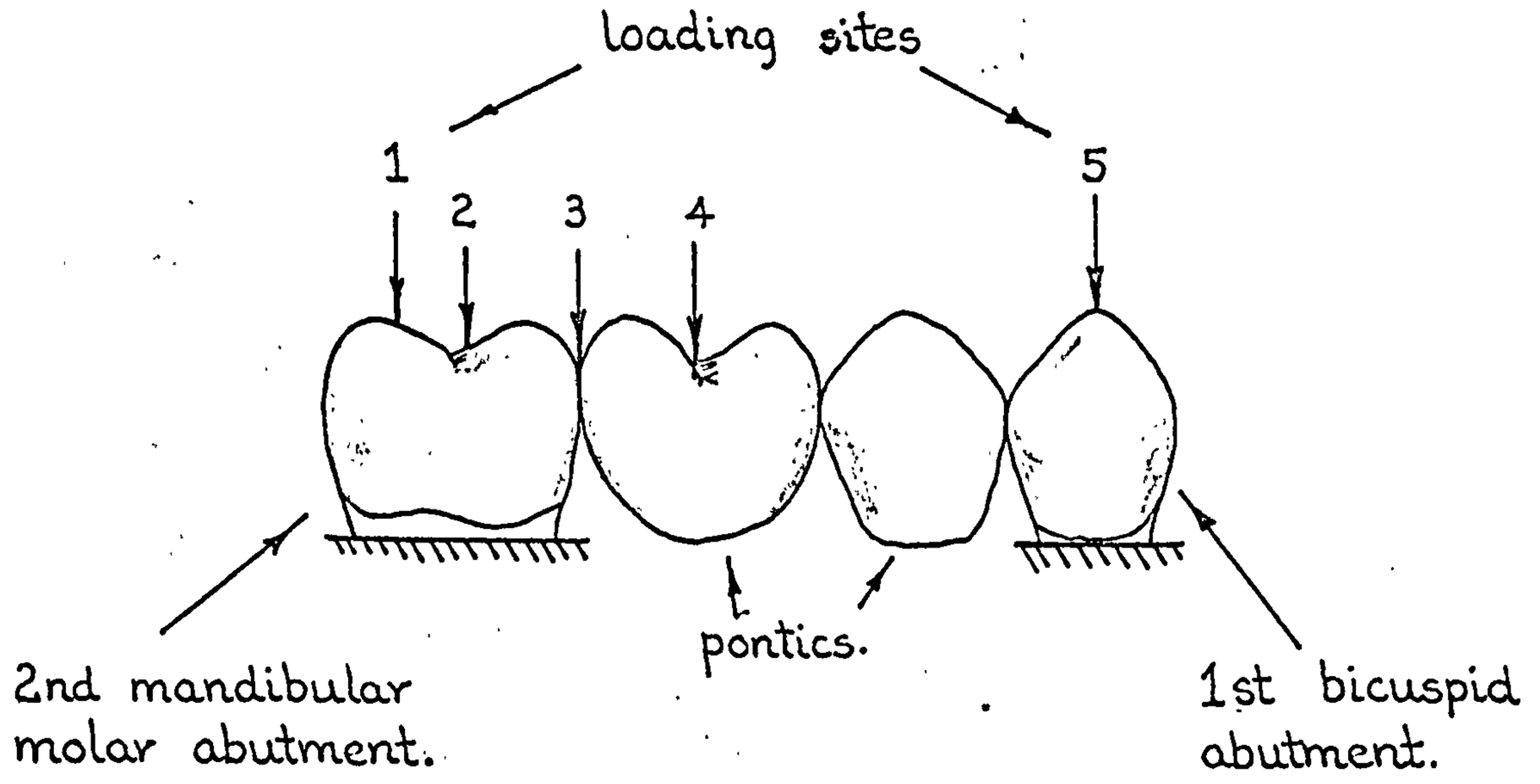


FIG. 5.8 A four unit bridge having two central pontics. Farah and Craig (63).

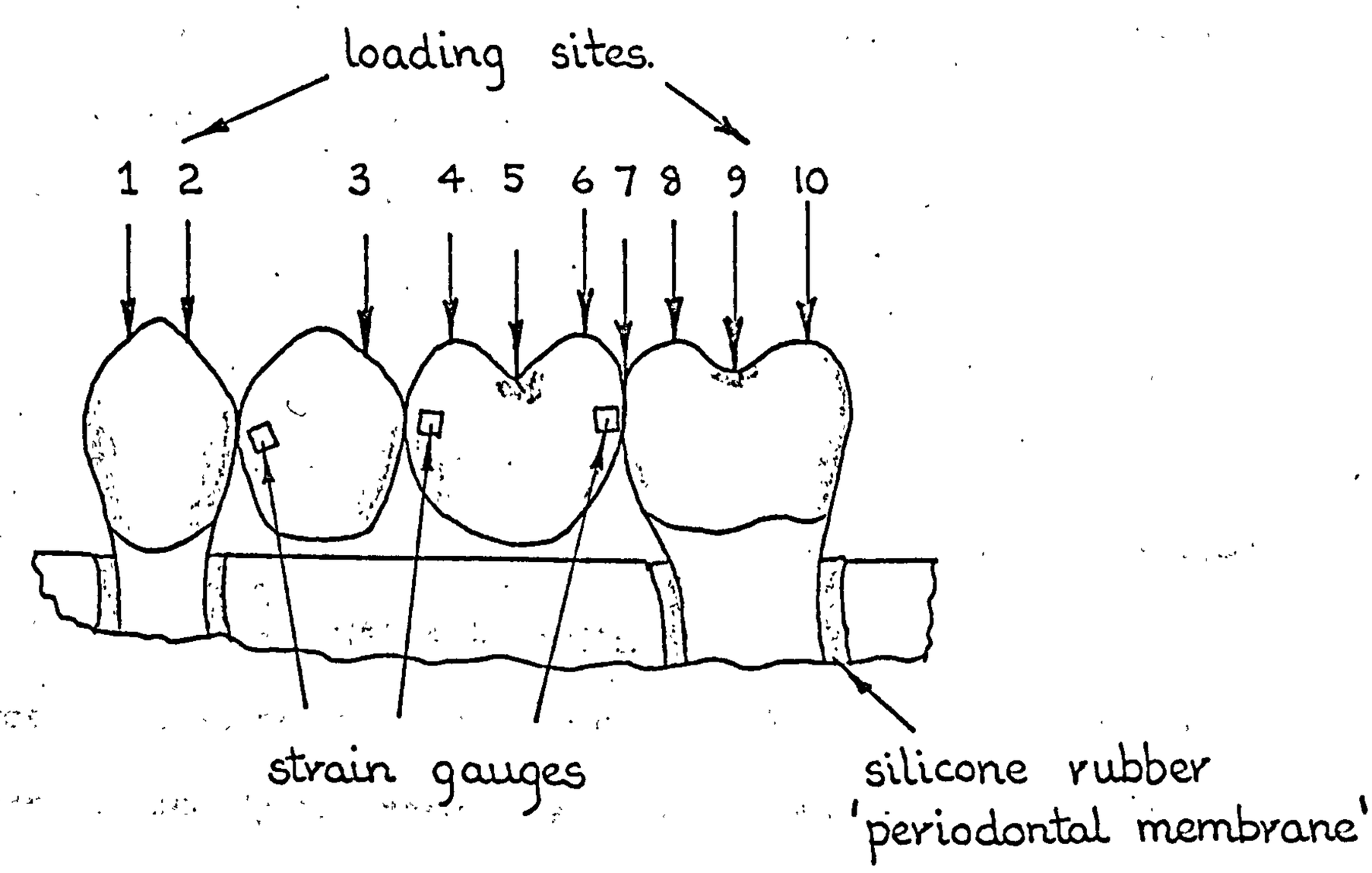


FIG. 5.9 Four unit bridge model containing three resistance strain gauges at the soldered joints. Tillitson et. al. (66).

it was simply coated with a uniform photoelastic layer. The bridge was loaded at the five different sites indicated, with static 100 pound loads and the resulting interference patterns observed at normal and obique incidence.

From their experiments, the authors concluded that the soldered joints of the bridge were subjected to the highest strains while the gingival areas of the pontics were almost strain free. However, Farah and Craig also pointed out that the overall bridge behaviour was critically dependent upon the support provided by the roots of the abutment teeth. Thus, it is apparent that in models of this kind the simulation of the periodontal membrane and alveolar bone support is of vital importance.

Sharry et al in 1960 (64), successfully employed the brittle lacquer coating technique to study the deformation behaviour of dried human skulls fitted with artificial dentures.
Each skull was supplied in turn with dentures which contained teeth having anatomical and non-anatomical forms. The dentures were separated from the bones of the skulls by a layer of rubber based material. The jaws of the skulls, which were sprayed with a coating of a brittle lacquer, were brought into 'occlusion' by forces applied statically in areas and in directions comparable to those applied by the normal masticatory musclature. Between the tests with dentures having anatomical and non-anatomical shaped teeth, the old brittle lacquer coating was removed and replaced with a new one.

From the crack patterns obtained from their tests,the authors agreed that the deformation of the alveolar bone was greater with dentures having anatomical shaped teeth than it was for the dentures having flattened or non-anatomical teeth. Sharry *et al* also concluded that deformation was also much less under heavy bone structure than it was under medium or light structures when they were subjected to the same loading conditions.

Craig and Peyton in 1965 (65), also employed the brittle lacquer coating technique to investigate the behaviour of fixed partial dentures. Three forms of gold alloy prosthesis were tested by attaching the bridge to plastic abutment teeth which were embedded in an acrylic 'alveolar' base support. Each partial denture was sprayed with a uniform layer of the brittle lacquer coating and was subjected to a particular loading condition. From their experiments the authors claimed that the stress and direction of the strains produced were a function of the magnitude of the load, position and direction at which the loads were applied and the design of the bridge and its supporting abutments.

The use of electrical resistance strain gauges was employed by Tillitson *et al* in 1970 (66), to study the structural behaviour of fixed partial dentures. Gold and chromium alloy four unit bridge models were constructed having two pontics and the same abutments as the experiment represented in FIG 5.8. However, in this series of experiments the abutment teeth were supported in an acrylic resin base on a 0.5 mm thick layer of

silicone rubber 'periodontal membrane'. Three strain gauges were cemented to the pontics and the surface strains were recorded for ten different loading conditions for both the gold and chromium alloy dentures, FIG 5.9. Although the strain gauges were attached to maximum strain areas, (as determined by a brittle lacquer coating study), the authors were unable, due to the physical size of the gauges and the surface curvatures of the structures, to attach gauges to the critical areas close to the soldered joints at the abutments.

## 5.5 THE FINITE ELEMENT METHOD

The advent of the high speed electronic digital computer has generated new and powerful methods of analysis. The Finite Element Method is one such technique. Although the method's rapid development can be attributed to its application in the field of structural stress analysis; i.e. for the analysis of aircraft structures, road and rail bridges, multi-storey building frames, reactor pressure vessels and arch dams, it is adaptable to solve other field type phenomena, e.g. fluid and heat flow problems.

The heart of the Finite Element Method lies in the manner in which the structure or body to be analysed can be represented as an assemblege of small individual portions or elements. FIG 5.10 shows the simple two-dimensional photoelastic model representation of a shoulderless mesioocclusodistal inlay (MOD) taken from the paper of Craig et al (51). In FIG 5.11,the same structure is shown subdivided into ninety straight-sided

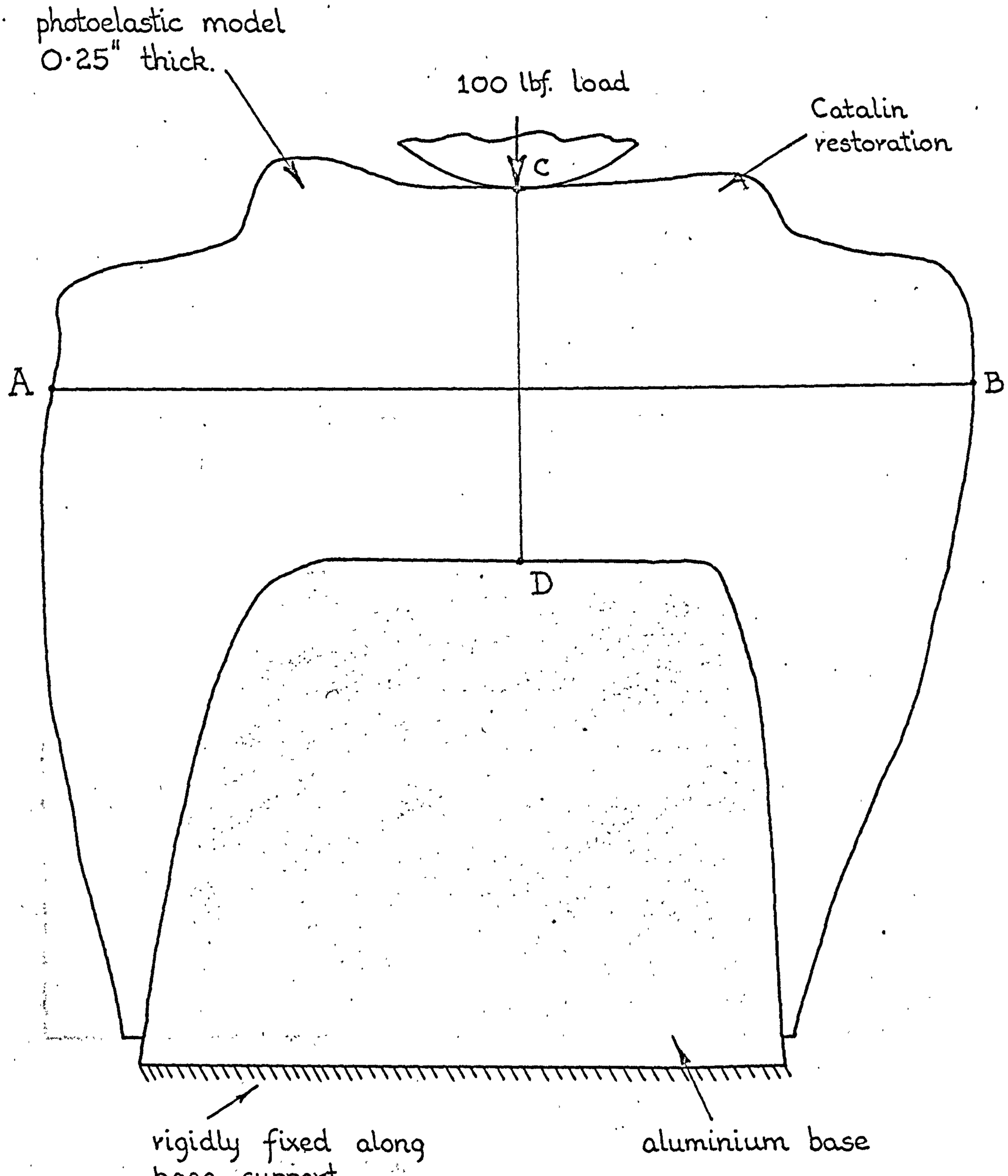


FIG.. 5.10 Two-dimensional photoelastic/aluminium M.O.D. restoration. Craig et. al. (51).

1*$PHOTOELASTIC CRAIG MODEL

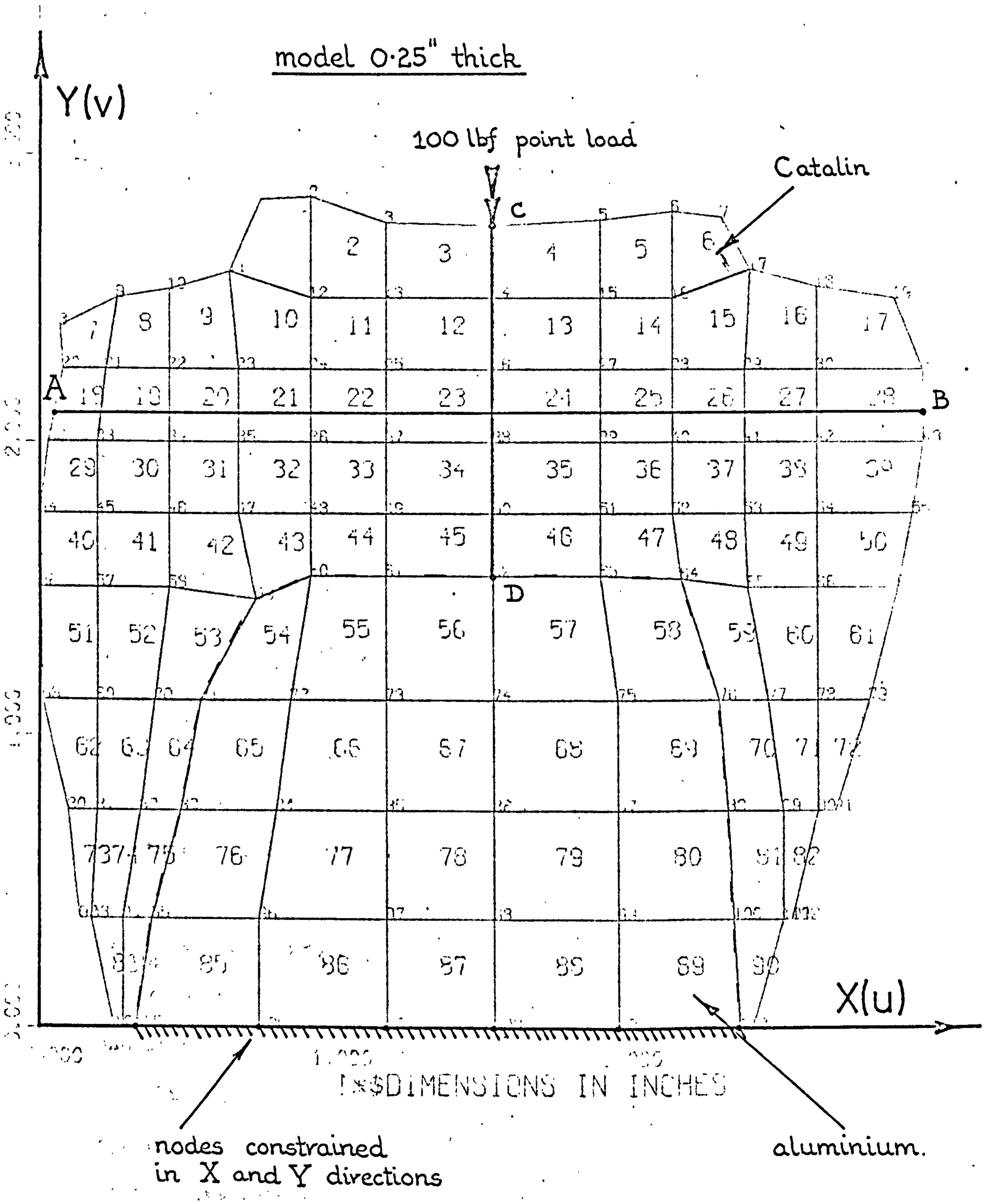


FIG. 5.11 Computer plot of Craig's model of a M.O.D. restoration constructed by ninety 4-noded 2-D finite elements.

quadrilateral shaped lamina elements of constant thickness. Each element is considered to be interconnected to each of its neighbours only at a number of discrete points, called nodes. These happen to be lines or line nodes in this instance.

Let us suppose that it is required to determine the stresses, strains and displacements throughout the structure due to the single static masticatory force shown in FIG 5.10. In order to obtain the stress and strain components, the displacement components of each of the nodes must first be calculated. That is the u and v displacements with respect to the corresponding X and Y Cartesian co-ordinate reference system. These can be determined by solving the equilibrium equations for the whole structure which can be derived using well known engineering principles of solid body mechanics. Obviously, the greater the number of nodes there are in the structure, the greater the number of equations there are to be solved. This necessitates the use of an electronic digital computer. Because stress and strain components are calculated from the nodal displacements, it follows that the larger the number of elements there are in the structure, (that is the finer the mesh), the more accurate are the stress and strain patterns obtained.

The equilibrium equations can be visualised as being 'cause and effect' relationships and relate the nodal force components of the structure to the corresponding nodal displacements by means of stiffness coefficients. In the same way that the individual elements combine together to form one structure,

so the set of stiffness coefficients for each of the separate elements can be assembled (superimposed), to form the stiffness coefficients of the whole structure.

In deriving the structural equilibrium equations,the actual mechanical properties of the materials involved are employed and so isotropic, anisotropic, non-linear elastic or even viscoelastic effects can be included. The mesh pattern is obviously constructed such that no element crosses a material boundary, e.g. between the Catalin and the aluminium (or enamel and dentine). Hence,elements on either side of the interface are assigned the appropriate material or tissue properties.

While the actual element arrangement takes care of the structure's geometry and layout, the relative size of the structure is incorporated in setting up the equilibrium equations by using the Cartesian co-ordinates of each node relative to some fixed datum.

Masticatory forces or known deformations are also easily simulated. These are simply applied at the appropriate node or nodes before the equilibrium equations are solved. (Fixed or constrained nodes are merely ascribed zero values of displacement). It is also a relatively simple matter to take into account thermal loading, (due to temperature gradients), or pre-stressing effects. First of all,the thermal or pre-stressing strains are calculated for each element. Then an equivalent set of element nodal forces are determined

such that they would produce the same strains in the element. These forces are then subsequently summed over all of the elements adjoining each node and the resulting force applied at the corresponding structural node as before.

Once the nodal displacements have been obtained it is a relatively simple task to calculate the stresses and strains at any point in the structure. These are calculated using the displacement components and the appropriate material properties at the particular point of interest.

To illustrate the application of the Finite Element Method,the two-dimensional MOD inlay model shown in FIG 5.10 will now be analysed and the results compared with the photoelastic results of Craig et al (51). The importance of matching the ratios of the photoelastic model properties with those of the simulated structure will also be investigated.

The nodal X and Y Cartesian co-ordinates; the aluminium and Catalin mechanical properties; the element node numbering sequence and the element thickness data are fed into the general two-dimensional finite element analysis program. In fact,FIG 5.11 is a computer plot of the nodal co-ordinates and the nodal and element numbering sequence. This 'regurgitation' is a necessary check to see that the data fed into the computer is correct. (It is an easy matter to make an error when measuring or punching the nodal coordinates of the structure.) The program then calculates in turn all the element stiffness coefficients and sets up the structural equilibrium equations. Finally, the masticatory load is 'applied' at node number 4 in

the Y coordinate direction and the nodes 105, 106, 107, 108, 109 and 110 are constrained, (ascribed zero valued displacements), to simulate the fixity of the aluminium base support. Once these boundary conditions have been applied,the structural equilibrium equations are solved and all the nodal displacement components are obtained. The program using these 'now known' displacements then derives the strain and stress components at the centroids of each of the ninety elements. FIG 5.12 a and b, shows the comparison between the finite element results and Craig's et al (51) photoelastic results for the vertical stress distribution across the lines AB and CD shown in FIG 5.10.

To investigate the effects of model materials the same structure is analysed with i) Enamel/dentine and ii) Gold/ dentine material combinations instead of the Catalin/aluminium materials. This is very easily accomplished using the finite element method by simply changing the material property data cards fed into the program.

The vertical stress distributions for the three cases analysed across AB and CD are compared in FIG 5.13. The finite element method also 'gives' the displacement components at every node in the structure. FIG 5.14 shows the vertical deformation across AB, obtained by plotting the nodal v displacements of node numbers 32, 33 ..... 42 and 43. It can be seen from these plots how the photoelastic model material results differ significantly from the natural dental tissue and material results. Clearly, the photoelastic model material properties must have the same ratios as the materials

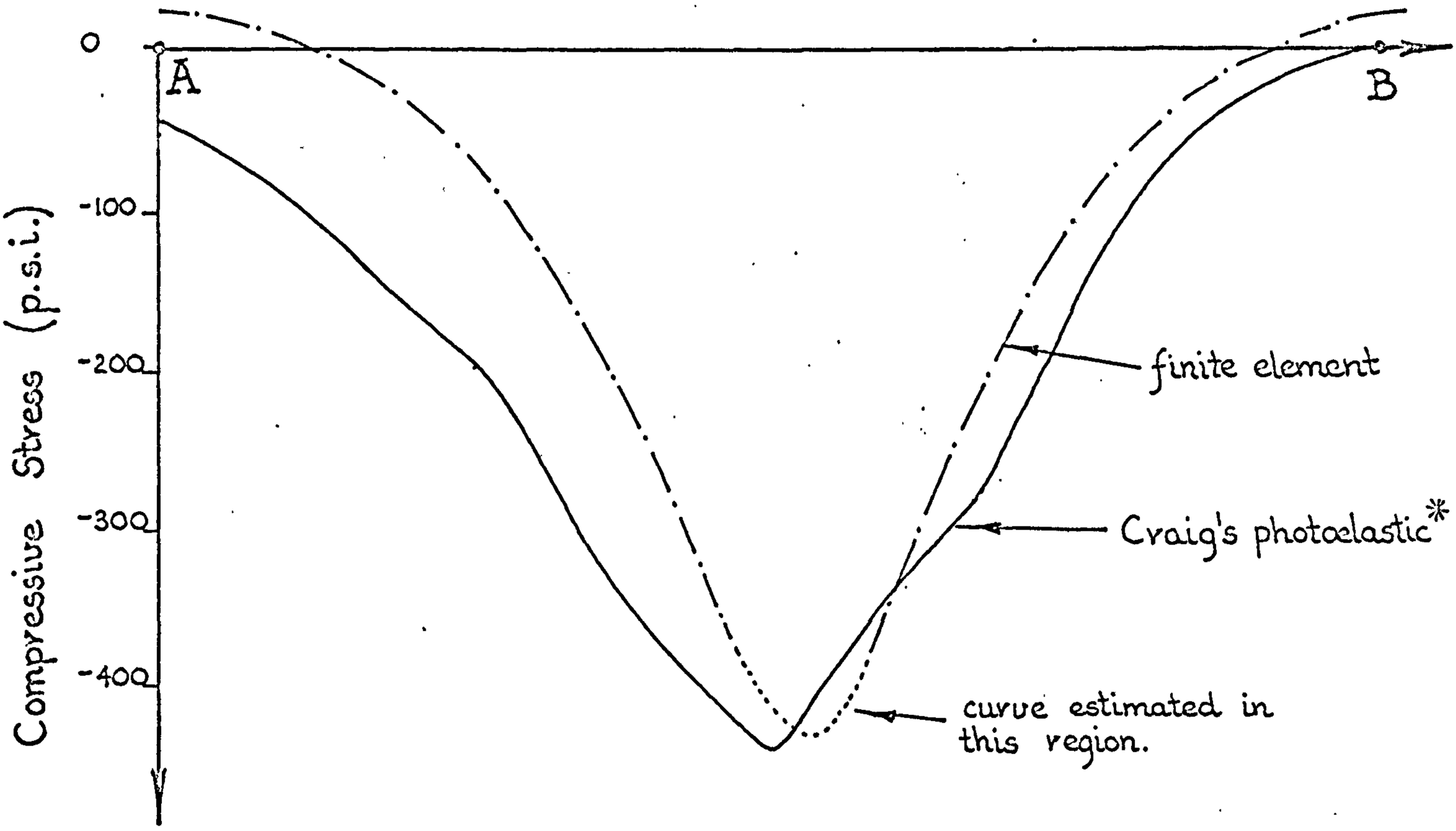


a) Vertical stress distribution across A-B

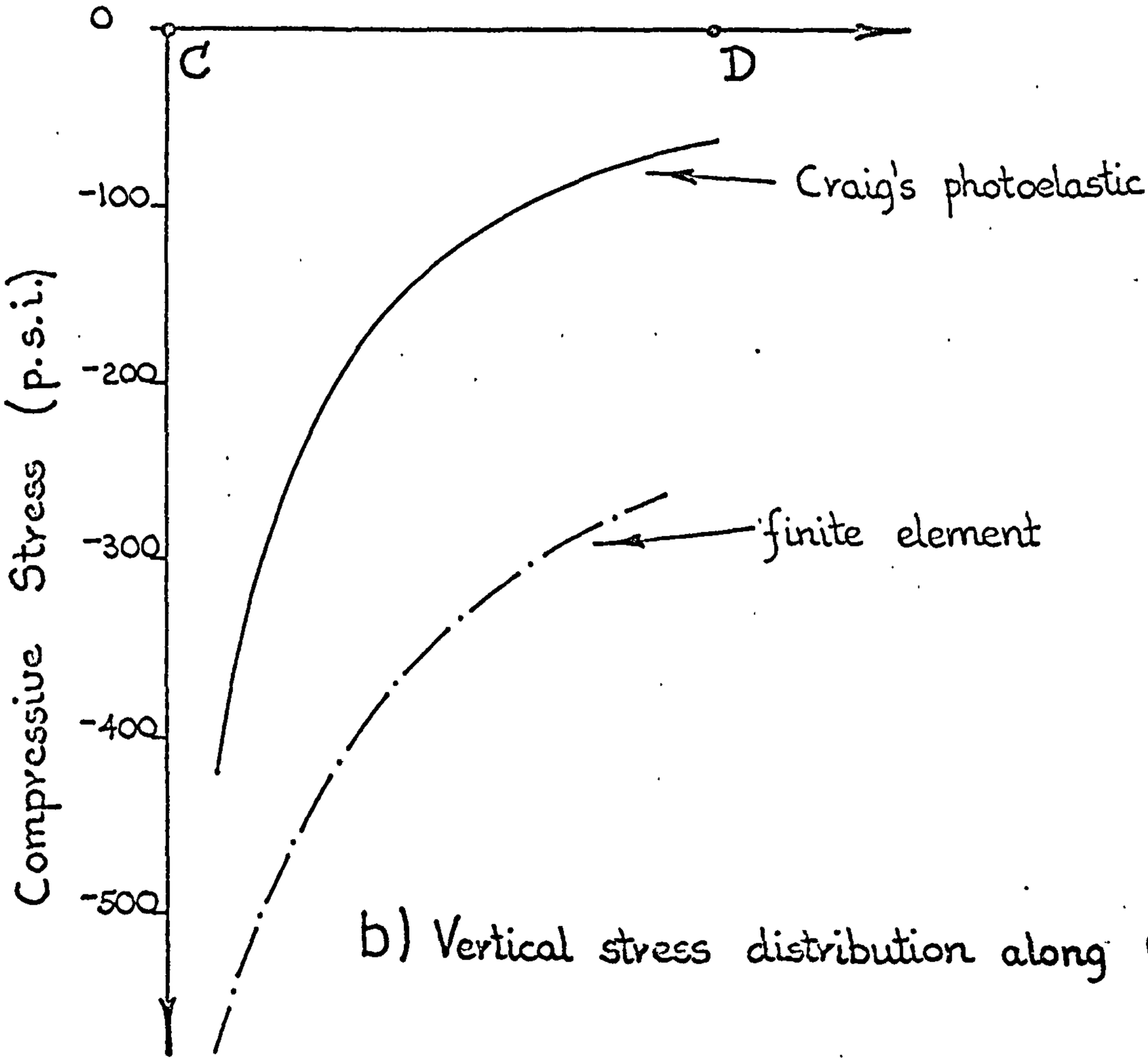


b) Vertical stress distribution along C-D

FIG. 5.12 Comparison of stress distributions obtained from the finite element and Craig et. al.(51) photoelastic models.

*Reference (51) values times four. Personal communication Craig et.al.

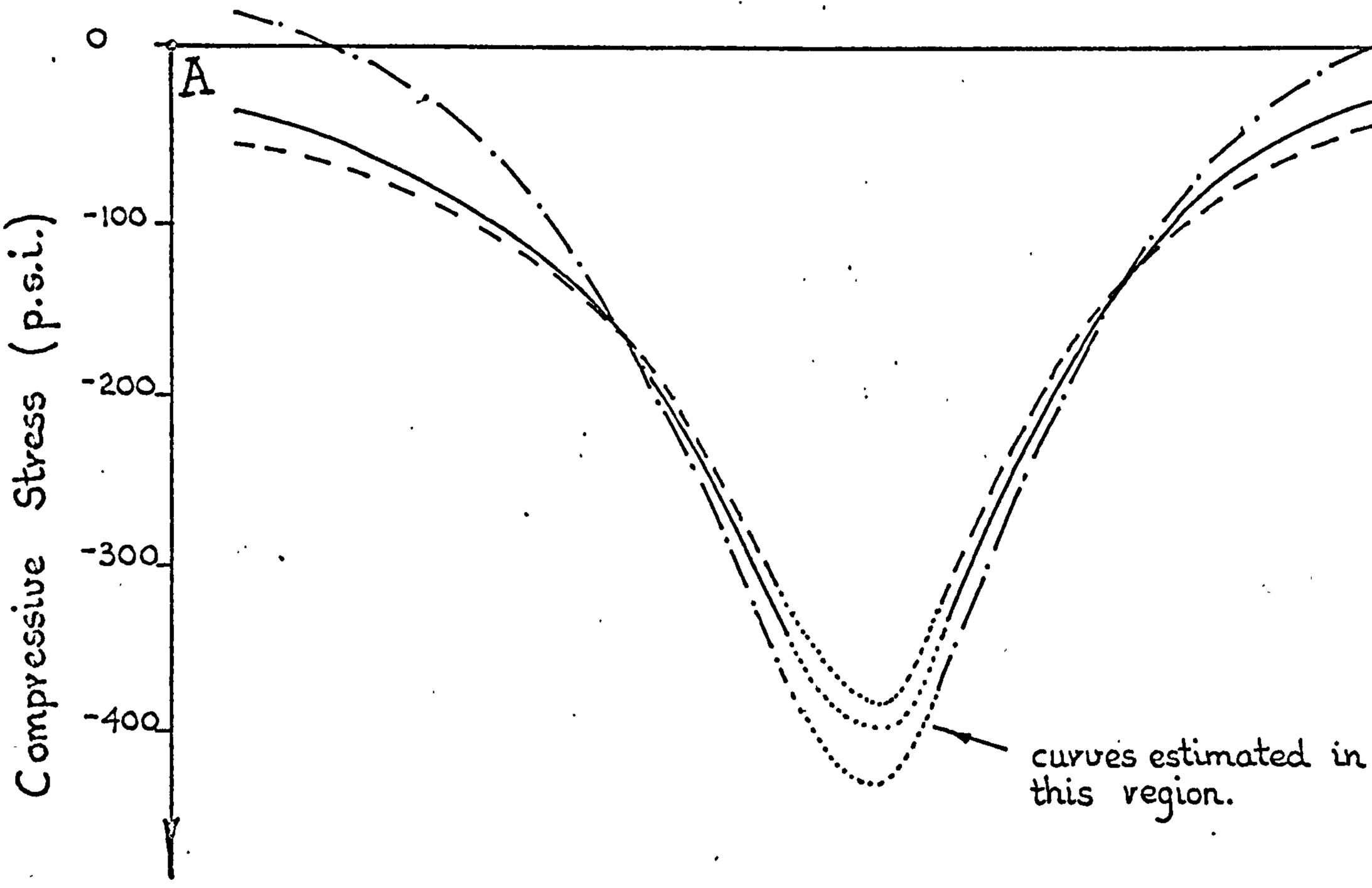


a) Vertical stress distribution across A-B

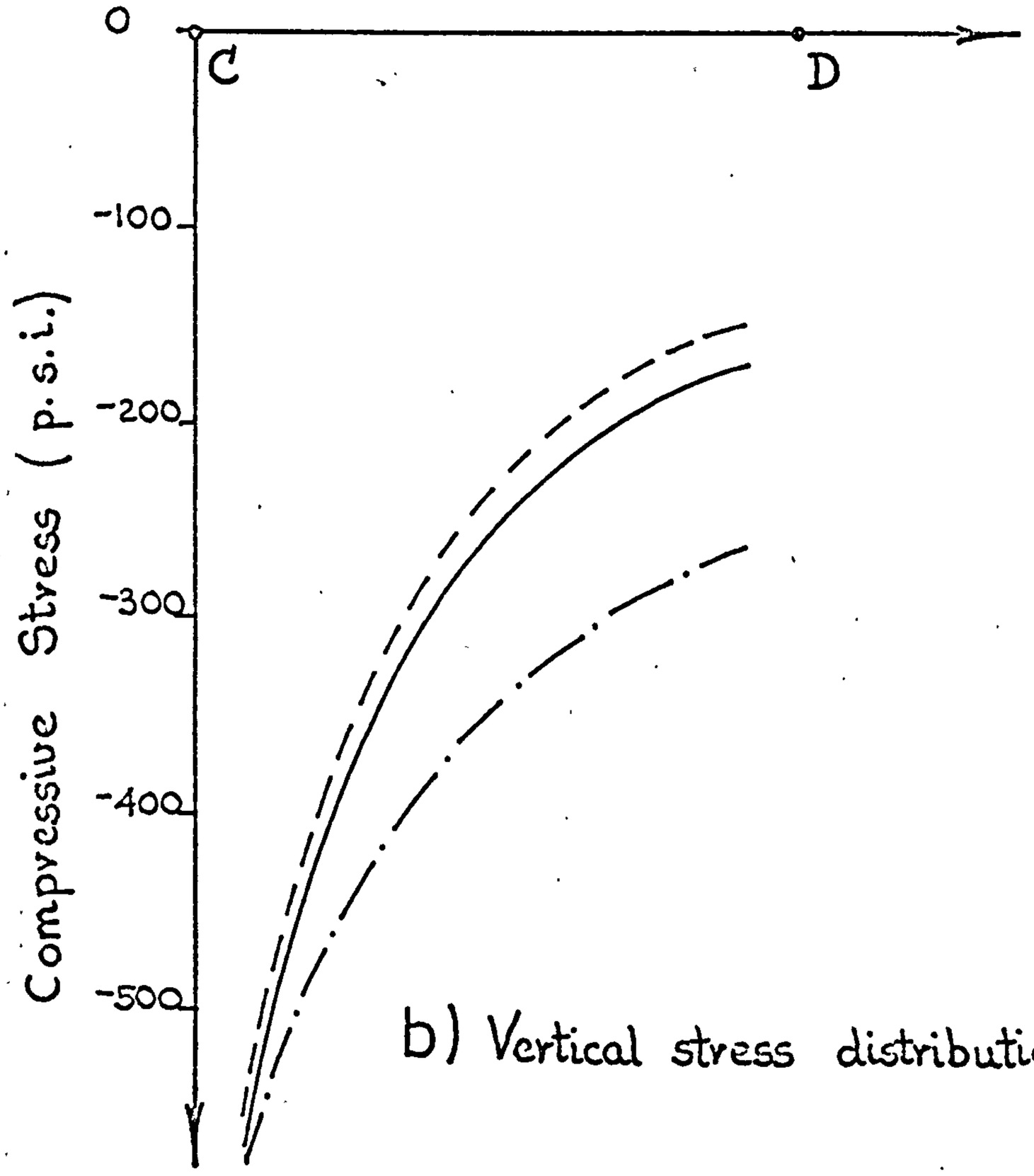


b) Vertical stress distribution along C-D

FIG. 5.13 Comparison of stress distributions obtained from the finite element model using different material combinations.

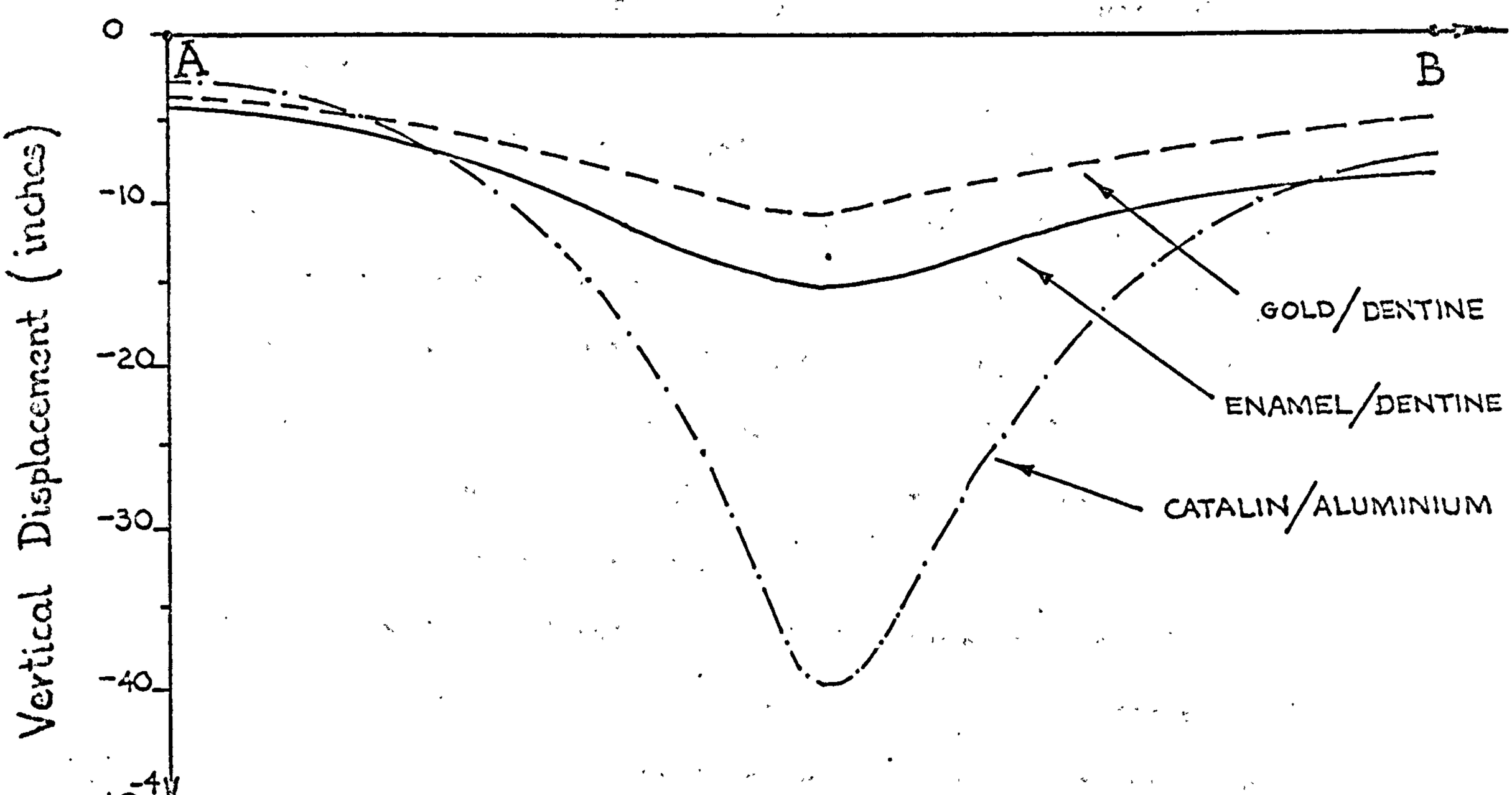


FIG. 5.14 Comparison of the vertical displacement distribution across A-B obtained from the finite element model using different material combinations.

## TABLE OF MATERIAL PROPERTIES.

| PROPERTY (ISOTROPIC) / MATERIAL | E (p.s.i.) | $\mu$ | G (p.s.i.) |
|---|---|---|---|
| CATALIN | $6{\cdot}15\times10^{5}$ | 0·365 | $2{\cdot}25\times10^{5}$ |
| ALUMINIUM | $10{\cdot}0\times10^{6}$ | 0·33 | $3{\cdot}76\times10^{6}$ |
| GOLD | $11{\cdot}3\times10^{6}$ | 0·3 | $4{\cdot}34\times10^{6}$ |
| ENAMEL | $6{\cdot}8\times10^{6}$ | 0·3 | $2{\cdot}61\times10^{6}$ |
| DENTINE | $1{\cdot}7\times10^{6}$ | 0·3 | $0{\cdot}654\times10^{6}$ |

of the simulated structure in order to obtain meaningful results.

The Finite Element Method is not restricted to two-dimensional structures. Axisymmetric and three-dimensional elements can also be employed, see FIG 5.15. Elements can also have curved boundaries or surfaces, (depending upon the number of nodes on the boundary or surface), and so, by using three-dimensional elements almost any dental structure can be modelled and analysed.

For a detailed and mathematical treatment of the Finite Element Method; the derivation of the element stiffness coefficients and the structural equilibrium equations; and the subsequent development and testing of the computer programs used in this project, the interested reader is referred to Volume Two of this thesis.

## 5.6 DISCUSSION

It can be appreciated from the previous five sections that the results obtained from the methods, models and techniques of analysis discussed, are no better than the assumptions, limitations and simplifications involved in their derivation.

Mathematical models, in order that they do not become too unwieldy are generally limited to simple shapes, e.g. cones or cylinders, and to simple forms of material behaviour.

While simulation techniques or models maintain a visual or physical appreciation of the problem, it is very difficult to simulate living tissues with inanimate materials,e.g. the

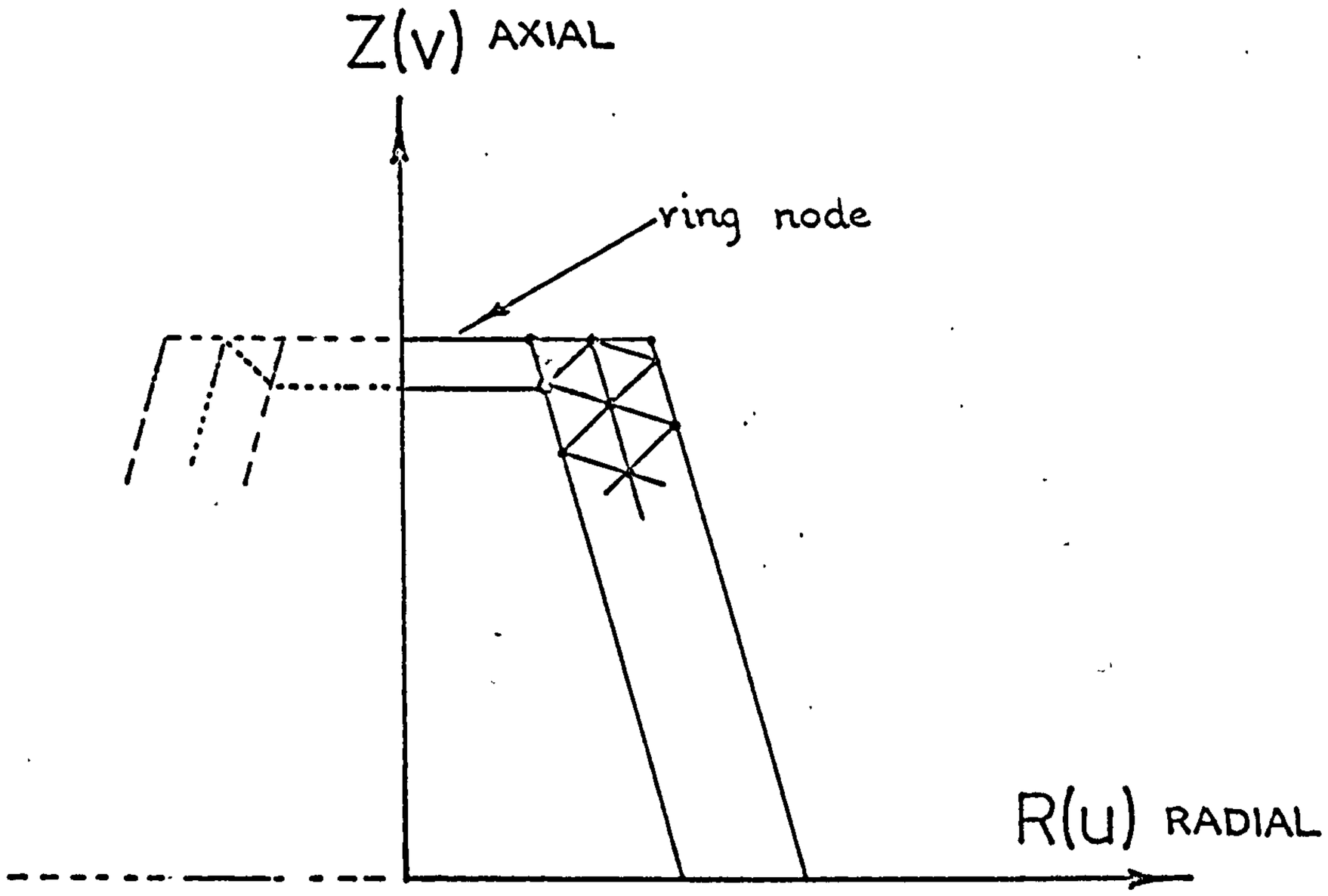


a) 3-noded axisymmetric or ring-type element.

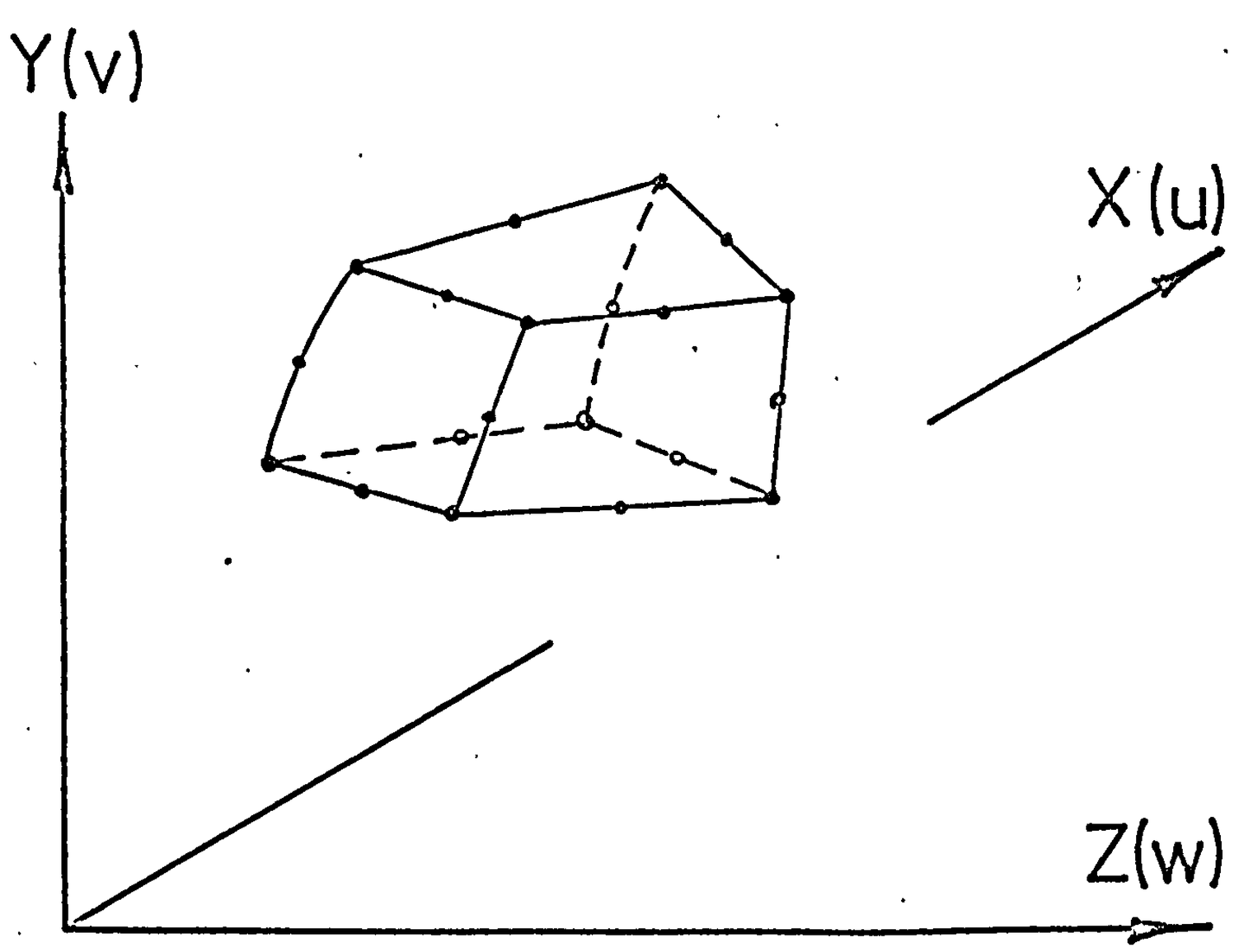


b) 20-noded three-dimensional finite element.

FIG. 5. 15 Illustrating typical axisymmetric and three-dimensional finite elements.

periodontal membrane with rubber.

Experimental methods also have their difficulties. Strain gauges are sometimes limited in their application due to their mere physical size and to environmental problems, e.g. adherence problems on wet materials. Again,while photoelastic techniques offer pictorial or physical appreciative advantages, they also have their drawbacks when composite structures are investigated. Relatively few materials are photoelastic and so the choice and range of the materials available is restrictive. Although attempts have been made to 'doctor' them and modify their mechanical properties, other problems,e.g. time effects,are usually introduced as well.

The Finite Element Method seems to offer many advantages over other techniques. (Always assuming of course that a large computer complex is available). Not only can three-dimensional structures be investigated but also fairly complex geometry and material behaviour can be included. While not eliminating the need for clinical experiments,the method can be employed as an exploratory research tool.

# CHAPTER SIX

# DETERMINATION OF MECHANICAL PROPERTIES OF TISSUES

# 6. DETERMINATION OF MECHANICAL PROPERTIES OF TISSUES

## 6.1 INTRODUCTION

To carry out any analytical static stress analysis it is generally necessary to know the type of behaviour and possibly also the associated mechanical properties of the particular materials concerned. The finite element method is no exception. Consequently, to analyse dental structures with this method it is required to know such data for all of the tissues and restorative materials involved. Although the finite element method is not confined to dealing with simple material characteristics, the work described later is restricted to analyses involving linear elastic, isotropic and orthotropic behaviour. Hence, the mechanical properties required are the elastic constants, namely, the Young's moduli, Poisson's ratios and the shear moduli, or, for simplicity, their pseudo equivalents, i.e. values derived by linearizing a non-linear material response.

Because of the lack of certain tissue property data, the finite element method has been used to obtain some overall values for these hitherto unknown mechanical properties. This has been accomplished by using the method in reverse. That is, instead of deriving the equilibrium equations for a structure of known geometry and material properties and determining the structural deformation due to a certain loading condition; the equilibrium equations have been derived by iterating the material properties in order to

achieve a 'known' structural deformation for a given loading configuration.

This chapter discusses two such experiments, the first determines some of the unknown elastic constants of cortical bone while the second investigates the behaviour and properties of the periodontal membrane.

## 6.2 CORTICAL BONE

### 6.2.1 Theoretical Considerations

It was concluded in Chapter 3 that cortical bone is approximately a linear elastic orthotropic material. A general orthotropic material has three axes of elastic symmetry which are all at right angles to one another. Consequently, the material has nine independent elastic constants, namely, three Young's moduli, (in the directions of the three elastic axes), three shear moduli, (relating to shear deformation in the three co-ordinate planes) and finally three Poisson's ratios, which are in cyclic permutation, the passive induced-strain in one co-ordinate direction with respect to the active stress-induced-strain in another co-ordinate direction, (i.e. $\mu_{xy}$, $\mu_{yz}$ and $\mu_{zx}$, subscript notation as defined in section 3.2.10).

One may wonder at this point why there are not six different Poisson's ratios, i.e. the above plus $\mu_{xz}$, $\mu_{yx}$ and $\mu_{zy}$. The reason for this seemingly reduced number of elastic constants can be argued either on a mathematical basis or by

a purely physical approach. A brief outline of the latter will be discussed here.

Consider an elementary cube of a general orthotropic material with its elastic axes of symmetry orientated in the X, Y, Z Cartesian coordinate directions as illustrated in FIG 6.1. The normal and shear components are shown with arrows indicating the assumed directions of the positive values. The three normal stresses, namely $\sigma_{xx}$, $\sigma_{yy}$ and $\sigma_{zz}$ not only produce active normal strains in their own coordinate directions but also passive normal strains in each of the other two coordinate directions as well, see section 3.2.3. For example $\sigma_{xx}$ induces a normal active strain in the X Cartesian coordinate direction equal to $\frac{\sigma_{xx}}{Ex}$ and passive strains in the Y and Z coordinate directions equal to

$\mu_{xy}\frac{\sigma_{xx}}{Ex}$ and $\mu_{xz}\frac{\sigma_{xx}}{Ex}$ respectively. This process can be similarly adopted for the other two normal stresses $\sigma_{yy}$ and $\sigma_{zz}$.

It has been found experimentally that the three normal strain components, when considered to be acting in the directions of the axes of elastic symmetry, do not affect the shear strains and neither do the shear strains interact with one another. Consequently, the shear strains are simply $\gamma_{xy} = \frac{\tau_{xy}}{Gxy}$, $\gamma_{yz} = \frac{\tau_{yz}}{Gyz}$ and $\gamma_{zx} = \frac{\tau_{zx}}{Gzx}$ respectively in the three coordinate planes.

Hence, the strain-stress relationship for all the stress and strain components acting on the orthotropic material shown in FIG 6.1 are:-

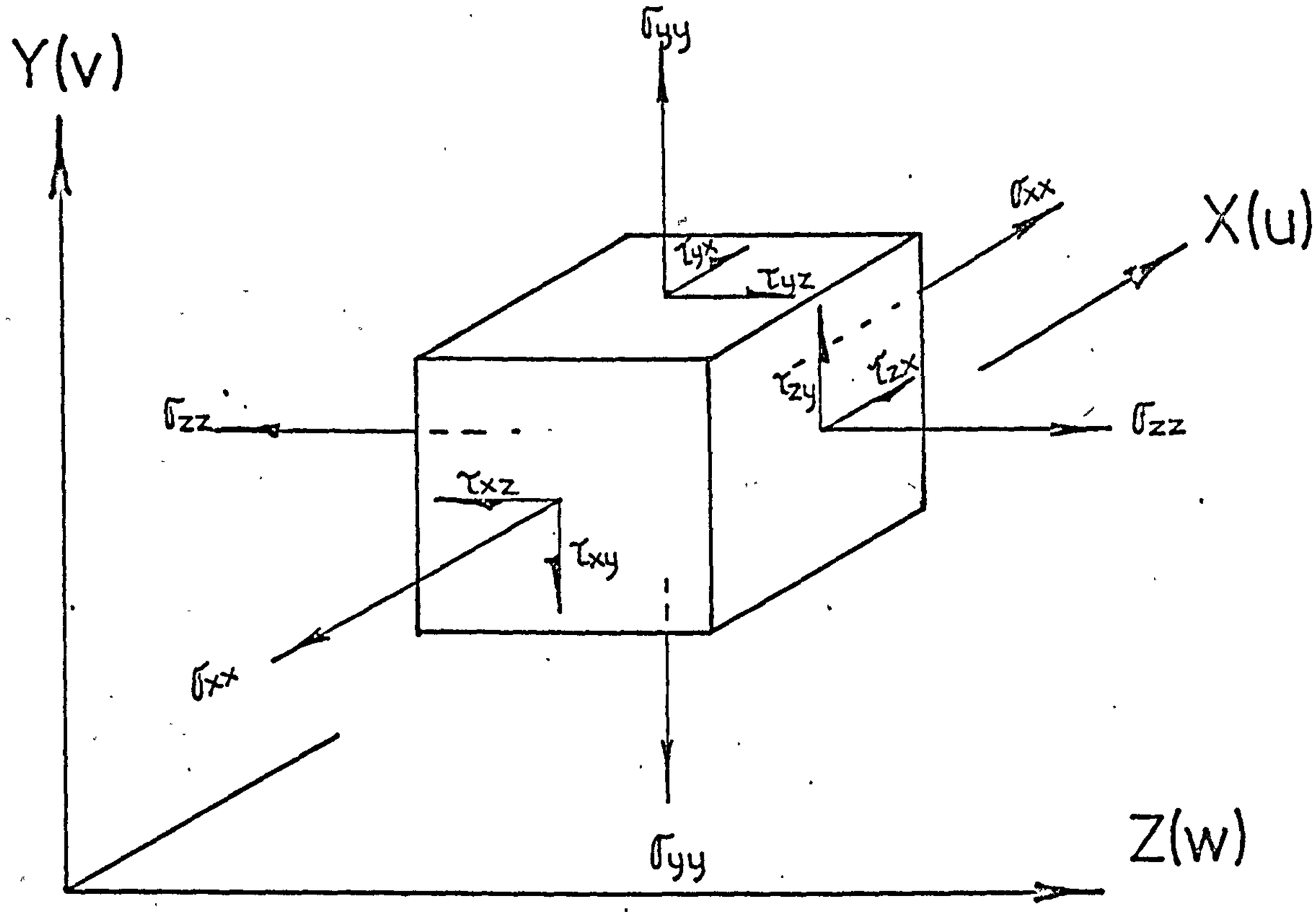


FIG. 6.1 Stress components acting on a cube of orthotropic material whose elastic axes coincide with the Cartesian axis reference system.

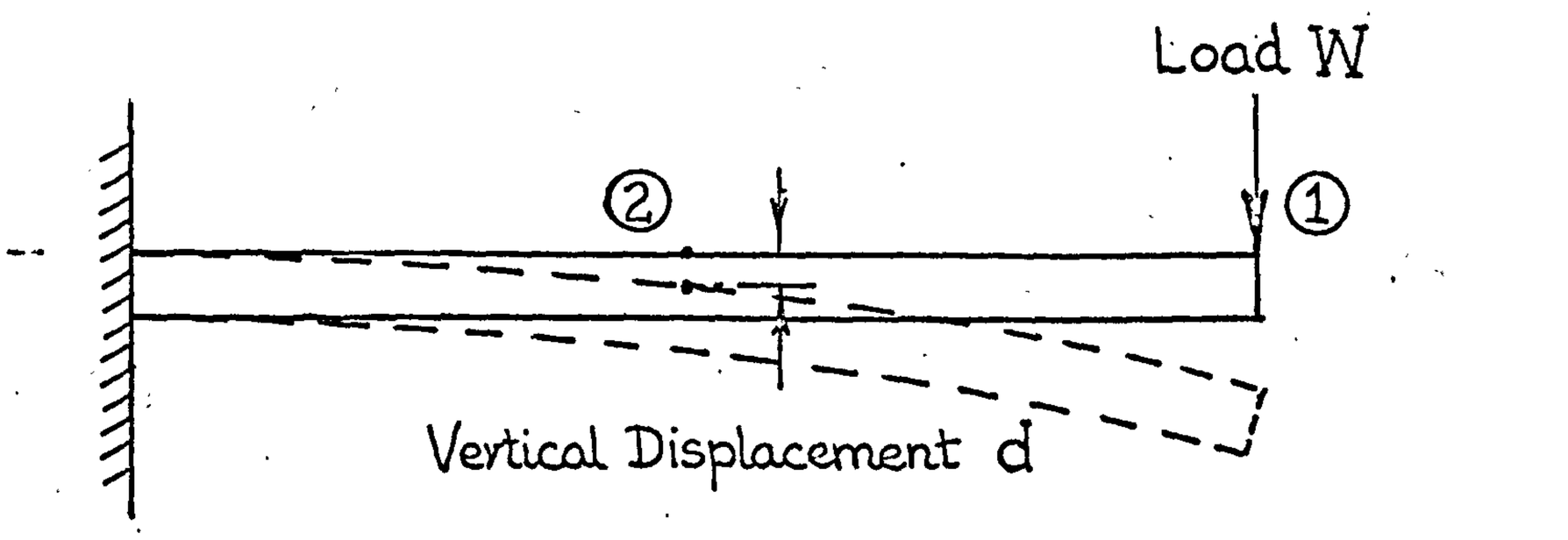


FIG. 6.2 Illustrating the Maxwell-Betti reciprocal relationship.

$$\varepsilon_{xx} = \frac{\sigma_{xx}}{Ex} - \mu_{yx}\frac{\sigma_{yy}}{Ey} - \mu_{zx}\frac{\sigma_{zz}}{Ez}$$

$$\varepsilon_{yy} = -\mu_{xy}\frac{\sigma_{xx}}{Ex} + \frac{\sigma_{yy}}{Ey} - \mu_{zy}\frac{\sigma_{zz}}{Ez}$$

$$\varepsilon_{zz} = -\mu_{xz}\frac{\sigma_{xx}}{Ex} - \mu_{yz}\frac{\sigma_{yy}}{Ey} + \frac{\sigma_{zz}}{Ez}$$

$$\gamma_{xy} = \frac{\tau_{xy}}{Gxy}$$

$$\gamma_{yz} = \frac{\tau_{yz}}{Gyz}$$

$$\gamma_{zx} = \frac{\tau_{zx}}{Gzx}$$

or more conveniently written in matrix form :-

$$\begin{Bmatrix} \varepsilon_{xx} \\ \varepsilon_{yy} \\ \varepsilon_{zz} \\ \gamma_{xy} \\ \gamma_{yz} \\ \gamma_{zx} \end{Bmatrix} = \begin{bmatrix} \frac{1}{Ex} & \frac{-\mu_{yx}}{Ey} & \frac{-\mu_{zx}}{Ez} & 0 & 0 & 0 \\ \frac{-\mu_{xy}}{Ex} & \frac{1}{Ey} & \frac{-\mu_{zy}}{Ez} & 0 & 0 & 0 \\ \frac{-\mu_{xz}}{Ex} & \frac{-\mu_{yz}}{Ey} & \frac{1}{Ez} & 0 & 0 & 0 \\ 0 & 0 & 0 & \frac{1}{Gxy} & 0 & 0 \\ 0 & 0 & 0 & 0 & \frac{1}{Gyz} & 0 \\ 0 & 0 & 0 & 0 & 0 & \frac{1}{Gzx} \end{bmatrix} \begin{Bmatrix} \sigma_{xx} \\ \sigma_{yy} \\ \sigma_{zz} \\ \tau_{xy} \\ \tau_{yz} \\ \tau_{zx} \end{Bmatrix}$$

In the above relationships the signs of the Poisson's ratios have been included so as to follow the normal or conventional notation. This implies that the material shrinks transversely when it is stretched in the third coordinate direction.

Although there are twelve different elastic constants in the above 6 x 6 matrix for the case of a general orthotropic material, the number of independent constants reduces to nine by virtue of the Maxwell-Betti reciprocal relationships, Bisplinghoff *et al* (67). This principle can be simply demonstrated by considering the cantilever illustrated in FIG 6.2. If the cantilever is loaded vertically at point 1 with a load of say W and the resulting vertical displacement at point 2 is d, then if the same vertical load W were applied at point 2 then the same vertical displacement d would be found to be produced at point 1. Employing the Maxwell-Betti reciprocal principle to the matrix of elastic constants gives:-

$$\frac{\mu xy}{Ex} = \frac{\mu yx}{Ey}$$

$$\frac{\mu xz}{Ex} = \frac{\mu zx}{Ez}$$

and

$$\frac{\mu yz}{Ey} = \frac{\mu zy}{Ez}$$

Hence, it can be seen that $\mu xy$, $\mu yz$ and $\mu xz$ are not independent of the other constants and therefore the total number of independent constants is nine. These are Ex, Ey, Ez, $\mu yx$, $\mu zy$, $\mu zx$, Gxy, Gyz and Gzx. (Obviously, the choice of the three independent Poisson's ratios is arbitrary, $\mu xy$, $\mu xz$ and $\mu yz$ could have been chosen).

Femoral cortical bone however, has been found to possess approximately the same Young's modulus in directions radial and tangential to the axis of the femur, i.e. in the Y and Z specimen coordinate directions as illustrated in FIG 6.3. Hence, considering the general anatomy of the tissue it therefore becomes apparent that cortical bone is approximately isotropic in the YZ plane. Consequently, the number of independent elastic constants for this simplified orthotropic material reduces from nine down to five. This is because:-

$Ey = Ez$ (perpendicular to bone grain)

$\mu yx = \mu zx$ (passive strains in grain direction due to stress induced strain in direction perpendicular to grain)

$Gxy = Gzx$ (in planes of bone grain)

and $Gyz = \frac{Ey}{2(1+\mu zy)}$ (bone isotropic in YZ plane)

or $Gyz = \frac{Ez}{2(1+\mu yz)}$

Thus, five independent elastic constants are:- Ex, Ey, $\mu yx$, $\mu zy$ and Gxy. Although the values of Ex, Ey and Gxy have been fairly well established, see Table 3.7, the Poisson's ratio $\mu xy$(or $\mu xz$) and $\mu yx$ (or $\mu zx$) determined by McLeish and Habboobi (3), violate the Maxwell-Betti reciprocal relationships, see section 3.5.5.

i.e. $\frac{\mu xy}{Ex} = \frac{\mu yx}{Ey}$

or $\frac{Ex}{Ey} = \frac{\mu xy}{\mu yx}$

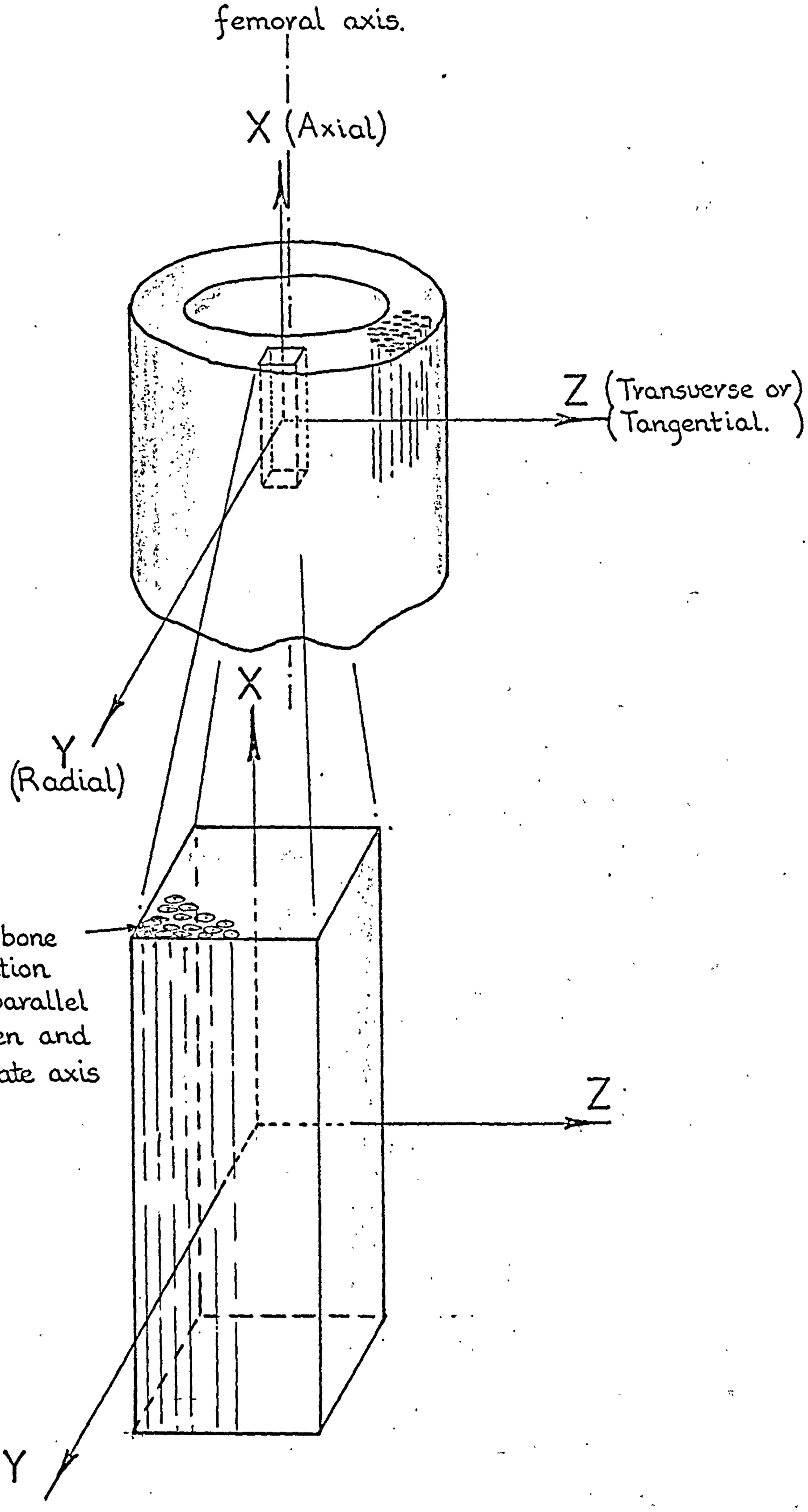


FIG. 6.3 Coordinate axis system employed in the determination of the mechanical properties of human cortical bone.

Assuming the values of the Young's moduli are correct, (this is the easier of the measurements to make), then from Table 3.7:-

$$\frac{Ex}{Ey} = 2$$

But according to McLeish and Habboobi,

$$\frac{\mu xy}{\mu yx} = \frac{0.29}{0.21} = 1.4$$

Therefore to uphold the reciprocal relationships,the Poisson's ratios must be modified. A reasonable estimate seems to be:-

$$\frac{\mu xy}{\mu yx} = 2 = \frac{0.3}{0.15}$$

This modification or rounding of the Poisson's ratios seems acceptable bearing in mind that McLeish and Habboobi inferred their values from experiments carried out on bovine material. Hence, the only property now required for the subsequent stress analyses is $\mu zy$, (or Gyz as they are not independent of each other).

Bonfield and Li (24),determined what they thought to be Gyz for bovine cortical bone from a torsion test experiment shown in FIG 3.8. By measuring tha angle of specimen rotation for a known value of applied torque,they calculated their Gyz value using the formula $\frac{T}{J} = \frac{G\phi}{L} = \frac{q}{r}$ (notation as illustrated in the figure). However, this formula is only applicable to specimens whose material properties are symmetrical about the axis of the applied torque. Obviously, this does not apply to the case in hand because as can be seen from FIG 3.8, the grain direction of the material at the sides of the specimen is different from that at the top and bottom surfaces. However,

using Bonfield and Li's results, their experiments can be simulated using the finite element method and consequently a value for Gyz obtained for the human tissue.

### 6.2.2 Analytical Procedure

The procedure employed to determine the unknown elastic constant of human cortical bone was to simulate the two torsion tests of Bonfield and Li(24) using the finite element Method. Thus by changing or iterating the property Gyz of the structural elements, the finite element results were made to converge to those obtained from their physical experiments.

Bonfield and Li carried out two torsion tests on cylindrical specimens of bovine cortical bone, one with the bone grain parallel to the axis of the test specimen and the other with the grain or osteons at right angles to the specimen axis, see FIG 3.8. The torsion specimen was represented by twenty three-dimensional orthotropic 20-noded finite elements as shown in FIG 6.4. The torque applied at the free end was determined by allowing for a maximum stress of 2000 p.s.i. to occur at the specimen surface, i.e.

$$\frac{T}{J} = \frac{q}{r}$$

$$\therefore \quad T = \frac{qJ}{r}$$

$$= \frac{2000 \times \pi \times 0.01^4}{0.005 \times 32} \text{ lbf. ins.}$$

$$\underline{\text{Torque} = 0.000393 \text{ lbf.ins}}$$

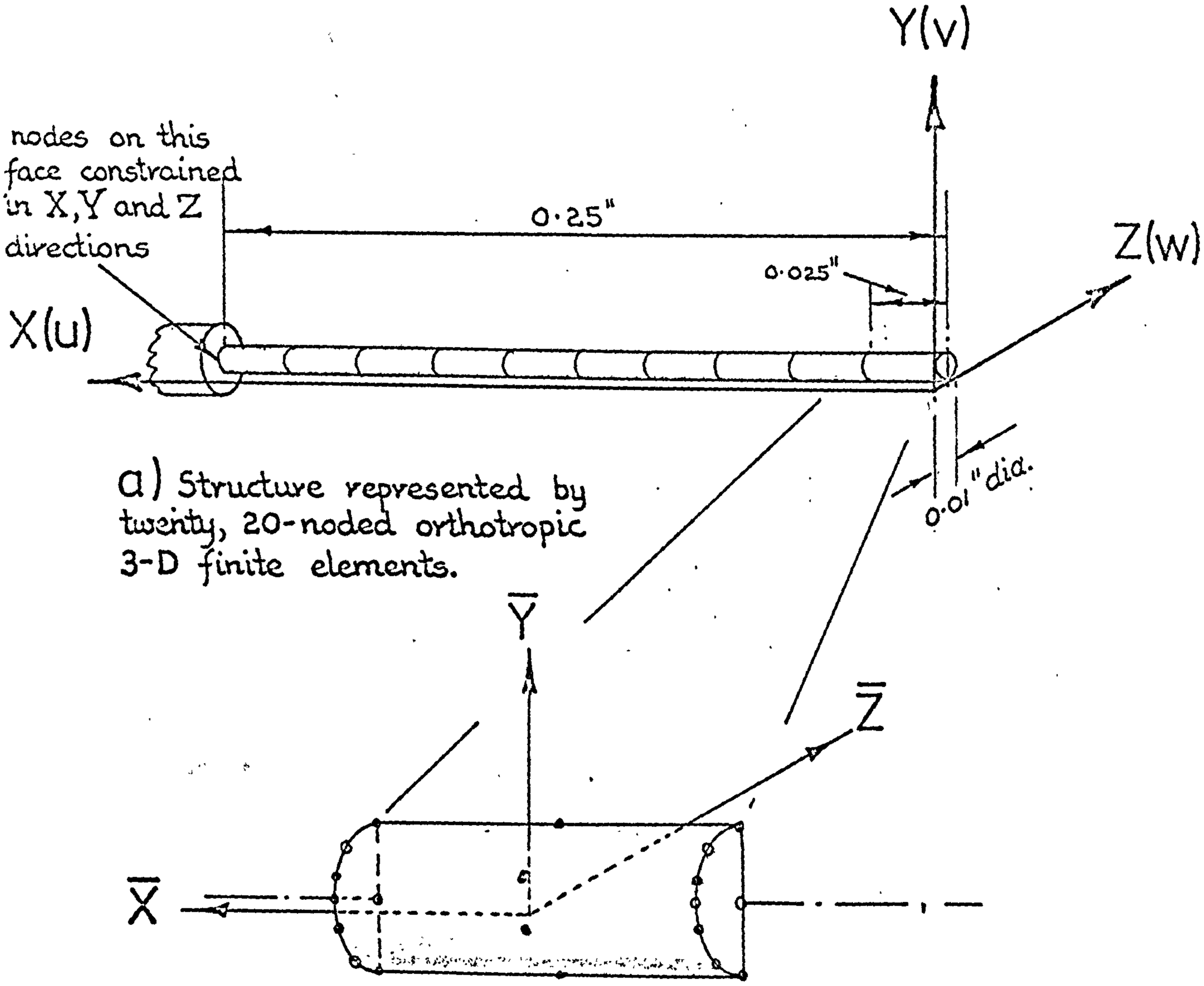


a) Structure represented by twenty, 20-noded orthotropic 3-D finite elements.

b) Typical element showing the orthogonal directions of the elastic axes.

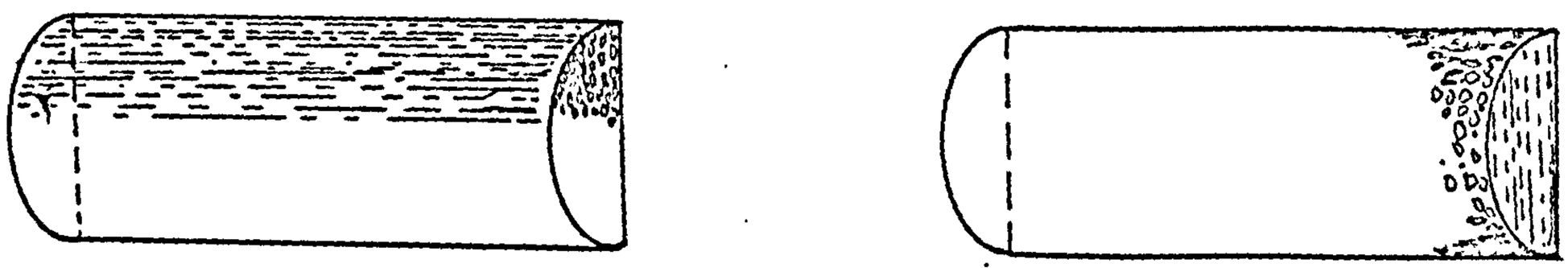

c) Bone grain parallel to specimen axis.

d) Bone grain transverse to specimen axis.

FIG. 6.4 Details of the finite element model used to simulate Bonfield and Li's (24) torsion experiments.

This was applied as illustrated in FIG 6.5, between four nodes such that no bending occurred in the finite element specimen. The nodes on the fixed end of the specimen were all rigidly clamped in the X,Y and Z coordinate directions by assigning the appropriate nodes zero-valued displacements.

From Bonfield and Li's results and by using the simple torsion formula,the rotation was calculated for this applied torque for both the parallel and transverse grain specimens. For the torsion test with the bone grain parallel to the specimen axis, FIG 6.4c, the authors obtained a G value of $0.85 \times 10^6$ p.s.i. This implies that the measured rotation must have been:-

$$\frac{T}{J} = \frac{G\phi}{L}$$

$$\text{i.e.} \quad \phi = \frac{TL}{JG}$$

$$= \frac{0.000393 \times 0.25 \times 32}{0.85 \times 10^6 \times \pi \times (0.01)^4} \text{ rads}$$

$$= 0.1177 \text{ rads}$$

$$\underline{\phi = 6.7 \text{ degrees}}$$

Similarly, for the transverse grain case, FIG 6.4d a G value of $1.9 \times 10^6$ p.s.i. was obtained by Bonfield and Li. Thus a rotation of:-

$$\phi = \frac{0.000393 \times 0.25 \times 32}{1.9 \times 10^6 \times \pi \times (0.01)^4} \text{ rads}$$

$$\underline{\phi = 3.0 \text{ degrees}}$$

must have been obtained in their experiment.

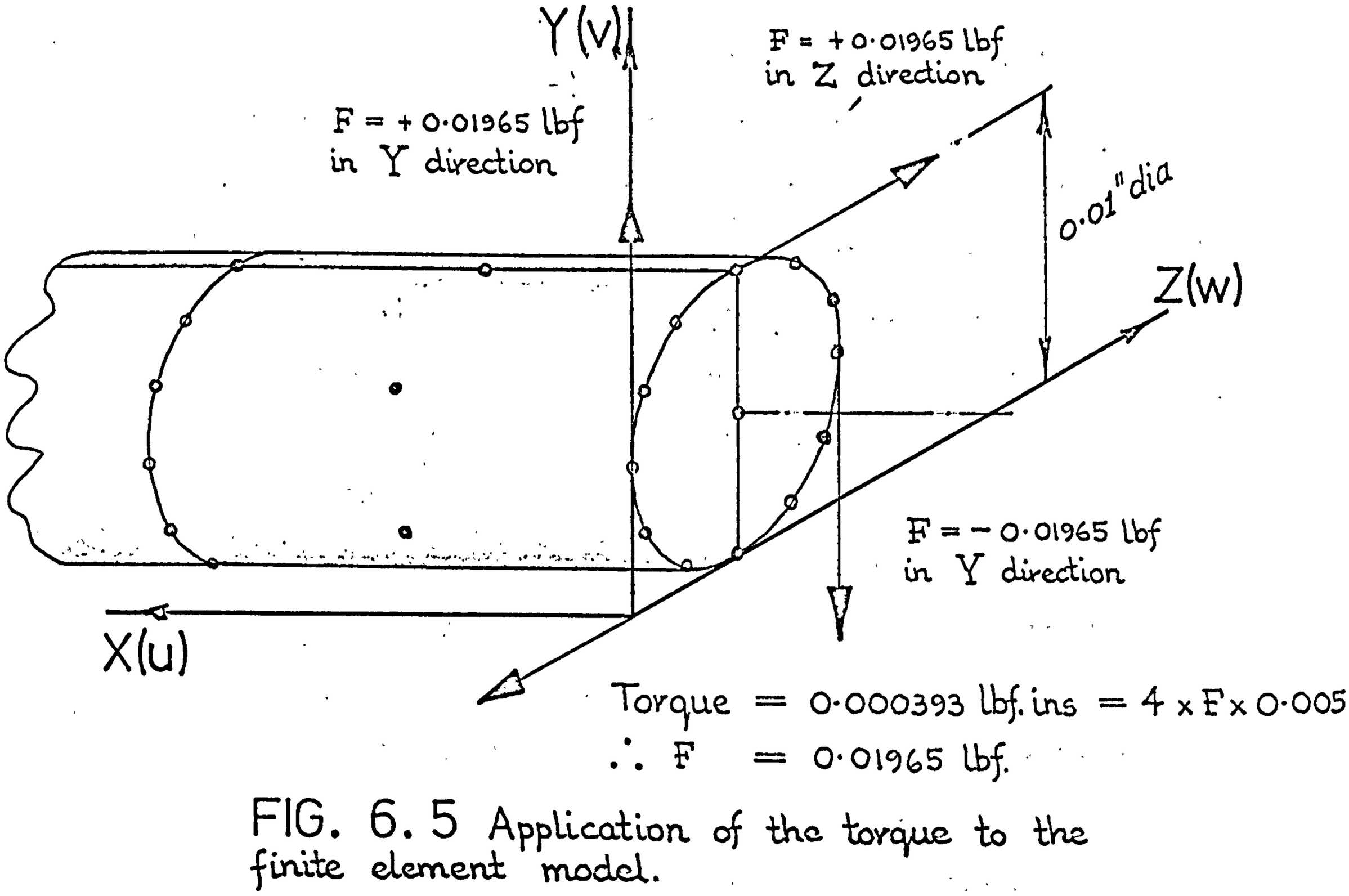


FIG. 6.5 Application of the torque to the finite element model.

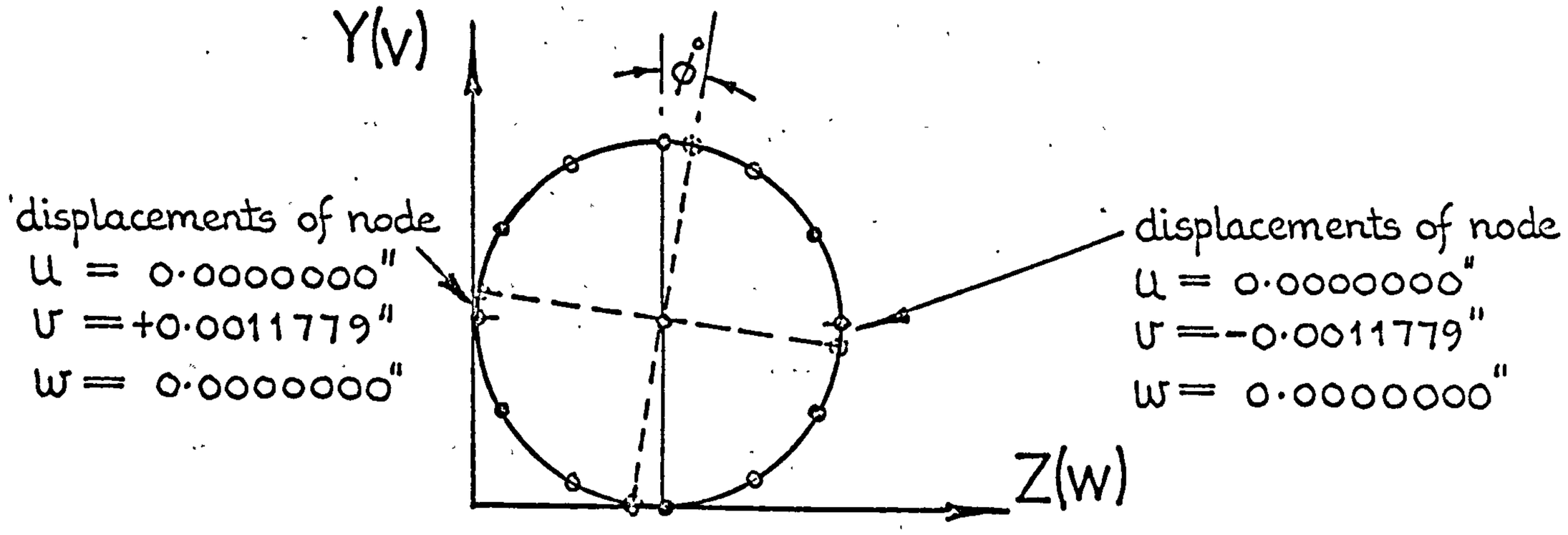


Rotation of specimen

$$\frac{\pi \times \phi^{\circ} \times r''}{180} = 0{\cdot}0011779''$$

$$\therefore \quad \phi = 13{\cdot}5^{\circ}$$

FIG. 6.6 Rotation of specimen for Run No. 1.

Although Bonfield and Li's experiments were carried out on bovine material, it is obviously the mechanical properties for human tissue that are required in this investigation. However, the consensus of opinion says that bovine material is twice as stiff as is the human counterpart and so for the same torsion experiments to be carried out on similar human tissue, rotations exactly twice those obtained from the bovine tests should be expected. Hence, for the parallel grain human specimen the end rotation for the same applied torque would be expected to be 13.4 degrees and for the transverse grain specimen 6.0 degrees. Thus, employing these two 'experimental' results and the known mechanical properties of human cortical bone, Gyz (and consequently $\mu zy$) was varied in the finite element analyses until the above displacements (i.e. rotations) were obtained.

In order to carry out the two different experiments, only the material data cards had to be changed in between computer runs. This involved simply changing the orientation of the elements' material property axes with respect to the structural coordinate axes X, Y and Z.

### 6.2.3 Results

The results for run number 1 with the bone grain assumed to be parallel with the specimen axis, see FIG. 6.4c, gave an end rotation of approximately 13.5 degrees for a guessed first value of Gyz of $0.4 \times 10^6$ p.s.i. (and $\mu zy = 0.25$), see FIG 6.6 and Table 6.1. This was a remarkable result as it

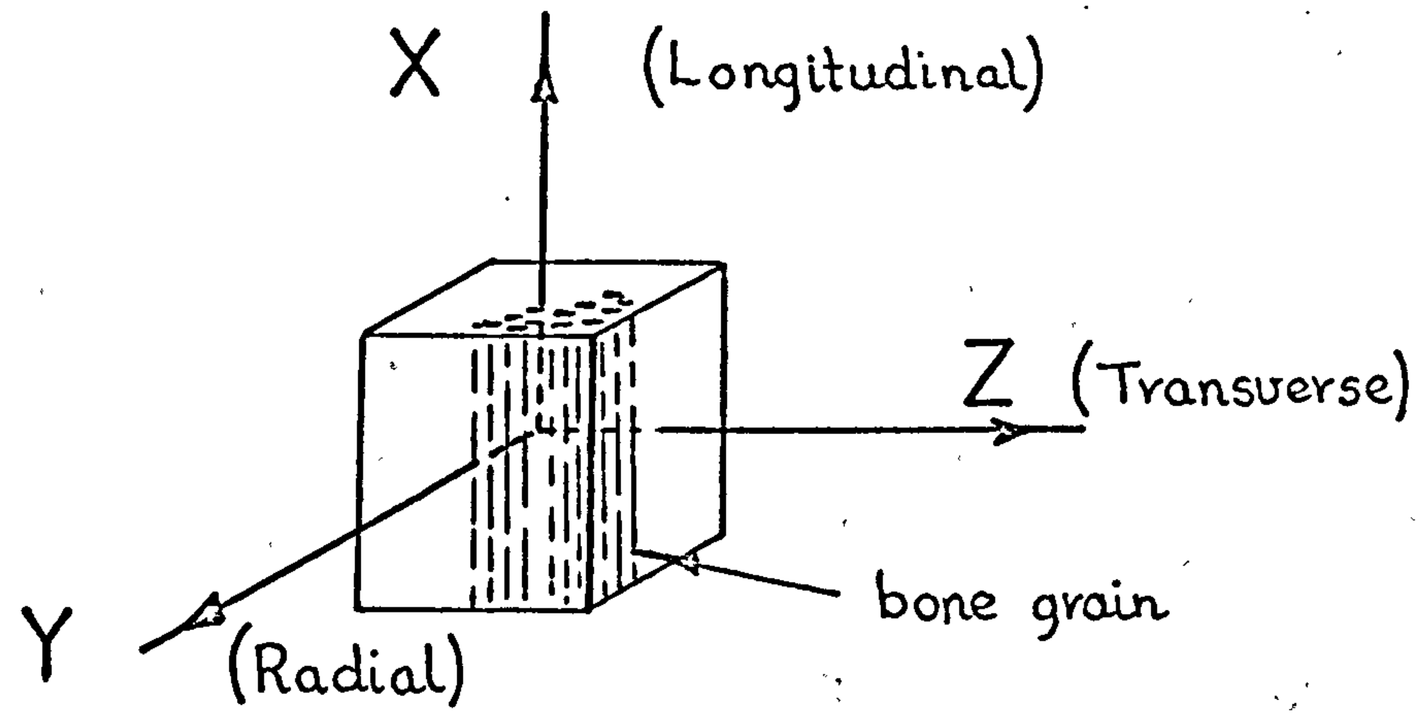


$$G_{yz} = \frac{E_y}{2(1+\mu_{zy})}$$

| RUN No. | $E_x$ p.s.i. $\times 10^6$ | $E_y$ p.s.i $\times 10^6$ | $E_z$ p.s.i $\times 10^6$ | $\mu_{yx}$ | $\mu_{zx}$ | $\mu_{zy}$ | $G_{xy}$ p.s.i $\times 10^6$ | $G_{yz}$ p.s.i. $\times 10^6$ | $G_{zx}$ p.s.i $\times 10^6$ | Rotation degrees. | REMARKS |
|---|---|---|---|---|---|---|---|---|---|---|---|
| 1 | 2 | 1 | 1 | 0·15 | 0·15 | 0·25 | 0·4275 | 0·4 | 0·4275 | 13·5 | Bone grain parallel to specimen axis. |
| 2 | 2 | 1 | 1 | 0·15 | 0·15 | 0·25 | 0·4275 | 0·4 | 0·4275 | 14·0 | Bone grain transverse to specimen axis |
| 3 | 2 | 1 | 1 | 0·15 | 0·15 | -0·375 | 0·4275 | 0·8 | 0·4275 | 10·4 | 〃 |
| 4 | 2 | 1 | 1 | 0·15 | 0·15 | -0·499 | 0·4275 | 1·0 | 0·4275 | 9·6 | 〃 |
| 5 | 2 | 1 | 1 | 0·15 | 0·15 | -0·499 | 0·5 | 1·0 | 0·5 | 8·6 | 〃 |
| 6 | 2 | 1 | 1 | 0·15 | 0·15 | -0·499 | 0·5 | 1·0 | 0·5 | 11·6 | Bone grain parallel to specimen axis. |

TABLE 6.1 Orthotropic mechanical properties of cortical bone obtained by simulating Bonfield and Li's (24) torsion experiments. Bone grain parallel and transverse to specimen axis, see FIG. 6.4.

was close to the required value. However, using exactly the same material properties in run number 2 for the transverse experiment, it can be seen that the rotation obtained was over two times too big and hence the structure was far too flexible in this mode. By doubling Gyz in run number 3, thereby making $\mu_{zy} = -0.375$ (hopefully to halve the specimen rotation), the displacement was reduced but only down to 10.4 degrees.

The significance of the negative Poisson's ratio will be reiterated here. As can be seen in FIG 6.7, the negative value for $\mu_{zy}$ implies that when a positive tensile stress stretches the bone in the Z coordinate direction, the bone expands in the Y coordinate direction, (remembering that the ZY plane is perpendicular to the bone grain). Although this behaviour is unusual for common engineering materials and seems physically irregular, it may be feasible for biological materials.

A further stiffening in run number 4, by increasing Gyz up to $1 \times 10^6$ p.s.i. and hence $\mu_{zy} = -0.499$, again only slightly reduced the end rotation. (In deriving the equilibrium equations for finite element analyses, the terms $(1 + 2\mu)$ and $(1 - 2\mu)$ are often encountered. Hence, Poisson's ratios of $\pm 0.5$ are avoided so as to prevent zero valued quantities and subsequent computer overflow, i.e. an infinite value being computed as a result of dividing by a zero quantity). It therefore seemed probable that other material constants would have to be changed in order to stiffen the structure sufficiently. In run number 5 the other shear moduli are slightly increased,

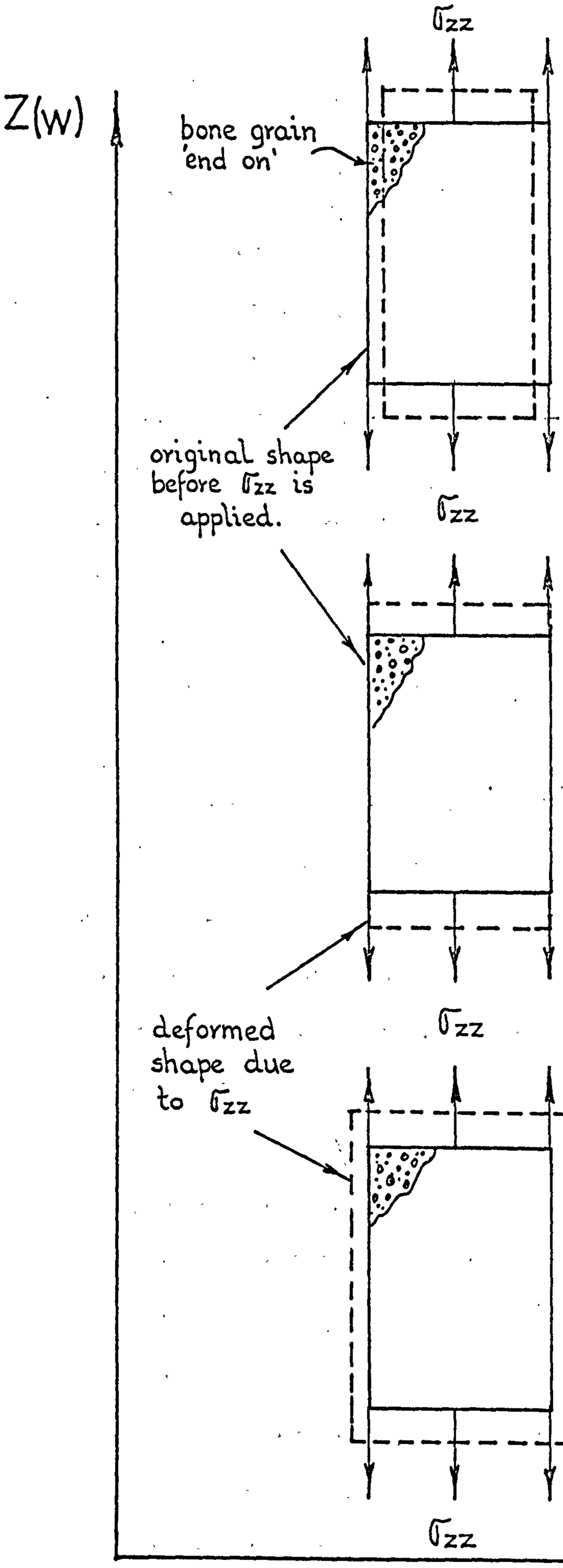


$0 < \mu_{zy} \leq 0.5$
decrease in lateral dimension or $\epsilon_{yy}$ = −ve

$\mu_{zy} = 0$
no change in lateral dimension or $\epsilon_{yy} = 0$

$-0.5 \leq \mu_{zy} < 0$
increase in lateral dimension or $\epsilon_{yy}$ = +ve

FIG. 6.7 Illustrating the significance of a negative value for the Poisson's ratio $\mu_{zy}$.
N.B. Conventional signs adopted

and, keeping Gyz = 1 x $10^6$ p.s.i. the desired effect is achieved. However, although the rotation of the transverse specimen is within reach of the required value the same properties when used for the longitudinal test, run number 6, reduces the end rotation for this case below that of the required value. Therefore, bearing in mind the limitations involved in this series of experiments, a reasonable value for the unknown mechanical property of human cortical bone seemed to be Gyz = 1 x $10^6$ p.s.i., (making $\mu_{zy}$ = -0.499).

## 6.3 PERIODONTAL MEMBRANE

### 6.3.1 Current Knowledge of the Physical Behaviour and Properties of the Periodontal Membrane

It can be seen from sub-section 3.4.4 that the current knowledge concerning the mechanical properties of the periodontal membrane is almost non-existent. However, this does not imply that little or no effort has been expended in connection with its study. In fact Muhlemann, Picton and many other investigators have examined the behaviour of the periodontal membrane in relation to tooth mobility studies and in particular, in connection with its possible implications to the onset of periodontal disease.

While the majority of tooth mobility studies have been conducted on animal subjects, (generally monkeys), a few experiments have been carried out on the human species. Most studies, due to the ease of access, have been concerned

with the incisor teeth and have involved the measurement of both axial and lateral tooth movements. Even so, it can be said that this work is still very much in its infancy and that the prime objective has been in elucidating the mechanism of tooth support rather than in determining the periodontal membrane's mechanical properties.

Basically, there are at present three different schools of thought concerning the supporting mechanism of the periodontal membrane. The two most popular theories propose that the membrane acts either as an hydrostatic cushion, compressible or incompressible, or as a fibre suspensionary system. The third idea is simply a combination of the other two.

In this sub-section some of the tooth mobility studies are reviewed and some of the data presented are used in subsequent finite element experiments to investigate the behaviour of the periodontal membrane. Using this approach some approximate overall mechanical properties of the membrane are determined.

### 6.3.2 Review of Some Tooth Mobility Studies

In 1954 Muhlemann (68), postulated that tooth mobility measurements might be useful as a diagnostic procedure for detecting the onset of periodontal disease. From his experiments on the labio-lingual movements of the crowns of the central incisors of monkeys, Muhlemann concluded that there were two distinct phases of tooth mobility. The first

phase gave rise to relatively large displacements for comparatively small applied forces whereas, in the second phase, the supporting mechanism was much stiffer. The tooth displacements in this phase were much smaller for further increases in load, see FIG. 6.8.

Tooth mobility, he proposed, was also influenced by the presence of interdental contact points and also by activation. Activation or exercise prior to mobility measurements, produced a slight but consistent increase in initial tooth mobility, FIG 6.8. In the third part of his paper Muhlemann suggested that the initial phase or initial tooth mobility was due to an intra-alveolar orientation of the periodontal membrane fibre bundles; fifty to one hundred grams being all that was required to prepare the membrane for functional readiness. Consequently, when forces larger than these were applied to the crowns of the teeth, the fibre bundles on the tension side resisted further tooth movement. This, he claims accounts for the sudden increase in the stiffness of the supporting structure.

Muhlemann in 1960 (69), published another paper in which he reviewed ten years of his tooth mobility work. In this paper he relates some of the observations made in his earlier publication to human clinical case studies.

Parfitt in 1960 (70), investigated the axial mobility of human central incisors under intermittent and continuously applied axial forces. Parfitt, like Muhlemann, concluded that tooth movement was relatively large for small forces but

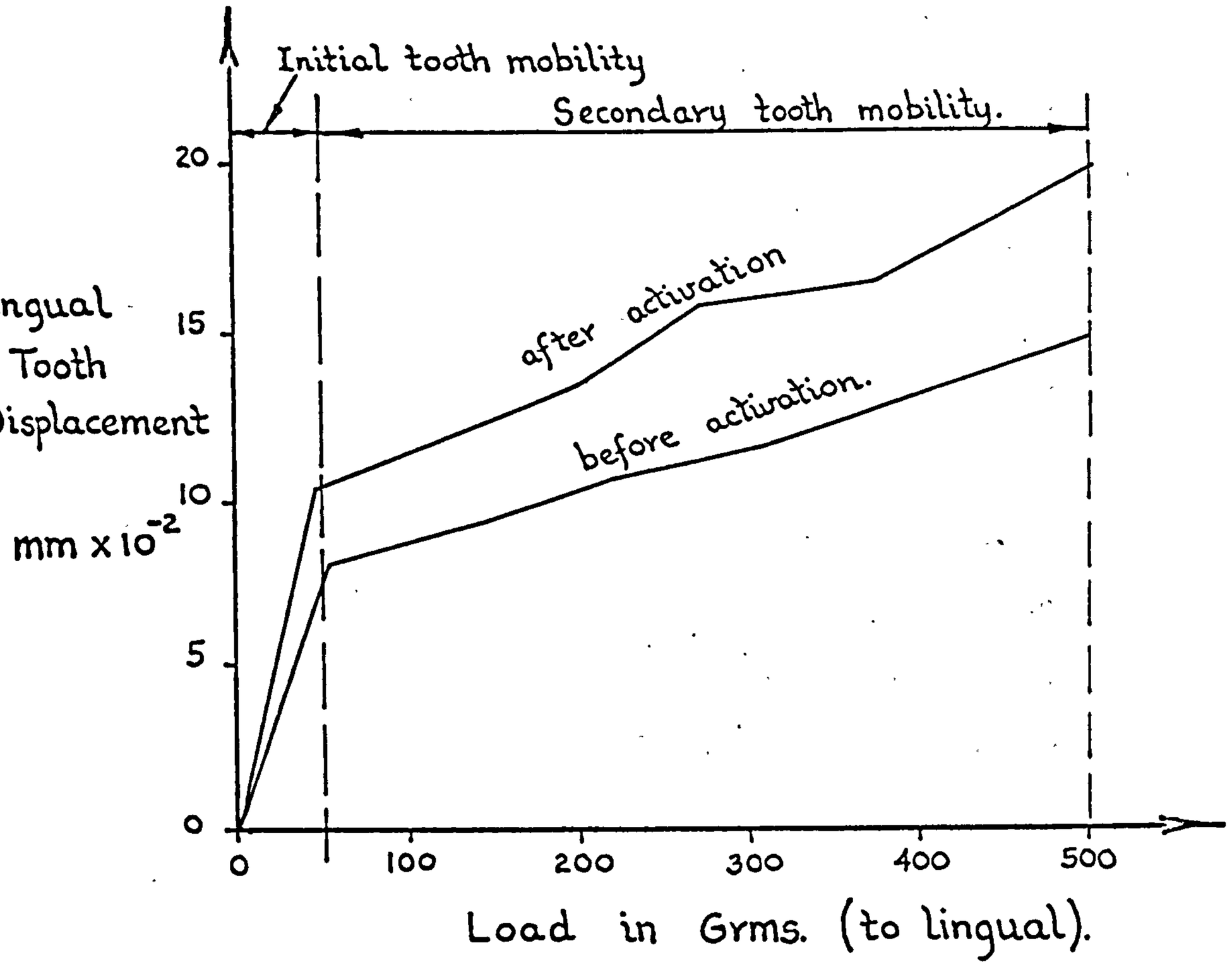


FIG. 6.8 Lingual mobility curves for monkey central incisors - before and after activation - Muhlemann (68).

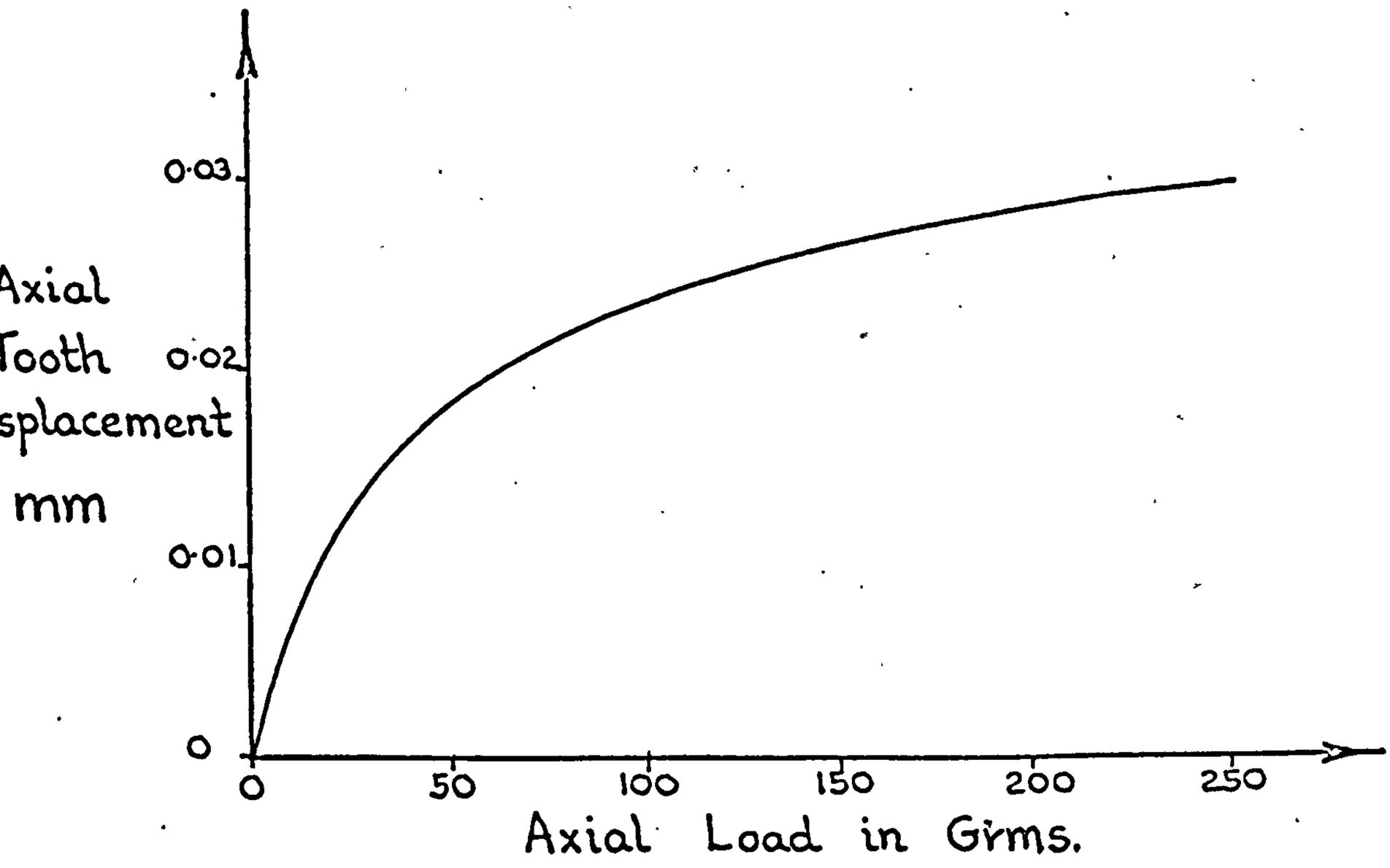


FIG. 6.9 Axial mobility curve for human central incisor~ before activation. - Parfitt (70).

that the resistance to movement became progressively greater for higher loads. Hence, he obtained a similar non-linear tooth displacement versus force response characteristic, FIG. 6.9. Parfitt also discovered that upon release of the applied load, the tooth regained its original position in two distinct phases. The first phase, upon load release, consisted of a rapid elastic type recovery which was subsequently followed by a slow exponential recovery phase. Under a continuously applied 500 gm. axial load however, the tooth moved apically a regular amount with each period of time until a limit was reached when no further displacement took place. This observation he concluded was indicative of a fluid support system. With low continuous axial forces,Parfitt detected a rise and fall in the teeth synchronous with the arterial pulse wave. This pulsation was found to be most strong between 2 and 4 gm. loads but disappeared altogether at loads above 15 gms.

In a later paper in 1961, Parfitt (71), investigated the displacement versus load characteristic of the human central incisor subjected to lateral or labio-lingual forces. As illustrated in FIG 6.10, the response was very similar to the one obtained for the application of intermittent forces for the axial case. However, the displacements in the lateral case were slightly larger than those obtained in the axial case for the same magnitude of applied load.

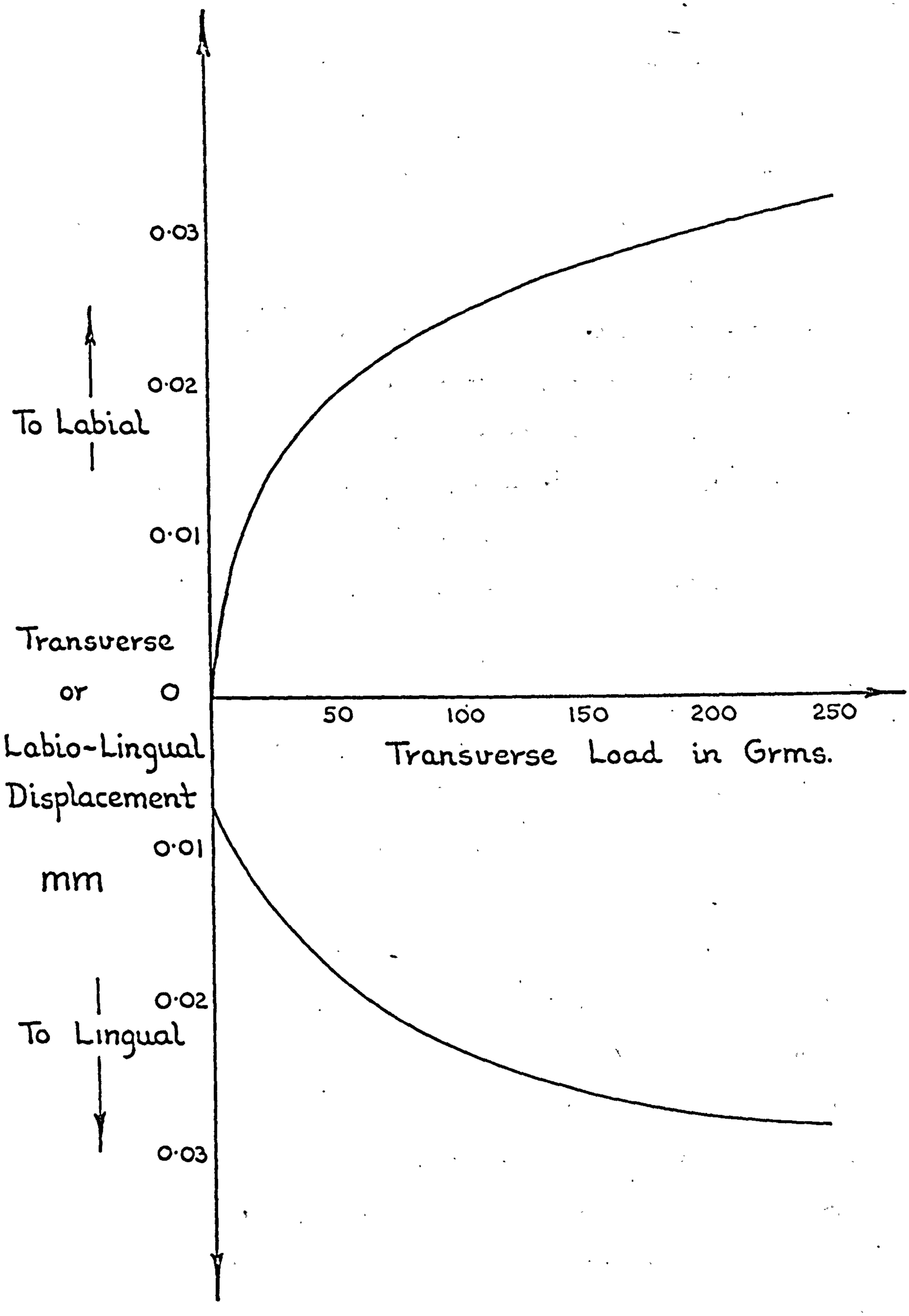


FIG. 6.10 Transverse or labio-lingual mobility curve for human central incisor. - Parfitt (71).

Picton in two papers in 1962 (72, 73), reported on work in which he had measured the movement of the teeth during biting. From his studies, he concluded that the anterior teeth were tilted labially and the posterior teeth tilted mesially under the forces of mastication. This observation explains the phenomenon of mesial drift and emphasizes why it is necessary to maintain contact points and full dental arches. The functioning of the arch as an integral unit was further demonstrated in another series of experiments in which it was shown how the teeth on one side of the arch were displaced when the teeth on the opposite side were loaded.

In 1964 Picton (74), published the results of some further experiments in which he examined the effect of loading frequency on the mobility of the teeth. For axial thrusts repeated at 5 second intervals, Picton found that tooth mobility gradually decreased. This, he claimed was due to the failure of the teeth to return to their initial positions in the sockets during the loading sequence. However, for thrusts repeated at 2 minute intervals, mobility was found to increase, thus indicating that the teeth not only returned to their original positions but actually extruded past them. Picton examined the implications of these results in a further paper in 1964 (75). Using the work of Anderson (76), he deduced that the average time interval between chewing thrusts during normal mastication was only 0.412 seconds. Hence, he concluded that the time interval between thrusts was

not sufficient to allow the teeth to regain or recover their original starting positions.

In a publication in 1965, Picton (77), reported on an investigation which had looked into the part played by the alveolar bone in tooth support. Using monkeys as subjects, he measured the distortion of the alveolar crests of central incisor teeth when they were loaded either axially or laterally. He concluded from the lateral case that the bone deflected for loads of less than 50 gms. but because of its smaller mass the labial plate deflected more than the corresponding lingual plate. However, no significant difference in the displacements of either plate could be detected whether the adjacent periodontal membrane was subjected to tensile or compressive stresses. This result, coupled with the observation that in the majority of cases the tooth sockets dilated when the teeth were subjected to axial intrusive forces, raises serious doubts as to the validity of the tension-fibre support theory.

Christiansen and Burstone (40) in 1969, determined the pattern of tooth tipping within the periodontal space under the action of simple but controlled lateral force systems. These authors carried out their experiments on the central incisors of human subjects and, by attaching extension pieces to the crowns of the teeth,measured the displacement of the extended crowns at two separate points. Consequently, they were able to determine the instantaneous centres of rotation of the teeth by the principle of similar triangles, see FIG 6.11.

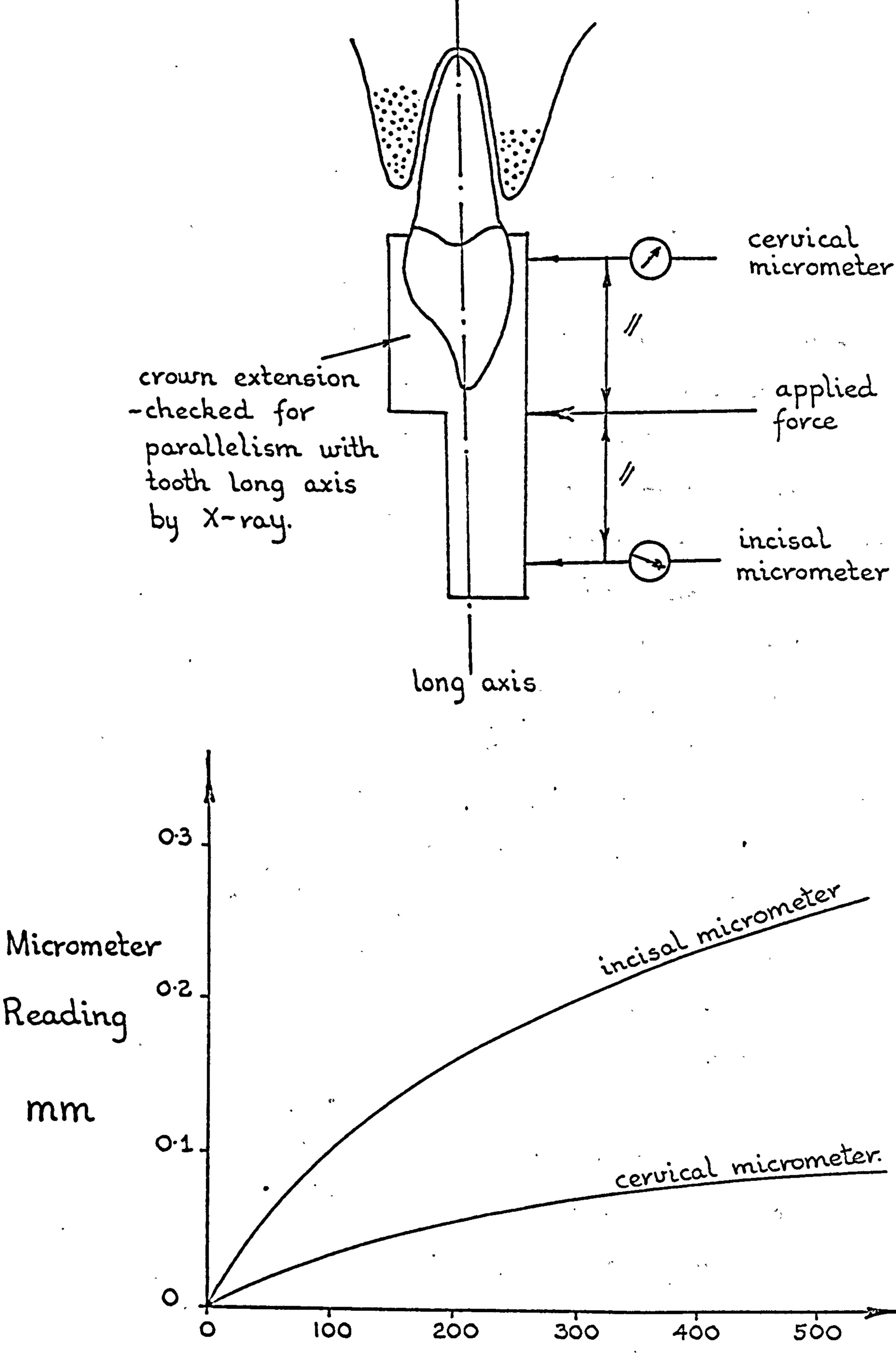


FIG. 6.11 Transverse or labio-lingual mobility curve for human central incisor.
- Christiansen and Burstone (40).

As can be seen from the figure their tooth displacement versus applied force response characteristic was very similar to that obtained by Muhlemann and Parfitt.

Picton and Davies in 1967 (78), continued the earlier work which investigated the general behaviour of the tooth-membrane-socket system. Again,using monkeys under Nembutal anaesthesia,the authors measured the relative displacement of the tooth and socket by passing a measurement probe through a small hole in the alveolar wall. Hence, from their recordings of the deflections of the tooth root and socket wall, Picton and Davies were able to ascertain the approximate position of the instantaneous centre of rotation. They observed that for some teeth the position of the instantaneous centre of rotation moved as the applied force was increased in magnitude. They again detected alveolar bone distortion for low force levels and also that it occurred irrespective of whether the periodontal membrane was under tensile or compressive stresses. However, as the authors themselves state, the extrapolation of these results to man must be proceeded with extreme caution. Because of the experimental difficulties of rigidly anchoring the instrumentation and of preventing jaw distortion caused by the head support, the data recorded must be viewed with some scepticism. Also to be borne in mind is the fact that the incisor teeth of the monkey are curved far more in the labio-lingual plane than are those of the human species.

In further studies,Picton in 1967 (79), and Picton and Slatter 1972 (80), investigated the effects of localised trauma on tooth mobility. Using monkey subjects under total anaesthesia, measurements were taken of lateral tooth displacements of central incisor teeth in the mesio-distal plane. This before and after localised trauma to selected areas of the gingival tissues had been administered. From their experiments they concluded that the cervical tissues play an important role in tooth support and that areas of the periodontal membrane under tensile and compressive stresses provide equal resistance to tooth displacement.

In the most recent publication of the research team, Wills, Picton and Davies 1972 (81), report on an investigation whereby the axial tooth mobility response of the central incisors of anaesthetized monkeys was considered to be viscoelastic in character. Following the idea put forward by Bien in 1966 (82), Wills et al proposed that the whole tooth-membrane-bone support system could be represented by a collection of Voigt elements, (a parallel connected dashpot-spring combination), coupled in series, FIG 6.12. Hence, by 'curve stripping' the tooth displacement time response characteristic,they were able to determine some of the spring and dashpot coefficients. However, disappointingly,the coefficients determined are in no way any indication of the actual viscoelastic properties of the periodontal membrane. Also, the studies are limited at present to investigations concerned purely with the response characteristics of the unloading phase.

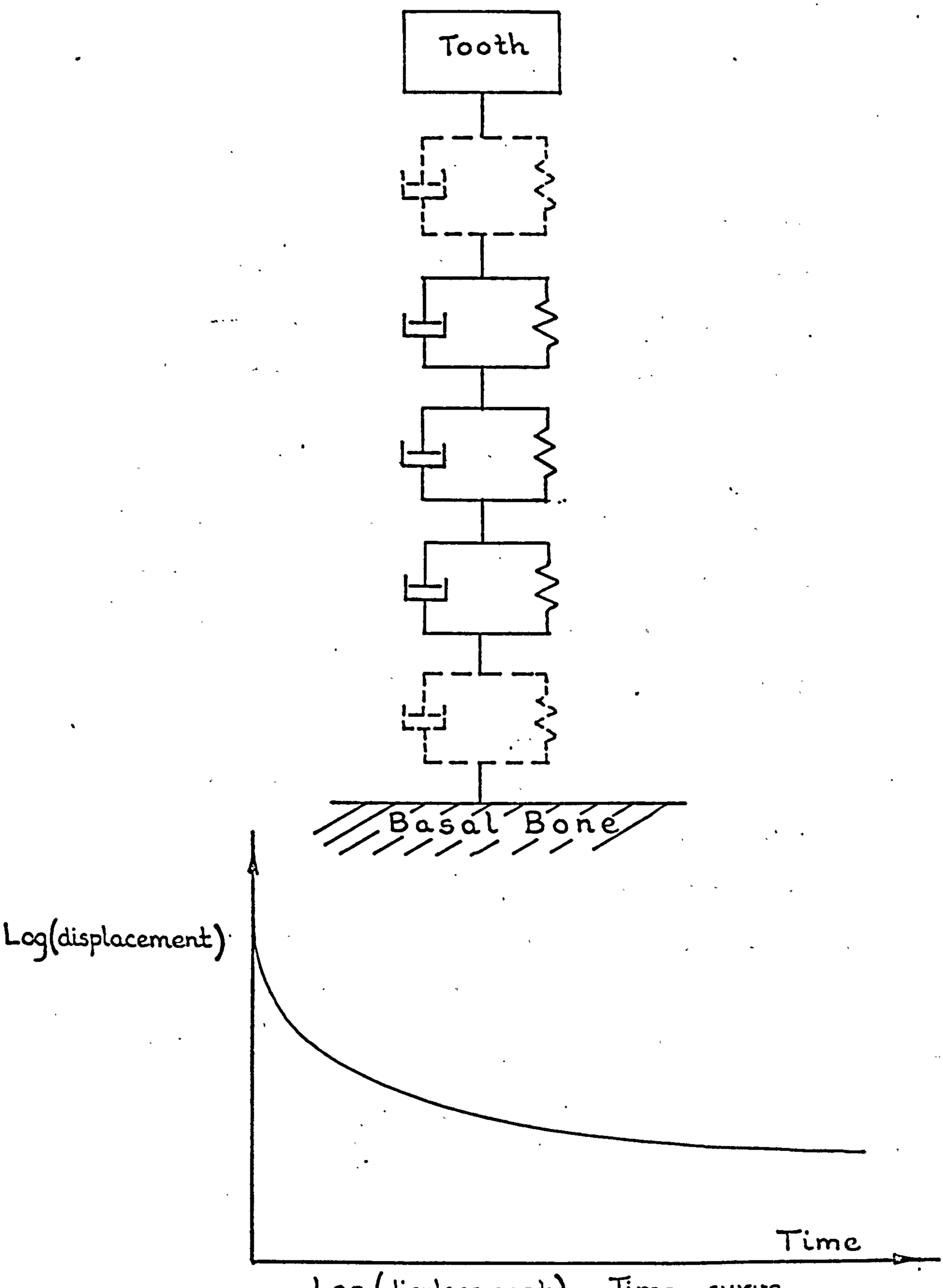


Log (displacement) - Time curve for unloading phase of monkey central incisor.

FIG. 6.12 Tentative model representing the periodontal tissues in the monkey during the unloading phase. - Wills, Picton and Davies (81).

### 6.3.3 Discussion

From the foregoing review it can be seen that the force versus displacement response of the human incisor teeth presents a non-linear form of characteristic. However, this response appears to be similar for both intrusive and lateral tooth movements although in the lateral mode, the larger displacements indicate a slightly more flexible structural behaviour. The areas examined in the current investigation are primarily concerned with the position and change in position of the instantaneous centres of rotation of the teeth,and with the stress and strain distributions occurring in the alveolar bone resulting from the application of small orthodontic forces. Consequently, tooth displacements corresponding to load magnitudes in the region of 30 gms., were selected for the determination of the periodontal membrane properties. Hence, from the measurements of Parfitt and of Christiansen and Burstone on human subjects, the following averaged data were selected:-

| | |
|---|---|
| Axial tooth displacements due to 30 gm. axial tooth load | = 0.015 mm (15 microns) |
| Lateral or transverse tooth displacements due to 30 gm lateral tooth load | = 0.018 mm (18 microns) |

It must be noted that for the lateral case, the position and direction of tooth loading and the point at which the crown excursions were measured were not documented in the literature. Consequently, it was assumed that the direction of the loading and recorded displacements were perpendicular to the tooth

long axis and approximately at the mid-point between the incisal edge and the cervical margin of the tooth.

Although the tooth mobility studies indicate that a certain amount of flow or creep occurs in the periodontal membrane, the analyses are restricted in this instance to consider the periodontium to react to orthodontic loading as a purely linear elastic system. However, as the finite element method is not restricted to analyses of this form, it may be possible in the future to extend the work and to consider time effects of the membrane when more clinical experimental data has been obtained.

### 6.3.4 Finite Element Test Procedure - Isotropic Periodontal Membrane

Tracings of the X-rays of the maxillary central incisor taken from a young patient before and after receiving crthodontic treatment are illustrated in FIG 6.13a and b. The treatment involved applying a load of 30 gm. to the labial surface of the crown of the tooth as indicated in FIG 6.13 a, This resulted in the eventual change of tooth position as shown in FIG 6.13b.

From the X-ray picture illustrated in FIG 6.13a, the tooth and supporting periodontal membrane and bone structure was meshed into three different finite element representations. The first model, simulating the combined tooth and support structure, was constructed using axisymmetric elements as shown in FIG 6.14. This configuration, (limited obviously

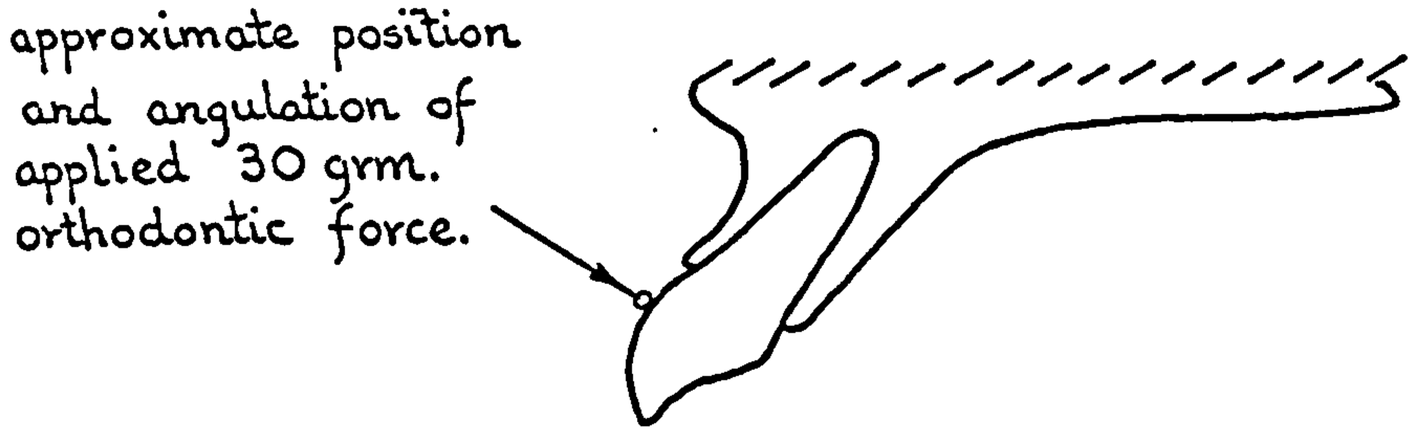


a) Before orthodontic treatment -

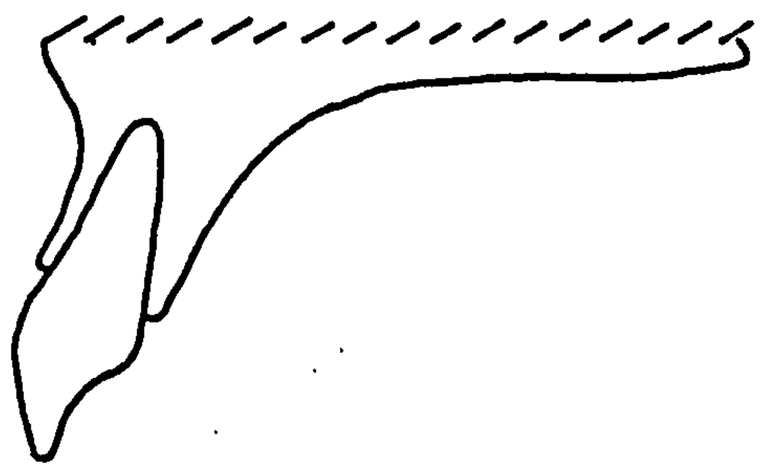

b) After orthodontic treatment

FIG. 6.13 Tracings of radiographs taken before and at the cessation of orthodontic treatment to a human maxillary central incisor.

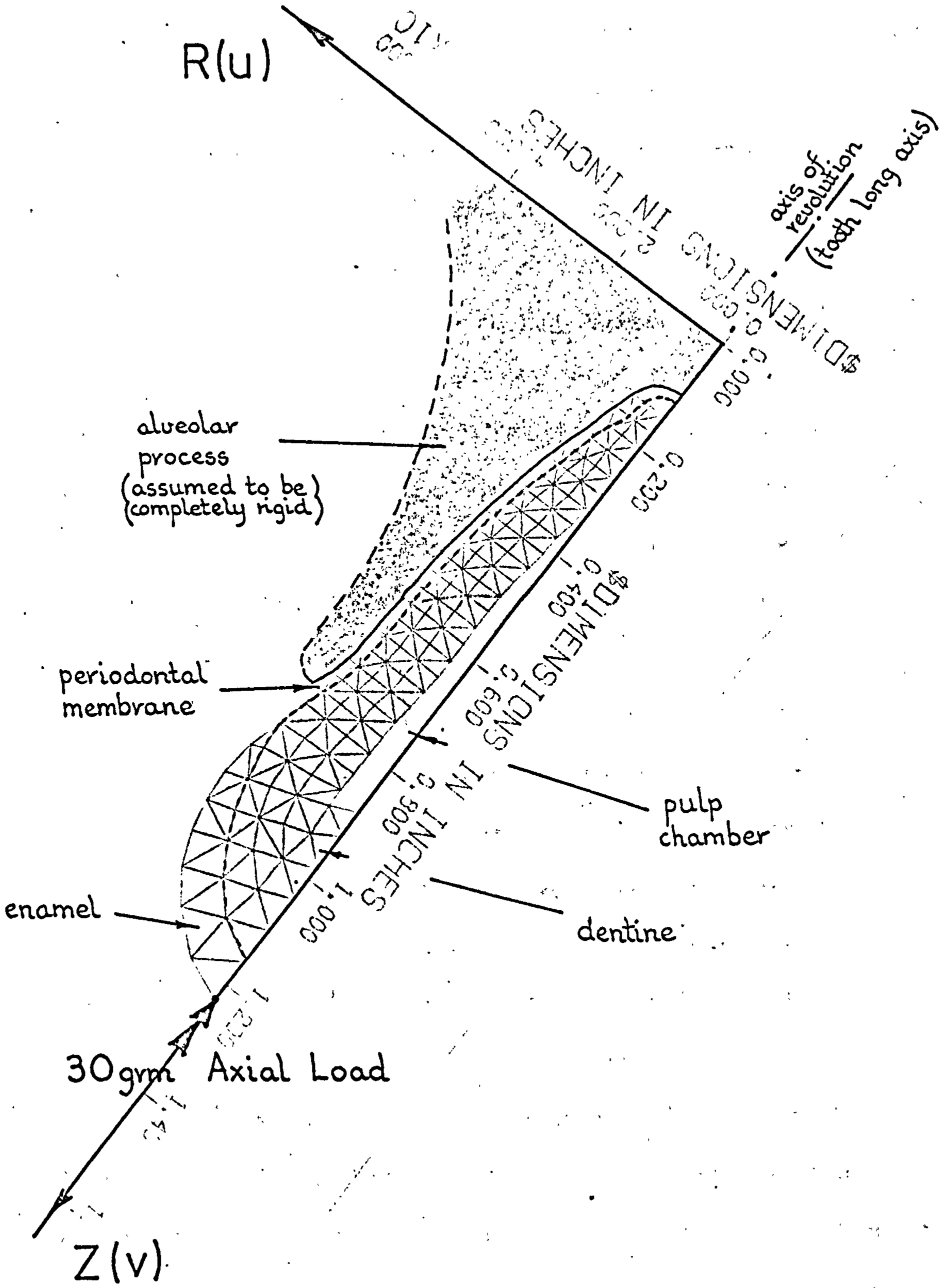


FIG. 6.14 Computer plot of axisymmetric representation of the maxillary central incisor

to considering axisymmetric loading), was employed to investigate the axial load condition. Of course, the model assumed the tooth, membrane and bone to have rotational symmetry about the tooth long axis. Also, to reduce the computational effort, the alveolar bone was assumed to be rigid under this condition of loading. Actually, it will deflect in real life but this will be relatively negligible. (This can be reasoned by considering the differences in the stiffnesses, i.e. the Young's moduli of the periodontal membrane and the supporting bone. Most of the tooth displacement takes place within the periodontal membrane space prior to any bone resorption and apposition).

The second model considered was the three-dimensional finite element simulation illustrated in FIG 6.15. As can be seen from the figure, the representation is very crude indeed. This was made so for economic reasons; the digital computer employed was relatively small and slow and hence, because of the vast number of stiffness coefficients and equilibrium equations involved with three-dimensional structures, the mesh was made very coarse. Again, to reduce the computation even further, the structure was assumed to be symmetric about the Y coordinate axis. (This simplification almost halves the computation required.) Consequently, the load applied to the half structure was similarly halved.

To enable a finer mesh to be constructed such that the non-symmetrically loaded structure could be investigated in greater detail, (particularly for the second part of this

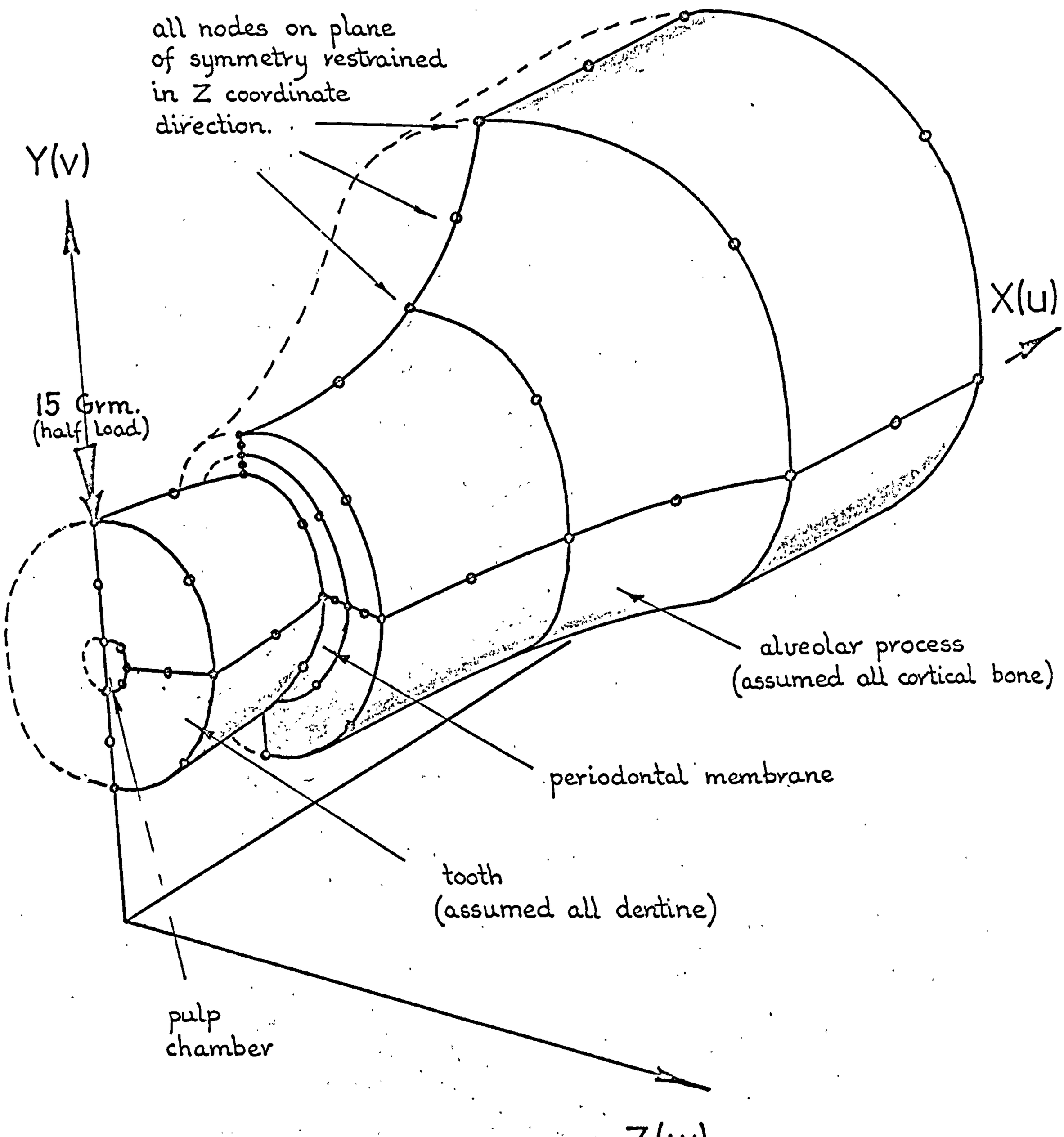


FIG. 6.15 Isometric sketch of 3-D maxillary central incisor representation using twenty, 20-noded finite elements.

section where orthotropic periodontal membrane properties are considered), the two-dimensional finite element representation was developed, see FIG. 6.16. Although,of course,the 3-D form of the structure has been lost, as demonstrated in Volume Two of this thesis, a two-dimensional representation does give a reasonable picture of the pattern of deformation and stress distribution occurring in the plane represented by the two-dimensional simulation. In order to portray the actual displacements of the axisymmetric and three-dimensional tooth models, an equivalent two-dimensional model slice thickness was derived. This was achieved by employing the mechanical properties determined for the periodontal membrane using the axisymmetric and three-dimensional models, and iterating the slice thickness until the sets of model displacements coincided.

### 6.3.5 Results

As a first approximation,the isotropic Young's modulus for the periodontal membrane for the axial load case was made equal to the value obtained by Dyment and Synge (15), from their experiments with membranes from lambs and calves, i.e. E = 210 p.s.i., see Table 3.3. In the first run of the axisymmetric model the periodontal membrane was also assumed to be incompressible, i.e. $\mu$ = 0.5. It can be seen from Table 6.2 that the resulting axial tooth displacement for the applied 30 gm. axial load is only 0.00024 mm., (0.24 microns). This implies that the membrane was made too stiff. As the

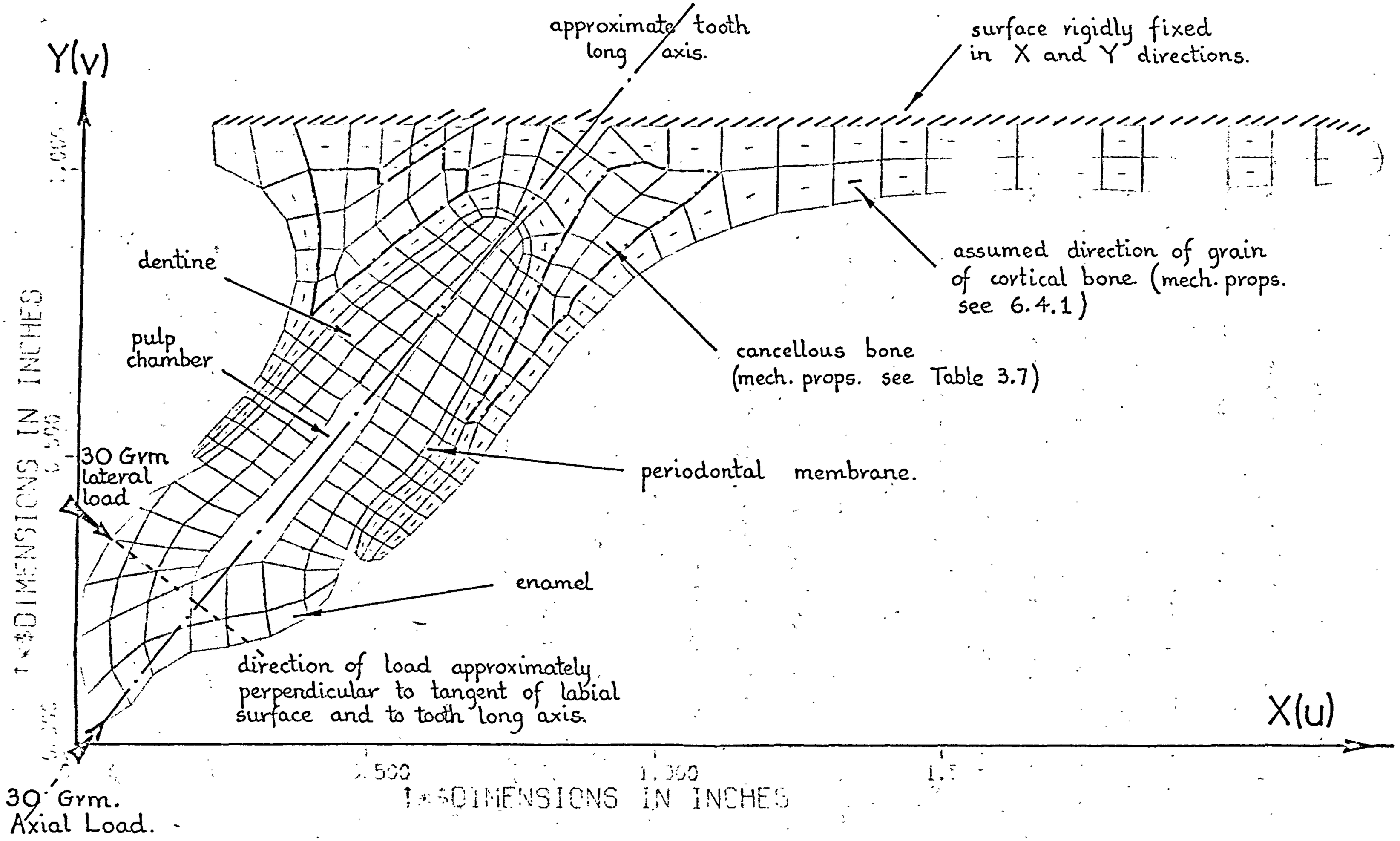


FIG. 6.16 Computer plot of 2-D representation of maxillary central incisor using 270 quadrilateral type finite elements.

axial tooth displacement required was 15 microns, the displacement was therefore $\frac{15}{0.24}$ = 68.2 times too small or the stiffness 68.2 times too high. Therefore, by making E equal to $\frac{210}{68.2}$ = 3.15 p.s.i. in run number 2, again assuming the membrane to be incompressible, the required axial tooth displacement of 15 microns was obtained. However, as can be seen from Table 6.2, the compressibility of the membrane, represented by the value of $\mu$, drastically affects its flexibility and consequently the resulting tooth displacement. This can be seen from run numbers 3 and 4 where the value of $\mu$ is varied for a constant value of E. Hence, if it is assumed at the onset that the periodontal membrane is compressible, (and a strong case can be made regarding the displaceable blood volume and the compressible components from which it is comprised), and $\mu$ is made equal to 0.3, a completely different E value is determined in order to obtain the required axial tooth displacement. This is clearly shown by run numbers 5 and 6 in Table 6.2. Again by varying the value of $\mu$, the flexibility of the periodontal membrane is greatly affected. From this set of results and from FIG 6.17, it is apparent that there exists numerous combinations of E and $\mu$ which would give the required axial tooth displacement.

Employing the mechanical properties obtained for the periodontal membrane in the axial analysis, run number 6 from Table 6.2, the transverse or lateral load condition was investigated using the three-dimensional finite element representation shown in FIG. 6.15. It can been seen from

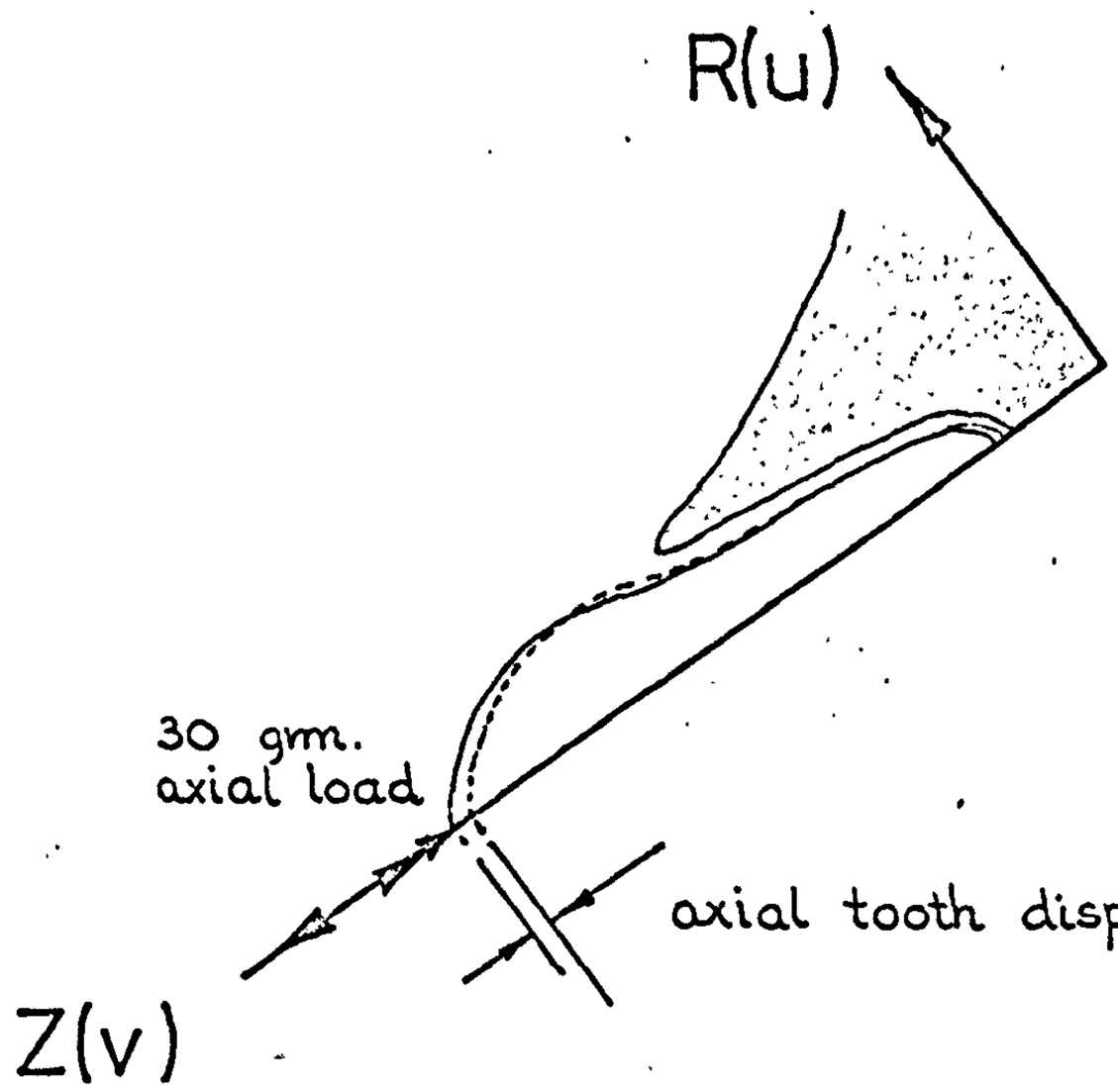


| RUN No. | E p.s.i. | $\mu$ | G p.s.i. | AXIAL TOOTH DISPLACEMENT microns | REMARKS |
|---|---|---|---|---|---|
| 1 | 210 | 0·5 | 70. | 0·24 | Membrane incompressible $\mu$= 0·499 in calculations |
| 2 | 3·15 | 0·5 | 1·10 | 15·0 | 11 |
| 3 | 3·15 | 0·45 | 1·15 | 34·2 | |
| 4 | 3·15 | 0·3 | 1·29 | 41·0 | |
| 4a | 3·15 | 0·1 | 1·43 | 37·0 | |
| 5 | 210 | 0·3 | 80·7 | 0·6 | |
| 6 | 8·7 | 0·3 | 3·35 | 14·8 | |
| 7 | 8·7 | 0·5 | 2·9 | 5·4 | Membrane incompressible $\mu$= 0·499 in calculations. |
| 8 | 8·7 | 0·45 | 3·0 | 12·4 | |
| 8a | 8·7 | 0·1 | 3·95 | 13·2 | |

TABLE 6.2 Axial tooth displacement results for 30gm. axial load applied to axisymmetric finite element idealisation of maxillary central incisor. Periodontal membrane assumed isotropic and the alveolar bone support rigid.

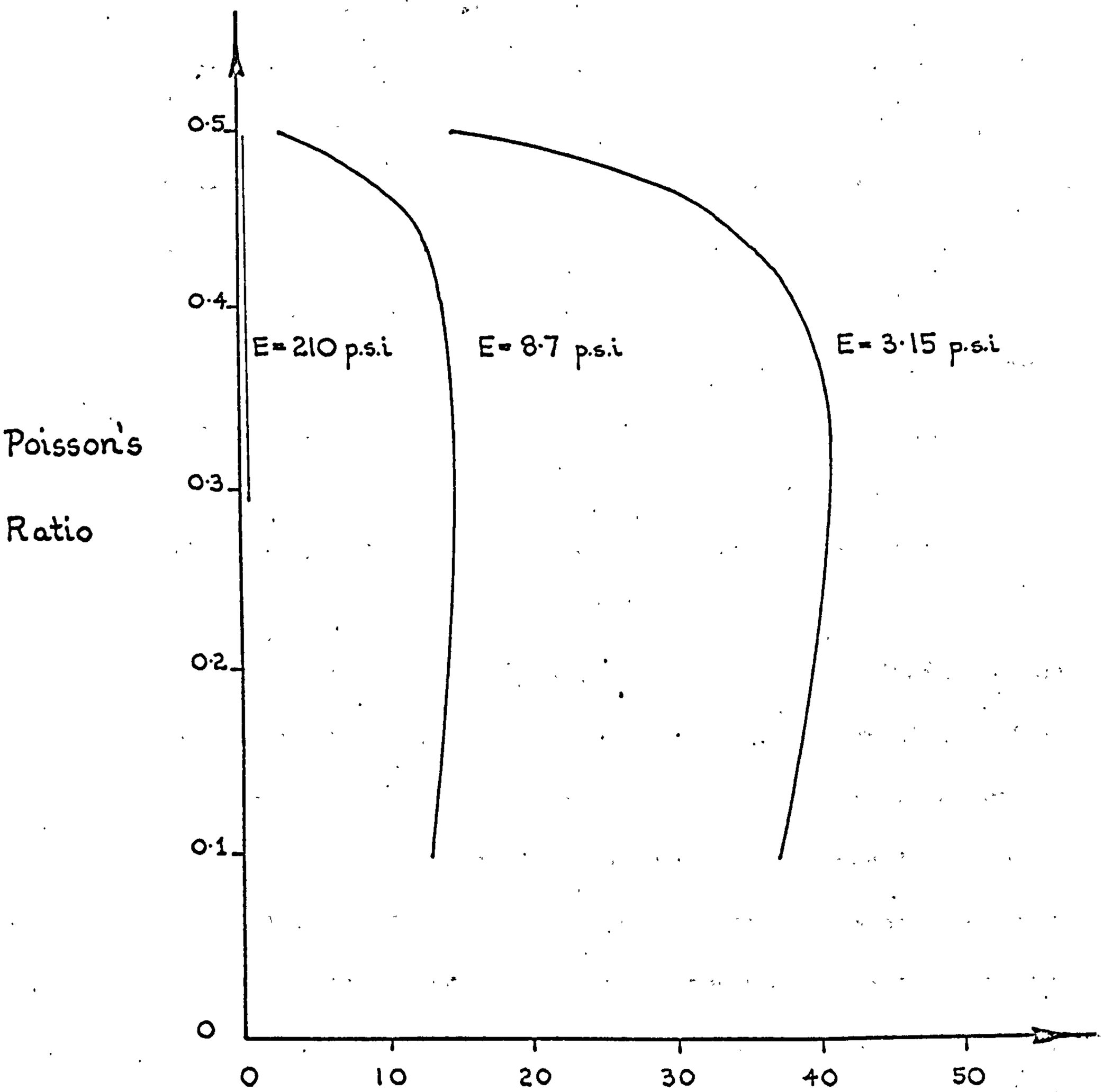


FIG. 6.17 Illustrating the change in axial tooth displacement as a result of varying the Poisson's ratio (compressibility) of the periodontal membrane.

run number 9 in Table 6.3, that the lateral tooth displacement, i.e. tooth displacement to lingual, for these isotropic properties is 0.051 mm. Hence, the displacement is very approximately three times too big. This indicates that the structural stiffness is nearly three times too low. Thus, stiffening the periodontal membrane by a factor of three, simply by increasing the value of the Young's modulus, and keeping the value assumed for the compressibility constant, a lateral tooth displacement of 17 microns is obtained, run number 10. This value is very close to that required for this loading condition. From this run the lateral deflection of the lingual alveolar crest was approximately 0.1 microns to lingual.

As previously mentioned, three-dimensional finite element analyses employing a small relatively slow digital computer, are not economical. Consequently, a two-dimensional model simulation of the maxillary central incisor was developed. This was achieved by using the axial and transverse periodontal membrane properties determined in the more realistic axisymmetric and three-dimensional analyses, and finding an equivalent two-dimensional model thickness which would give the same axial and lateral tooth displacements for the same axial and lateral orthodontic 30 gm. loads. (As shown in Volume Two of this thesis, the stiffness of a 2-D planestress finite element structure is directly proportional to the model thickness. Hence, the displacement of the model tooth is a linear function of the slice thickness.)

Run number 11 considered the axial load case of the 2-D model illustrated in FIG 6.16. Using the periodontal membrane values of run number 6 from Table 6.2 and selecting a slice thickness of 1.0 inch,the axial tooth displacement obtained was approximately 5.2 microns. This result indicates that the 2-D model stiffness was too high and so,to obtain the required axial displacement the stiffness, i.e. the model thickness, was reduced. As the displacement was $\frac{15}{5.2}$ = 2.9 times too small, by reducing the thickness to $\frac{1}{2.9}$ ≏ 0.345 ins., the required axial tooth displacement was obtained, run number 12.

By following a similar procedure,the lateral load versus displacement condition was also investigated. For this case,the lateral periodontal membrane properties determined in run number 10 Table 6.3 were used,together with the equivalent model thickness (0.345 ins) obtained above. The lateral tooth displacement determined for the 30 gm. lateral load was 17.2 microns, run number 13, which of course is very close to that required for this particular loading arrangement.

### 6.3.6 Finite Element Test Procedure-Orthotropic Periodontal Membrane

The two-dimensional finite element model illustrated in FIG. 6.16, having an equivalent slice thickness of 0.345 ins., was employed to investigate the fibre support theory of the periodontal membrane under axial and lateral 30 gm. tooth loads respectively. To do this the elements defining the

| RUN No. | E p.s.i. | $\mu$ | G p.s.i | LATERAL TOOTH DISPLACEMENT microns | REMARKS |
|---|---|---|---|---|---|
| 9 | 8·7 | 0·3 | 3·35 | 51·0 | See note below* |
| 10 | 26·1 | 0·3 | 10·05 | 17·0 | " |

* Tooth displacement to lingual, in a direction perpendicular to the tooth long axis.

TABLE 6.3 Lateral tooth displacement results for 30 gvm lateral load applied to 3-D finite element idealisation of maxillary central incisor. Periodontal membvane assumed isotvopic.

| RUN No. | AXIAL OR LATERAL 30 GRM LOAD | 2-D SLICE EQUIVALENT THICKNESS inches | E p.s.i | $\mu$ | G p.s.i. | CORRESPONDING AXIAL OR LATERAL DISPLACEMENT microns. |
|---|---|---|---|---|---|---|
| 11 | AXIAL | 1·0 | 8·7 | 0·3 | 3·35 | 5·2 |
| 12 | AXIAL | 0·345 | 8·7 | 0·3 | 3·35 | 15·12 |
| 13 | LATERAL | 0·345 | 26·1 | 0·3 | 10·05 | 17·2 |

TABLE 6.4 Axial and lateral tooth displacement results for 30gvm. axial and lateral loads respectively applied to 2-D finite element idealisation of maxillary central incisor. Periodontal membvane assumed isotvopic.

periodontal membrane were ascribed orthotropic mechanical properties with the major orthotropic material axis being made coincident with the known direction of the principal fibres in the membrane for each of the separate elements, FIGS. 6.18 and 6.19. The directions assumed for the principal fibres of the membrane were obtained by averaging the rather sketchy data given in standard anatomy texts, see for example the works of Scott and Symons and of Tylman and Tylman, (titles listed under general references).

The periodontal membrane orthotropic mechanical properties were then varied by trial and error in an attempt to obtain the required axial and lateral tooth displacements corresponding to the respective axial and lateral 30 gm. loads.

It must be remembered that in estimating the orthotropic properties, the Maxwell-Betti reciprocal relationships have to be observed. These are for two-dimensions:-

$$\varepsilon_{xx} = \frac{\sigma_{xx}}{Ex} - \mu_{yx}\frac{\sigma_{yy}}{Ey}$$

$$\varepsilon_{yy} = -\mu_{xy}\frac{\sigma_{xx}}{Ex} + \frac{\sigma_{yy}}{Ey}$$

$$\gamma_{xy} = \frac{\tau_{xy}}{Gxy}$$

with $$\frac{\mu_{xy}}{Ex} = \frac{\mu_{yx}}{Ey}$$

Hence, there are four independent elastic constants Ex, Ey, $\mu_{xy}$, (or $\mu_{yx}$) and Gxy. Obviously, the values and corresponding number of permutations which can be selected for these four independent variables is legion. Also, the selection of one set of values which may give the required tooth displacements

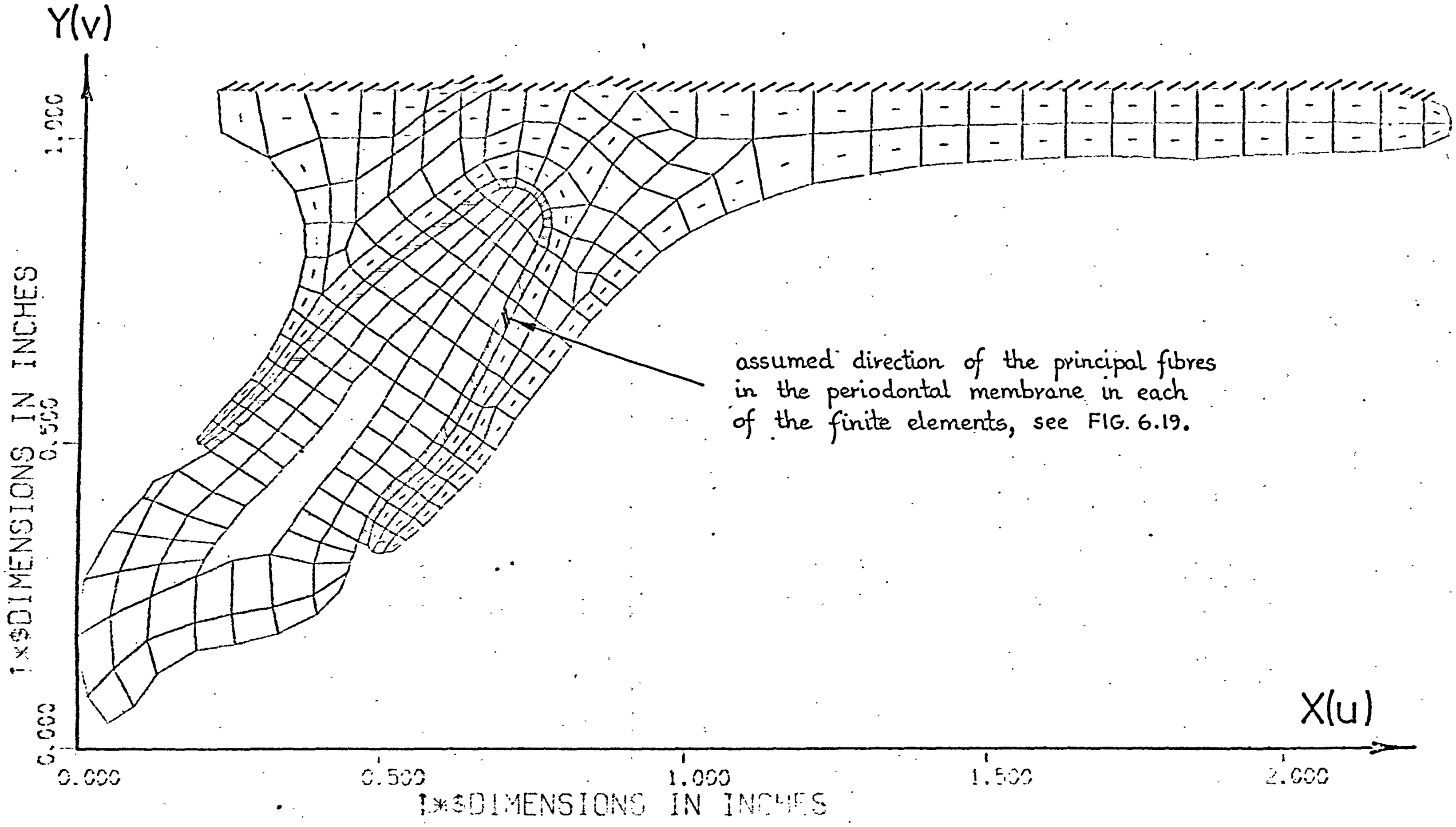


FIG. 6.18 Computer plot of 2-D vepresentation showing assumed direction of the principal fibres of the periodontal membrane ~(major orthotropic material axis.)

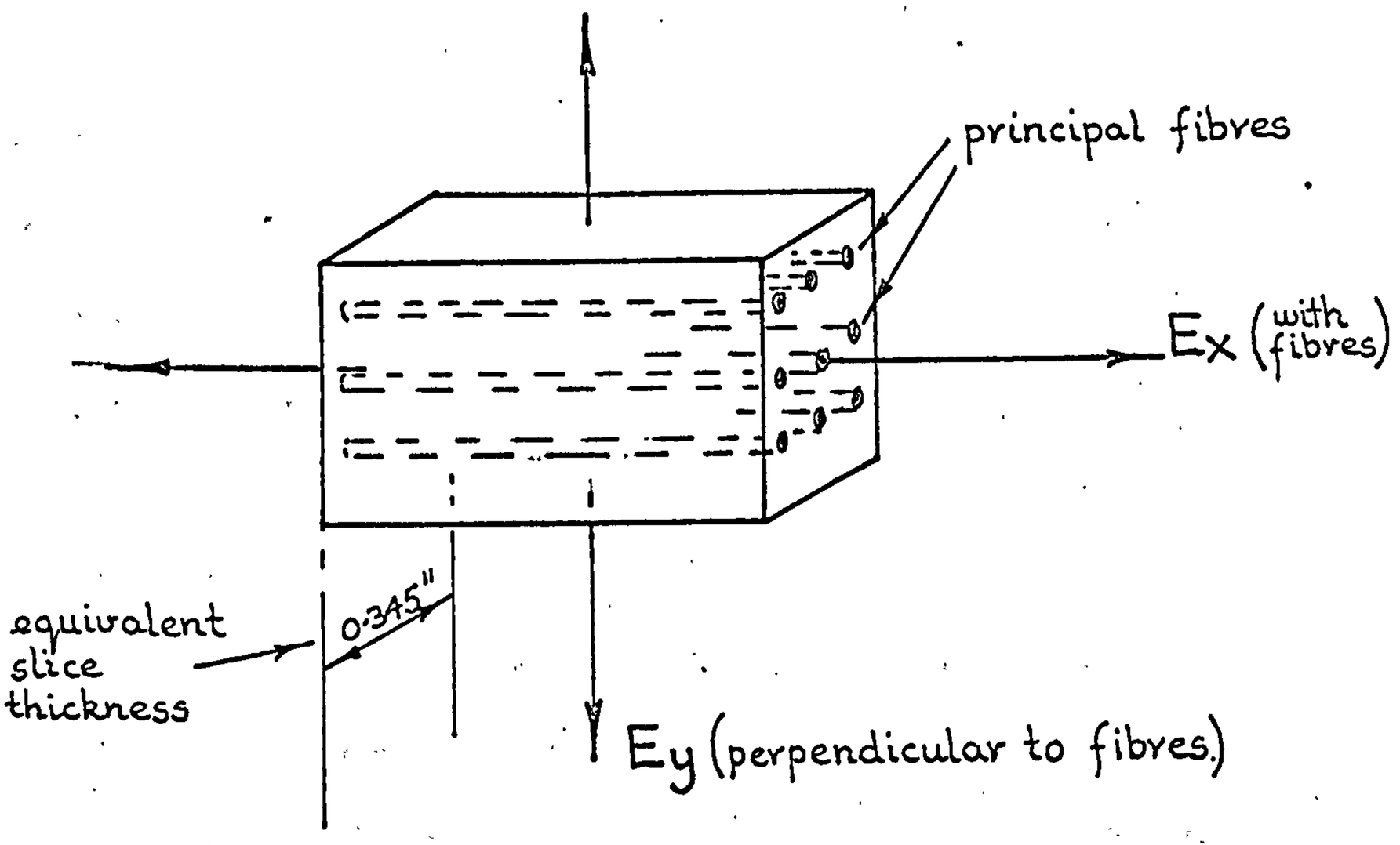


FIG. 6.19 Typical periodontal membrane element showing the principal fibres and the legend employed for defining the orthotropic mechanical properties in Table 6.5

| RUN No. | 30 GRM. LOAD AXIAL OR LATERAL | Ex p.s.i. | μxy | Ey p.s.i. | μyx | Gxy p.s.i. | TOOTH DISPLMT. AXIAL OR LATERAL | REMARKS |
|---|---|---|---|---|---|---|---|---|
| 14 | AXIAL | 32 | 0·24 | 4 | 0·03 | 3·35 | 6·8(μm) | |
| 15 | LATERAL | 32 | 0·24 | 4 | 0·03 | 3·35 | 31·6(μm) | |
| 16 | AXIAL | 32 | 0·24 | 4 | 0·03 | 1·68 | 7·1(μm) | |
| 17 | AXIAL | 16 | 0·24 | 8 | 0·12 | 10 | 8·7(μm) | Alveolar crest tips converge. |
| 18 | LATERAL | 16 | 0·24 | 8 | 0·12 | 10 | 28(μm) | |
| 19 | AXIAL | 16 | 0·24 | 8 | 0·12 | 10 | 10·6(μm) | Apical membrane elements made "soft." |

TABLE 6.5 Orthotropic mechanical properties of the periodontal membrane for orthodontic levels of axial and lateral tooth loading.

may only be one of many such sets. Consequently, for these and economic reasons only a few runs were undertaken in order to ascertain whether or not the periodontal membrane is orthotropic for this fairly low level of loading.

### 6.3.7 Results

In the first axial experiment, run number 14, Table 6.5, the ratio of the Young's moduli with and against the principal fibres was made equal to eight. This implied a comparatively high element stiffness in the direction of the collagenous fibres. Hence, as the value of the Young's modulus for the laterally loaded isotropic case was found to be 26.1 p.s.i., a value of Ex = 32 p.s.i. was selected. The Poisson's ratios similarly had to have the ratio of eight, and for ease and convenience $\mu xy$ was made equal to 0.24. Hence, the only other arbitrary elastic constant required was Gxy. This was prescribed the value of 3.35 p.s.i.; it was the value required in the axial isotropic experiment and from physical reasoning seemed the property most concerned with axial tooth displacement. The axial tooth displacement obtained from this analysis was only 6.8 microns, a value considerably below that required. However, using exactly the same properties for the lateral load condition, run number 15, the lingual displacement obtained was 31.6 microns. a value almost twice that required. Hence, paradoxically, the lateral load condition required property adjustments to stiffen the structure while the axial load

condition required adjustments in order to make the structure more flexible. It was mentioned earlier that the shear modulus seemed physically more significant in the axial displacement mode, however, halving the value of Gxy in run number 16 only slightly increased the flexibility. It therefore seemed apparent that the Young's modulus Ex must be the dominant property and so it was reduced in value by half. This would of course have increased the displacement for the transverse case which was already too big. Hence, Ey was increased by a factor of two and so the ratio of $\frac{Ex}{Ey}$ was reduced to two. Similarly, $\mu yx$ was modified so as to obey the reciprocal relationships. Because changing Gxy in run number 16 only marginally affected the axial tooth displacement, it also was increased to the value determined in the lateral mode for the isotropic experiment. However, although these changes result in an increase in tooth displacement for the axial case, run number 17, and a decrease in tooth displacement for the lateral case, run number 18, the relative changes in the displacements are small. For run number 19,the same properties were employed as in runs 17 and 18 but in this experiment the membrane elements in the apical region of the tooth were made very soft, thereby implying that the principal fibres provide no compressive support. Although the increase in axial displacement is encouraging,if this feature were to be applied to the transverse case, i.e. allowing the elements in the compression areas of the membrane to assume very little stiffness, then the lateral tooth displacement would obviously be drastically increased.

## 6.4 DISCUSSION AND CONCLUSIONS

### 6.4.1 Cortical Bone

The values of certain mechanical properties for human cortical bone have been suggested by various researchers. These have been compared and reasonable compromise values selected and used in order to determine those properties for which no values have been hitherto published.

While the Young's moduli values for bovine bone were found experimentally to be approximately twice those of the human equivalent, it was assumed in the finite element analyses that the shear moduli values were twice as large too. Hence, the end rotations obtained by Bonfield and Li from their bovine torsion tests were simply doubled for the equivalent human specimens. However, bearing in mind the limitations in the procedure adopted,the following mechanical properties for wet human cortical bone are proposed, (legend as given in Table 6.1).

$$E_x = 2.0 \times 10^6 \text{ p.s.i.}$$

$$E_y = 1.0 \times 10^6 \text{ p.s.i.}$$

$$E_z = 1.0 \times 10^6 \text{ p.s.i.}$$

$$\mu_{yx} = 0.15$$

$$\mu_{zx} = 0.15$$

$$\mu_{zy} = -0.5$$

$$G_{xy} = 0.4275 \times 10^6 \text{ p.s.i.}$$

$$G_{yz} = 1.0 \times 10^6 \text{ p.s.i.}$$

$$G_{zx} = 0.4275 \times 10^6 \text{ p.s.i.}$$

The negative value obtained for the Poisson's ratio $\mu_{zy}$, raises an interesting point. The negative sign, (remembering the normal sign convention), implies that a specimen of human cortical bone expands in the Y material coordinate direction when it is extended in the Z material coordinate direction. Although this effect is highly unusual for engineering materials, and on the face of it, seems highly irregular physically, it none the less may be feasible for biological materials. In fact, Haines (10) and the results of Renson (14), suggest that human dentine may have a negative Poisson's ratio. (Unfortunately, these authors made no comment regarding the physical implications of this anomaly.) After all, the two shear moduli obtained for human cortical bone are approximately half the magnitude of the two Young's moduli. This result seems reasonable when comparisons are made with published values for engineering orthotropic composite materials. For example, for two-dimensional glass fibre and boron fibre reinforced plastics, the in-plane shear moduli are almost exactly, in each case, half the magnitude of the smaller of the Young's moduli, Greszczuk (83).

### 6.4.2 Periodontal Membrane - Isotropic

Tooth mobility studies indicate that the tooth supporting structures possess a non-linear force-displacement response characteristic and also that they are probably time dependent. However, tooth force-displacement curves obtained from human subjects have been employed to determine overall isotropic

linear elastic mechanical properties for the periodontal membrane.

Using an axisymmetric finite element idealisation of a maxillary central incisor, the 'axial' mechanical properties of an assumed isotropic periodontal membrane were determined by matching finite element model displacements with those obtained from in-vivo mobility measurements made under the same level of axial loading. A similar approach, this time using a three-dimensional finite element model, was employed to determine the lateral membrane isotropic mechanical properties for the same tooth structure under a similar 30 gm. orthodontic level of lateral loading. It was found from the analyses that the periodontal membrane was very flexible relative to the other tissues comprising the periodontium. Consequently, in the 30 gm. force range considered here, tooth displacement takes place almost entirely within the periodontal space, i.e. with very little alveolar bone distortion. The results also show that if the membrane is considered to be isotropic, then the whole structure is approximately only $^1/3$ as stiff for axial tooth displacements, i.e. intrusion, as it is for lateral tooth displacements. This is reflected in the values determined separately for the isotropic mechanical properties of the periodontal membrane in the axial and lateral tooth displacement modes.

i.e. E (axial tooth loading = 8.7 p.s.i. ( $\mu$ = 0.3
30 gm load) G = 3.35 p.s.i.)

E (lateral tooth loading 30 gm. orthodontic load) = 26.1 p.s.i. ( $\mu$ = 0.3
G = 10.05 p.s.i.)

Hence, it can be concluded that the periodontal membrane must exhibit some degree of anisotropy in order to compensate for this 3 to 1 difference in stiffness required for the axial and lateral loading conditions. Moreover, it was shown in the axial case how compressibility drastically affected the flexibility of the periodontal membrane and consequently the resulting tooth displacement. However, the accuracy of the finite element results for Poisson's ratios greater than 0.45 is questionable. This is because in the derivation of the equilibrium equations, coefficients involving the quantity $\frac{1}{1 - 2\mu}$ arise. Hence, as $\mu$ approaches 0.5, this term approaches zero and the coefficient becomes infinite. (For the runs which considered the membrane to be incompressible, $\mu$ was made equal to 0.499 so as to avoid a zero term). Even so, the results demonstrate that numerous combinations of E and $\mu$ could be obtained in order to simulate the axial mobility studies. However, bearing in mind the displaceable blood volume contained within the periodontal membrane and the compressible components, e.g. collagen, constituting its structure, a Poisson's ratio of 0.3 seems a reasonable value to accept for the 30 gm. load range.

### 6.4.3 Periodontal Membrane - Orthotropic

The fibre support theory basically implies that the tooth is suspended in its socket by a system of principal fibres. Hence, because the fibres are assumed to be purely tension members, tooth loads are transmitted to the supporting alveolar

bone in the form of tensile stresses acting on the surface of the socket wall.

Although the finite element method employed in the analyses did not allow only tensile stresses to occur in the direction of the fibres in the periodontal membrane, it was contrived to give the major stiffness, i.e. the Young's modulus, to the elements in the direction of these principal fibres. Likewise, because of the Maxwell-Betti reciprocal relationships, the two Poisson's ratios were limited to the same ratio as that of the two Young's moduli. Even so, throughout the series of experiments the major Poisson's ratio was maintained around the value of 0.3 for the reasons discussed in sub-section 6.4.2.

Because of the limited number of experiments conducted in this section, no concrete conclusions can be drawn to either support or contradict the fibre suspensionary theory. Obviously, the two-dimensional finite element idealisation drastically simplifies the true situation and it may therefore be unfounded to make serious comment employing such a restrictive model. Although the model can simulate the principal membrane fibres, these are assumed to run parallel with the plane of the slice and not circumferentially as is believed to be the case, (Scott & Symons), see FIG 6.20. Also, the effect of compressibility which was found to be of major significance in the isotropic membrane experiments was not investigated.

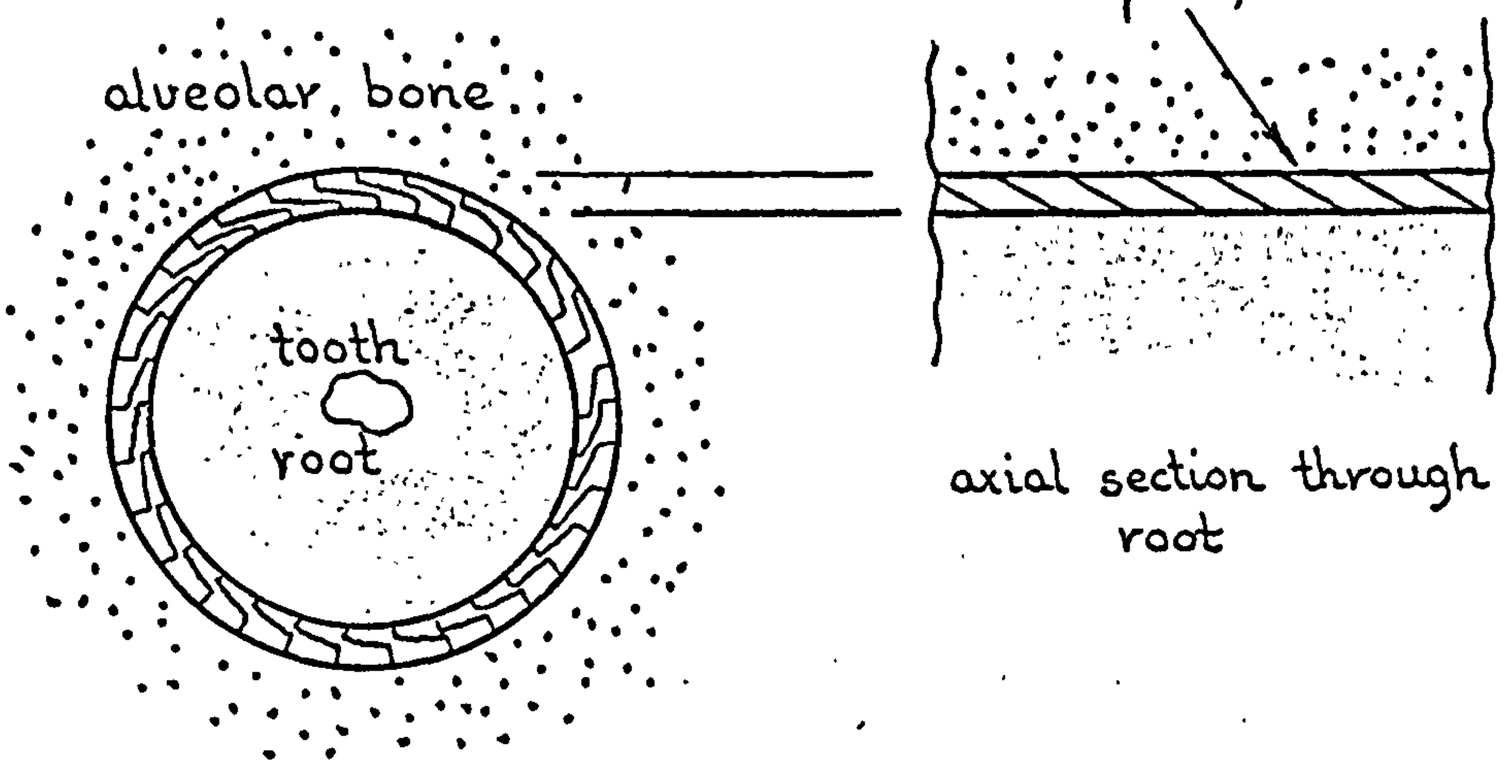


a) Normal model.

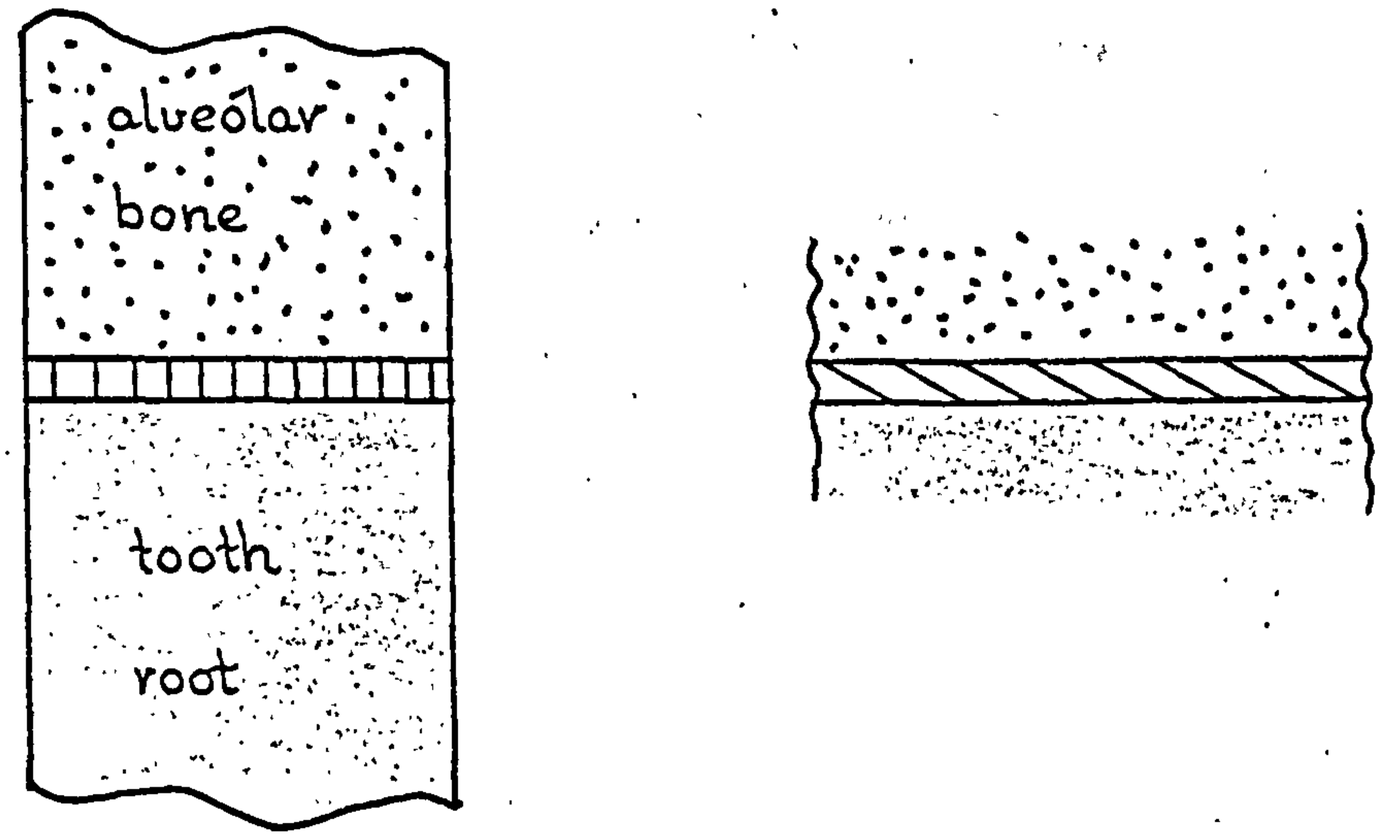


b) 2-D finite element model

FIG. 6.20 Illustrating the believed principal fibre orientation in the 'oblique' portion of the periodontal membrane and the corresponding finite element model simulation.

# CHAPTER SEVEN

# ANALYSIS OF THE CROWNS OF NORMAL AND RESTORED TEETH

# 7. ANALYSIS OF THE CROWNS OF NORMAL AND RESTORED TEETH

## 7.1 INTRODUCTION

Both normal mastication and the introduction of certain commonly employed restorations, generate considerable reactionary stresses in the teeth and supporting dental tissues. Already,some references have been discussed where this area of dental structural behaviour has been investigated, e.g. Hoppenstand and McConnell (41), Craig et al (51 and 52) and El-Ebrashi et al (53, 54, 55, 56 and 57). Here however, three distinct problems are considered. First, the design of the crown of a normal tooth is considered in an attempt to understand how the masticatory forces are reacted by the natural enamel-dentine tooth structure. In the second problem, the same tooth form, subjected to identical loading conditions, is considered but this time with the structure containing a full crown type restoration.

The final problem investigated is a class I amalgam restoration. This is considered with the view of determining the stress patterns generated in the restored structure as a result of the normal setting expansion of the amalgam. This is then extended to investigate the case where the amalgam restoration is exposed to a temperature increase such as may be experienced in vivo due to the ingestion of hot foodstuffs.

## 7.2 ANALYSIS OF THE CROWN OF A NORMAL TOOTH SUBJECTED TO MASTICATORY LOADING

While various authors have employed diverse techniques in order to study the structural behaviour of restored teeth, very few have attempted to examine the behaviour or structural response of normal teeth. Logically, this seems a somewhat unusual situation, for unless one has an understanding of the normal, how can one assess the effectiveness, or more important, diagnose possible causes of failure in the abnormal?

### 7.2.1 Finite Element Model and Test Procedure

The model employed for this problem was a two-dimensional pseudo bucco-lingual slice of a second mandibular premolar having an equivalent thickness of 0.345 inches, see FIG. 7.1. While the general external shape of the tooth was taken from the work of Wheeler (84), the internal structural arrangement was averaged from sections prepared from several normal healthy teeth which had been extracted for orthodontic reasons. The reason for selecting this particular tooth is that a great deal of the later work is concerned with it, e.g. the investigation into the force distribution on the tooth root as a result of various bridge loadings. Hence, the subsequent studies

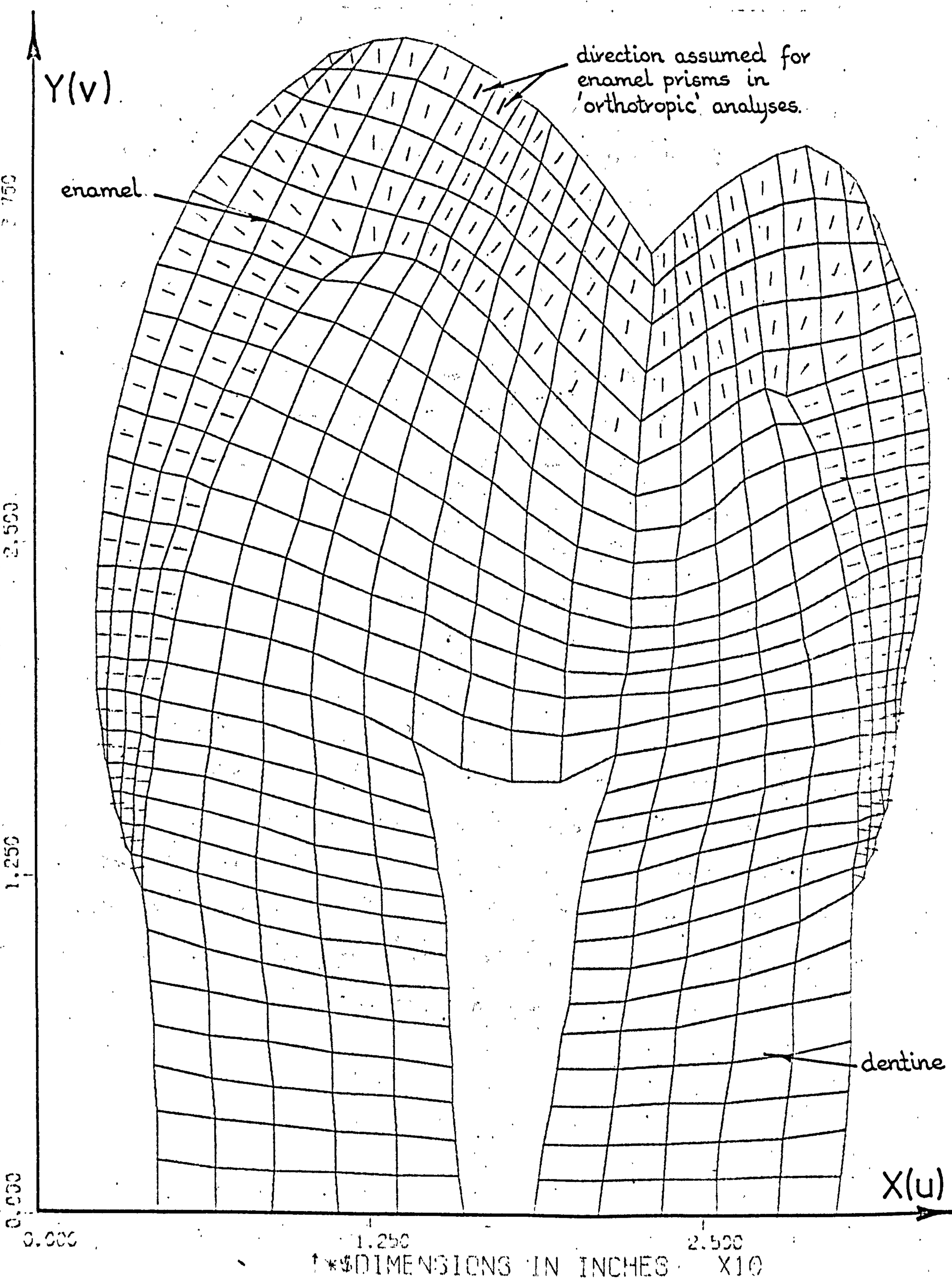


FIG. 7.1 Computer plot of pseudo bucco-lingual section of the crown of a second mandibular premolar. Model comprised of 508 quadrilateral 2-D finite elements.

will complement this investigation and so an overall tooth response from the point of loading through to periodontal membrane and alveolar bone support will be achieved.

The finite element model was restrained in both the X and Y co-ordinate directions at all the nodes lying on the X axis. Although this is of course an unnatural fixation, i.e. the tooth would normally be intruded and/or tipped under masticatory forces, because the investigation is concerned with the structural behaviour at the enamel-dentine-cusp region, this form of restraint does not affect the overall response in this area. (This is due to Saint-Venant's principle, see Chou and Pagano (85) pages 84 - 85).

7.2.2 Results

In the first experiment, the enamel was assumed to be isotropic and was ascribed a value of E equal to $6.8 \times 10^6$ p.s.i. The Poisson's ratio was made equal to 0.3 and so G was calculated from the formula $G = \frac{E}{2(1+\mu)}$. The dentine, an isotropic tissue, was given an E value of $1.7 \times 10^6$ p.s.i., see Table 3.7, and it too was ascribed a Poisson's ratio of 0.3. Although

there is no experimental evidence to justify the value of 0.3, it is a fact that the Poisson's ratio does not significantly affect the stress distribution in two-dimensional analyses. Consequently, a value common to general engineering isotropic materials was adopted.*

Forces were applied to the model at two points as indicated in FIG. 7.2. Even though the model is not strictly a bucco-lingual slice of a normal tooth, this form of loading was devised to simulate the cleavage type action of active centric occlusion. (In a normal tooth, the points of intercusp contact on the buccal and lingual cusps would not occur in the same bucco-lingual plane). FIG. 7.2 shows a plot of the contours of constant minimum principal stress under this loading condition and FIG. 7.3, the corresponding contours of constant maximum principal stress. These results are combined in FIG. 7.4 which gives a clearer physical appreciation of how the loads 'flow' through the tooth structure. In this figure, the magnitudes of the maximum and minimum principal stresses are represented by the lengths of the lines and the directions in which they act by their respective orientation. Thick lines represent compressive stresses and thin lines tensile stresses. Because of the scale chosen to represent the stress magnitude, values below 10 p.s.i. are not plotted.

*Two papers dealing with the finite element stress analysis of dental structures which have been published during the preparation of this thesis have also employed similar values for Poisson's ratio, Thresher and Saito (87) and Farah et al (88).

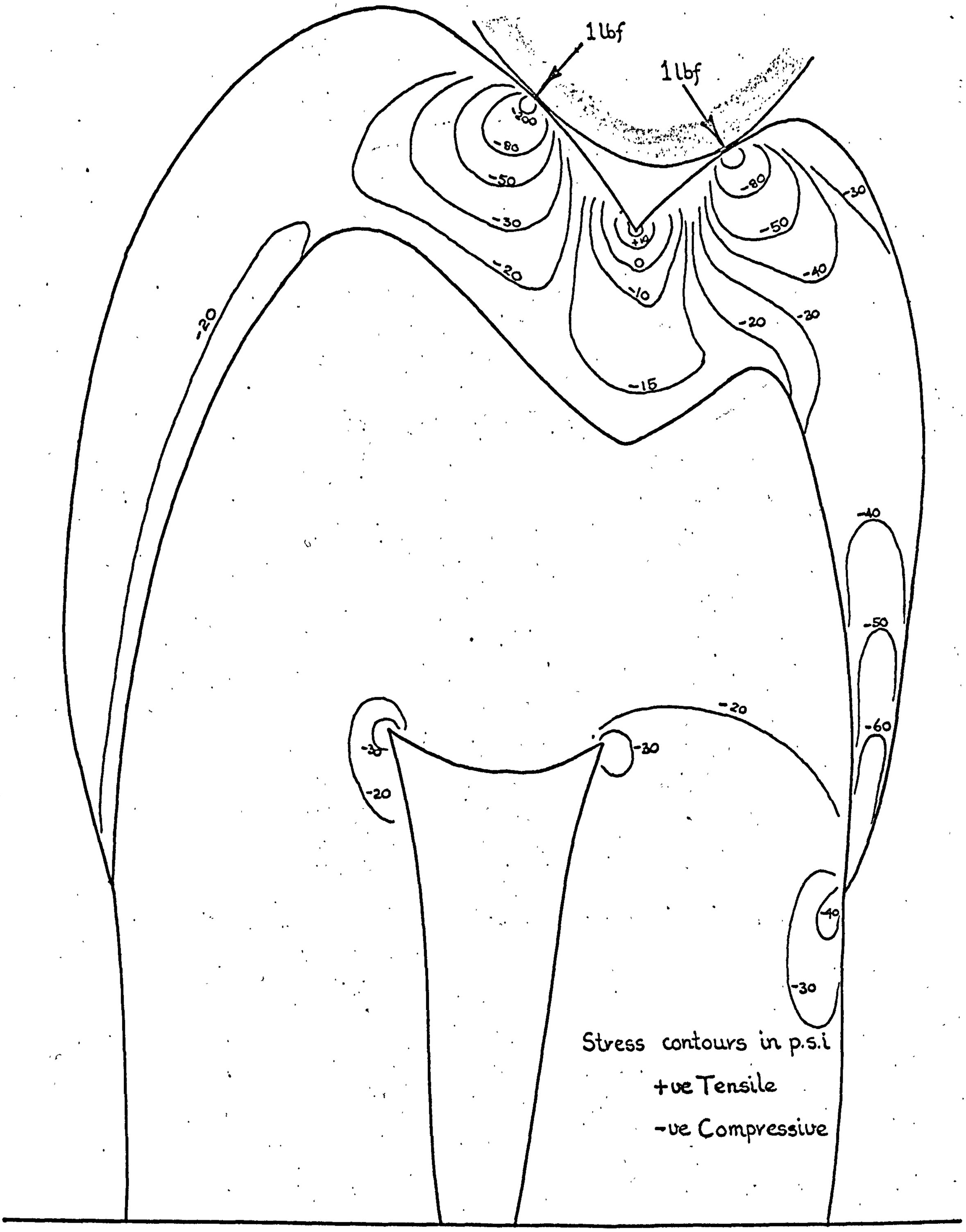


FIG. 7. 2 Contours of constant minimum principal stress. Isotropic enamel with two point loading.

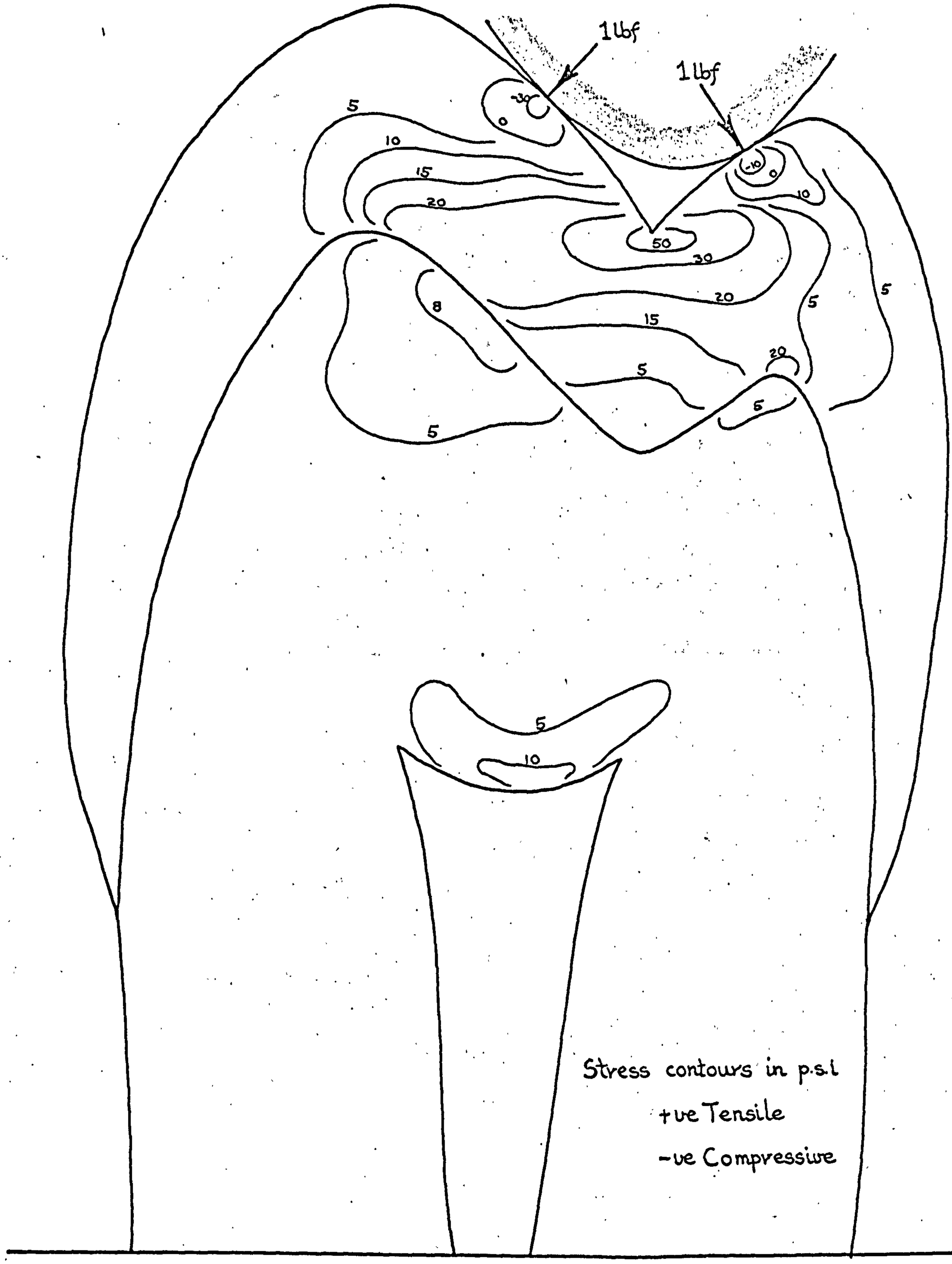


FIG. 7.3 Contours of constant maximum principal stress. Isotropic enamel with two point loading.

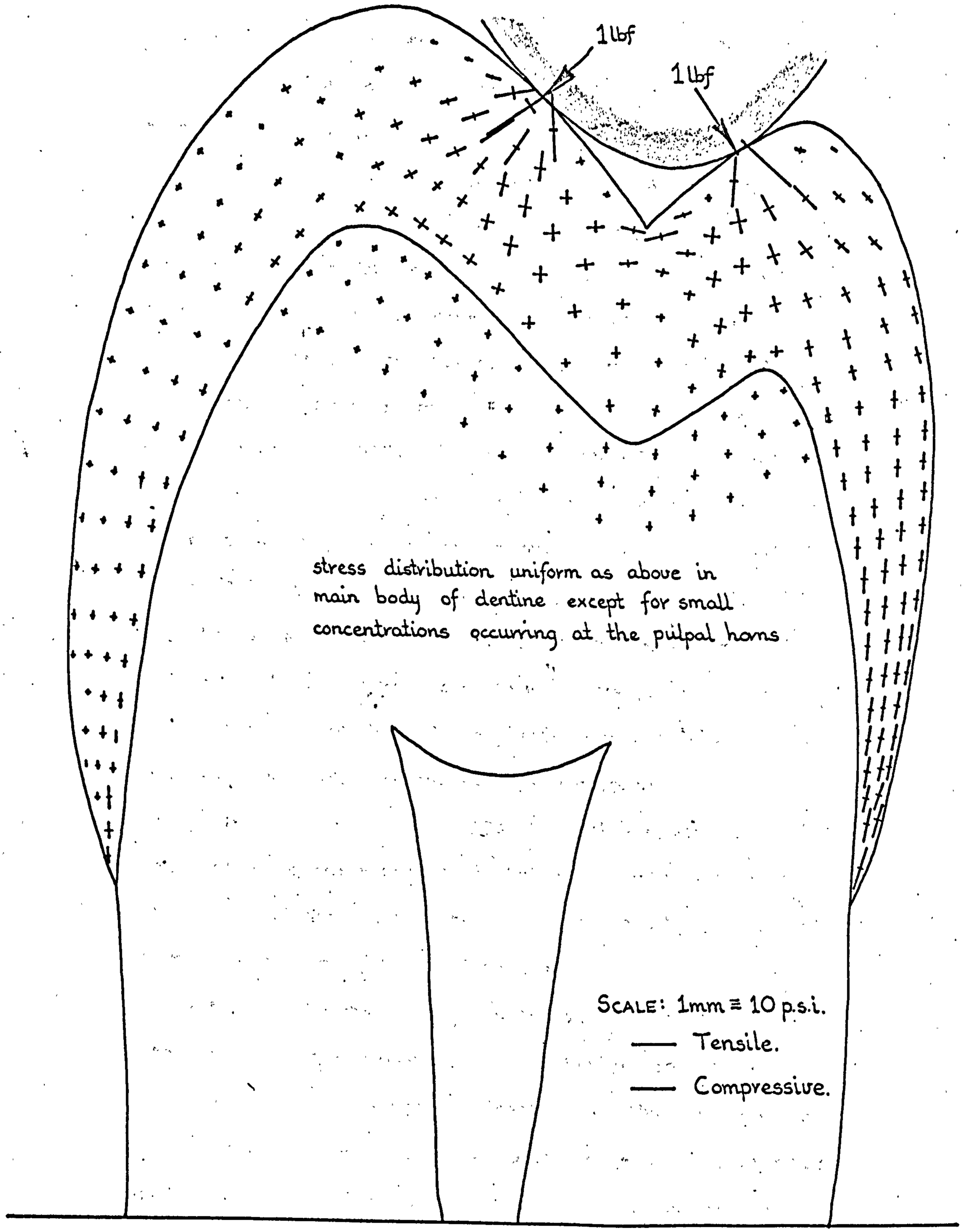


FIG. 7.4 Principal stress distribution for two point occlusal type loading. Enamel assumed to be isotropic.

The enamel in the second experiment was ascribed orthotropic mechanical properties; the long axis of the prisms being taken as the primary or stiffer material direction. The line in the centre of the enamel elements in FIG. 7.1, indicates the direction assumed for the prisms in that particular element. While the mechanical properties of the dentine were maintained at the values used in the previous experiment, the properties ascribed to the enamel were as shown in FIG. 7.5. The Young's moduli, taken from Table 3.7, have a ratio of 3 to 1, and so, to obey the Maxwell-Betti reciprocal relationships, the Poisson's ratios were similarly proportioned. While the primary Poisson's ratio was set at 0.3, the value of Gxy was obtained by halving the smaller of the Young's moduli.

In the first instance the structure was loaded in a manner identical to that of the previous experiment, i.e. two point loads simulating intercuspation. This arrangement is illustrated in FIG. 7.6 which shows the resulting principal stress distribution occurring in the tooth structure. Hence, by comparing FIGS. 7.4 and 7.6, the effect of enamel anisotropy can be ascertained.

A final experiment was conducted on this model structure with the mechanical properties of the tissues remaining at the values used in the previous test. However, in this case, the structure was only subjected to a single point load which was applied to the lingual side of the buccal cusp of the 'tooth' as illustrated in FIG. 7.7. This figure also depicts the resulting principal stress distribution in the structure under this particular loading regime.

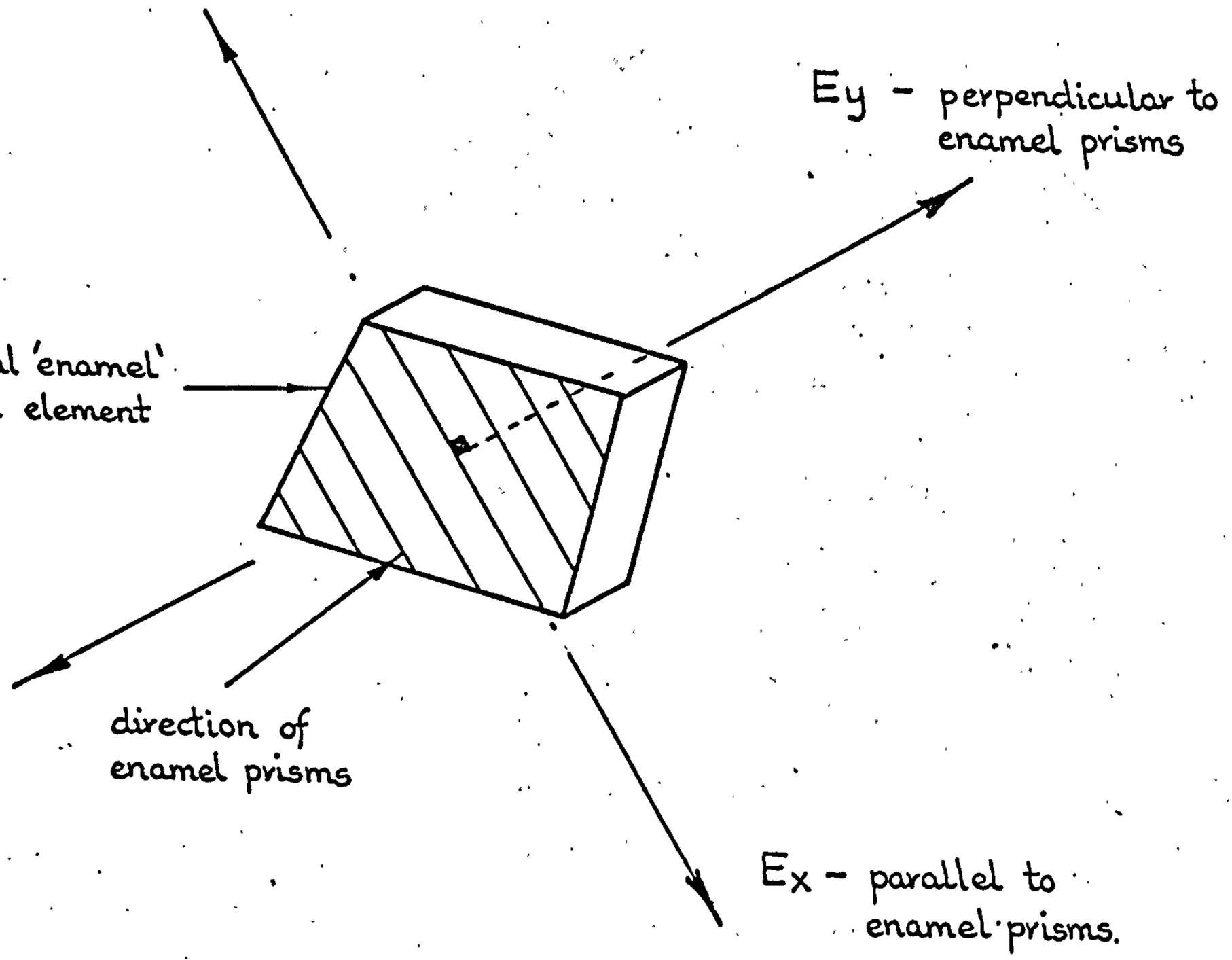


| Ex (parallel to enamel prisms) p.s.i. | μxy | Ey (perpendicular to enamel prisms) p.s.i. | μyx | Gxy p.s.i. |
|---|---|---|---|---|
| $10.2 \times 10^6$ | 0.3 | $3.4 \times 10^6$ | 0.1 | $1.7 \times 10^6$ |

FIG. 7.5 Values ascribed to the orthotropic mechanical properties of the enamel.

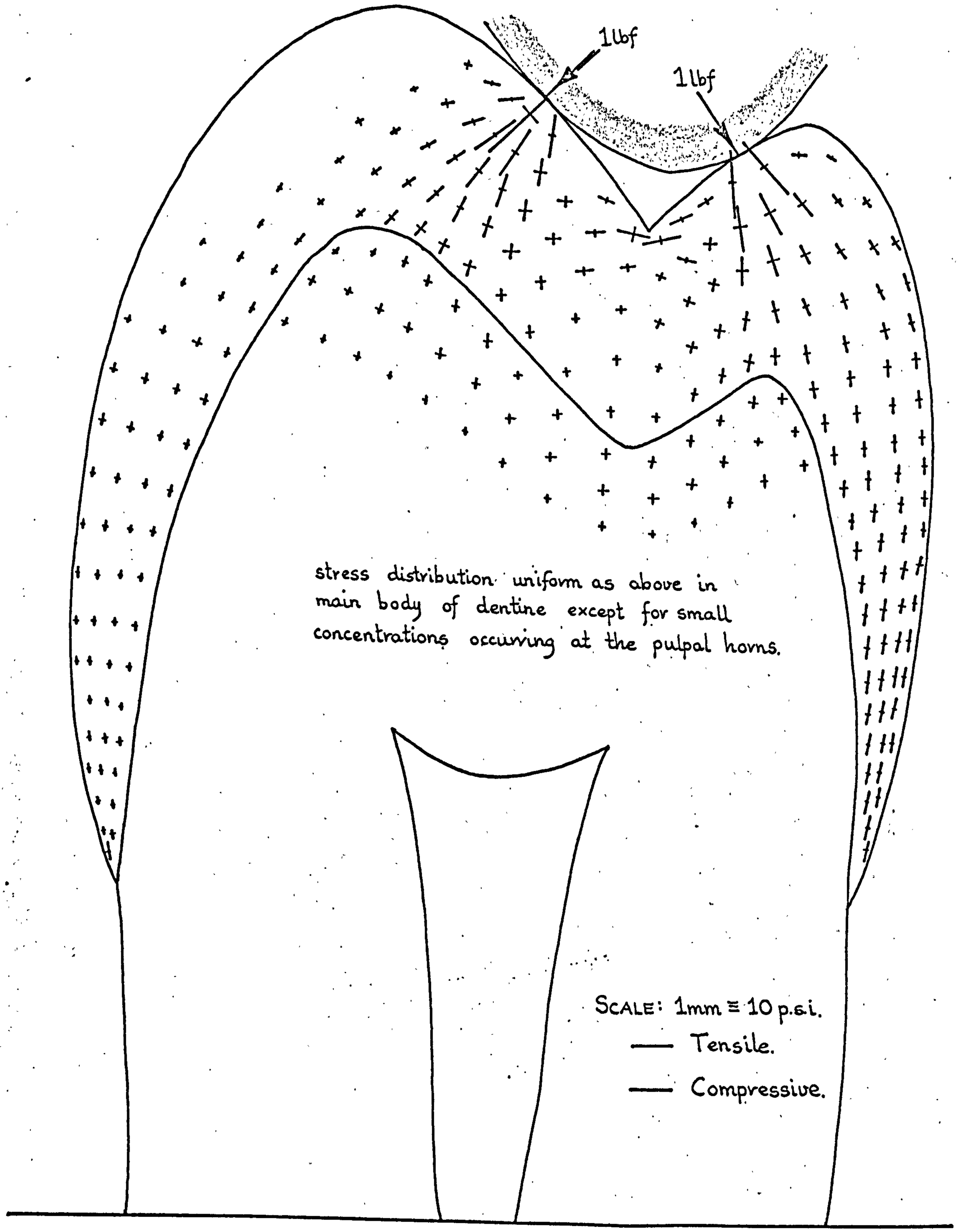


FIG. 7.6 Principal stress distribution for two point occlusal type loading. Enamel assumed to be orthotropic.

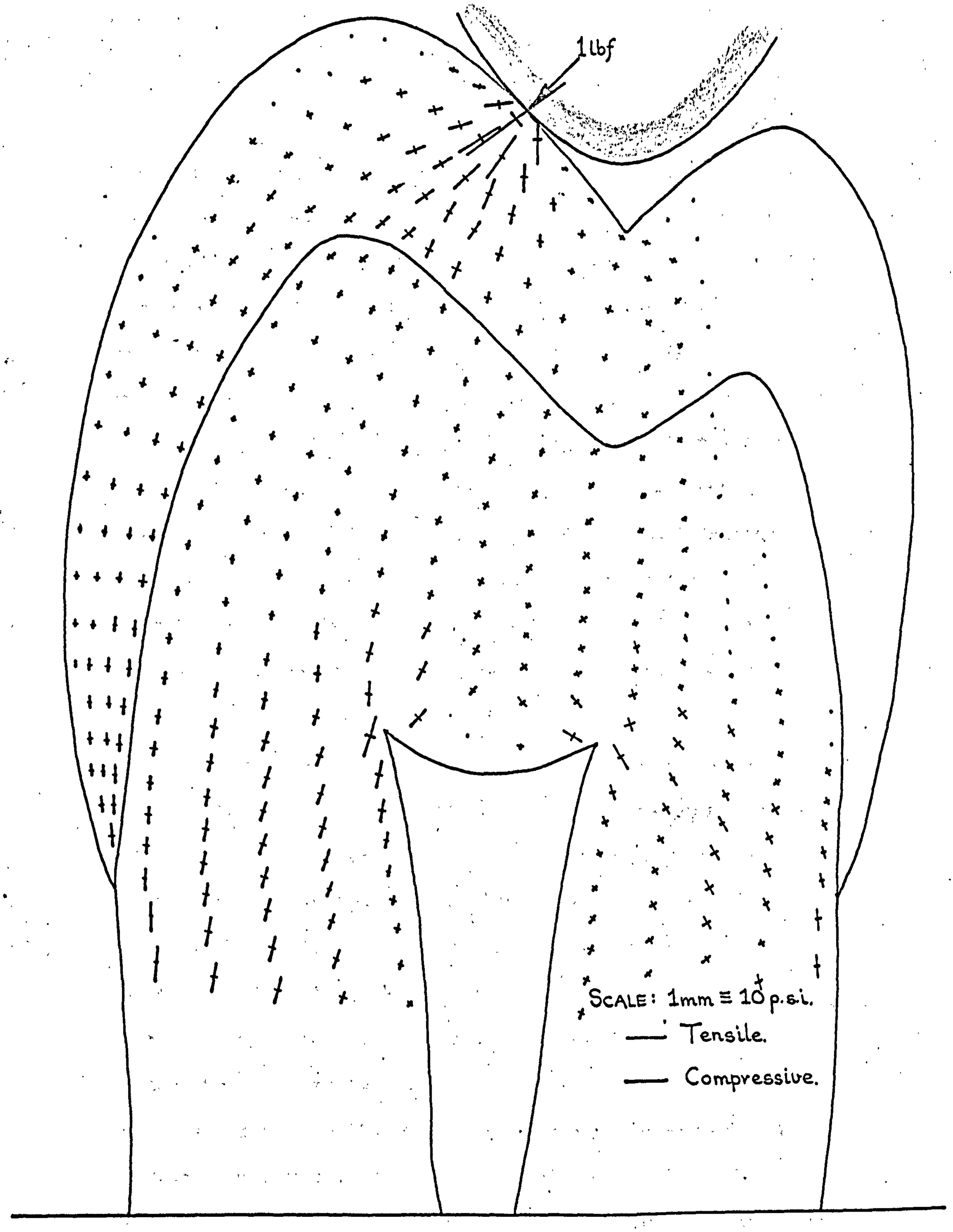


FIG. 7.7 Principal stress distribution for single point occlusal type loading. Enamel assumed to be orthotropic.

### 7.2.3 Discussion of Results

The results of all three experiments in the preceeding sub-section clearly demonstrate the role played by the enamel in reacting the forces of mastication. Even in the first experiment, where the enamel was assumed to be isotropic, its greater stiffness over that of the dentine enabled it to react the larger proportion of the applied loads. (This result agrees with the experimental observation made by Lehman and Meyer (60), who noticed this behaviour in their work with three-dimensional tooth models composed of an epoxy resin - silicone rubber combination. Their enamel-dentine material simulation which had a Young's moduli ratio of 6 to 1, was very similar to that used in the finite element isotropic experiment). Hence, masticatory forces tend to 'flow' around the enamel cap as illustrated in FIG. 7.8, while the dentine core remains relatively lightly stressed. This in fact is seen to be the case for all three experiments for isotropic or orthotropic enamel under single or two point loading, see FIGS. 7.4, 7.6 and 7.7. Consequently, the enamel near the amelo-cemental junction is very highly stressed because the reacted forces have to flow into and through this thin wedge of tissue in order for them to be transmitted into the root of the tooth and subsequently into the supporting alveolus. It is therefore evident that restorations inserted into the cervical region of the teeth can be subjected to high compressive stresses even though these areas are not susceptible to the direct contact stresses of mastication. Indeed, it may be that these high stresses are

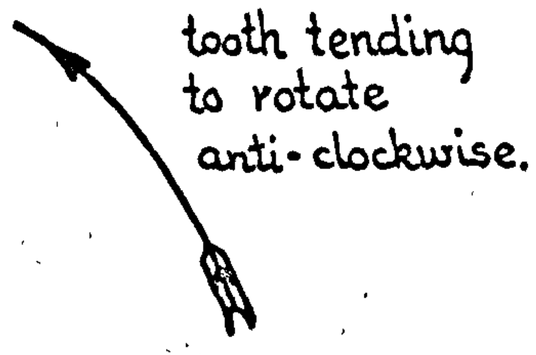


FIG. 7.8 Illustrating the flow of masticatory type forces through the enamel-dentine tooth structure.

responsible for the pain often experienced by patients who have received cervically placed restorations.

Another important feature demonstrated by the experiments is the relatively high tensile stresses which are generated in the fossa under masticatory type loading. Although these stresses do not seem to be as large in magnitude as those induced near the amelo-cementad junction, they could have far more serious consequences.. It can be seen from FIGS. 7.4 and 7.6, that these tensile stresses would tend to pull apart the enamel prisms in this region and may thereby assist the attack of caries in the fossae of premolar and molar teeth once the chemical demineralisation of the enamel has been initiated. The distraction of the cusps would also tend to open up the margins of any restbration placed between the two contact points. Any increase in the marginal gap would obviously encourage the seepage of harmful material into these spaces and consequently, may assist in the breakdown of the margins of restorations placed in this area.

## 7.3 ANALYSIS OF A FULL CROWN RESTORATION SUBJECTED TO MASTICATORY LOADING

### 7.3.1 Finite Element Model and Test Procedure

The removal of the enamel cap from a tooth and its subsequent replacement with a full cast gold crown, is a type of restoration often employed when large areas of the crown are affected by caries. Therefore, in this section, the

mechanical behaviour of this type of restoration is compared with the response obtained in the previous section for a normal tooth under identical loading conditions. A scaled computer plot of the full crown model is shown in FIG. 7.9 and its likeness in form to the normal tooth model can easily be seen on comparison with FIG. 7.1. The occlusal surface of the full crown was made identical to that of the original normal tooth surface. It was designed, having 5 degree axial wall angles and with rounded shoulder type proximal margins. The thickness of the gold restoration at the proximal margins was made approximately 1.25 mm.

7.3.2 Results

For the two experiments conducted on this model, both the gold and the dentine were assumed to be isotropic materials. The dentine was ascribed the same value for its Young's Modulus as for the previous problem, i.e. $E=1.7\times10^6$ p.s.i., while the gold was given the value of $E=11.3\times10^6$ p.s.i., see Table 3.7. Both materials were given the value of 0.3 for their Poisson's ratio and their respective shear moduli were subsequently calculated using the familiar formula $G=\frac{E}{2(1+\mu)}$.

Forces were applied to the model in the first experiment at two points, the same as for the previous problem simulating active centric occlusion. FIG. 7.10a shows the resulting principal stress plot under this system of loading, again the lengths of the lines indicate the magnitude of the stresses and their orientation, the direction in which the stresses act. Thick lines represent compressive stresses and thin lines tensile stresses.

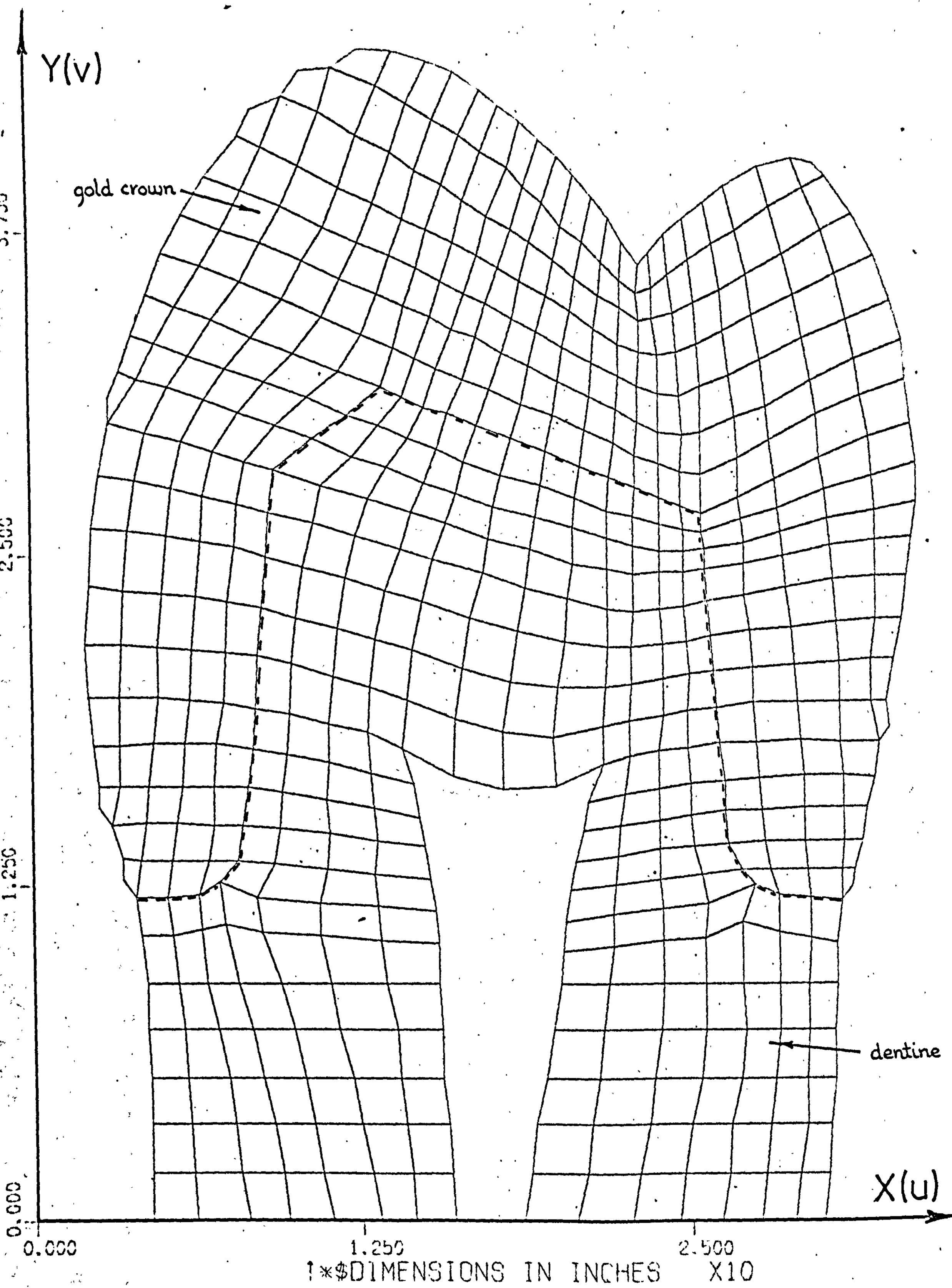


FIG. 7.9 Computer plot of pseudo bucco-lingual section of a second mandibular premolar containing a full cast gold crown restoration. Model comprised of 518 quadrilateral 2-D finite elements.

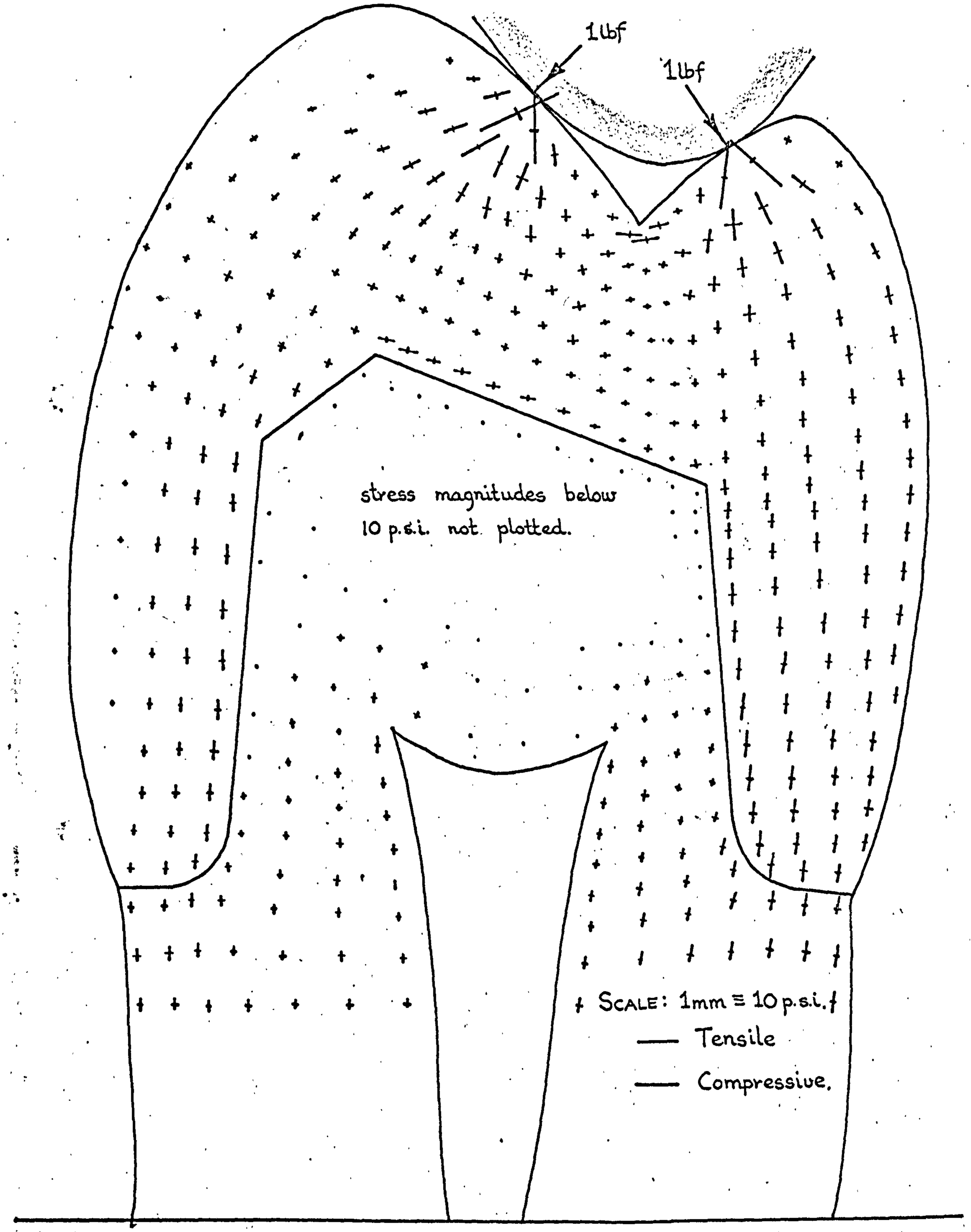


FIG. 7.10a Principal stress distribution for a full cast gold crown restoration under two point occlusal type loading.

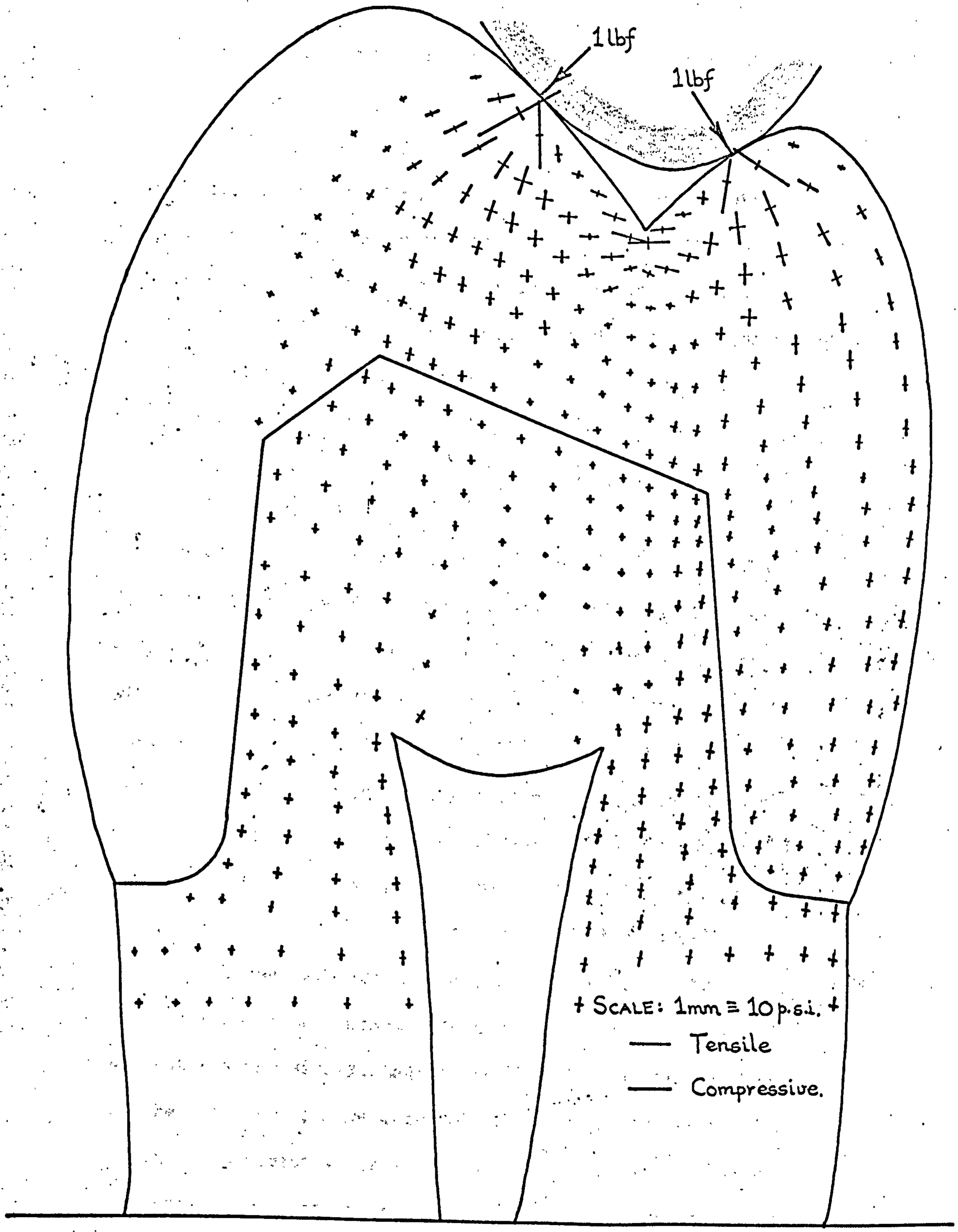


FIG. 7. 10b Principal stress distribution for an acrylic resin full crown restoration under two point occlusal type loading.

In the second experiment with this model, a 'masticatory' load was applied at a single point as before and as shown in FIG. 7.11. This figure also shows the principal stress distribution resulting from this tipping type loading whereas FIG. 7.12 shows the distortion or displacement of the loaded structure. This picture was obtained by plotting, to a suitably enlarged scale, the calculated nodal point displacements of the model at the perimeter and at the interface between the different materials.

### 7.3.3 Discussion of Results

The principal stress distribution shown in FIG. 7.10a for the full cast gold crown restoration under the centric occlusion type loading, is in many respects similar to the plot of FIG. 7.4 for the enamel-dentine structure under identical loading conditions. In both cases, the occlusally applied loads are transmitted around the very much stiffer gold or enamel cap material as illustrated earlier in FIG. 7.8. Hence, the gold crown is playing remarkably well the role of an improvised enamel. This is perhaps hardly surprising as the stiffness of the gold material is practically the same as that of the enamel tissue which it is replacing. To demonstrate the significance of the likeness in the stiffness of the gold restorative material and that of the enamel, a further experiment was performed. For this test the same geometric crown structure under identical loading and support conditions was employed. However, for this case the full crown restoration was ascribed a stiffness (approximating

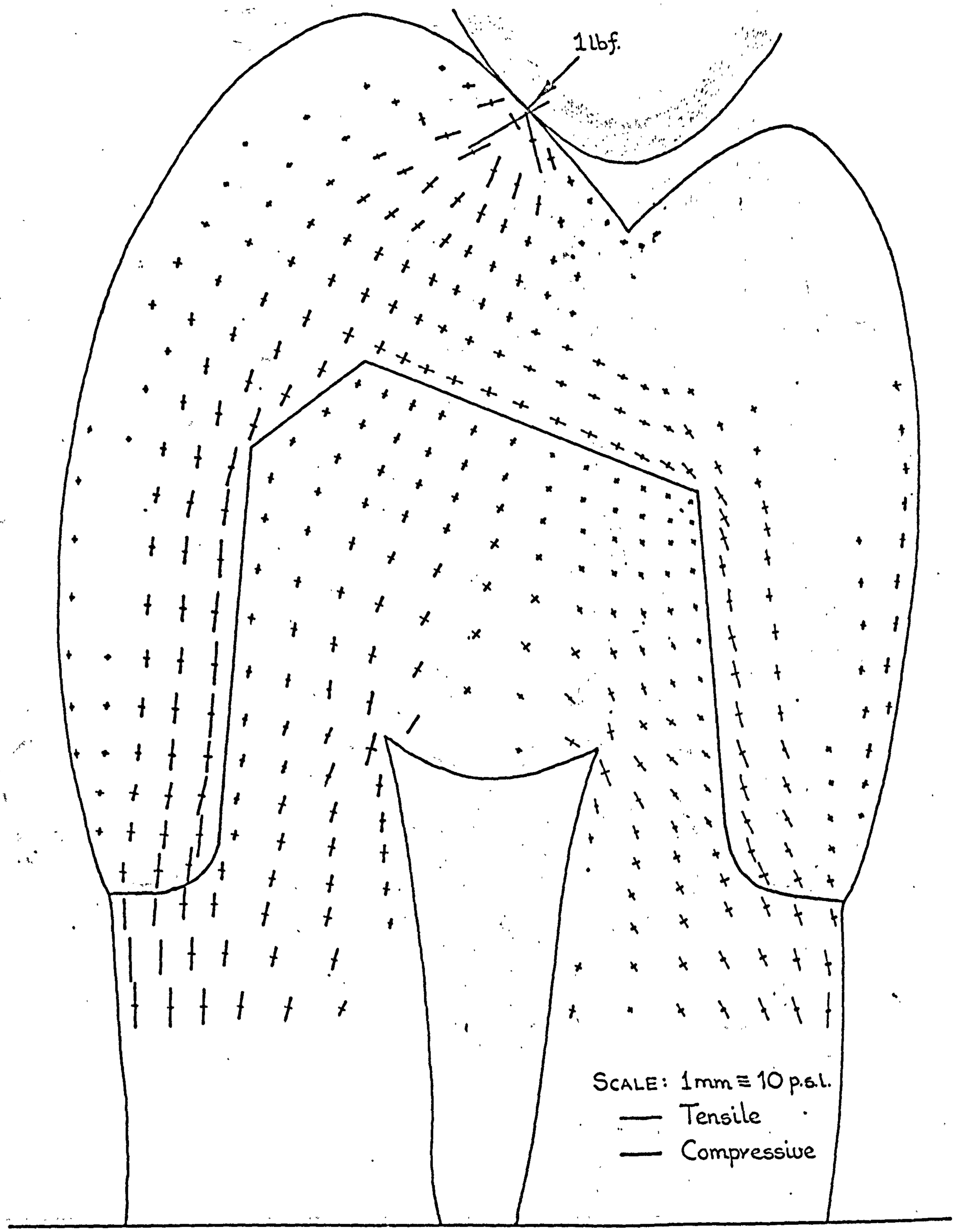


FIG. 7.11 Principal stress distribution for a full cast gold crown restoration under single point occlusal type loading.

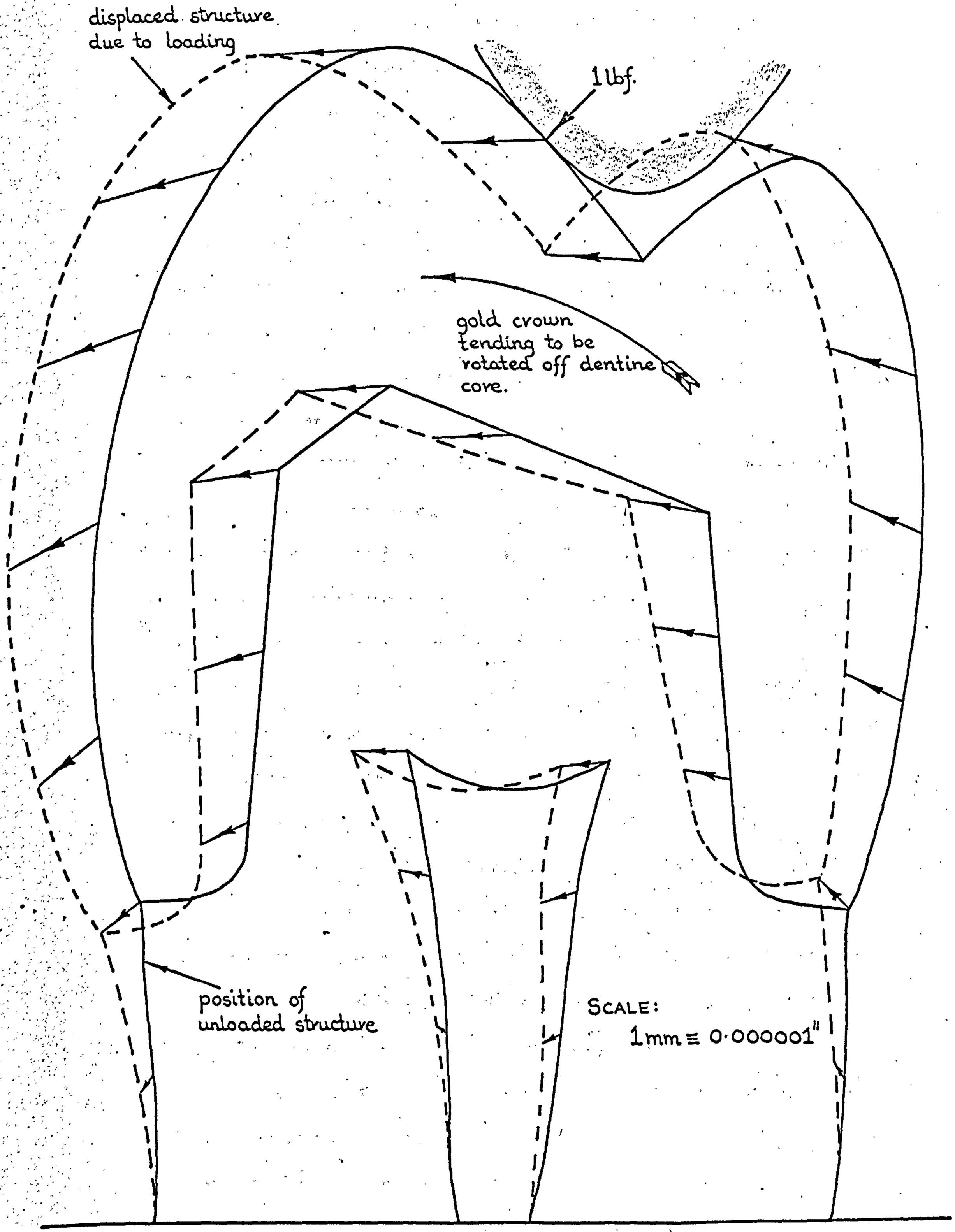


FIG. 7. 12 Displacement of the full cast gold restoration due to the single point turning type occlusal loading.

to that of polymethylmethacrylate), equal to half the value ascribed to that of the dentine core. FIG. 7.10b gives the resulting principal stress distribution for this structure. It can been seen from this figure that the less-stiff crown restoration is not by-passing the occlusal loads around the dentine above the pulp chamber as did the gold crown restoration shown in FIG. 7.10a. Instead, more of the load is flowing through the dentine 'crown', which is consequently more highly stressed than it was with either the gold restoration or with the natural enamel crown.

The major difference between the cast gold crown restoration and the enamel of the normal tooth structure, lies in the design of the gold crown's proximal margins. Whereas the enamel thins down to feather edges, the gold crown model stands on two broad legs over the tooth's dentine core. In fact, the design of the full gold crown restoration in this region becomes very critical when the single point tipping type load is applied to the lingual aspect of the buccal cusp. It can be seen from FIGS 7.11 and 7.12 that this loading condition is trying to rotate the gold crown in an anticlockwise sense off the dentine core. This is indicated by the high compressive stresses generated at right angles to the shoulder at the proximal margin in the buccal leg of the crown and by the correspondingly high tensile stresses in the lingual leg. The reason why these high stresses are induced in this model is that the finite element analysis technique employed here rigidly connects the gold to the dentine at all the nodes along the materials' interface. In an actual tooth however, if either the tensile or compressive strength of the cemented joint between the gold crown and the dentine were below the stress level generated,

the margin would of course fail and would consequently allow the ingression of unwanted materials. Although studies concerned with the strength of dental cements have been reported, see for instance the work of Peyton *et al* listed under general references, no work has been traced which deals with the tensile or compressive strength of complete cemented joints. Obviously, failure of a cemented joint will occur along the weakest path. This could possibly be at the mechanical bond between either the dentine and cement or between the gold and cement. Consequently, investigations concerned with dental cements should be carried out on complete joints as well as on the individual cement materials themselves.

Because the tipping type load is trying to rotate the gold crown off the dentine stump, it would be beneficial from the mechanical point of view if the contour of the occlusal surface of the crown was flattened. This would reduce the magnitude of the lateral or turning force component. Although at present the occlusal surfaces of crowns are 'flattened' clinically, this is done purely so that the surfaces produced are self-cleansing.

Although the two-dimensional model undoubtedly accentuates the rotational effect, it is evident that the design of the proximal margins of crown restorations, the stabilizing height and parallelism of the axial walls and the form of the occlusal surface must be carefully considered. The examination of these various aspects of restoration design presents the ideal problem to which the finite element method is particularly well suited.

## 7.4 ANALYSIS OF A CLASS 1 AMALGAM RESTORATION SUBJECTED TO SETTING AND THERMAL EXPANSION

### 7.4.1 Finite Element Model and Test Procedure

Although numerous authors have investigated different aspects of amalgam restoration design, no references have been found where the structural effects of the amalgam setting (i.e. pre-stress) and thermal expansions have been examined. It was therefore the aim of this sub-section to look at the structural behaviour of a tooth restored with typical class 1 type amalgam restorations and subjected to these two internally generated force systems.

The tooth selected for this series of experiments was again the second mandibular premolar. However, instead of using the two-dimensional simulation as in the previous set of experiments in this chapter, this time an axisymmetric representation was employed. FIG. 7.13 shows a computer plot of the model divided up into 662 three-noded, straight-sided, triangularly shaped annuli type finite elements. Obviously, the shape of the tooth in this model has been modified in order for it to possess rotational symmetry. Although of course this therefore represents an unnatural structure, this idealisation should not limit the applicability of the analyses for this type of structural loading. As can be seen from the figure the mesh or finite element division has been arranged so that the depth of the cavity, and consequently the depth of the filling and lining materials, can easily be changed so that different sizes and forms of

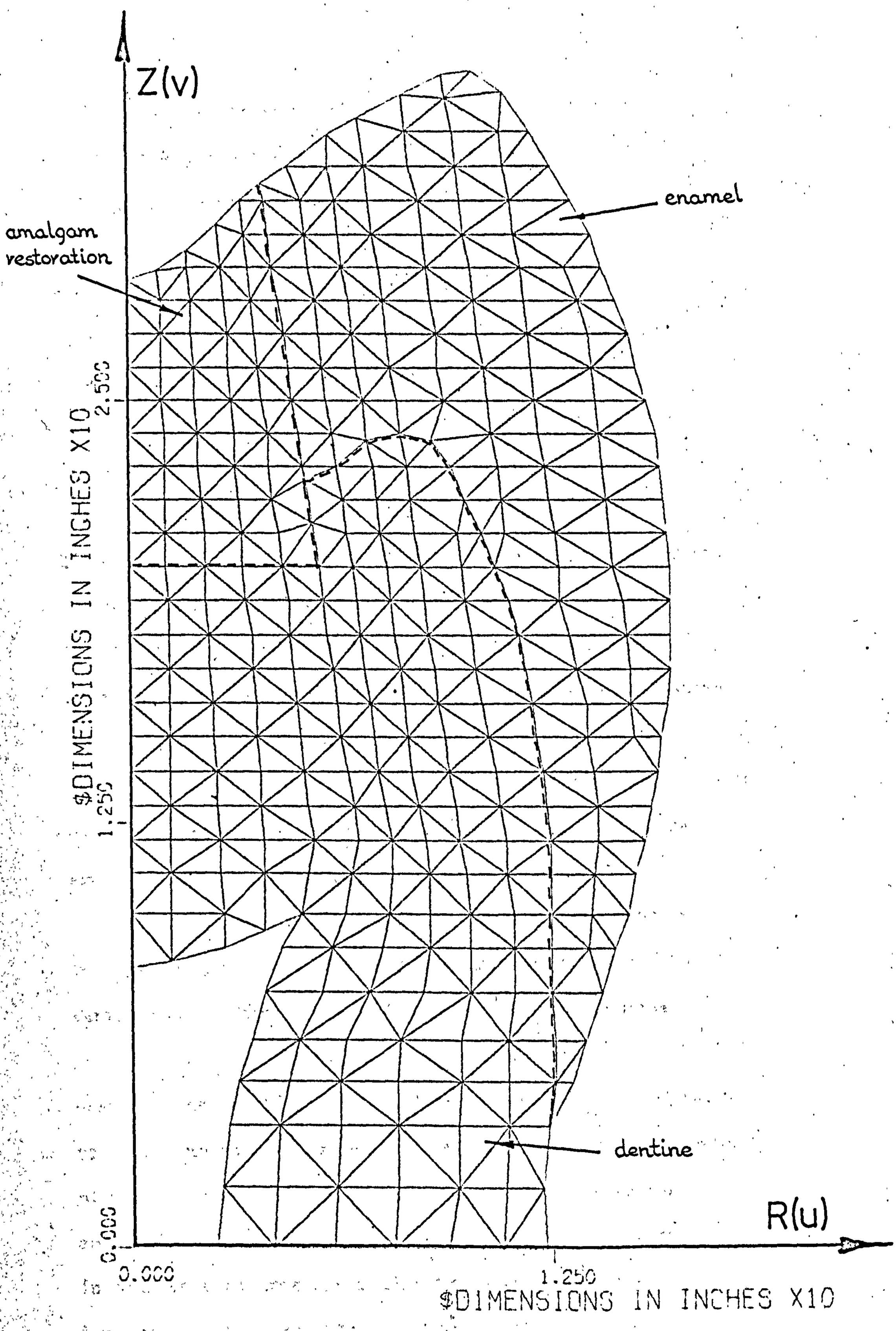


FIG. 7.13 Computer plot of axisymmetric representation of a mandibular second premolar containing a shallow class I amalgam restoration. Model comprised of 662 triangular section annular finite elements.

restoration can be examined. The mean diameter of the cavity is approximately 2 mm with the axial wall diverging 7.5 degrees from the occlusal surface. The boundary conditions applied to the model were to restrain all the nodes on the axis of rotation from movement in the radial direction and the pulpal surface node on the radial axis from movement in the Z co-ordinate direction.

The normal amount of setting expansion recommended for an amalgam lies generally between 3 and 20 microns per centimetre length of the restoration. Hence, as the linear dimensions of the restoration under consideration are approximately 2 mm, the amount of setting expansion can be prescribed as shown in FIG. 7.14. From this figure it is evident that a uniform temperature increase of 40 degrees Centigrade in the amalgam, produces a 'free' expansion of the restoration equivalent to that produced by the unrestrained setting expansion of the same restoration for a pre-stress amounting to 10 microns per centimetre length.

In the mouth, the teeth and restorations are subjected to temperature variations ranging from 0 up to 60 degrees Centigrade, Pickard (30). Consequently, as the normal mouth temperature is 37 degrees C, the upper limit is 23 degrees C above this datum. Usually however, the extremes of this temperature range are never realized for long periods of time in the mouth but rather represent the peaks or amplitudes of the fluctuations. Hence, the variations in oral temperatures are really transients with the temperature, whether from above or below 37 degrees C, always tending to return to this equilibrium or datum value,

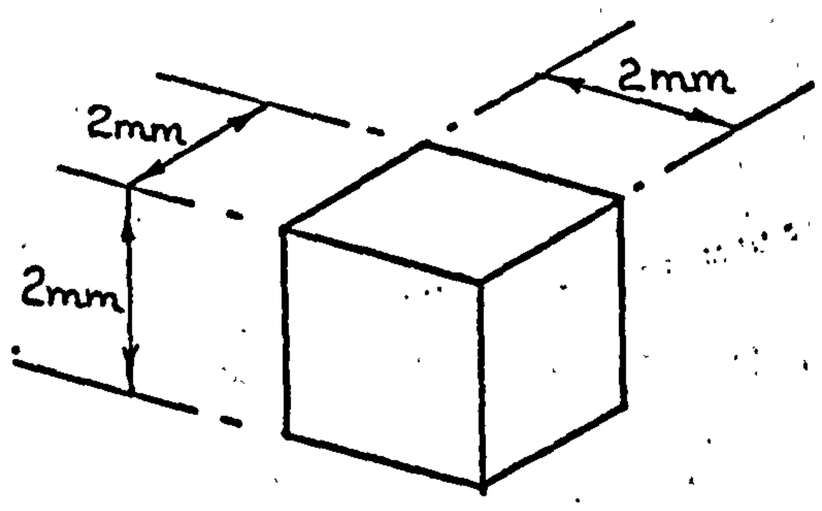


Linear dimension of amalgam restoration $\simeq$ 2 mm

Amount of pre-stress required @ 10 microns per centimetre length of restoration. i.e $= 0{\cdot}001$ mm/mm

But linear dimension of restoration is 2 mm

Therefore, pre-stress required for this restoration $= 0{\cdot}002$ mm

Now the change in a linear dimension as a result of an increase in body temperature is equal to, see sub-section 3.2.12.

$$\delta l = \alpha \times l \times \text{Temp. rise.}$$

Hence, in this case

$$0{\cdot}002 = \alpha \times l \times \text{Temp. rise.}$$

Now $\alpha$, the coefficient of linear thermal expansion, is equal to $25 \times 10^{-6}$ mm/mm per °C for amalgam, see Table 3.7. Therefore, substituting in the equation above gives the equivalent temperature rise required to produce the same amount of setting expansion in the amalgam restoration.

$$\text{i.e. Equivalent Temp. rise} = \frac{0{\cdot}002}{25 \times 10^{-6} \times 2} \,^{\circ}C$$

$$\underline{\text{Equivalent temperature rise}} = \underline{40\,^{\circ}C}$$

FIG. 7. 14 Determination of the equivalent temperature rise required to produce a 10 micron/cm setting expansion in an amalgam restoration.

It is in this context that the thermal conductivity of the restorative material has its major significance. Obviously, a material which is a good thermal conductor will conduct heat more quickly through the restoration towards the dental pulp even if the oral temperature is only increased momentarily. (Braden (86), shows in his work on the efficiency of lining materials that thermal diffusivity, a quantity involving the thermal conductivity, density and specific heat of the material, was the parameter most relevant to transient conditions).

In the finite element experiments an endeavour was made to take into account the transient temperature variation. This was achieved by prescribing the occlusal surface of the restoration to have a temperature increase of 20 degrees C above datum, i.e. above 37 degrees C, while the pulpal surface of the restoration was prescribed a temperature of 0 degrees above datum. The temperature distribution through the depth of the filling was then assumed to be linear as illustrated in FIG. 7.15. Although of course this situation may never actually occur in in vivo it was thought that this was a reasonable simulation. In the analysis procedure, the elements in each layer were simply assigned the temperature above datum appertaining to that particular level.

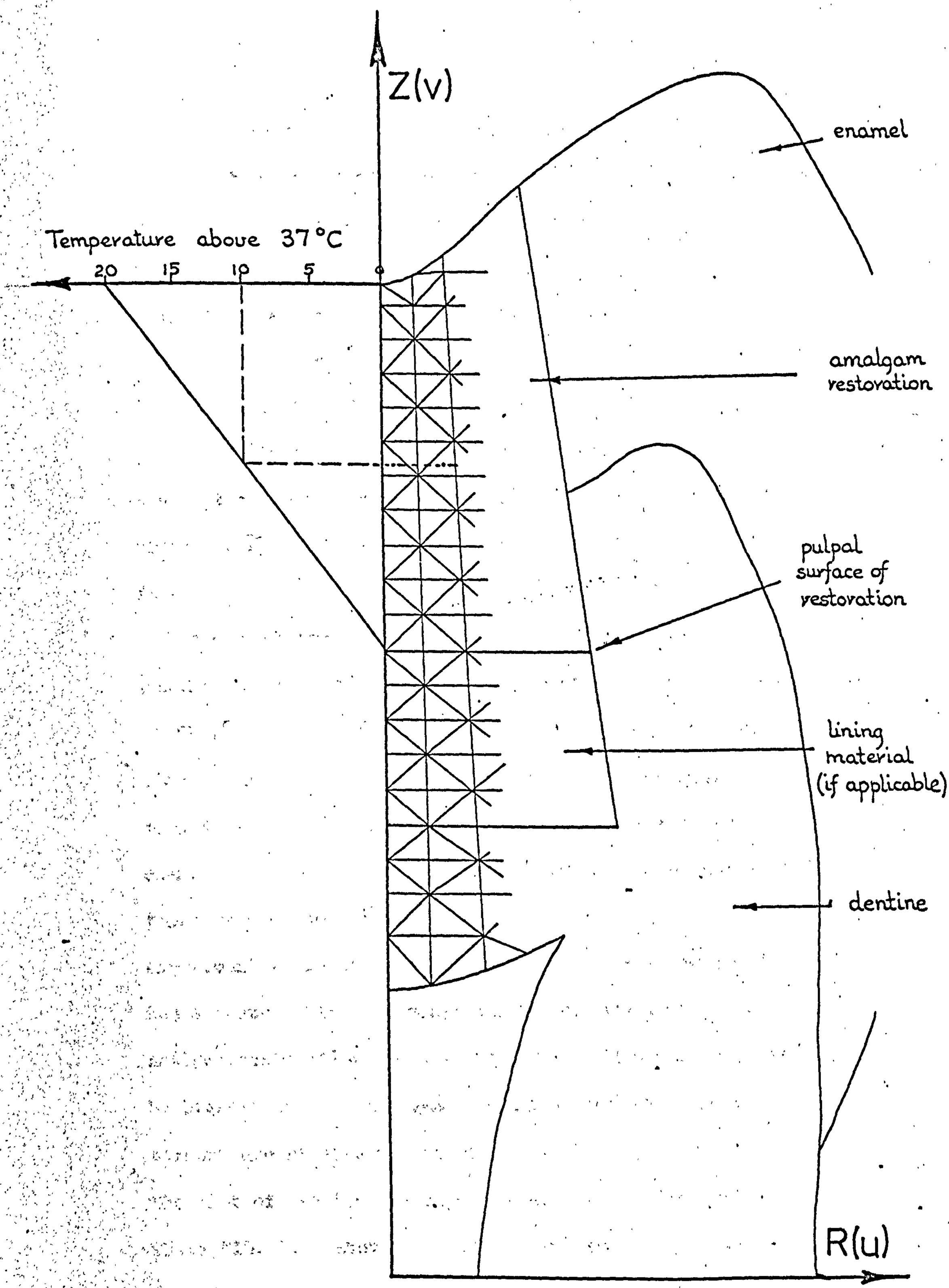


FIG. 7. 15 Illustrating the linear temperature distribution in an amalgam restoration.

### 7.4.2 Results

For this series of experiments the enamel, dentine and amalgam were ascribed the mechanical properties given in Table 3.7.

i.e. E enamel = $6.8 \times 10^6$ p.s.i., $\mu = 0.3$

E dentine = $1.7 \times 10^6$ p s.i., $\mu = 0.3$

E amalgam = $2.0 \times 10^6$ p.s.i., $\mu = 0.3$

$\alpha$ amalgam = $25 \times 10^{-6}$ cm/cm per degree C

Again, because the materials were all assumed to be isotropic their respective shear moduli were calculated using the formula

$$G = \frac{E}{2(1+\mu)}$$

The model for the first series of experiments was constructed with a cavity having a depth of 2 mm, as illustrated in FIG. 7.13. This cavity, being of shallow form, was not lined with an insulating material as the pulpal floor was considered to be of sufficient distance away from the pulp chamber. However, its design is such that the entire cavity floor reaches down into sound dentine. In the first experiment with this model, the behaviour or response of the structure was determined purely for the effects of the amalgam restoration setting expansion. This was achieved by prescribing the amalgam the equivalent 40 degree C temperature rise as determined in FIG. 7.14. FIG 7.16 shows the plot of the resulting principal stress distribution while FIG. 7.17 shows the actual structural deformation. As before, the lengths of the lines represent the magnitudes of the stresses and the axis of the lines their respective

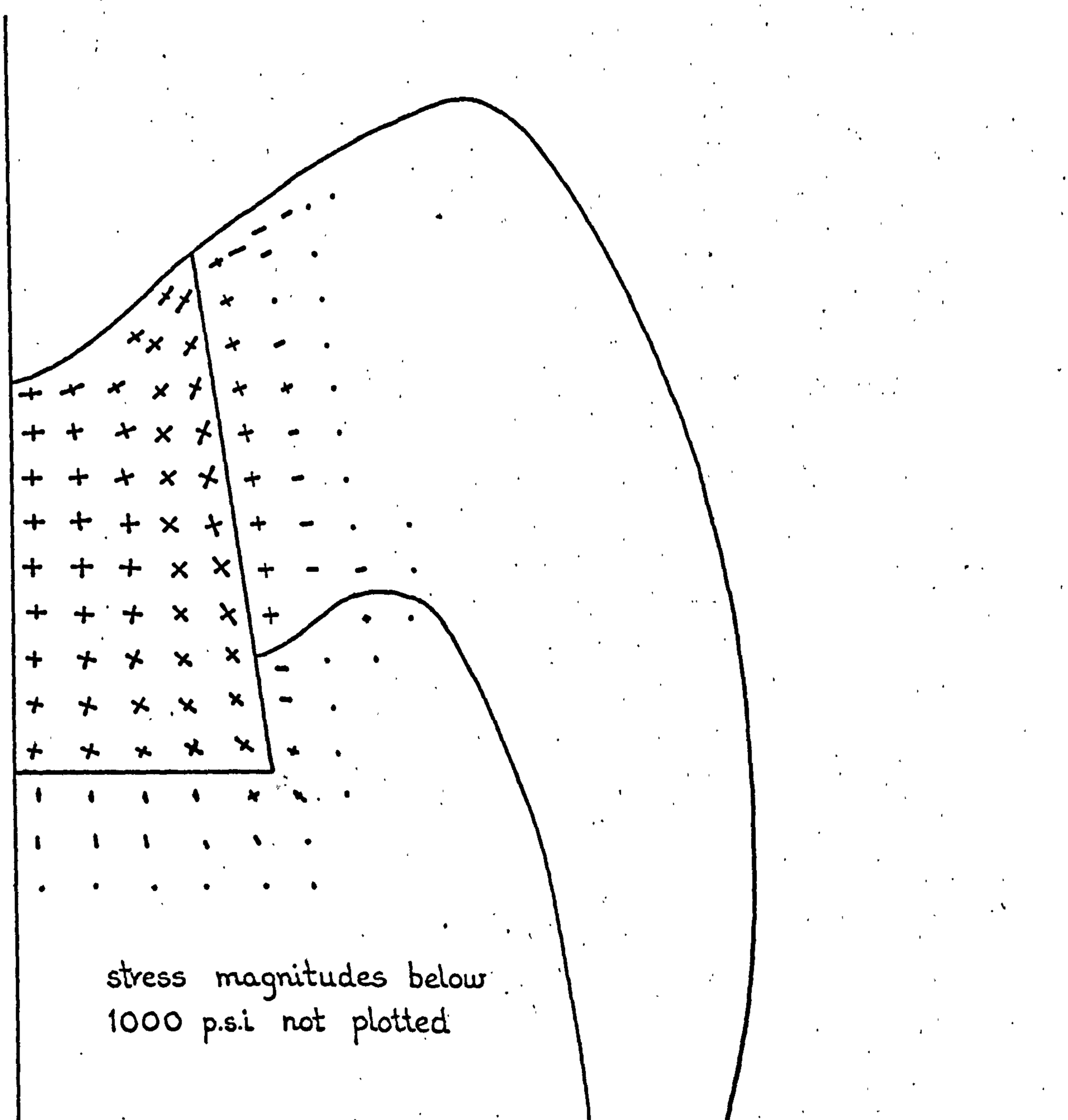


FIG. 7. 16 Principal stress distribution for a 2mm deep amalgam restoration subjected to the filling setting expansion.

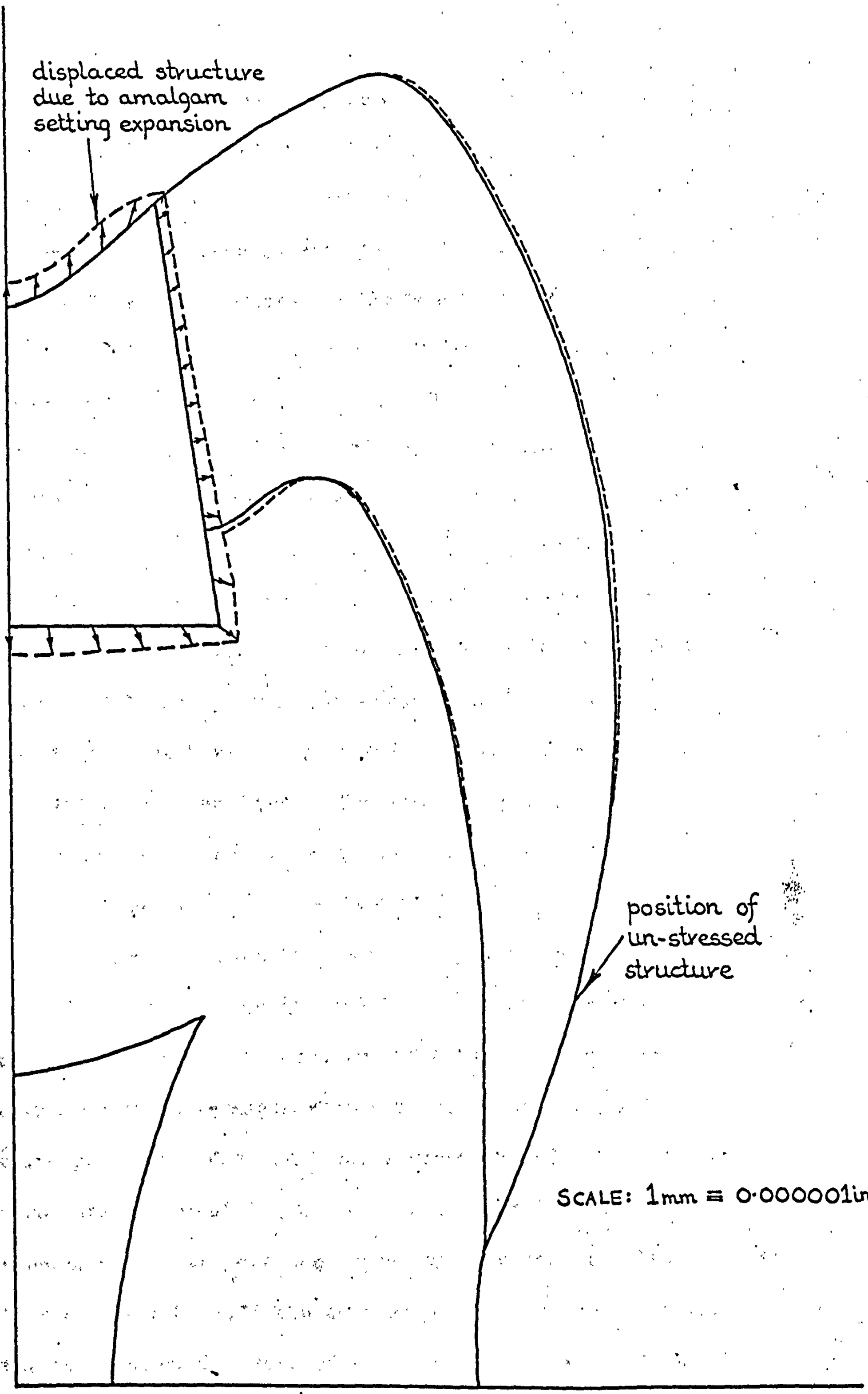


FIG. 7. 17 Displacement of the structure due to the setting expansion of the 2mm deep amalgam restoration.

directions. Thick lines represent compressive stresses while thin lines signify tensile stresses. The second experiment with this model included both the setting and the temperature expansion effects. This was achieved by prescribing the restoration surface, a temperature increase of 20 degrees C, reducing linearly down to zero temperature increase at the pulpal surface, i.e. at the 2 mm depth. FIG. 7.18 gives the principal stress distribution and FIG. 7.19 the resulting structural distortion for this condition.

For the second series of experiments the finite element model was constructed with a class 1 cavity having a total depth of 3.75 mm. This deep cavity was first lined with a 1.25 mm thick base layer of zinc phosphate cement and then filled with amalgam. The zinc phosphate cement was assumed to be an isotropic material, having the mechanical properties given in Table 3.7.

i.e.E zinc phosphate cement = $1.3 \times 10^6$ p.s.i., $\mu = 0.3$.

As with the shallow cavity model, the first experiment with this structure investigated the effects of the setting expansion of the amalgam restoration. The resulting principal stress distribution is given in FIG. 7.20 and the structural deformation in FIG. 7.21. For the second experiment, the temperature expansion effects were also included. As shown in FIG. 7.15 the surface of the amalgam was ascribed the temperature increase of 20 degrees C while the pulpal surface, 2.5 mm below, was given a zero increase, FIGS. 7.22 and 7.23 show respectively the principal stress distribution and structural deformation for this case.

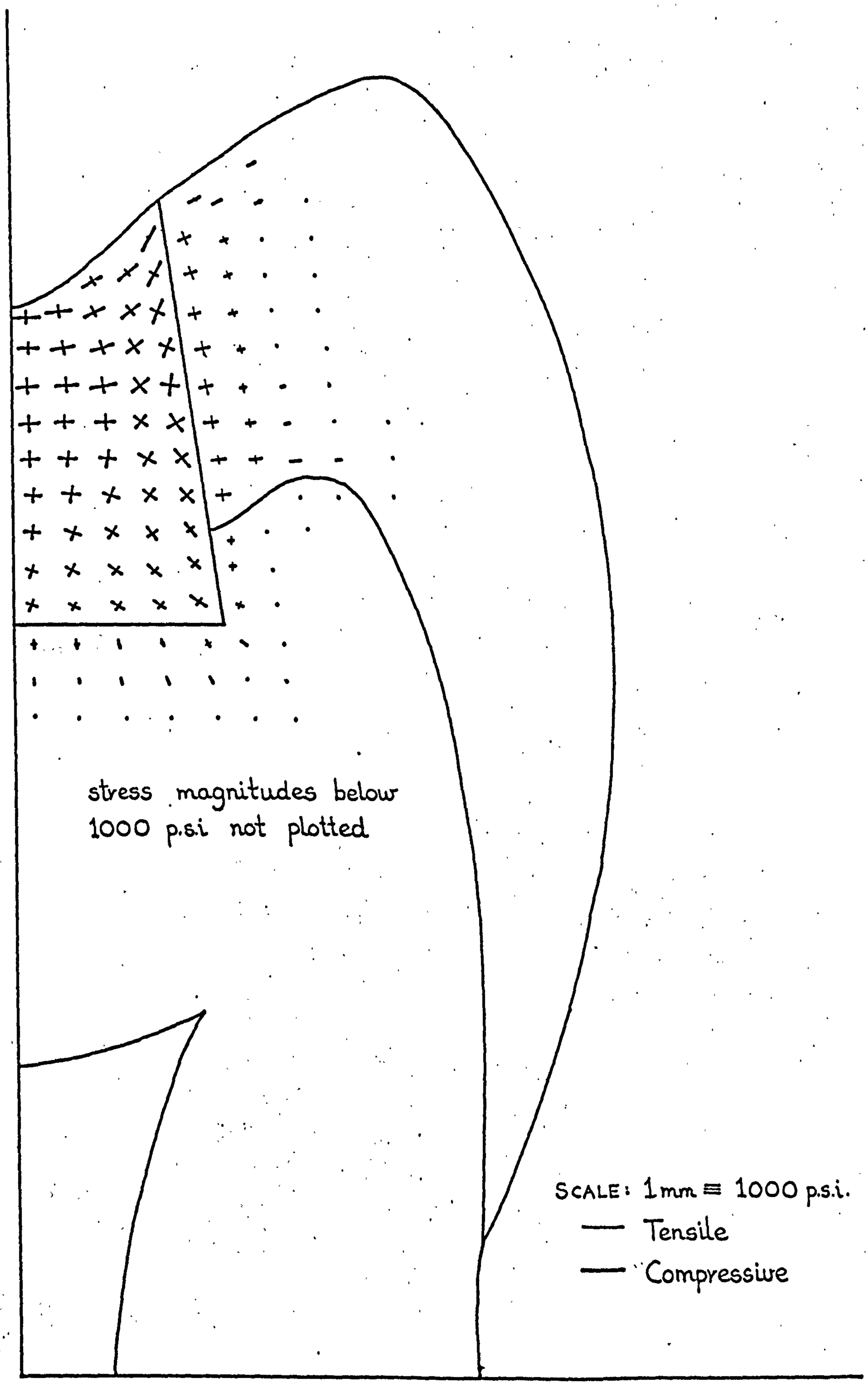


FIG. 7.18 Principal stress distribution for a 2mm deep amalgam restoration subjected to both setting and temperature gradient expansion effects.

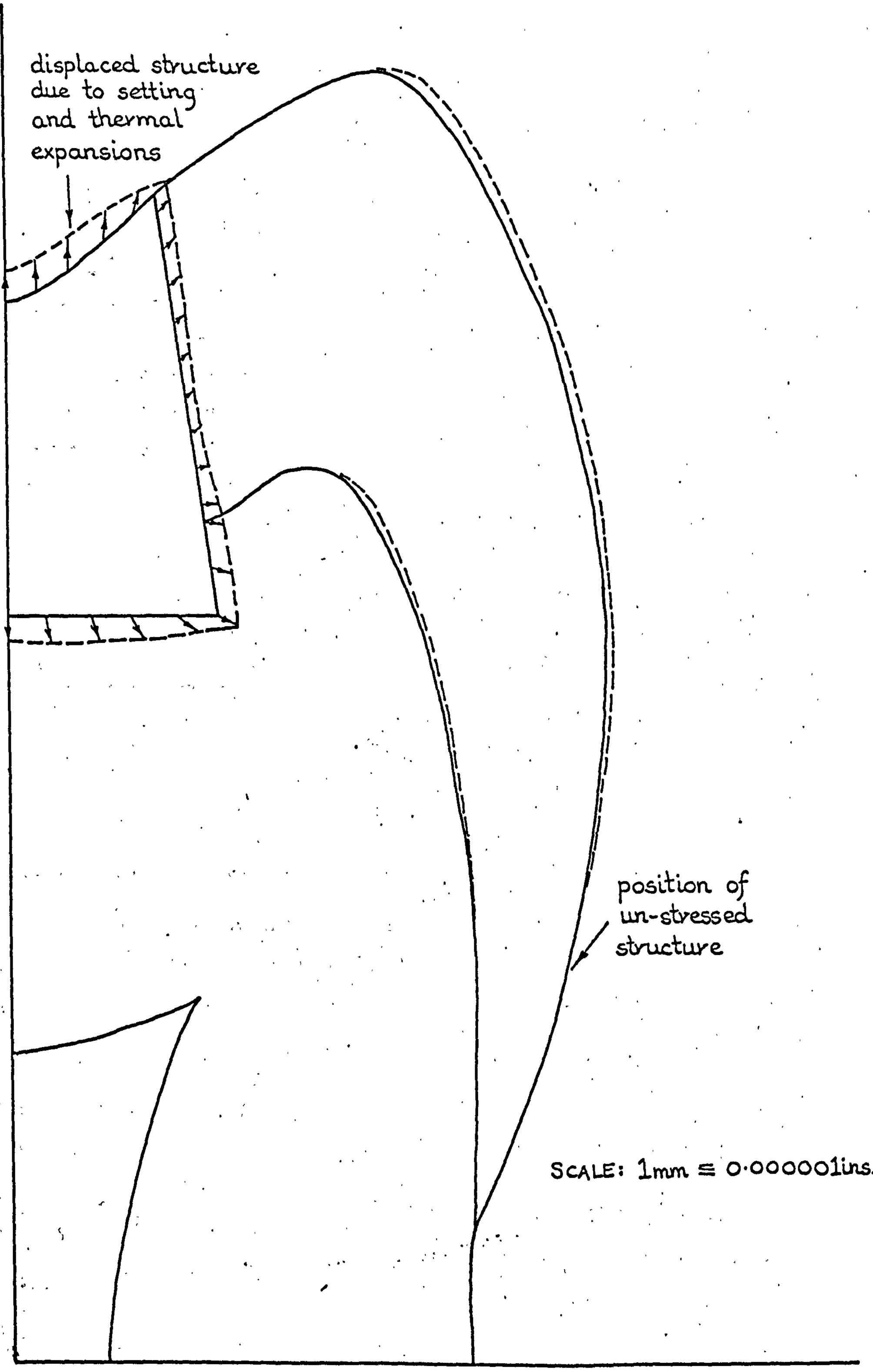


FIG. 7. 19 Displacement of the structure due to both the setting and thermal expansion of the 2mm deep amalgam restoration.

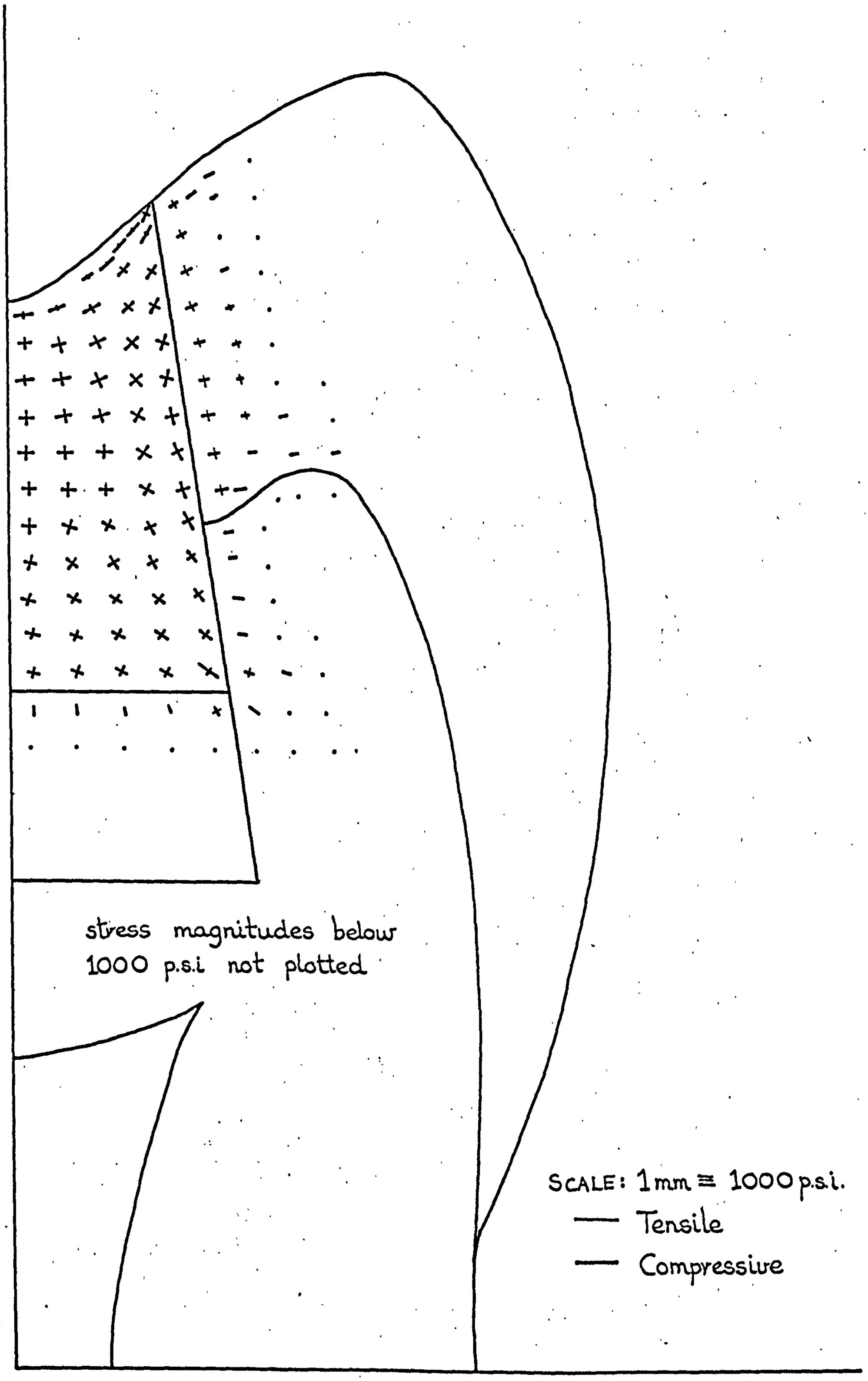


FIG. 7. 20 Principal stress distribution for a 2·5 mm deep amalgam restoration on a 1·25mm deep zinc phosphate lining. Structure subjected to the filling setting expansion.

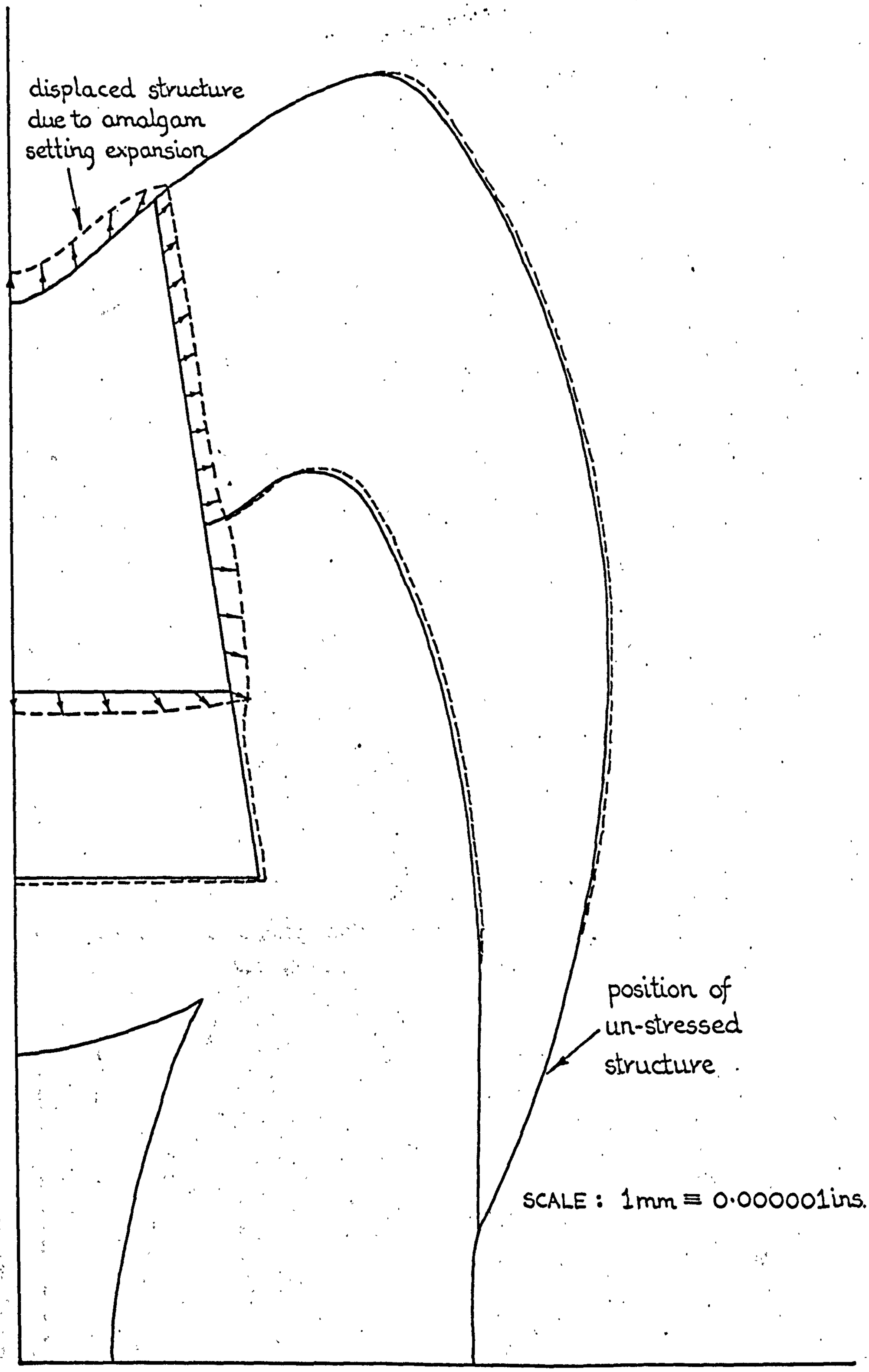


FIG. 7. 21 Displacement of the structure due to the setting expansion of the 2·5mm deep amalgam restoration.

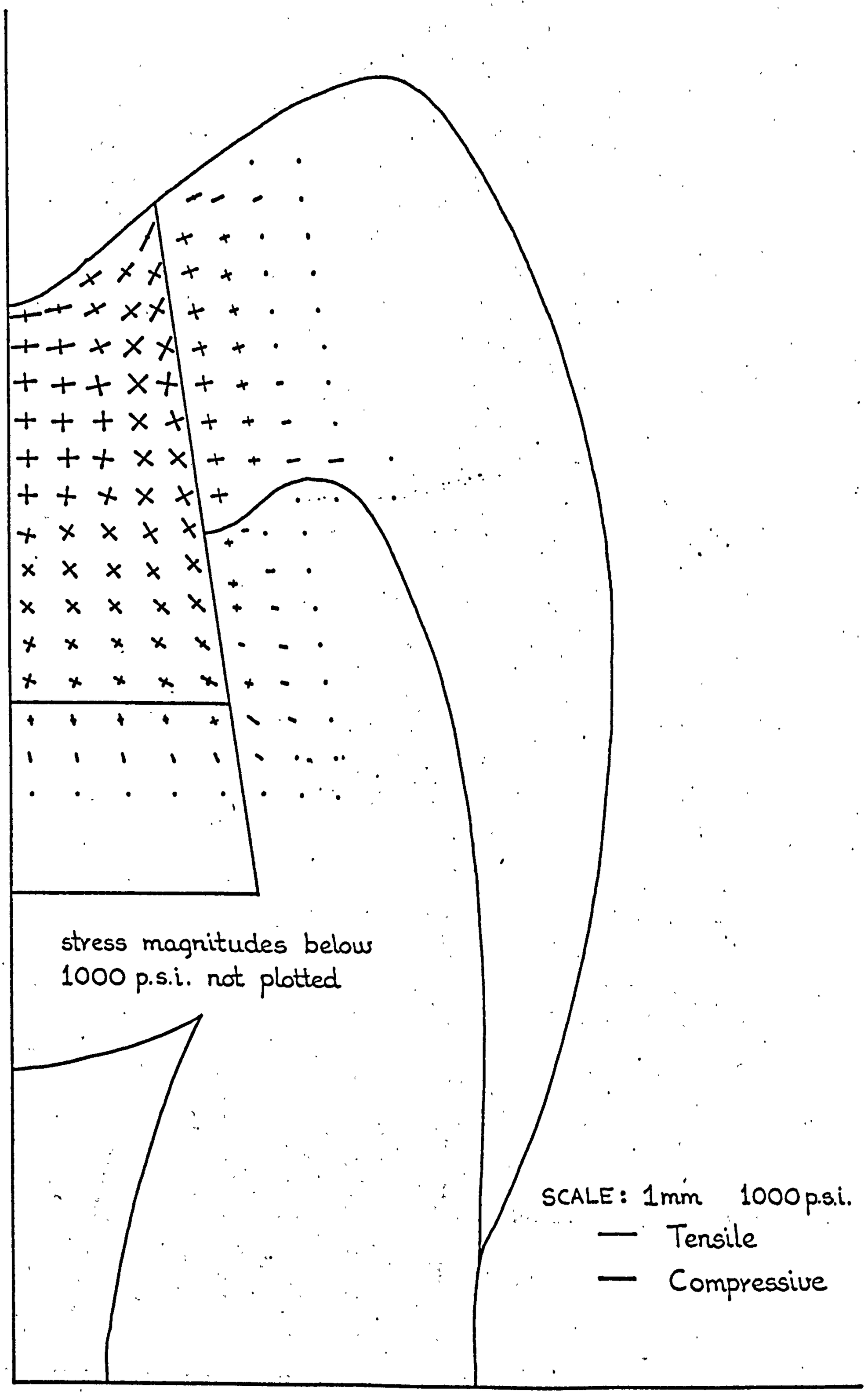


FIG. 7.22 Principal stress distribution for a 2·5mm deep amalgam restoration on a 1·25 mm deep zinc phosphate lining. Structure subjected to both setting and temperature gradient expansion effects.

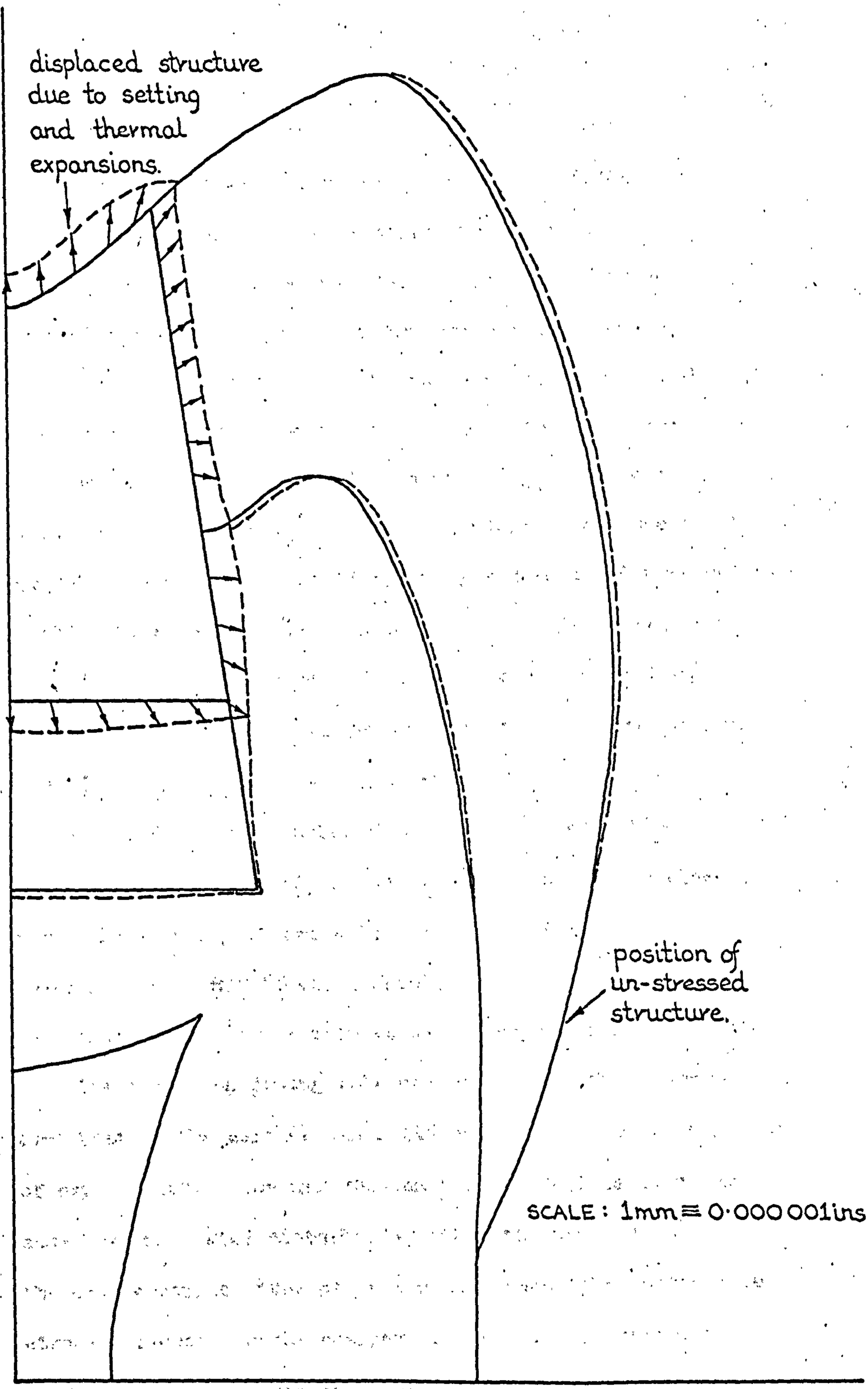


FIG. 7. 23 Displacement of the structure due to both the setting and thermal expansion of the 2·5 mm deep amalgam restoration.

### 7.4.3 Discussion of Results

A 'free' amalgam setting expansion of 10 microns per centimetre length of restoration was shown to be equivalent to an unrestrained thermal expansion in the same retoration resulting from a uniform temperature increase of 40 degrees C. Hence, it is reasonable to assume that by lowering the normal mouth temperature of the amalgam restoration from 37 degrees C down to 0 degrees C, e.g. by the ingestion of very cold foods or drinks, the pre-stress initially induced is almost completely removed. Consequently, in order to eliminate the possibility of marginal leakage occurring,it would be advisable if the amount of setting expansion employed for amalgam restorations was never allowed to be less than 10 microns per centimetre.

Although movement between the amalgam restoration and the tooth tissue probably occurs in vivo, the finite element simulations employed here allow for no slippage to take place. However, this simplification should not impair too greatly the significance of the results of the experiments.

The major supporting role of the high stiffness enamel over that of the dentine was again demonstrated in this series of experiments. The deformation plots in all cases clearly show how the enamel distorts less than the dentine under the same expansion type of loading. Hence, the compressive stresses induced in the amalgam adjacent to the enamel or constricted region, are far higher than those induced in the portion of the restoration lying in the more flexible dentine. Because the Young's modulus of the zinc phosphate

lining material is similar to that of the dentine, it is mechanically (as well as thermally), a very good substitute for this tissue.

Although the assumed linear temperature distribution in the amalgam restoration does not affect the overall patterns of the stress and displacement components occurring in the structure, the magnitudesof the stresses and displacements are substantially increased. In fact, both FIG. 7.18 and FIG. 7.22 indicate that very high stress levels are developed in the wedged shaped region of the amalgam at the occlusal margin for the shallow and deep cavities respectively when they are subjected to both the setting and thermal expansions. Even though any slippage at the margin would drastically alter the stress patterns induced, it is evident that it would be advisable to design this margin of the restoration to have as obtuse an angle as possible. Preferably, the included angle should be 90 degrees such that the strength of the margin of the restoration is not gained at the expense of the strength of the enamel margin. Of course, any masticatory loading applied to, or adjacent to, the restoration would not only affect the resulting stress distribution around this critical region but would also undoubtedly increase the stress magnitudes to an even higher level.

## 7.5 CONCLUSIONS

The stresses generated in natural teeth as a consequence of a point contact form of loading obviously 'flow' out in

three-dimensions. Consequently, the magnitudes of the stresses obtained from two-dimensional finite element analyses are only relative; their values are dependent on the thickness of the model slice employed. (Also of course, the stress components occurring in the normal structure at right angles to the model plane are ignored altogether in two-dimensional simulations). Although an equivalent slice thickness was obtained in Chapter Six which produced similar in-plane model displacement magnitudes as observed in experiments on natural teeth in vivo, the stress magnitudes are not so easily matched. However, while the stress magnitudes are therefore somewhat unnatural, the form of the stress distributions or patterns obtained from the analyses are, with certain reservations, significant, in that they do represent general trends of the overall structural response in the plane of the two-dimensional simulation.

Under the loading conditions imposed in the experiments, it was found that the enamel of normal teeth, being very much stiffer than the underlying dentine, absorbs a greater proportion of the masticatory loads. (In fact, a similar effect was seen to occur irrespective of whether the enamel was assumed to be an isotropic or an orthotropic material). Consequently, the reactionary stresses induced in the enamel tend to flow around the cap as illustrated in FIG. 7.8. Therefore, as the enamel thins down at the amelo-cemental junction, the load carried by the cap has to pass through the diminishing amount of enamel tissue and into the dentine of the root in order for it to be dissipated in the supporting

tissues. Hence, high compressive stresses are induced in the cervical regions of teeth under normal masticatory loading and restorations placed in this area would obviously be subjected to these stresses. In fact, it is suggested that these stresses may well be responsible for the pain often experienced by patients who have had restorations placed in this area.

No reference has been traced which reports on any work being carried out to determine the mobility of a tooth in the mesial-distal direction while the tooth has been physically restrained in this plane by its neighbouring teeth. However,it is probable that the mobility of a tooth situated in a complete arch is a great deal less in this plane than it is in the corresponding buccal-lingual plane, see Chapter Six. Consequently, it would be interesting, using a 'normal' tooth model, to see what effect the restraint imposed by the interdental contact points has on the stress distribution around the cervical region of a tooth subjected to 'normal' masticatory loading. This situation could easily be simulated using the finite element method simply by restraining the interdental contact point node on the enamel surface in the appropriate direction.

While high compressive stresses are being induced in the cervical region of a tooth under masticatory loading, equally high tangentially directed tensile stresses are simultaneously being induced around the tooth's fossa. These tensile stresses tend to separate the enamel prisms in this area and it is therefore suggested that these stresses may

assist the spread of dental caries in the fossae of teeth.

The same tensile stresses discussed above would also tend to separate the enamel tissue from any restorative margin positioned below the intercuspation contact points. Clinically,the position of a margin is governed by the philosophy of conserving as much as possible of the healthy tooth tissue while at the same time providing a secure and stable restoration which is inherently self-cleansing. However, the results suggest that from the mechanical standpoint no restorative margin should be positioned below the intercuspation points as the tensile stresses generated may well be instrumental in causing marginal breakdown and the subsequent failure of the restoration.

While bearing in mind the previously discussed limitations of two-dimensional analyses, the results obtained from the full cast gold crown experiments highlighted several fundamental points. First of all, the cast gold which has a similar stiffness to that of the enamel, was shown mechanically to be a remarkably good substitute for the tissue it was replacing. Under near axial loading, the gold restored tooth behaved similarly to that of a normal tooth under identical loading conditions with the gold cap reacting a greater proportion of the applied load. The gold crown's share of the load was seen to flow around the restoration in a fashion similar to that seen in the natural enamel tissue. However, when a material with a stiffness significantly lower than that of the enamel was employed for the crown restoration, the whole stress pattern was seen to change. For this case,the

load did not flow around the crown but instead passed vertically downwards and through into the dentine forming the roof of the pulp chamber.

When the cast gold restoration was subjected to lateral or tipping loads,the crown was seen to have the tendency to rotate off the dentine base. This tendency could of course lead to the breakdown of the proximal margins of the restoration. Consequently, flattening the cusps on the occlusal surface of restorations is recommended as this would reduce the magnitude of the turning force component. Although this re-contouring procedure is practised clinically for self-cleansing purposes, it also has therefore mechanical advantages by helping simultaneously to protect the integrity of the proximal margins.

The design of the axial walls with regard to both their height and angulation,and also the form of the proximal margins themselves,will obviously affect the mechanical stability of the restoration. Consequently,it is suggested that these aspects should be further investigated using the finite element method. Although a considerable amount of data has been collected with regard to the strength of the dental cements employed in this type of restoration, no account can be found where the strength of a complete cemented joint has been investigated. Of course,if this information were known;the finite element analyses would be able to indicate the sort of loading conditions under which marginal failure could be expected to occur.

It was shown that a setting expansion of amalgam of 10 microns per centimetre length of restoration was approximately equivalent to a free thermal expansion resulting from a uniform temperature rise of 40 degrees C. Consequently, even bearing in mind the fact that the amalgam will both flow upon setting and will also slightly expand the prepared cavity, it is suggested that a setting expansion below this level should never be employed. This minimum level of setting expansion, (which is substantially higher than the minimum level generally recommended), would therefore reduce the possibility of a marginal breakdown occurring in a class 1 cavity as a result of the restoration shrinking due to the lowering of the amalgam temperature to an 'ice-cream' level.

It was also shown that very high stresses are induced at the occlusal margin of an amalgam class 1 restoration when the amalgam is subjected to both setting and thermal expansions. These stresses could result in the edges of the filling breaking away and the formation of pockets which could subsequently lead to the failure of the restoration. Consequently, it is suggested that further finite element experiments should be carried out with regard to the structural design of this margin.

# CHAPTER EIGHT

## DETERMINATION OF THE INSTANTANEOUS CENTRES OF ROTATION OF TEETH

# 8 DETERMINATION OF THE INSTANTANEOUS CENTRES OF ROTATION OF TEETH

## 8.1 INTRODUCTION

When a rigid body moves from one position to another, the path of motion of the body at any particular instant in time can be considered to be along the arc of a circle. Consequently, the movement of the body at each particular instant in time constitutes to a pure rotation of the body about some fixed point. FIG. 8.1 illustrates a two-dimensional body which is considered to move from an initial position A to a final position B. At a particular instant during this movement, i.e. when the body is at point C, the body is assumed to move an infinitesimal distance, i.e. from C to D, during an equally infinitesimal period of time dt. (In FIG. 8.1, the infinitesimal distance is drawn for clarity to a very much enlarged scale). From the reference line marked on the body, which indicates the direction of the body's motion in both its C and D positions, perpendiculars are erected which are found to intersect at some point in space. The reference line marked on the body is now seen to form tangents to a circle having as its centre the intersection of the two lines. This point is known as the instantaneous centre of rotation of the body during its infinitesimal movement from position C to position D.

Obviously, this same procedure could be adopted for any instant of time during the body's movement from A to B and a series of positions of the instantaneous centre of rotation determined. The locus of all such positions forms a path

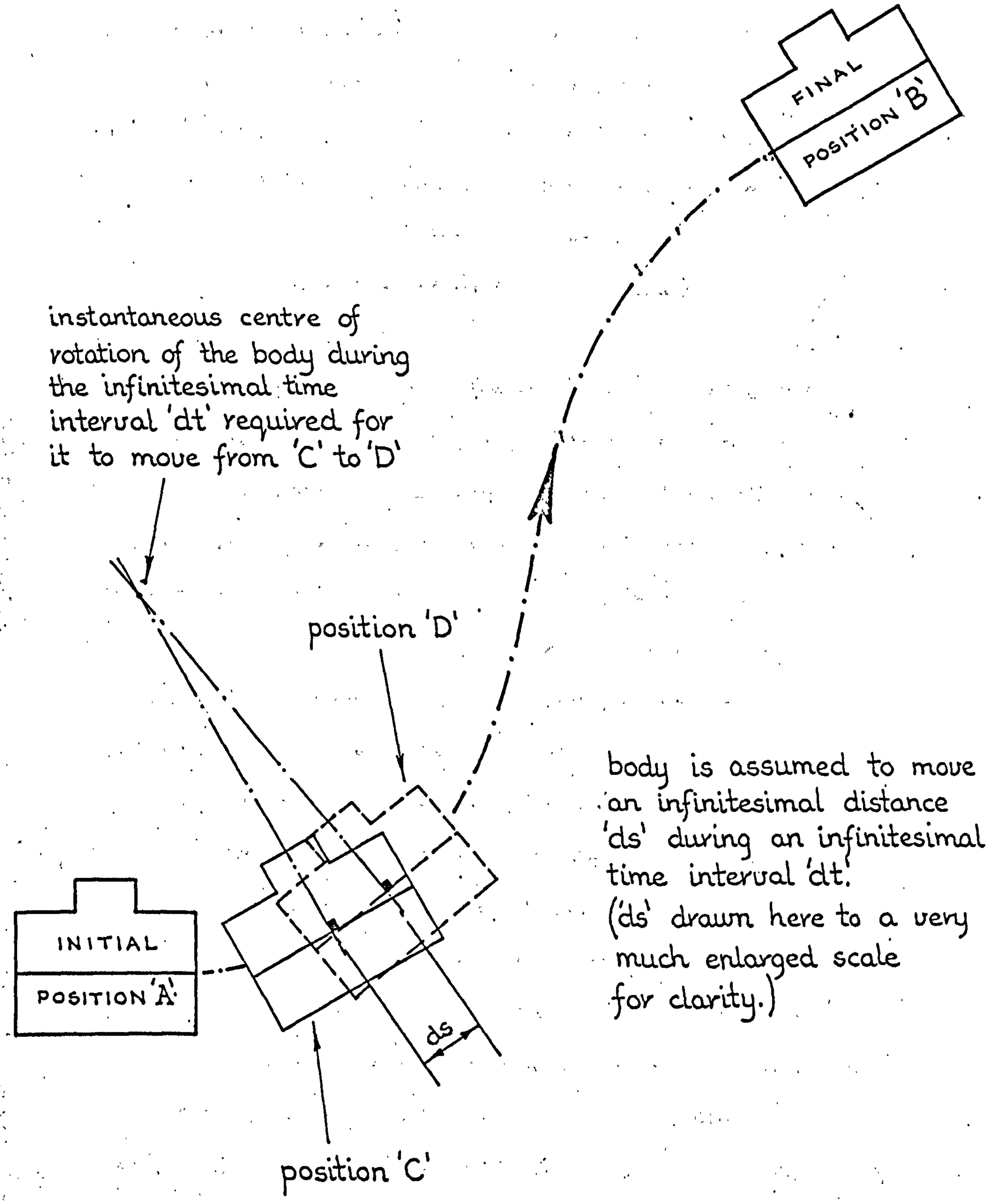


FIG. 8.1 Illustrating the definition of the instantaneous centre of rotation of a rigid body during it's movement in 2-D space.

in space, (unless of course the body is undergoing purely rotary motion in which case the path reduces down to a single point), and this path is called a space centrode. The actual path taken by the body in moving from C to D depends upon a number of factors. These include the forces acting on the body and giving rise to its movement, and also the kind and form of resistances which may be opposing the body's motion.

When very small forces or loads in the order of a few grammes are applied to a tooth, the tooth moves as a rigid body within the socket a very small amount. The distances involved, i.e. a few microns, (see section 6.3 which deals with tooth mobility studies), can be considered as being infinitesimal in comparisen with the overall dimensions of the tooth. Consequently, the theory of the instantaneous centre of rotation of a rigid body discussed above, can be applied to the movement of a tooth which is subjected to relatively small loads. In fact, the determination of the instantaneous centres of rotation of teeth subjected to various loading regimes has been the subject of numerous investigations. The main reason for these studies is that it is thought that a correlation exists between the instantaneous centre of rotation of a tooth, subjected to orthodontic loads, and the subsequent remodelling of the alveolar bone and periodontal membrane. Although it is known that the movement of a tooth, as the result of the application of an orthodontic force, disturbs the equilibrium of the supporting tissues, the type and form of the stimulus which excites the

tissue remodelling response still remains a mystery. Various stimuli for exciting alveolar bone resorption and deposition have been suggested. High compressive stresses above unknown but so-called 'physiological limits' and the changes in surface curvature of the alveolar bone, are probably the two most favoured currently held theories, see Chapters Nine and Ten. However, the lack in understanding the phenomenon of bone resorption and deposition with respect to the alveolar process subsequent to orthodontic treatment, can probably be attributed to the lack in knowledge and understanding of the behaviour and function of the periodontal membrane. Returning to the disaussion on FIG. 8.1, it was stated that the actual motion of the body was dependent upon the forces and resistances opposing the body's movement. Consequently, the resistance afforded by the periodontal membrane to the tooth under orthodontic loading will obviously affect the resulting movement of the tooth. Hence, until an understanding of the nature and supporting mechanism of the periodontal membrane is attained, the type and mode of tooth movement resulting from orthodontic treatment will remain purely conjecture. As an example, FIG. 8.2 illustrates the mechanical response of the periodontal membrane when it is considered to act either as a compressible or incompressible elastic membrane and as a tensional suppensionary support system, under both intrusive and lateral tooth loading conditions.

While bearing in mind the points put forward in the above

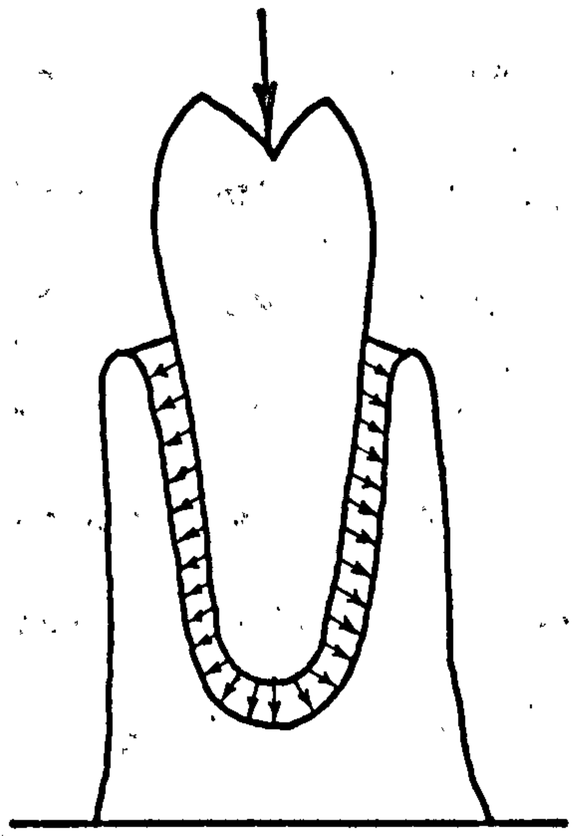

Vertical load producing compressive stresses on lamina dura

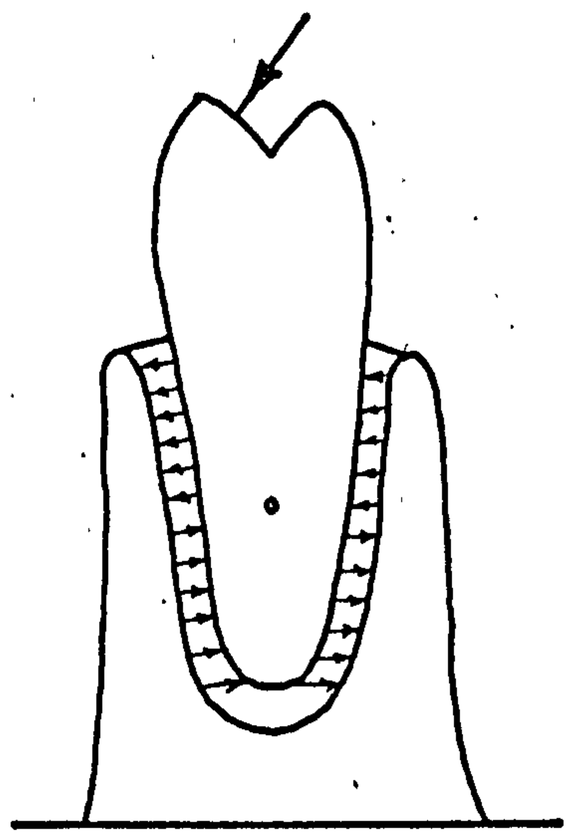

Lateral load producing tensile and compressive stresses on lamina dura.

a) Response of an incompressible or compressible elastic membrane.

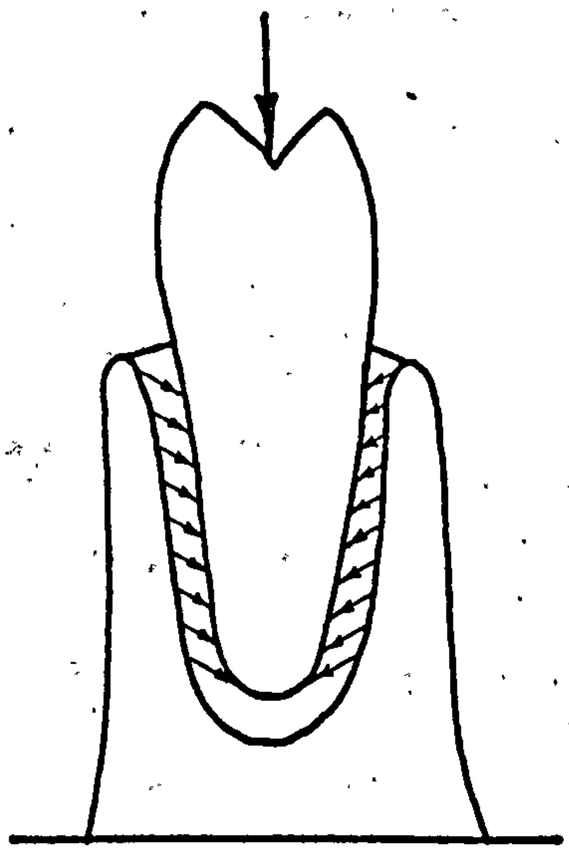

Vertical load producing tensile stresses on lamina dura.

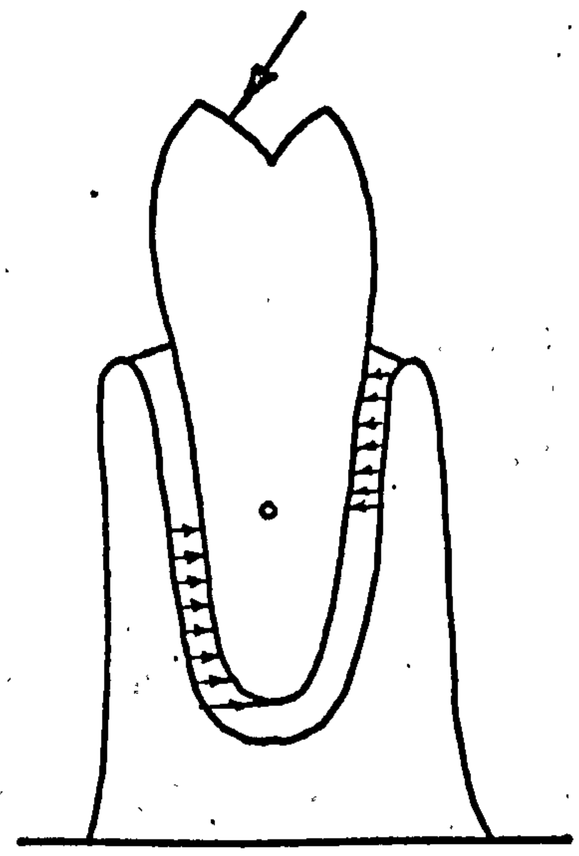

Lateral load producing tensile stresses on lamina dura.

b) Response of a tensional support membrane system.

FIG. 8.2 Diagrammatic illustration of the response of the periodontal membrane when considered a) as an incompressible or compressible elastic system and b) as a tensional support system.

discussion, the purpose of this chapter was to determine the instantaneous centres of rotation of teeth under the action of various loading conditions. Thus, it would be possible to examine some of the factors which were considered to influence the resulting tooth displacement. Factors investigated included the effect of the type of model employed in the analytical determination of the instantaneous centres of rotation; the effect of the position and direction of the loading imposed; the difference between isotropic compressible and orthotropic tensional periodontal membrane support systems and the effect of the height and stiffness of the alveolar bone. Although this chapter is concerned with the analysis of single rooted tooth models, the finite element analysis technique is capable of dealing with the movements of multi-rooted teeth.

## 8.2 VARIATION IN THE POSITION OF THE INSTANTANEOUS CENTRE OF ROTATION OF A TOOTH AS A RESULT OF EMPLOYING DIFFERENT FINITE ELEMENT MODELS

Nearly all the published work concerned with the determination of the instantaneous centres of rotation of teeth, whether by analytical or by experimental means, has been carried out using two-dimensional models, e.g. Burstone (39) and Haack and Weinstein (43). In general, the plane of these models has been selected to coincide with the plane of the force systems which are applied to the actual teeth being simulated. However, it is not certain that the three-dimensional nature of the real periodontium does not give a substantially

different form of support to the teeth than does a two-dimensional substitute. Hence, the instantaneous centre of rotation of a tooth determined from a simple two-dimensional model simulation could be significantly different from that of the real structure. In this section, the effect of employing two and three-dimensional models for the determination of the position of the instantaneous centre of rotation of a maxillary central incisor subjected to lateral orthodontic loading was investigated.

### 8.2.1 Finite Element Models and Test Procedure

The two and three-dimensional finite element models used in these comparison tests were the same maxillary central incisor models employed in Chapter Six. The 0.345 inch equivalent thickness two-dimensional model is illustrated in FIG. 6.16 and the three-dimensional model in FIG. 6.15. Apart from the obvious difference between the forms of the two models, the only other significant variation occurred in the simulation of the alveolar processes. Whereas the two-dimensional model simulated the areas of cancellous bone, the three-dimensional model did not. The reason for this omission was purely to minimise the number of elements in the three-dimensional model.

### 8.2.2 Results

In these experiments the enamel and dentine, and the cancellous bone for the two-dimensional model were ascribed

the isotropic mechanical properties given in Table 3.7.
For both models the periodontal membrane was also assumed to be isotropic and the mechanical properties associated with the tooth's lateral force versus displacement relationship were employed.
i.e. $E = 26.1$ p.s.i., $\mu = 0.3$ and $G = \frac{E}{2(1+\mu)}$
(see Chapter Six).
However, while the cortical bone grain was assumed to 'run' as indicated by the directions of the lines in the centres of the cortical bone elements in FIG. 6.16 for the two-dimensional model, the grain was assumed to 'run' as illustrated in FIG. 8.3 for the three-dimensional model, i.e. parallel to the X co-ordinate axis.

The two and three-dimensional models were each loaded with a 30 gm. orthodontic force applied at a similar position on their respective labial surfaces. The positions of the instantaneous centres of rotation under this loading, obtained by plotting the model tooth's nodal displacements and constructing the appropriate perpendiculars as illustrated in FIG. 8.1, are shown in FIG. 8.4a. Also shown in this figure is the position of the instantaneous centre of rotation obtained using Burstone's formula (39 and 40), see section 5.2. However, this formula assumes the root area, i.e. the area between the root apex and the alveolar crests, to be of the form of a parabola.

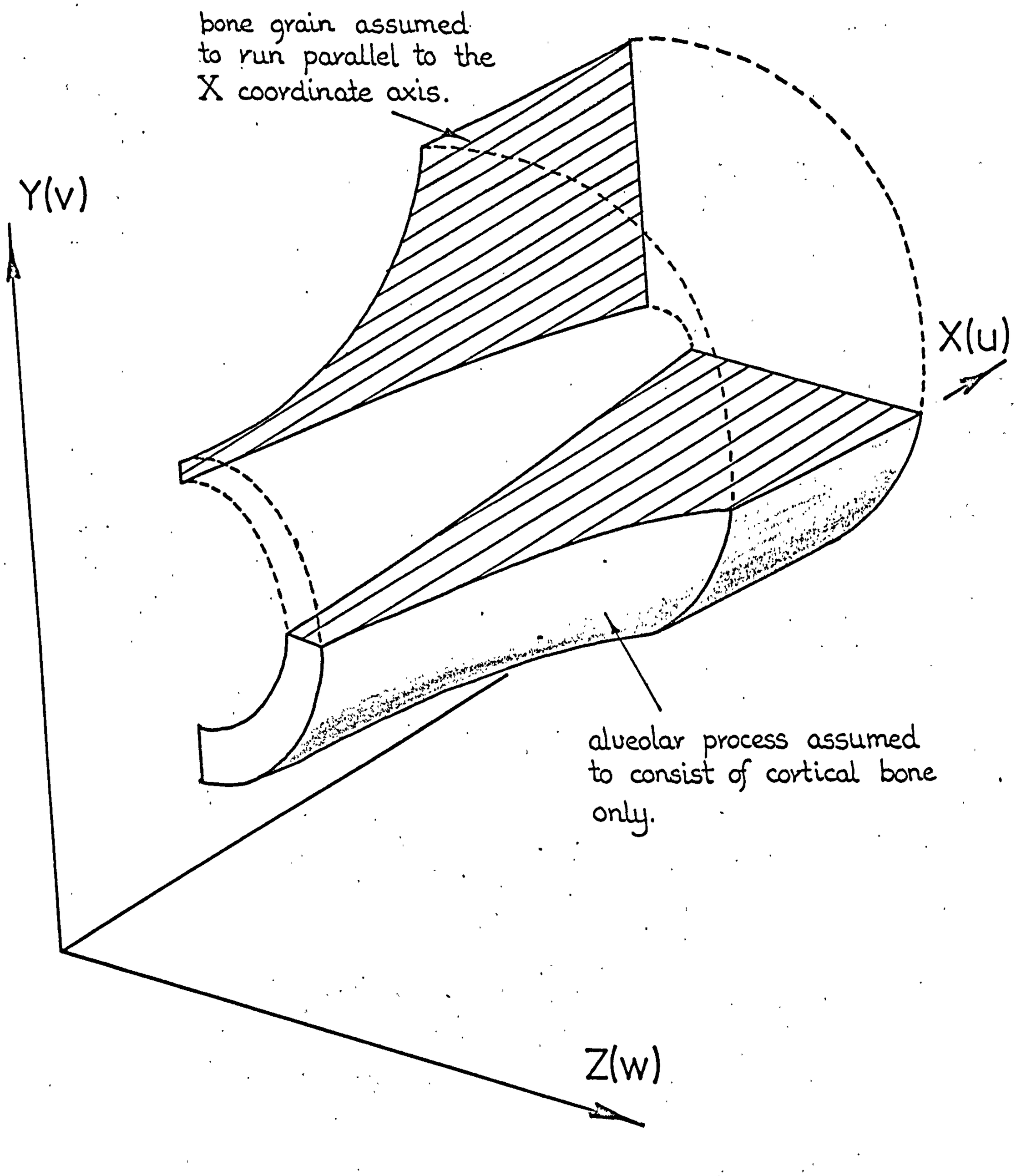


FIG. 8.3 Illustrating the direction assumed for the 'grain' of the cortical bone in the three-dimensional finite element model.

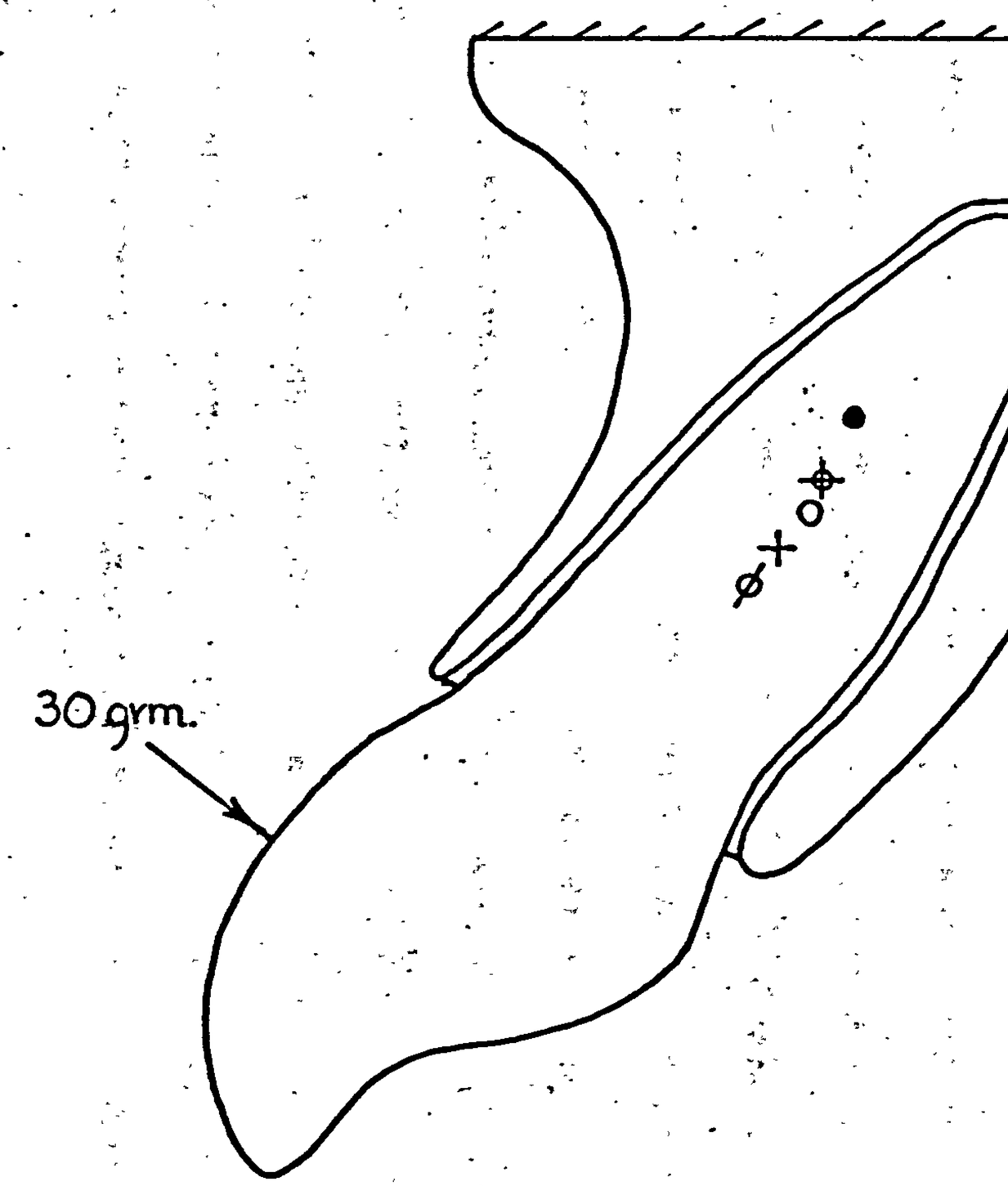


KEY:

- • Instantaneous centre of rotation for 2-D finite element model, see FIG. 6.16.
- ⌖ Instantaneous centre of rotation for 3-D finite element model, see FIGS. 6.15 and 8.3.
- o Instantaneous centre of rotation using Burstone's formula, see section 5.2
- \+ Centroid of root area if assumed to be of parabolic form.
- ⌀ Centroid of actual root area, i.e. between root apex and alveolar crest tips.

FIG. 8.4a Positions of the instantaneous centres of rotation obtained from the 2 and 3-D models for a 30grm lateral orthodontic load applied to the tooth's labial surface.

### 8.2.3 Discussion of Results

The positions determined for the instantaneous centres of rotation for the two and three-dimensional finite element models of the maxillary central incisor under lateral orthodontic loading, can be seen from FIG. 8.4a to be significantly different. In fact, their relative position, when measured from the root apex and expressed as a percentage of the distance between the root apex and the alveolar crest tips,, are 38% for the two-dimensional model and 48% for the three-dimensional model respectively. It is therefore apparent that the form of the finite model employed to simulate the structure considerably affects the overall displacement behaviour of the tooth. As expected, the three-dimensional model provides a far stiffer periodontium support to the tooth than does the two-dimensional equivalent thickness model. In the case of the latter, the alveolar bone plates deform and behave as simple cantilevers. This is readily appreciated by looking at the deflections of the lingual alveolar crest tips. For the three-dimensional model, the displacement to lingual was only 0.1 microns whereas for the two-dimensional model, the crest tip displacement was approximately 1 micron. Consequently, although in the determination of the isotropic lateral mechanical properties of the periodontal membrane the same lateral tooth movement was obtained for both model types, it is evident that in the case of the two-dimensional model more of this movement was associated with bone deformation. However, even for the more flexible two-dimensional model the alveolar bone

displacement contributes only to approximately 5% of the total tooth movement. Therefore, it can be concluded that because of the relative low stiffness of the periodontal membrane in comparison with that of the alveolar bone, the tooth displacement for the low level of loading considered here, takes place almost entirely within the tooth socket and is therefore governed primarily by the stiffness of the periodontal membrane. However, this point will be considered in greater depth later.

The instantaneous centre of rotation for the three-dimensional finite element model, i.e. at a position 48% of the distance between the root apex and the alveolar crest tips measured from the root apex, occurs nearer to the root apex than does the positions determined analytically by Synge (31) and Hay (32), for their three-dimensional models, see section 5.2. Their values were 72% and 66% of the root apex to alveolar crest distance respectively, see FIG. 5.2, However, both these authors employed a conical shaped root model which was loaded laterally at the incisal edge and whose supporting alveolar bone was assumed to be completely rigid. Also, the values employed for the elastic constants of the periodontal membrane were much higher than were the values used here, i.e. G = 230 p.s.i. by Synge and G = 70 p.s.i. by Hay. Therefore, it seems from the results of these two authors and from the three-dimensional finite element experiment that an increase in the stiffness of the periodontal membrane raises the level of the position of the instantaneous centre of rotation

in the tooth root.

A rather surprising feature of the results of the experiments is the similarity between the instantaneous centre of rotation obtained for the three-dimensional finite element model and that determined using the formula derived by Burstone (39 and 40) for a two-dimensional analytical model. Even though a cross-section of the tooth model conforms to the assumed parabolic form required by the formula, see FIG. 8.4a,the closeness of the positions determined for these two completely different models is quite astonishing.

Burstone, like Synge and Hay, did not take into account the flexibility of the alveolar bone in his two-dimensional analytical model. Consequently, his tooth supporting structure would be stiffer than the equivalent two-dimensional finite element model employed here. Therefore, to see whether the flexibility of the alveolar bone alone affected the position of the instantaneous centre of rotation of the two-dimensional finite element model, a further experiment was performed. In this experiment the alveolar bone was stiffened and was made almost rigid by simply clamping all the nodes on the external surfaces of the cortical bone-plates, see FIG. 8.4b. The tissue mechanical properties and the labial 30 gm. load were applied as before. The instantaneous centre of rotation for this condition is shown in FIG. 8.4b It can be seen that the position determined is identical to that obtained from the two-dimensional model which took into account the flexibility of the alveolar bone. This therefore again demonstrates that the flexibility of the

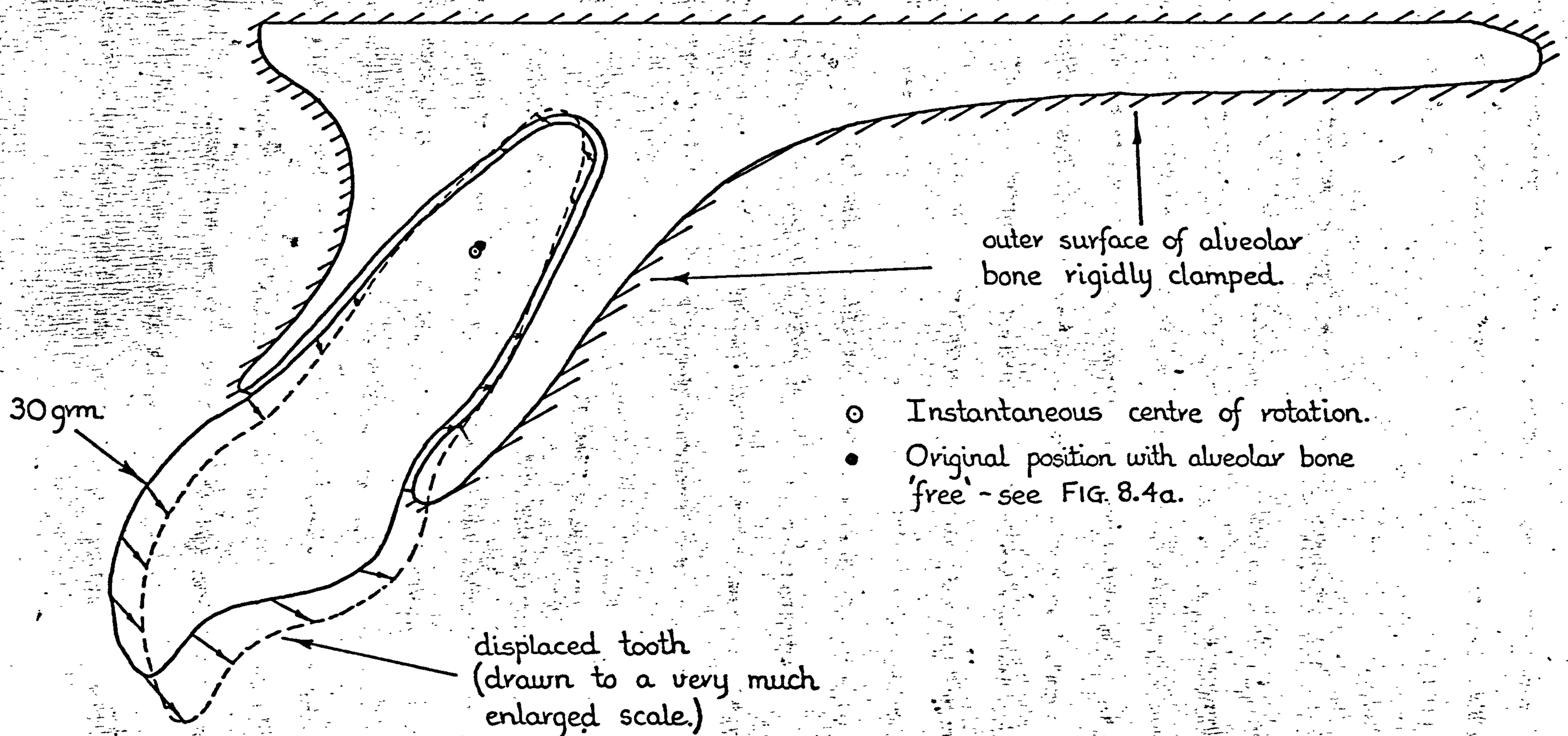


FIG. 8.4b Position of the instantaneous centre of rotation of the 2-D model for a 30 gm lateral load with the outer surface of the cortical bone rigidly clamped.

alveolar bone plays very little part in the initial orthodontic tooth displacement. Tooth movement under the action of these low magnitudes of force occurs almost entirely within the alveolus.

## 8.3 VARIATION IN THE POSITION OF THE INSTANTANEOUS CENTRE OF ROTATION OF A TOOTH AS A RESULT OF EMPLOYING DIFFERENT PERIODONTAL MEMBRANE MECHANICAL PROPERTIES

While the majority of authors have employed two-dimensional models to study the instantaneous centres of rotation of teeth, certainly all the references encountered have considered the periodontal membrane to behave as an isotropic material. Even though the work carried out in Chapter Six was inconclusive with regard to obtaining satisfactory orthotropic mechanical properties for the periodontal membrane, the aim of this section was to see what effect, if any, non-isotropic mechanical properties of the membrane would have on the position determined for the tooth's instantaneous centre of rotation.

### 8.3.1 Finite Element Models and Test Procedure

The finite element model used for these experiments was the same two-dimensional simulation of the maxillary central incisor shown in FIG. 6.16. For the orthotropic periodontal membrane test, the principal fibres were assumed to 'run' as illustrated in FIG. 6.18. Both figures show the areas of the cancellous bone simulated in the alveolar processes, also the directions assumed for the grain of the cortical tissue. The 0.345 inch equivalent slice thickness model was employed for both tests and hence, the mechanical properties

of the periodontal membrane previously determined in Chapter Six.

### 8.3.2 Results

As with the previous set of experiments the enamel, dentine and cancellous bone were ascribed the isotropic mechanical properties given in Table 3.7 and the cortical bone, the orthotropic properties determined in Chapter Six. For the isotropic test, the periodontal membrane was assigned the properties relating to the tooth's lateral force versus displacement relationship determined in sub-section 6.3.5. These were as follows:-

$E = 26.1$ p.s.i., $\mu = 0.3$, and $G = \frac{E}{2(1+\mu)}$

For the non-isotropic experiment, the periodontal membranes orthotropic mechanical properties determined in sub-section 6.3.7 were employed. These are listed in Table 6.5 under run numbers 17, 18 and 19 and are

| Ex (p.s.i.) | $\mu xy$ | Ey (p.s.i.) | $\mu yx$ | Gxy (p.s.i.) |
|---|---|---|---|---|
| 16 | 0.24 | 8 | 0.12 | 10 |

As before, the principal Young's modulus value Ex, applies to the direction of the principal fibres of the membrane, the arrangement of which is illustrated in FIG. 6.18.

A lateral 30 gm orthodontic force was applied to the labial surface of both models in a direction approximately prependicular to the long axis of the tooth, see FIG. 8.5. Again, the upper region of the maxilla was assumed not to deform under the action of the loading. Consequently, this was

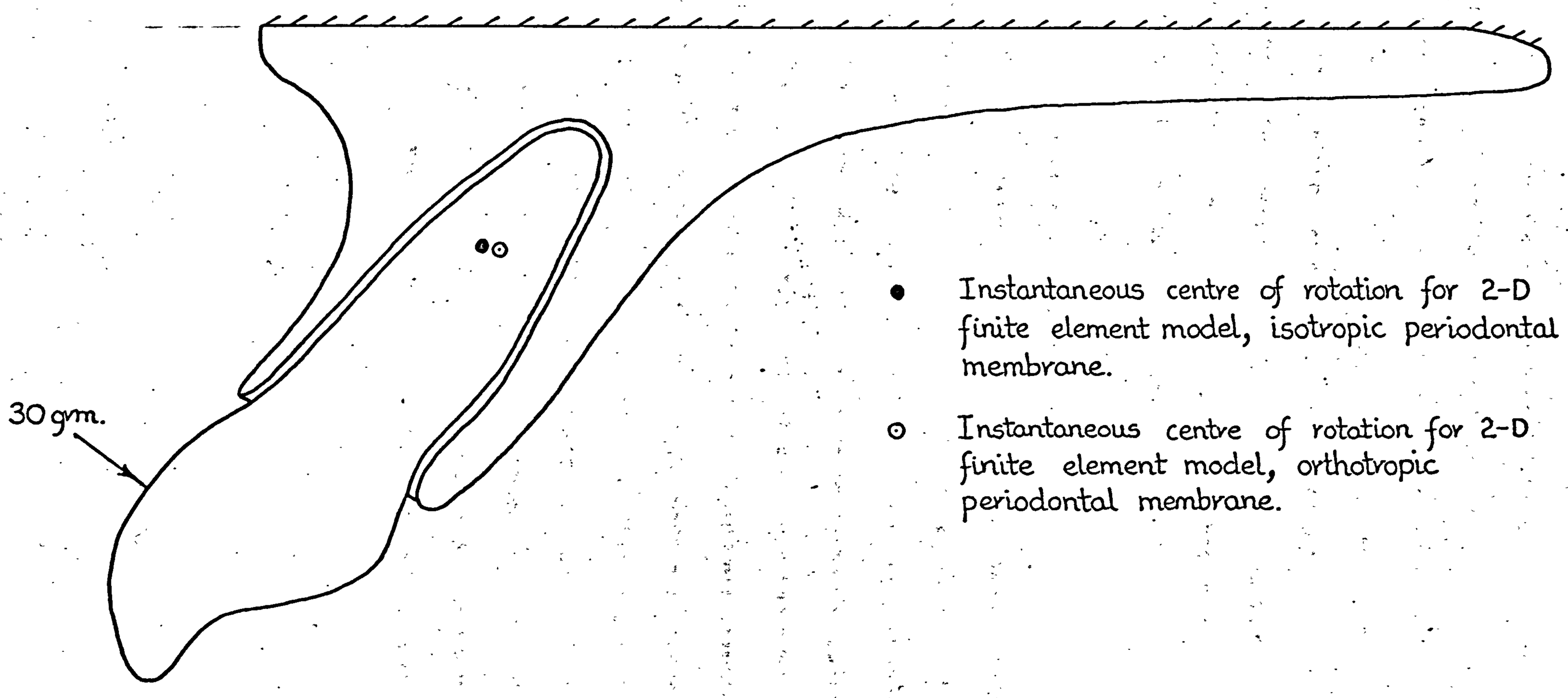


● Instantaneous centre of rotation for 2-D finite element model, isotropic periodontal membrane.

⊙ Instantaneous centre of rotation for 2-D finite element model, orthotropic periodontal membrane.

FIG. 8. 5 Positions of the instantaneous centres of rotation obtained from the 2-D model having isotropic and orthotropic periodontal membrane.

simulated in the analyses by rigidly clamping all the nodes in both the X and Y co-ordinate directions on the maxilla's top surface, i.e. ascribing these nodes zero-valued displacements. The resulting nodal displacements obtained from the analyses were plotted and from them the position of the instantaneous centre of rotation of the tooth determined for both the isotropic and orthotropic periodontal membrane structures. These are shown in FIG. 8.5.

### 8.3.3 Discussion of Results

The difference between the positions determined for the instantaneous centre of rotation of the maxillary central incisor supported in either an isotropic or an orthotropic periodontal membrane, can be considered as being insignificant, see FIG. 8.5. Obviously, the difference in the overall tooth support afforded by the isotropic and orthotropic periodontal membranes ,simulated in the models of these experiments, was insufficient to seriously alter the displacement behaviour of the tooth under purely lateral type loading. However, due allowance must be made in the clinical interpretation of these results due to the limitations of the two-dimensional orthotropic membrane model already enumerated in sub-section 6.4.3.

## 8.4 VARIATION IN THE POSITION OF THE INSTANTANEOUS CENTRE OF ROTATION OF A TOOTH AS A RESULT OF CHANGING BOTH THE POSITION AND DIRECTION OF THE APPLIED LOAD

The orthodontist must be aware of the effects that the type, position and direction of applied orthodontic forces have on the bcdily movement and tipping of teeth. This knowledge would not only enable him to select the most appropriate type of appliance to employ for each particular treatment, e.g. fixed or removable, but would also allow him to determine both the position and direction of the forces which the selected appliance must provide in order to induce the desired tooth displacement. Consequently, the aim of this section was to see how the rotation of the maxillary central incisor is affected by changing the position and direction of the applied orthodontic load.

### 8.4.1 Finite Element Model and Test Procedure

The model employed for this series of experiments was again the two-dimensional simulation of the maxillary central incisor illustrated in FIG. 6.16. As for the previous tests, the model was assigned the 0.345 inch equivalent slice thickness.

### 8.4.2 Results

The enamel, dentine and cancellous bone of the structure were again ascribed the isotropic mechanical properties given in Table 3.7 and the cortical bone, the orthotropic properties determined in Chapter Six. Although the directions of the

30 gm. orthodontic forces applied at four positions on the crown were not exactly at right angles to the tooth's long axis, the periodontal membrane was assigned the isotropic mechanical properties determined in section 6.3 for purely lateral loading, i.e. E = 26.1 p.s.i. etc. FIG. 8.6 shows the five independent loading positions selected for which the instantaneous centres of rotation of the tooth were determined. As can be seen from this figure, the loads were all acting perpendicularly to the enamel surface. Hence, the loads possessed both lateral and either intrusive or extrusive components at four of the positions analysed. The position of the instantaneous centre of rotation determined for each of the five load cases is shown in FIG. 8.6.

### 8.4.3 Discussion of Results

The positions of the instantaneous centre of rotation determined in the experiments were all found to occur at the same level in the tooth root, measured from the root apex. Nevertheless, the actual positions of the five instantaneous centres did vary along this common level. The two cervically positioned loads, one on each of the labial and lingual aspects, had similar extrusive components. These produced instantaneous centres of rotation which were symmetrically positioned either side of the instantaneous centre determined for the purely lateral load case. However, while the force, approximating the direction of the natural occlusal force, produced an instantaneous centre of rotation comparable to the other three results, the force applied to the labial surface of

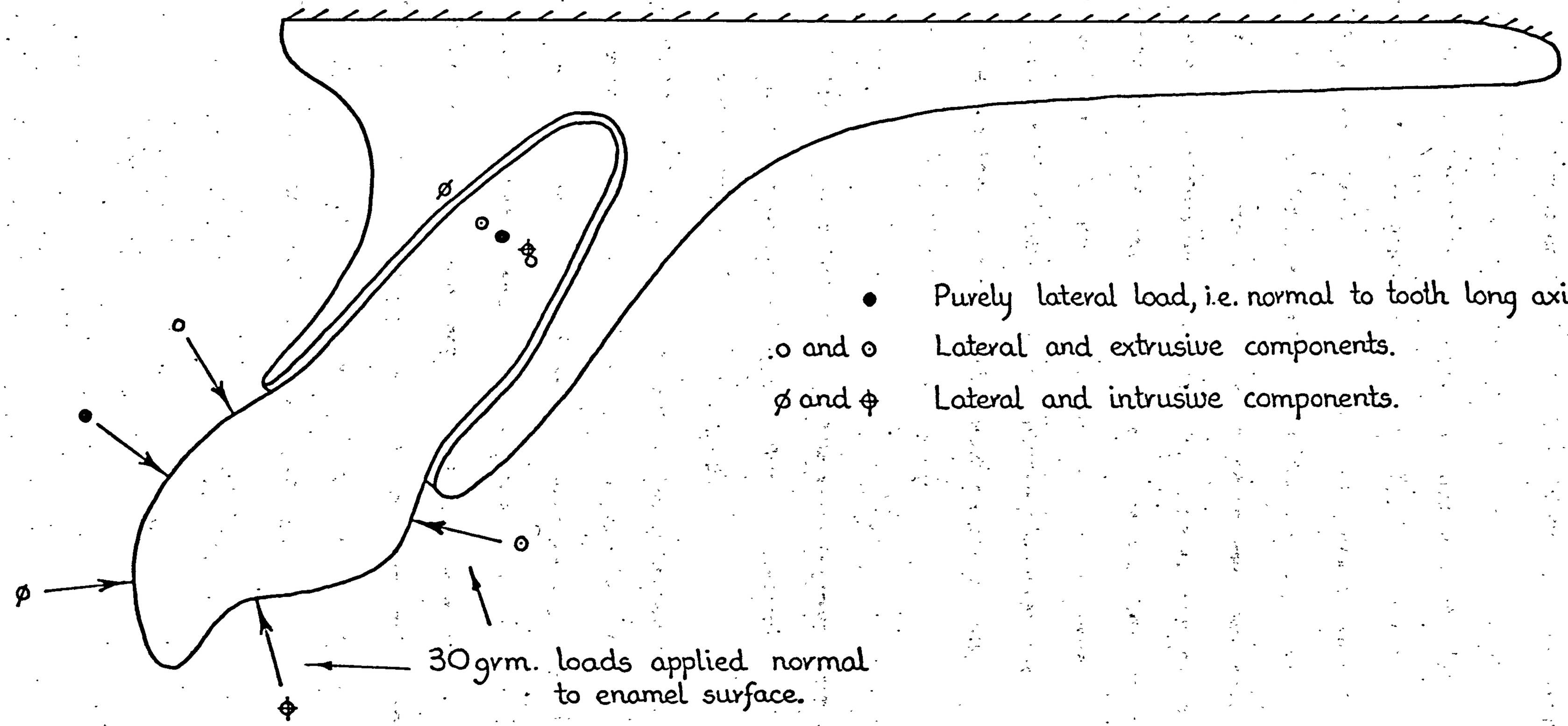


FIG. 8.6 Positions of the instantaneous centres of rotation obtained from the 2-D model for various positions of 30grm loading.

thetooth and possessing both palatal and intrusive components produced a completely different form of result. In this case,the position of the instantaneous centre of rotation was outside the tooth's root and instead,fell within the labial alveolar bone. This indicated that the tooth had not undergone a simple rotation about the long axis but had experienced a considerable intrusive movement as well. Although this effect was not unexpected, the extrapolation of this phenomenon to actual dental structures must be undertaken with caution. As mentioned earlier the applied force possessed a significant intrusive component whereas the properties employed for the periodontal membrane were determined from purely lateral loading.

## 8.5 VARIATION IN THE POSITION OF THE INSTANTANEOUS CENTRE OF ROTATION OF A TOOTH AS A RESULT OF CHANGING THE POSITION ONLY OF THE APPLIED LOAD

In the last section,the effect of both the position and the direction of the applied load on the position of the instantaneous centre of rotation was investigated. However, in this section,the object was to see what effect the load's position alone had on the centresof rotation determined. This was achieved by varying the load's point of application on the labial surface and by maintaining the load's direction relative to the long axis of the central incisor.

### 8.5.1 Finite Element Model and Test Procedure

The same central incisor two-dimensional finite element model employed in the previous section and shown in FIG. 6.16 was also adopted for this series of experiments.

### 8.5.2 Results

As in the previous section, the isotropic mechanical properties for the enamel, dentine and cancellous bone listed in Table 3.7 were employed. Again, the cortical bone and the periodontal membrane were assigned their respective orthotropic and lateral isotropic mechanical properties as derived in Chapter Six.

FIG. 8.7 shows the three labial surface loading positions, for which the instantaneous centre of rotation of the tooth was determined. Each load is clearly seen to be acting approximately at right angles to the tooth's long axis and hence constitutes purely lateral loading. The three instantaneous centres of rotation determined for the three load cases shown, are depicted in FIG. 8.7.

### 8.5.3 Discussion of Results

Whereas, in the previous set of experiments, the positions of the instantaneous centres of rotation remained at the same level in the tooth root, (i.e. at a level 38% of the distance between the root apex and the cervix, measured from the apex of the tooth), this set of experiments produced centres of rotation at different levels. FIG. 8.7 clearly shows how the position of the instantaneous centre of rotation moves

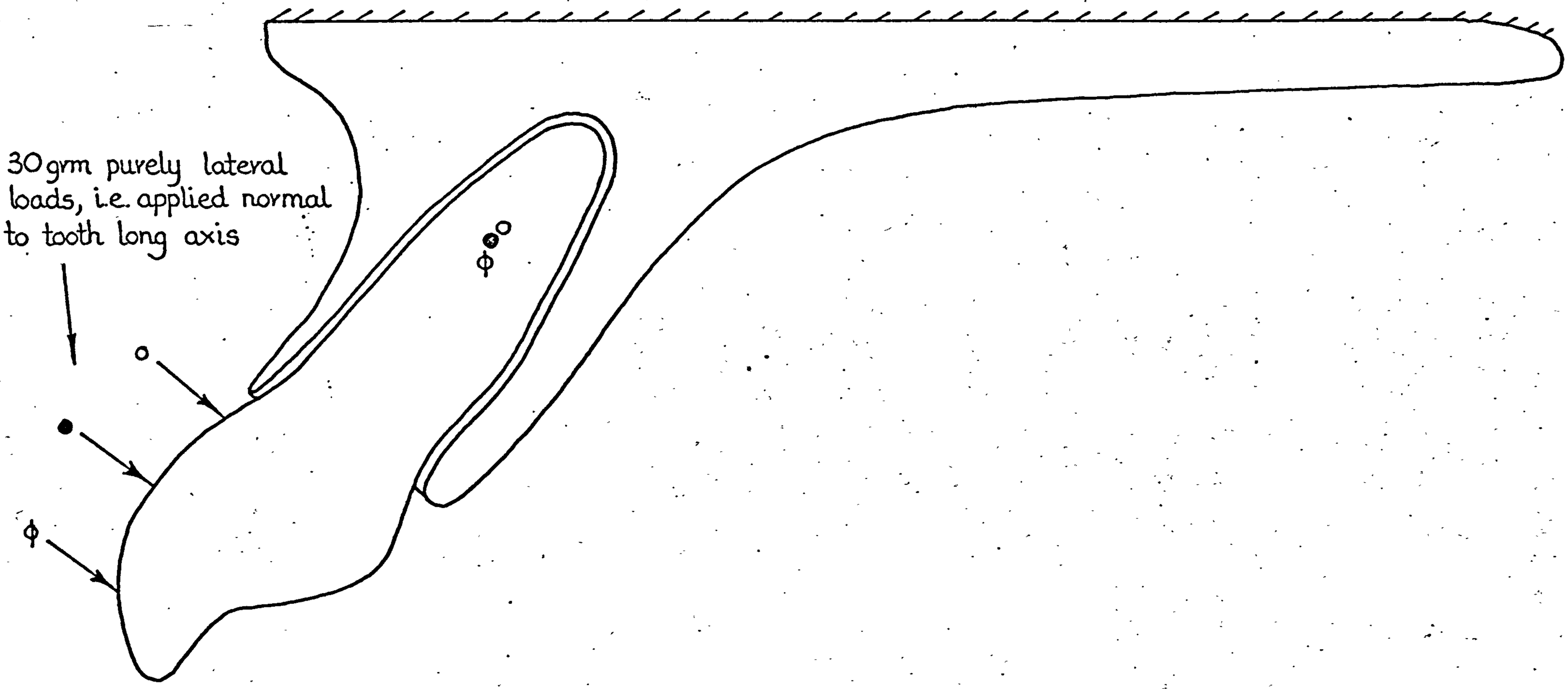


FIG. 8.7 Positions of the instantaneous centres of rotation obtained from the 2-D model for various positions of 30 grm. loading. Loads applied normal to tooth long axis.

towards the incisal edge of the tooth as the position of the applied load moves in a similar manner.

The results of this series of experiments are probably more realistic than are those of the previous section. This is because the loads act laterally and therefore conform to the type of loading for which the properties of the periodontal membrane were originally determined. Therefore, it can be concluded that for the purely lateral type of loading, the position of the instantaneous centre of rotation of the tooth moves in phase with the position of the applied load. However, the relative movement of the position of the instantaneous centre of rotation determined is quite small in comparison with the differences separating the positions at which the corresponding loads were applied.

## 8.6 RELATIVE CHANGE IN THE POSITION OF THE INSTANTANEOUS CENTRE OF ROTATION OF A TOOTH DURING ORTHODONTIC TREATMENT

The aim of this section was to see whether the position of the instantaneous centre of rotation of a tooth changed during the course of orthodontic movement. This was achieved by first considering a model of the tooth structure in the initial state prior to orthodontic treatment, and subsequently, a second model of the modified tooth structure at the cessation of treatment. During the period of movement, the shape and size of the tooth was assumed to remain constant. Also, the 30 gm. orthodontic load was considered to act at the same point on the labial surface of the tooth and in the same direction, (i.e. normal to the tooth's long axis), for both

finite element models. Although clinically both the magnitude of the orthodontic force and its direction relative to the tooth's long axis may change very slightly during treatment, it was felt that these changes would not significantly alter the outcome of the experiments.

### 8.6.1 Finite Element Model and Test Procedure

The tracings shown in FIGS. 6.13a and 6.13b in Chapter Six, were made from X-ray pictures of a maxillary central incisor taken before and after the tooth had received orthodontic treatment. The model employed in many of the earlier experiments, and shown in FIG. 6.16, is in fact a finite element simulation of the tooth in its initial position, i.e. derived from FIG. 6.13a. On the other hand, FIG. 8.8 shows the two-dimensional equivalent thickness finite element model derived from FIG. 6.13b; the tooth structure at the end of the treatment period. Hence, the simulations shown in FIG. 6.16 and FIG. 8.8 were the two models that were employed for this series of experiments.

### 8.6.2 Results

The isotropic mechanical properties for the enamel, dentine and cancellous bone were employed for both models. These were taken as before from Table 3.7. Likewise, the orthotropic cortical bone and lateral isotropic periodontal membrane properties derived in Chapter Six were similarly employed.

Both finite element models were loaded with a 30 gm. lateral orthodontic load; the positions and directions of

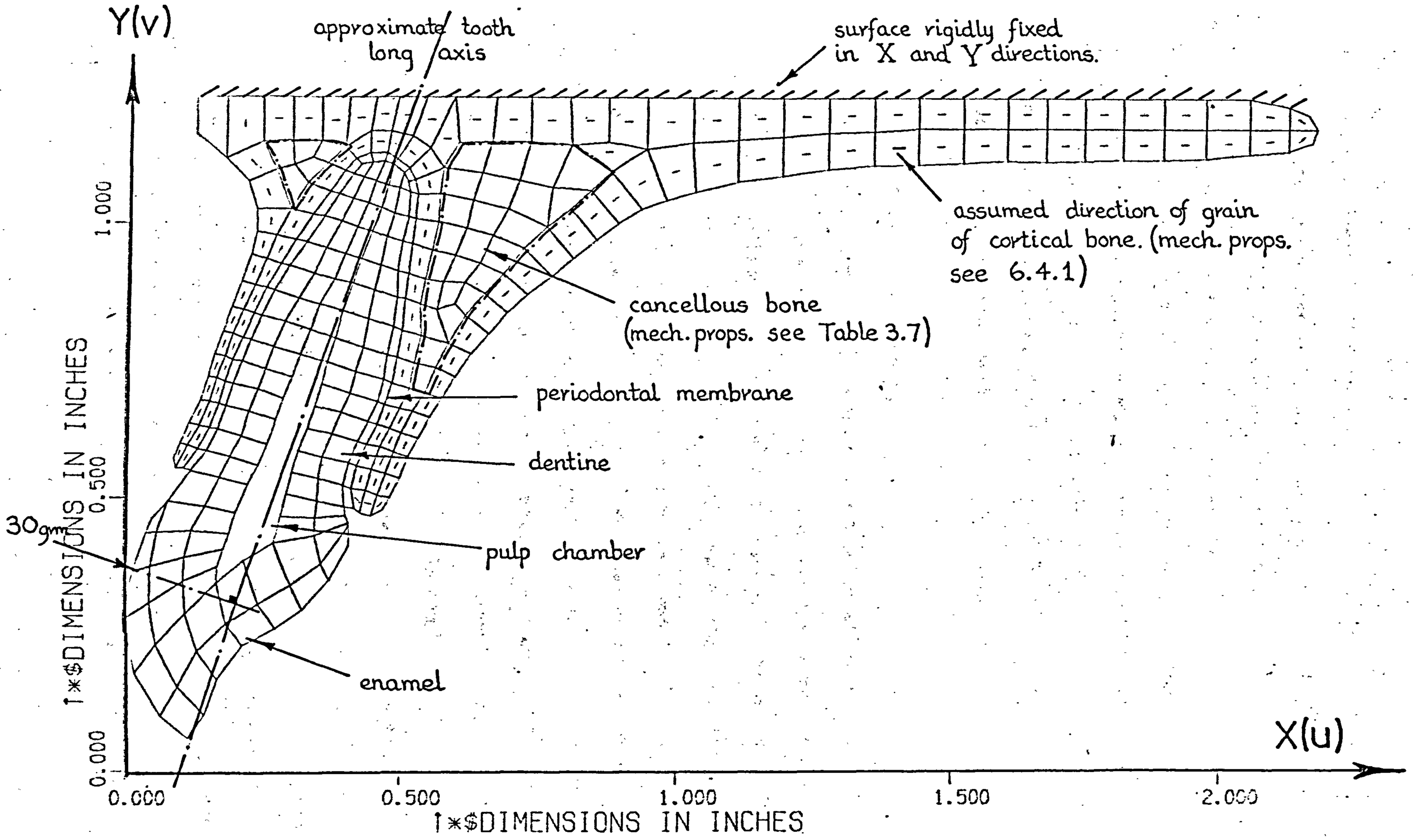


FIG. 8.8 Computer plot of 2-D representation of maxillary central incisor at the cessation of orthodontic treatment. Model comprised of 275 quadrilateral type finite elements.

these are shown in FIGS. 8.8 and 8.9. It was assumed that the magnitude of the orthodontic spring force did not change during the period of treatment and also that the direction of the force remained at right angles to the tooth's long axis.

The position determined for the instantaneous centre of rotation of the maxillary central incisor after treatment is shown in FIG. 8.9. Also shown in this figure is the corresponding position of the centre of rotation of the tooth obtained before orthodontic treatment.

### 8.6.3 Discussion of Results

Although the instantaneous centre of rotation was only determined for the tooth in the initial and final positions, the intermediate positions during the course of the orthodontic movement have been estimated. The locus of these positions, i.e. the space centrode of the tooth, is shown in FIG. 8.9. Even so, the results obtained from this series of experiments clearly show that there is practically no change in the position of the instantaneous centre of rotation, relative to the tooth, of the incisor model during the course of orthodontic treatment, i.e. the body centrode of the tooth. Although FIG. 8.9 shows that considerable alveolar bone remodelling has taken place, the height of the alveolar crest tips relative to the tooth's root has remained almost constant. Therefore, bearing in mind the fact that the orthodontic load was applied at the same position and in the same direction relative to the tooth's long axis for both finite element models, this result is consistent with those obtained from the earlier tests.

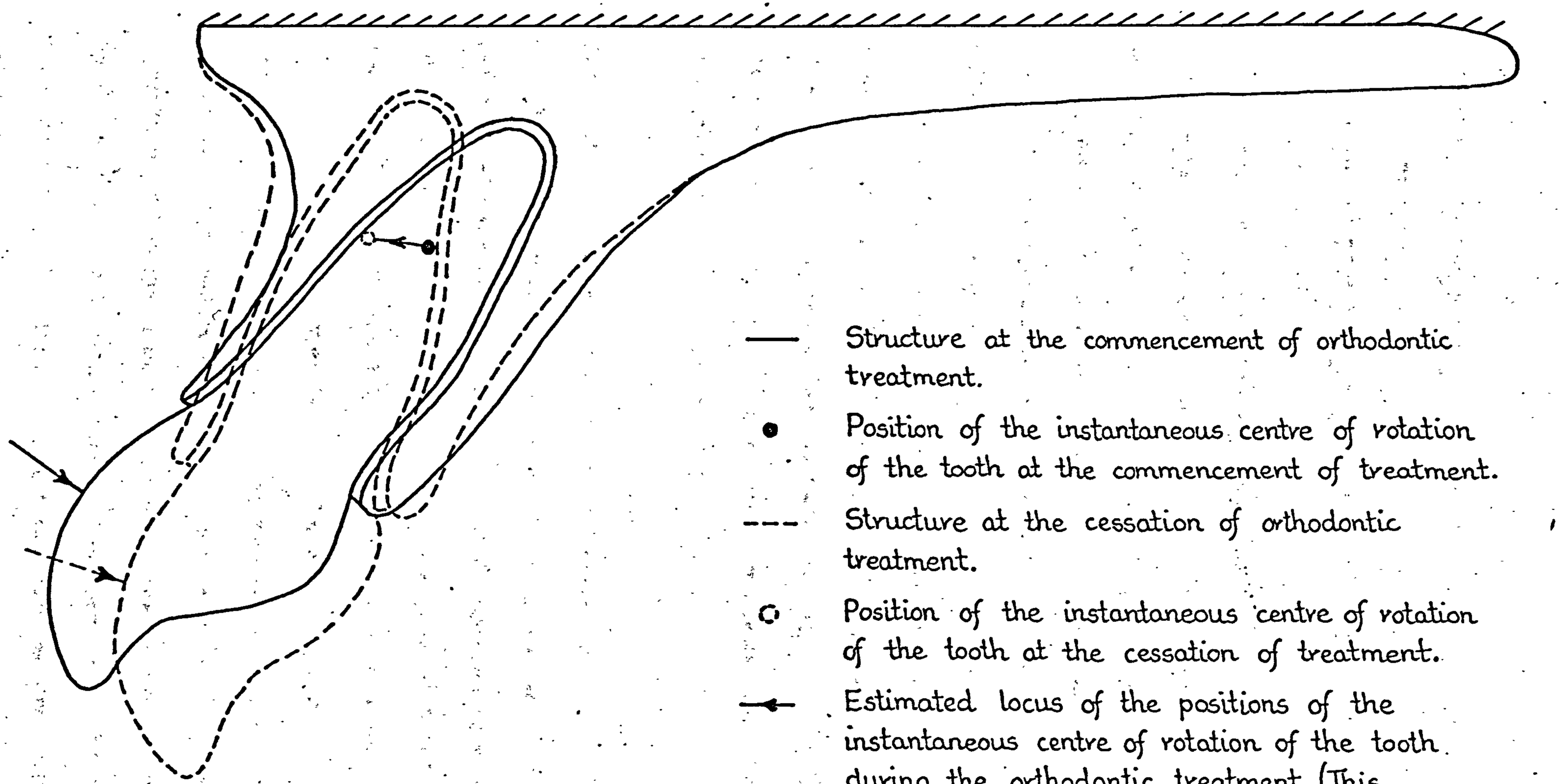


FIG. 8.9 Position of the instantaneous centre of rotation obtained from the 2-D finite element models of the maxillary central incisor at the commencement and at the cessation of orthodontic treatment.

## 8.7 CHANGE IN THE POSITION OF THE INSTANTANEOUS CENTRE OF ROTATION OF A TOOTH AS A RESULT OF VARYING THE DIRECTION OF THE APPLIED LOAD AND THE HEIGHT OF THE SUPPORTING ALVEOLAR BONE

In section 8.4 of this chapter, the effect of both the position and direction of the applied load on the instantaneous centre of rotation of the maxillary central incisor was investigated. Subsequently, the effect of the position of the applied load alone on the rotation of the same tooth was looked at in section 8.5. Consequently, the object of this section was to explore the effect, if any, that changing the direction of the applied load had on the instantaneous centre of rotation. The effect of the height of the supporting alveolar bone on the rotation of the tooth model was also investigated in this study.

### 8.7.1 Finite Element Model and Test Procedure

The finite element model used for this series of experiments was a two-dimensional bucco-lingual slice section of a mandibular second premolar having an equivalent thickness of 0.345 inches, see FIG. 8.10. This model is an extension of the crown model employed in Chapter Seven. As with the maxillary central incisor model, the alveolar process was constructed having both cortical and cancellous bone tissue. The assumed direction of the grain of the cortical bone is again indicated by the axis of the lines located in the centres of the cortical bone elements. The finite element mesh was so arranged around the alveolar crest areas such that it would be a relatively

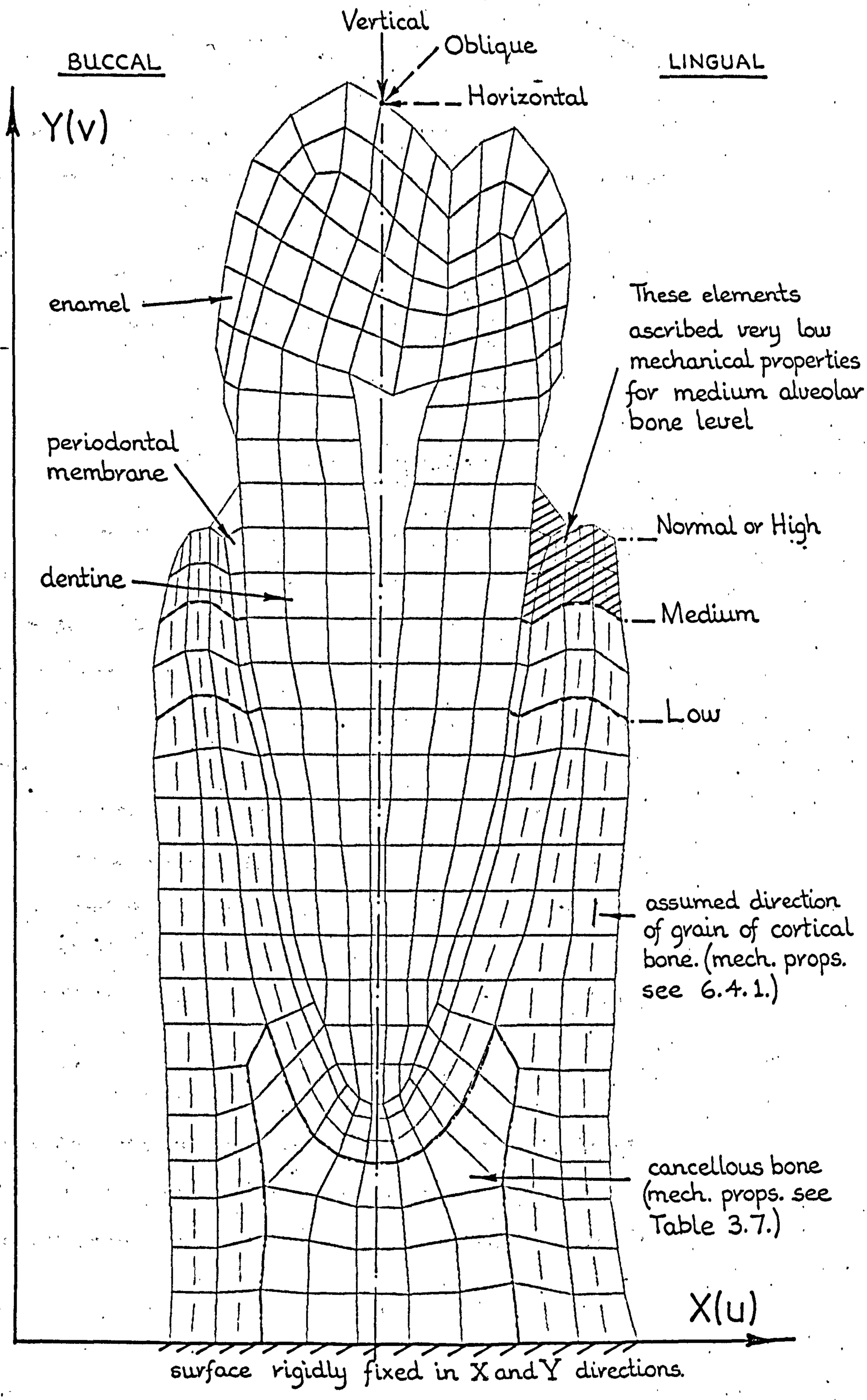


FIG. 8.10 Computer plot of 2-D representation of a bucco-lingual section of a mandibular second premolar having either a normal (high), medium or low level of alveolar bone support.

easy matter to change the effective height of the bone tips. The aim of this series of experiments was to investigate the effects of three different levels of alveolar bone height. These were:-

1) Normal or high alveolar bone height, extending up to within 2 mm of the amelo-cemento junction.

2) Medium bone height, extending up to within 4 mm of the amelo-cemento junction.

and 3) Low bone height, extending up to within 6 mm of the amelo-cemento junction.

The high, medium and low levels of alveolar bone considered are indicated in FIG. 8.10. For the medium and low bone analyses, the appropriate alveolar and periodontal membrane finite elements extending above the level under consideration were simply ascribed very low, (i.e. very flexible,) mechanical properties.

The mandibular second premolar was loaded on the lingual aspect of the buccal cusp with one of the following different loading regimes. These were:-

1) A 30 gm vertical intrusive load.

2) A 30 gm oblique load at an angle of 45 degrees to the vertical, i.e. bucco-intrusive.

and 3) A 30 gm horizontal load applied in the buccal direction.

The whole tooth structure was rigidly supported at the base of the model by clamping the cortical bone nodes lying along the horizontal X axis, in both the X and Y co-ordinate directions.

### 8.7.2 Results

The enamel, dentine and cancellous bone of the model were in each test assigned the appropriate isotropic mechanical properties listed in FIG. 3.7 and the cortical bone, the orthotropic properties derived in Chapter Six. However, the periodontal membrane was ascribed the isotropic mechanical properties given in FIG. 8.11. As can be seen from this figure, the properties employed for the vertical and horizontal, ( i.e. lateral) load cases were those derived in Chapter Six for the maxillary central incisor under similar loading conditions. However, the properties for the intermediate oblique load case were obtained by linearly interpolating the vertical and lateral values.

The height of the alveolar crests was varied between the high, medium and low model levels depicted in FIG. 8.10. Subsequently, the three models, each assigned with the appropriate periodontal membrane properties, were analysed under the action of the vertical, oblique and horizontally applied loads respectively. The positions of the instantaneous centres of rotation obtained from the nine experiments are tabulated in FIG. 8.12.

### 8.7.3 Discussion of Results

The results obtained from this series of experiments, see FIG. 8.12, show that although the position of the instantaneous centre of rotation of the tooth changes with respect to the height of the alveolar bone, its relative position remains

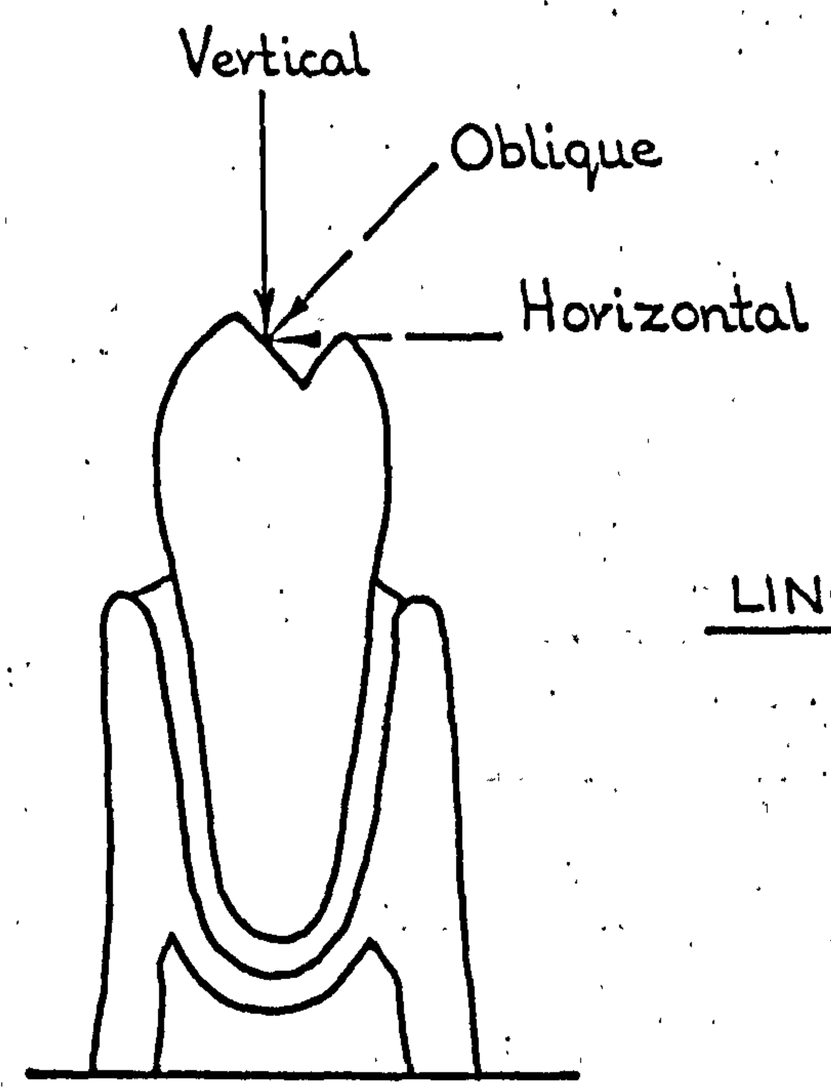


| LOAD CASE | MECHANICAL PROPERTIES | | |
|---|---|---|---|
| | E p.s.i. | $\mu$ | G p.s.i. |
| Vertical | 8·7 | 0·3 | 3·35 |
| Oblique | 17·4 | 0·3 | 6·7 |
| Horizontal | 26·1 | 0·3 | 10·05 |

FIG. 8.11 Isotropic mechanical properties for the periodontal membrane for the three different load cases.

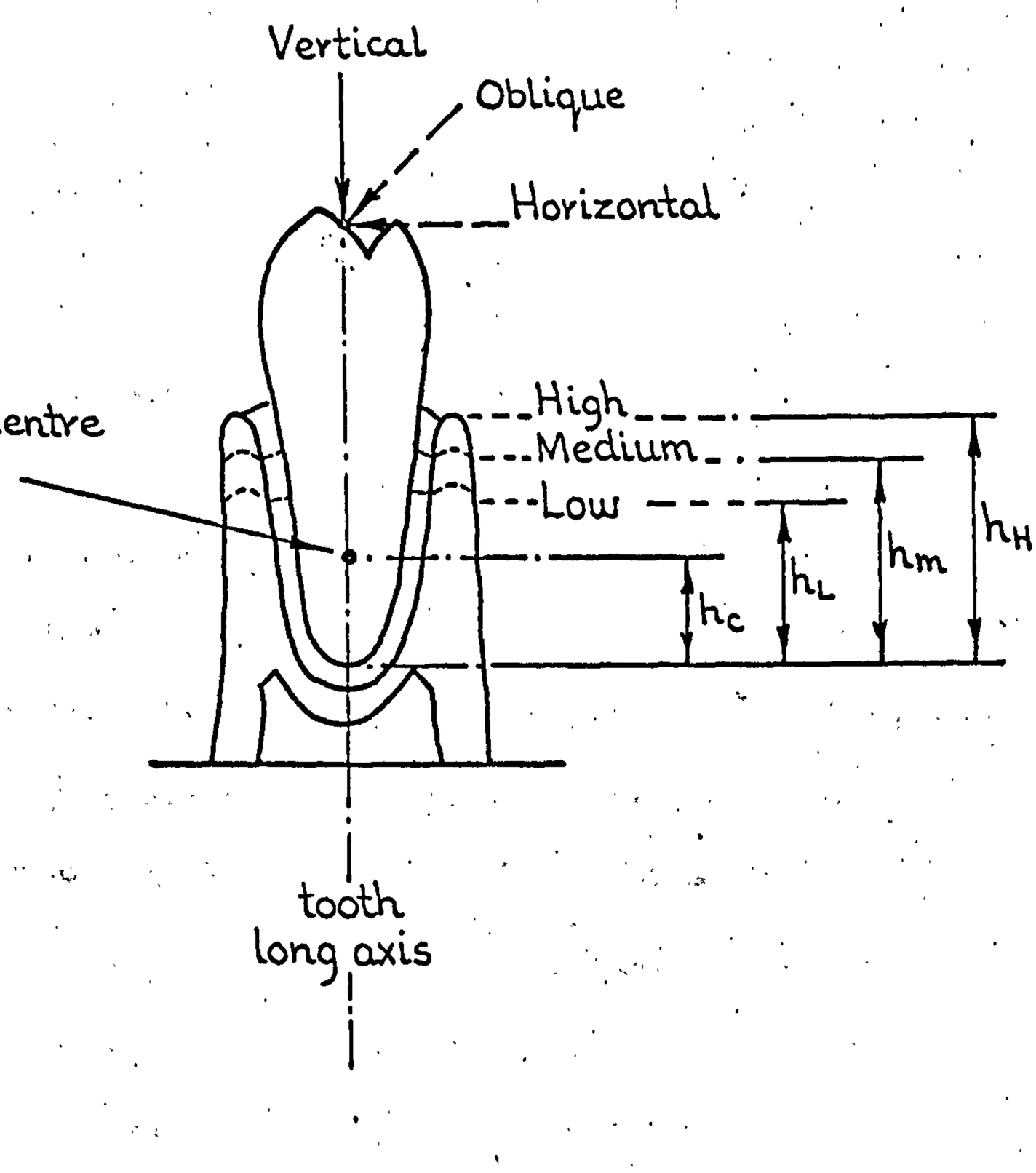


| ALVEOLAR BONE HEIGHT | APPLIED LOAD DIRECTION | | | RELATIVE POSITION OF INSTANTANEOUS CENTRE OF ROTATION | |
|---|---|---|---|---|---|
| | $h_c$ for 30grm Vertical | $h_c$ for 30 grm Oblique | $h_c$ for 30 grm Horizontal | 30 grm. Oblique | 30 grm Horizontal |
| High ($h_H$ 104mm) | — | 42·5 mm | 43·5 mm | $\frac{h_c}{h_H} = 41\%$ | $\frac{h_c}{h_H} = 42\%$ |
| Medium ($h_m$ 91mm) | — | 36·0 mm | 39·5 mm | $\frac{h_c}{h_m} = 39\%$ | $\frac{h_c}{h_m} = 43\%$ |
| Low ($h_L$ 74mm) | — | 30·0 mm | 30·5 mm | $\frac{h_c}{h_L} = 40\%$ | $\frac{h_c}{h_L} = 41\%$ |

FIG. 8. 12 Positions and relative positions, with respect to alveolar bone height, of the instantaneous centre of rotation of the second mandibular premolar under vertical, oblique and horizontal 30grm forces.

practically constant. In fact, the position of the centre of rotation remains at a level of approximately 40 percent of the root apex to alveolar crest dimension, measured from the root apex. Obviously, the vertical load does not rotate the tooth but merely translates it down into the socket. (It must be borne in mind that in this series of tests, the position of the load application occurred at a point which lay very close to the tooth's long axis). Therefore,these results are consistent with those obtained in the earlier work even allowing for the fact that in this series of tests an attempt was made to simulate the periodontal membrane's, mechanical properties for each of the vertical, oblique and laterally applied loads respectively.

## 8.8 CONCLUSIONS

If a body, located in a Cartesian co-ordinate system moves an infinitesimal distance, the motion of the body can be considered to constitute a pure rotation of the body about some fixed point. This fixed point, known as the instantaneous centre of rotation of the body during the body's very small displacement, need not necessarily lay inside or on the body. In fact, it can occur at any point within the co-ordinate system.

The initial or instantaneous* movement of a tooth upon the application of an orthodontic force is very small indeed.

* Initial or instantaneous tooth movement is implied here to be displacement immediate to load application as opposed to any subsequent tooth movement resulting from the tissue remodelling process.

Hence, the rigid body instantaneous centre of rotation theory can be applied to this particular problem. (Indeed, the theory upon which the finite element analyses employed here are based, is known as 'small displacement theory', i.e. the theory is only applicable for very small tooth displacements and structural deformations). It follows therefore that the instantaneous centre of rotation of a tooth, which has been moved by the application of an orthodontic load may not lay within the tooth itself.

Although the majority of authors have employed two-dimensional models in order to determine the instantaneous centres of rotation of teeth, it was shown that the positions obtained using these simplified models predicted centres of rotation which were significantly different from those obtained using the more realistic three-dimensional models. One notable exception however, was the two-dimensional model of Burstone (39, 40); the results produced using this author's approach were very close to those determined using the three-dimensional finite element model. However, because of the need for economy, the majority of experiments reported on in this chapter were carried out using two-dimensional finite element models. Indeed, the main aim was to look at overall trends and effects and not at specific or absolute values.

Because the stiffness of the alveolar bone is very high in comparison with that of the periodontal membrane for the orthodontic loads considered here, it has very little effect on the initial tooth displacement. However, it was apparent

from the literature and from the finite element results that the stiffness of the periodontal membrane drastically affects the position determined for the instantaneous centre of rotation. Indeed, the stiffer the periodontal membrane, the higher up the tooth root the position of the instantaneous centre of rotation occurred. This suggests therefore that because the stiffness of the periodontal membrane increases, with increase in tooth load, see FIG. 6.10., the position of the instantaneous centre of rotation of a tooth would be expected to be dependent upon the magnitude of the applied load. The indications were that the position would occur higher up the tooth's root for larger orthodontic forces. However, the linear elastic type analyses employed here presuppose that the magnitude of the orthodontic loading does not qualitatively affect the resulting structural displacement. Thus, the form of the tissues' cellular response would also similarly be assumed to remain constant. In fact, several researchers substantiate this as they have shown clinically that the magnitude of the orthodontic force does not affect the remodelling process, Utley (89) and Hermanson (90).

When the tooth was subjected to identical loading conditions it was found that as the height of the alveolar crest tips approached the amelo-cemento junction, so the position of the instantaneous centre of rotation moved away from the root apex. Although the results showed that the absolute position of the instantaneous centre of rotation of the tooth varied with varying alveolar bone heights, they also showed that under the same loading conditions the relative position, with respect to the

actual alveolar crest height did not, see FIG. 8.12. The constancy of the position of the instantaneous centre of rotation of the tooth during orthodontic movement, where both the height of the alveolar bone and the orthodontic load is considered to remain constant, further emphasises the significance of the bone level as a governing parameter. Nevertheless, with a constant alveolar bone height, the position of the instantaneous centre of rotation was found to move in phase with the position of the point of load application as it was moved along the labial surface. However, the differences in the positions of the instantaneous centres of rotation determined were very small.

When the orthodontic force was applied in a direction normal to the enamel surface, the position of the point of load application did not affect the general level of the centre of rotation in the tooth. Although its position across the tooth did vary, it seemed that the intrusive or extrusive components of these normally applied forces compensated for any small changes in position which were expected to occur as the result of the change in the position of the point of the load application. However, as can be seen from FIG. 8.6, the instantaneous centre of rotation was found in one instance to lay completely outside the tooth's root in the labial plate of the alveolar bone.

Although the orthotropic periodontal membrane simulation portrays a somewhat inadequate representation, the experiments

showed that little change occurred in the position of the instantaneous centre of rotation. It seems again to indicate therefore that the position of the centre of rotation depends mainly upon the height of the periodontal membrane - alveolar bone attachment, and on the overall flexibility of the periodontal membrane itself. It should be noted however, that in reality, the flexibility of the periodontal membrane is not linear; its supporting mechanism might well change significantly with increasing magnitude of load, tooth displacement and time. Also, the principal fibre system may not present an equal mechanical response to both tensile and compressive stresses as was assumed in the model simulation employed. In fact, the principal periodontal membrane fibre support system may not even be operative in the clinical situation immediately after the application of the very low orthodontic loads considered here.

For all the two-dimensional finite element models employed in this chapter, the positions of the instantaneous centres of rotation occurred generally at a level about 40% of the distance between the root apex and the alveolar crest tips (measured from the root apex.) Therefore, bearing in mind that the position of the instantaneous centre of rotation was found to be even higher, (approximately 50%), for the more realistic three-dimensional finite element model, these results agree with the recent observations made clinically by Stephens (91). Both the results here and Stephens' work indicate that the instantaneous

centre of rotation of a tooth loaded by a removable type of appliance occurs well towards the centre of the root apex to alveolar crest tip distance. This challenges the currently held view that the position of the instantaneous centre of rotation occurs at approximately one third of the root apex to crest tip distance for a removable type of appliance. Consequently, this finding raises a serious doubt as to the validity of existing ideas concerned with certain methods employed for orthodontic treatment.

# CHAPTER NINE

# BONE RESORPTION AND DEPOSITION

# 9. BONE RESORPTION AND DEPOSITION

## 9.1 INTRODUCTION

The ability of the skeletal system of man to adapt itself to meet the structural demands placed upon it, has intrigued and perplexed the minds of scientists from time immemorial. Even though numerous theories have been put forward to explain the phenomenon of bone remodelling*, a study of the relevant literature shows that a universally accepted theory of the fundamental mechanism or mechanisms which regulates bone resorption and deposition is still a very long way away. Obviously, an understanding of the process of bone remodelling is desirable as this would enable better and more efficient orthodontic and orthopaedic diagnoses and treatment to be attained.

## 9.2 REVIEW OF IDEAS ON BONE RESORPTION AND DEPOSITION

Although several different theories have been postulated to explain the phenomenon of bone resorption and deposition, only the commonly cited theory proposed by Wolff in 1870 (92) and further elaborated in a monograph in 1892 (93), has so far stood the test of time. Wolff's Law, as it is now commonly called, states that bone responds to the mechanical demands placed upon it. That is to say, for an increase in function or demand the bone responds with deposition and for a decrease in function or demand it responds with resorption.

* In this chapter, bone remodelling refers to the changes occurring in bones resulting from a change in either bone shape or the quantity of bone substance. Used in this context, bone remodelling is a completely different phenomenon from the normal and continuous process of bone turnover.

Nett loss of bone substance has been shown to occur in patients who have undergone long periods of bedrest and more recently, it has been discovered that astronauts subjected to prolonged periods of weightlessness and physical inactivity, also suffer from a similar process.

Although D'arcy Thompson in his classic work "On Growth and Form" (94) and most other subsequent authors have accepted Wolff's Law, certain doubts concerning this theory do exist. For example, there is strong clinical evidence to suggest that bone 'melts away' from around certain orthopaedic screws and implants where 'excessive' stress concentrations are expected to occur*. This tends to suggest therefore that bone may be either sensitive to the type of demand placed upon it or it may possess an upper demand cut-off level above which it fails to respond. Similarly, Wolff's Law has been shown not to govern the initial form taken by whole bones. Fell, (95) in a review paper in 1956 reported that cartilaginous rudiments of bones taken from embryos long before their eventual form was apparent, developed in tissue culture to their normal characteristic form. This proved that the initial bone form must somehow be coded into the cells such that they were able to initiate osteogeneses <u>in vitro</u> as in this environment they were devoid of all mechanical as well as neural and circulatory influences. Consequently, the process of initial bone development and construction has had to be separately defined and Wolff's Law modified to include this contingency. For

* Another possible explanation for bone resorption around metal devices employed in orthopaedic surgery may be that the resorption process is triggered off by the irritation of the cells which results from either mechanical fretting or material incompatability.

instance Bassett's interpretation is (96) ''The form of the bone being given, the bone elements place or displace themselves in the direction of the functional pressure and increase or decrease their mass in order to reflect the amount of functional pressure''. This statement implies that the mechanical demand implied by Wolff's Law is the pressure, or in other words the stresses, acting on the bone during function. Furthermore, Bassett states that ''regions under compression, which tend to be concave, are usually negatively charged while regions under tension, which tend to be convex, are usually positively charged.'' Bassett also states that ''it is known both clinically and experimentally that a concave region of a bone will be built up and a convex region torn down''.

Other authors have made slightly different interpretations of the surface curvature idea. Chamay and Tschantz (97) for example, state that ''when a bone is bent under a mechanical load it modifies its structure by bony deposition in the cancavity and by resorption in the convexity''. However, Epker and Frost (98), who were the originators of the surface curvature regulating mechanism theory, proposed that bony formation only occurs at bone surfaces in areas that are <u>becoming more concave</u> under load, and bone resorption in areas that are <u>becoming more convex</u>.

Epker and Frost arrived at their conclusion by considering the two most frequently discussed cases of orthodontic tooth movement and the so-called straightening of the malaligned fractured long bone, see FIG.9.1a. These authors believed that "naturewas consistent" and hence assumed that the same

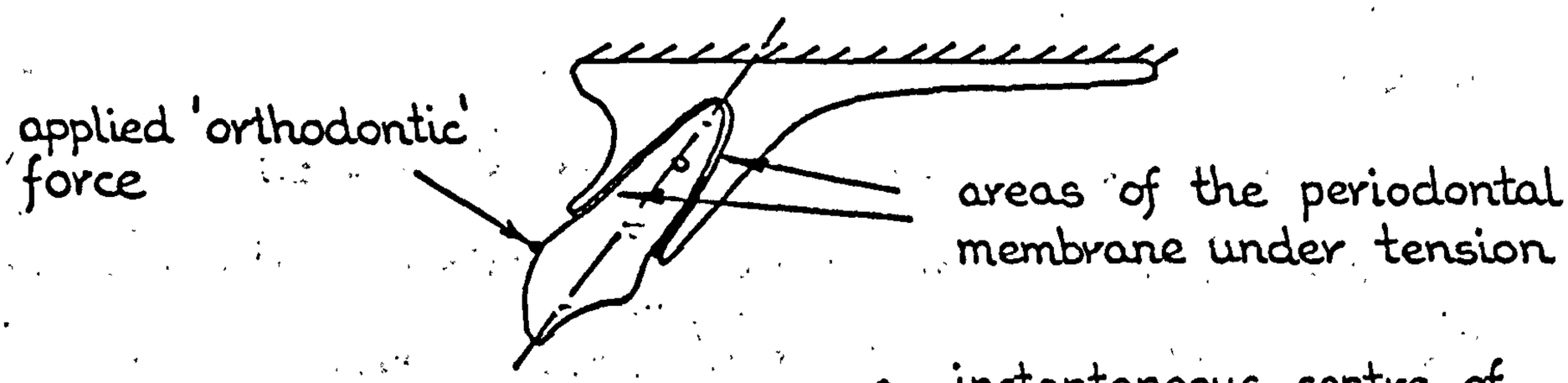


Above :- Orthodontic case of bone resorption and deposition to reorientate tooth.

Below:- Orthopaedic case of bone resorption and deposition to correct malalignment in a long bone.

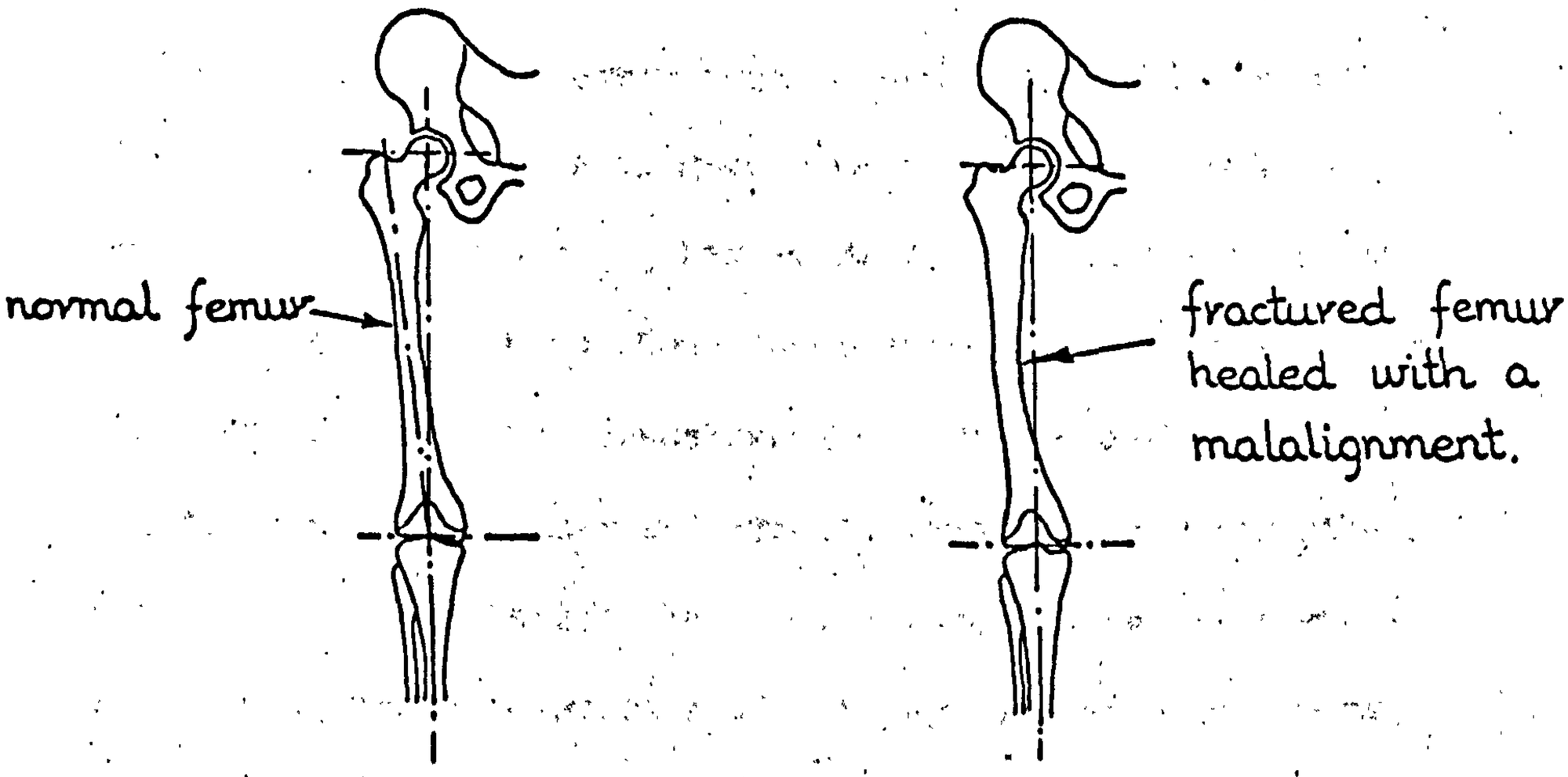


FIG. 9.1a Classic orthodontic and orthopaedic cases of bone resorption and deposition.

regulating mechanism governed both cases.

Currey in 1968 (122), challenged both Bassett's,and Epker and Frost's theories. Bassett's theory, he claimed,did not hold true for tubular bone remodelling. Currey argued that if a malalignment in a long bone was subjected to a combined compressive and bending moment type of loading as shown by FIG.9.1b, then the cortex on the right hand side of the figure would be under compressive stresses while the left hand side of the cortex would be under tensile stresses. Thus, Currey claims, the remodelled bone as predicted by Bassett's "compression equals deposition" theory would be as shown in FIG.9.1b. This he believes is clinically untrue. Although Currey's argument is a very convincing one, it must be pointed out that Bassett never stated whether he considered the same mechanical stimulus to be equally effective at both the periosteal and endosteal bone surfaces.

Currey also proposed that Epker and Frost's theory would not hold true if a tubular bone was subjected to net tensile loading. The example Currey used in his argument is shown in FIG.9.1c in which the malaligned bone is subjected to a net tensile load. This loading regime produces both a straightening effect on the kink in the bone and a predominantly tensile stress distribution across the cross-section. Consequently, Currey claims, by applying Epker and Frost's remodelling theory,the malalignment would tend to be 'self-enhancing' as is shown by the figure. Again however, although Currey's argument seems sound, it is open to serious doubt as to whether bones are ever subjected to net tensile loading, Frost (123) and Oxnard (124). Consequently,Currey's criticism of Epker and Frost's theory

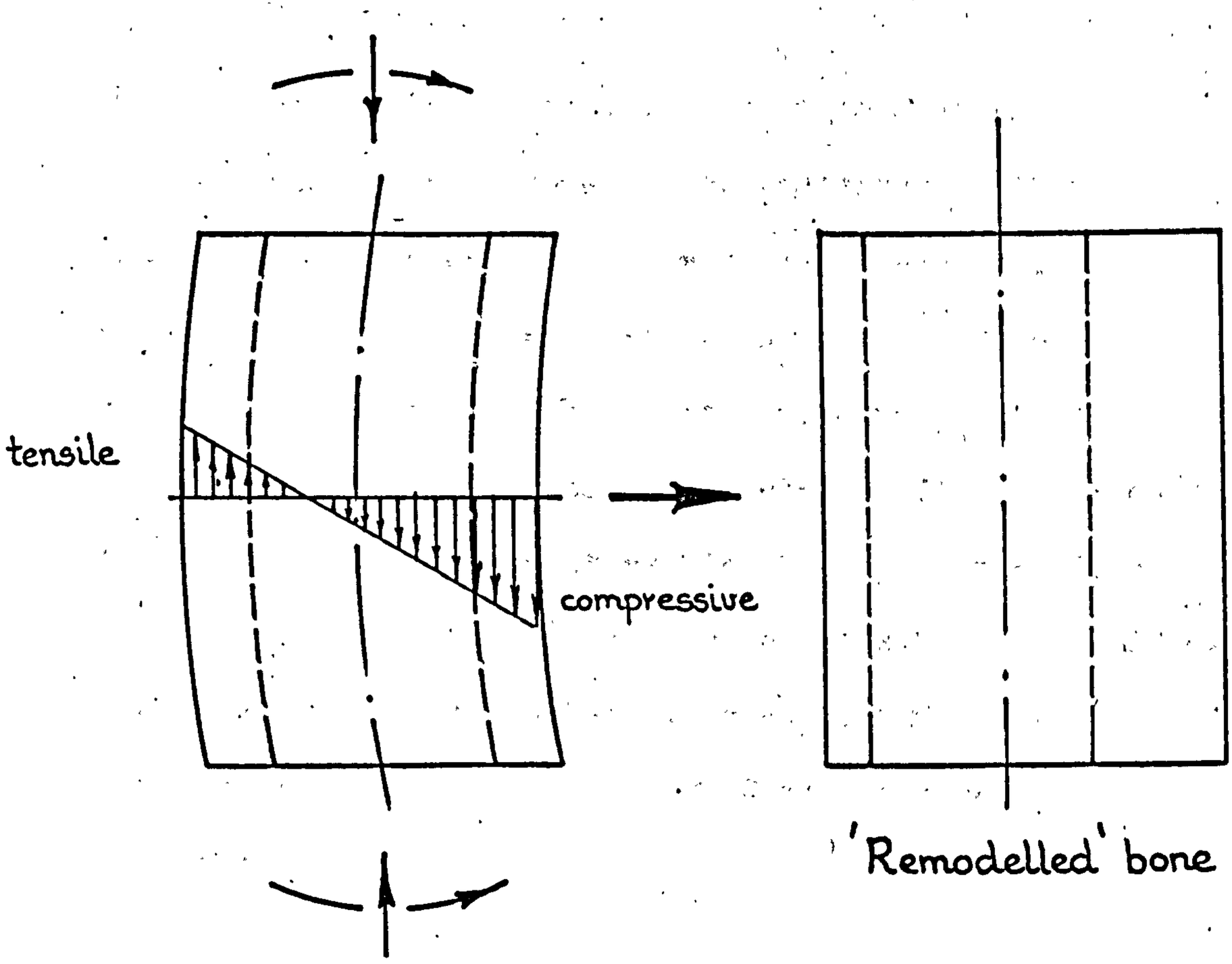


FIG. 9. 1b Bassett's remodelling theory applied to a malaligned long bone subjected to combined compressive and bending loading conditions.

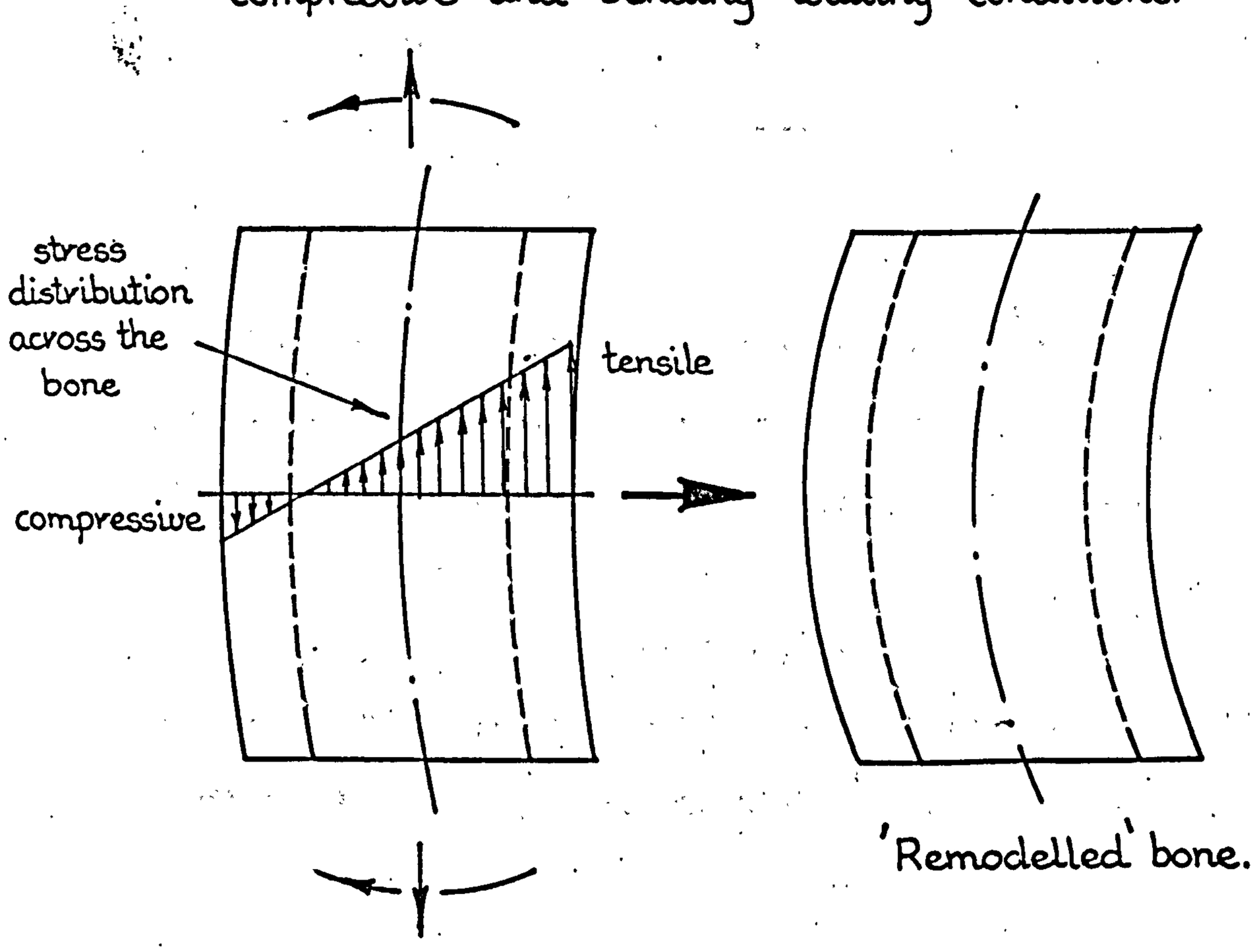


FIG. 9. 1c Epker and Frost's remodelling theory applied to a malaligned long bone subjected to Currey's "net tensile" loading conditions.

on the basis of this case may be open to question.

Because of the apparent shortcomings of both the Bassett and Epker and Frost remodelling theories, Currey proposed another approach which, he claims, covers all clinical situations. This theory requires that the net stress on the bone be known (however, it is difficult to interpret what is meant explicitly by the term ''net stress''). Once this ''net stress'' has been determined, C or T according to whether it is net compression or tension, the remodelling process Currey claims is as follows:-

| | C | T |
|---|---|---|
| C > | A | S |
| C < | S | A |

where C> signifies that the local stress on the bone surface is more compressive than it is underneath etc., and A and S signify whether bone is Added or Subtracted at the bone surface.

Although Currey's theory 'predicts' a remodelling correction of the malaligned bone shown in FIG. 9.1c, possible schemes of loading the bone can be drawn up

which tend to challenge this theory, see FIG. 9.1d. (In this figure it is assumed in each case, that the system of loading produces a remodelling response which tends to correct the malalignment.) Indeed, it can be seen that various situations can be 'devised' which can in fact contradict Bassett's, Epker and Frost's, and Currey's theories in turn. Thus, the warning from this exercise is that it can be misleading to propose possible hypothetical cases such as those shown in FIG. 9.1d on which to test theories, when such cases have not been examined biomechanically and are not backed up with sufficient clinical evidence.

Generally speaking, although the two bone remodelling situations depicted in FIG. 9.1a have been examined by numerous researchers, albeit more frequently they have been considered in isolation. Indeed, it is when they are considered together that there appears to be a discrepancy between the ideas which are commonly held regarding each case. For instance, the orthopaedic viewpoint is that an increase in compressive stress causes bone formation or growth, that is, in the concavity on the periosteal surface of the malaligned femur shown in FIG. 9.1a and that an increase in tensile stress results in bone resorption, i.e. on the convex periosteal surface of the femur shown in FIG. 9.1a. On the other hand, the

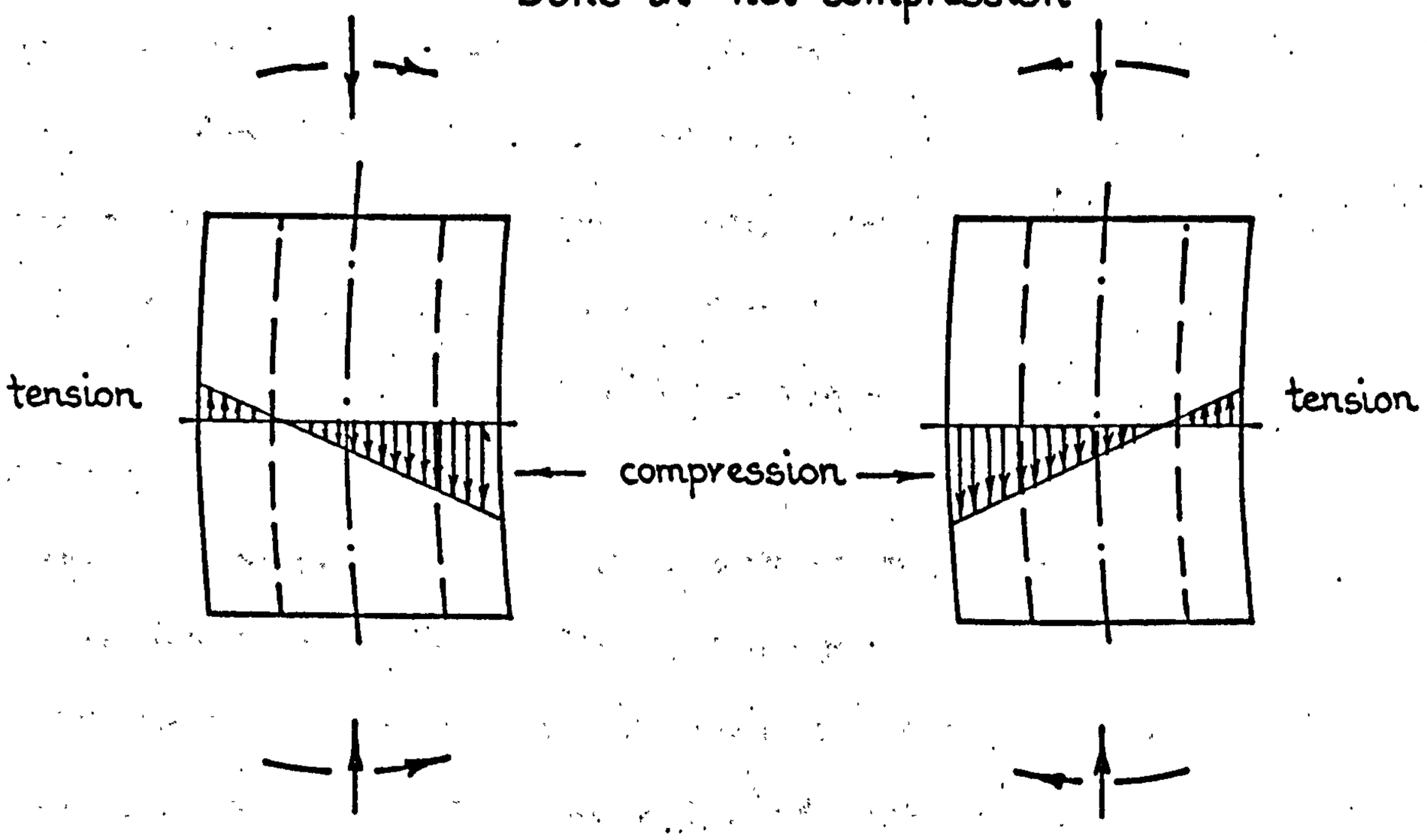


FIG. 9.1d Speculative loading schemes applied to a malaligned long bone.
'Yes' - remodelling theory predicts correction of malalignment
'No' - remodelling theory does not predict correction of malalignment.

orthodontist's view is to the contrary. His conception is that when the tooth is loaded as shown in FIG. 9.1a, the various areas of the periodontal membrane above and below the instantaneous centre of rotation are subjected to the action of either tensile or compressive stresses. Subsequently, it is the bone which is adjacent to the areas of the periodontal membrane under compression which is resorbed, whereas bone formation occurs on the socket wall which is adjacent to the areas of the periodontal membrane which is under the action of tensile stresses.

Although work has been published by Baumrind (99) which unjustly repudiates this theory, see Chapter Ten, the hypothesis relating the pressure-tension areas in the periodontal membrane to the areas of alveolar bone resorption and deposition respectively, has found wide support. (In fact, it is because of this theory that so much importance and attention has been focussed on the problem of determining the centres of rotation of teeth under orthodontic loading, see previous Chapter.) Reitan in particular has published numerous papers on histological studies in which he has examined the periodontal membranes of both animals and man which have been subjected to orthodontic tooth movements, (100, 101, 102 and 103). This author showed that the pressure zones created in the periodontal membrane may result in the formation of hyalinized or cell-free areas.

Subsequently, it is the lamina dura adjacent to these hyalinized areas which Reitan has observed to be resorbed. On the other hand, in the zones of the periodontal membrane which are subjected to tensile stresses, he believes there occurs a general increase in cellular elements and the formation of osteoid tissue. Reitan found that eventually new bony spicules eminated from, and attached the stretched principal fibre bundles of the periodontal membrane to the lamina dura in this osteod layer.

Further support for the pressure-resorption hypothesis has been supplied by Ackerman et al (104). These authors implanted matched pairs of magnets having differing attractive force strengths on either side of the sternums of pigeons. They found that the breast bone resorbed away from between the opposing faces of the active magnet pairs but that little change occurred between the inactive controls. However, bone resorption was not found to be dependent upon the magnitude of the pressure over the range of attractive forces employed in the tests. Instead, it was found to be dependent upon the duration of the experiments.

Although the evidence seems overwhelmingly in support of the pressure equals resorption and tension equals deposition hypothesis, this theory does not obviously apply to the bone remodelling which takes place outside the tooth socket during orthodontic treatment. FIG. 9.2 shows both the areas of bone formed and resorbed during the orthodontic movement of the maxillary central incisor depicted in FIGS. 6.13 and 8.9.

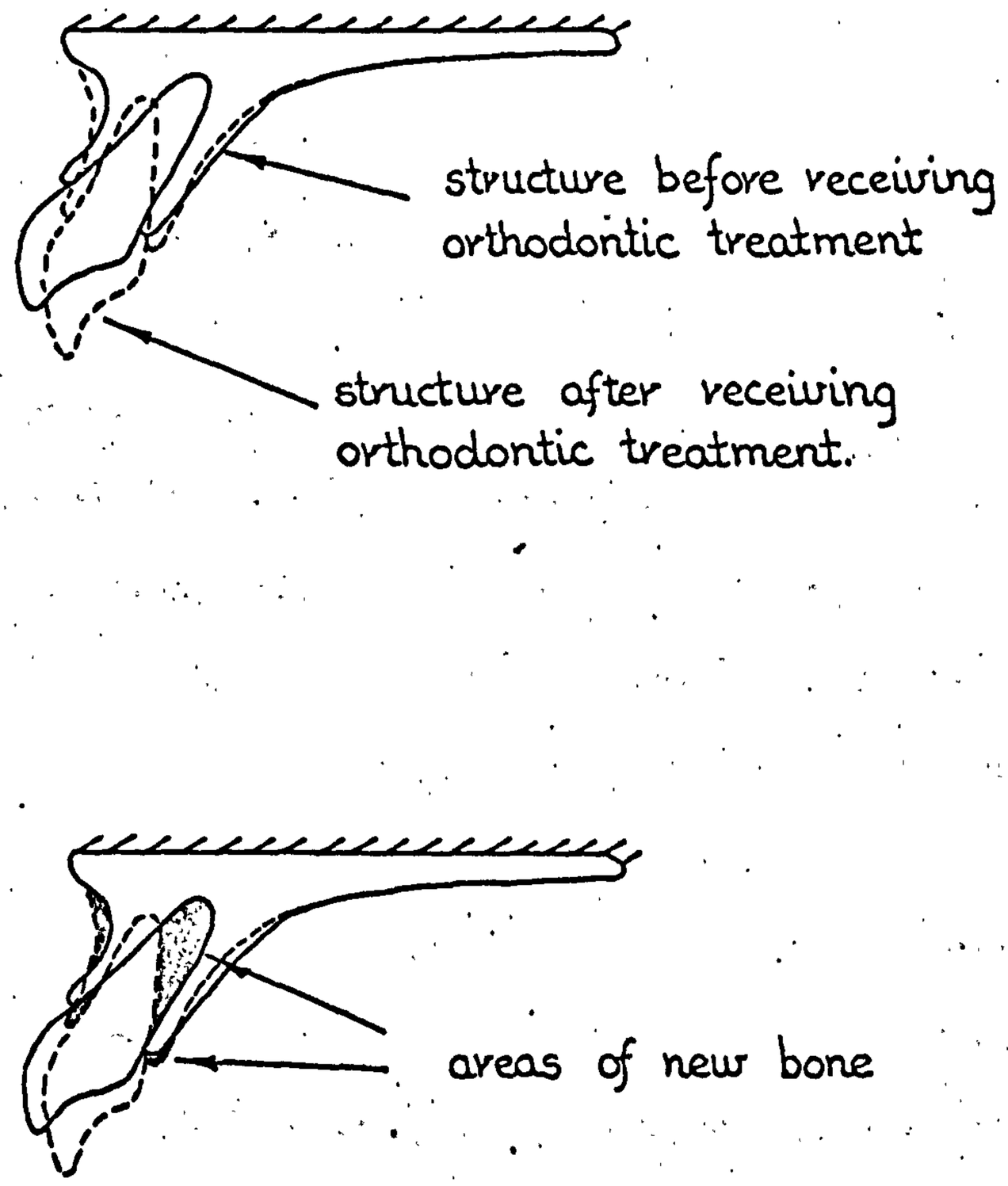


FIG. 9.2 Superimposed tracings of radiographs taken of a maxillary central incisor before and after receiving orthodontic treatment to show the areas where bone resorption and deposition have taken place.

It can be seen that significant areas of bone are formed and resorbed on the outer surfaces of the alveolar processes. Clearly, the periodontal membrane pressure-tension hypothesis does not apply to these areas.

It is pertinent to point out at this juncture that for the remodelled orthopaedic and orthodontic structures considered above, the direction of the stresses involved in the discussion have not been taken into account. In fact, in the case of the long bone the compressive stress 'producing' bone formation in the concavity of the periosteal surface must be acting in a direction approximating to that of the long axis of the femur itself. However, in the orthodontic case, (and also for the experiments conducted on the pigeons), the compressive stresses implied are acting in a direction almost perpendicular to the lamina dura and bone surfaces, see chapter ten. Logically, it seems reasonable to expect that the direction (as well as the type) of stresses acting on the bone tissue is an important factor to consider. (This must be so, especially if cognizance is taken of the proposed bioelectrical transducer mechanism).

Another important difference between the two cases discussed above lies in the manner in which the two structures are loaded. In the case of the incisor tooth a very small continuous force is applied, whereas for the long bone it is believed that it is the heavy intermittent forces resulting from locomotion that provide the stimulus for the remodelling process. Therefore, the stresses generated in the bone as a consequence of locomotion are many orders of magnitude greater

than the stresses generated in the alveolar bone in response to the orthodontic appliance loading. Consequently, purely from a logical viewpoint it seems reasonable to suspect that the stimulating stresses in the femur may not be those produced by locomotion. Instead,the stimulus could possibly be attributed to quite small muscle forces whose equilibrium and balance has been disrupted by the malalignment in the bone. However, at the moment little is known about the directions and magnitudes of the muscle forces during locomotion and even less about whether residual or disturbed muscle forces really exist. Of course, if they do exist then it is possible that they would tend to straighten the malalignment in the long bone,illustrated in FIG. 9.3 and would thereby create a completely different stress system to the one created by the force system shown in the figure.

The arguments supporting the theory that it is small continuous forces which provide the stimuli for bone remodelling are very strong indeed. After all, it has been shown by many authors that orthodontic tooth movement is independent of the magnitude of the forces applied and also that the forces required need be but very small, Weistein (105) and Hermanson (90). Also, it was shown in the previous chapter see section 8.4, that the masticatory force applied to the central incisor produced a very similar tooth rotation as did the orthodontic type force. However, in the orthodontic case the supporting tissues are stimulated to remodel whereas under the masticatory loading no structural modification appears to take place. Of course, it could be argued that for the latter situation, the

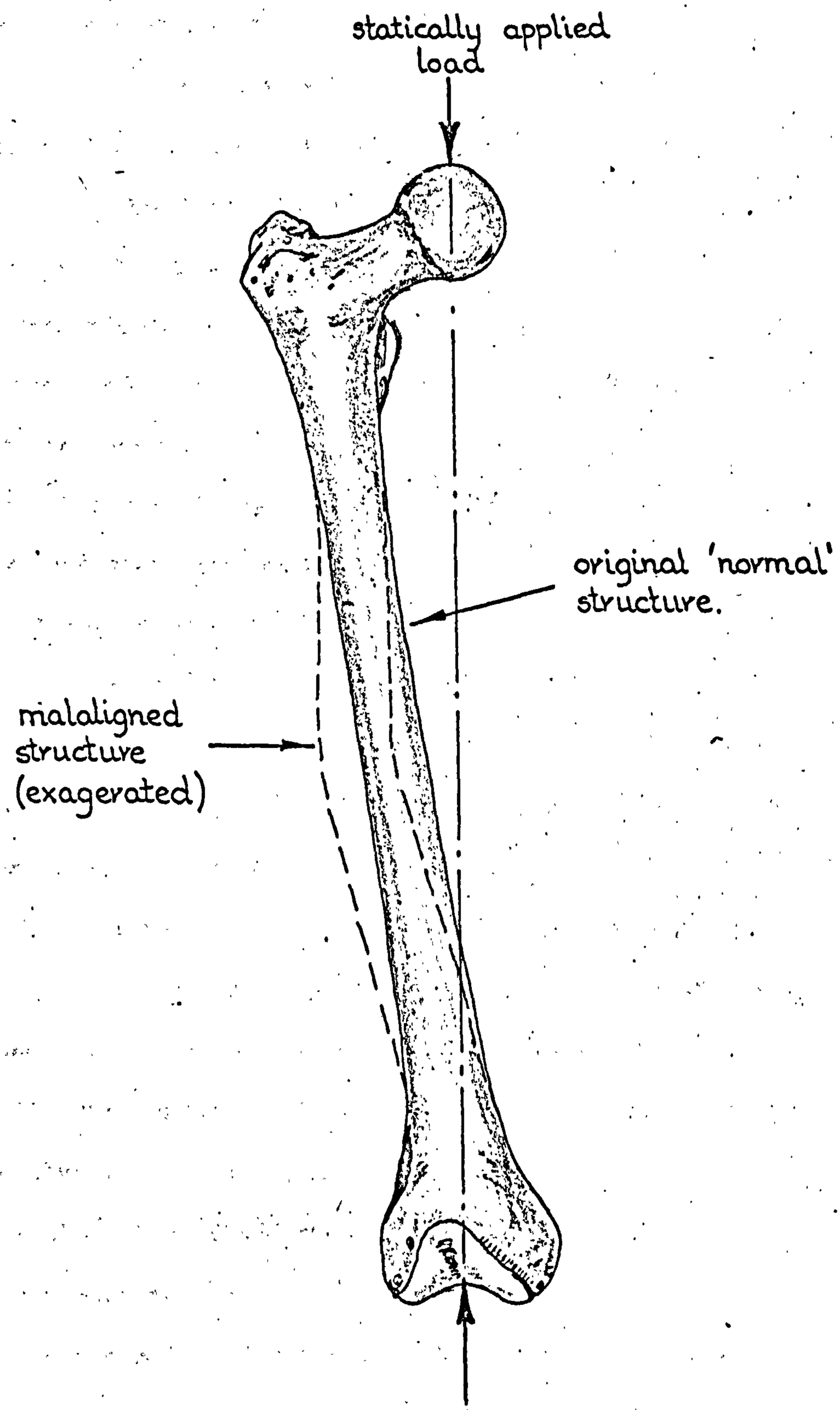


FIG. 9.3 Normal and malaligned femur subjected to a single statically applied compressive point load.

entire maxillary arch is in a state of dynamic balance, i.e. masticatory forces in equilibrium with the resulting interdental contact, tongue and cheek forces. Even so, it could be that the frequency of the masticatory forces, (which incidentally is very similar to the frequency of the femoral forces resulting from locomotion), is above the threshold frequency required to stimulate the bone cells in order for remodelling to occur.

Yet another example against the theory that it is the compressive stresses 'generated' in the concavity of the malaligned femur which gives rise to the bone deposition can be cited from the field of orthopaedics. Here, cases are frequently encountered where bone resorption has occurred in areas of high stress concentration, for example from around nails, screws and implants such as the early hip prostheses. Even though the stress is apparently of a compressive nature, the bone is often seen to simply 'melt away'.* However, too much emphasis must not be placed on these observations as other factors already mentioned earlier in this section, may be involved.

Since 1957 when Fukada and Yasuda (106) postulated that bone was a piezoelectric material, a great deal of research has been carried out to investigate the bioelectric properties of the human tissues. While Shamos and Lavine (107) and Braden et al (108) using small bone and dentine samples agreed that the phenomenon was one of classical piezoelectricity,

* Private communication. Dr. J.T. Scales, Dept. Biomedical Engineering, Institute of Orthopaedics, Stanmore.

Bassett and Becker (109) proposed that bone's inherent electrical characteristics could not be totally explained in terms of this phenomenon. Instead, they proposed that the tissue's electrical response, could best be described in terms of a solid state p-n junction theory. Similarly, other authors have found that this electrical phenomenon is also present in complete biological structures, for instance, Cochran et al (110) in slices of bovine mandible and tooth sections and McElhaney (111) in whole human femora. However, much of the data so far published has been obtained from experiments which have been carried out using de-fatted and/or dried specimen material, Fukada and Yasuda (106), Shamos and Lavine (107), Braden et al (108) and McElhaney (111). Consequently, it is extremely doubtful whether the electrical effects observed by these workers are comparable with the effects which may be present in an in vivo situation.

The conclusions of Braden et al (108) who found no bioelectrical effect in enamel but did so in dentine is extremely interesting. This result backs up the suggestion of Fukada and Yasuda who proposed that it was the collagen fibres in the bone tissue which were responsible for the electrical effects. Consequently, if this is so it is imperative that investigations concerned with the bioelectrical phenomenon must take into account the directions of the collagen fibres in the tissues in relation to the directions of the applied stresses. In fact, Gjelsvik (112 and 113), in two recent publications proposes a piezoelectric model for compact bone which takes into account the 'material direction' from the macroscopic viewpoint. Gjelsvik uses his model to examine the malaligned long bone problem and claims that his model agrees well with clinical observation.

Clearly, the field of bioelectricity in tissues is both an expanding and an exciting development. However, piezoelectricity, or possibly whatever bioelectrical phenomenon is responsible for the bone remodelling mechanism, is dependent upon the strain and consequently stress fields generated in the tissue. Therefore, the understanding of the particular phenomenon involved and all its possible implications may well be governed by the ability of the researcher to determine the stress or strain fields appertaining to the clinical situation. Consequently, it is the aim here using the finite element method, to investigate the mechanical behaviour of the orthodontic and orthopaedic cases previously discussed. The results from these analyses are also compared with the clinical observations in the areas where bone remodelling occurs. This was to see if any of the mechanical responses, i.e. stress, strain or displacement components, correlated with the tissues cellular response of resorption or deposition.

## 9.3 ANALYSIS OF A MALALIGNED LONG BONE SUBJECTED TO A STATICALLY APPLIED LOAD

Many authors have studied either analytically or experimentally the mechanical behaviour of a normal or malaligned long bone subjected to statically applied loads. Koch (114) in 1917 carried out one of the earliest analyses by employing a simple beam type model. He determined the vertical stress distributions on different horizontal planes taken through a normal femur which was loaded as shown in FIG. 9.3. Koch considered the femur to be in the form of a tube and employed simple isotropic mechanical properties for the bone tissue. Fessler (115) on

the other hand, analysed a normal femur using a two-dimensional photoelastic approach. However, in Fessler's model the femoral shaft was assumed to be solid with the whole 'bone' being constructed of the same photoelastic material; no distinction was made between the 'cortical' and 'cancellous' tissues.

Williams and Svensson (116) also employed the photoelastic approach. However, although these authors constructed a three-dimensional frozen stress model, their simulation unrealistically modelled the long bone as a solid structure. Even so, Williams and Svensson did try and take into account the effects of some muscle forces in their analysis. This was achieved by casting 'hair pin' ligament and muscle attachments into the plastic model and by subsequently applying the appropriate forces at these points as determined by Paul (117).

Rybicki et al (118) in their work also allowed for both the femoral head and muscle attachment forces. Like Fessler, these authors carried out their continuum analyses using a two-dimensional plane stress solid homogeneous model. Nevertheless, they concluded from their studies that while the simple beam type approach gave adequate and 'acceptable' results at the mid-shaft of the long bone, the approach was inadequate for the femoral head and neck regions. Consequently, they disagreed with Koch's results in these areas and concluded that a more realistic representation of the internal anisotropy was required. They proposed therefore, that this must be done before the theory that the 'bony trabecula network in the head and neck regions is coincident with the internal stress trajectories' could be verified.

More recently Gjelsvik (112 and 113) also employed a simple beam type analysis technique for a malaligned long bone. Static loads were applied to the model such that the concavity in the malaligned region increased. Epker and Frost (98) also looked at the same problem. Their model femur was similarly loaded as shown in FIG. 9.3, so as to increase the hollow or concavity at the malalignment.

For the work reported here,the main area of interest was in the malaligned region of the femur where bone remodelling is clinically experienced to take place. Consequently, the long bone was considered to consist solely of cortical tissue in this region. The femur was represented by three-dimensional finite elements with cognizance being taken of the collagen fibre or grain orientation. This was achieved by considering the bone to be an orthotropic material. The femur was statically loaded as shown in FIG. 9.3. Hence, the concavity at the malalignment was increased under this regime of loading in the same manner as considered by Gjelsvik and by Epker and Frost.

### 9.3.1 Finite Element Models and Test Procedure

To obtain greater definition in the results of finite element analyses for a particular region in a structure, it is generally necessary to have a finer meshwork of elements in that area. However, as will be shown in Volume Two of this thesis the number of elements that can be employed in any one analysis is governed both by the size, or storage capacity,of the computer employed and also by the amount of computer time available. Three-dimensional structures generally take a very

long time to analyse and so the number of elements should, for economic reasons, be kept to a minimum. Consequently, in order to obtain greater definition in the results of the malaligned region of the femur, illustrated in FIG. 9.3, two separate models were employed.

To reduce the size of the structure into one of managable proportions, the shaft of the femur was assumed to be symmetric both with respect to the malalignment in the horizontal plane and also to the frontal plane, see FIG. 9.4b. The shaft, the shape and size of which was assumed to remain uniform throughout, was considered to consist purely of a tube of cortical bone, FIG. 9.4c.

In the first finite element model the one quarter femur was subdivided into 112 eight-noded three-dimensional elements. The mesh consisted of 14 layers with each layer containing 8 different elements, FIGS, 9.4d and e. Because of the simple uniform shape assumed for the femur, some elements in one layer were identical to the corresponding elements in other layers. This simplification considerably reduced the computational effort required.

The bone 'grain' in the model was assumed to run parallel to the axis of the shaft of the femur. Hence, the orthotropic mechanical properties of cortical bone, derived in Chapter Six, were appropriately employed.

i.e. E (in grain direction) $= 2.0 \times 10^6$ p.s.i.
E (perpendicular to direction of bone grain) $= 1.0 \times 10^6$ p.s.i.
(see sub-section 6.4.1)

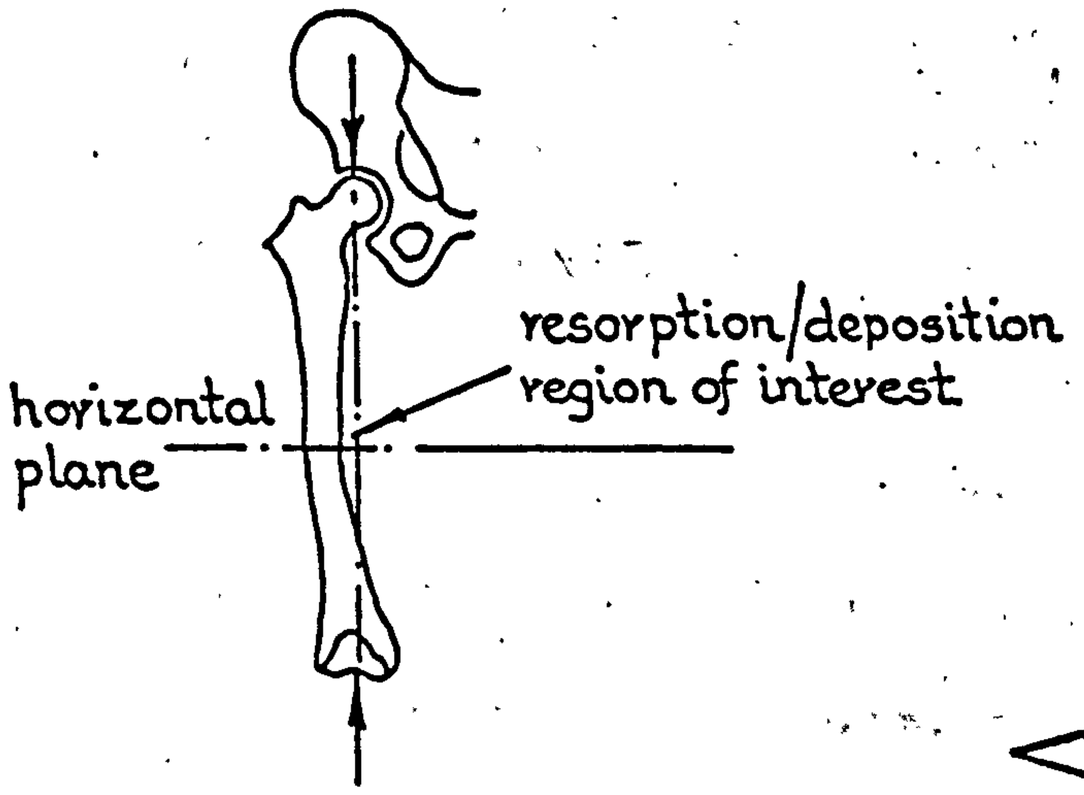


a) Malaligned femur.

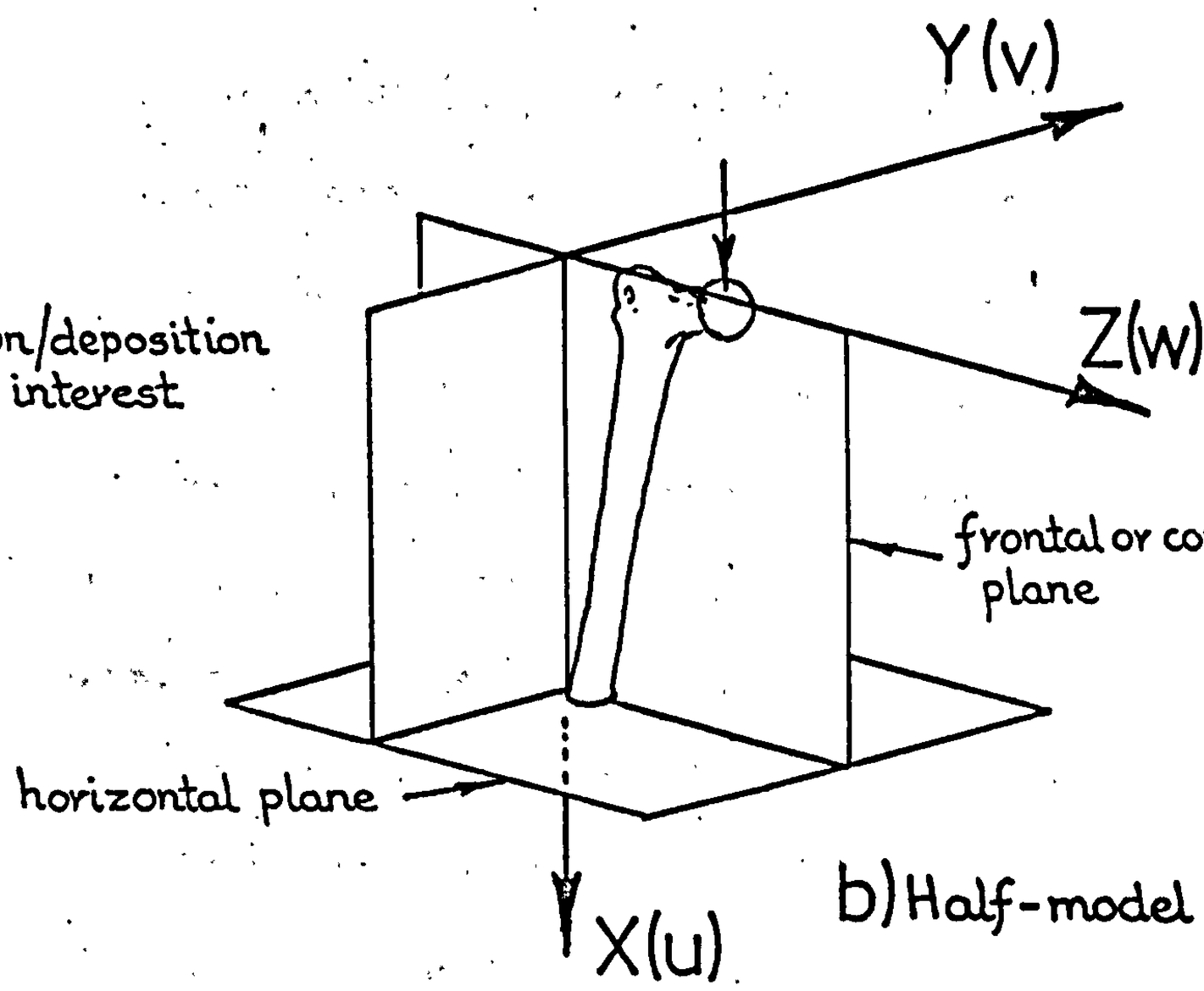


b) Half-model

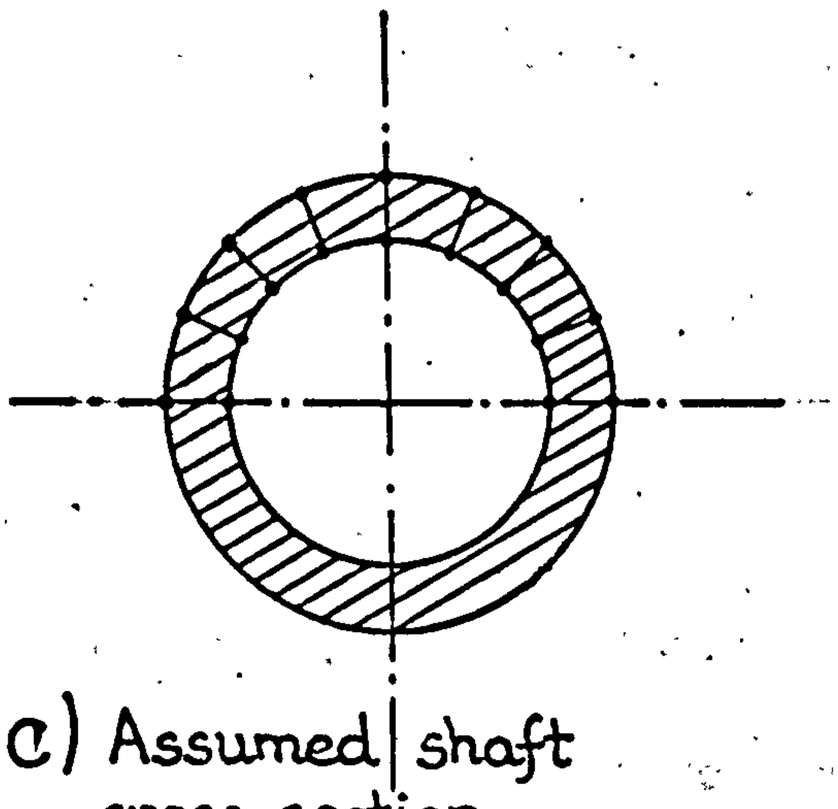

c) Assumed shaft cross-section.

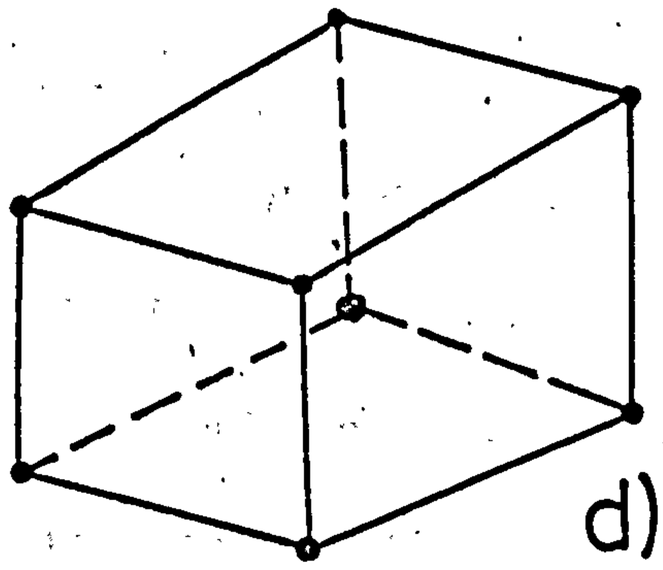

d) Typical 8-noded finite element.

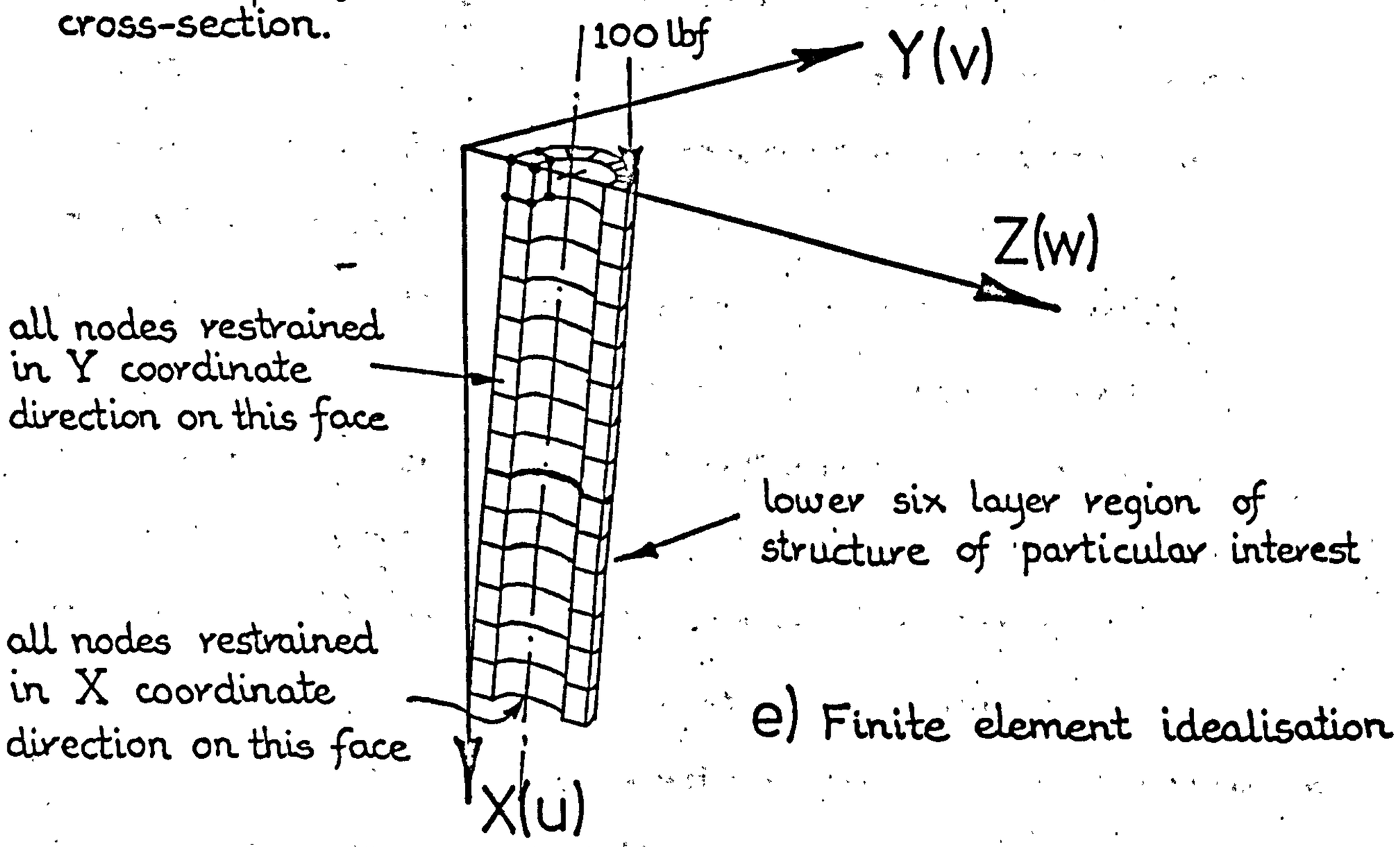


e) Finite element idealisation

FIG. 9.4. One-quarter finite element representation of malaligned femur. Model comprised of 112 eight-noded 3-D finite elements.

The model femur was loaded with a single 100 pound compressive point load (corresponding to a 200 pound load for the whole femur), with the two faces which lie on the planes of symmetry being restrained in the appropriate directions, see FIG. 9.4d. Although the load applied to the model did not possess the same lever arm as the more natural femur type loading shown in FIG. 9.4a,(and therefore did not apply the same level of bending moment), this would not affect the directional sense of the deformation and stress responses.

To increase the definition of the results obtained from the analysis of the rather coarse first finite element simulation, a second more refined model was devised. For this model, the region of the femur containing the malalignment, (corresponding to the lower six layers of elements in the coarse model), was subdivided into sixteen 20-noded finite elements as shown, in FIG. 9.5a. This subdivision, a computer plot of which is illustrated in FIG. 9.5b, consisted of four layers of elements with each layer containing four separate elements. Even though this is a coarser meshwork of elements than the original equivalent eight-noded element subdivision, because the 20-noded element is more 'refined' than its 8-noded counterpart, it is more able to interpret rapidly varying stress fields. (For a detailed explanation of this point, the reader is again referred to Volume Two of this thesis where the theory behind the various finite elements is discussed in detail).

As with the 8-noded element model, the bone 'grain' was assumed to run parallel to the axis of the shaft and the tissue's orthotropic mechanical properties listed in sub-section 6.4.1 employed. Again,the symmetric or mirror image faces were

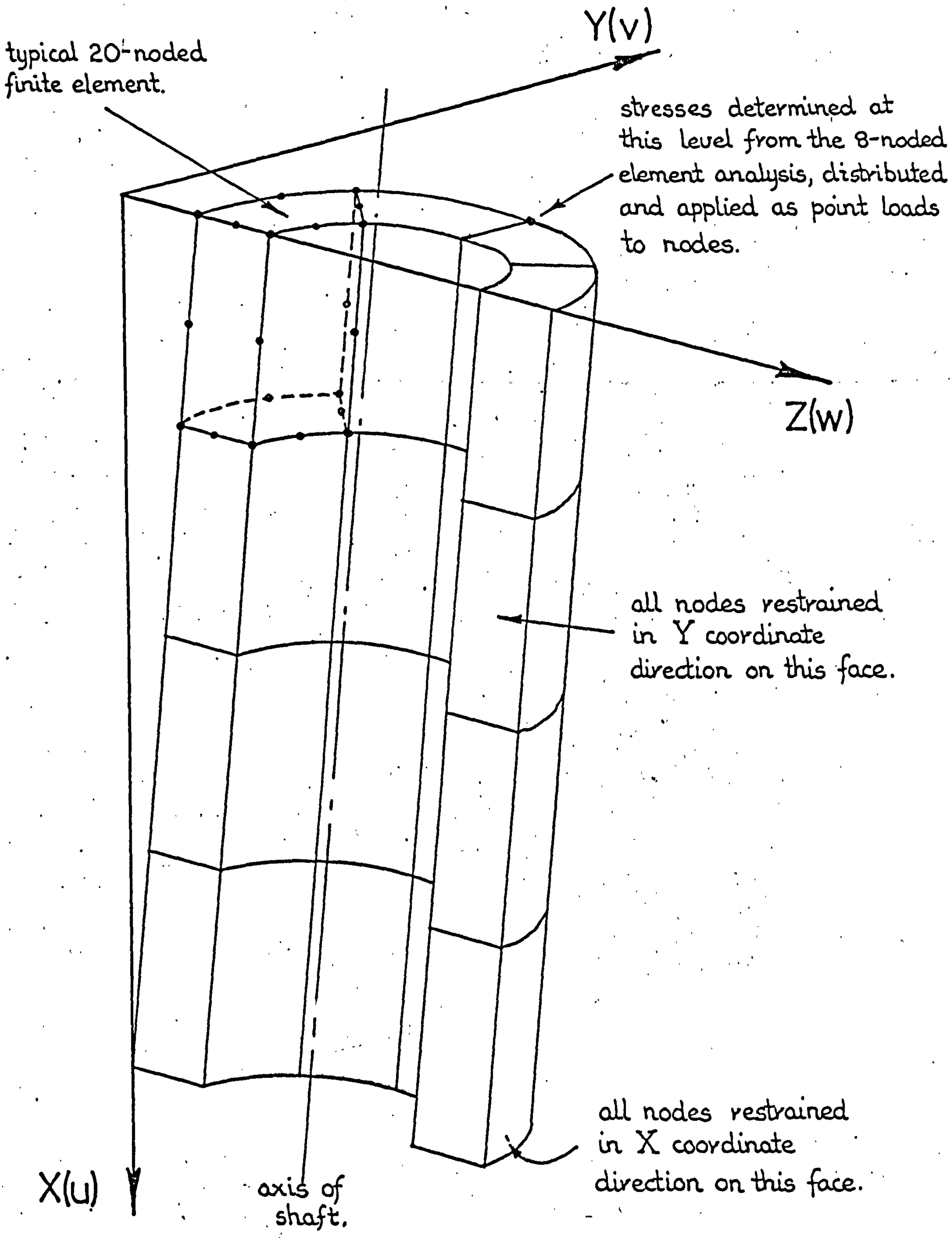


FIG. 9.5a Sixteen 20-noded finite element idealisation of malaligned region of femur. (This corresponds to lower six layers of 8-noded model.)

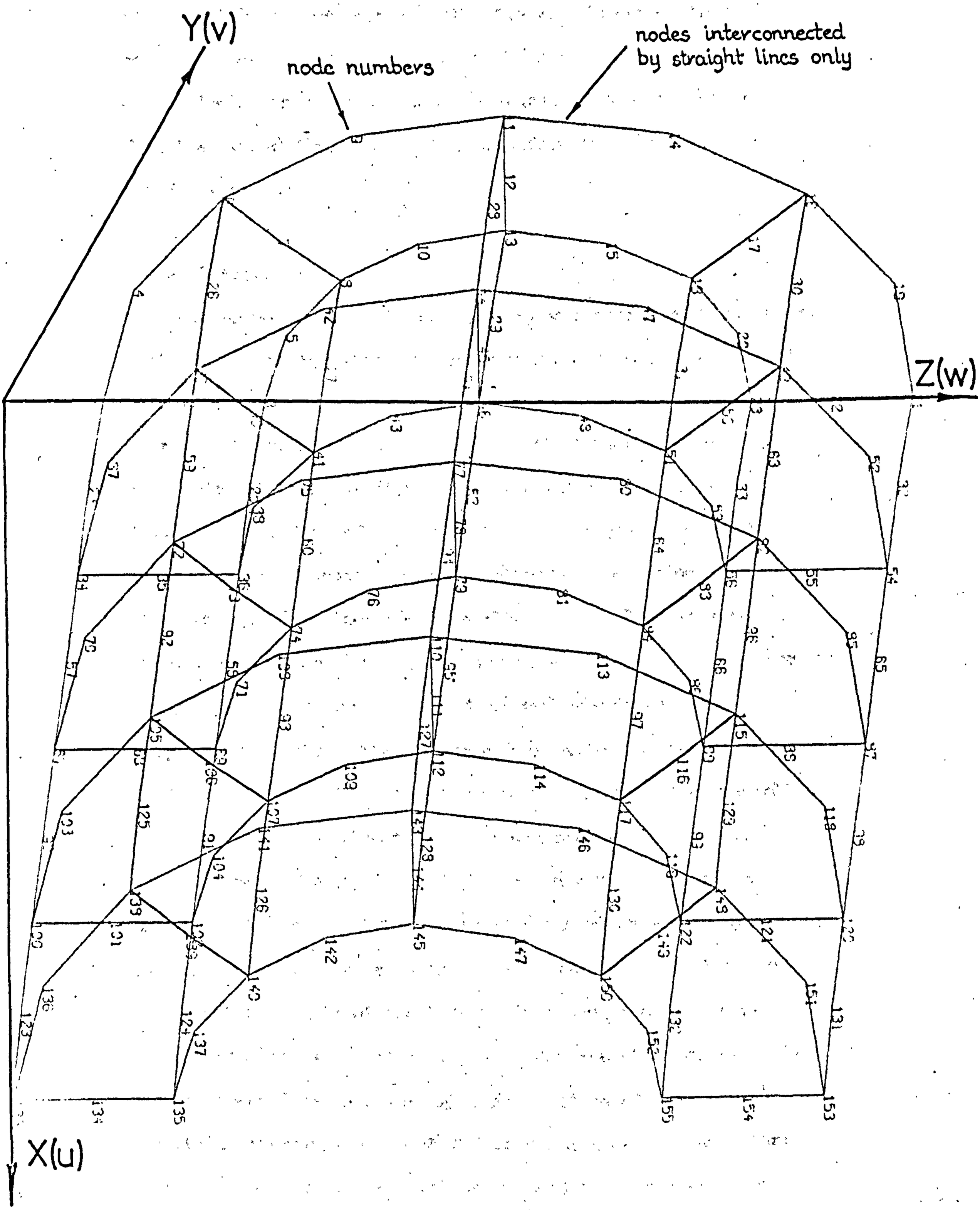


FIG. 9.5b Computer plot of the 3-D idealisation of the lower region of the malaligned femur.
Model comprised of sixteen, 20-noded finite elements.

restrained in the appropriate directions. However, for this model the loading applied to the upper surface of this part of the femur was determined, as outlined in the next sub-section, from the stress distribution obtained from the first 8-noded element analysis.

### 9.3.2 Results

The prime purpose of the first 8-noded finite element coarse analysis was to calculate the stresses acting on the horizontal plane at the sixth element layer of the malaligned femur model, so that the applied nodal loading for the 20-noded element simulation of the bone at this level could be calculated. FIG. 9.6 shows the deflection (drawn to a very much enlarged scale), of the 8-noded element model under the action of the 100 pound vertical load shown in FIG. 9.4d. The deflected structure, obtained by plotting the u, v and w nodal displacements (corresponding to the X, Y and Z co-ordinate directions respectively), shows how the femur bows under the regime of loading imposed. This bowing or bending of the femur resembles the deformation of a beam which is subjected to a bending moment type of loading. FIG. 9.7 which gives the vertical stress distribution of the femur at the sixth element layer level also clearly shows this. The stress pattern shows how the right hand side of the tube is in compression, while the left hand side is in tension. The fact that the neutral axis of the femur (the axis through which a state of zero stress exists), is assymmetric with the cross-section, indicates that the structure is not only subjected to a bending moment but carries also a direct compressive load as well.

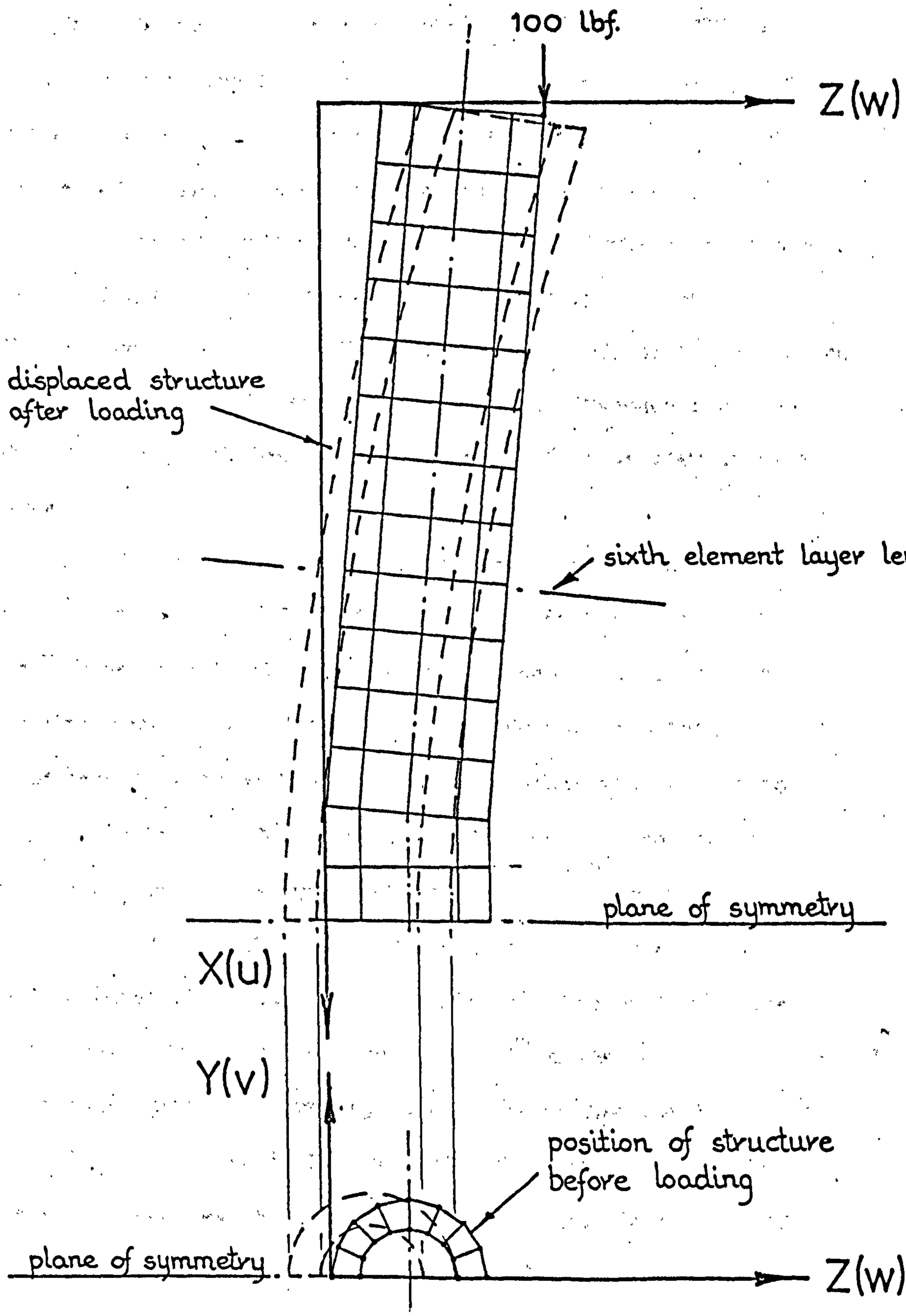


FIG. 9.6 Displaced or deflected 8-noded finite element model of the malaligned femur due to a 100 lbf. static point load.

From the vertical stress distribution shown in FIG. 9.7, the equivalent system of vertical nodal forces, to be applied to the 20-noded finite element model shown in FIG. 9.5, was determined. This was achieved by averaging the vertical stress components of the two 8-noded elements which corresponded to the single 20-noded replacement element in the second finite element model, see FIG. 9.8a and b. Using these average stress values and the surface areas of the 20-noded elements, the total vertical load applied to each of these elements was computed.

The distribution of the total element force amongst the eight surface nodes of the 20-noded element has to obey the principles of solid body mechanics and cannot be carried out by simply uniformly distributing or 'lumping' the total load equally between the eight nodes. That this is not so can easily be seen from studying FIG. 9.8c. Here, some of the loads seem to be wrong but they do in fact represent a 'consistent' equivalent system of loads. For the derivation and explanation of this load distribution the reader is again referred to Volume Two of the thesis where the topic is considered in greater depth. However, it must be pointed out here that the signs of the equivalent set of nodal forces so derived have all been reversed, see FIG. 9.8c. This is because of the co-ordinate system employed for the finite element model. Normally, it is assumed that a positive applied force produces a positive or tensile stress. However, for the 20-noded model it is a negatively applied force which is required to produce a positive or tensile stress.

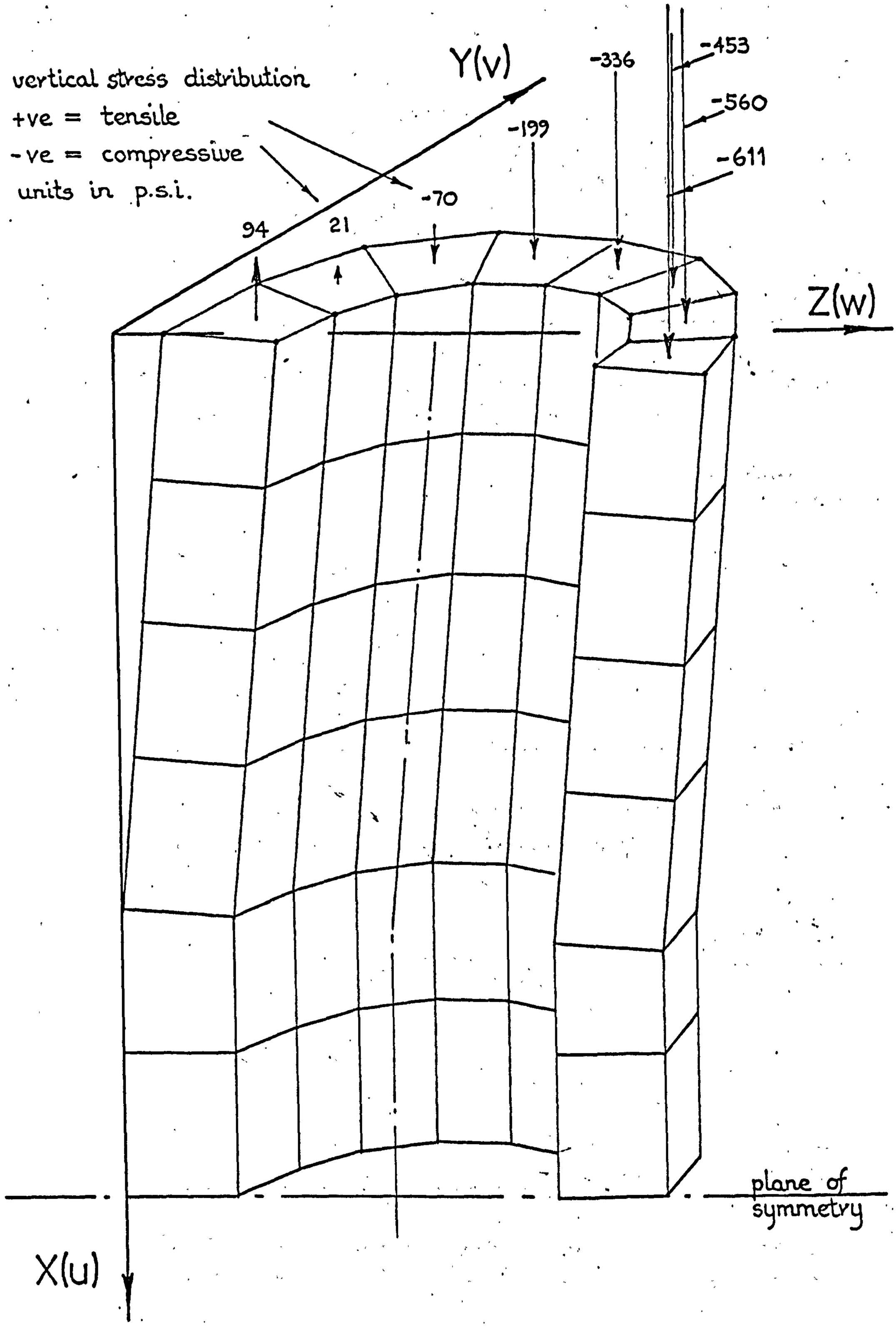


FIG. 9.7 Vertical stress distribution in the 8-noded finite element model of the malaligned femur at the sixth element layer level.

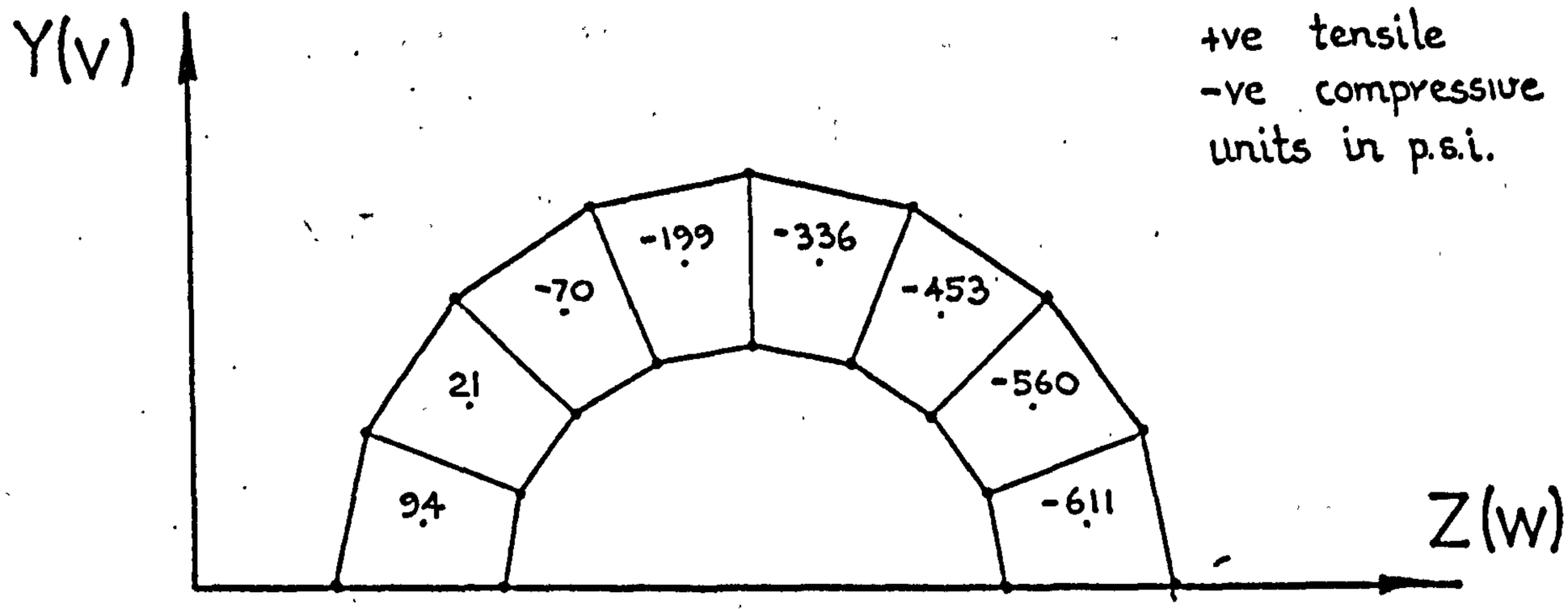


a) Vertical stress distribution from the 8-noded finite element model at the sixth element layer.

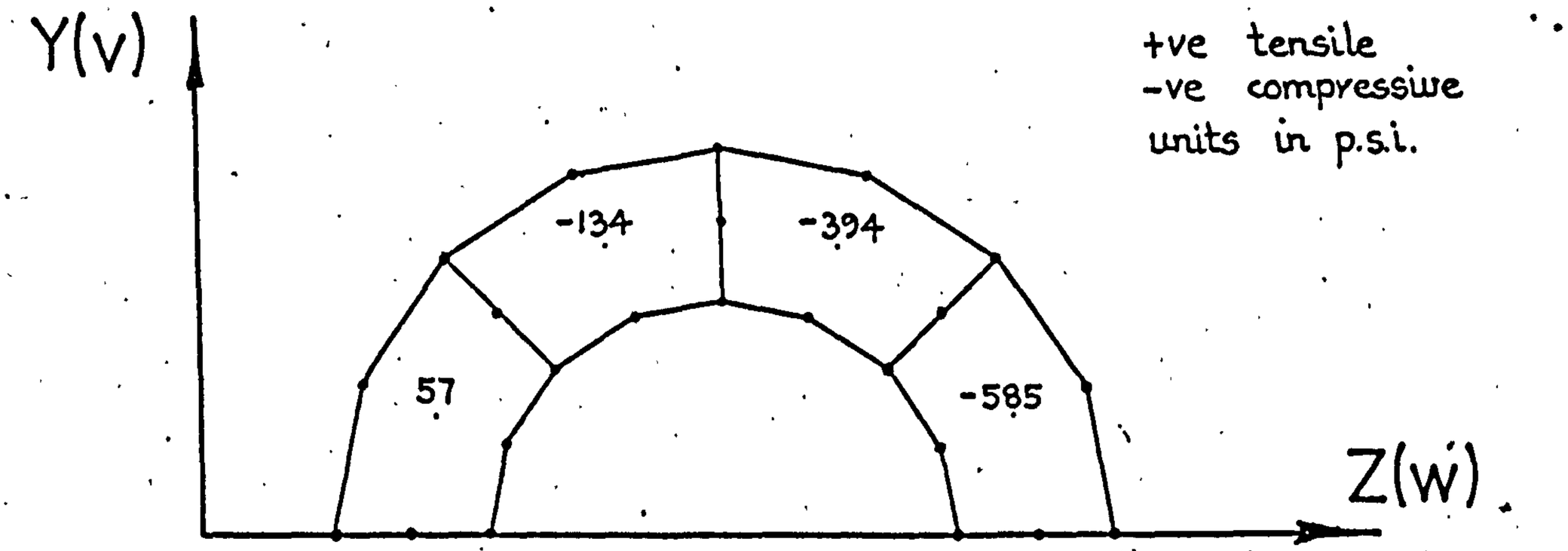


b) Eqivalent vertical stress distribution derived for the 20-noded finite element model.

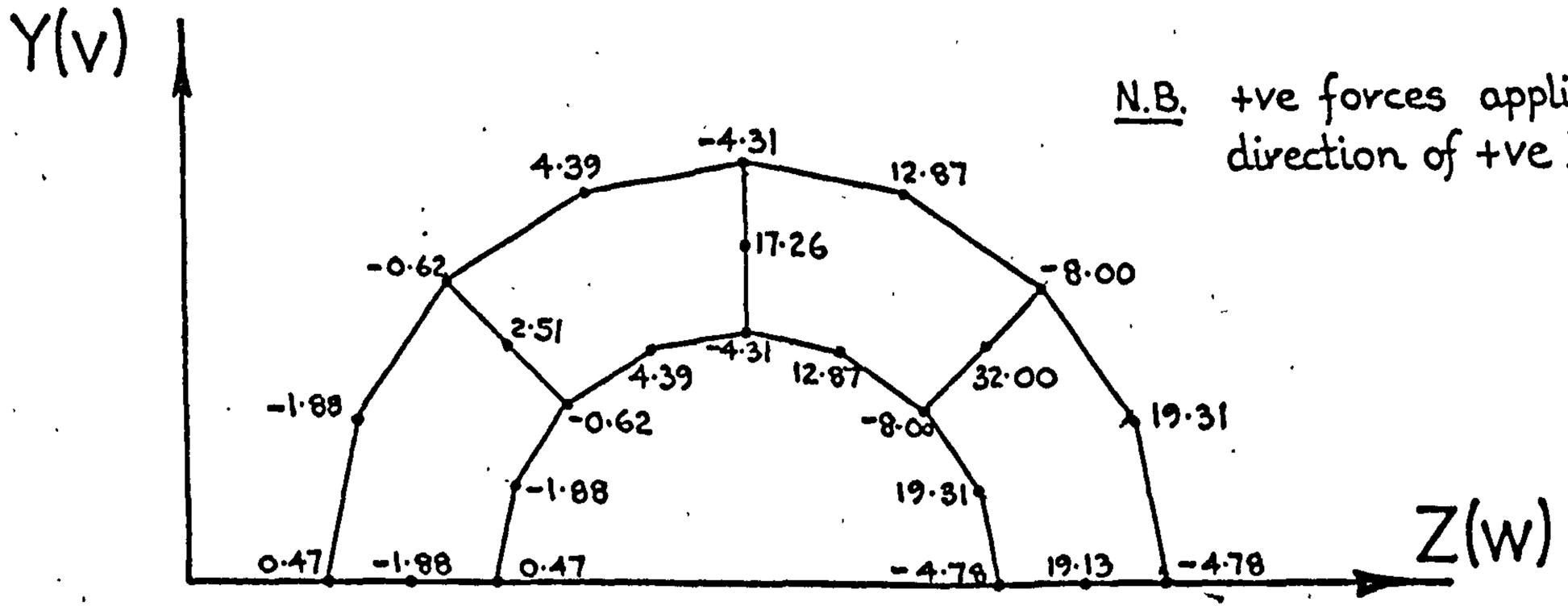


c) 'Consistent' set of vertical nodal forces derived for the 20-noded finite element model from b). above.

FIG. 9.8 Derivation of the equivalent or 'consistent' set of nodal forces for the 20-noded model from the stress distribution obtained from the 8-noded analysis.

If the loads shown in FIG. 9.8c are summed, they add up to a total net applied load of +103.56 lbf. Consequently, as the originally applied load to the 8-noded finite element model was +100.0 lbf, vertical equilibrium (which should exist at each and every horizontal plane in the femur), has approximately been maintained at this section. It must be remembered however, that only the vertical stress components obtained from the 8-noded element model analysis were employed to determine the equivalent set of vertical loads for the 20-noded element model. Theoretically, all the stress components acting on the upper surface of the sixth element layer should have been included in the determination of the equivalent nodal force system. However, because all the other components were very small in comparison with the vertical stresses these were ignored in the analysis here.

Using the vertical load distribution shown in FIG. 9.8c, the stress, strain and displacement distributions were determined for the 20-noded finite element idealisation in the critical regions of the periosteal and endosteal surfaces of the malaligned femur. FIG. 9.9a shows the vertical stress distribution in the critical areas of the malalignment and FIG. 9.9b, the corresponding hoop stress distribution. The radial stress components, while being obviously zero at the periosteal and endosteal surfaces, were found to be very small indeed throughout the entire thickness of the cortex. Hence, these have not been plotted. On the other hand, FIGS. 9.10a and b show the corresponding vertical and hoop strain components respectively for the same positions in the femur. Whereas the radial stresses were zero at the periosteal and endosteal

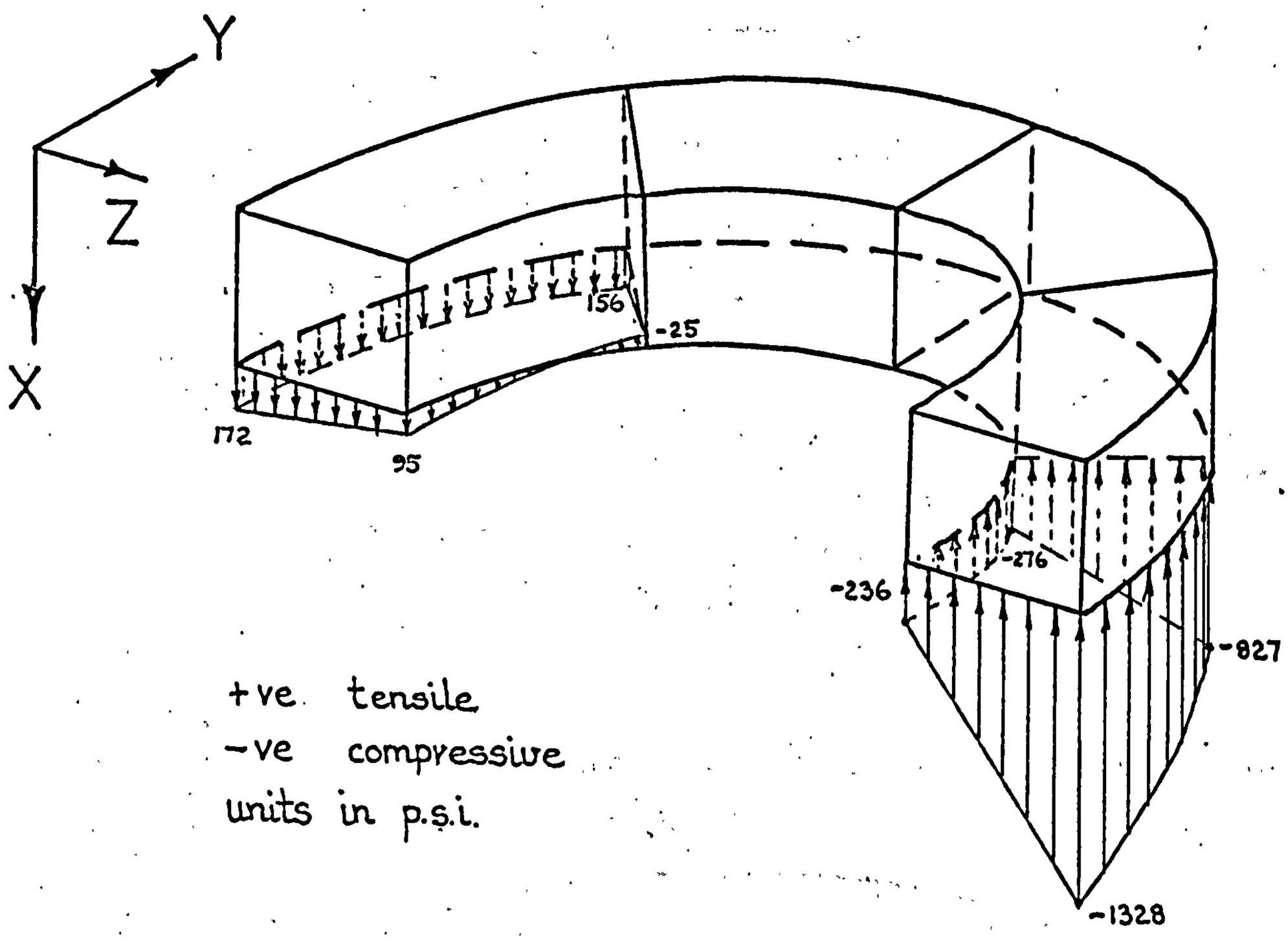


a) Vertical stress distribution ($\sigma_{xx}$) on horizontal plane of symmetry in critical areas.

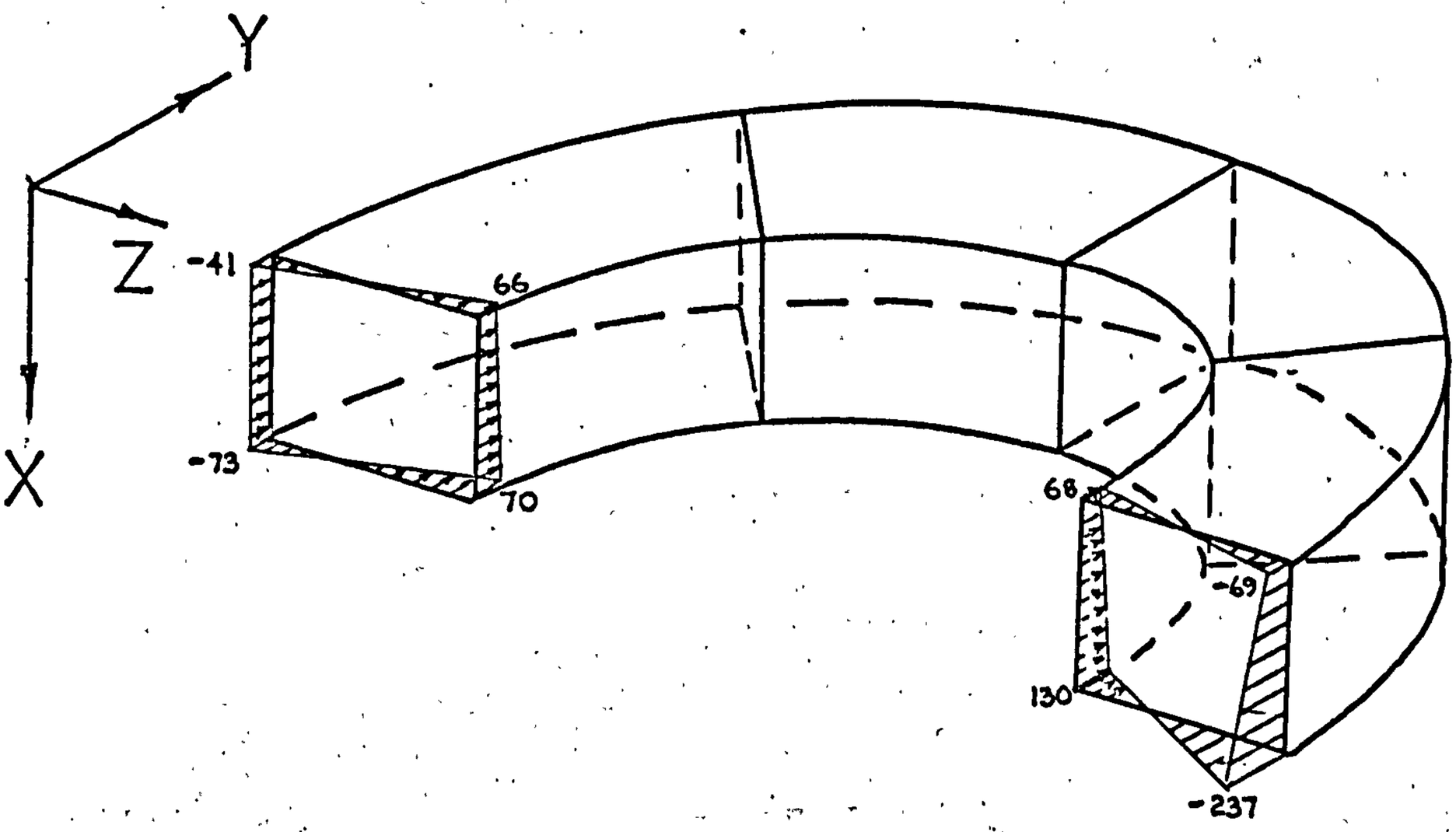


b) Hoop stress distribution ($\sigma_{yy}$) on frontal plane of symmetry in critical areas.

FIG. 9.9 Vertical and hoop stress distributions in critical areas of malaligned femur.

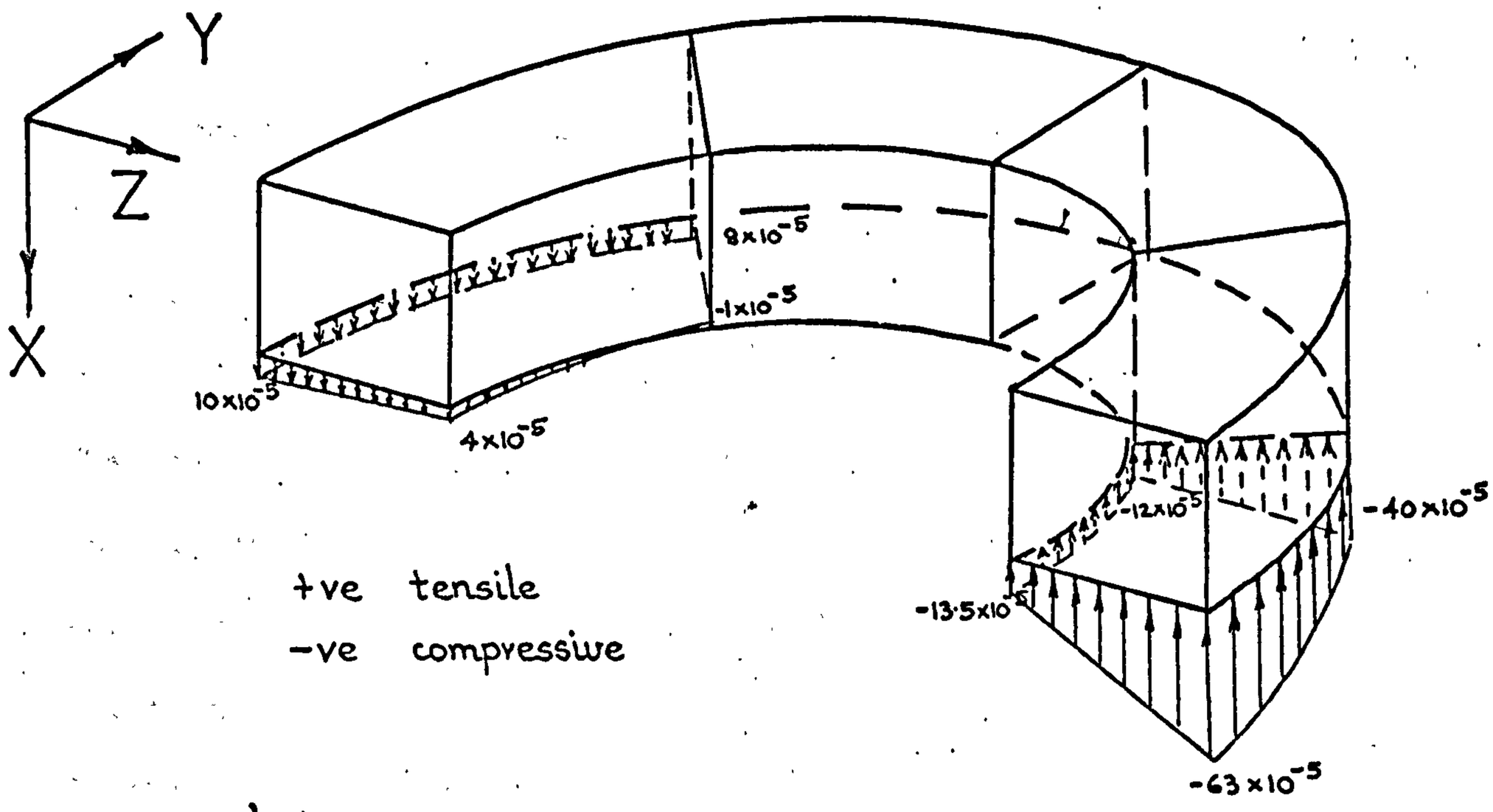


a) Vertical strain distribution ($\epsilon_{xxc}$) on horizontal plane of symmetry in critical areas.

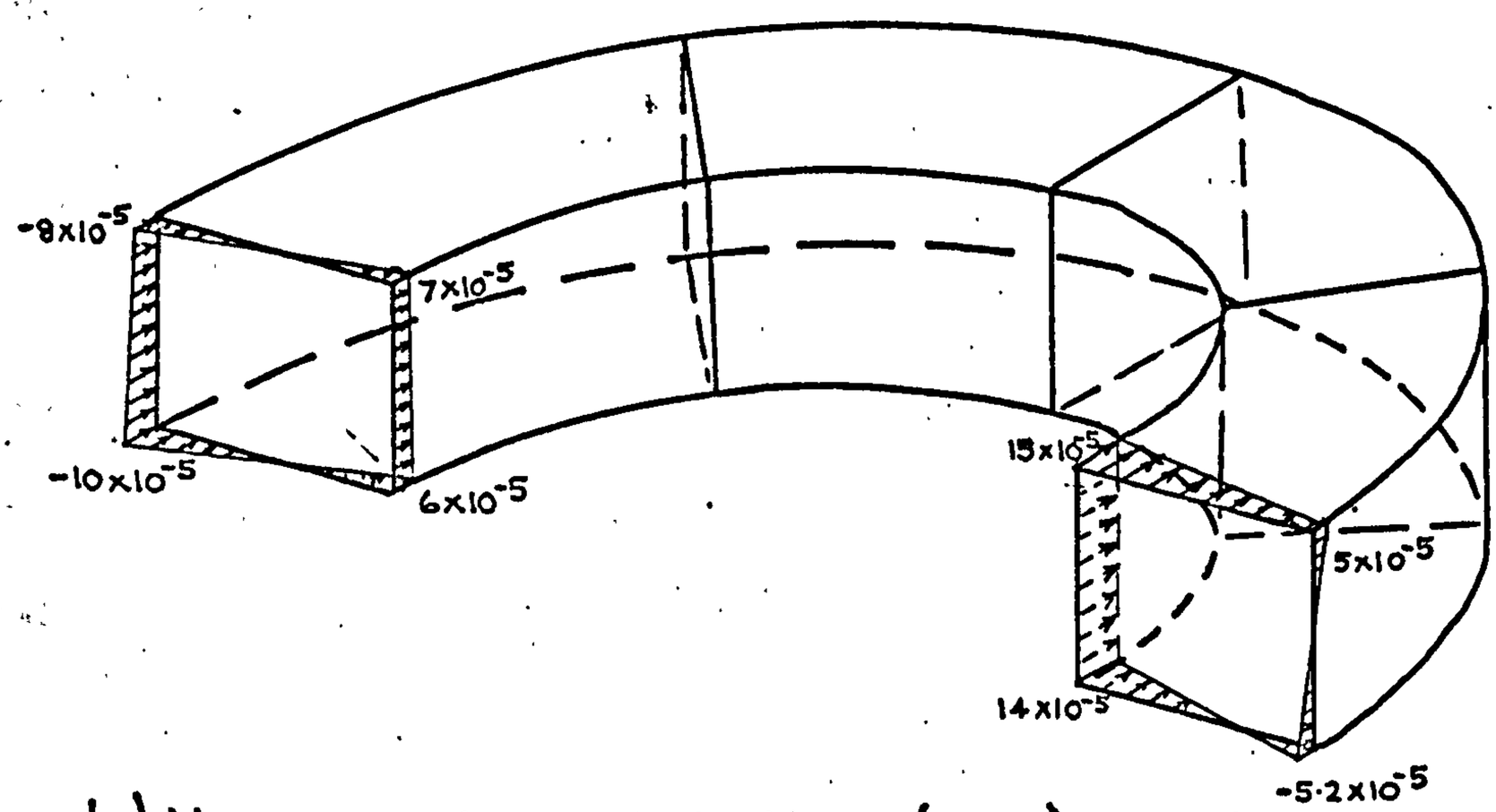


b) Hoop strain distribution ($\epsilon_{yy}$) on frontal plane of symmetry in critical areas.

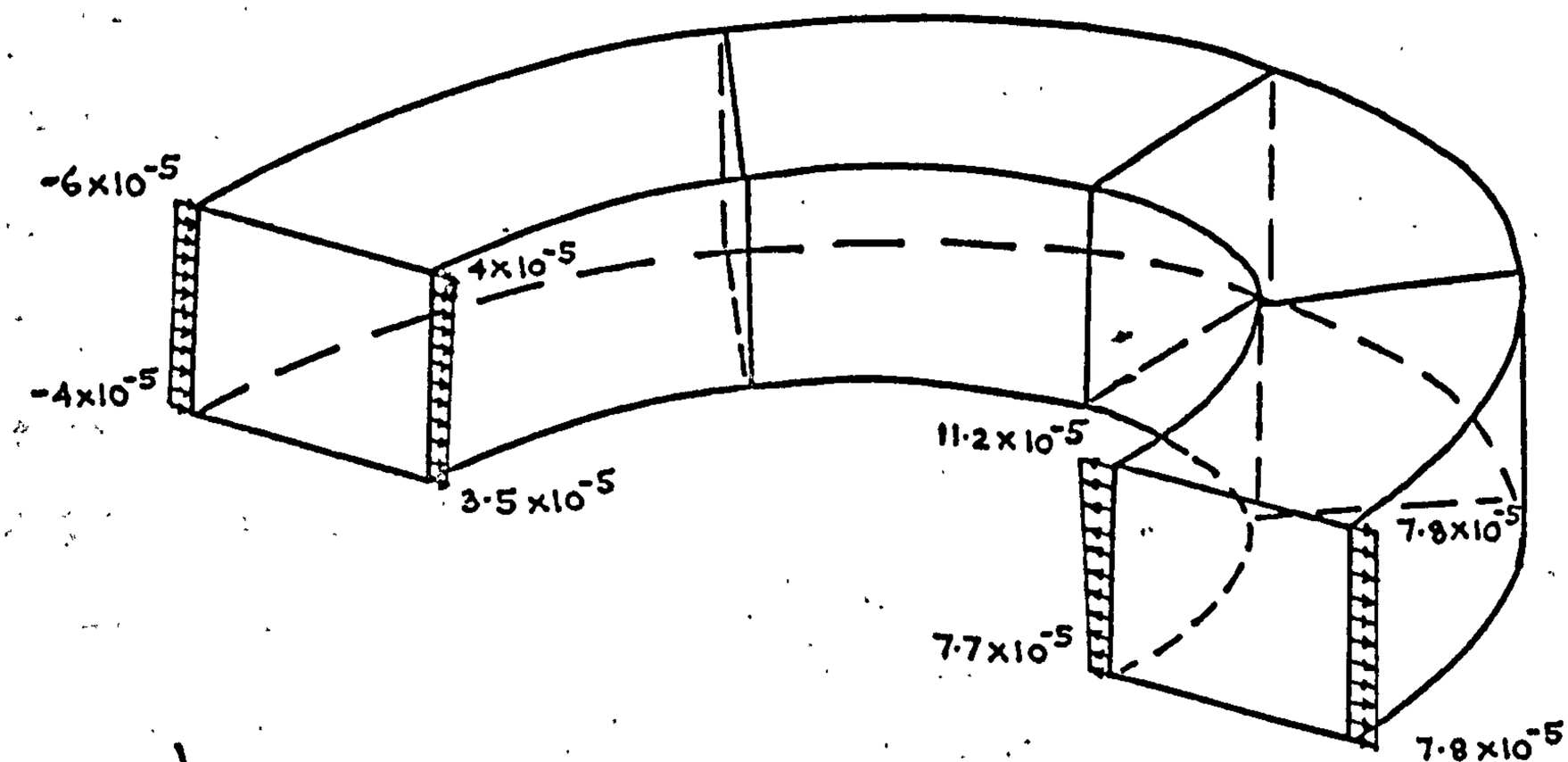


c) Radial strain distribution ($\epsilon_{zz}$) on periosteal and endosteal surfaces on frontal plane of symmetry.

FIG. 9.10 Strain distributions in critical areas of malaligned femur.

surfaces, the corresponding radial strains are not necessarily zero too. This is because of the Poisson's ratio effect of the material. In fact, for this problem, the radial strains were indeed significant and are plotted in FIG. 9.10c. The distortion of the femur under the vertical type loading is illustrated in FIG. 9.11. Here the displacements of the nodes lying on the vertical and horizontal planes of symmetry are plotted to a very much enlarged scale. Consequently, by comparing the new or displaced positions of these nodes with their original positions, the change in the curvature of the periosteal and endosteal surfaces of the femur in the critical areas of the malalignment in both these planes were determined.

For convenience, all the results obtained from the analysis and relating to the critical areas of the malalignment of the femur where bone resorption and deposition is clinically observed to take place, are displayed in FIG. 9.12.

### 9.3.3 Discussion of Results

The results displayed in FIG. 9.12 show the mechanical response of a femur which, having healed in a malaligned or bowed form, is subjected to a statically applied compressive load. This loading, which is intended to simulate the loading on the femur during part of the walking cycle, was applied so as to increase the bow or concavity in the malaligned region, see FIGS. 9.3 and 9.4. Hence, it was presumed at the outset that it was this compressive type loading, generated during locomotion, which was responsible for invoking the cellular response of the

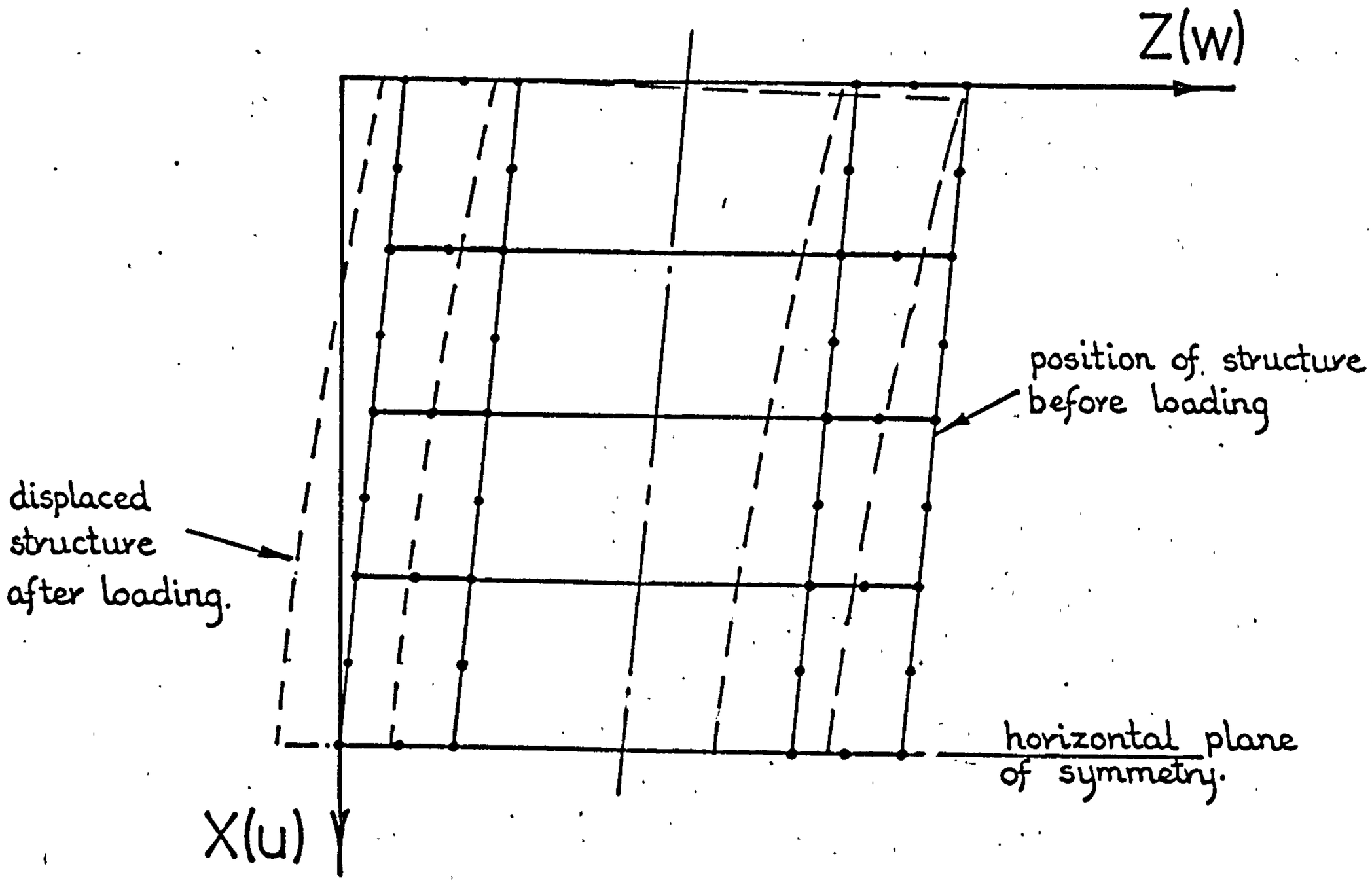


a) Displacement distribution on frontal plane of symmetry.

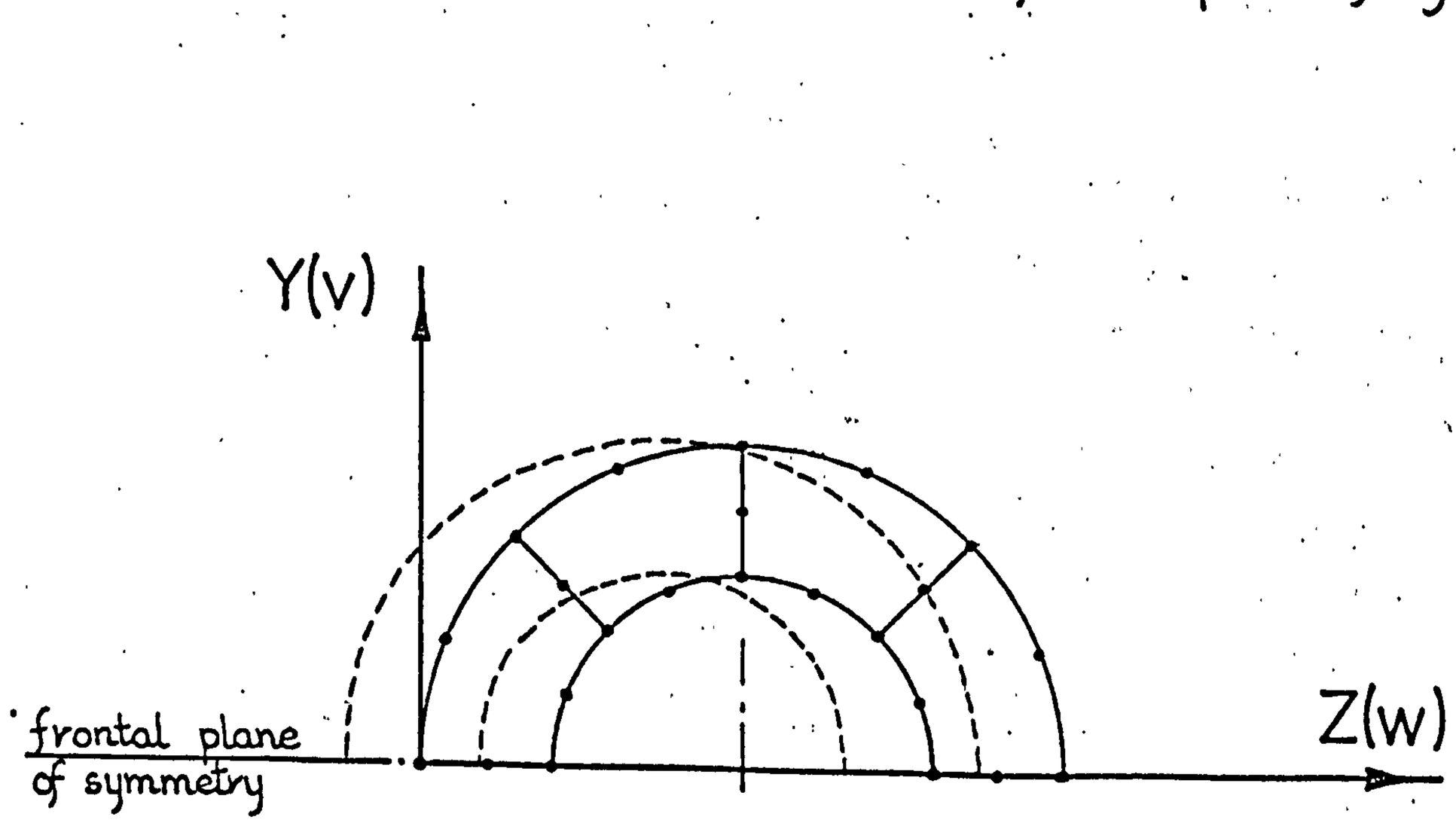


b) Displacement distribution on horizontal plane of symmetry.

FIG. 9.11 Displacement or distortion of the periosteal and endosteal surfaces of the malaligned femur.

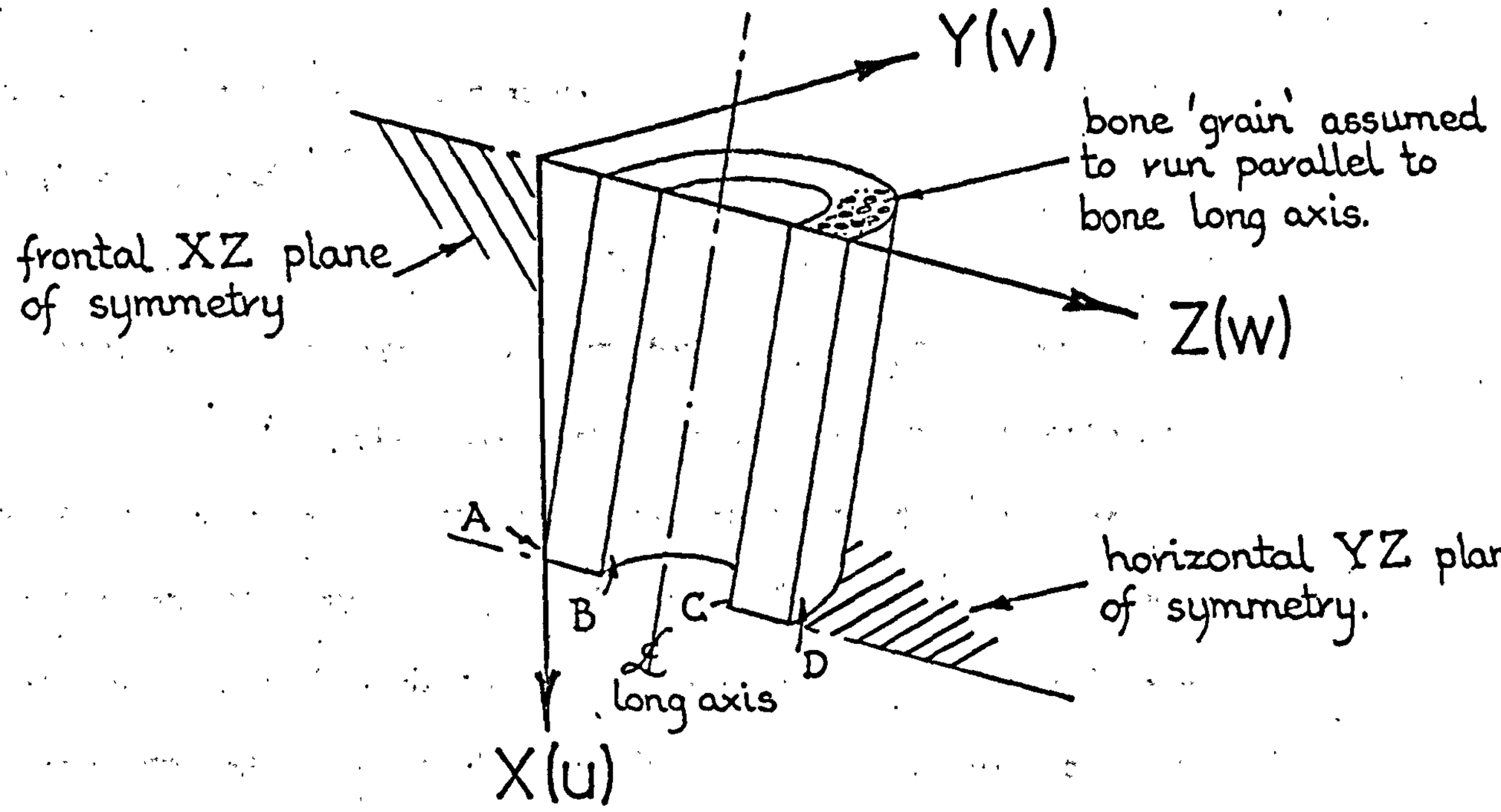


| | PERIOSTEAL A | ENDOSTEAL B | ENDOSTEAL C | PERIOSTEAL D |
|---|---|---|---|---|
| $\sigma_{xx}$ - vertical stress - in direction of bone 'grain'. | Tensile. | Tensile | Compress. | Compress. |
| $\sigma_{yy}$ - hoop stress - tangential to bone 'grain' | Compress. | Tensile | Tensile | Compress. |
| $\sigma_{zz}$ - radial stress - normal to bone 'grain' | Zero | Zero | Zero | Zero |
| $\epsilon_{xx}$ - vertical strain - in direction of bone 'grain' | Tensile | Tensile | Compress. | Compress. |
| $\epsilon_{yy}$ - hoop strain - tangential to bone 'grain' | Compress. | Tensile | Tensile | Very small Com. or Ten? |
| $\epsilon_{zz}$ - radial strain - normal to bone 'grain' | Compress. | Tensile | Tensile | Tensile |
| Change in surface curvature in frontal XZ plane | $\overrightarrow{\text{Convex}}$ | $\overrightarrow{\text{Concave}}$ | $\overrightarrow{\text{Convex}}$ | $\overrightarrow{\text{Concave}}$ |
| Change in surface curvature in horizontal YZ plane. | $\overrightarrow{\text{Concave}}$ | $\overrightarrow{\text{Convex}}$ | $\overrightarrow{\text{Convex}}$ | $\overrightarrow{\text{Concave}}$. |
| Clinically observed Remodelling response | Resorption | Deposition | Resorption | Deposition |

N.B. $\overrightarrow{\text{Concave}}$ ≡ surface becoming more concave

FIG. 9.12 Qualitative results obtained from the finite element analyses of the malaligned femur.

bone and surrounding tissues and for regulating the bone resorption and deposition process.

From a study of FIG. 9.12,it can be seen that when the mechanical behaviour is broken down into separate qualitative component responses, only one type of response correlates with the clinically observed bone response on both the periosteal and endosteal surfaces. This mechanical response was the change in the surface curvature of the bone in the direction parallel to the femur's long axis. For the finite element model employed here,this direction also coincided with that of the assumed bone grain. Therefore, these results indicate that the malaligned femur might well respond to an increasing concavity on the periosteal and endosteal surfaces with bone deposition and on the surfaces which tend to become more convex with bone resorption. This conclusion agrees exactly with the thecry proposed by Epker and Frost (98).

If only the periosteal surfaces are considered, four separate mechanical response components were found to correlate. In addition to the curvature already discussed, both the stress and strain components in the direction of the bone grain and the radial strain component, all correlated with the biological response. For the mechanical components in the direction of the bone grain, represented by $\sigma_{xx}$ and $\varepsilon_{xx}$ in FIG. 9.12, tensile stresses and strains both corresponded to areas of bone resorption whereas compressive stresses and strains corresponded to regions of bone deposition. However, for the case of the radial strain component,the nature of the correlation was

found to be reversed. In this case, compressive radial strains were found to correspond to bone resorption and tensile radial strains to bone deposition.

It is apparent from FIG.9.12 that if both the periosteal and endosteal bone surfaces are considered then Bassett's theory, as Currey suggested, does not hold. However, if only the periosteal bone surfaces are considered then indeed the compressive stress $\sigma_{xx}$ on face D and the corresponding tensile stress $\sigma_{xx}$ on face A do in fact correlate with the bone deposition and resorption responses respectively. On the other hand, if again both periosteal and endosteal surfaces are considered and the femur is assumed to be loaded in net compression, then it can be seen from FIGS. 9.9a and 9.12 that Currey's theory (if this case coincides with Currey's understanding of the term "net compression") like that of Epker and Frost, predicts the bone's remodelling response in the form generally assumed.

## 9.4 ANALYSIS OF A MAXILLARY CENTRAL INCISOR SUBJECTED TO A STATICALLY APPLIED ORTHODONTIC LOAD

Bone resorption and deposition in tooth supporting structures undergoing orthodontic treatment has been discussed and investigated by numerous research workers. Even so, no comparative analyses, whether experimental or otherwise, have been conducted into the stress and strain response of orthodontic problems as has been carried out for the case of the long bone.

Although Epker and Frost (98) considered the stress and strain systems which they believed to occur in the socket wall, the model upon which they based their discussion exhibits a very poor simulation of the tooth - periodontal membrane - alveolar bone combination. In particular, their analogue representing the cancellous tissue supporting the lamina dura was very dubious indeed. Consequently, their conclusions must be viwed with a great deal of scepticism. Epker and Frost's work also contained a very serious theoretically based error. They assumed in their discussion that tensile and compressive stresses gave rise to tensile and compressive strains respectively. This of course is not necessarily true. The type of strains induced depends upon the structural geometry and the mechanical properties of the materials, in particular on the value of the Poisson's ratio.

In most cases, the work carried out on this problem has in general been confined to determining the stresses occurring in the periodontal membrane. Consequently, these studies have been primarily concerned with 'externally' applied stresses to the surfaces of the lamina dura rather than with the 'internal' stresses actually induced in the alveolar bone itself, Baumrind (99), Storey (119), Reitan (100, 101, 102 and 103) and Edwards (120). However, for the work reported herein, finite element analyses were carried out on 'complete' dental structures in which the teeth were subjected to statically applied orthodontic forces. Therefore, an attempt was made to determine the displacement behaviour of the entire structure as well as the 'internal' stress and strain responses of the alveolar processes. For the finite element models, the teeth, periodontal membrane and supporting alveolar bone were simulated more realistically with cognizance being taken where possible, of the differences between the areas of cancellous and cortical bone. The anisotropy of the cortical bone was also taken into consideration in the models. This was simulated as an orthotropic material.

### 9.4.1 Finite Element Models and Test Procedure

In order to investigate possible correlations between mechanical behaviour and bone resorption and deposition in tooth supporting structures undergoing orthodontic treatment, two-dimensional models were considered to be inadequate. Consequently, to obtain a more realistic picture of the displacement, stress and strain fields in the areas of the alveolar bone

where remodelling is clinically observed to take place, three-dimensional finite element models were employed. However, because of the limited storage capacity of the computer available, it was found necessary to develop two separate three-dimensional models.

The first of the three-dimensional models employed for this work was the same as the idealisation which was used in previous analyses, see FIG. 6.15. To reduce the computational effort required, the structure was considered to be symmetrical about the sagittal plane passing through the tooth's long axis. Even then, in order to reduce the size of the structure into one of managable proportion, it was found necessary to assume that the alveolar processes consisted solely of cortical bone. However, the cortical tissue was modelled as an orthotropic material with the principal grain directions being taken as indicated in FIG. 8.3. The mechanical properties ascribed to the cortical bone were as listed in sub-section 6.4.1. On the other hand, the periodontal membrane was assumed to be isotropic and was therefore ascribed the corresponding transverse or lateral type loading mechanical properties derived in chapter six. While the external nodes in the deeper regions of the cortical tissue were constrained in all three coordinate directions, all the other nodes lying on the plane of symmetry were constrained in the Z direction only. Also, because of the 'mirror image' symmetry assumed, only half of the orthodontic force was applied to the model, see FIG. 6.15.

Because of the small number of elements contained in the three-dimensional finite element model shown in FIG. 6.15, and consequently the large spacing resulting between the nodal points, the changes in the curvatures of the periosteal surfaces were difficult to determine. Hence, a second less refined or pseudo three-dimensional model was developed. This consisted of a slice type model, similar in form to the two-dimensional models discussed earlier, but in this case the elements employed were the 20-noded variety, see FIG. 9.14. Even though this model does not accurately simulate the actual dental structure, it was anticipated to give slightly superior results than would be obtained from a similar model which consisted only of two-dimensional elements. Although the slice or pseudo three-dimensional model contained practically the same number of elements as did the three-dimensional model, (16 as opposed to 20), it had the advantage that the nodal points were very much closer together, see FIG. 9.15. As for the three-dimensional model proper, the slice type model was assumed to be symmetric about a sagittal plane passing through the long axis of the tooth and the alveolar processes assumed to consist entirely of cortical bone. Again, the periodontal membrane was ascribed the transverse type loading isotropic mechanical properties determined in chapter six and the cortical bone, the orthotropic properties given in sub-section 6.4.1. However, the principal bone grain directions in the alveolar processes have not been clearly identified in the literature. Consequently, two distinctly different grain orientations were devised. The first, indicated in FIG. 9.14a, assumed the grain to flow approximately parallel to the periosteal surfaces whereas

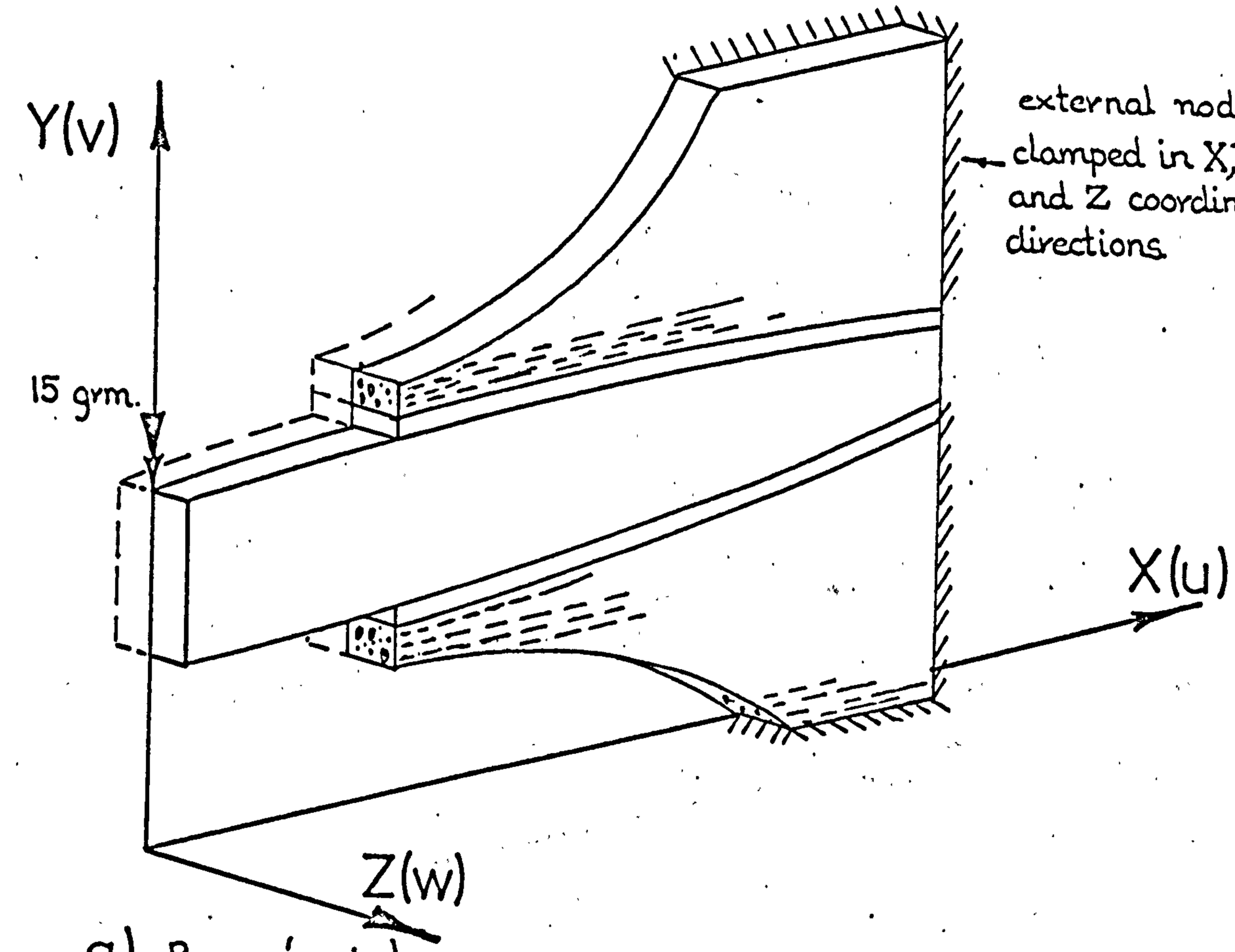


a) Bone 'grain' assumed to run parallel to X coordinate axis.

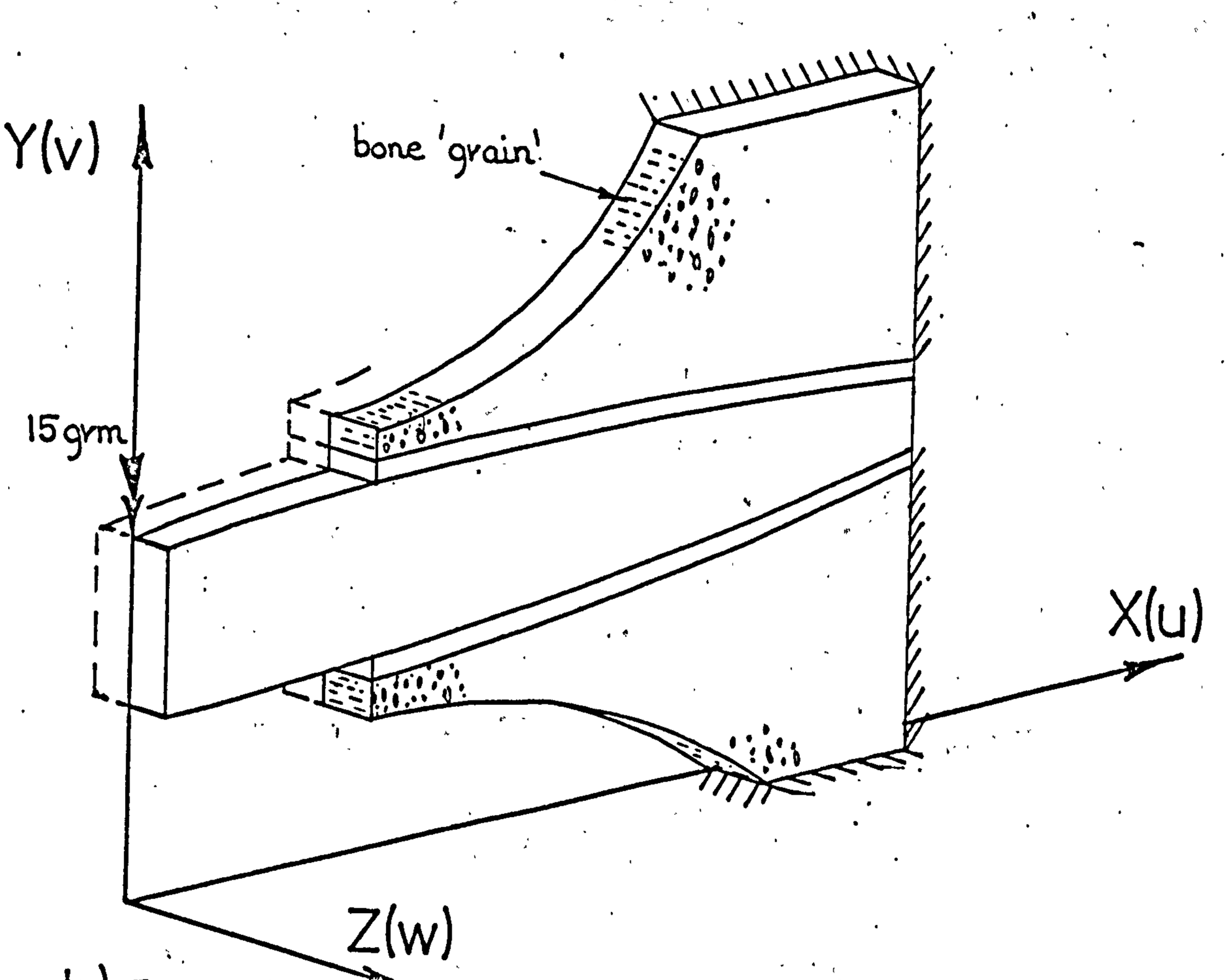


b) Bone 'grain' assumed to run parallel to Z coordinate axis.

FIG. 9.14 Pseudo 3-D models of maxillary central incisor consisting of sixteen 20-noded elements.

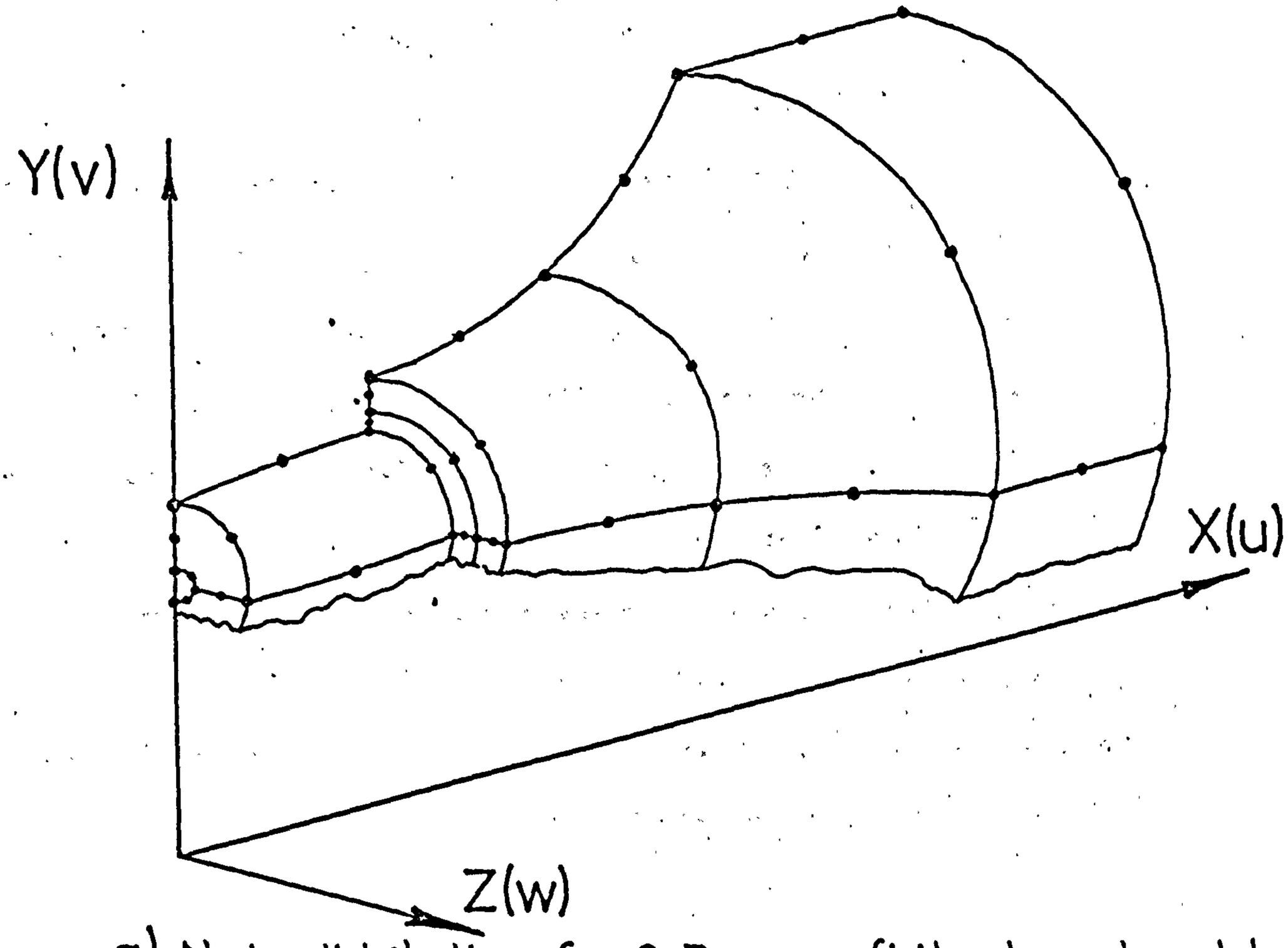


a) Node distribution for 3-D proper finite element model.

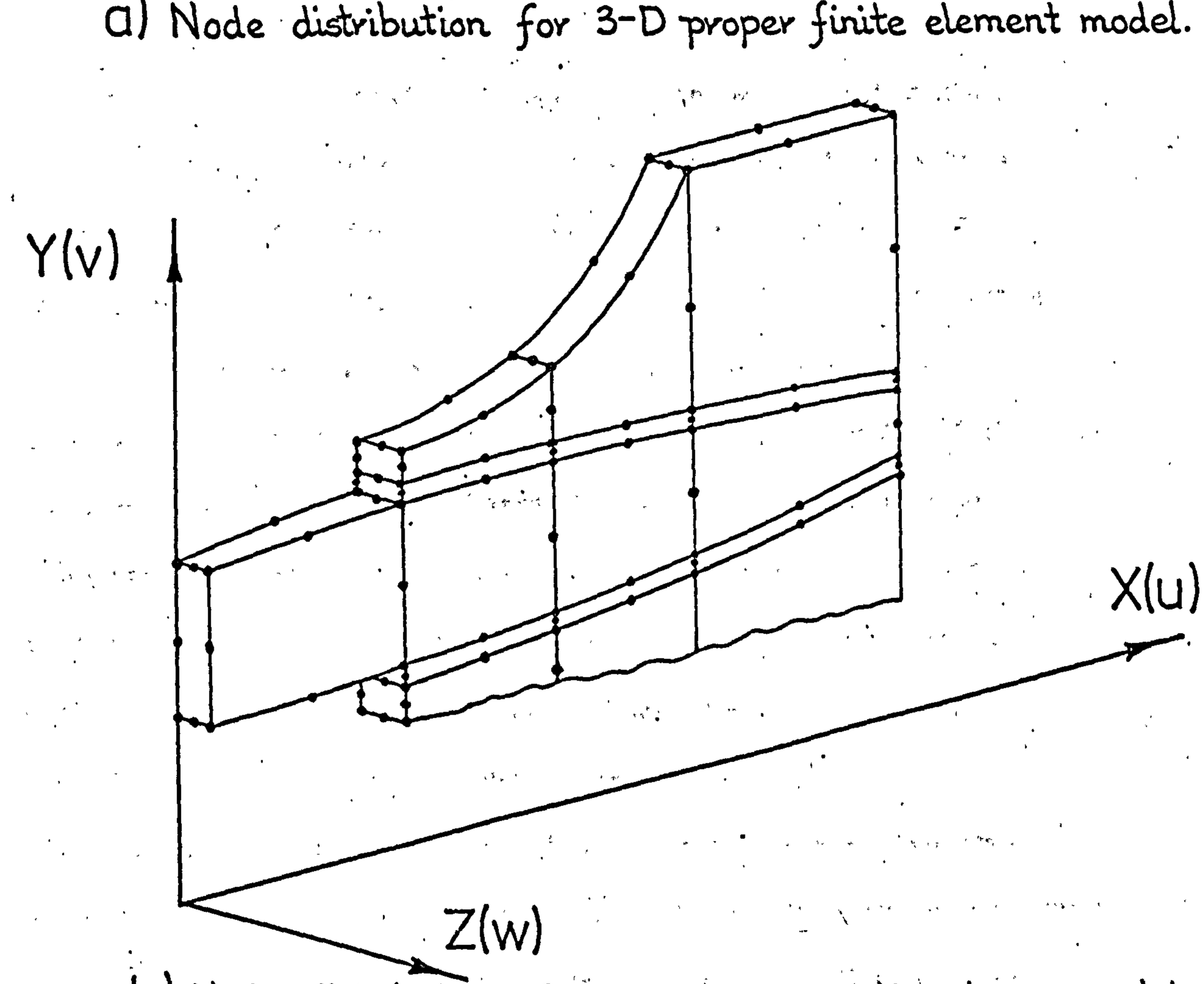


b) Node distribution for pseudo 3-D slice type model.

FIG. 9.15 Comparison of the node distributions for the 3-D finite element models of the maxillary central incisor.

the second arrangement, assumes the grain direction to be at right angles to the plane of the model, FIG. 9.14b. The former configuration, indicated by Tappen (121) who worked on monkey skulls using the split-line technique, probably gives the more realistic simulation. Even so, the grain of actual alveolar bone probably follows a gnarled and twisted course and is more likely to be a conglomeration of polydirectional seams. Again, as with the proper three-dimensional model, the deeper external alveolar process nodes were totally constrained whereas the mirror image nodes were only constrained in the Z co-ordinate direction. Also, only half the total orthodontic load was applied because of the half structure simulation.

### 9.4.2 Results

The stress and strain components obtained from the three-dimensional model analysis are tabulated in qualitative form in FIG. 9.16. The four areas considered are the critical regions of the alveolar processes which are observed to undergo either bone resorption or deposition during orthodontic treatment. However, because of the coarse mesh employed, the nodal points are spaced at large distances from one another. Consequently, the change occurring in the curvature of the surface at the four points in question could not be assessed with any confidence. This was in fact the reason why the second pseudo three-dimensional model was developed.

The mechanical responses of the pseudo three-dimensional model structure were determined for both the bone grain configurations assumed. These are displayed qualitatively in FIG. 9.17 and FIG. 9.18. Even though the spacing of the nodes allowed the

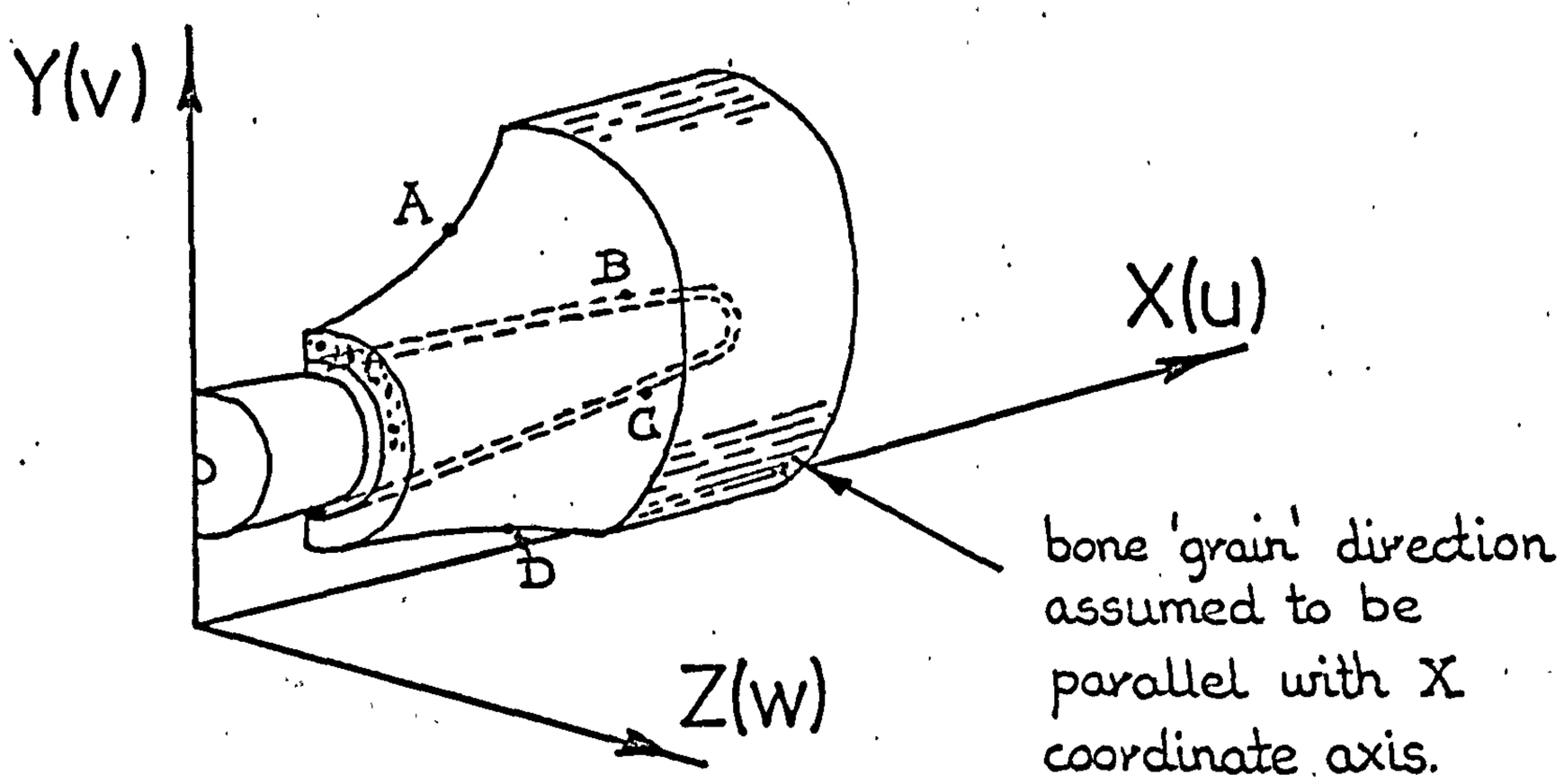


| | PERIOSTEAL A | PERIOD. MEM. B | PERIOD. MEM. C | PERIOSTEAL D |
|---|---|---|---|---|
| $\sigma$ - stress in the direction of assumed 'bone grain'. | Tensile | Tensile | Tensile | Compress. |
| $\sigma$ - stress in direction approx normal to bone surfaces. | Zero | Compress. | Tensile | Zero |
| $\sigma$ - hoop or circumferential stress | Mesh of model too coarse for an accurate assessment | | | |
| $\epsilon$ - strain in the direction of assumed 'bone grain'. | Tensile | Very small Comp. or Tens? | Tensile | Compress. |
| $\epsilon$ - strain in direction approx. normal to bone surfaces. | Compress. | Compress. | Compress. | Tensile. |
| $\epsilon$ - hoop or circumferential strain. | Mesh of model too coarse for an accurate assessment | | | |
| Change in surface curvature in XY plane. | Node distribution on bone surfaces too coarse to permit an accurate assessment. | | | |
| Change in surface curvature circumferentially, YZ plane. | | | | |
| Clinically observed Remodelling response | Deposition | Resorption | Deposition | Resorption. |

FIG. 9. 16 Qualitative results obtained from the 3-D proper finite element analysis of the maxillary central incisor.

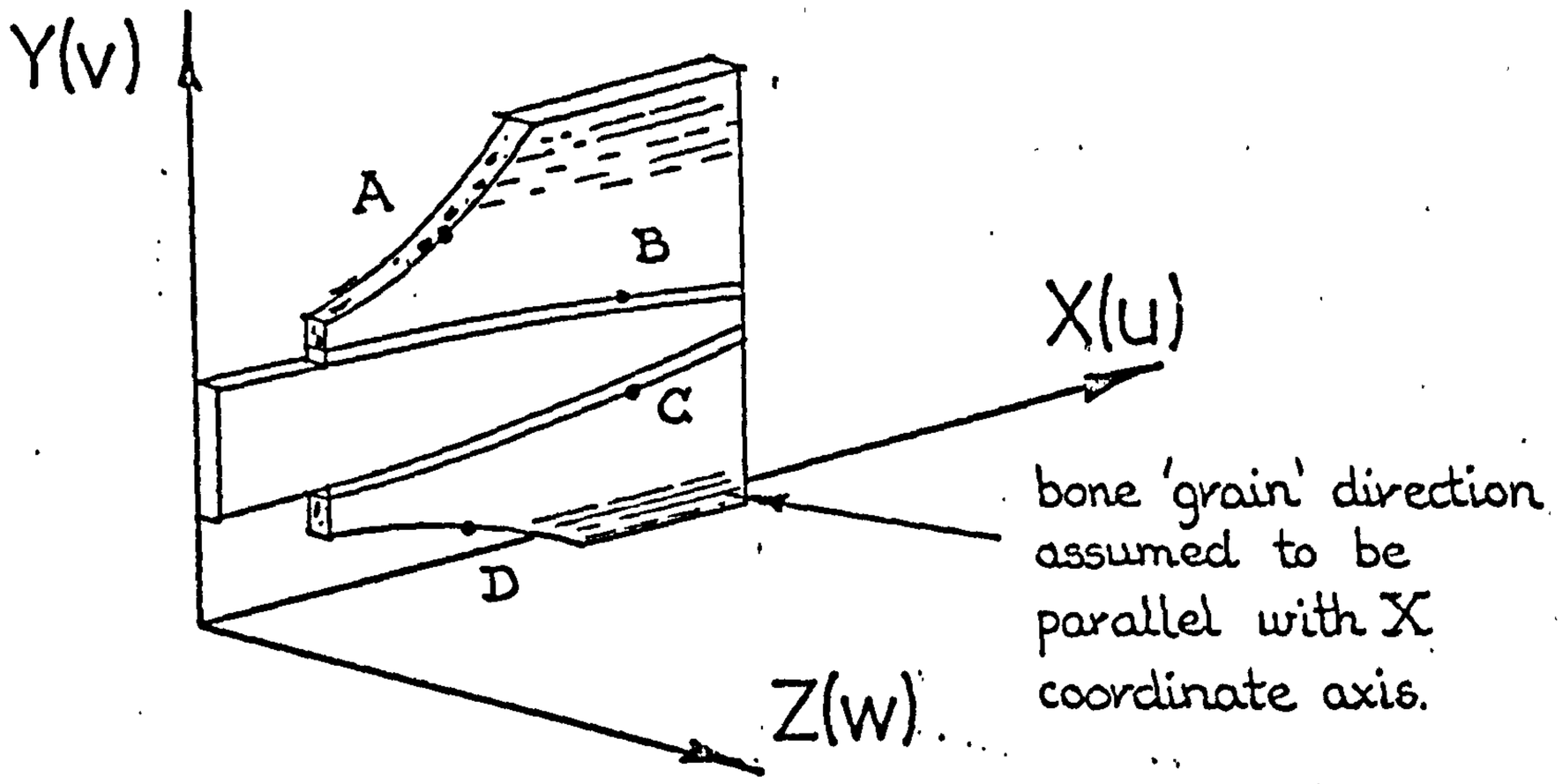


| | PERIOSTEAL A | PERIOD. MEM. B | PERIOD. MEM. C | PERIOSTEAL D |
|---|---|---|---|---|
| $\sigma$- stress in direction of assumed 'bone grain'. | Tensile | Compress. | Tensile | Compress |
| $\sigma$- stress in direction approx. normal to bone surfaces | Zero | Compress. | Tensile | Zero |
| $\sigma$- hoop stress $\perp$r. to model | Compress. | Compress. | Compress. | Tensile |
| $\epsilon$ - strain in direction of assumed 'bone grain'. | Tensile | Compress. | Tensile | Compress. |
| $\epsilon$ - strain in direction appx normal to bone surfaces. | Compress. | Compress. | Tensile | Tensile |
| $\epsilon$- hoop strain $\perp$r. to model. | Zero | Zero | Zero | Zero |
| Change in surface curvature in XY plane. | $\overrightarrow{\text{Convex}}$ | $\overrightarrow{\text{Concave}}$ | $\overrightarrow{\text{Convex}}$ | $\overrightarrow{\text{Concave}}$ |
| Change in surface curvature in YZ plane. | No change * | $\overrightarrow{\text{Concave}}$ * | $\overrightarrow{\text{Concave}}$ * | $\overrightarrow{\text{Convex}}$ * |
| Clinically observed Remodelling response. | Deposition | Resorption | Deposition | Resorption |

* results tentative only

$\overrightarrow{\text{Convex}}$ ≡ surface becoming more convex.

FIG. 9. 17 Qualitative results obtained from the pseudo 3-D finite element analysis of the maxillary central incisor. Bone grain parallel to X coordinate direction.

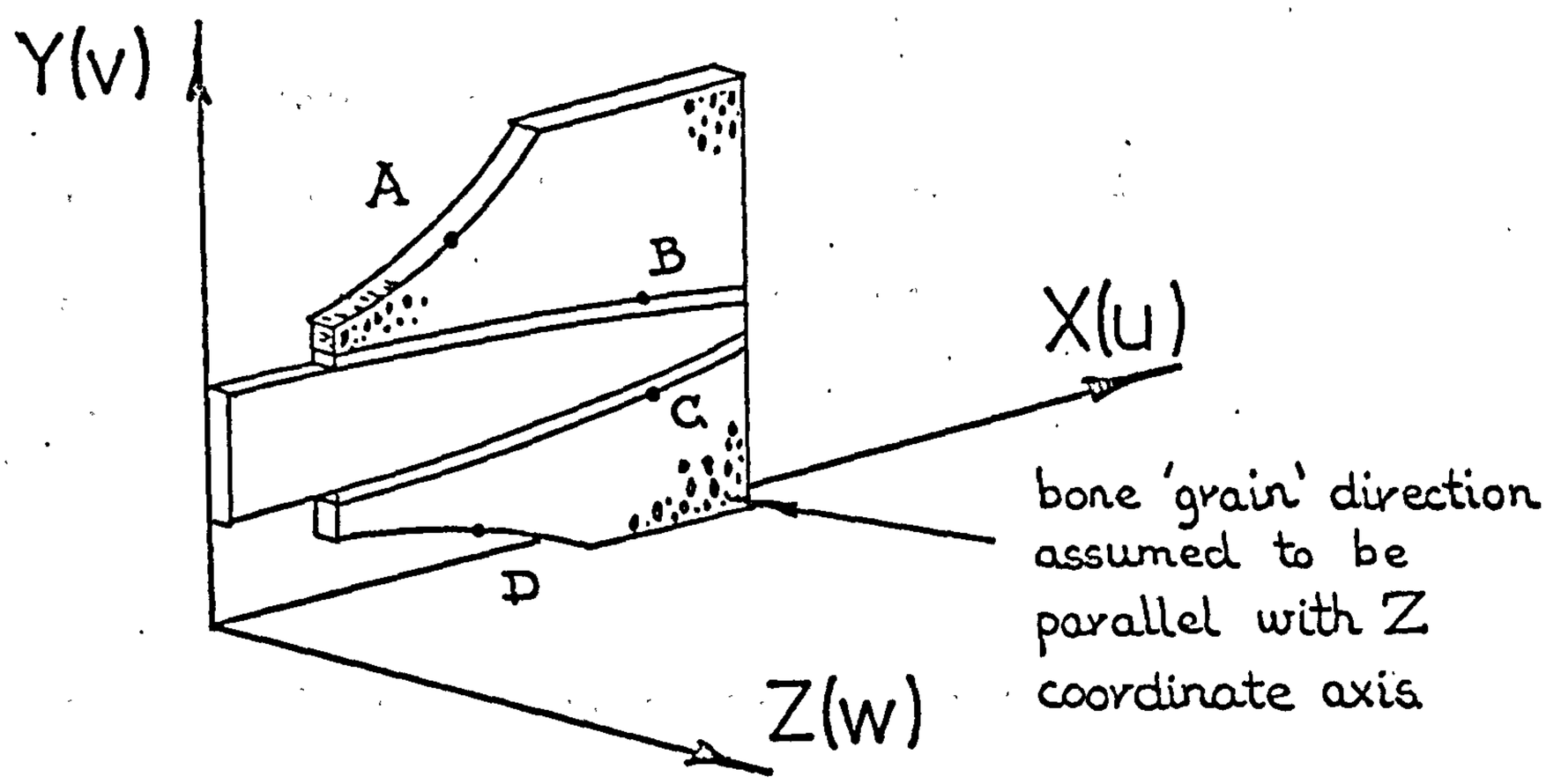


| | PERIOSTEAL A | PERIOD. MEM. B | PERIOD. MEM. C | PERIOSTEAL D |
|---|---|---|---|---|
| $\sigma$- stress tangential to assumed bone 'grain' | Tensile | Compress. | Tensile | Compress. |
| $\sigma$- stress in direction approx normal to bone surfaces. | Zero | Compress. | Tensile | Zero |
| $\sigma$- hoop stress, $\perp$r to model in direction of bone 'grain'. | Tensile | Compress. | Tensile | Compress. |
| $\epsilon$- strain tangential to assumed bone 'grain'. | Tensile | Compress. | Tensile | Compress. |
| $\epsilon$- strain in direction appx normal to bone surfaces. | Tensile | Compress. | Tensile | Compress. |
| $\epsilon$- hoop strain, in direction of bone 'grain'. | Zero | Zero | Zero | Zero |
| Change in surface curvature in XY plane. | $\overrightarrow{\text{Concave}}$ | $\overrightarrow{\text{Convex}}$ | $\overrightarrow{\text{Concave}}$ | $\overrightarrow{\text{Convex}}$ |
| Change in surface curvature in YZ plane. | $\overrightarrow{\text{Convex}}$ * | $\overrightarrow{\text{Convex}}$ * | $\overrightarrow{\text{Concave}}$ * | $\overrightarrow{\text{Concave}}$ * |
| Clinically observed Remodelling response | Deposition | Resorption | Deposition | Resorption |

* results tentative only
$\overrightarrow{\text{Concave}}$ ≡ surface becoming more concave.

FIG. 9.18 Qualitative results obtained from the pseudo 3-D finite element analysis of the maxillary central incisor. Bone grain parallel to Z coordinate direction

change in curvature of the periosteal surfaces to be estimated, the obvious limitations and inadequacies of the models employed must be borne in mind when assessing the value and accuracy of the results.

### 9.4.3 Discussion of Results

A major difference between the orthodontic tooth models and the model of the malaligned femur is that two of the critical areas on the socket wall cannot be strictly classified as either periosteal or endosteal surfaces. Also, the coarse mesh employed for the three-dimensional analysis did not enable some of the individual mechanical responses of the alveolar bone to be ascertained. Consequently, a complete discussion regarding all the aspects of this analysis is not possible. However, it can be seen from FIG. 9.16 that for the mechanical responses which were evaluated, none correlated completely with the clinically observed occurrences of bone resorption and deposition. Although the normal stress components in the periodontal membrane correlated, i.e. compression equals resorption and tension equals deposition, the normal stresses acting on both the outside alveolar surfaces were obviously zero. Even so, in an actual tooth structure these surfaces are covered with soft tissues and consequently their presence may create normal stresses on the alveolar bone in these areas in an <u>in vivo</u> situation.

Because it was impossible to determine accurately the changes in the surface curvatures of the 'remodelled' areas, Epker and Frost's theory could not be examined against the

three-dimensional analysis results. However, it is apparent from FIG. 9.16 that Bassett's theory that compressive stresses in the bone lead to deposition and tensile stresses to bone resorption does not hold. On the other hand, if a section is taken through the points A,B,C,D across the alveolar processes and the bone exposed is assumed to be under net tension, Currey's theory once again seems to predict the correct biological response.

From the results obtained for the rather limited pseudo three-dimensional models, several mechanical responses were found to correlate. For the first model where the bone grain was assumed to run approximately parallel to the periosteal surfaces, see FIG.9.17, three individual parameters were found to suit for all four critical areas. These were the stress and strain components acting parallel to the periosteal and socket wall surfaces, (and consequently parallel to the direction of the assumed bone grain), and the change in the curvature of the surface in the plane of the model slice. (The change in the curvature of the surface in the hoop or circumferential direction could not be determined with sufficient accuracy due to the limitation of the finite element model). However, the curvature correlation with this model was contradictory to the correlation experienced with the femur analysis. For this case,the increase in surface CONVEXITY was associated with bone DEPOSITION and increase in CONCAVITY with bone RESORPTION. As well as the correlation already mentioned,the normal stress components in the periodontal membrane were again found to suit. Once again though, the normal stress component did not correlate on the two external alveolar surfaces for the same

reasons which were enumerated for the three-dimensional analysis proper.

On examining the results depicted in FIG.9.17, both the remodelling theories proposed by Bassett and by Epker and Frost were found not to hold. Also, because of the model employed and the resulting alternate compressive - tensile nature of the stresses produced in the four critical regions, it is not at all clear as to whether the bone is in net compression or tension. Consequently, it is difficult to examine the validity of Currey's theory. However, if each of the alveolar processes is considered separately, the labial process would have to be considered as being in net tension (as the tensile stress at A is greater in magnitude than the compressive stress at B). Similarly, due to the same reasoning, the lingual process would have to be considered as being in net compression. Applying Currey's theory subsequently leads to a correct remodelling prediction for the labial process but an incorrect one for the lingual process.

For the second pseudo three-dimensional model where the bone grain was assumed to run perpendicular to the plane of the model slice, see FIG.9.18, even more correlations were found to exist. In this case,five complete correlations occurred, i.e. correlations on all four bone surfaces, as well as the partial correlation of the normal stress component in the periodontal membrane as before. These consisted of both the stress and strain components acting parallel to the periosteal and socket wall surfaces (and now in a direction tangential to the assumed bone grain), the hoop or circumferential stress component, the strain component acting in a direction normal to the periosteal surfaces, and finally as before, the

change in the curvature of the alveolar bone surfaces in the plane of the model slice. It is very interesting to note that the change in the curvature of the surfaces is completely reversed in character in comparison with the type of curvature change experienced using the same model but having the previous parallel grain orientation. As for the femur analysis, the surface curvature change now indicates that an increase in surface CONCAVITY is associated with bone DEPOSITION while an increase in surface CONVEXITY is associated with bone RESORPTION. This particular feature alone emphasizes the effect that the direction assumed for the bone grain has on the results obtained.

If the results shown in FIG. 9.18 are examined in conjunction with the three remodelling theories, it can be seen that only Epker and Frost's approach coincides with the biological response. However, as already mentioned, the direction of the assumed bone grain runs at right angles to the direction of the curvature changes. This of course is contrary to that of the case of the malaligned femur analysis.

## 9.5 CONCLUSIONS

A study of both the literature and the results obtained from the experiments reported here, reveals that the biological response of bone tissue to mechanical stimuli is a very complex process. Indeed, it is suggested that the remodelling or regulating ability of bone tissue may not be the result of simply one process but may in fact be due to various different phenomena. Hence, the remodelling response of the orthopaedic and orthodontic structures widely discussed in the literature and examined here may not be due to the same form of stimulus.

For the orthopaedic problem, it is questionable purely from intuitive reasoning, whether the loads applied to the malaligned femur as a result of locomotion can alone stimulate the resorption and deposition response of the bone tissue. Even though the forces generated during locomotion are both dynamic and cyclic in character, their precise magnitudes and directions at each particular instant during the walking cycle are unknown. The forces applied to the femur are not simply a proportion of the total body weight. In addition to the body weight force components, there are considerable and constantly varying forces, torques and bending moments being exerted by the surrounding complex system of muscles. As an example, the hip joint alone is engulfed by a system of over twenty separate muscles. Each one of these muscles can act either independently or with any of the other muscles. Even from simple mechanical considerations, it is apparent that some of these muscles must develop forces in excess of the magnitude of the body weight force during a normal walking activity. Hence, it is extremely doubtful whether it is merely the simple force (which is always considered in the literature to be applied to the femoral head as illustrated in FIG. 9.3), which is solely responsible for the remodelling process. In fact, it is suggested here that the mechanical stimulus which invokes the remodelling response could be created by the rearrangement of the musclature as a result of the malalignment in the bone. However, the only possible way of determining whether there are any residual stresses set up in the malaligned femur as a result of muscle rearrangement,

would be by the implantation of some strain gauge device so that the required information could be transmitted via some telemetering system.

Another point which is usually never considered very seriously is whether the bone response is the same for an endosteal surface as it is for a periosteal one. Afterall, it may be that the endosteal surface is either much less responsive than its periosteal counterpart or is in fact merely a sleeping partner in the remodelling process. This fact seems to warrant further study.

Bearing in mind the possible fallacies in the arguments used in the literature to explain the bone remodelling phenomenon, the analyses presented in this chapter throw some light on the problem even though the finite element models employed are somewhat limited. Firstly, it is apparent from the maxillary central incisor analyses, that the direction of the bone grain must be known and taken into account. It can be seen from FIGS. 9.17 and 9.18, that by simply changing the direction of the Haversian systems, and thereby the direction of the principal stiffness axis, the form of the changes in the curvature of the alveolar bone surfaces are reversed for the two bone grain orientations considered. (This point is also particularly important when the bioelectric effects of the bone tissue are being discussed). Secondly, it is vitally important that like is compared with like and that the directions of the stress, strain or displacement components being discussed are clearly specified. In many papers, the compressive stresses in the compressed areas of the periodontal membrane are treated as

the same as the compressive stresses generated in the concave cortex of the malaligned femur. Of course, the compressive stresses generated in the membrane are acting in a direction which is approximately normal to the bone surface of the alveolus whereas the compressive stresses in the cortex of the femur are acting within the bone tissue itself and in a direction approximating to that of the bone grain.

If the periosteal, endosteal and socket surfaces of the malaligned femur and alveolar bone in the critical areas are considered, only one mechanical feature correlates with the clinically observed bone remodelling response. This feature is the change in the curvature of the surface which occurs in the longitudinal planes of the femur and tooth socket respectively. This result agrees with the theory put forward by Epker and Frost (98), who proposed that bone deposition occured only in areas of increasing surface concavity and resorption in areas of increasing surface convexity. However, this only applies here provided that the grain in the alveolar bone runs circumferentially around the alveolus as shown in FIG.9.18. Nevertheless, these results are inconsistent in that for the case of the femur, the curvature change is 'with' the direction of the bone grain whereas for the socket wall, the change in the curvature of the surface is 'across' the assumed direction of the alveolar bone grain.

Therefore, although Epker and Frost did not take the bone grain orientation into account in their distussion, it seems, in the light of all the evidence available that the internal structure of the bone should play a significant role in the remodelling process. Consequently, it seems doubtful whether their theory, as it stands is entirely satisfactory. Similarly, Bassett's theory even if it is restricted to periosteal bone surfaces, fails to predict the 'required' remodelling responses for two cases considered. On the other hand, even though Currey's interpretation of the concept of net tensile or compressive stress is not clearly defined, the results obtained here do tend to support his hypothesis. However, it is abundantly clear that a great deal more research, both biomechanical and clinical is required before any firm conclusions can be drawn.

# CHAPTER TEN

# DETERMINATION OF SOME FORCE DISTRIBUTIONS ON THE PERIODONTAL MEMBRANES OF TEETH

# 10. DETERMINATION OF SOME FORCE DISTRIBUTIONS ON THE PERIODONTAL MEMBRANES OF TEETH

## 10.1 INTRODUCTION.

When a tooth is intruded, extruded or rotated by a system of masticatory or orthodontic loads, the periodontal membrane, which is attached to both the root of the tooth and to the lamina dura, is both distorted and displaced. Indeed, it is the distortion, e.g. the compression and extension of the periodontal membrane, which enables it to distribute the reactive forces required to equilibrate the system of applied loads.

A considerable number of clinical research workers believe that it is the stresses which are set up in the periodontal membrane which, by regulating that tissue's blood supply, stimulates the remodelling process of the alveolar bone, Reitan (101, 102 and 103). The theory widely acknowledged to govern this process is that compressive stresses in the membrane lead to bone resorption and tensile stresses to bone deposition. Compressive stresses undoubtedly reduce and restrict the blood supply in the membrane in the areas under compression. Hence, it is believed that the reduced vitality leads subsequently to the hyalinization of the membrane tissue and this in turn to the resorption of the adjacent alveolar bone. Conversely, it is believed that the areas of the periodontal membrane subjected to tensile stresses experience an increase in their blood supply. This increased vitality is thought to be followed by the formation of osteoid tissue which in turn is believed to be eventually calcified to form new bone.

Baumrind(99) in 1969, challenged this hypothesis on the basis of some observations he had made from experiments carried out on rats. This author examined histological specimens taken from two areas of the periodontal membrane of a molar tooth during orthodontic movement. The two areas he believed were under compressive and tensile stresses respectively. However, Baumrind's findings are somewhat misleading. In fact, he seems to have made a serious error in his calculations regarding the narrowing and widening of the periodontal membrane at the positions from which he obtained his histological specimens. Re-working correctly the figures tabulated in his paper, indicates that the areas he selected for examination were BOTH under compression, i.e. a narrowing of the membrane tissue. Consequently, the conclusions drawn from this work are completely invalid.

Another conclusion arrived at by Baumrind was that the alveolar bone deformed more readily than the periodontal membrane tissue. Baumrind's so-called bone bending of the alveolar processes is in complete contrast to the findings of the earlier chapters. It is also very difficult to believe this proposal in the light of the finding of other workers, unless of course Baumrind applied forces which were so great that the tooth actually touched the socket wall. Even so, if this were the case his conclusions would not be applicable for orthodontic work, as treatment in this category generally relies upon small forces.

Because of the keen interest shown by clinicians in the stress distributions which occur in the periodontal membrane, this chapter is devoted to looking at the mechanical behaviour of this tissue under various forms of tooth loading. However, it must be pointed out at the outset that the nature or supporting mechanism assumed for the periodontal membrane will govern the type and form of its mechanical response. Indeed, the discussion concerning this aspect which was dealt with earlier and illustrated in FIG. 8.2, is equally applicable to the work reported on in this chapter. Nevertheless, although this point must be borne in mind it should not affect the conclusions drawn from the analyses.

The first problem investigated here was to see what effect the direction of an occlusally applied load and the height of the supporting alveolar bone have on the resulting force distribution on the periodontal membrane. This is then followed by a study of the force distributions which occur on the membranes of teeth which are employed either as tooth stabilizers or as bridge abutments. Finally, a simple experiment is carried out in order to assess the stress distribution which occurs around an endosseous pin implant. In this case of course, no periodontal membrane is involved. Instead, the metal implant is in direct contact with the alveolar bone.

## 10.2 CHANGES IN THE FORCE DISTRIBUTION ON THE PERIODONTAL MEMBRANE OF A TOOTH AS A RESULT OF VARYING THE DIRECTION OF THE APPLIED LOAD AND THE HEIGHT OF THE SUPPORTING ALVEOLAR BONE

A generally held view is that the periodontal membrane and supporting alveolar bone structure is built primarily to react axial tooth loading and only to a very limited degree lateral or tipping type forces. Indeed, it is believed that lateral forces, due to their lever actions, generate 'excess' stresses in the membrane tissue and thereby precipitate tooth movement and possibly alveolar bone resorption.

Alveolar bone resorption invariably manifests itself as a lowering of the alveolar crests. Hence, the effective support given to the tooth by the alveolar process against the offending tipping or lateral forces is consequently reduced. Therefore, a 'snowball' situation can be created in which the loosening and sometimes even the eventual loss of the tooth occurs, Sometimes in fact, tooth loosening occurs clinically as a result of orthodontic treatment in which the force levels applied have been too high. This of course implies that bone resorption occurs either ahead of bone deposition or at a faster rate. However, from clinical observations it has been postulated e.g. Storey (119), that when orthodontic forces are too large, bone resorption occurs behind on the cancellous side of the laminar dura. This 'undermining' type of resorption is characterised by sudden and erratic tooth movements. For small orthodontic forces it is believed that resorption occurs on the socket side of the lamina dura adjacent to the compression areas in the periodontal membrane, and deposition on the cancellous side. (Deposition also occurs

on the socket side of the lamina dura adjacent to the tension areas of the periodontal membrane). However, for heavy forces, although the small initial tooth movement is experienced as before, the tooth moves suddenly and more drastically once the lamina dura has been undermined. It is this process which it is believed results in the eventual instability and loosening of the tooth.

In this section, the aim was to see how the periodontal membrane reacted both axial and lateral type forces, and also, to investigate the effect of the height of the supporting alveolar bone.

### 10.2.1 Finite Element Model and Test Procedure

The finite element model used in this series of experiments was the two-dimensional bucco-lingual slice section of the second mandibular premolar shown in FIG. 8.10. Indeed, the model and test procedure was identical to that described in sub-section 8.7.1. However, for this series of tests the computer program was written such that the nodal point forces which were effectively being applied to the periodontal membrane via the root of the tooth were determined.

### 10.2.2 Results

The mechanical properties ascribed to the tissues involved were the same as those employed in section 8.7. Again, the vertical, oblique and horizontal loads were applied in turn to the occlusal surface of the tooth while the height of the alveolar crests was varied between the high, medium and low levels, see FIG. 8.10.

The force distributions on the periodontal membrane obtained for the nine cases considered, are illustrated in FIGS 10.1 up to 10.9. Note that for the vertical load cases, i.e. FIGS. 10.1, 10.4 and 10.7, the force distribution plots are drawn to a scale which is ten times greater than it is for the other plots in the series.

### 10.2.3 Discussion of Results

Because of the limitations of the two-dimensional model employed, the nodal force distributions obtained can only be discussed on a purely qualitative basis. Nevertheless,it is apparent from the figures (bearing in mind the ten times scale factor difference in FIGS. 10.1, 10.4 and 10.7), that the force distribiton on the periodontal membrane is less severe for the cases where the tooth was loaded axially. Not only are the magnitudes of the forces a great deal smaller, but the whole membrane is more uniformly loaded. The nodal forces are all of a compressive nature and are therefore tending to compress the periodontal membrane.

When the same tooth load is applied in a non-axial manner, the magnitudes of the forces acting on the periodontal membrane are greatly increased. The magnitudes increase as the loading on the tooth becomes more oblique. The worst condition therefore, occurs when the load is applied at right angles to the tooth's long axis.

The largest periodontal membrane forces,for non-axial tooth loads, are seen to occur at the alveolar crest tips and around the root apex. Unlike the distributions obtained for the axial load cases, the forces produced in these regions can be

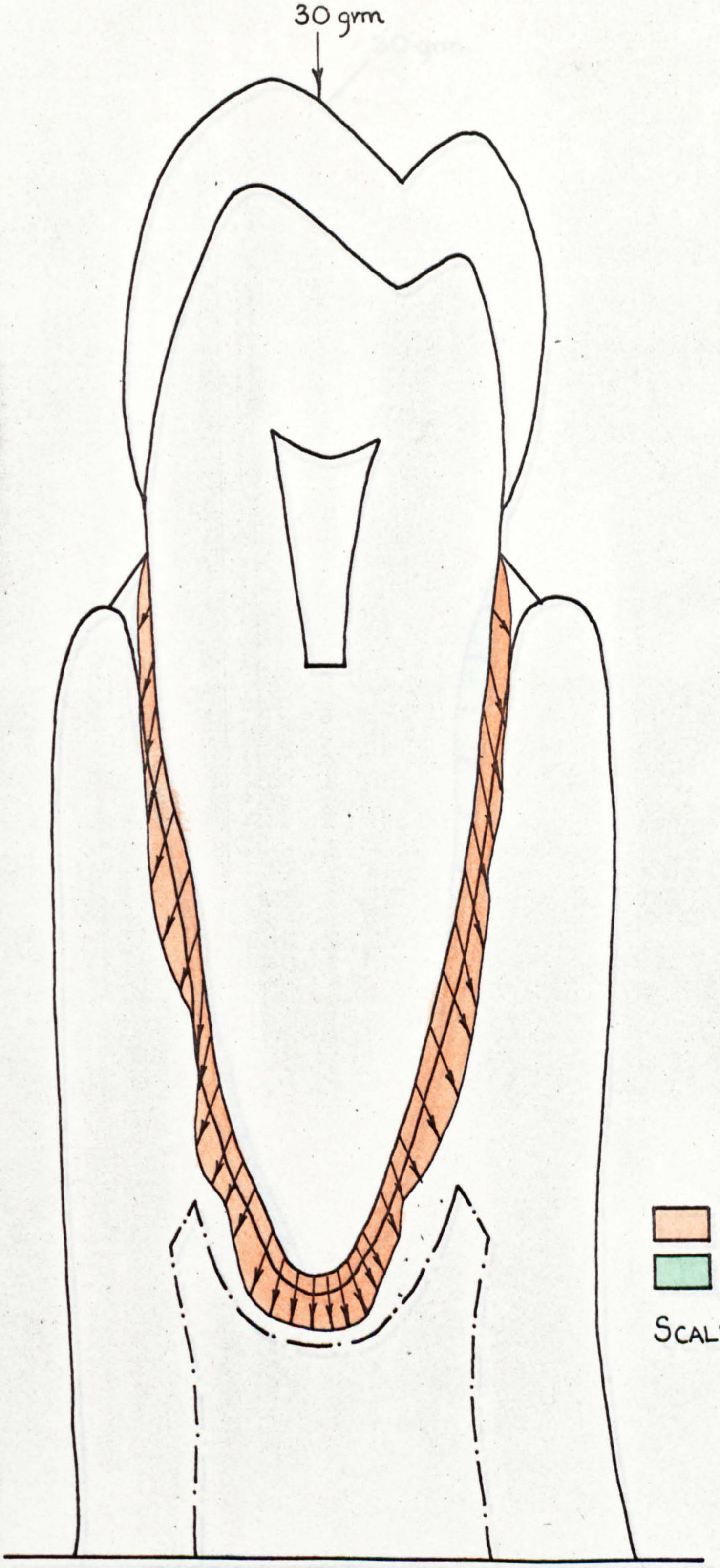


FIG. 10. 1 Force distribution on the periodontal membrane of a tooth loaded with a 30 grm. vertical load. High or normal alveolar bone support height.

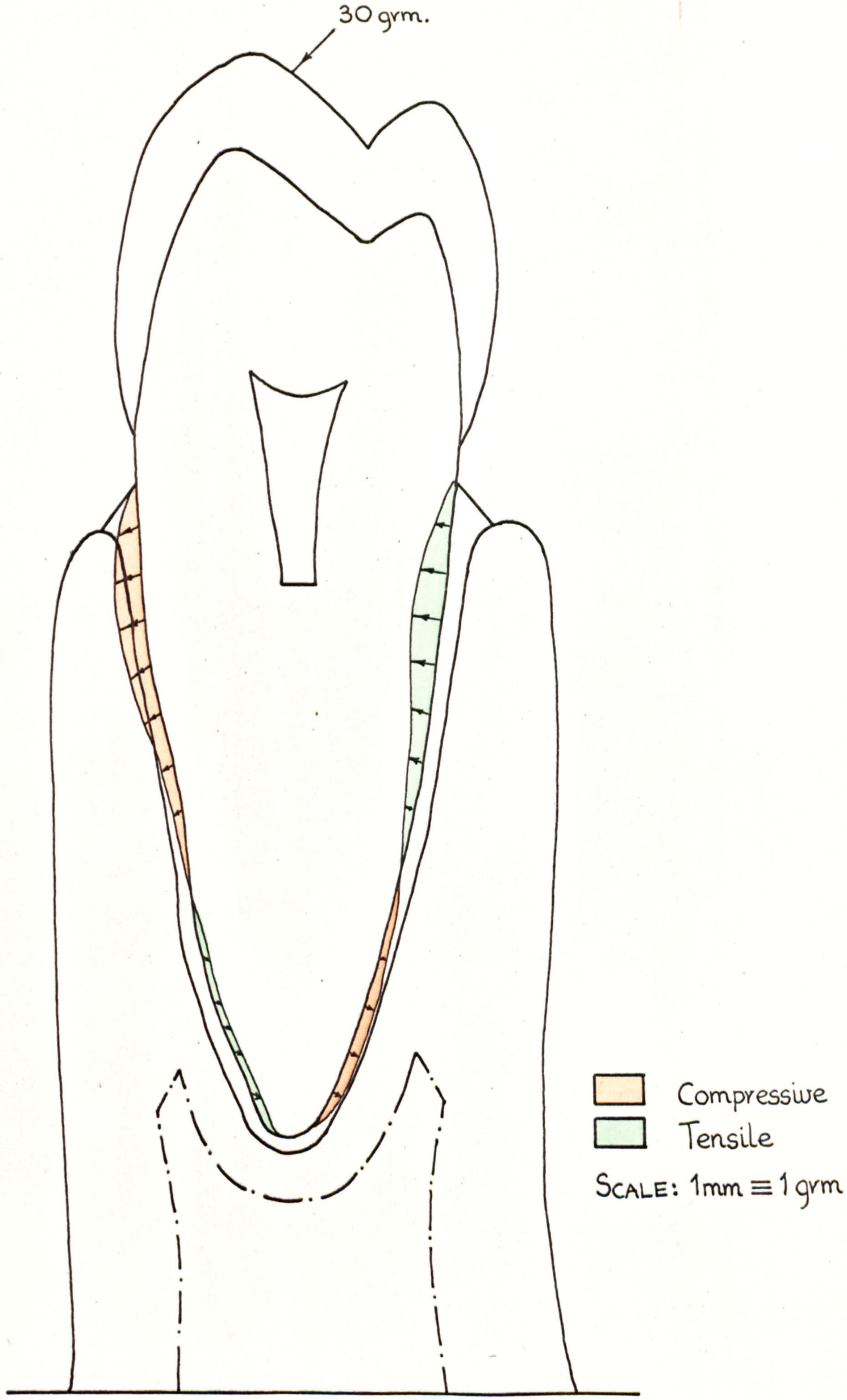


FIG. 10.2 Force distribution on the periodontal membrane of a tooth loaded with a 30 grm. oblique load. High or normal alveolar bone support height.

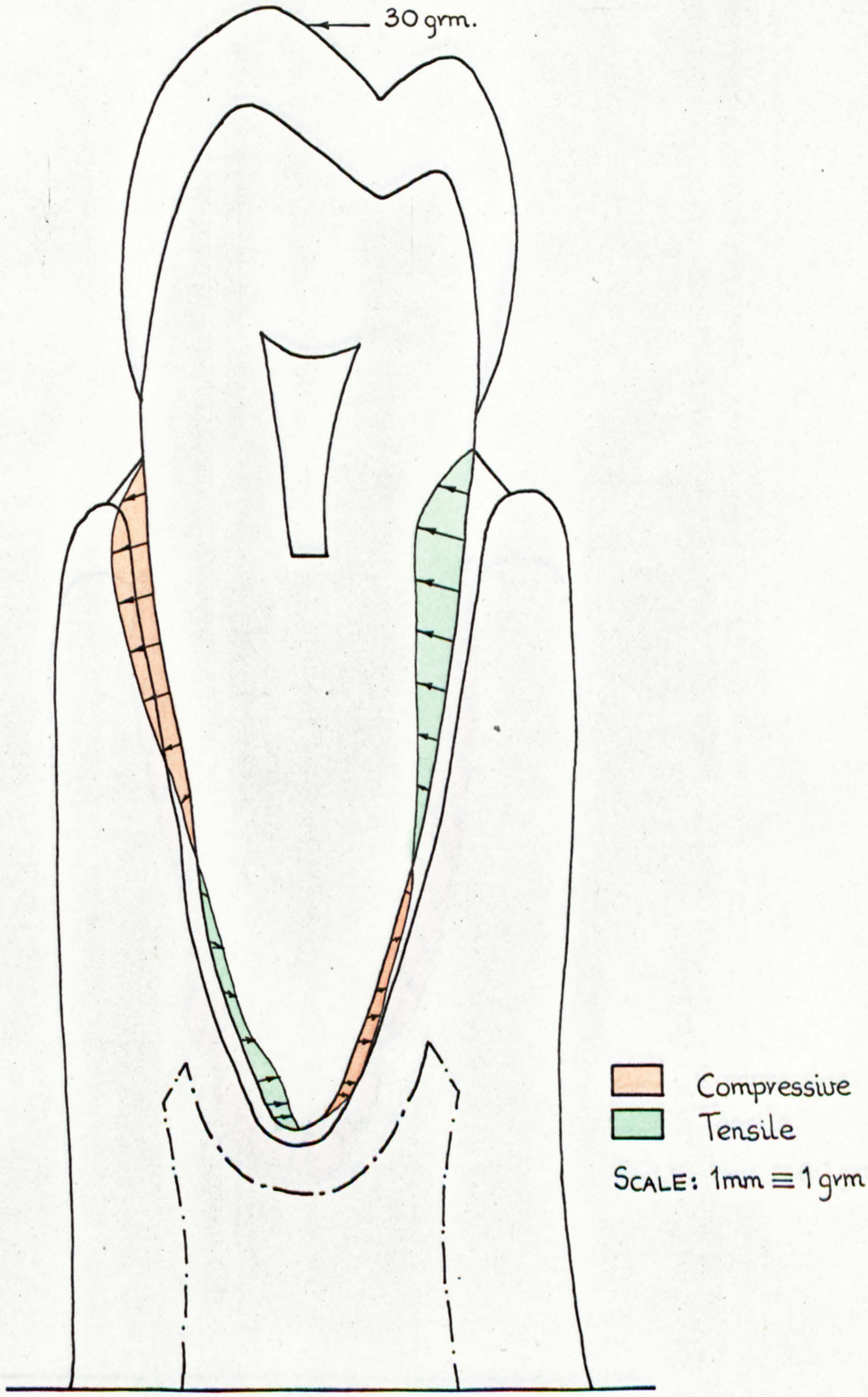


FIG. 10.3 Force distribution on the periodontal membrane of a tooth loaded with a 30grm. horizontal load. High or normal alveolar bone support height.

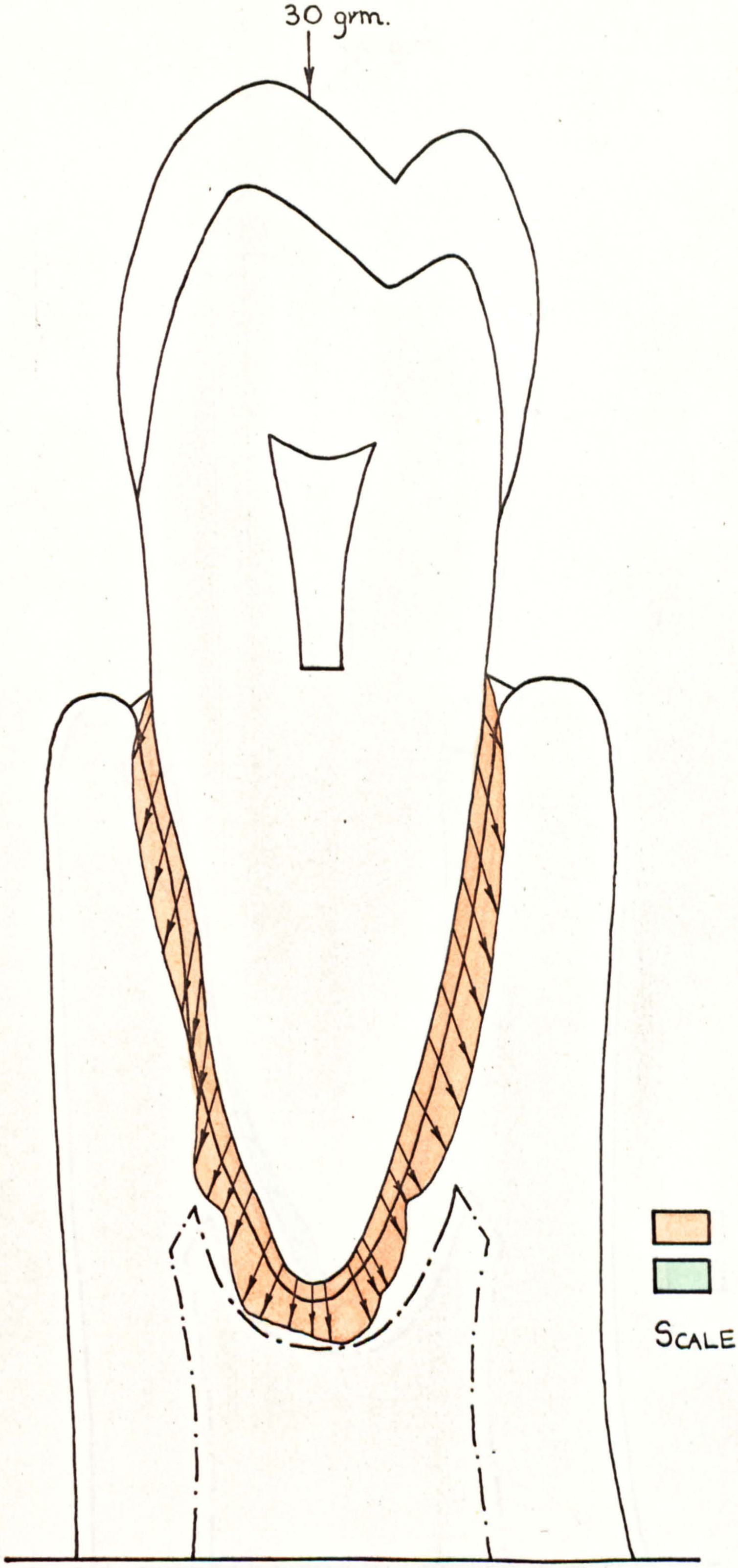


FIG. 10.4 Force distribution on the periodontal membrane of a tooth loaded with a 30 grm. vertical load. Medium alveolar bone support height.

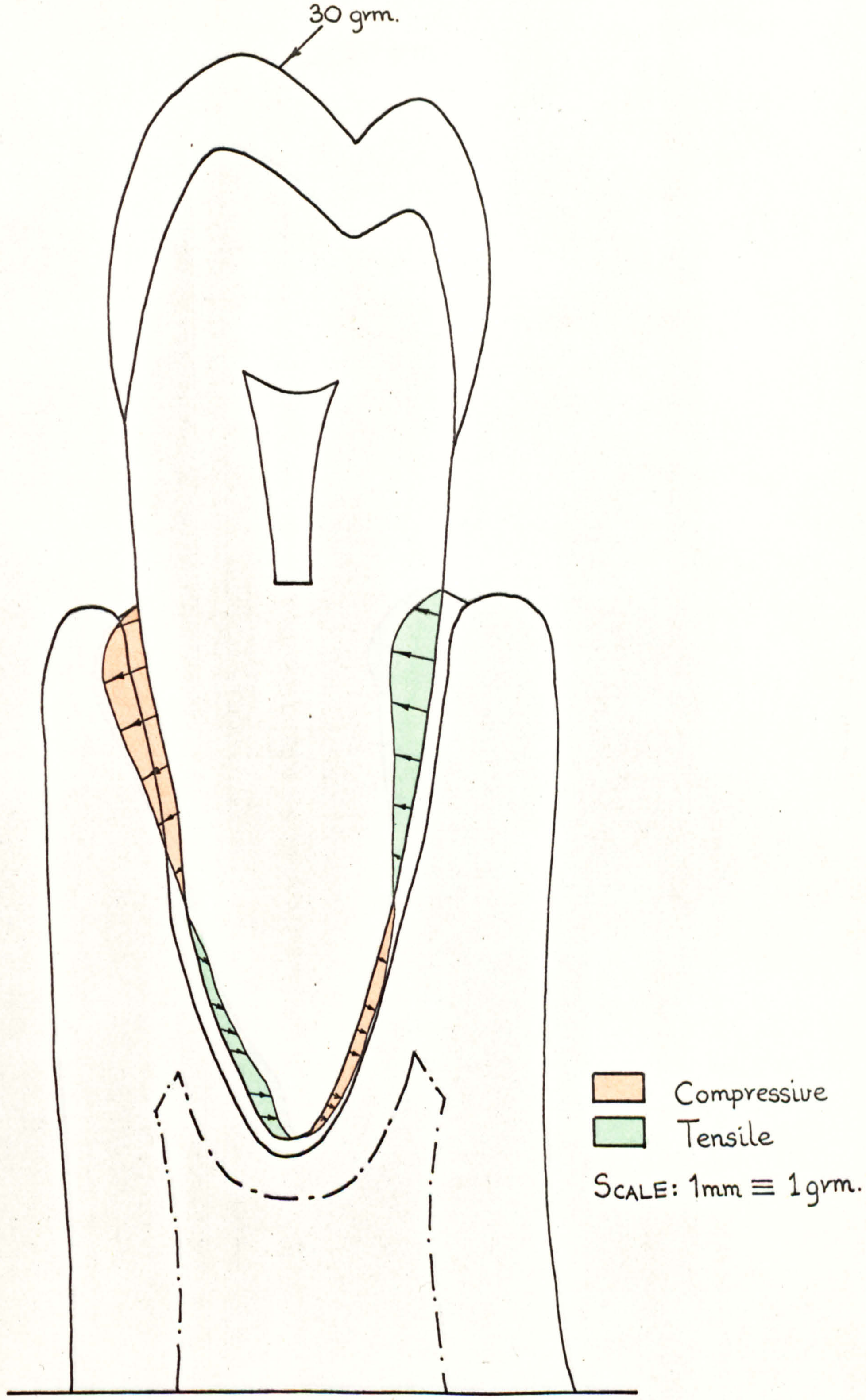


FIG. 10.5 Force distribution on the periodontal membrane of a tooth loaded with a 30 grm. oblique load. Medium alveolar bone support height.

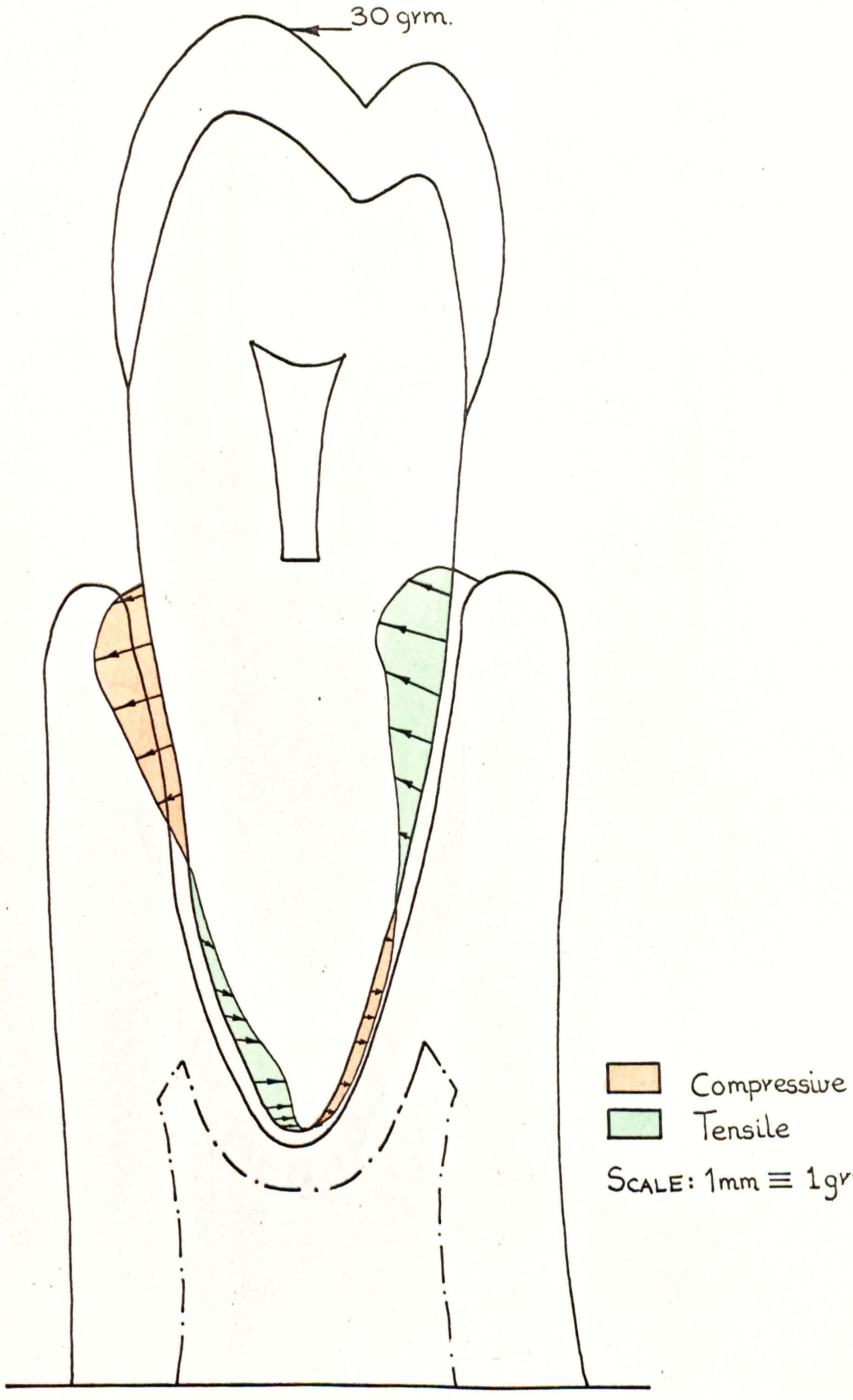


FIG. 10.6 Force distribution on the periodontal membrane of a tooth loaded with a 30 grm. horizontal load. Medium alveolar bone support height.

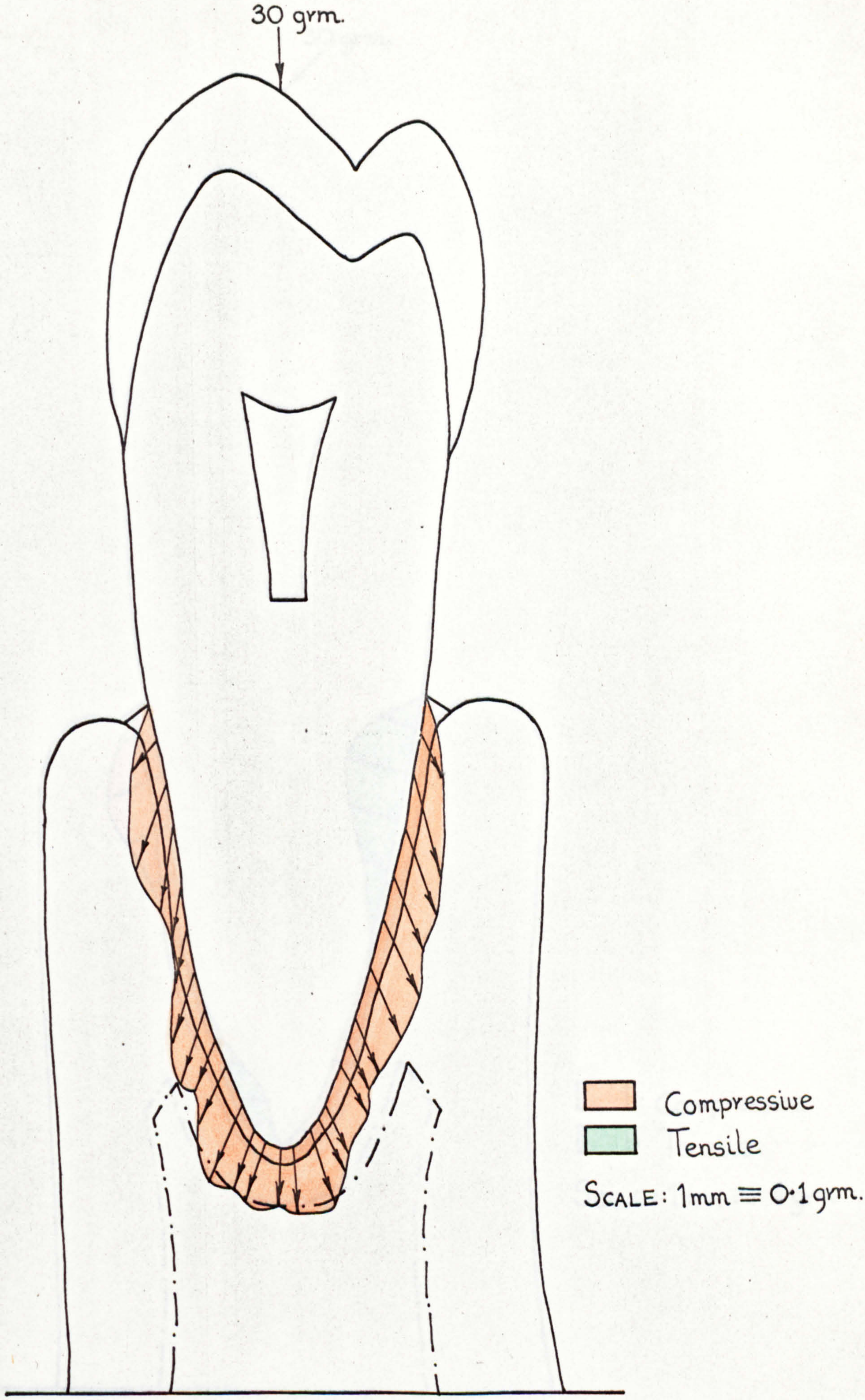


FIG. 10.7 Force distribution on the periodontal membrane of a tooth loaded with a 30 grm vertical load. Low alveolar bone support height.

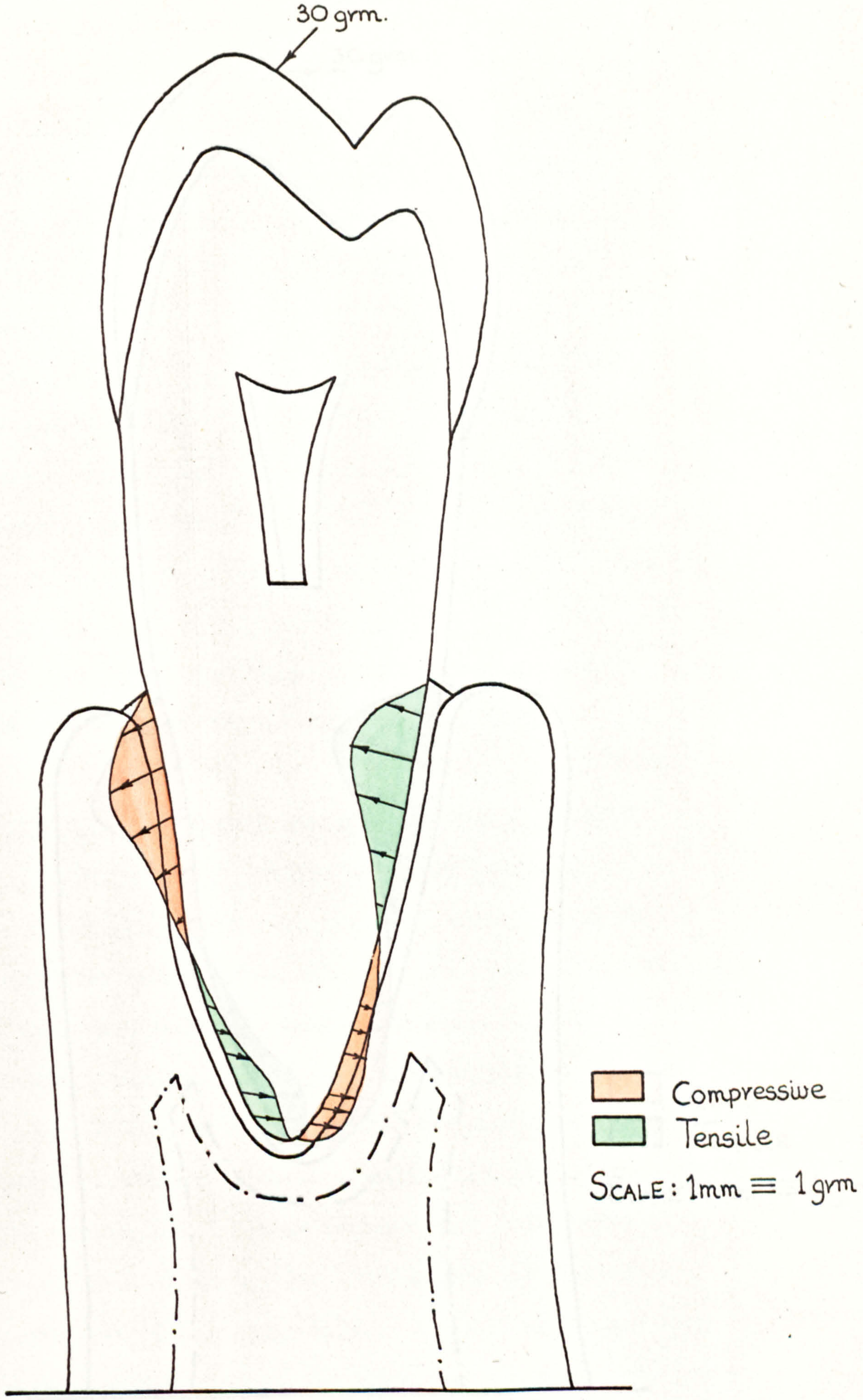


FIG. 10.8 Force distribution on the periodontal membrane of a tooth loaded with a 30 grm oblique load. Low alveolar bone support height.

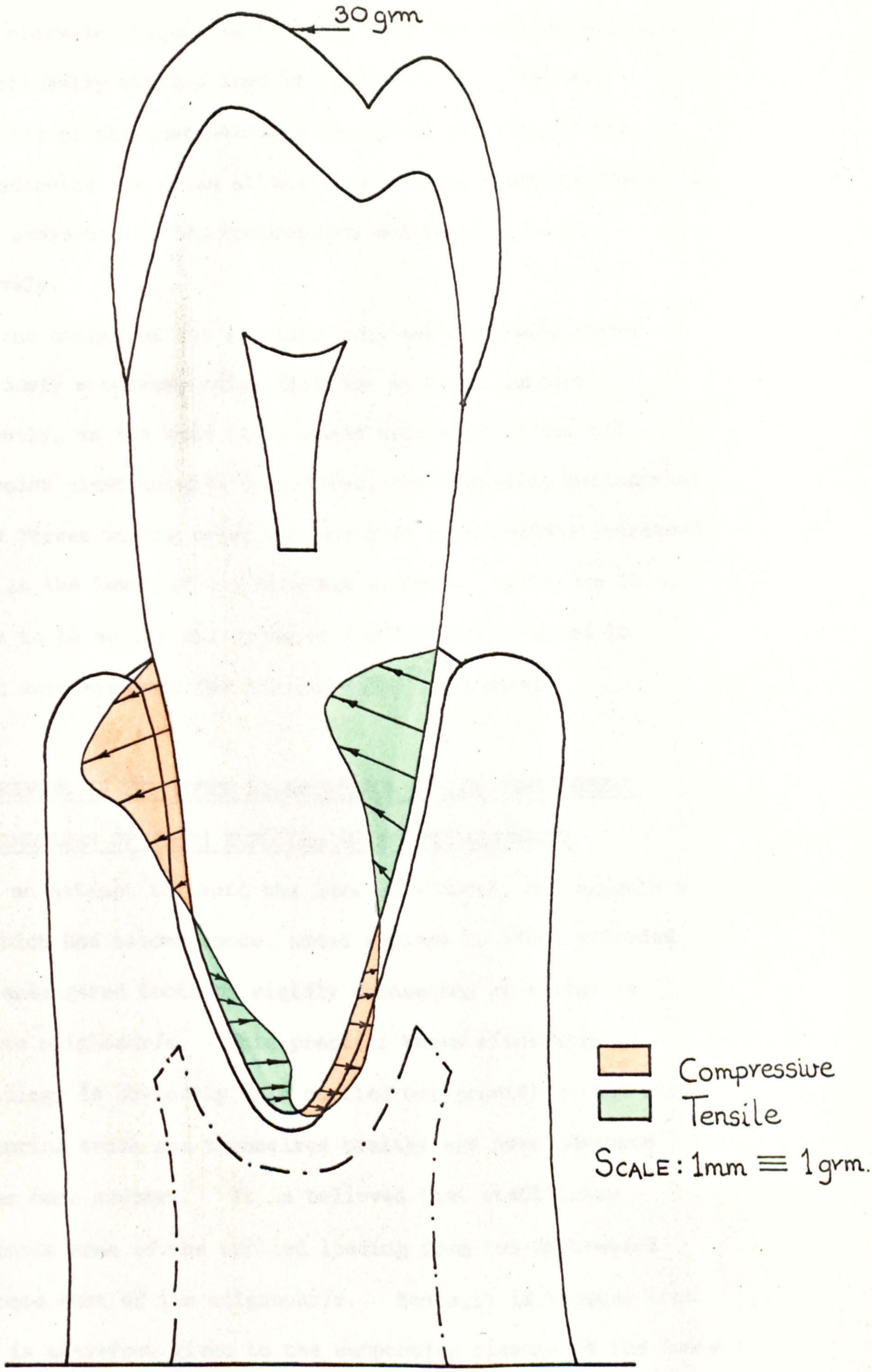


FIG. 10.9 Force distribution on the periodontal membrane of a tooth loaded with a 30 grm horizontal load. Low alveolar bone support height.

either compressive or tensile in character. This is of course,a necessary requisite in order that the turning moment of the occlusally applied load is equilibrated. Indeed, the position of the instantaneous centre of rotation of the tooth, indicates the areas of the periodontal membrane which would be subjected to the compressive and tensile forces respectively.

As the height of the alveolar bone was decreased,there was obviously a corresponding decrease in tooth support. Consequently, as the same tooth loads were applied for all the alveolar crest heights considered, the resulting periodontal membrane forces in the crest tip and root apex regions increased greatly as the level of the bone was reduced. Although this, was seen to be so for all types of loading investigated it was much more apparent for the non-axial load cases.

## 10.3 CHANGES IN THE FORCE DISTRIBUTION ON THE PERIODONTAL MEMBRANES OF TEETH EMPLOYED AS BRIDGE ABUTMENTS

In an attempt to avoid the loss of a tooth, for example a tooth which has become loose, added support is often afforded to the endangered tooth by rigidly connecting or splinting it to its neighbour/s. This practice known clinically as stabilizing, is obviously only carried out providing that the neighbouring teeth are themselves healthy and have adequate alveolar bone support. It is believed that stabilizing distributes some of the applied loading from the distressed tooth onto that of its neighbour/s. Hence,it is thought that relief is therefore given to the supporting tissues of the loose tooth which thereby gives its surrounding alveolar bone time to recuperate.

When a single tooth or sometimes even when several teeth are unfortunately lost, their positions are usually 'filled' with artificial or false teeth. Sometimes the familiar partial dentures or plates can be avoided, (providing that the remaining teeth are healthy and strong), by attaching or connecting the replacement teeth to the remaining natural teeth. The supporting teeth therefore provide abutments for the replacement teeth or pontics which span or 'bridge' the empty sockets left by the lost teeth. Again, for restorations of this type it is often felt desirable to employ more than a single tooth as an end abutment. Indeed, two adjacent teeth are frequently 'splinted' together in an attempt to distribute the bridge loading over a greater root support area. Indeed, simple formulae have been derived whereby the number of abutment teeth required for a particular bridge construction can be determined.

Because an ever increasing amount of bridgework is being carried out in the clinic, the aim in this section was to try and investigate the forces which are being exerted on the periodontal membranes of abutment teeth employed for this type of resotration. The effect of employing more than one tooth as an abutment was also included in the study.

### 10.3.1 Finite Element Model and Test Procedure

The finite element model employed for this series of experiments was a two-dimensional mesio-distal slice section of the first and second mandibular premolars. A computer plot of the model, which has an equivalent slice thickness of 0.345 inches, is shown in FIG. 10.10. As for the earlier

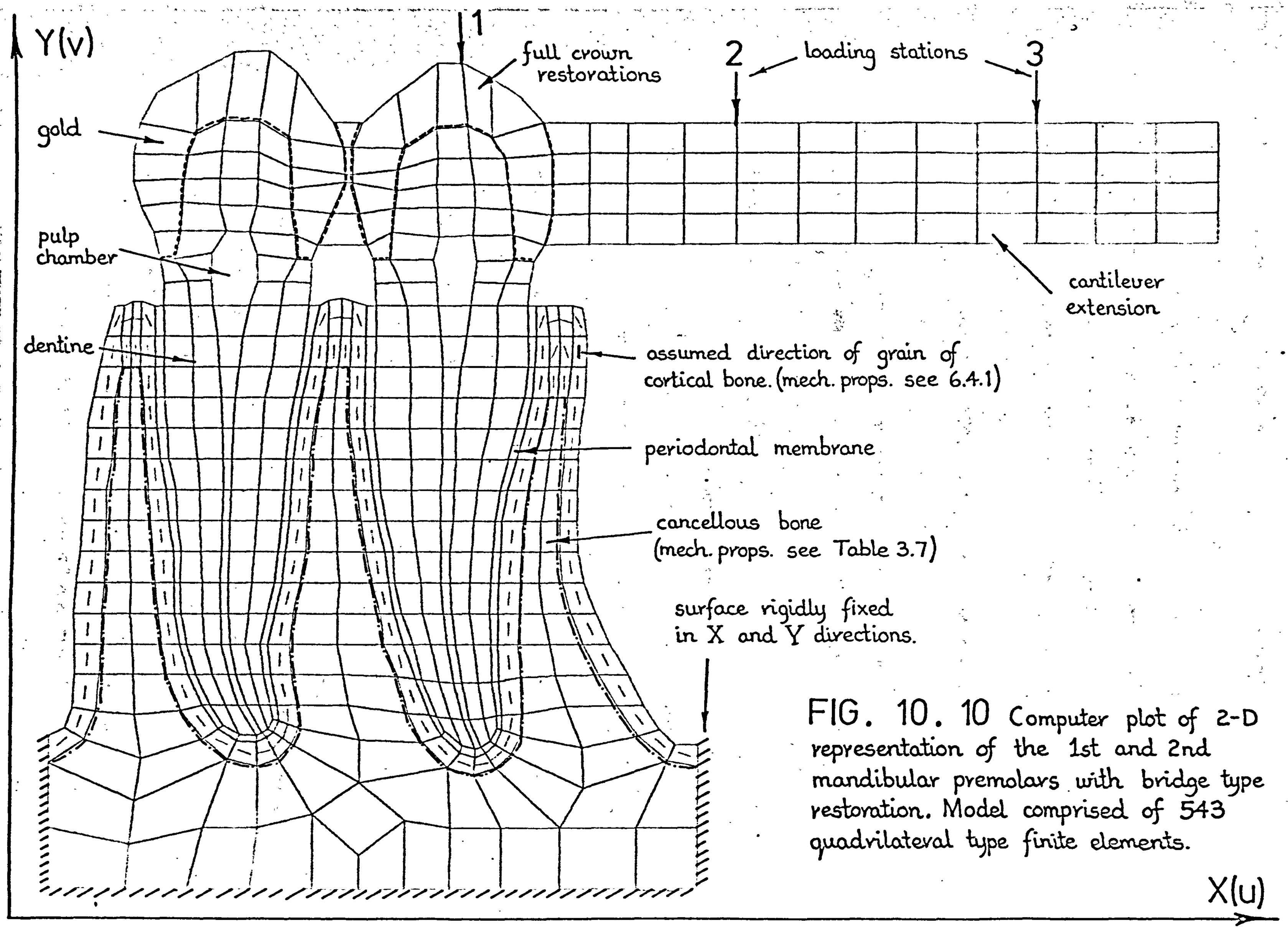


FIG. 10. 10 Computer plot of 2-D representation of the 1st and 2nd mandibular premolars with bridge type restoration. Model comprised of 543 quadrilateral type finite elements.

two-dimensional models the alveolar process was constructed having both cortical and cancellous tissues. The assumed direction of the grain of the cortical bone is indicated by the lines located in the centres of the cortical bone elements. The cancellous tissue was extended to a distance at which the effect of any occlusally applied loading was thought to remain constant.

As can be seen from FIG. 10.10, the first and second premolars were constructed having full gold crown restorations. The crown of the second mandibular premolar however,also included an extension piece which was in the form of a cantilever. Hence, via this lever arm,loading of a bridge at for example mid-span, could easily be simulated.

The gold crowns of the two teeth were joined together by means of five interconnecting elements. Consequently, by simply ascribing the mechanical properties of either gold or a very flexible material to these five elements, completely different structures could be simulated. If the properties of gold were employed then the two teeth would effectively be rigidly joined or 'splinted' together. However, if the five elements were made very flexible, then the two teeth could effectively be considered as being independent of each other. On the other hand, if only the central element of the five was made of gold and the other four of a very flexible material, then the form of the connection between the two teeth would resemble that of a pin joint, i.e. a joint through which no bending moment can be transmitted.

The object here was to determine the force distributions occuring on the periodontal membranes of abutment teeth used in

bridgework. Because of the lack of mechanical property data for the periodontal membranes of teeth subjected to masticatory levels of loading, the mechanical properties of the membrane associated with orthodontic levels of loading were employed. Hence, the membrane mechanical properties derived earlier in Chapter Six were adopted. Thirty gramme point loads were applied to the structure in turn, at the three positions indicated in FIG. 10.10, i.e. the stations marked by 1, 2 and 3 respectively. However, for each of these three load positions, different forms of connection between the two abutment teeth were examined.

For all the experiments in this series, the nodes lying on the perimeter of the alveolar process, shown cross-hatched in FIG. 10.10, were rigidly held by restraining them in both the X and Y co-ordinate directions.

### 10.3.2 Results

The elements representing the areas of the dentine, gold and cancellous bone in the model were ascribed the appropriate isotropic mechanical properties listed in TABLE 3.7, and the cortical bone elements the orthotropic properties derived in Chapter Six. Although the loads applied at the positions labelled 2 and 3 in FIG. 10.10 are not purely axial, because no membrane data was available concerning the tooth mobility under these conditions of loading, the axial properties of the tissue derived in Chapter Six were employed.

In the first series of experiments, the five elements connecting the first and second premolars were made very soft, i.e. given very small stiffness coefficients. Hence, the second premolar could therefore be considered as being 'free'

and independent of its neighbour. The thirty gramme vertical load was applied in turn, at the three positions shown in FIG. 10.10 and the resulting nodal force distributions on the periodontal membrane determined. These are plotted in the FIGS. 10.11 to 10.13.

For the second series of experiments, the five connecting elements between the two premolars were given the mechanical properties of the gold crown material. Consequently, the two teeth were therefore rigidly connected or 'splinted' together. The 30 gm. vertical load was then applied in sequence at the three positions as before and the periodontal membrane force distributions (this time for both teeth), obtained. These are depicted in FIGS. 10.14 to 10.16.

In the final experiment with this bridge model, an attempt was made to see what effect a pin type connection between the two teeth would have on the periodontal membrane's force distribution. This was achieved by simply ascribing the very narrow centre element of the five connecting elements the mechanical properties of gold, while the four remaining connecting elements were made very soft. It was hoped that this simulation, while allowing shear forces to be transmitted across the joint, would prevent any bending moments from being transferred. The structure was loaded by a single 30 gm. point load which was applied at the station 3. The resulting periodontal membrane force distribution for this configuration is illustrated in FIG. 10.17.

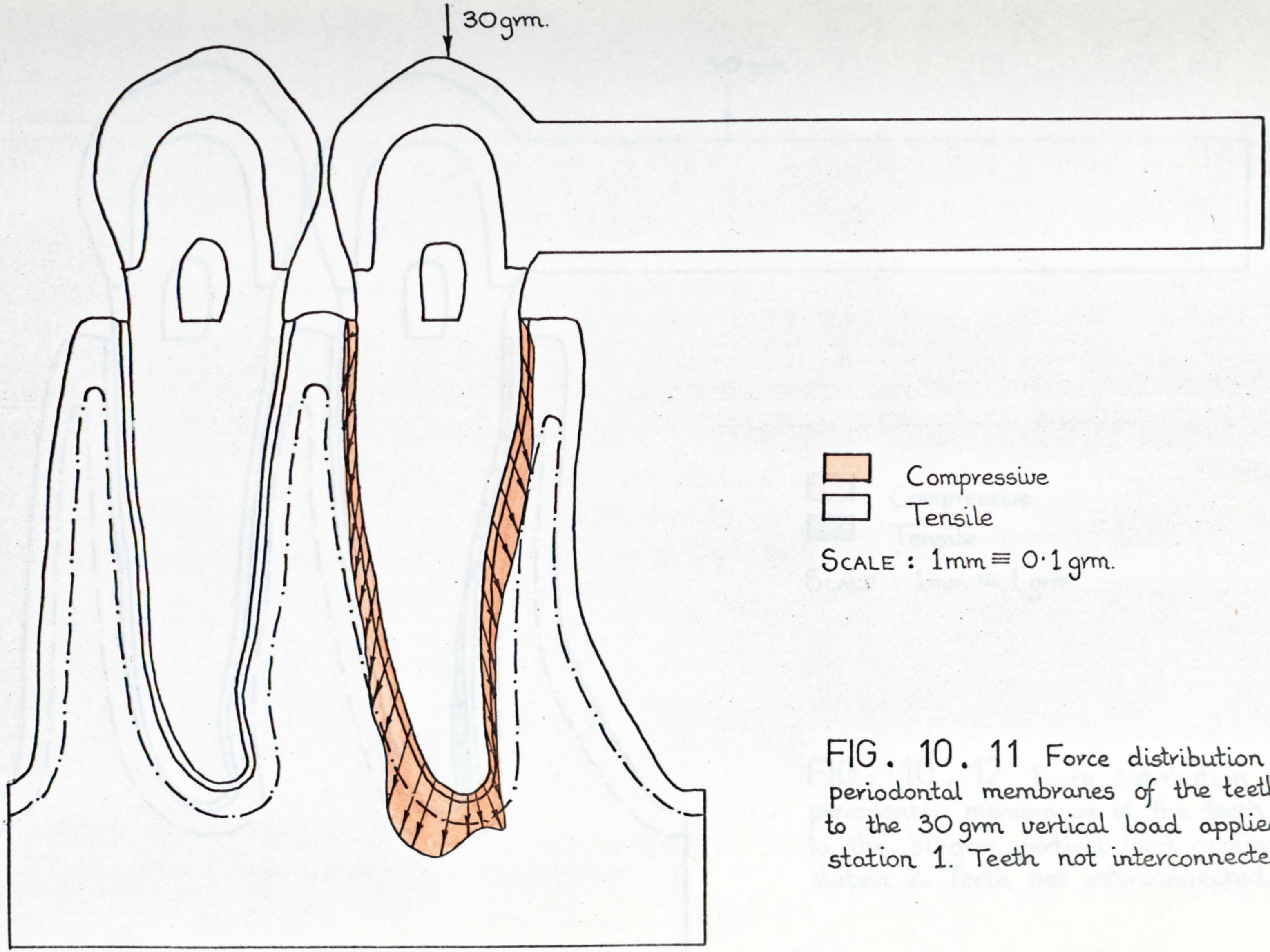


FIG. 10. 11 Force distribution on the periodontal membranes of the teeth due to the 30 grm vertical load applied at station 1. Teeth not interconnected.

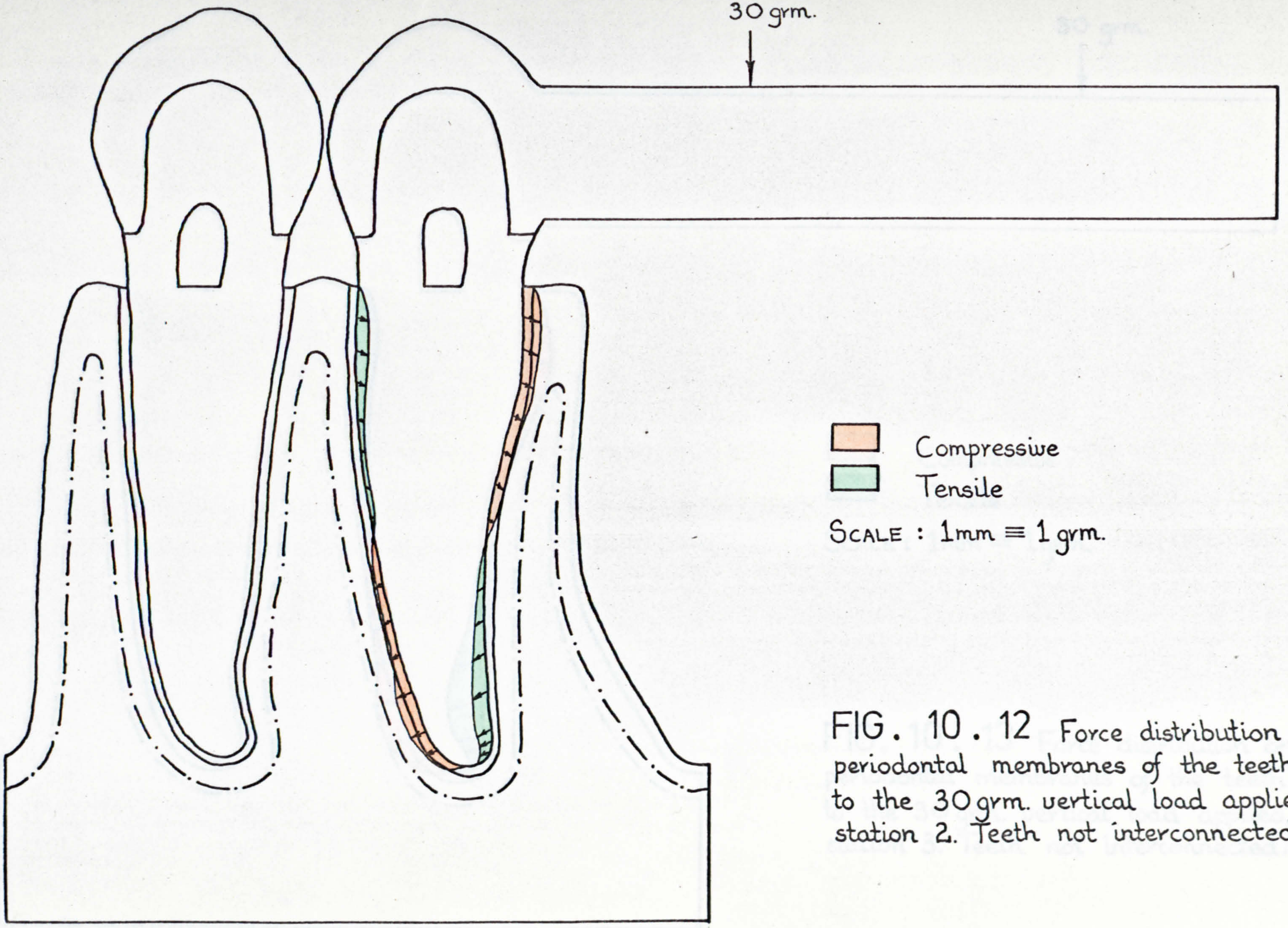


FIG. 10.12 Force distribution on the periodontal membranes of the teeth due to the 30 grm. vertical load applied at station 2. Teeth not interconnected.

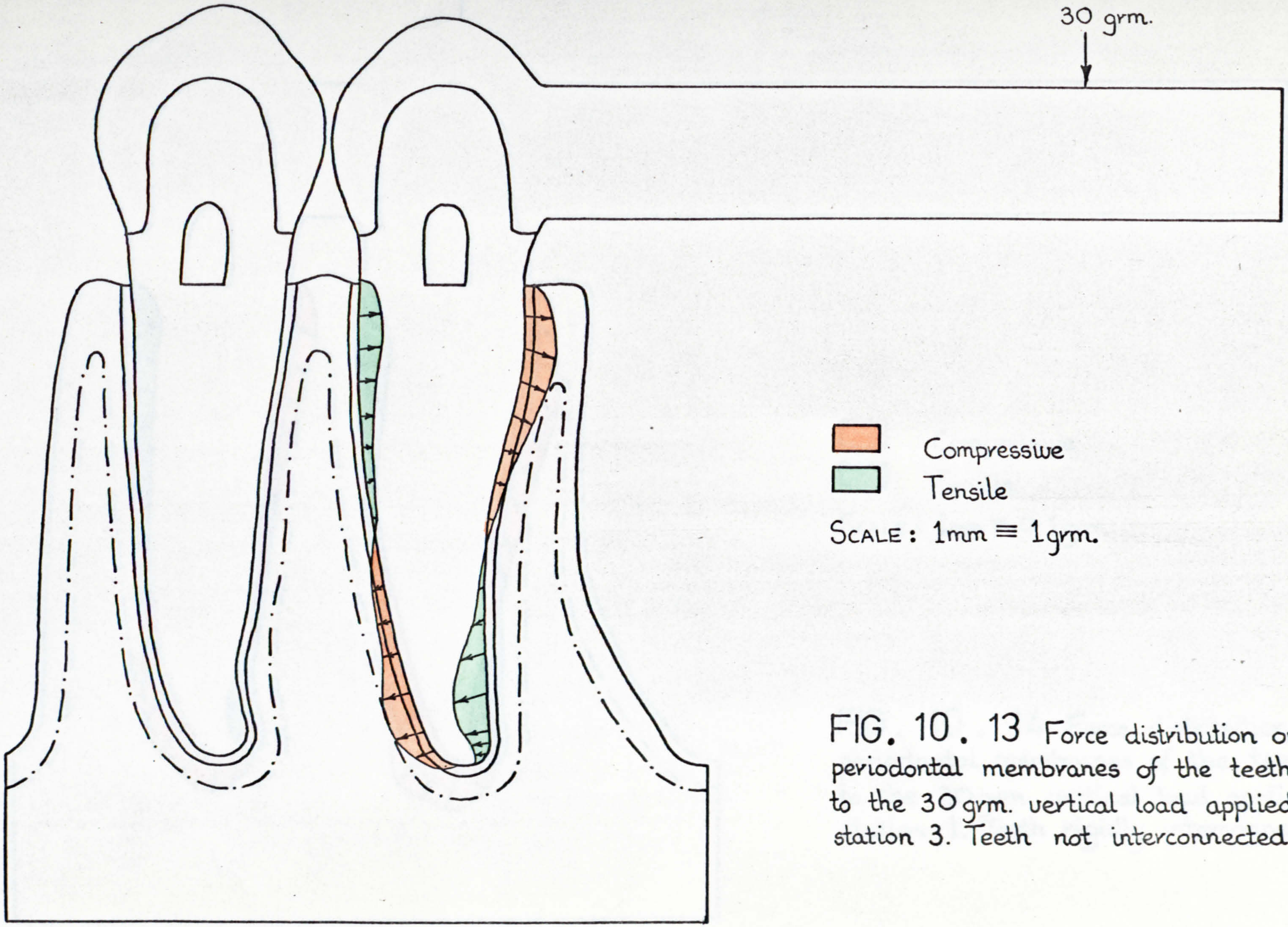


FIG. 10.13 Force distribution on the periodontal membranes of the teeth due to the 30 grm. vertical load applied at station 3. Teeth not interconnected.

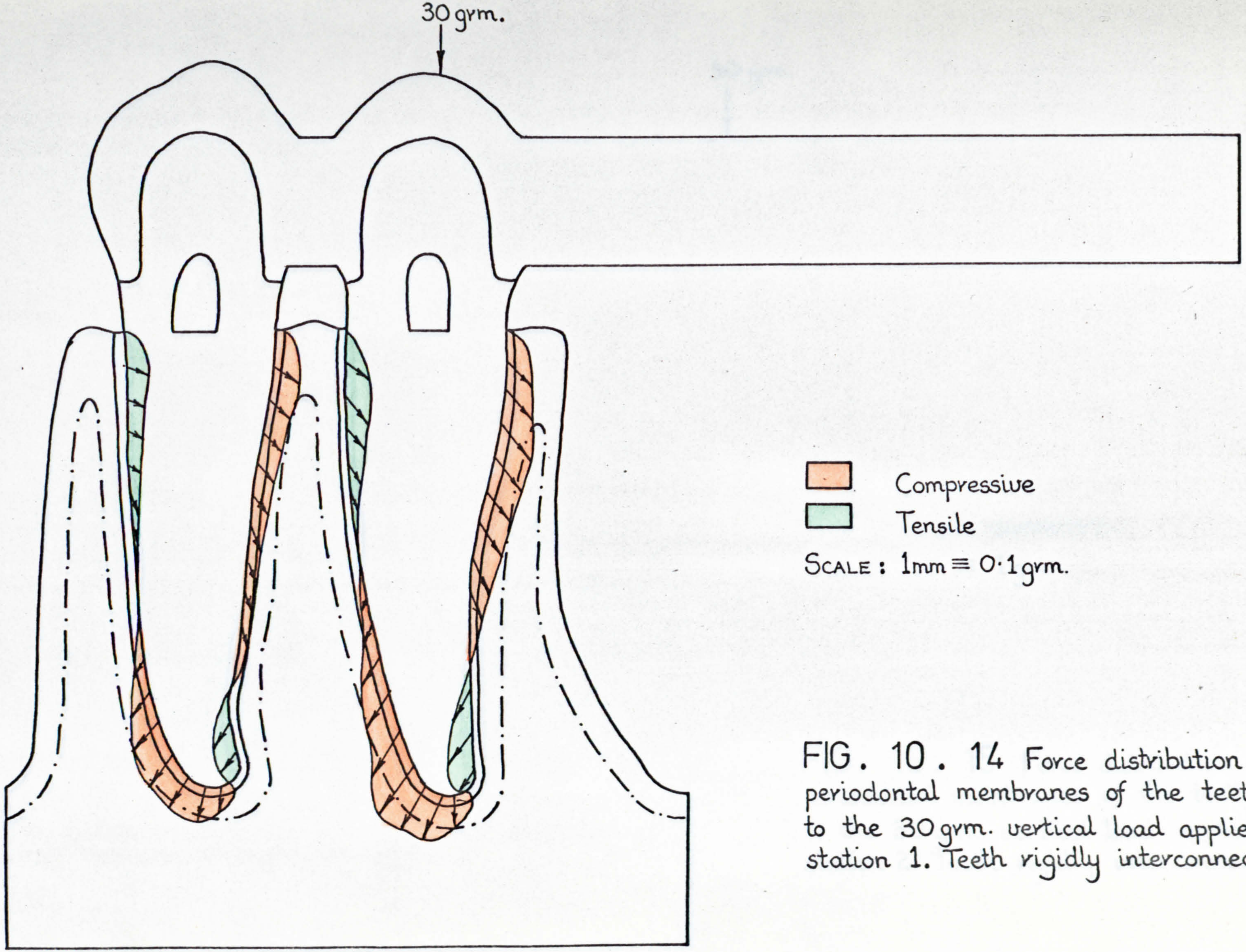


FIG. 10. 14 Force distribution on the periodontal membranes of the teeth due to the 30 grm. vertical load applied at station 1. Teeth rigidly interconnected.

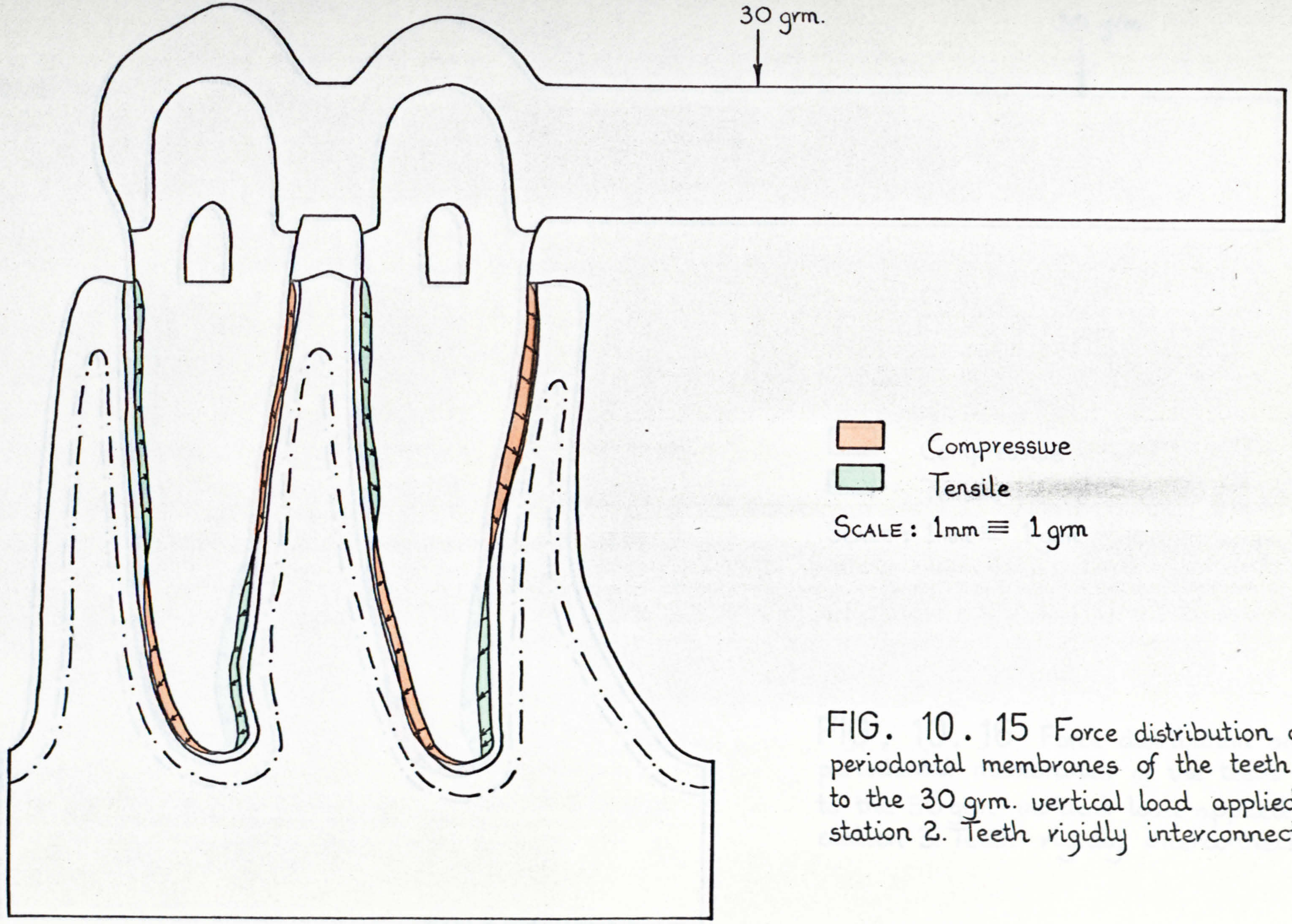


FIG. 10. 15 Force distribution on the periodontal membranes of the teeth due to the 30 grm. vertical load applied at station 2. Teeth rigidly interconnected.

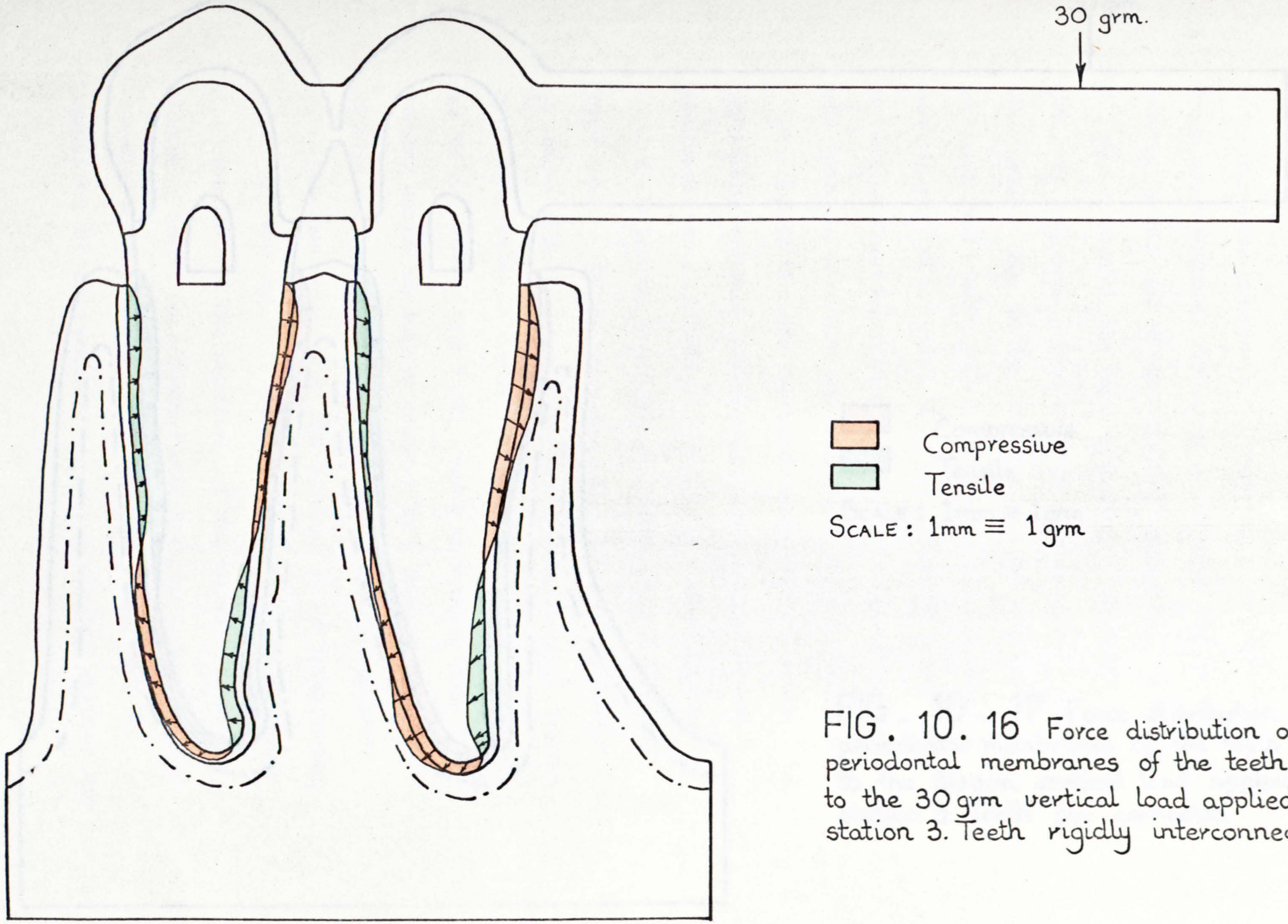


FIG. 10. 16 Force distribution on the periodontal membranes of the teeth due to the 30 grm vertical load applied at station 3. Teeth rigidly interconnected.

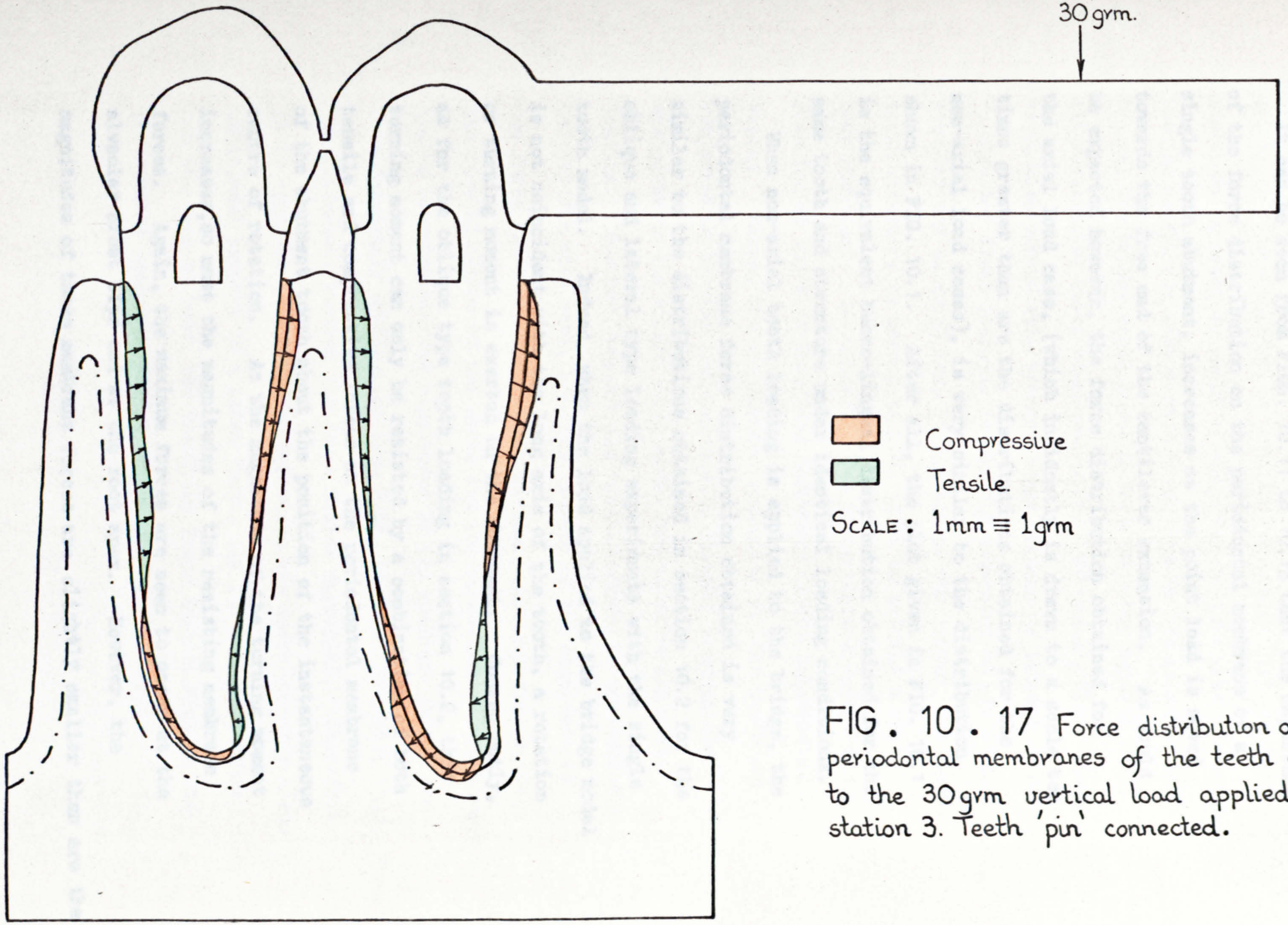


FIG. 10.17 Force distribution on the periodontal membranes of the teeth due to the 30 grm vertical load applied at station 3. Teeth 'pin' connected.

### 10.3.3 Discussion of Results

It can be seen from FIGS. 10.11 to 10.13 that the magnitude of the force distribution on the periodontal membrane of a single tooth abutment, increases as the point load is moved towards the free end of the cantilever extension. As would be expected however, the force distribution obtained for the axial load case, (which incidently is drawn to a scale ten times greater than are the distributions obtained for the non-axial load cases), is very similar to the distribution shown in FIG. 10.1. After all, the plot given in FIG. 10.1 is the equivalent bucco-lingual distribution obtained for the same tooth and structure under identical loading conditions.

When non-axial tooth loading is applied to the bridge, the periodontal membrane force distribution obtained is very similar to the distributions obtained in section 10.2 for the oblique and lateral type loading experiments with the single tooth model. Indeed, when the load applied to the bridge model is not coincident with the long axis of the tooth, a rotation or turning moment is exerted on the abutment. Consequently, as for the oblique type tooth loading in section 10.2, this turning moment can only be resisted by a combination of both tensile and compressive forces on the periodontal membrane of the abutment tooth about the position of the instantaneous centre of rotation. As the magnitude of the turning moment increases, so must the magnitudes of the resisting membrane forces. Again, the maximum forces are seen to occur at the alveolar crest tips and at the root apex. However, the magnitudes of these membrane forces are slightly smaller than are the

ones obtained for the oblique and lateral load cases for the single tooth model, compare FIGS. 10.12 and 10.13 with FIGS 10.2 and 10.3. Nevertheless, it must be remembered that the bridge structure in practice would be subjected to much more stringent loading conditions than were imposed here in the experiments. In use, the bridge would probably have to carry several point and distributed loads simultaneously. Of course, these loads would also undoubtedly involve large oblique or lateral components.

When the first premolar is rigidly connected to the second premolar and an axial load is applied to the latter, the double tooth structure is seen from FIG. 10.14 to undergo a rigid body rotation. Consequently, the instantaneous centre of rotation of the structure lies somewhere in the interdental septum. Hence, the periodontal membranes of both teeth are subjected to tensile and compressive forces; a situation analogous to the single tooth model subjected to non-axial loading. However, because the turning moment is considerably smaller for this case, i.e. the product of the magnitude of the force and the perpendicular distance measured from between the line of action of the force and the structure's instantaneous centre of rotation, the magnitudes of the membrane forces are correspondingly smaller, compare FIGS. 10.2 and 10.3 with 10.4. (Note the difference between the force scales employed). Therefore, it is apparent that although splinting two teeth together gives additional support to a loose tooth, say the second premolar for the case at hand, the resulting force distribution on the periodontal membranes will be of an undesirable form.

The two-teeth abutment arrangement for the bridge loaded at either positions 2 or 3, can be seen to be beneficial on comparing FIGS. 10.15 and 10.16 with FIGS 10.12 and 10.13. Indeed, the turning moment applied to the bridge is, for these cases, resisted by both the abutment teeth. Consequently, the magnitudes of the membrane forces on any one tooth are therefore considerably smaller than they would have been had only one abutment tooth been employed, compare FIGS. 10.13 and 10.16.

The periodontal membrane force distribution obtained for the pin connected simulation, see FIG. 10.17, shows little difference to the distribution shown for the equivalent rigidly connected structure in FIG. 10.16. However, the reason for this is probably because the magnitude of the loading considered here was very small. Hence,the 'pin connection' was sufficiently stiff such that it behaved simply as a rigid connection.

## 10.4 STRESS DISTRIBUTIONS AROUND AN ENDOSSEOUS PIN IMPLANT

In order to avoid the use of dentures or plates, dental implants are increasingly being employed as an alternative means of 'artificial' tooth fixation. A dental implant can be considered as being a device which is constructed from a non-biological material and is embedded in the living tissues. However, the term dental implant is usually considered to imply the particular types of devices which are either driven or screwed into the alveolar processes. It is these devices or implants that are employed to form abutments for the

"artificial" teeth*.

Generally speaking, dental implants which are driven into the bone can be either in the form of a pin or a blade, see FIG. 4.4. Being constructed from metal, the pin or blade implant is very much stiffer than either the cortical or the cancellous tissue. Consequently, when masticatory forces are applied to the artificial tooth superstructure, stress concentrations inevitably occur in the alveolar bone. This is a consequence of the uneven load transfer which occurs across the interfaces of materials having vastly different stiffness moduli. Hence, the aim of this section was to investigate the type of stress distribution which occurs around a single pin implant when it is subjected to a typical turning moment type of loading.

10.4.1 Finite Element Model and Test Procedure

The finite element model employed for this series of experiments was a two-dimensional slice section of an area of cortical and cancellous tissue which, contained in its centre a parallel pin implant, see FIG. 10.18. It can be seen from this figure, that the finite element mesh was arranged such that it was a relatively easy matter to change the configuration of the model. For instance, the thickness of the cortical bone skin could be changed by simply ascribing the cortical bone mechanical properties

* Research workers are currently investigating the use of porous materials for dental implants. Such materials would encourage the ingrowth of the biological tissues into the pores of the implant and would thereby provide a much more efficient and stable fixation.

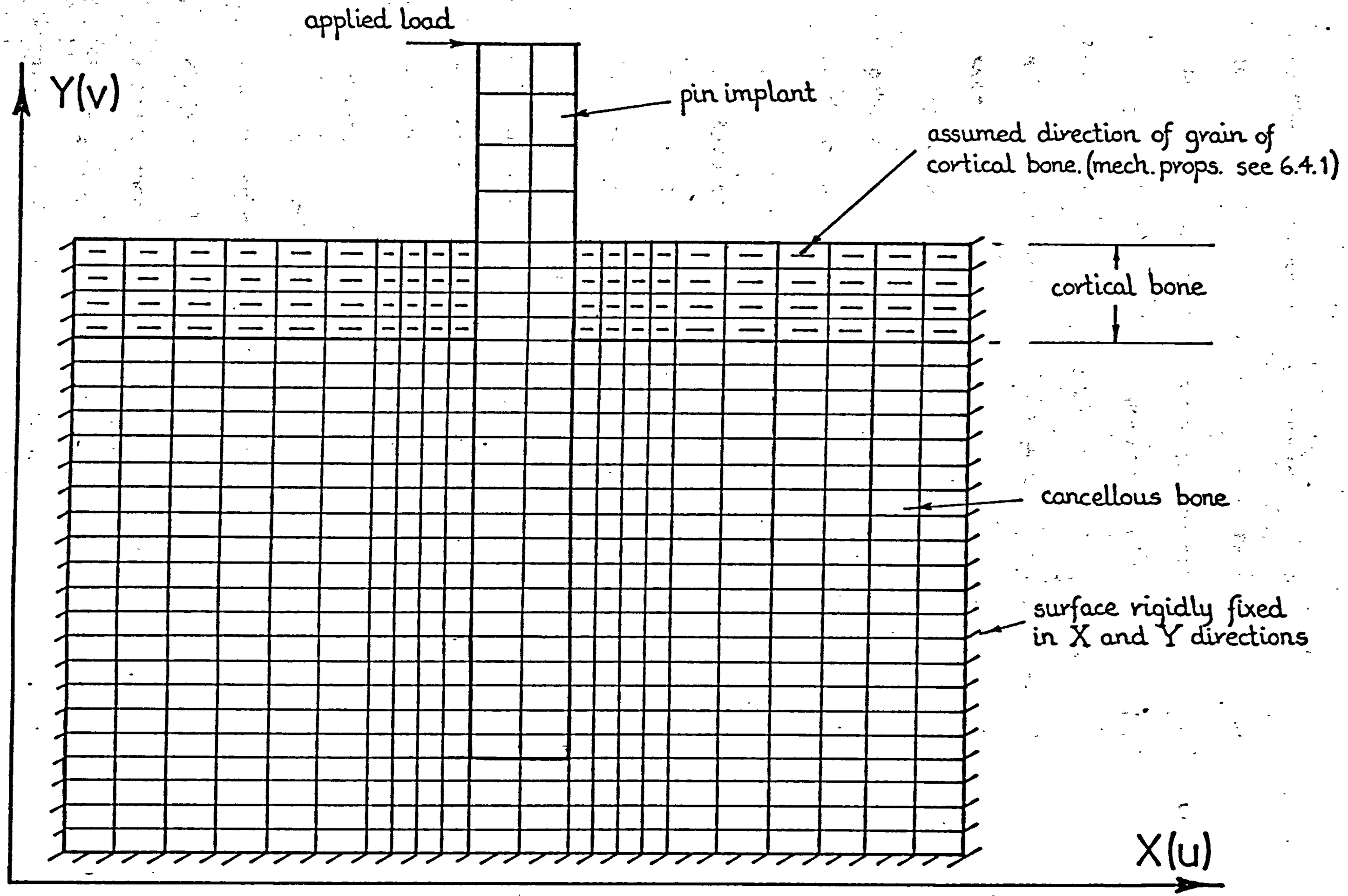


FIG. 10.18 2-D slice section model of endosseous pin implant and the supporting alveolar process. (558 elements.)

to the appropriate element layers. The direction assumed for the grain of the cortical tissue is again indicated by the lines shown in the centres of the cortical bone elements, see FIG. 10.18. This figure also clearly shows the pin implant which was constructed 2 mm wide. Finally, as with all the other two-dimensional models, the whole structure was ascribed the equivalent model slice thickness of 0.345 inches.

In order to subject the structure to the turning type of loading which proved so severe for the natural tooth models analysed earlier, a single laterally directed point load was applied to the 'free' end of the pin as illustrated in FIG. 10.18. This type of loading could be envisaged to occur when the 'artificial' tooth superstructure, attached to the pin implant, is itself subjected to an oblique or laterally directed load.

It can be argued that the bone surrounding a dental implant is under compression and that it is these reactive stresses generated by the bone, which retain the implant in position. Undoubtedly, the bone applies some retaining influence on the implant even though in some cases the cortical bone is cut with a dental burr before the implant is inserted. However, it can also be argued that the bone can react to these concentrated stresses by local resorption around the implant and thereby relieve some or all of these compressive stresses. Therefore, it is impossible to estimate the form and magnitude of the local compressive stresses which are generated in the alveolar bone as a result of inserting the implant. Consequently, in the analyses here, they have been ignored completely. Indeed, the implant and supporting tissues have been assumed to be completely stress-free prior to the application of the apical load.

For all the experiments which were carried out using this model, the boundary or perimeter nodes lying within the bone tissue were all constrained in both the X and Y Cartesian co-ordinate directions.

### 10.4.2 Results

The finite elements representing the cancellous tissue were ascribed the appropriate isotropic mechanical properties listed in Table 3.7. However, the cortical bone was assumed to be an orthotropic material and was therefore ascribed the orthotropic properties derived in Chapter Six. The final component in the structure was the pin implant. This was assumed to be made from surgical stainless steel type 316 S12, see BS3531 (1968), and was consequently ascribed the modulus of elasticity given in this publication. Although the other mechanical properties required for the analyses were not given, a Poisson's ratio value of 0.3 was assumed; a value typical for stainless steels. Consequently, because stainless steel is an isotropic material, the shear modulus was determined using the familiar property relationship $G = \frac{E}{2(1+\mu)}$

For the first analysis, the cortical bone skin was assumed to be 1 mm thick. The normal stress distribution on the alveolar process resulting from the application of the single horizontally applied load is shown in FIG. 10.19. However, it must be pointed out here how this particular stress distribution was obtained.

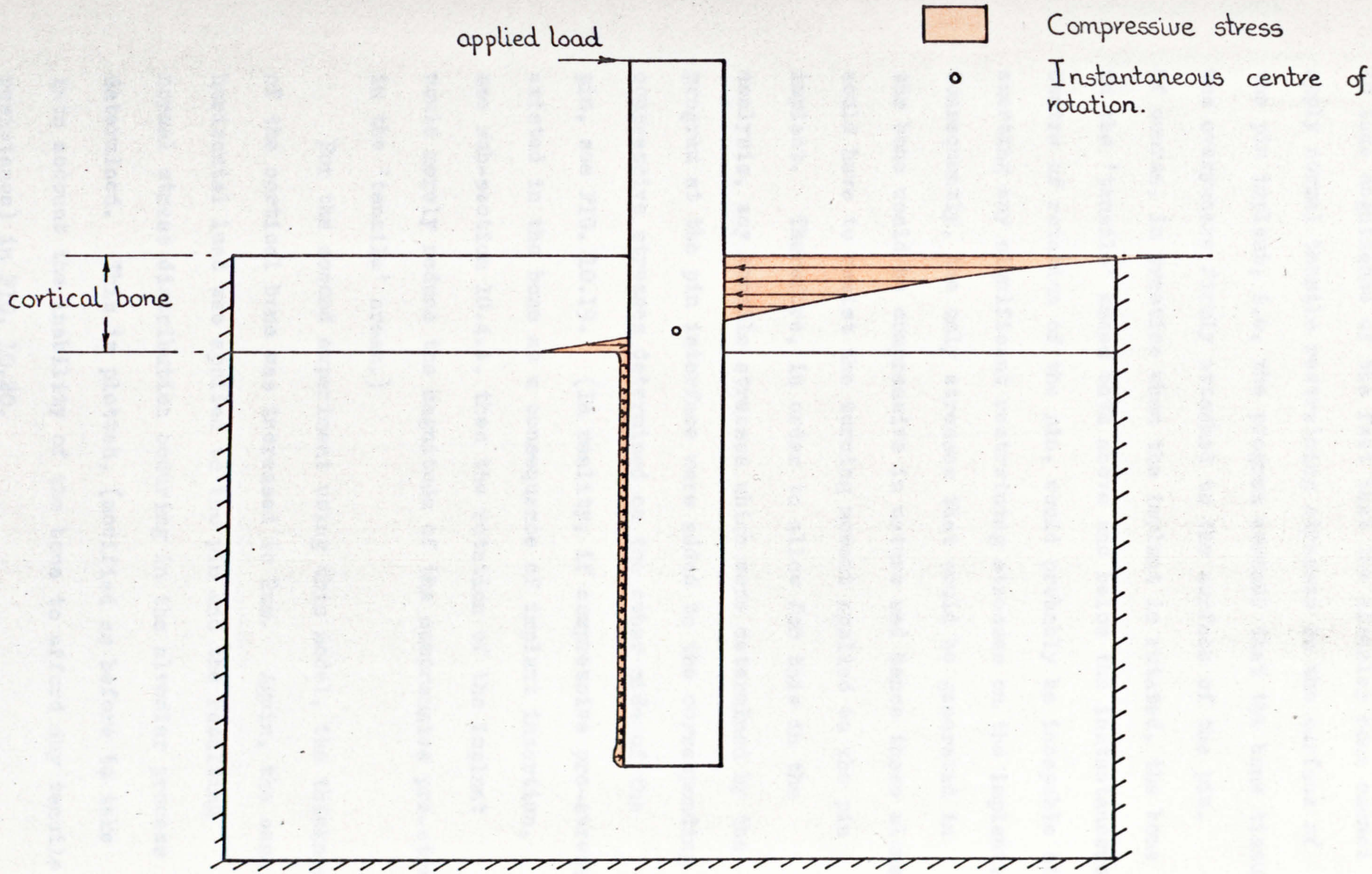


FIG. 10. 19 Normal stress distribution on the alveolar process as a consequence of applying a lateral load to the pin implant. Cortical bone 1mm thick.

The finite element analysis program employed was unable to take cognizance of the fact that the alveolar bone cannot apply normal tensile restraining stresses to the surface of the pin implant, i.e. the program assumed that the bone tissue was everywhere firmly attached to the surface of the pin. Of course, in practice when the implant is rotated, the bone in the 'tensile' areas both above and below the instantaneous centre of rotation of the pin, would probably be incapable of exerting any significant restraining stresses on the implant. Consequently, the only stresses that would be generated in the bone would be compressive in nature and hence these alone would have to resist the turning moment applied to the pin implant. Therefore, in order to allow for this in the analysis, any tensile stresses which were determined by the program at the pin interface were added to the corresponding compressive stresses determined on the other side of the pin, see FIG. 10.19. (In reality, if compressive pre-stress existed in the bone as a consequence of implant insertion, see sub-section 10.4.1, then the rotation of the implant would merely reduce the magnitude of the compressive pre-stress in the 'tensile' areas.)

For the second experiment using this model, the thickness of the cortical bone was increased to 2mm. Again, the same horizontal load was applied to the pin and the resulting normal stress distribution occuring in the alveolar process determined. This is plotted, (modified as before to take into account the inability of the bone to afford any tensile resistance) in FIG. 10.20.

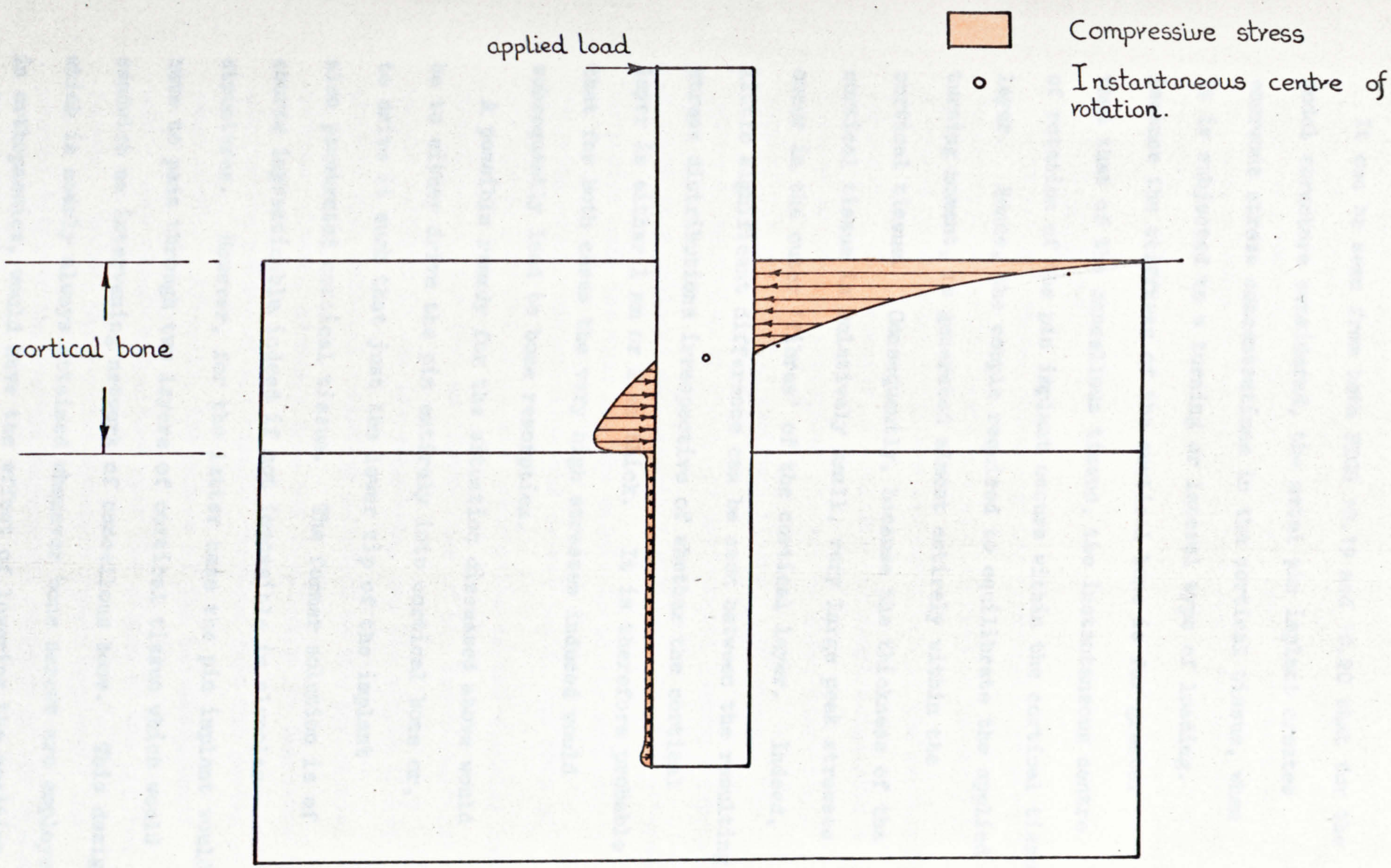


FIG. 10. 20 Normal stress distribution on the alveolar process as a consequence of applying a lateral load to the pin implant. Cortical bone 2mm thick.

### 10.4.3 Discussion of Results

It can be seen from both FIGS 10.19 and 10.20 that for the model structure considered, the metal pin implant creates enormous stress concentrations in the cortical tissue, when it is subjected to a turning or lateral type of loading. Because the stiffness of the cortical bone is far greater than that of the cancellous tissue, the instantaneous centre of rotation of the pin implant occurs within the cortical tissue layer. Hence, the couple required to equilibrate the applied turning moment, is generated almost entirely within the cortical tissue. Consequently, because the thickness of the cortical tissue is relatively small, very large peak stresses occur in the outer 'fibres' of the cortical layer. Indeed, little significant difference can be seen between the resulting stress distributions irrespective of whether the cortical layer is either 1 mm or 2 mm thick. It is therefore probable that for both cases the very high stresses induced would subsequently lead to bone resorption.

A possible remedy for the situation discussed above would be to either drive the pin entirely into cortical bone or, to drive it such that just the lower tip of the implant also penetrated cortical tissue. The former solution is of course impracticable, indeed if not impossible in alveolar structures. However, for the latter case the pin implant would have to pass through two layers of cortical tissue which would sandwich an intervening network of cancellous bone. This design, which is nearly always attained whenever bone screws are employed in orthopaedics, would have the effect of lowering the position

of the instantaneous centre of rotation of the pin such that it would occur somewhere between the two cortical bone layers. Thus, the necessary reacting couple required would be generated with the lever arm a greater distance apart and therefore the peak stresses in the cortical bone would be considerably reduced.

## 10.5 CONCLUSIONS:

With natural dental structures the orthodontic or masticatory forces applied to the teeth are equilibrated or balanced by a system of stresses which are generated within the periodontal membrane. Consequently, a complete and complicated stress pattern is created throughout the entire three-dimensional form of the periodontal membrane tissue. Of course, the nature or mechanism by which the periodontal membrane supports a tooth is a critical and important factor. It will afterall, determine both the type and the magnitude of the membrane's reacting stress distribution and consequently, the form of the stress patterns which are transmitted to the alveolar bone. Nevertheless, the obvious limitations of the two-dimensional models employed in the investigation, and the simple linear elastic type material behaviour ascribed to the periodontal membrane tissue, probably does not invalidate the character or qualitative nature of the results obtained from the series of experiments. Afterall, the planes of the two-dimensional models were always coincident with the planes of the applied forces. Hence, the results obtained should represent the general trend of the overall mechanical response of the equivalent dental structure.

The generally held view that the natural teeth are 'designed' to carry only axial type loading was substantiated by the experiments. It can be seen from the axial load plots, namely FIGS 10.1, 10.4 and 10.7, that the magnitudes of the resulting force distributions occuring on the periodontal membranes are more uniform and considerably smaller than those obtained for the non-axial or oblique type loading conditions. The reason for this, is that for the axial loads, the whole membrane is under compression. Consequently, each small piece of the tissue reacts a small portion of the occlusally applied load. However, when a load of the same magnitude is applied obliquely, the membrane not only has to react the same load but also has to equilibrate a large turning moment as well. The turning moment is reacted by the membrane generating a couple about a point called the instantaneous centre of rotation of the tooth. This couple or push-pull system of forces, is probably the result of the periodontal membrane generating alternate regions of tensile and compressive stresses above and below the instantaneous centre of rotation. However, the ability of the membrane to generate both compressive and tensile resistances, depends upon the nature of its structure and on its support mechanism. Nevertheless, it is clearly seen from the figures that the peak or maximum forces acting on the membrane occur in the alveolar crest tip and root apex regions. Therefore, if the periodontal membrane is only capable of generating either tensile or compressive resistances, then the magnitudes of the stress or force patterns would be considerably increased. Hence, it is apparent from the analyses that teeth should be

preferably subjected to only axial forms of loading and that oblique or lateral loads should be kept to a minimum.

When the level of the supporting alveolar bone is reduced, the magnitude of the reacting forces of the periodontal membrane to the same occlusally applied loads, considerably increases. (This was seen to be so, even for the axial load cases). Therefore, if bone destruction is a consequence of the high stress concentrations generated in the periodontal membrane, then once initiated the resorption process would gather momentum as the height of the supporting bone decreased. Hence, excess lateral forces may perhaps be instrumental in a tooth becoming loose and subsequently in its eventual loss.

Although the bridge model investigated was perhaps a rather unrealistic representation of a clinical reconstruction, the results showed several definite features which have a direct clinical significance. The force patterns which occured on the periodontal membranes of the abutment teeth for non-axial tooth loading of the bridge, are indeed very similar to those obtained for the oblique load cases on the single tooth model. This was true whether one or two teeth were employed for the bridge abutment. However, because the bridge structure would be subjected to more severe loading than would a single normal tooth, the magnitude of the membrane forces would consequently be far greater. Therefore it is apparent, purely from the mechanical standpoint, that a cantilever bridge having an overhang greater than one tooth would not be a viable clinical proposition.

When two teeth are 'splinted' together; say to provide extra support for a loose tooth, the instantaneous centre of rotation of the combined structure occurs somewhere within the interdental septum. Consequently, both teeth are effectivelyrotated when either tooth is simply subjected to a pure axial type load. However, because of the position of the instantaneous centre of rotation of the structure, the magnitude of the turning moment which can result from this situation is relatively small. In fact, due to the position of the instantaneous centre of rotation, the turning moment which can be produced when either tooth in the structure is subjected to an oblique type load could be very small indeed and sometimes, even zero. (This occurs when the line of action of the load passes through the instantaneous centre of rotation of the structure.) Therefore, it can be concluded that the procedure of splinting two teeth together is, from the mechanical point of view, a very desirable practice.

It is concluded from the endosseous pin experiments that this type of implant should never be employed. Although in clinical practice three pins are usually deployed in a tripod arrangement, it is difficult to see how they can react normal masticatory forces without creating enormous stress concentrations in the cortical alveolar bone. This type of implant could in fact only function satisfactorily provided that it is either embedded completly within cortical tissue or, is implanted such that it is supported in cortical tissue in at least two points which are a considerable distance apart. However, because of the very nature and configuration of the alveolar processes, it is very difficult to see how this can be achieved.

# CHAPTER ELEVEN

## SUMMING UP AND GENERAL CONCLUSIONS

# 11 SUMMING UP AND GENERAL CONCLUSIONS

It was shown in Chapter Five that unless the relative stiffnesses of the materials comprising multi-material structures are accurately simulated, completely erroneous results can be obtained. Consequently, it is difficult to see how the results obtained from composite photoelastic model analyses employing materials having ''unmatched'' mechanical properties, can be anything but misleading.

When human cortical bone is considered to be a linear elastic orthotropic material and it is assumed that the mechanical properties are equal in directions mutually perpendicular to the osteon direction, five independent constants are required to describe its mechanical behaviour. Although only three of these constants have been documented, it was possible using the finiteelement method, to simulate some of the published work and to obtain estimates of the other two hitherto unknown properties. These were found to be, see legend in Table 6.1,

$$G_{yz} = 1 \times 10^{6} \text{ p.s.i.}$$

$$\text{and } \mu_{zy} = -0.499$$

It is apparent that the force versus displacement response curves of a human maxillary central incisor, present a similar non-linear form of characteristic for both intrusive (axial) and labio-lingual (lateral) tooth movements. There are also indications that the periodontal membrane flows or creeps

under continous loading. Nevertheless, by simulating published tooth mobility experiments using equivalent finite element models, estimates of pseudo linear elastic isotropic mechanical properties for the periodontal membrane under conditions of light static intrusive and lateral loading were determined. These were found to be:-

30gm intrusive loading $E = 8.7$p.s.i., $\mu = 0.3$

30gm lateral loading $E = 26.1$p.s.i., $\mu = 0.3$.

It was therefore concluded that the periodontal membrane must exhibit some degree of anisotropy in order to compensate for this apparent 3:1 difference in the stiffness required for these conditions of loading. The anisotropy was investigated in an attempt to examine the fibre support theory, by representing the periodontal membrane in the finite element models as an orthotropic material. However, these studies proved inconclusive due to the inadequacy of the finite element representation and to the lack of the experimental physical data available. Nevertheless, it was apparent from the finite element experiments that for the level of loading considered, nearly all of the tooth movement occurs within the tooth socket. This is contrary to the view held by some authors, who believe that the tooth displacement is due mainly to the deflection of the alveolar bone.

The tooth enamel, being very much stiffer than the underlying dentine, reacts masticatory type loads by transmitting the forces around the enamel cap, as shown in FIG.7.8. Consequently, very high compressive stresses are induced in the diminishing wedge of enamel tissue at the amelo-cement$_{al}$ junction and therefore restorations placed in the cervical

region of teeth would be affected by these stresses.

The wedging type action of occlusion induces very high tensile stress concentrations in the fossae of teeth. This, therefore tends to separate the enamel prisms in this area in normal teeth, and to open up the margins of restorations placed on the fossa aspect of the intercuspation contact points. This finding suggests that it would be beneficial from the mechanical standpoint if restorative margins were not positioned in this high tensile stress region.

It was also shown in Chapter Seven that gold, (because it has a very similar stiffness to that of enamel), is mechanically an excellent restorative material in that it behaves in a manner similar to that of the enamel tissue. However, when a material of a much lower stiffness is employed to replace the enamel, such as for example an acrylic or an epoxy resin, the masticatory forces are not transmitted around the cap in the normal manner and so the underlying dentine is subjected to abnormally high stresses.

For cast gold full crown restorations, it was found that it was beneficial mechanically if the cusps on the restoration were 'reduced'. This practice would tend to lessen the magnitude of any turning type forces on the restoration and would therefore help to protect the integrity of the proximal margins.

A minimum setting expansion of 10 microns per centimetre length should be adopted for all amalgam restorations. This value, which is substantially higher than the minimum value generally recommended, would reduce the possibility of marginal breakdown occurring due to the contraction of the restoration upon cooling. In addition, because of the very high stresses

induced in the occlusal margins of class I type amalgam restorations as a consequence of the setting and differential thermal expansion of the restorative material, these margins must be designed to have the maximum strength characteristics.

It was shown using the three-dimensional finite element model, that the instantaneous centre of rotation of a maxillary central incisor occurs at approximately 50% of the root apex to alveolar crest height distance when the tooth is loaded by a removable type of appliance. Although this finding is in agreement with some very recent work reported by Stephens (91), this challenges the generally held view that the position occurs nearer to the root apex at about 33% of the total apex to crest distance.

The position of the instantaneous centre of rotation of the incisor, depends primarily upon the height of the supporting alveolar bone and upon the overall flexibility of the periodontal membrane. For higher alveolar crest tips and a stiffer periodontal membrane, the further the position of the instantaneous centre of rotation moves from the root apex. Consequently, because the stiffness of the membrane is non-linear and is probably dependent upon the magnitude of the applied loading, the position of the instantaneous centre of rotation is undoubtedly dependent on the magnitude of the orthodontic forces applied.

Although with a constant alveolar bone height, the position of the instantaneous centre of rotation of the tooth moved in phase with the position of the point at which a purely lateral load was applied, the overall variation

was found to be very small. However, when the direction of the orthodontic force was applied,normal to the enamel surface, locations on the crown of the tooth were found at which the resulting position of the instantaneous centre of rotation occurred completely outside the root of the tooth.

Although the finite element models employed for the malaligned femur and the tooth socket analyses were limited, the results failed to show any consistent correlation to exist between a particular mechanical stimulus and the corresponding clinically observed biological remodelling response. Indeed, of the three bone remodelling hypotheses examined, only Currey's theory may possibly correlate for the two cases considered. However, a definitive comment on Currey's theory must necessarily appear inconclusive as it is not clear what this author implies by the term 'net stress'. This is important as this term forms the keystone to Currey's hypothesis.

Bassett's theory that bone deposition occurs in areas of compression,and resorption in areas of tension,was shown not to hold even if the theory was restricted to periosteal bone surfaces. Similarly, because surface curvature changes were found to be highly dependent upon the bone grain orientation, Epker and Frost's theory that bony deposition only occurs in areas which become more concave under load, was also considered to be suspect. Although the effect of the bone grain has frequently been ignored in the literature,it was apparent from the analyses that the osteon direction could play a significant role in the tissue remodelling response. It is considered that this would be particularly important

if the regulating mechanism is proved to be one of an 'electrical' nature.

In view of the fact that the type and magnitude of the loading applied to the two structures is completely different, it is suggested that the bone remodelling regulating mechanism may be due to two different phenomena for the cases considered. In addition, it is proposed that it is extremely doubtful whether the single force generally considered to be acting in the case of the malaligned long bone is the primary and/or only stimulus in the remodelling process. It is suggested that the stimulus could arise from quite small muscle forces which could be created due to the rearrangement of the tissues as a direct result of the malalignment.

It was shown that the tooth supporting structures are best equipped to react vertical or axial tooth loads. When either oblique loads to a single tooth or offset loads to a cantilever type bridge construction are applied, high stress concentrations are created in the periodontal membrane. This is because of the necessity of equilibrating the considerable turning moments. Consequently, it is apparent that turning moments applied to teeth must be kept to a minimum. Indeed, if the stress concentrations created by the turning moments are responsible for alveolar bone resorption, then once initiated,the process will escalate as a lowering of the crest tips will accentuate the level of the stress concentrations. However, the splinting of two teeth together will help to distribute the stresses created by any turning moments and will therefore provide added support.

Very high stress concentrations are created in the cortical bone of the alveolar process when an endosseous pin implant is subjected to lateral type loading. Consequently, it is concluded, that this type of implanted device should never be employed for transmitting masticatory forces to the alveolar processes.

# CHAPTER TWELVE

## SUGGESTED FURTHER RESEARCH IN DENTAL STRUCTURAL BEHAVIOUR

## 12 SUGGESTED FURTHER RESEARCH IN DENTAL STRUCTURAL BEHAVIOUR

Owing to the difficulties of obtaining a direct measurement of the value of $G_{zy}$, it is probable that the measurement of $\mu_{zy}$, offers the most reasonable approach of determining the unknown orthotropic mechanical properties of human cortical bone experimentally. The negative value obtained for $\mu_{zy}$ in the finite element experiments was surprising, and physically represents an unusual type of material behaviour. However, although this characteristic may be possible for biological materials, a direct measurement of this property would provide a very useful check on the value obtained here.

Further, more detailed studies are required to examine more carefully the fibre support theory of teeth. To achieve this, a full three-dimensional finite element analysis model is required which would allow the principal fibres of the periodontal membrane to accept only tensional type stresses. In addition, further tooth mobility studies are required to obtain more accurately the directions of the applied tooth forces and the corresponding tooth displacements on a three-dimensional basis. Indeed, in order to obtain the actual movement of the tooth due to a particular force, the displacement of the tooth should be measured simultaneously at two different positions. This data would enable more accurate orthotropic mechanical properties to be determined for the periodontal membrane. Consequently, it would then

be possible to examine further, the effects that various types of simulated orthodontic forces have on the position of the instantaneous centre of rotation.

The effect on the stress distribution in the crowns of normal teeth subjected to masticatory type loading as a result of imposing interdental contact restraints, could also be examined using the finite element method. This could be achieved by simply rigidly clamping the appropriate nodes on the enamel surface in the mesio-distal direction. Alternatively, a spring type element could be attached to these nodes which, by varying the stiffness coefficients, could allow a certain amount of flexibility or 'give' in this direction.

The design of full crown type restorations could also be investigated using the finite element method. In particular, the angulation of the axial walls and the shape and size of the proximal margins should be examined. The optimum design of the occlusal margins of Class 1 type amalgam restorations also warrants further study using a similar approach.

# SELECTED REFERENCES

## SELECTED REFERENCES


1. SKINNER, E.W. and PHILLIPS, R.W.
The Science of Dental Materials.
W.B. Saunders Co., 6th Ed. 1967.

2. SWANSON, S.A.V. and FREEMAN, M.A.R.
Is Bone Hydraulically Strengthened ?
Med. and Biol. Engng. 4 : 433-438, 1966.

3. McLEISH, R.D. and HABBOOBI, S.
Strain Gauge Techniques for Cadaveric Bone.
Engng. in Med. 1(2) : 36-40 and 47, 1971.

4. EVANS, F.G. and LEBOW, M.
Regional Differences in Some of the Physical Properties of the Human Femur.
J. App. Phys. 3 : 563-572, 1951.

5. TYLDESLEY, W.R.
The Mechanical Properties of Human Enamel and Dentine.
Br. Dent. J. 106(8) : 269-277, 1959.

6. STANFORD, J.W. et al.
Determination of Some Compressive Properties of Human Enamel and Dentine.
J.A.D.A. 57 : 487-495, 1958.

7. McELHANEY, J.H.
Dynamic Response of Bone and Muscle Tissue.
J. App. Phys. 21 : 1231-1236, 1966.

8. STANFORD, J.W., et al.
Compressive Properties of Hard Tooth Tissues and Some Restorative Materials.
J.A.D.A. 60 : 746-756, 1960.

9. CRAIG, R.G., et al.
Compressive Properties of Enamel, Dental Cements and Gold.
J. Dent. Res. 40(5) : 936-945, 1961.

10. HAINES, D.J.
Physical Properties of Human Tooth Enamel and Enamel Sheath Material Under Load.
J. Biomech. 1 : 117-125, 1968.

11. LEES, S. and ROLLINS, F.R.
Anisotropy in Hard Dental Tissues.
J. Biomech. 5 : 557-566, 1972.

12. PEYTON, F.A., et al.
Physical Properties of Dentine.
J. Dent. Res. 31 : 366-370, 1952.

13. CRAIG, R.G. and PEYTON, F.A.
Elastic and Mechanical Properties of Human Dentine.
J. Dent. Res. 37 : 710-718, 1958.

14. RENSON, C.E.
An Experimental Study of the Physical Properties of Human Dentine.
A Thesis submitted to the University of London for the degree of Doctor of Philosophy, November 1970.

15. DYMENT, M.L. and SYNGE, J.L.
The Elasticity of the Periodontal Membrane.
Oral Health (Toronto). 25 : 105-109, 1935.

16. McELHANEY, J.H., et al.
Mechanical Properties of Cranial Bone.
J. Biomech. 3 : 495-511, 1970.

17. WOOD, J.L.
Dynamic Response of Human Cranial Bone.
J. Biomech. 4 : 1-12, 1971.

18. KRAUS, H.
On the Mechanical Properties and Behaviour of
Human Compact Bone.
Advances in Biomedical Engineering and
Medical Physics.
Editor S.N. Levine, Volume 2, 1968.

19. WELCH, D.O.
The Composite Structure of Bone and it's Response
to Mechanical Stress.
Recent Advances in Engineering Science.
Editor A.C. Eringen, Volume 5, Part 1, 1968.

20. SWANSON, S.A.V.
Biomechanical Characteristics of Bone.
Advances in Biomedical Engineering.
Editor R.M. Kenedi, Volume 1, 1971.

21. SEDLIN, E.D.
A Rheologic Model for Cortical Bone.
Acta. Ortho. Scand. Supplement No. 83, 1965.

22. DEMPSTER, W.T. and LIDDICOAT, R.T.
Compact Bone as a Non-isotropic Material.
Am. J. Anat. 91 : 331-362, 1952.

23. BONFIELD, W. and LI, C.H.
Deformation and Fracture of Bone.
J. of App. Physics. 37(2) : 869-875, 1966.

24. BONFIELD, W. and LI, C.H.
Anisotropy of Non-elastic Flow in Bone.
J. of App. Physics. 38(6) : 2450-2455, 1967.

25. CARTWRIGHT, A.G.
The Effects of Histological Variation on the
Tensile Properties of Cortical Bone.
A Thesis submitted to the University of Surrey for
the degree of Doctor of Philosophy, September 1971.

26. YOKOO, S.
Compression Test of the Cancellated Bone.
J. Kyoto Pref. Med. Univ. 51 : 273-276, 1952.

27. HOWELL, A.H. and BRUDEVOLD, F.
Vertical Forces Used During Chewing Food.
J. Dent. Res. 29(2) : 133-136, 1950.

28. YURKSTAS, A. and CURBY, W.A.
Force Analysis of Prosthetic Appliances
During Function.
J. Pros. Den. 3(1) : 82-87, 1953.

29. CHARNLEY, J.
Biomechanics in Orthopaedic Surgery.
Biomechanics and Related Bio-Engineering Topics
Proceedings of a Symposium held in Glasgow in 1964.
Editor R.M. Kenedi, Pergamon: 1965.

30. PICKARD, H.M.
A Manual of Operative Dentistry.
Oxford University Press. 3rd Edition, 1970.

31. SYNGE, J.L.
The Tightness of the Teeth, Considered as a Problem concerning the Equilibrium of a Thin Incompressible Elastic Membrane.
Phil. Trans. Roy. Soc. (A)231 : 435-477, 1933.

32. HAY, G.E.
Stress in the Periodontal Membrane.
Oral Health. 29 : 257-261, 1939.

33. HAACK, D.C. and HAFT, E.E.
An Analysis of Stresses in a Model of the Periodontal Ligament.
Int. J. Engng. Sci. 10 : 1093-1106, 1972.

34. GABEL, A.B.
A Mathematical Analysis of the Function of the Fibres of the Periodontal Membrane.
J. of Periodontology. 27 : 191-198, 1956.

35. LEDLEY, R.S.
Theoretical Analysis of Displacement and Force Distribution for the Tissue-Bearing Surface of Dentures.
J. Dent. Res. 47(2) : 318-322, 1968.

36. LEDLEY, R.S. and HUANG, H.K.
Linear Model of Tooth Displacement by Applied Forces.
J. Dent. Res. 47 : 427-432, 1968.

37. LEDLEY, R.S. and HUANG, H.K.
Numerical Experiments with a Linear Force-Displacement Tooth Model.
J. Dent. Res. 48 : 32-37, 1969.

38. TSAO, D.H.
Designing Occlusal Rests using Mathematical Principles.
J. Prosth. Dent. 23(2) : 154-163, 1970.

39. BURSTONE, C.J.
Mechanics.
Vistas in Orthodontics, Chap. 5.
Ed. Kraus, B.S. and Riedel, R.A., H. Kimpton, 1962.

40. CHRISTIANSEN, R.L. and BURSTONE, C.J.
Centres of Rotation within the Periodontal Space.
Amer. J. Orthod. 55(4) : 353-369, 1969.

41. HOPPENSTAND, D.C. and McCONNELL, D.
Mechanical Failure of Amalgam Restorations with Zinc Phosphate and Zinc Oxide/Eugenol Cement Bases.
J. Dent. Res. 39 : 899-905, 1960.

42. MAHLER, D.B., et al.
Evaluation of Techniques for Analysing Cavity Design for Amalgam Restorations.
J. Dent. Res. 40(3) : 497-503, 1961.

43. HAACK, D.C. and WEINSTEIN, S.
Geometry and Mechanics as Related to Tooth Movement Studied by Means of Two-dimensional Models.
J.A.D.A. 66 : 157-164, 1963.

44. DEMPSTER, W.T. and DUDDLES, R.A.
Tooth Statics.
J.A.D.A. 68 : 652-666, 1964.

45. HENDERSON, D. et al.
The Cantilever Type of Posterior Fixed Partial Dentures.
A Laboratory Study.
J. Pros. Dent. 24 : 47-67, 1970.

46. DICKSON, R.L.
Mechanical Analysis of Posterior Teeth in Centric Closure.
J. Pros. Dent. 27(4) : 358-363, 1972.

47. HOLISTER, G.S.
Experimental Stress Analysis.
Pub. Cambridge University Press 1967.

48. FROCHT, M.M.
Photoelasticity. Vols. 1 and 2.
Pub. Wiley, New York. 1957.

49. MAHLER, D.B. and PEYTON, F.A.
Photoelasticity as a Research Technique for Analysing Stresses in Dental Structures.
J. Dent. Res. 34 : 831-838, 1955.

50. MAHLER, D.B.
An Analysis of Stresses in a Dental Amalgam Restoration.
J. Dent. Res. 37 : 516-526, 1958.

51. CRAIG, R.G. et al.
Experimental Stress Analysis of Dental Restorations.
Part 1. Two-dimensional Photoelastic Stress Analysis of Inlays.
J. Pros. Dent. 17(3) : 277-291, 1967.

52. CRAIG, R.G. et al.
Experimental Stress Analysis of Dental Restorations.
Part 2. Two-dimensional Photoelastic Stress Analysis of Crowns.
J. Pros. Dent. 17(3) : 292-302, 1967.

53. EL-EBRASHI, M.K. et al.
Experimental Stress Analysis of Dental Restorations.
Part 3. The Concept of the Geometry of Proximal Margins.
J. Pros. Dent. 22(3) : 333-345, 1969.

54. EL-EBRASHI, M.K. et al.
Experimental Stress Analysis of Dental Restorations.
Part 4. The Concept of Parallelism of Axial Walls.
J. Pros. Dent. 22(3) : 346-353, 1969.

55. EL-EBRASHI, M.K. et al.
Experimental Stress Analysis of Dental Restorations.
Part 5. The Concept of Occlusal Reduction and Pins.
J. Pros. Dent. 22(5) : 565-577, 1969.

56. EL-EBRASHI, M.K. et al.
Experimental Stress Analysis of Dental Restorations.
Part 6. The Concept of Proximal Reduction in Compound Restorations.
J. Pros. Dent. 22(6) : 663-670, 1969.

57. EL-EBRASHI, M.K. et al.
Experimental Stress Analysis of Dental Restorations.
Part 7. Structural Design and Stress Analysis of Fixed Partial Dentures.
J. Pros. Dent. 23(2) : 177-186, 1970.

58. TANNER, A.N.
Factors Affecting the Design of Photoelastic Models for Two-dimensional Analysis.
J. Pros. Dent. 27(1) : 48-62, 1972.

59. NALLY, J.N. et al.
Experimental Stress Analysis of Dental Restorations.
Part 9. Two-dimensional Photoelastic Stress Analysis of Porcelain Bonded to Gold Crowns.
J. Pros. Dent. 25(3) : 307-316, 1971.

60. LEHMAN, M.L. and MEYER, M.L.
Relationship of Dental Caries and Stress: Concentrations in Teeth as Revealed by Photoelastic Tests.
J. Dent. Res. 45(6) : 1706-1714, 1966.

61. JOHNSON, E.W. et al.
Stress Pattern Variations in Operatively Prepared Human Teeth, Studied by Three-dimensional Photoelasticity.
J. Dent. Res. 47(4) : 548-558, 1968.

62. LEHMAN, M.L.
Stress Distribution in the Alveolar Bone.
J. Biomech. 1 : 139-145, 1968.

63. FARAH, J.W. and CRAIG, R.G.
Reflection Photoelastic Stress Analysis of a Dental Bridge.
J. Dent. Res. 50(5) : 1253-1259, 1971.

64. SHARRY, J.J. et al.
Influence of Artificial Tooth Forms on Bone Deformation Beneath Complete Dentures.
J. Dent. Res. 39(2) : 253-266, 1960.

65. CRAIG, R.G. and PEYTON, F.A.
Measurement of Stresses in Fixed-Bridge Restorations Using a Brittle Coating Technique.
J. Dent. Res. 44(4) : 756-762, 1965.

66. TILLITSON, E.W. et al.
Experimental Stress Analysis of Dental Restorations.
Part 8. Surface Strains on Gold and Chromium Fixed Partial Dentures.
J. Pros. Dent. 24(2) : 174-180, 1970.

67. BISPLINGHOFF, R.L., MAR, J.W. and PIAN, T.H.H.
Statics of Deformable Solids.
Pub. Addison-Wesley, 1965.

68. MUHLEMANN, H.R.
Tooth Mobility.
J. Periodont. Part 1 25(JAN) : 22-29, 1954.
J. Periodont. Part 2 25(APR) : 125-128, 1954.
J. Periodont. Part 3 25(APR) : 128-137,153, 1954.

69. MUHLEMANN, H.R.
10 Years of Tooth-Mobility Measurements.
J. Periodont. 31 : 110-122, 1960.

70. PARFITT, G.J.
Measurement of the Physiological Mobility of Individual Teeth in an Axial Direction.
J. Dent. Res. 39(3) : 608-618, 1960.

71. PARFITT, G.J.
The Dynamics of a Tooth in Function.
J. Periodont. 32 : 102-107, 1961.

72. PICTON, D.C.A.
Tilting Movements of the Teeth During Biting.
Arch. Oral Biol. 7 : 151-159, 1962.

73. PICTON, D.C.A.
Distortion of the Jaws During Biting.
Arch. Oral Biol. 7 : 573-580, 1962.

74. PICTON, D.C.A.
The Effect of Repeated Thrusts on Normal Axial Tooth Mobility.
Arch. Oral Biol. 9 : 55-63, 1964.

75. PICTON, D.C.A.
Some Implications of Normal Tooth Mobility During Mastication.
Arch. Oral Biol. 9 : 565-573, 1964.

76. ANDERSON, D.J.
Measurement of Stress in Mastication.
Part 1. J. Dent. Res. 35 : 664-670, 1956.
Part 2. J. Dent. Res. 35 : 671-673, 1956.

77. PICTON, D.C.A.
On the Part Played by the Socket in Tooth Support.
Arch. Oral Biol. 10 : 945-955, 1965.

78. PICTON, D.C.A. and DAVIES, W.I.R.
Dimensional Changes in the Periodontal Membrane of Monkeys (Macara Irus) due to Horizontal Thrusts applied to the Teeth.
Arch. Oral Biol. 12 : 1635-1643, 1967.

79. PICTON, D.C.A.
The Effect on Tooth Mobility of Trauma to the Mesial and Distal Regions of the Periodontal Membrane in Monkeys.
Helv. Odont. Acta. 11 : 105-112, 1967.

80. PICTON, D.C.A. and SLATTER, J.M.
The Effect on Horizontal Tooth Mobility of Experimental Trauma to the Periodontal Membrane in Regions of Tension or Compression in Monkeys.
J. Periodont. Res. 7 : 35-41, 1972.

81. WILLS, D.J., PICTON, D.C.A., and DAVIES, W.I.R.
An Investigation of the Viscoelastic Properties of the Periodontium in Monkeys.
J. Periodont. Res. 7 : 42-51, 1972.

82. BIEN, S.M.
Hydrodynamic Damping of Tooth Movement.
J. Dent. Res. 45(3) : 907-914, 1966.

83. GRESZCZUK, L.B.
Effect of Material Orthotropy on the Directions of the Principal Stresses and Strains.
From Orientation Effects in the Mechanical Behaviour of Anisotropic Structural Materials.
A.S.T.M., S.T.P. No. 405 : 1-13, 1965.

84. WHEELER, R.C.
Tooth Form. A Manual on Drawing and Carving.
Pub. W.B. Saunders Co., 1939.

85. CHOU, P.C. and PAGANO, N.J.
Elasticity.
Pub. D. Van Nostrand Co., 1967.

86. BRADEN, M.
Heat Conduction in Teeth and the Effect of Lining Materials.
J. Dent. Res. 43 : 315-322, 1964.

87. THRESHER, R.W. and SAITO, G.E.
The Stress Analysis of Human Teeth.
J. Biomech. 6 : 443-449, 1973.

88. FARAH, J.W. et al.
Photoelastic and Finite Element Stress Analysis of a Restored Axisymmetric First Molar.
J. Biomech. 6 : 511-520, 1973.

89. UTLEY, R.K.
The Activity of Alveolar Bone Incident to Orthodontic Tooth Movement as Studied by Oxytetracycline-induced Fluorescence.
Am. J. of Orthod. 54(3) : 167-201, 1968.

90. HERMANSON, P.C.
Alveolar Bone Remodelling Incident to Tooth Movement.
Angle Orthod. 42(2) : 107-115, 1972.

91. STEPHENS, C.D.
A Preliminary Report of a Cephalometric Appraisal of Incisor Movement During Orthodontic Treatment.
British J. of Orthod. 1(2) : 44, 1974.

92. WOLFF, J.
Ueber die innere Architectur der Knochen und ihre Bedeutung fiir die frage vom Knochenwachstum.
Virchow's Arch Path. Anat. 50 : 389-453, 1870.

93. WOLFF, J.
Das Gasetz der Transformation der Knochen.
Berlin (Monograph). 1892.

94. THOMPSON, D'Arcy W.
On Growth and Form.
Pub. Cambridge Univ. Press. 1952.

95. FELL, H.B.
In Biochemistry and Physiology of Bone.
Editor G.H. Bourne, 1st Edition.
Pub. Academic Press.

96. BASSETT, C.A.L.
Electrical Effects in Bone.
Scientific America. 213 : 18-25, 1965.

97. CHAMAY, A. and TSCHANTZ, P.
Mechanical Influences in Bone Remodelling.
Experimental Research on Wolff's Law.
J. Biomech. 5 : 173-180, 1972.

98. EPKER, B.N. and FROST, H.M.
Correlation of Bone Resorption and Formation with the Physical Behaviour of Loaded Bone.
J. Dent. Res. 44(1) : 33-41, 1965.

99. BAUMRIND, S.
A Reconsideration of the Propriety of the " Pressure-Tension" Hypothesis.
Am. J. Orthod. 55(1) : 12-22, 1969.

100. REITAN, K.
Some Factors Determining the Evaluation of Forces in Orthodontics.
Am. J. Orthod. 43(1) : 32-45, 1957.

101. REITAN, K.
Bone Formation and Resorption during Reversed Tooth Movement.
From Vistas in Orthodontics.
Editors B.S. Kraus and R.H. Reidel.
Pub. H. Kimpton 1962.

102. REITAN, K.
Effects of Force Magnitude and Direction of Tooth Movement on Different Alveolar Bone Types.
Angle Orthod. 34(4) : 244-255, 1964.

103. REITAN, K.
Clinical and Histological Observations on Tooth Movement During and After Orthodontic Treatment.
Am. J. of Orthod. 53(10) : 721-745, 1967.

104. ACKERMAN, J.L. et al.
The Effects of Quantified Pressure on Bone.
Am. J. Orthod. 52(1) : 34-46, 1966.

105. WEINSTEIN, S.
Minimal Forces in Tooth Movement.
Am. J. Orthod. 53(12) : 881-903, 1967.

106. FUKADA, E. and YASUDA, I.
On the Piezoelectric Effect of Bone.
J. Physical Soc. of Japan. 12(10) : 1158-1162, 1957.

107. SHAMOS, M.H. and LAVINE, L.S.
Physical Bases for the Bioelectric Effects in Mineralised Tissues.
Clin. Orthop. 35 : 177-188, 1964.

108. BRADEN, M. et al.
Electrical and Piezoelectric Properties of Dental Hard Tissues.
Nature. 212 : 1565-1566, 1966.

109. BASSETT, C.A.L. and BECKER, R.O.
Generation of Electrical Potentials by Bone in Response to Mechanical Stress.
Science. 137 : 1063-1064, 1962.

110. COCHRAN, G.V.B. et al.
Stress Generated Electrical Potentials in the Mandible and Teeth.
Arch. Oral Biol. 12 : 917-920, 1967.

111. McELHANEY, J.H.
The Charge Distribution on the Human Femur Due to Load.
J. Bone and Joint Surgery. 49(8) : 1561-1571, 1967.

112. GJELSVIK, A.
Bone Remodelling and Piezoelectricity (1).
J. Biomech. 6 : 69-77, 1973.

113. GJELSVIK, A.
Bone Remodelling and Piezoelectricity (2).
J. Biomech. 6 : 187-193, 1973.

114. KOCH, J.C.
The Laws of Bone Architecture.
Am. J. Anat. 21 : 177-298, 1917.

115. FESSLER, H.
Load Distribution in a Model of a Hip Joint.
J. Bone and Joint Surgery. 39(1) : 145-153, 1951.

116. WILLIAMS, J.F. and SVENSSON, N.L.
An Experimental Stress Analysis of the Neck of the Femur.
Med. and Biol. Eng. 9 : 479-493, 1971.

117. PAUL, J.P.
Forces Transmitted by Joints in the Human Body.
Proc. Inst. Mech. Eng. 181(3J) : 8-15, 1967.

118. RYBICKI, E.F. et al.
On the Mathematical Analysis of Stress in the Human Femur.
J. Biomech. 5 : 203-215, 1972.

119. STOREY, E.
Bone Changes Associated with Tooth Movement.
A Radiographic Study.
The Australian J. of Dent. 57(2) : 57-64, 1953.

120. EDWARDS, J.G.
A Study of the Periodontium During Orthodontic
Rotation of Teeth.
Am. J. of Orthod. 54(6) : 441-476, 1968.

121. TAPPEN, N.C.
Main Patterns and Individual Differences in Baboon Skull Split-lines and Theories of Causes of Split-line Orientation in Bone.
Am. J. Phys. Anthrop. 33(1) : 61-71, 1970.

122. CURREY, J.D.
The Adaption of Bones to Stress.
J. Theoret. Biol. 20 : 91-106, 1968.

123. FROST, H.M.
The Laws of Bone Structure.
Pub. Charles C. Thomas, Springfield.

124. OXNARD, C.E.
Tensile Forces in Skeletal Structures.
J. of Morphology. 134 : 425-436, 1971.

125. HRENNIKOFF, A.
Solution of Problems of Elasticity by the Framework Method.
J. App. Mech. 63 : A-169-175, 1941.

126. YETTRAM, A.L. and ROBBINS, K.
Space-Framework Method for Three-dimensional Solids.
J. Eng. Mech. Div. A.S.C.E. EM 6, 21-36, 1967.

127. TURNER, M.J. et al.
Stiffness and Deflection Analysis of Complex Structures.
J. Aero. Sci. 23 : 805-823, 1956.

128. DESAI, C.S. and ABEL, J.F.
Introduction to the Finite Element Method.
Pub. Van Nostrand Reinhold Co., 1972.

129. ZIENKIEWICZ, O.C.
The Finite Element Method in Engineering Science.
Pub. McGraw-Hill, 1971.

130. ERGATOUDIS, J.G.
Isoparametric Elements in Two and Three-dimensional Analysis.
Ph. D. Thesis, University of Wales, Swansea, 1968.

131. BROOKS, D.F. and BROTTON, D.M.
Computer Systems for Analysis of Large Frameworks.
J. of the Structural Division, Proc. A.S.C.E.
93(ST6) : 1-23, 1967.

132. YETTRAM, A.L. and HIRST, M.J.S.
The Solution of Structural Equilibrium Equations by the Conjugate Gradient Method with Particular Reference to Plane Stress Analysis.
Int. J. Num. Meth. Eng. 3 : 349-360, 1971.

133. I.C.L. Technical Publication 4087,
Graph Plotter 1900 series, 1970.

134. TIMOSHENKO, S. and GOODIER, J.N.
Theory of Elasticity.
Pub. McGraw-Hill, 2nd Edition, 1951.

135. IRONS, B.M.
A Frontal Solution Program for Finite Element Analysis.
Int. J. Num. Meth. Eng. 2 : 5-32, 1970.

136. KOPAL, Z.
Numerical Analysis.
Pub. Chapman and Hall, London 1955.

137. CLOUGH, R.W.
Comparison of Three-dimensional Finite Elements.
From Proceedings of a Symposium on the Application of Finite Element Methods in Civil Engineering.
A.S.C.E. Nov. 13-14 : 1969.

138. IRONS, B.M.
Quadrature Rules for Brick Based Finite Elements.
Int. J. Num. Meth. Eng. 3 : 295-296, 1971.

139. McKINNON, V.
Matrix Analysis of Plates and Plated Grillages Using Equivalent Framework Idealisations.
Ph. D. Thesis, Leeds University, 1970.

140. ZIENKIEWICZ, O.C.
Private Communication.

141. EDWARDS, J.
Physical Characteristics of Articular Cartilage.
Paper 6. Proc. Inst. Mech. Eng. 181(3J) 16-24, 1967.

142. LEE, E.H.
Stress Analysis in Viscoelastic Materials.
J. App. Physics. 27(7) : 665-672, 1956.

143. ZIENKIEWICZ, O.C. et al.
A Numerical Method of Viscoelastic Stress Analysis.
Int. J. Mech. Sci. 10 : 807-827, 1968.

144. GHISTA, D.N. et al.
Computerised Left Ventricular Mechanics and Control System Analysis Models Relevant for Cardiac Diagnosis.
Comput. Biol. Med. 3 : 27-46, 1973.

145. MATTHEWS, F.L. and WEST, J.B.
Finite Element Displacement Analysis of a Lung.
J. Biomech. 5 : 591-600, 1972.

# GENERAL REFERENCES

## GENERAL REFERENCES


ANDERSON, G.M.
Practical Orthodontics.
Henry Kimpton, London. 7th Ed. 1948.

HANCOX, N.M.
Biology of Bone.
Cambridge University Press. 1972.

HEMLEY, S.
Orthodontic Thecry and Practice.
Grune and Stratton, N.Y. 2nd Ed. 1953.

PEYTON, F.A., et al.
Restorative Dental Materials.
Henry Kimpton, London. 2nd Ed. 1964.

SCOTT, J.H. and SYMONS, N.B.B.
Introduction to Dental Anatomy.
E. and S. Livingstone, Edinburgh and London. 3rd Ed. 1961.

SICHER, H.
Oral Anatomy.
Henry Kimpton, London. 1949.

TYLMAN, S.D., and TYLMAN, S.G.
Theory and Practice of Crown and Bridge Prosthodontics.
Mosby Co., St. Louis. 4th Ed. 1960.

Mechanisms of Hard Tissue Destruction:
Symposium of the American Association for the Advancement of Science. Dec., 29th and 30th, 1962.
Editor R.F. Sognnaes.
Publication no. 75 of the A.A.A.S.

The American Textbook of Operative Dentistry.
Edited by A.B. Gabel.
Henry Kimpton, London. 9th Ed. 1954.